Australian Geomechanics Society

ENGINEERS AUSTRALIA

Resilient Geotechnics

Proceedings of the 2014 AGS Symposium
Friday 7th November 2014

Photos Taken by Tim Mote from Arup

Platinum Sponsor: TERRATEST

Gold Sponsors: Coffey, JK Geotechnics, Menard Bachy

Silver Sponsors: GHD, DGSI, VIBROPLIE, Golder Associates, MACQUARIE GEOTECH

ISSN 0818-9110

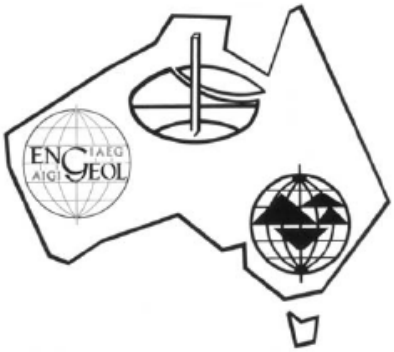

Australian Geomechanics Society

ISSN 0818-9110

Resilient Geotechnics

PROCEEDINGS OF THE 2014 AGS SYMPOSIUM

HELD IN

AUSTRALIAN NATIONAL MARITIME MUSEUM, DARLING HARBOUR, NSW

ON

October 7th 2014

Organising Committee: H. Khabbaz, C. Rujikiatkamjorn, S. Mirlatifi, C. McColgan and M. van Uden,

Editors: H. Khabbaz and C. Rujikiatkamjorn

Published by
The Australian Geomechanics Society,
National Secretariat,
P.O. Box 955, ST IVES, NSW 2075

The Australian Geomechanics Society (AGS) is jointly sponsored by: Engineers, Australia and The Australasian Institute of Mining and Metallurgy

Australian Geomechanics Society

Geomechanics is the application of engineering principles to the earth sciences to improve continually the accuracy, efficiency, cost-effectiveness and safety of construction projects both above and below ground, including the recovery of the earth's mineral resources. It remains an imprecise discipline due to the infinite variety of conditions in the earth's crust but correspondingly offers a fascinating and rewarding field of research and practice.

The Australian Geomechanics Society was founded in 1970. Its origins lie in the National Committee of Soil Mechanics of the Institution of Engineers, Australia, established in 1953 and the call for a corresponding society in rock mechanics. In 1973 the society was expanded to include the third discipline of engineering geology and has remained substantially unchanged since that date.

The society is affiliated to the International society of Soil Mechanics and Foundation Engineering (ISSMFE), the International Society for Rock mechanics (ISRM) and the International Association for Engineering Geology and the Environment (IAEG).

The AGS is jointly sponsored by the Engineers Australia and the Australian Institute of Mining and Metallurgy.

CORPORATE MEMBERSHIP OF THE AGS

$770.00 and look at what your organisation gets -
Membership for two nominees who each receive:

- Membership fee ($209)
- Membership of the three International Societies ($176)
- IAEG Bulletin ($44)

An extra copy of *Australian Geomechanics* for company library ($154)

Acknowledgement in front section of every issue of *Australian Geomechanics*

Total benefit is $836 All prices include GST.

Contact Peter Robinson on secretary@australiangeomechanics.org or go to www.australiangeomechanics.org **for application forms and more information**.

Australian Geomechanics Society

2014 AGS Symposium
Resilient Geotechnics

Friday 7 November 2014
Australian National Maritime Museum, Darling Harbour, Sydney

Program

8:30 Registration
9:00 Welcome and opening address

Morning (part 1)

9:05 **Keynote Lecture:** Resilience and vulnerability to climate change through the prism of soil-water interactions: challenges of temporal and geographical scales for geotechnical engineering
Abbas El-Zein (University of Sydney)

9:40 **Invited Lecture:** Ingenuity and intelligent risk assessment for resilient geotechnics
David Oliveira (Coffey)

10:05 Understanding liquefaction triggering risk: an Australian geotechnical design perspective
Tim Mote (Arup Australia)

10:25 *Questions*
10:40 ***Morning tea***

Morning (part 2)

11:10 **Invited Lecture:** Design and construction of a resilient motorway on difficult ground
Richard Kelly (Coffey)

11:35 **Invited Lecture:** Pipe jacking through a rail embankment
Jeff Hsi (SMEC Australia)

12:00 Application of compound deep cement mixed walls for retaining structures in excavations
Samanathika Liyanapathirana (Uni. of Western Sydney)

12.20 Resilient foundations: building in repair capability
Y. Duraisamay and D. Airey (Uni. of Sydney)

12:40 *Questions*
12:55 ***Lunch***

Afternoon (part 1)

13:45 **International Invited Lecture:** Limitations on geotechnical risk management: designing for resilience
Tim Davies (University of Canterbury, NZ)

14:10 **Invited Lecture:** Resilient geotechnics - past failures and future success
Philip Davies (Golder Associates)

14:35 A one pass synthetic fibre reinforced shotcrete tunnel lining for a very shallow cover tunnel, north Strathfield rail underpass
Ted Nye (Mott MacDonald)

14:55 Innovative design of reinforced soil wall on a steep slope subject to land slip risks
Jim Yang (Hyder Consulting)

15:15 *Questions*
15:30 ***Afternoon tea***

Afternoon (part 2)

15:50 Towards a resilient design: L-shaped barrier-impact load modelling on reinforced soil wall structure
Philip Wanis (The Reinforced Earth Company)

16:10 Design challenges of road widening in soft grounds: characterisation to numerical analysis
Saman Zargarbashi (Golder Associates)

16:30 Sustainability considerations for ground improvement techniques using controlled modulus columns
Harry Nguyen (Uni. of Technology Sydney)

16:50 Risk based approach in a spillway upgrade
Jayantha Sinha (State Water Corporation)

17:10 *Questions*
17:25 *Closing address*
17:30 ***Close***

Platinum Sponsor

Celebrating 50 Years TERRATEST

Gold Sponsors

coffey

MENARD BACHY

JK Geotechnics
GEOTECHNICAL & ENVIRONMENTAL ENGINEERS
www.jkgeotechnics.com.au

Silver Sponsors

Golder Associates

MACQUARIE GEOTECH

GHD

DGSI
DURHAM GEO SLOPE INDICATOR

VIBROPILE
EXPERIENCE IS THE BEST FOUNDATION


Terratest
Now with CPT
terratest.com.au

Photograph by Andrew Worssam

JK Geotechnics
GEOTECHNICAL & ENVIRONMENTAL ENGINEERS
www.jkgeotechnics.com.au

JK Geotechnics completed a comprehensive geotechnical investigation for the ITE building located on Broadway. JK Geotechnics completed 2D FE modelling to assess the potential impacts of the proposed development on the existing Transgrid cable tunnel and the proposed Metro West twin railway tunnel. JK Geotechnics were heavily involved in the construction stage of the project during installation of shoring piles, drilling and stress testing of temporary ground anchors, inspection of rock cut faces, detailing rock face stabilisation measures and confirming the adopted high design bearing pressures for the building footings.

EIS

EIS, the environmental division of the JK Group, undertook the preliminary Stage 1 Environmental Site Assessment for the UTS Broadway Precinct. EIS subsequently completed the Stage 2 Environmental Assessment for the ITE building in conjunction with JK Geotechnics.

Symposium – Friday 7 November 2014

RESILIENT GEOTECHNICS

PREFACE

This document contains papers for the 18th annual symposium organised by the Sydney Chapter of the Australian Geomechanics Society. It is hoped that the symposium will keep practicing geotechnical engineers, engineering geologists and other engineering professionals informed of recent developments in this field. It also recognises the need to gather together the experience of those practicing throughout Australia and to allow transfer of knowledge and sharing of their experiences.

These symposia continue to be one of the best forms for bringing together the key stakeholders of the Australian geotechnical community. The main objective of the symposium, held on 7 November 2014, is to advance the knowledge in design and construction towards more resilient infrastructure.

Contributors include academics, designers, suppliers and contractors. The papers present novel design and construction technologies for the performance monitoring and prediction of resilient geotechnical structures, risk management strategies, numerical modelling, deep basement analysis, the use of new materials for infrastructures, the state-of-the-art practices, innovative technologies as well as new research results and case histories on construction and design aspects of green and resilient infrastructure, considering climate change adaptation, natural disaster risk reduction and sustainability.

This symposium is the cooperative effort of many authors. The editors and organising committee wish to thank the authors, who have generously contributed their time to prepare the various papers and the colleagues of the authors, who have assisted with time, secretarial, drafting and other facilities. Appreciation is also extended to our sponsors for their support. Without them the Symposium would not be possibly the best ongoing forum for the Australian Geomechanics community.

Hadi Khabbaz, Cholachat Rujikiatkamjorn, Sam Mirlatifi, Cillian McColgan and Mark van Uden

On behalf of the AGS Symposium Organising Committee, and
The Australian Geomechanics Society, Sydney Chapter

Annual Seminars of AGS Sydney Chapter

No.	Date	Topic	Chairman & Organising Team
1	1997	Pavement Design Beyond 2000	A Leventhal
2	1998	Recent Developments in Piling Practice in Sydney	P Andrews
3	1999	Flexible Retaining Walls: Design to Prevent Failure	P Andrews and P Hewitt
4	2000	Computer Methods	P Hewitt and J Carter
5	2001	Excavation Retention	T Walker and P Hewitt
6	2002	Landslide Risk Management	B Walker and T Walker
7	2003	Geotechnical Instrumentation and Construction Works Compliance Testing	G Scholey and T Walker
8	2004	The Engineering Geology of the Sydney Region – Revisited	G Scholey, M Parmar, G Young and G McNally
9	2005	Geotechnical Aspects of Tunnelling	H Buys and T Gourlay
10	2006	Soft Ground Engineering	H Buys, R Moyle and P Hewitt
11	2007	Engineering Advances in Earthworks	R Moyle, R Lindbeck and H Liu
12	2008	Foundation Design and Construction	R Moyle, R Lamont and B Ewers
13	2009	Geosynthetics – New Materials for Modern Infrastructure	B Ewers, H Buys and H Liu
14	2010	Seismic Engineering- Design for Management of Geohazards	C Rujikiatkamjorn, J McIlveen, R Lamont and M Haysler
15	2011	Coastal and Marine Geotechnics- Foundations for Trade	C Rujikiatkamjorn, J McIlveen, G Blumberg, J Smith and C Y Tey
16	2012	Advances in Geotechnical Aspects of Roads and Railways	H Khabbaz, C Y Tey, O Stahlhut and C Rujikiatkamjorn
17	2013	Retaining Structures: Recent Advances and Past Experiences	H Khabbaz, C Rujikiatkamjorn, M van Uden, C McColgan and S Mirlatifi
18	2014	Resilient Geotechnics	H Khabbaz, C Rujikiatkamjorn, S Mirlatifi, C McColgan and M van Uden

TABLE OF CONTENTS

[All papers have been refereed in accordance with the full DETYA review process, unless stated otherwise.]

RESILIENCE AND VULNERABILITY TO CLIMATE CHANGE THROUGH THE PRISM OF SOIL-WATER INTERACTIONS: CHALLENGES OF TEMPORAL AND GEOGRAPHICAL SCALES FOR GEOTECHNICAL ENGINEERING

Abbas El-Zein[1]
[1]*Associate Professor*
School of Civil Engineering, University of Sydney, Sydney NSW 2006, Australia

ABSTRACT

The interaction between water and soil particles lies at the heart of the work of geotechnical and geo-environmental engineers. The water content of the subsurface is an important state variable influencing soil behaviour in relation to strength and stability, hydrologic and chemical insulation, sediment budgets and transport, and support for biological life. The capacity of many soils to maintain high shear strength and withstand loads applied to them without significant deformation, crushing or erosion; their ability to insulate contaminated sites and filter heavy metals and organic chemicals out of polluted water; and their effectiveness in supporting healthy biological life for food production and other ecosystem services, are all examples of vital, and sometimes conflicting services, that soils provide and which are critically dependent on water content.

Three major sources of ecological and social change are reasonably certain in the 21st century:

a) increased urbanisation with more demands placed on subsurface systems and structures, by the energy, transport, mining and environmental sectors;
b) increased frequencies, magnitude and duration of droughts and floods as a result of anthropogenic climate change, with likely changes to patterns of precipitation and water retention; and
c) significant rise in sea levels as a result of thermal expansion and melting of glaciers, leading to higher risks of erosion of coastal land and weakening of coastal foundations with possible damage to private properties and critical water, wastewater, telecommunications and transport infrastructure.

The paper's goal is threefold. First, different pathways for the impacts of climate change on subsurface systems are described through the lens of soil-water and land-ocean interactions. Second, a case study from Callala beach in Shoalhaven is presented to illustrate the complexity of making adaptation choices at the interface between land and water, especially as a result of uncertainty and unusual temporal and geographical scales of the problems. Third, the readiness of geotechnical education and practice to deal with these problems is discussed in the context of the difference between risk and vulnerability and the emerging distinction between incremental and transformational adaptation. The paper calls on the geotechnical community to engage more fully in the debate on adaptation to climate futures, going beyond the technical assessment of the integrity of infrastructure systems, and identifying long-term strategies for the conflicting demands we place on the subsurface. This will require innovations and possibly some extension of the spatial and temporal scopes of our experimental, analytical and theoretical methodologies.

1 INTRODUCTION

In 1925, Austrian engineer Karl von Terzaghi proposed the concept of effective stress, ultimately linking the strength and deformation of soil to the way the burden of applied load is shared between soil particles and pore water. Since then, the science of soil mechanics has come a long way, developing fully functioning theories of soil behaviour—including Maurice Biot's poro-mechanics—with their associated experimental and analytical tools and protocols. As a result, we are now able to account for a large number of observed soil phenomena and use that knowledge in geotechnical design and construction. It was clear from early on that, in almost every geotechnical endeavour, the proportion of water relative to soil minerals in a soil sample—known as either gravimetric or volumetric water content, depending on how it is measured—is a key parameter that has significant bearing on the shear strength of soil, its deformability as well as its ability to conduct liquids, chemicals, heat and electricity. For example, in unsaturated soil mechanics, water content strongly influences the way soil particles are held together by capillary menisci and the extent to which soil water is free to move or become bonded to the surface of soil grains (Fredlund et al., 2012). As a result,

water content plays a critical role in such problems as soil compaction, slope stability and landslides, foundation settlement, road pavement design and failures, and low-conductivity clay for waste repositories.

Water content itself is the outcome of environmental and engineering variables that can change in space and time, in the short- and longer terms. Indeed, the most important factors affecting the quantity and physico-chemical state of water in soil are rainfall, runoff, temperature-dependent rates of evaporation and transpiration, water table levels, soil water retention properties, soil hydraulic conductivity and structure and type of soil. All but the last (type of soil) are likely to be affected, at least to some extent, by climate change. Over the last century, a 19 cm rise in global sea levels has been recorded and changes to patterns of precipitation and frequencies of extreme weather events have occurred and are projected to continue, and possibly accelerate, over the course of the 21st century (IPCC, 2013). While the rate and pace of change will depend on scenarios of greenhouse gas emissions, an increase of 2^{o}C in global average temperatures and a 30cm rise in sea levels by 2100 now appear inevitable, with some possibility of larger changes (IPCC, 2013).

Climate change can impact, and be affected by, the work of geotechnical engineers in two major ways. First, the production and distribution of energy is a central focus of the emerging global effort to wean society off GHG-intensive modes of living and economic production and growth. Mining for lower greenhouse gas intensive sources of energy such as natural gas, extracting and distributing renewable energy from geothermal sources or waste bioreactors, and geo-sequestrating carbon dioxide emitted by coal-burning power-plants are examples of three areas of climate change mitigation in which geotechnical engineers have a central contribution to make (e.g., Fragaszy et al., 2011; Basu et al., 2013). Second, natural and engineered subsurface systems (including infrastructure components in the transport, housing, telecommunication, electricity, water and wastewater sectors) can be impacted by changes in key climatic indicators and extreme weather events (e.g., Yasuhara et al., 2012). For example, the integrity of railway and road systems, water and wastewater pipelines, as well as foundations of houses and buildings are likely to be affected by projected changes in rainfall, temperature and sea levels—including associated events such as heatwaves, droughts, flash floods, cyclones and storm surges. With cities in Australia historically developing as port towns and more than 80% of Australians living along the coast today, the effects of sea level rise in particular are expected to be important (Cechet et al., 2011). Furthermore, climate change should be viewed in the context of continuing urbanisation in Australia and overseas, and more demands placed on subsurface systems and structures (State of Australian Cities 2013a; State of Australian Cities 2013b).

This paper is concerned with the second of these connections, i.e., the vulnerability of sub-surface systems to changes in climate. It has three objectives. First, different pathways for the impacts of climate change on geotechnical systems are described through the lens of soil-water and land-ocean interactions. Second, a case study from Callala beach in Shoalhaven is presented to illustrate the complexity of geotechnical and coastal adaptation problems, emanating from their unusual temporal and geographical scales. Finally, the readiness of geotechnical education and practice to deal with these problems is discussed in the context of the emerging distinction between incremental and transformational adaptation.

2 WATER CONTENT, INFRASTRUCTURE AND CLIMATE CHANGE

Climate change may impact subsurface systems[1] in at least three different ways, shown in Figure 1. Pathway 1 refers to the direct impact of a single extreme weather event. For example, a flash flood can alter soil hydro-mechanical properties, decrease suction and strength and temporarily raise the water table. This can cause slope instability (e.g., Briggs, 2010; Yellishetty and Darlington, 2011) or a temporary rise of water table increasing the risk of soil liquefaction (e.g., Take et al., 2014) and/or dissolution of contaminants stored near or below the surface (e.g., Stadler et al., 2012). Under pathways 2 and 3, on the other hand, long-term changes in climatic variables and repeated occurrences of extreme weather events, respectively, may lead to changes in key soil characteristics and consequently failures of engineered or natural subsurface systems. Examples of pathway 2 are the reduction in average precipitation and infiltration and increase in average temperatures and rates of evaporation which may result in a gradual, long-term decline in water table levels and soil water contents and, therefore, seawater intrusion and soil deformation (e.g., Comegna et al., 2012). An instance of pathway 3 is a repetitive occurrence of storm surges over a number of years eroding beach dunes and weakening foundations of foreshore properties (e.g., Suanez et al., 2012; Li et al., 2014). Another example is repeated flash flood events and pore pressure oscillations which may lead to the ―softening" of

[1] By ―subsurface systems" I mean that part of the lithosphere that is directly relevant to the work of geotechnical and geoenvironmental engineers; they include engineered foundation and underground systems, as well as engineered and non-engineered plant cover, topsoil, aquitards and aquifers; this definition does *not* include deeper geological formations and the earth crust which, with the exception of the effects tectonic-plate movements and earthquakes, are much less relevant to geotechnical engineering. For a review of the effects of climate on the deeper geosphere, the reader is referred to Liggins et al. (2010).

plastic clay, with corresponding loss of strength and progressive failure (e.g., Fan et al., 2014). In many instances, the three pathways may be active simultaneously (e.g., an extreme event triggering slope failure along pathway 1, in a soil that has been undergoing long-term change along pathways 2 and 3).

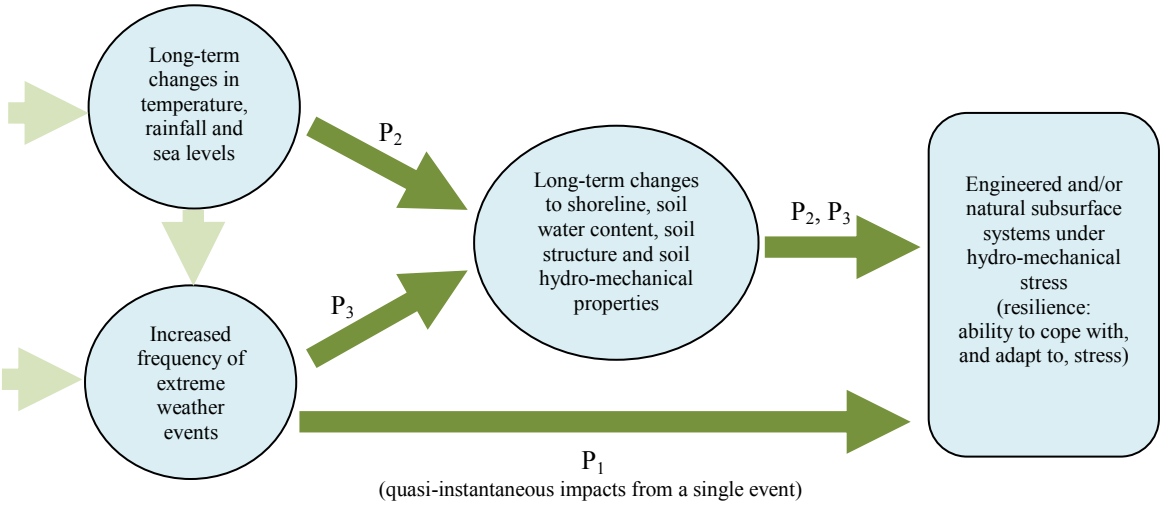

Figure 1. Three pathways (P_1, P_2 and P_3) of impacts of climate change on subsurface systems

Pathway 1 can be analysed and understood by assessing the sensitivity of soil properties and states to key environmental variables, over a time scale of seconds to days or, at most, a season. For example, in many shrink-swell failure problems related to oscillations of suction in the unsaturated zone, the water table is deep and reasonably stable and the pore pressures are hence essentially determined by micro-climate variables, such as rainfall, vegetation and temperature (e.g., Briggs, 2010; Nguyen et al., 2010). It is indeed possible to quantify and manage this sensitivity by means of theoretical, experimental and numerical techniques and tools that are already well-honed in the geotechnical profession.

Studying pathways 2 and 3, on the other hand, raises a number of issues, not least of which is the need to monitor and predict the variability over years and decades of key soil hydro-mechanical variables. Furthermore, given that the principal drivers of the hazards in question are environmental, geographically-widespread (rather than site-specific) risk factors, the above-mentioned variables need to be mapped on large spatial scales of kilometres or more. By contrast, geotechnical and geoenvironmental engineering—like soil science but unlike geography—are disciplines whose methods and theories are premised, by and large, on site-specific information measured on a scale ranging from a few millimetres to a few kilometres.

One soil moisture indicator developed in geography and adopted to some extent in geotechnical engineering is the Thornthwaite Moisture Index (TMI). The TMI measures the balance of soil moisture from rainfall, runoff, evaporation and transpiration and lends itself well to geographical mapping. It has been used for global climate classifications, as an indicator of climate change and for the study of drought, water availability and some aspects of forestry and agriculture (Keim, 2010). Its applications in geotechnical engineering include its use as a proxy for fluctuations in suctions when designing footings or assessing slope stability (e.g., Fityus et al., 1998; Fityus and Buzzi, 2008; Coe, 2012), and road pavement failure (e.g., Austroads, 2004; Philp and Taylor, 2012). Leao (2014) studied the change in TMI in the state of Victoria over 100 years and found a pattern of long-term decline, indicating that a significant proportion of Victorian soils are experiencing long-term drying, consistently with climate change predictions for the state (Climate Change in Victoria, 2008). However, the implications of such trends for the hydro-mechanical behaviour of the subsurface are yet to be elicited. While some studies have attempted to bridge the gap between global climate predictions and specific hazards such as landslides (e.g., Collison et al., 2000; Jomelli et al., 2009; Oku and Nakakita, 2013), there is a dearth of studies about impacts along pathways 2 and 3.

Clearly, such an effort is expensive and would likely require the kind of partnership between industry, research organizations and government that are not readily achievable or easy to sustain. While other geotechnical endeavours in the past have successfully conducted large-scale, multi-party, long-term investigations (e.g., study and design of radioactive waste repositories in Europe and the US), some aspects of adaptation to climate change—especially in relation to temporal and geographical scales, as well as uncertainty—add significant complexity to the problem. These aspects will be illustrated next through a case study of Callala beach in Shoalhaven, south of Sydney.

3 ADAPTATION TO CLIMATE CHANGE: CALLALA BEACH AS A CASE STUDY

Background

Settled coastlines in Australia and overseas have always experienced some morphological and structural change as a result of both natural and man-made processes. However, the magnitude of the projected sea level rise and associated hazards, as well as the relatively small time span over which it is happening—decades rather centuries and millennia—present major challenges to coastal communities and planners. Callala beach is located in Callala bay, along the northern shoreline of Shoalhaven, in the state of New South Wales on the east coast of Australia (see figures 2 and 3). The beach is around five kilometres long, made of quartz sand and characterized by relatively dense development. It is of one eight beaches, identified by the Shoalhaven City Council (SCC) as especially exposed to the effects of sea level rise and associated problems of short- and long-term shoreline erosion, as well as single-event and repeated storm surges and flooding (Adamantidis and Glatz, 2009; Nicholls, 2011; Tonmoy et al., 2012; Royal Haskoning DHV, 2013). In other words, the subsurface at Callala beach and surroundings is set to experience impacts along all 3 pathways shown in Figure 1. Over the next 50 to 100 years, the beach is at high risk of loss of beach width and dunes. The erosion demand (based on extreme storms that occurred in 1974 and 1978) is estimated at 120 m^3/m and the long-term recession rate is 0.05m/year (Adamantidis and Glatz, 2009). Storm-surge erosion is believed to be more significant than long-term erosion. Although, risks of slope instability at bluffs and headlands are present at a number of locations in Shoalhaven, they do not seem to be an issue at Callala beach (Rheinberger & Malorey, 2008).

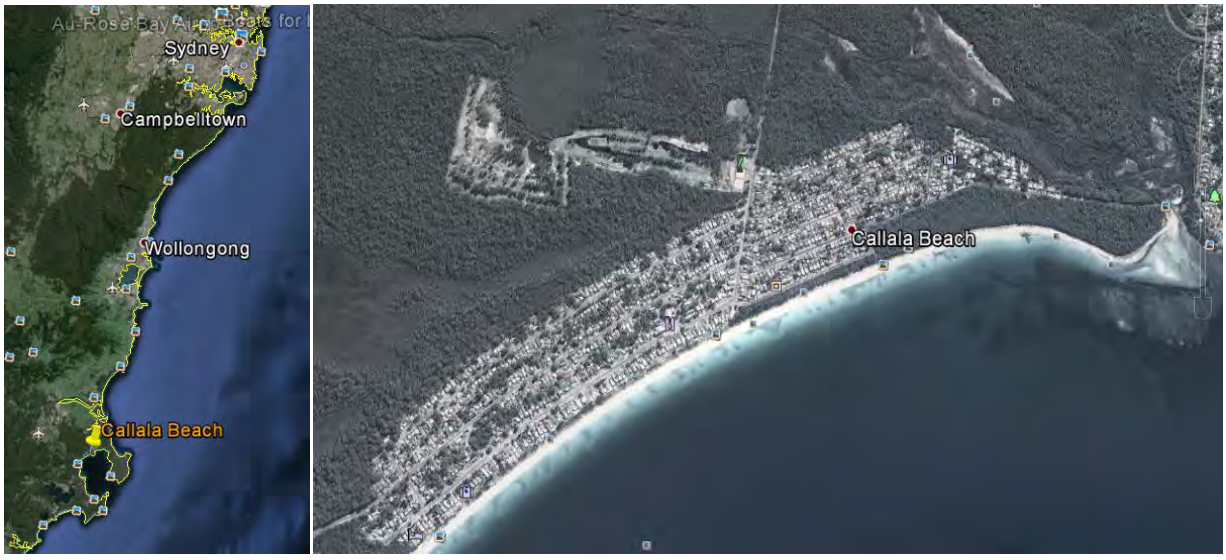

Figure 2. Location and map of Callala beach in the Shoalhaven region south of Sydney (from Google Earth)

Figure 3. Callala beach after a period of heavy rainfall; close-up photo shows erosion of sand dunes (photos taken by author on 9 September 2014)

Properties at or close to the beach—private dwellings as well as a publicly-owned community centre and public roads—are exposed to the risk of weakening of foundation, submersion and damage from storm surges. Estimated cost of private properties under threat by 2050 is A$150 million in today's monetary value. The total value of public infrastructure at risk by 2050—roads and the community centre—is A$230,000 in today's values, which grows to $1.1million if risk by 2100 is considered. These forecasts are based on a rise in sea levels, relative to 1990, of 40cm and 90cm, by 2050 and 2100, respectively, which is the best technical advice provided by the New South Wales government to the SCC (Umwelt, 2012). On the positive side, a number of adaptation options, shown in table 1, are available and generally fall under one of three well-known categories of responses, namely protection, accommodation and evacuation/retreat (Nicholls, 2011; Yasuhara et al., 2012). The SCC is currently considering some of these options in consultation with the community and no decision has yet been made.

Table 1. Examples of adaptation options for Callala beach including some of their advantages and drawbacks

Option[1]	Likely Advantages	Some Drawbacks
Revetment seawalls	Protects properties	Negative impact on beach width; visual impact
Revetment seawalls with a degree beach nourishment	Protects properties	Visual impact; financially costly
Breakwaters	Protects properties	Effect on shoreline and beach width; visual impact; financially costly
Beach nourishment	Protects properties and beach	Costly to public funds; impact on source of sand
Beach nourishment with groyne	Protects properties and beach	Financially costly; impact on source of sand; visual impact
Shoreline stabilisation	Protects properties and beach	Not effective in the long-term; visual impact
Acquisition of private assets by the SCC; compulsory and publicly funded	Eliminates exposure	Financially costly; moral hazard[2]; breakup of community
Voluntary relocation of assets and community; publicly funded	Eliminates exposure	Breakup of community
Rezoning and staged retreat; compulsory and funded by property owners	Eliminates exposure	Financially costly; impacts on community; costly to owners
Managing risk through information and emergency temporary evacuation plans	No engineering cost incurred; flexibility kept for future options	Risk to communities and the SCC

1: options shown are partly based on Royal Haskoning DHV (2013) and reflect the opinion of the author, not necessarily those of the SCC or the Callala beach community; 2: refers to the SCC acting as an insurer of last resort which would encourage risk-taking behaviour.

The question is how best to make a choice between these options, a combination of them (or indeed others that might be added to the list)? It is possible, in theory, to design for a scenario combining worst-case storm surges, long-term erosion and sea level rise. Cost-effectiveness or cost-benefit analyses could be conducted to help in choosing between a number of solutions, aiming to minimize the risk to individuals, properties and public infrastructures, as well as maintain the ecological integrity and amenity of the beach. In other words, the problem can be approached through multi-criteria or multi-objective decision analysis methods. However, the application of conventional decision-making approaches is rendered difficult by a number of elements which add unusual complexity to the issues considered, not least the uncertainty of impacts and the temporal and geographical scales of the problem. These are discussed next.

Multiple Uncertainties and Expanded Range of Solutions

Based on future predictions of Global Circulation Models (GCMs) and past records of sea level rise (over the last few decades), the risks faced by Callala beach are highly significant but the probabilities of their magnitude (as well as those of associated processes of short- and long-term erosion and storm surges) are very difficult to establish. This is because of the multiple chain of causality between, on the one hand, global socio-economic greenhouse gas emission scenarios and, on the other hand, regional and local impacts of climate change—all of which add different levels and types of uncertainty to future predictions. A detailed discussion of the various sources of uncertainty is beyond the scope of this paper and the reader is referred to Smith and Stern (2011) for an excellent discussion of the topic. However, despite the uncertainty, the relationships between global sea level rise and the risks faced by Callala beach are generally monotonic, i.e., higher sea levels always indicate higher risks and there is no uncertainty about the *direction* of the impacts (unlike, for example, hazards associated in many instances with increased or decreased rainfall).

There is a need to consider a range of solutions (as shown in table 1) that are based on technological protection (e.g., seawalls, groynes), ecological modification (e.g., beach nourishment, shoreline stabilisation) and social and institutional behaviour (e.g., relocation, setting up of emergency systems)—all within the same analytical framework that would

allow us to make comparisons between them. This range of solutions is broader than the ones normally encountered in engineering projects and requires rigorous integration of community consultation into the different stages of decision-making, since it is difficult in this case to separate the technological and social elements of the interventions considered (El-Zein and Hedemann, 2013; El-Zein, 2014). Choosing between protection, accommodation and retreat is clearly not just a matter of objective management of physical risk because some options can have a significant impacts on the livelihoods of the community. Therefore, scientific and engineering information, as well as choices, values and norms of the community (including the importance of Callala beach itself in the life of the community living close to it) will need to be considered in any adaptation process. For example, the community of Currarong beach—a 15 min drive from Callala bay and experiencing severe erosion problems—expressed a clear preference for beach nourishment when presented with a number of options (Currarong Progress Association, 2013). Likewise it is expected that seawalls and their visual impacts on the beach would face with some opposition within the Callala beach community. Indeed, different interventions might prove to be more suitable depending on whether priority is given to maintaining beach width for recreational, touristic and surfing purposes or achieving cost-effective protection to houses and their foundations. Whether one or the other is preferred is not just a question of scientific merit, but a matter of social choice, politics and values.

For all these reasons (i.e., uncertainty in magnitude of future impacts with no probabilities available, expanded range of solutions and importance of social values and norms in the decision-making process), it is difficult to apply conventional cost-benefit analyses as a decision-making tool. The difference in focus of the different interventions and the fact that at least some of the decision criteria will not be reducible to monetary values will require the deployment of other methods from decision science (e.g., Preston et al., 2013; Kontogianni et al., 2014; El-Zein and Tonmoy, 2015).

Temporal Scale

Two choices related to time, not usually encountered in geotechnical engineering, need to be made in the case of climate adaptation action in Callala beach (and generally coastal adaptation problems).

First, gradual sea-level rise is projected to continue into the next century and the hazard against which protection is required is likely to *worsen* over time. Hence, the choice of time horizon in the analysis and design of the different engineering adaptation options acquires additional importance: it indicates the extent to which possible changes in environmental and/or social conditions affecting the use of the development under consideration are to be incorporated. For example, shoreline stabilisation might be the most cost-effective solution if the time horizon is chosen to be a decade or two, or if sea levels were no longer increasing (Preston et al., 2013). However, it is unlikely to work in the longer term and may even prove counterproductive by conveying a false sense of safety to individuals and communities making long-term decisions about their assets. Hence, a choice of time horizon is no longer just a reference to internal changes to the built structure affecting its performance—as is usually the case in engineering projects—but changes in the social and environmental conditions of its deployment as well. Figure 4 shows the different zones of reduced foundation capacity (ZRFC) prevailing in 2025, 2050 and 2100 and shows that the area at risk will be expanding. Implicit in the choice of the time horizon is a question of intergenerational equity: how much of the cost of adaptation should we choose to pass on to future generations (i.e., generations who will benefit from, and/or carry the burden of, the development beyond the chosen horizon)?

Another time-related decision that needs to be made, is *when* to initiate any adaptation intervention (Tonmoy and El-Zein, 2012; Preston et al., 2013; Lin et al., 2013). This is essentially a voluntary choice and entirely different to the unavoidable lead time required to initiate and execute any engineering project. Intervention time can be designed, in principle, to optimise the outcomes of the intervention. The reason for considering an intervention time other than zero (i.e., other than as soon as possible) is that current arrangements for managing risk might be deemed acceptable, but are not expected to remain so in the future. If, say, a sea wall is found to be the best option for protection against a storm surge under higher sea levels, building one at a given time t in the future (option b) compared to today (benchmark option a), may be more or less desirable. On the negative side for option b are all the lost benefits (i.e., damages) accruing between now and t. These may be significant because of the often irreversible nature of shoreline changes and the possibility of extreme weather events occurring in this period. In addition, there may be added construction difficulties under option b, when sea levels are higher. On the other hand, option b has a few potential advantages over option a. In addition to the financial benefits from a discounted future expenditure, option b leaves the possibility open, between now and t, for the emergence of new technology, as well as some flexibility in case new knowledge becomes available suggesting a different course of action. It is important to keep in mind, however, that option b does not necessarily make the choice of time horizon easier, because there is no guarantee that future projections from time t onwards will be less uncertain than they are now.

Figure 4. Hazard lines for 2025, 2050 and 2100 at Callala beach (adapted from a production by SMEC in Umwelt, 2012; the hazard lines reflect zones of reduced foundation capacity (ZRFC) under conditions of worst storm surge ever recorded and long-term erosional changes occurring between now and the given time horizon; the photo to the right is a zoom-in of the 2050 hazard line and shows position of water and wastewater lines)

Clearly, depending on the choice of time horizon, very different combinations of solutions and intervention times may emerge as optimal at Callala beach. In addition, the uneven distribution of uncertainty in hazard evolution (with near-term projections enjoying a higher level of confidence than longer-term predictions), the robustness of estimates of adaptation benefits may be very different for different time horizons and intervention times. This will make the choice of a course of action undoubtedly more difficult.

Geographical Scale

Is the problem at Callala beach, including its geotechnical elements, a local one? On the one hand, it is possible to give an affirmative answer because:

a) the problem concerns a reasonably well-defined community occupying a surface area of a few kilometre squares in Callala Bay;
b) the engineering solutions being considered are located more or less within that same geographical area;
c) institutionally, the public agency responsible for managing the risks and making adaptation decisions is the local SCC.

On the other hand, three elements of the problem impart on it larger spatial/institutional (i.e., geographical) scales. First, some of the solutions listed in Table 1, such as breakwater, beach nourishment and relocation of the community, may have an impact on localities and systems, beyond the Callala beach area. This is due to the effects on marine ecosystems of breakwaters and beach nourishment (assuming the sand is sourced offshore) and the footprint of the community at destination, in the case of relocation.

Second, it is obvious that the SCC operates within a wider regulatory state and federal coastal management system which places constraints on its actions and can provide direction and resources including funding. For example, the NSW Office of Environment and Heritage has advised the SCC that, as a general rule, protective measures for an individual house can be approved when the erosion escarpment is within 20m of the property in question, an event considered likely today at Callala beach under storm conditions (Royal Haskoning DHV, 2013). The advantage of the rule is that it allows residents some freedom of action in protecting their properties; however, it may also promote mal-adaptation since a large number of protective measures at the level of individual assets is likely to sub-optimal. Hence, unsurprisingly, the wider legal and regulatory framework—over which the local Callala community has little control—can significantly skew the choice of adaptation options.

A third and most important factor is that, given the rise in sea levels and density of settlements along the East Coast of Australia, hazards similar to those faced by Callala Beach and its community are encountered at a large number of beaches along the coast (Kinsela and Hanslow, 2013). This is not, in other words, one isolated problem emanating from the particular characteristics of a particular place. While the question for the Callala beach community is how to protect the Callala beach and adjacent properties, competing priorities can shift the emphasis somewhat for the SCC and other state and federal government agencies, with some level of authority over the beach. For example, decisions about resource allocation must be made and questions about comparative risks in different coastal areas have to be answered before specific action at a specific locality is taken (Preston et al., 2013). From the Shoalhaven City Council perspective, a number of other beaches (e.g., Currarong, Collingwood, Mollymook) are experiencing significant erosional risks too (Adamantidis and Glatz, 2009; Umwelt, 2012; Tonmoy et al., 2012). Implicit in the allocation of resources is a question of intra-generational equity, i.e. which social and environmental priorities should take precedence in public expenditures. In addition, measures of costs and benefits are often scale-dependent (i.e., solutions that are beneficial or ‗cost-effective' at a local scale may not be so at a higher scale) and economies of scale may be achieved when considering problems at larger geographical scales (e.g., Adger et al., 2005; Hallegatte and Corfee-Morlot, 2010; Kontogianni et al., 2014). For example, as indicated earlier in discussing the 20m distance rule, optimal strategies of beach protection or retreat are bound to be different depending on whether they are considered for individual properties or beaches, for the Shoalhaven area or for the state of New South Wales as a whole.

4 RISK, VULNERABILITY AND INCREMENTAL VERSUS TRANSFORMATIONAL ADAPTATION

The rise in sea levels, together with changes to precipitation patterns and increases in the frequencies of extreme weather events, projected to occur within this century, amount to a re-negotiation of long-established boundaries and dynamics of interaction between land and water. How should the risks, unfolding over years and decades rather than weeks and months, be managed and what kind of adaptation will work best? Clearly, the answer depends on specific contexts and specific hazards and on the factors we choose to consider in characterizing the word ―best". However, given the extent of change, interventions that go beyond conventional engineering protective measures may well be required and, as was shown through the case study, the choices we make will depend on the temporal and geographical scales we adopt and the values and norms we prioritize.

A useful distinction here is between risk and vulnerability. If risk is conventionally construed as the likelihood of exposure to the hazard, multiplied by its impacts, the concept of vulnerability incorporates both exposure and impacts and goes beyond them, attempting to account for the differential abilities of individuals, communities, ecosystems, economic sectors and institutions to cope with, and/or adapt to, the hazard in question (e.g., Adger, 2006; Smit and Wandel, 2006; Füssel, 2007; Tonmoy et al., 2014). A shift from *risk* to *vulnerability* in geotechnical engineering would be beneficial in the context of long-term planning for subsurface systems. Such a shift would mark a change of emphasis, moving from the structural integrity and performance of subsurface infrastructure systems to the *services* they provide and the *well-being* of the communities they serve. It would, at the very least, help us avoid narrowly technological perspectives, operate within an expanded range of solutions and better take into account social and institutional factors of adaptations.

Another useful distinction is emerging in the literature between different forms of adaptation. Pelling (2011) defines adaptation as either *resilience*, *transition* or *transformation*. Adaptation as resilience, from this perspective, is the ability to ―support the continuation of desired systems functions into the future through enabling changes in social organisation and the support of technology" (p. 56 of Pelling, 2011). According to Kates et al. (2012), merely *incremental* adaptations are extensions of existing actions or behaviours, whereas *transformational* adaptations are ―those that are adopted at a much larger scale or intensity, those that are truly new to a particular region or resource system, and those that transform places and shift locations." For example, choosing to strategically relocate human settlements from areas of high risk along parts of the Australian coastline as a way of sustainably managing the hazards associated with higher sea levels—should this be considered a sound course of action at a given stage—would require changes in governance, laws, techno-social interactions and ways of thinking about risk management that can be said to amount to a transformational adaptation. Another example is the significant departure from past flood management policies in the Netherlands that are premised on a network of engineering protection systems, replaced by the new so-called ―room-for-the-river" policies which allow, selective and periodic flooding and multi-functional usage of land (e.g., Fliervoet et al., 2013).

An important point here is that resilience and transformational adaptation can sometimes operate *in opposition* to each other, ie the more resilient a system is, the more resistant to transformational adaptation it might be, even when the

latter is desirable or essential in the long term (Pelling, 2011). For example, Cooper and Pile (2014) distinguished between adaptation actions that focus on changing human behaviour (e.g., re-settlement; development constraints) from those that aim to change the physical environment in order to minimize impacts on human behaviour (e.g., building defences or nourishing beaches). They argued that the latter is a form of resistance that can delay or prevent adaptation by creating a false belief in technological fixes, whereas the former tends to be a more sustainable response to sea level rise. Conducting a cost-benefit analysis of adaptation options in the eThekwini district in South Africa which includes the city of Durban, Cartwright et al. (2013) found that socio-institutional interventions carried higher benefit-cost ratios than adaptations involving changes to ecosystems or infrastructure systems. On the other hand, there are, and will be in the future, many contexts in which technological adaptation is more sustainable. For example, Koks et al. (2013) studied flood risks in Belgium and found that upgrading defences appears to work generally better than land zoning. However, the point here is that resilience, while often a powerfully positive system property to be reinforced, may be more or less desirable depending on context and scales.

In light of the above discussion, are geotechnical and geo-environmental practice and education well placed to provide sound advice to policy- and decision-makers on issues of long-term adaptation? Clearly, there are no simple answers to the question. However, two points can be made tentatively:

1. The geotechnical profession can draw on strong expertise and well-developed methods and tools to study the sensitivity to extreme events of the hydro-mechanical behaviour of subsurface systems at any given site and, to this extent, it is possible to give an affirmative answer to the question above. There is already a rich body of knowledge on the effects of heavy rainfall and drought on slope stability and the deformation and failure of roads and embankments. We should continue to refine this knowledge and apply it to the management of the risk to infrastructure systems. One of the challenges here is to incorporate in our studies the compound effects of multiple hazards. Two recent examples are the study of the effect of sea level rise in San Francisco on land subsidence, seawater intrusion into groundwater and the inability to drain stormwater and wastewater by gravity (Hanak & Moreno, 2011); and the combined effects of land subsidence and storm surges on levees and seawalls in Shanghai (Wang et al., 2012).

2. Our theoretical and experimental methods and tools for studying long-term changes to subsurface systems are less well developed than they need to be. It is therefore important to incorporate in geotechnical education and practice, far more than we have done so far, the measurement and study of indicators at larger geographical scales—as opposed to site-specific data—in order to be able to make better judgments about long-term adaptation. This would necessarily include stronger reliance on, and better understanding of, Geographical Information Systems (GIS), remote sensing technologies and methods characterising spatial and temporal uncertainty. What geotechnical engineers could then bring to the field is a powerful understanding of subsurface phenomena at multiple scales. For example, geographical studies attempting to develop regional landslide or flooding vulnerability maps tend to make highly simplistic assumptions about failure mechanisms (e.g., Joyce et al., 2014). Geotechnical engineers can clearly enrich these methods by adding a more sophisticated understanding of transport processes and hydro-mechanical failure mechanisms. However, this can only happen if geotechnical education and practice are able and willing to engage with larger geographical scales and longer time frames. Interestingly, Chowdhury and Flentje (2008), examining geo-hazards in the context of growing populations in a globalised world, reached similar conclusions about the importance of multi-disciplinary approaches incorporating methods traditionally more present in the realm of geosciences and geography.

Pursuing these recommendations would place the profession in a better position to play an active role in adaptation to climate change. It would allow geotechnical engineering to provide its input more upstream of the policy-making and planning processes, than is currently the case.

5 CONCLUSIONS

Projected changes to the climate over the next few decades will alter the hydro-mechanical behaviour of many subsurface systems, leading in some cases to higher risk of failure. The sensitivity of key infrastructure systems—such as roads, embankments and slopes—to extreme weather events and fluctuations in soil water content and suction have been assessed in a range of studies in Australia and overseas. However, as shown in this paper, the multiple pathways through which climate can impact subsurface systems, and the unusual temporal and multiple spatial and institutional scales of the problems, add significant complexity to adaptation responses. Our ability as geotechnical engineers to tackle the unprecedented changes likely to be experienced by the subsurface, inland and along the coast, depends on

whether we can embrace and/or develop experimental and theoretical tools at different scales to the ones we have mostly worked with so far.

Over the last decade, geomechanics research has made significant advances in developing a better understanding of soil behaviour based on fundamental laws of physics on scales smaller than the representative element volume, from millimetres to micro and nanometres. This research will continue, as it should, and one element of its success lies in the willingness of geotechnical engineering researchers to engage with methods and theories from scientific disciplines that have long-standing experiences with smaller scales, such as physics, chemistry and thermodynamics. Given the changes affecting our planet today, it is now equally important that we extend our interests, and those of our students, towards the larger spatial scales and associated disciplines that will help us better tackle the challenges lying ahead.

6 ACKNOWLEDGEMENTS

Dr Fahim Tonmoy and honours thesis students, Mr Matthew Brown and Ms Peta Polydoropoulos, from the School of Civil Engineering of the University of Sydney, helped by providing data and conducting simulations of flash floods in Callala beach. I am grateful to Ray Massie and Isabelle Ghetti from the Shoalhaven City Council for useful discussions and provision of data. Prof David Airey kindly read the manuscript and gave generous feedback. I am, of course, solely responsible for the opinions expressed in the article.

7 REFERENCES

Adamantidis, C., & Glatz, M. (2009). *Shoalhaven Coastal Zone Management Plan*. Retrieved from https://www.shoalhaven.nsw.gov.au/demosite/environment/coastal/documents/Report - Shoalhaven Coastal Zone Management Plan - SMEC Australia_reduced.pdf

Adger, A. W., Arnell, N. W., & Tompkins, E. L. (2005). Successful adaptation to climate change across scales. *Global Environmental Change*, *15*(2), 77–86. doi:10.1016/j.gloenvcha.2004.12.005

Adger, W. N. (2006). Vulnerability. *Global Environmental Change*, *16*(3), 268–281. doi:10.1016/j.gloenvcha.2006.02.006

Austroads. (2004). *Impact of climate change on road infrastructure* (p. 123). Retrieved from https://www.onlinepublications.austroads.com.au/items/AP-R234-04

Basu, D., Misra, A., Puppala, A. J., & Chittoori, C. S. (2013). Sustainability in Geotechnical Engineering. In *Proceedings of the 18th International Conference on Soil Mechanics and Geotechnical Engineering, Paris 2013* (pp. 3171–3174).

Briggs, K. (2010). Charing Embankment : Climate change impacts on embankment hydrology, 28–31.

Cartwright, a., Blignaut, J., De Wit, M., Goldberg, K., Mander, M., O'Donoghue, S., & Roberts, D. (2013). Economics of climate change adaptation at the local scale under conditions of uncertainty and resource constraints: the case of Durban, South Africa. *Environment and Urbanization*, *25*(1), 139–156. doi:10.1177/0956247813477814

Cechet, B., Taylor, P., Griffin, C., & Hazelwood, M. (2011). Australia's coastline : adapting to climate change. *AusGeo News-Geoscience Australia, Australian Government*, (101), 1–9.

Chowdhury, R., & Flentje, P. (2008). Strategic Approaches for Management of Risk in Geomechanics. *Proceedings of The 12th International Conference of International Association for Computer Methods and Advances in Geomechanics (IACMAG)*.

Climate Change in Victoria : 2008 Summary. (2008). Retrieved from http://www.climatechange.vic.gov.au/__data/assets/pdf_file/0020/73172/DSEstatesummaryWEB.pdf

Coe, J. a. (2012). Regional moisture balance control of landslide motion: Implications for landslide forecasting in a changing climate. *Geology*, *40*(4), 323–326. doi:10.1130/G32897.1

Collison, A., Wade, S., Gri, J., & Dehn, M. (2000). Modelling the impact of predicted climate change on landslide frequency and magnitude in SE England, *55*, 205–218.

Comegna, L., Picarelli, L., Bucchignani, E., & Mercogliano, P. (2012). Potential effects of incoming climate changes on the behaviour of slow active landslides in clay. *Landslides*, *10*(4), 373–391. doi:10.1007/s10346-012-0339-3

Cooper, J. a. G., & Pile, J. (2014). The adaptation-resistance spectrum: A classification of contemporary adaptation approaches to climate-related coastal change. *Ocean & Coastal Management*, *94*, 90–98. doi:10.1016/j.ocecoaman.2013.09.006

El Zein, A. & Hedemann, C. (2013). Engineers as Problem Solvers: A Deficient Self-Definition for the 21st Century. *Engineering Education for Sustainable Development 2013 (EESD13)*, Cambridge, United Kingdom: University of Cambridge.

El-Zein, A. (2014). Risk and social vulnerability: how engineering can engage more effectively with climate change. *Frontiers of Environmental Science-Interdisciplinary Climate Studies,* in review.

El-Zein, A., & Tonmoy, F. N. (2015). Assessment of vulnerability to climate change using a multi-criteria outranking approach with application to heat stress in Sydney. *Ecological Indicators*, *48*, 207–217. doi:10.1016/j.ecolind.2014.08.012

Fan, L., Smethurst, J., Powrie, W., & Sellaiya, a. (2014). Seasonal slope surface deformation measured with TLS. *IOP Conference Series: Earth and Environmental Science*, *17*, 012264. doi:10.1088/1755-1315/17/1/012264

Fityus, S. G., Walsh, P. F., & Kleeman, P. W. (1998). The Influence of CLimate as Expressed by the Thorthwaite Index on the Design Deoth of Moisture Change of Clay Soils in the Hunter Valley. In *Conference on geotechnical engineering and engineering geology in the Hunter Valley* (pp. 251–265).

Fliervoet, J. M., Van den Born, R. J. G., Smits, a J. M., & Knippenberg, L. (2013). Combining safety and nature: a multi-stakeholder perspective on integrated floodplain management. *Journal of Environmental Management*, *128*, 1033–42. doi:10.1016/j.jenvman.2013.06.023

Fragaszy, R. J., Santamarina, J. C., Amekudzi, a., Assimaki, D., Bachus, R., Burns, S. E., … Tsouris, C. (2011). Sustainable development and energy geotechnology — Potential roles for geotechnical engineering. *KSCE Journal of Civil Engineering*, *15*(4), 611–621. doi:10.1007/s12205-011-0102-7

Füssel, H.-M. (2007). Vulnerability: A generally applicable conceptual framework for climate change research. *Global Environmental Change*, *17*(2), 155–167. doi:10.1016/j.gloenvcha.2006.05.002

Hallegatte, S., & Corfee-Morlot, J. (2010). Understanding climate change impacts, vulnerability and adaptation at city scale: an introduction. *Climatic Change*, *104*(1), 1–12. doi:10.1007/s10584-010-9981-8

Hanak, E., & Moreno, G. (2011). California coastal management with a changing climate. *Climatic Change*, *111*(1), 45–73. doi:10.1007/s10584-011-0295-2

Jomelli, V., Brunstein, D., Déqué, M., Vrac, M., & Grancher, D. (2009). Impacts of future climatic change (2070–2099) on the potential occurrence of debris flows: a case study in the Massif des Ecrins (French Alps). *Climatic Change*, *97*(1-2), 171–191. doi:10.1007/s10584-009-9616-0

Joyce, K. E., Samsonov, S. V., Levick, S. R., Engelbrecht, J., & Belliss, S. (2014). Mapping and monitoring geological hazards using optical, LiDAR, and synthetic aperture RADAR image data. *Natural Hazards*, *73*(2), 137–163. doi:10.1007/s11069-014-1122-7

Kates, R. W., Travis, W. R., & Wilbanks, T. J. (2012). Transformational adaptation when incremental adaptations to climate change are insufficient. *Proceedings of the National Academy of Sciences of the United States of America*, *109*(19), 7156–61. doi:10.1073/pnas.1115521109

Keim, B. D. (2010). the Lasting Scientific Impact of the Thornthwaite Water-Balance Model. *Geographical Review*, *100*(3), 295–300. doi:10.1111/j.1931-0846.2010.00035.x

Kinsela, M., & Hanslow, D. (2013). Coastal Erosion Risk Assessment in New South Wales: Limitations and Potential Future Directions. In *22nd NSW Coastal Conference 2013* (pp. 1–28). Retrieved from http://www.coastalconference.com/2013/papers2013/NSWCC_Kinsela_Hanslow_2013.pdf

Koks, E. E., de Moel, H., Aerts, J. C. J. H., & Bouwer, L. M. (2013). Effect of spatial adaptation measures on flood risk: study of coastal floods in Belgium. *Regional Environmental Change*, *14*(1), 413–425. doi:10.1007/s10113-013-0514-7

Kontogianni, a., Tourkolias, C. H., Damigos, D., & Skourtos, M. (2014). Assessing sea level rise costs and adaptation benefits under uncertainty in Greece. *Environmental Science & Policy*, *37*, 61–78. doi:10.1016/j.envsci.2013.08.006

Leao, S. (2014). Mapping 100 Years of Thornthwaite Moisture Index: Impact of Climate Change in Victoria, Australia. *Geographical Research*, *52*(3), 309–327. doi:10.1111/1745-5871.12072

Li, F., Gelder, P. H. a. J. M. Van, Vrijling, J. K., Callaghan, D. P., Jongejan, R. B., & Ranasinghe, R. (2014). Probabilistic estimation of coastal dune erosion and recession by statistical simulation of storm events. *Applied Ocean Research*, *47*, 53–62. doi:10.1016/j.apor.2014.01.002

Liggins, F., Betts, R. a, & McGuire, B. (2010). Projected future climate changes in the context of geological and geomorphological hazards. *Philosophical Transactions. Series A, Mathematical, Physical, and Engineering Sciences*, *368*(1919), 2347–67. doi:10.1098/rsta.2010.0072

Lin, B. B., Khoo, Y. B., Inman, M., Wang, C.-H., Tapsuwan, S., & Wang, X. (2013). Assessing inundation damage and timing of adaptation: sea level rise and the complexities of land use in coastal communities. *Mitigation and Adaptation Strategies for Global Change*, *19*(5), 551–568. doi:10.1007/s11027-013-9448-0

Nguyen, Q., Fredlund, D. G., Samarasekera, L., & Marjerison, B. L. (2010). Seasonal pattern of matric suctions in highway subgrades. *Canadian Geotechnical Journal*, *47*(3), 267–280. doi:10.1139/T09-099

Nicholls, R. J. (2011). Planning for the impacts of sea level rise. *Oceanography*, *24*(2), 144–157. doi:10.5670/oceanog.2011.34.COPYRIGHT

Oku, Y., & Nakakita, E. (2013). Future change of the potential landslide disasters as evaluated from precipitation data simulated by MRI-AGCM3.1. *Hydrological Processes*, *3340*(April), n/a–n/a. doi:10.1002/hyp.9833

Philp, M., & Taylor, M. (2012). Beyond Agriculture : Exploring the application of the Thornthwaite Moisture Index to infrastructure and possibilities for climate change adaptation infrastructure and possibilities for climate change adaptation, (October).

Preston, B. L., Maloney, M., Thomsen, D., Smith, T., Mangoyana0, R., & Conlon, B. (2013). *A Multi-Criteria Analysis of Coastal Adaptation Options for Local Government* (p. 89). Retrieved from http://www.sydneycoastalcouncils.com.au/sites/default/files/MCA_of_Coastal_Adaptation_Options_for_Local_Government.pdf

Rheinberger, T., & Malorey, D. (2008). *Shoalhaven City Council Coastal Zone Management Study and Plan Coastal Slope Instability Hazard Study* (p. 69).

Royal Haskoning DHV. (2013). Shoalhaven Authorised Locations Coastal Erosion Remediation Options. Callala Beach. *Report to Shoalhaven City Council*, (March). Retrieved from https://www.shoalhaven.nsw.gov.au/demosite/environment/coastal/documents/rp8A0101_gpb_240213_Callala_Rev2.pdf

Smit, B., & Wandel, J. (2006). Adaptation, adaptive capacity and vulnerability. *Global Environmental Change*, *16*(3), 282–292. doi:10.1016/j.gloenvcha.2006.03.008

Smith, L. a, & Stern, N. (2011). Uncertainty in science and its role in climate policy. *Philosophical Transactions. Series A, Mathematical, Physical, and Engineering Sciences*, *369*(1956), 4818–41. doi:10.1098/rsta.2011.0149

Stadler, S., Tredoux, G., & Wrabel, J. (2012). Identification of sources and infiltration regimes of nitrate in the semi-arid Kalahari : Regional differences and implications for groundwater management, *38*(2), 213–224.

State of Australian Cities 2013-Introduction. (2013) (p. Chapter 1, p 9–23). Retrieved from https://www.infrastructure.gov.au/infrastructure/pab/soac/files/2013_05_INFRA1782_MCU_SOAC_CHAPTER_1_WEB_FA.pdf

State of Australian Cities 2013-Population and settlement. (2012) (p. Chapter 2, p 25–82). Retrieved from https://www.infrastructure.gov.au/infrastructure/pab/soac/files/2013_06_INFRA1782_MCU_SOAC_CHAPTER_2_WEB_FA.pdf

Suanez, S., Cariolet, J.-M., Cancouët, R., Ardhuin, F., & Delacourt, C. (2012). Dune recovery after storm erosion on a high-energy beach: Vougot Beach, Brittany (France). *Geomorphology*, *139-140*, 16–33. doi:10.1016/j.geomorph.2011.10.014

Take, W. A., Beddoe, R. a., Davoodi-Bilesavar, R., & Phillips, R. (2014). Effect of antecedent groundwater conditions on the triggering of static liquefaction landslides. *Landslides*, (October 2013). doi:10.1007/s10346-014-0496-7

Tonmoy, F., El-Zein, A., Ghetti, I., & Massie, R. (2012). Vulnerability to sea level rise of 8 beaches in shoalhaven: a new multi-dimensional assessment methodology. In *21st NSW Coastal Conference* (pp. 1–13). Retrieved from http://www.coastalconference.com/2012/papers2012/Abbas El-Zein Full Paper.pdf

Tonmoy, F. N., El-Zein, A., & Hinkel, J. (2014). Assessment of vulnerability to climate change using indicators: a meta-analysis of the literature. *Wiley Interdisciplinary Reviews: Climate Change*, n/a–n/a. doi:10.1002/wcc.314

Umwelt. (2012). *Coastal Zone Management Plan for the Shoalhaven Coastline*. Retrieved from http://projects.umwelt.com.au/shoalhaven-coastline/home.php#view-draft-plan

Yasuhara, K., Komine, H., Murakami, S., Chen, G., Mitani, Y., & Duc, D. M. (2012). Effects of climate change on geo-disasters in coastal zones and their adaptation. *Geotextiles and Geomembranes*, *30*, 24–34. doi:10.1016/j.geotexmem.2011.01.005

Yellishetty, M., & Darlington, W. J. (2011). Effects of monsoonal rainfall on waste dump stability and respective geo-environmental issues: a case study. *Environmental Earth Sciences*, *63*(6), 1169–1177. doi:10.1007/s12665-010-0791-0

INGENUITY AND INTELLIGENT RISK ASSESSMENT FOR RESILIENT GEOTECHNICS

D.A.F. Oliveira

Associate Geotechnical Engineer, Coffey, Sydney and Research Fellow, University of Wollongong, Australia,

ABSTRACT

Geotechnical engineering is a risky business and there is much that can, and does, go wrong. It is often said that the single most common cause of failure in construction (including delays and additional costs) is in the ground. This would indicate that the logical path to design more resilient infrastructure would be the adoption of over-conservative designs. However, the in-ground structures that collapse often have a number of fundamental and basic design flaws. In reality, most in-ground structures move considerably less than predicted at design stage, suggesting that they were, in fact, over-designed. Over-design can also be considered a form of failure as it can add cost and delays in construction. It is generally accepted that a resilient piece of infrastructure is not necessarily one that does not fail upon a catastrophic event, i.e. one that is overdesigned to withstand such event. Otherwise the concepts of sustainability and resiliency would be conflicting. A resilient design is one that does not cause significant disruption to the community and can function effectively as quickly as possible after the catastrophic event.

So, how can geotechnical engineers achieve resilient infrastructure designs? The best approach seems to be associated with intelligent risk assessment that is based on an in-depth understanding of how such a design will perform before, during and after a catastrophic event. This approach requires good knowledge of the fundamental principles of geotechnical engineering such as solid mechanics, geology, failure mechanisms and so on. This paper will discuss some of the requirements for intelligent risk assessment and presents a practical example of an approach that could be adopted for the design of resilient infrastructures. Its primary focus is on the anticipated performance during a potential failure and the intelligent risk assessment forming the basis of the entire design.

1 INTRODUCTION

The International Tunnelling Association (ITA-AITES), in its 2013 Global Perspective Programme – "Deciding on Better and Resilient Cities", stated that the world today is facing many challenges. One of these is that the world‟s cities will need to accommodate 6 billion people by 2050 and by then it is estimated that 70% of the world‟s population will live in urban areas. This fact alone poses a major challenge for urban planners. Imagine the world‟s population now, all living in cities - this is what the figure of 70% in 2050 represents. Rapid urbanisation is one of the world‟s major challenges. Natural disasters and the changing climate are the second major challenge facing the world. The effects of climate change, notably as freak weather occurrences, are now a recurring global phenomenon. This has enormous impact on mega cities. Earthquakes, tsunamis, major storms and flooding on a massive scale, are threatening the fabric of society and cause massive disruption. Cities need to learn to cope with this challenge and ask themselves how resilient they are to such events.

These challenges have been identified by the United Nations as major issues that require policies and action at a global level. UN Habitat is running the World Urban Campaign which has the theme „Better City, Better Life‟. The basis of this programme is not only to raise awareness but it is also a true call to action. It requires engaging the public at large, the civil society, the business sector, the research community and governments in a global movement. The campaign includes a vision of what sustainable urban development requires. However, sustainable urban development calls for resilient cities and asks cities to consider and prepare for natural disasters. It also asks cities to plan for these events. How does this affect geotechnical engineering?

Geotechnical engineering is a risky business and there is much that can, and does, go wrong. It is often said that the single most common cause of failure in construction (including delays and additional costs) is in the ground. This would indicate that the logical path to design more resilient infrastructure would be the adoption of over-conservative designs . However, the in-ground structures that collapse often have a number of fundamental and basic design flaws. In reality, most in-ground structures move considerably less than predicted at design stage, suggesting that they were, in fact, over-designed. Over-design can also be considered a form of failure as it can add cost and delays in construction. As a result, it is also generally accepted that a resilient piece of infrastructure is not necessarily one that does not fail upon a catastrophic event, i.e. one that is overdesigned to withstand such event. Otherwise the concepts of sustainability and resiliency would be conflicting. So what is resilient infrastructure design?

A resilient design is one that does not cause significant disruption to the community and can function effectively as quickly as possible after the catastrophic event. So, the third question is, how can geotechnical engineers achieve resilient infrastructure design?

Joan Clos, the United Nations Under-Secretary-General, Executive Director of UN-Habitat in 2013, made a statement that contains the essence of the answer:

> *"We need to demonstrate that change is possible through the genius, creativity and audacity of people and decision-makers to make the wisest choices for our urban future.*"

As cities face the task of climate change adaptation and focus on resiliency, creative thinking is required. Contemporary solutions no longer provide the answers. In geotechnical engineering, the answer seems to be associated with two words: ingenuity (in agreement with Joan Clos above) and intelligent risk taking.

Intelligent risk assessment requires in-depth understanding of how a geotechnical design will perform before, during and after a catastrophic event. This approach requires good knowledge of the fundamental principles of geotechnical engineering such as solid mechanics, geology, failure mechanisms and so on. This paper presents an example of such design approach that was adopted for a temporary case but has, in its essence, the concept of intelligent risk assessment and therefore could be adopted for the design of resilient infrastructure. Its primary focus was on its anticipated performance during a potential failure and the risk assessment forming the basis of the entire design.

2 THE IMPORTANCE OF FUNDAMENTALS

As mentioned above, intelligent risk assessment requires in-depth understanding of the basics and fundamental concepts of geotechnical engineering. On one hand, the collapse of in-ground structures exposes severe flaws in understanding of fundamental concepts of ground behaviour and geotechnical engineering. On the other, most in-ground structures move considerably less during construction and operation than predicted at design stage, suggesting that they were in fact over-designed - also a form of failure. According to Atkinson (2008), the relatively high incidence of failures in geotechnical engineering indicate that geotechnical engineers are not as competent as they should be, or as we would like them to be.

When asked to define the typical characteristics of sands and clays, most geotechnical engineers would say that sands are granular and frictional and clays are cohesive. They would also answer that, upon rapid loading, sands would behave in a drained manner and clays undrained. These concepts, although generally accepted for most practical purposes, seem to be easily challenged by everyday experiences, including those we have as children. For example, Figure 1a, would seem to indicate a cohesive sand while the dry area around the footprint in Figure 1b demonstrates the undrained behaviour of a dense sand. The former is a demonstration of pore water suction and the latter a demonstration of the concepts of constant volume shearing generating negative excess pore-pressures due to a dilative behaviour. As a result, the terms granular and cohesive to describe soils are misleading (Atkinson, 2008). Both sands and clays are granular, i.e. they both consist of individual particles, and both may have "cohesive" strength. Soils should be described as coarse-grained or fine-grained as grain size (strictly pore size) is the fundamental aspect that controls suction and drainage and therefore their behaviour.

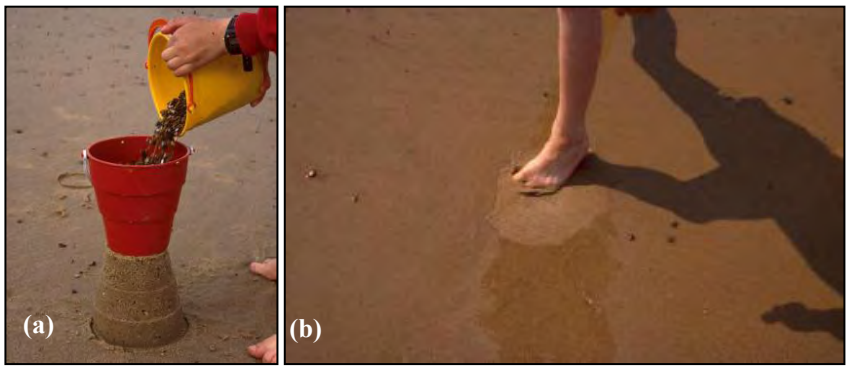

Figure 1: (a) Unconfined compression of sand. (b) Undrained shearing of dense sand (after Atkinson, 2008).

Another concept that is fundamental to geotechnical engineering is the principle of effective stress and geotechnical engineers must have a clear knowledge of it. They must understand the difference between drained loading, undrained loading and consolidation. They must know when to carry out analyses in terms of total or effective stress.

In other words, the principle of effective stress underpins all geotechnical engineering but its application is often misunderstood. A well-known example is the 2004 collapse of the cut and cover structure for the Circle Line Stage 1 adjacent to the Nicoll Highway in Singapore. One of the main contributing factors was the incorrect application of a numerical model involving the assessment of undrained strength through effective strength parameters. The original design analysis of soil-structure interaction was carried out using finite element methods with a linear-elastic perfectly plastic Mohr-Coulomb (MC) model representing the soil behaviour. The use of this soil model together with drained effective stress strength parameters (c', ϕ'), in an undrained setting, greatly overestimated the undrained shear strength of the local marine clay leading to a serious underestimation of computed wall deflections, bending moments and mobilization of forces in the jet grout pile-raft at the base of the excavation (Whittle and Davies, 2006). The overestimation of the undrained strength is associated with the uncoupled shear and volumetric behaviour of elastic-plastic models underestimating the generation of excess pore-pressures and resulting in a vertical effective stress path in isotropic elastic models as depicted in Figure 2 below.

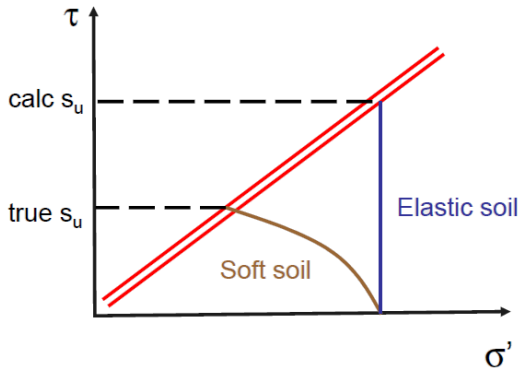

Figure 2: Effective stress path for an isotropic elastic soil compared to true soft soil behaviour.

Soils and rocks behave differently under different applications and there are a variety of combinations of parameter values and factors applicable to different design limit states. Geotechnical engineers are often unclear about the relationships between, for example, peak, critical state and residual strengths and factors of safety and load factors (Atkinson, 2008).

It is important to note that there is no discussion in this section about the correct use of standards or codes of practice. The discussion above is around basic competencies. Competence requires the engineer to get the basics right; it does not require the engineer to follow a code or standard. Without these basic competencies, the target of resilient geotechnical design is unattainable.

3 INTELLIGENT RISK ASSESSMENT

As discussed above, a resilient piece of infrastructure does not need to be over-designed to fully withstand a catastrophic event but to have the extent and magnitude of any impact caused by a failure controlled such that it does not cause significant disruption to the community and can function effectively as quickly as possible after the event. To achieve such controlled failure it is essential to have good knowledge of the fundamental principles of geotechnical engineering, such as ground behaviour, failure mechanisms, as discussed in the previous section. Once these basic competencies are achieved, the geotechnical engineer has the tools to appropriately assess the problem at hand and adopt a more risk based design which focuses on delivering a resilient piece of infrastructure.

2.1 RISK BASED DESIGN

Risk is part of every human endeavour. From the moment we get up in the morning, drive or take public transport to school or to work, until we get back into our beds (and perhaps even afterwards), we are exposed to risks of varying degrees. What makes the study of risk fascinating is that while some of this risk bearing may not be completely voluntary, we seek out some risks on our own (speeding on the highways or gambling, for example) and enjoy them. While some of these risks may seem trivial, others make a significant difference in the way we live our lives. It can be argued that every major advance in human civilization, from the caveman's invention of tools to gene therapy, has been made possible because someone was willing to take a risk and challenge the status quo. This seems reasonably in line with the statement of Joan Clos cited above regarding the "*…genius, creativity and audacity of people…*". Although it seems reasonable to accept that to combine sustainability and resiliency in infrastructure projects, risk taking is essential this should be based on a thorough understanding of the likelihoods and consequences involved in a potential failure, i.e. intelligent risk taking.

2.2 PRACTICAL EXAMPLE

In order to illustrate the concept above, a practical example of a risk based design is presented here. This example is based on a remedial design carried out by Coffey for a 35 m high existing slope/embankment supporting a highway that was assessed to have unacceptable risk levels (low factor of safety against instability of around 1 to 1.1), though not all design details are provided herein.

The design focused on a temporary solution using a sheet pile wall that would address the risks associated with a potential failure of the embankment without necessarily improving its overall stability (i.e. global factor of safety in the vicinity of one was still accepted as long as the risks were mitigated) allowing the construction of remedial measures that would improve the global stability of the embankment to acceptable levels in the long term. The results of the geotechnical analysis of the existing embankment and sheet pile wall were then used as input to a risk assessment approach (RTA, 2011) adopted to evaluate the effectiveness of the design as a temporary solution.

Although the example presented here is for a temporary solution, a similar approach is possible when assessing catastrophic events where it is practically impossible to design against a failure without overdesigning and conflicting with the concept of sustainable design, but where the design solution should manage the risks associated with a potential failure during such events.

2.2.1 Design philosophy

Generally, the purpose of any support measure is to provide a minimum factor of safety, typically between 1.2 and 1.3 for a temporary condition (often acceptable for a catastrophic event, e.g. earthquakes), such that there is a low probability of failure. In other words, in the conventional design of support measures it is necessary to target a sufficiently low risk of failure, particularly if life is at risk. Under this philosophy, there are circumstances (e.g. catastrophic events) where the support measure may not provide such factors of safety due to the nature of the disaster or possibly the scale of the problem.

A new design philosophy was proposed which focuses on managing the risks of a potential failure mechanism by mitigating the likely consequences. The solution would no longer aim to improve the overall factor of safety of the slope but to force the path of least resistance against slope instability downslope of a sheet pile wall to be installed close to the crest of the slope. As a result, the upper section of the slope, which contains the highway, would be retained by the sheet pile wall for sufficient time to allow for emergency response, such as a road closure, if required. This approach achieved a Roads and Maritime Services (RMS) Assessed Risk Level (ARL) of 4 for "Loss of Life" for a short duration while the permanent solution of an earthfill stability berm was constructed. The design philosophy aims to provide a temporary sheet pile wall such that:

- In the event of a failure downslope of the temporary sheet pile wall, movement is expected to be at a rate such that there will be enough warning for emergency response, if necessary.
- A detailed program of real-time monitoring is implemented to reduce the risk to construction workers and road users of embankment failure.

It is important to note that although the above philosophy is not a design approach typically adopted even for temporary solutions, it is based on conventional engineering principles which mainly focus on addressing the risks of progressive collapse. For instance, fire and earthquake engineering often do not aim to avoid a building collapse but target for enough time during such events to allow for evacuation.

Following such principles, the US National Institute of Standards and Technology (NSIT, 2007) recommends that to reduce the potential for progressive collapse in buildings, the design should consider the assessment of alternate load paths whereby a review of the strength and ductility of key structural elements is required to investigate whether the structure would be able to "bridge" over the initial damage, i.e. to redistribute stresses, but with enough ductility to avoid brittle failure and its propagation. This approach typically requires specific attention to the structure's redundancy, ductility and capacity.

As a result, the proposed sheet pile wall promotes redundancy within the embankment reducing the probability of failure propagating towards the carriageway even though the overall factor of safety remains the same as before implementing any temporary measures. For example if a substantial slope failure in front of the sheet piles (mechanism A) is assessed to have a factor of safety (FS) = 1.1 with "Likelihood" L3 in accordance with the RMS Guide, i.e. an annual probability $P(A) = 10^{-2}$, and the likelihood of the sheet pile wall failure before the highway can be closed with sufficient warning (mechanism B) is assessed as $P(B) = 10^{-3}$, the probability of the failure propagating to the carriageway will be lower than $P(B) = 10^{-3}$ as it is a function of both probabilities. As a result, the probability of a failure propagating to the highway and causing loss of life would be significantly reduced even though the minimum FS = 1.1, i.e. lower than generally targeted in design.

2.2.2 Preliminary design of sheet pile wall

As discussed above, the main design concept of the sheet pile wall is to force the path of least resistance against slope instability downslope of the sheet pile wall, i.e. a slope failure can still occur but the slip surface with the lowest factor of safety is located in front of the temporary sheet pile wall. In addition, adverse impacts on the highway resulting from a slope failure are managed. As a result of this potential failure, a large volume of soil would move downslope, thereby forming a batter which is flatter than the pre-failure slope angle. The upper portion of the slope would then have to be temporarily supported by the sheet pile wall to avoid propagation of the failure towards the carriageway. This mechanism is depicted in Figure 3 below.

The simplified method for estimating failure induced embankment deformation as proposed by Khalili *et al*. (1996) has been adopted. A slow failure mode was assumed based on the rate of movements observed on site. The dynamics of a slow failure mode is represented schematically in Figure 4. In this figure, an unstable soil mass is shown at its initial and final condition, i.e. before and after failure, where the centre of gravity moves from point *A* to *B*. The weight of the soil mass is represented by *W* with *O* and *R* being the centre and radius of the slip surface, respectively.

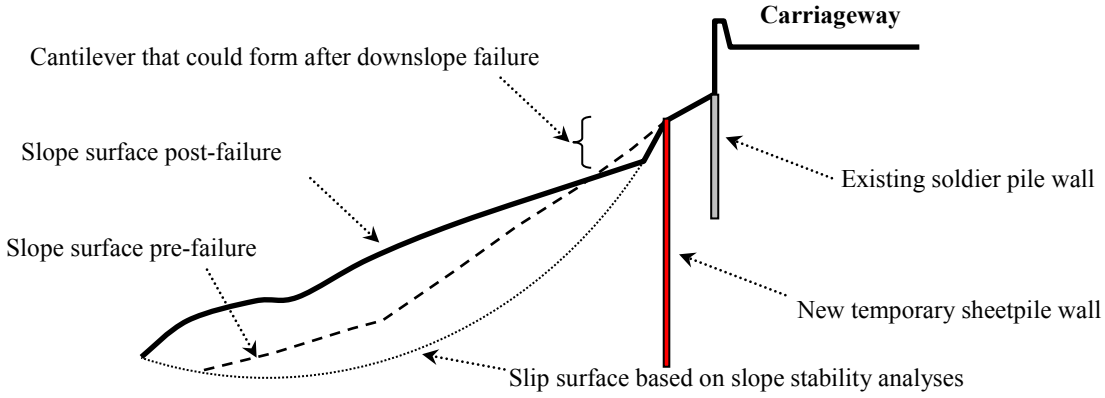

Figure 3: Sheetpile wall concept.

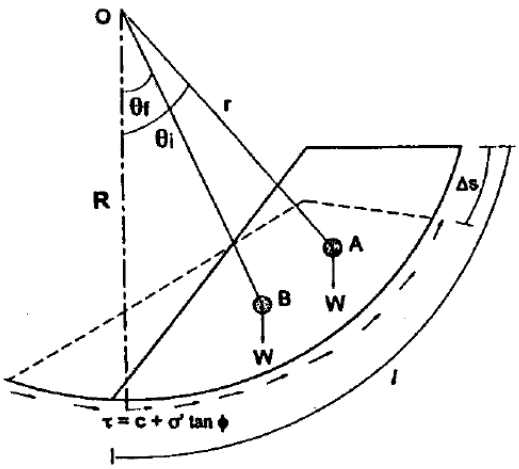

Figure 4: Failure induced slope deformation model (Khalili *et al*., 1996)

For a slow mode, inertia forces resulting from the movement of the sliding mass can be assumed as negligible, thus, the unbalanced mass will gradually move down the slope until it attains a new stable condition with a factor of safety of unity. Under such large movements the final factor of safety is related to the residual shear strength of the soil. Therefore, the final angular position of the centre of gravity of the unbalanced soil mass, θ_f, can be estimated if the initial angular position, θ_i, and the residual factor of safety, $FS_{residual}$, are known. The final slope geometry may then be estimated from the assessed value of θ_f. It is important to note that $FS_{residual}$ is the factor of safety using the residual shear strength but for the original slope geometry, i.e. prior to failure.

Adopting residual strength parameters considered appropriate for the prevailing ground conditions, a minimum factor of safety $FS_{residual} = 0.73$ was assessed such that the volume of unstable soil mass was considered to be significant, i.e. with scale of failure S1 and volume, $V > 20{,}000\ m^3$, with potential significant adverse impact on the highway (Figure 5).

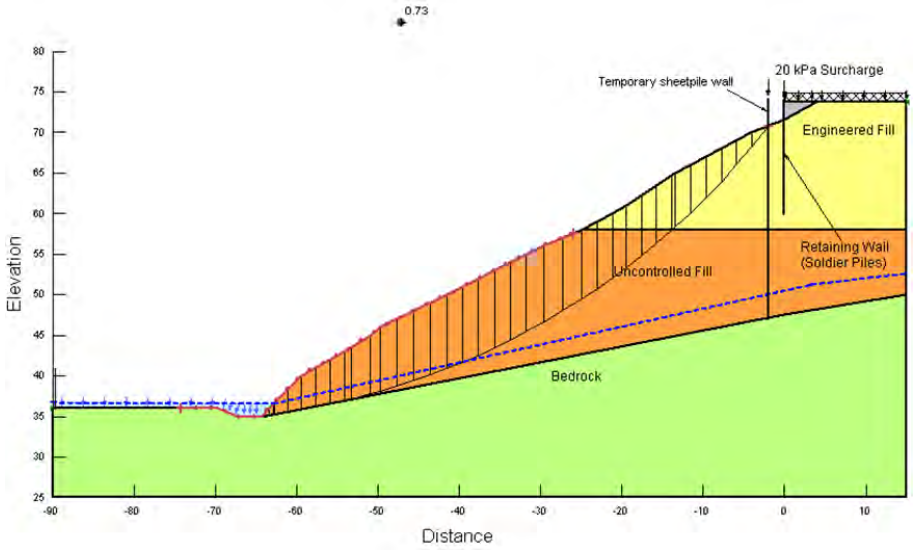

Figure 5: Residual factor of safety for design of sheetpile wall.

Adopting the value of $FS_{residual} = 0.73$ and the slip circle geometry from Figure 5, the failure induced displacements can be assessed using the simplified method proposed by Khalili *et al*. (1996). This assessment indicates that the failed soil mass would reach limiting equilibrium when the slope achieves an average angle of approximately 20º to the horizontal. Considering further failure immediately in front of the sheet pile wall, a cantilever height of up to 6.5 m was considered possible to develop as a result of the movement of the failed soil mass. A 6.5 m high cantilever sheet pile wall within sloping ground was then modelled using the commercial computer program WALLAP. The simplified model is shown in Figure 6 below.

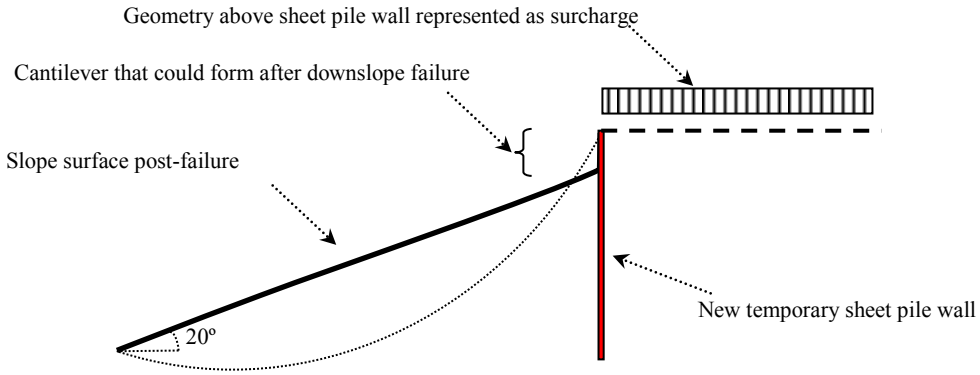

Figure 6: Simplified temporary sheet pile wall model adopted in WALLAP

The soil properties used in WALLAP were assumed to be the peak values as the residual values would only be applicable to the shear zone (i.e. in the vicinity of the slip surface). However, potential strain softening outside the shear zone (i.e. within the embankment) was further investigated through 3-dimensional (3D) numerical modelling, as briefly discussed in the following section. The sheet pile wall was assessed to be subjected to an ultimate bending moment of up to approximately 1,150 kN.m/m and an ultimate shear force of up to 305 kN/m with horizontal movements at the pile head of up to 250 mm. Under such conditions, the sheet pile wall option was considered feasible.

It is important to note that significant simplifications were made to allow assessment using WALLAP. The entire geometry could not be modelled, particularly the section above the sheet pile wall which was simplified to a surcharge as illustrated in Figure 6. Another important limitation of the analysis is that it is based on small strain theory which may be of limited application for large soil movements associated with slope failure. In addition, the methodology

adopted assumes that the failed soil mass moves as a rigid body ignoring its own deformation. It was therefore considered that a more sophisticated analysis was required using 3D numerical modelling techniques.

2.2.3 3D numerical modelling of sheet pile wall

In order to address the limitations of the preliminary design stage, a 3D numerical analysis was carried out for the critical section of the embankment, as shown in Figure 5 above, using the commercial Finite Difference computer program FLAC3D.

It is not the intention of this paper to fully describe the numerical analysis. However, the main objective of the numerical analysis was to more accurately model the geometry and loading conditions of the problem, to account for strain-softening effects of the soil materials and to assess the effect of large strain deformation on the sheet pile structural elements.

A Shear Strength Reduction (SSR) technique was adopted to confirm that the sheet pile wall induces the path of least resistance against slope failure to be downslope of the embankment similar to the limit equilibrium approach shown in Figure 5. The model was then allowed to fail under large displacements as shown in Figure 7.

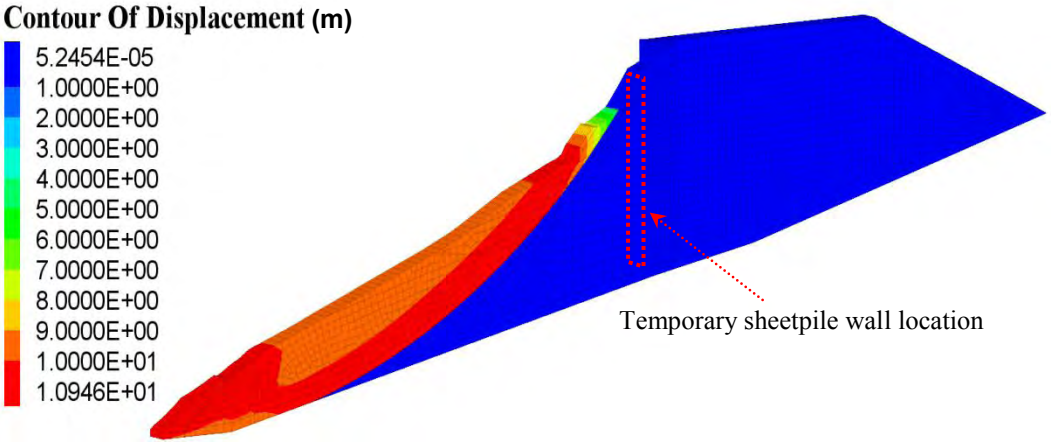

Figure 7: Large scale slope failure.

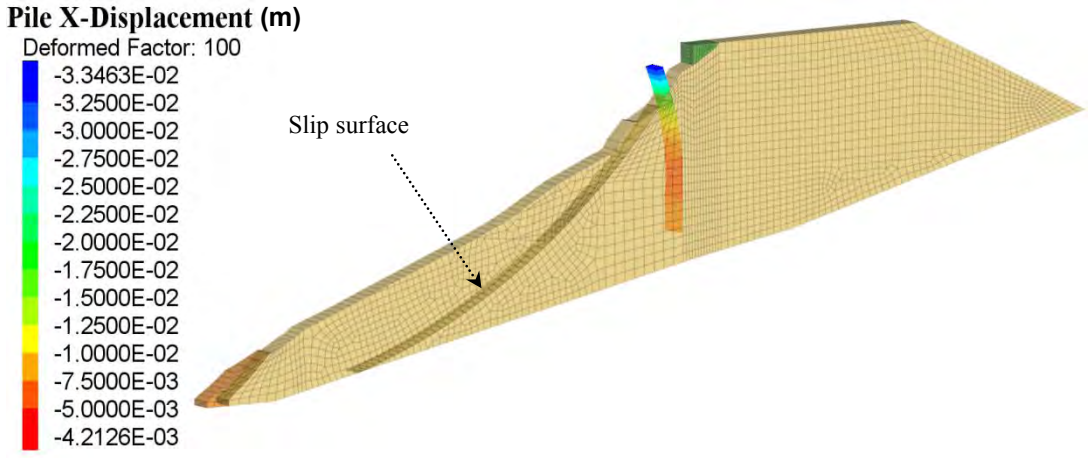

Figure 8: Sheet pile wall deflections after large scale failure (piles exaggerated 100x).

A total displacement of up to 11 m is estimated for the failed soil mass (Figure 7) which reaches equilibrium at a slope angle similar to that assessed using the method after (Khalili *et al.*, 1996). Movements of up to 95 mm horizontal and 100 mm vertical were assessed at the carriageway level as a result of the large scale slope failure when the sheet pile wall is in place. If the sheet pile wall is not installed, collapse of the carriageway occurs upon the same large scale slope failure. This modelling outcome clearly indicated the benefits of the temporary measure in controlling the displacements at highway level.

The 3D model indicated that progressive erosion and loosening could cause the development of a cantilever length within the upper 3 m of the sheet pile wall, in contrast to the 6.5 m high cantilever assessed in preliminary analysis. This scenario was then induced in later stage of the 3D model by removal of the upper 3 m of material in front of the sheet piles. An additional 28 mm of horizontal displacement and 23 mm of vertical displacement were estimated at the carriageway level as a result of this progressive failure.

Although the 3D model indicated the formation of a 3 m cantilever height for the sheet pile wall after downslope failure, an unlikely extreme event was considered that would result in a total cantilever length of 6.5 m, consistent with the analytical preliminary assessment. Under such conditions, large movements were estimated from the 3D analysis. These movements were larger than those estimated by the analytical method possibly due to the large strain approach of the numerical model which increases the bending of the sheet pile wall. Settlement of up to 650 mm was observed at the carriageway level with horizontal displacements of up to 800 mm. These movements indicate a potential collapse of the carriageway with the sheet pile wall yielding, however it is important to note that this condition was assessed to be an extreme event and these movements would be expected to be slow and would still allow enough time for emergency responses to be actioned.

2.2.4 Risk assessment

In order to evaluate the effectiveness of the proposed solution, the RMS ARLs (RTA, 2011) were compared for the two cases, i.e. with and without the remedial measures.

For the condition without the sheet pile wall, different failure mechanisms and associated likelihoods and consequences were considered. The assessed RMS ARLs are presented in Table 1 for the various failure mechanisms. Large scale slope failures typically present low frequency/likelihood with the “Likelihood” rating increasing with decreasing scale of failure. As a result, the likelihood of the different failure mechanisms has been assumed to vary by one order of magnitude between each failure mechanism, commencing with L5 for a large scale failure of 20,000 m^3 as shown in Table 1. The “Vulnerability” rating is a measure of the probability of loss of life resulting from a failure. It is associated with traffic speed as well as the “Failure Mechanism”.

The ARLs for loss of life indicated that for the condition without the sheet pile wall, the assessed risk level would be at ARL3 or worse (i.e. potentially ARL2 when a traffic speed of 100 km/h is considered). The slow lane of the highway is located within the potentially affected failure zone and has traffic volume of approximately 25,000 vehicles per day. The fast lane was more than 7 m from the embankment crest, and was assessed to be outside the immediate zone most likely impacted by a failure of the embankment. This condition resulted in a “Temporal Probability” rating of T1 which is the maximum in the RMS rating. In quantitative terms, however, the “Temporal Probability” would double if the two traffic lanes could be severely affected by a failure. The “Vulnerability” rating is the rating associated with the risk of a fatality given a failure. The “Property Damage and Consequential Effects” rating is the rating associated with damage to the highway given the failure.

The ARLs presented in Table 1 indicate that the existing embankment had a “high” risk.

As discussed above, the sheet pile wall remedial measure targeted to reduce the short term adverse impacts of a large scale failure propagating to the highway, so as to provide sufficient time for monitoring data to be evaluated and the road closed (if required) to reduce the risk of fatality resulting from a failure. As a result, it was considered that the “Likelihood” rating should relate to the movements at the road surface resulting from deflection of the sheet pile wall caused by failure of the embankment downslope of the sheet pile wall. These movements were based on the previous analyses.

The “Likelihood” rating was also based on the assumption that real time monitoring is implemented as part of the temporary measures (which allows for early warning of large movements that may adversely impact road users).

As a result, it was assessed that upon installation of the sheet pile wall and real-time monitoring, an ARL5 could be assigned (Table 2 below) which needs to be continuously revised based on the results of the real-time monitoring. Based on this assessment, the benefits of the construction of short term measures (e.g. installation of a sheet pile wall) including the real time monitoring of the embankment were evident and therefore recommended.

It is important to note that the risk assessment required on-going real time monitoring due to the temporary characteristic of the design which still carried the risk that the highway would have to be closed if adverse conditions were revealed by the monitoring data. This would be similar to a catastrophic event which may not have had on-going monitoring but would require inspections for damage assessment after the event.

The ARLs presented in Table 2 were considered to be applicable only for the temporary condition, up until closure of the highway to traffic in the event of a failure occurring downslope of the temporary sheet pile wall. Should a significant failure of the embankment batter occur there would be loss of lateral support to the sheet pile wall with the

slope below the wall being in a meta-stable condition. Progressive failure may then take place due to adverse conditions such as rainfall and erosion. The ARL associated with loss of life is no longer applicable following road closure, and the ARL associated with property damage and consequential effects for some of the mechanisms is likely to become ARL1 following a significant failure. Therefore, the sheet pile wall could not be accepted as a long-term solution nor would be considered a solution to avoid failure under a natural disaster.

Table 1: Risk assessment for condition without sheet pile wall.

Ratings		**Failure Mechanism**			
		Large scale S1 Vol. >20,000 m^3	**Medium scale S2 Vol. >2,000 m^3**	**Small scale S3 Vol. >200 m^3**	**Minor scale S4 Vol. >20 m^3**
Velocity of failure		R5 – very slow	R5 – very slow	R5 – very slow	R5 – very slow
Likelihood(1)		L5	L4	L3	L2
Temporal probability		T1 – heavy urban traffic	T1 – heavy urban traffic	T1 – heavy urban traffic	T1 – heavy urban traffic
Vulnerability (vehicle crossing embankment failure)	Hazard	Deep narrow void	Shallow void (0.2 – 0.5 m step)	Stepped surface (0.1 – 0.2 m steps)	Irregular surface (< 0.1 m steps)
	60 km/h	V2	V3	V4	V5
	100 km/h	V1	V2	V3	V5
Consequence for loss of life	60 km/h	C1	C2	C3	C4
	100 km/h	C1	C1	C2	C4
Assessed Risk Level for loss of life	**60 km/h**	**ARL3**	**ARL3**	**ARL3**	**ARL3**
	100 km/h	**ARL3**	**ARL2**	**ARL2**	**ARL3**
Consequence for Property Damage and Consequential Effects		C1	C1	C2	C2
Assessed Risk Level for Property Damage and Consequential Effects		**ARL3(2)**	**ARL2(2)**	**ARL2(2)**	**ARL1**

Notes:

(1) Relates to the likelihood of failure and resulting movement of the road carriageway

(2) After a significant failure, the ARL associated with property damage and consequential effects for some of the mechanisms is likely to become ARL1.

Table 2: Risk assessment for condition with sheet pile wall.

Ratings		**Failure Mechanism**			
		Large scale S1 Vol. >20,000m^3	**Medium scale S2 Vol. >2,000m^3**	**Small scale S3 Vol. >200m^3**	**Minor scale S4 Vol. >20m^3**
Velocity of failure		R5 – very slow	R5 – very slow	R5 – very slow	R5 – very slow
Likelihood(1)		L5	L5	L5	L5
Temporal probability		T1 – heavy urban traffic	T1 – heavy urban traffic	T1 – heavy urban traffic	T1 – heavy urban traffic
Vulnerability (vehicle crossing embankment failure)	Hazard	Stepped surface (0.1 – 0.2 m steps)	Irregular surface (< 0.1 m steps)	Irregular surface (< 0.1 m steps)	Irregular surface (< 0.1 m steps)
	60 km/h	V5	V5	V5	V5
	100 km/h	V4	V4	V5	V5
Consequence for loss of life	60 km/h	C4	C4	C5	C5
	100 km/h	C3	C3	C4	C4
Assessed Risk Level for loss of life	**60 km/h**	**ARL5(2)**	**ARL5(2)**	**ARL5(2)**	**ARL5(2)**
	100 km/h	**ARL5(2)**	**ARL5(2)**	**ARL5(2)**	**ARL5(2)**
Consequence for Property Damage and Consequential Effects		C1	C1	C2	C2
Assessed Risk Level for Property Damage and Consequential Effects		**ARL3(3)**	**ARL3(3)**	**ARL4(3)**	**ARL4(3)**

Notes:

(1) Relates to likelihood of induced movements on road surface following a failure downslope of the sheetpile wall. The likelihood is dependent on the probability of movement occurring behind the sheetpile wall as well as the probability of failure of the embankment batter downslope of the sheetpile wall, and also the probability that an early warning system installed fails to detect the failure prior to road closure with respect to the risk assessment on loss of life.

(2) These ARLs for loss of life applies only to the temporary condition up to closure of the road (if required) based on the real time monitoring data.

(3) After a significant failure downslope of the sheetpile wall, the ARL associated with property damage and consequential effects for some of the mechanisms is likely to become ARL1

4 CONCLUSIONS

Sustainable and resilient geotechnical designs call for a different thinking from engineers that moves away from the traditional design approaches where nothing is allowed to physically fail.

In order to achieve this objective it is necessary that the primary focus of any geotechnical design is to get the basics right and only then apply the correct use of standards or codes of practice. The combination of strong basic competencies and the need for different thinking will drive engineers to ingenuity. According to Poulos (2014) "ingenuity" does not necessarily mean the application of new or emerging technology, although it may do. The key ingredients are:

- It draws upon multiple and diverse sources (individuals, disciplines, bodies of knowledge) for ideas and inspiration.
- It sees alternative ways to view or define problems and is not constrained by thoughts or approaches of others.
- It combines ideas in unique ways making connections between disparate concepts to deliver results.
- It applies current know how and capability in new and creative ways.
- It meets client's expectations of value which may not necessarily be technically novel.

In addition, risk is part of every human endeavour. As a result, it is essential that the "different thinking" involves not only ingenuity but also intelligent risk taking, i.e. one where the likelihoods and consequences of a potential failure are well understood. A practical example was presented where a risk based approach was adopted and where the solution did not focus on avoiding failure but on managing the risks of a potential failure mechanism by mitigating the likely consequences. With a similar approach, the geotechnical engineer can target reduced disruption to the community and infrastructure that can function effectively as quickly as possible after a catastrophic event, thus attaining a resilient design.

5 ACKNOWLEDGEMENTS

The author of this paper would like to acknowledge the important contribution and guidance of Patrick Wong and Frances Badelow through the design example discussed above. Both provide continuous guidance and mentoring to the author. It is also important to acknowledge the assistance and contribution of Daniel Gorman. The author is also thankful to Frances Badelow for her review of this paper.

6 REFERENCES

Atkinson, J.H. (2008). Keynote Lecture: What should geotechnical engineers be able to do and how should they acquire these skills? Proc. 1st Int Conf. on Education and Training in Geo-engineering. Constantza.

Khalili, N., Fell, R. and Tai, K.S. (1996). "A simplified method for estimating failure induced deformation". Proc. Seventh Int. Symp. On Landslides. Editor K. Sennesett, Balkema, Rotterdam, pp.1263-1268.

NSIT (2007). Best Practices for Reducing the Potential for Progressive Collapse in Buildings. Report NISTIR 7396.

Poulos, H. (2014). Internal Coffey memorandum.

RTA (2011). RTA Guide to Slope Risk Analysis Version 4.

Whittle, A.J. and Davies R.V. (2006). Nicoll Highway Collapse: Evaluation of Geotechnical Factors Affecting Design of Excavation Support System. Proc. International Conference on Deep Excavations 28-30 June, Singapore.

UNDERSTANDING LIQUEFACTION TRIGGERING RISK - AN AUSTRALIAN GEOTECHNICAL DESIGN PERSPECTIVE

Timothy Mote and Minly So
Arup Australia

ABSTRACT

Resilience is the ability to quickly recover during an adverse event. Following an earthquake the resilience of a community can be directly related to working infrastructure. Geotechnical resilience design must consider liquefaction from future large earthquakes.

Although Australia is considered a stable continental region with relatively low seismic hazard, earthquakes do occur and where susceptible geological conditions exist, liquefaction can occur. In fact, liquefaction has been documented in Australia on at least three occasions. In 1897, liquefaction was observed during a large (Ms 6.5) earthquake near Beachport, south-eastern South Australia (Collins et al., 2004); in the 1903 Warrnambool, Victoria (Ml 5.3) earthquake (Mitchell and Moore, 2007); and in 1968, numerous „sand blows" were observed following the Ms 6.8 earthquake at Meckering in Western Australia (Collins et al., 2004).

Liquefaction is a credible geohazard considered in current Australian geotechnical engineering practice, and infrastructure planning desk studies in Australia commonly identify liquefaction as a geohazard where susceptible soils exist within the project footprint. Further assessments are required in subsequent feasibility and detailed design phases. Accurately assessing the liquefaction triggering potential is an essential part of geotechnical design considerations.

The low seismicity of Australia creates a situation where liquefaction triggering is marginal at design hazard levels. This low level of seismic hazard makes the liquefaction trigger assessment very sensitive to the derivation of the seismic inputs. The lack of guidance on liquefaction from AS1170.4 requires interpretation of the basis seismic hazard inputs.

This paper explored the sensitivity to seismic inputs in low seismicity hazard Australia, to better understand liquefaction triggering risk in Australian geotechnical design. The components of the seismic hazard inputs are reviewed. A case study is presented showing that for liquefaction assessments in low seismicity regions, liquefaction triggering is sensitive to the selection of design magnitude and the calculation of the ground motions through the soil profile.

1 INTRODUCTION

Resilience is the ability to quickly recover during an adverse event. Lesson learned from recent earthquakes show that the resilience of a community can be directly related to the performance of its infrastructure. With transport, power and water functional communities are able to respond and recover quicker.

When considering the geotechnical resilience of infrastructure during earthquakes, liquefaction is a significant risk. Liquefaction is a soil behaviour in which saturated soil experiences a reduction in strength due to pore pressure increase during dynamic loading, such as earthquake ground shaking. Consequences of liquefaction include settlement, lateral displacement, loss of bearing capacity, and uplift of buried structures. The historic impact of liquefaction to society is well known from historic earthquakes including billions of dollars in damage from 1994 Northridge, 1995 Kobe, 1989 Loma Prieta (San Francisco) and most recently 2011 Christchurch.

Geotechnical earthquake engineering practice"s understanding of liquefaction is increasing with every real world example earthquakes from the early 1990"s to the current findings coming out of the 2011 Christchurch event. The nascence of understanding has meant that as a practice, liquefaction risk has been missed in design of many high importance/high consequence infrastructure, such as San Francisco"s Bay Area Rapid Transit Tunnel, the Massey Tunnel in Vancouver, San Pablo Dam in the East Bay of San Francisco and even the water and sewer network of the low lying suburbs of Christchurch. These significant structures considered earthquake ground shaking, but not liquefaction and had significant retro-fits or rebuilds.

Current building codes do not focus on earthquake resilience, but rather life safety. This means significant damage is allowed as long as the code objective is met. It is therefore not surprising that when a major earthquake strikes an urban region the losses are large and the general public is left to wonder why. The Christchurch earthquake in February 2011 is a prime example of this. As design focuses on resilience and beyond life safety, understanding risk is critical.

Although Australia is considered a stable continental region with relatively low seismic hazard compared to active tectonic areas of the world, earthquakes do occur and where susceptible geological conditions exit, liquefaction can trigger. In fact, liquefaction has been documented in Australia on at least three occasions. In 1897, liquefaction was observed during a large (Ms 6.5) earthquake near Beachport, south-eastern South Australia (Collins et al., 2004); in the 1903 Warrnambool, Victoria (Ml 5.3) earthquake (Mitchell and Moore, 2007); and in 1968, numerous „sand blows" were observed following the Ms 6.8 earthquake at Meckering in Western Australia (Collins et al., 2004). Note that liquefaction was not observed in the 1989 Newcastle Event, the colloquial reference design earthquake event for many Australian geotechnical practitioners.

Liquefaction is a credible geohazard considered in current Australian geotechnical engineering practice. Infrastructure planning desk studies in Australia commonly identify liquefaction as a geohazard where susceptible soils exist within the project footprint. Further assessments are required in subsequent feasibility and detailed design phases. Accurately assessing the liquefaction potential is an essential part of geotechnical design considerations.

The low seismicity of Australia creates a situation where liquefaction triggering is marginal at design hazard levels. This low level of seismic hazard makes the liquefaction trigger assessment very sensitive to the derivation of the seismic inputs. AS1170.4 (2007) – Earthquake Actions, does not provide liquefaction guidance or details from the seismic hazard analysis basis to support rigour in liquefaction assessments in Australia without an interpretation of the seismic inputs. In typical geotechnical engineering liquefaction assessments, focus is on characterising the ground conditions and characterising variation and material properties of ground conditions ultimately providing design advice against liquefaction risk. The seismic hazard inputs out of AS1170.4 are often taken for granted without understanding of application or implicit uncertainty in application of liquefaction assessment.

This paper explores the sensitivity to seismic inputs in low seismicity hazard Australia, to understand liquefaction triggering risk in Australian geotechnical design.

2 LIQUEFACTION TRIGGERING ANALYSIS METHODOLOGY

Liquefaction assessment methodology has been well established in earthquake engineering practice following Seed and Idriss (1971) and refinement over the last 40 years. The resistance to liquefaction depends on the relationship between the in-situ density of the soil with its critical state, as well as the behaviour of the soil under earthquake-induced cyclic loading.

Seed and Idriss (1971) proposed a simplified procedure for evaluation of liquefaction triggering that compare the soils" resistance to liquefaction, termed cyclic resistance ratio (CRR), with the cyclic stress caused by an earthquake, termed cyclic stress ratio (CSR), expressed as the factor of safety (FS_{liq}) against triggering liquefaction.

$$FS_{liq} = CRR/CSR$$

A FS_{liq} less than 1.0 implies that liquefaction triggering is likely.

The CRR for liquefaciton of in-situ deposits is evaluated from the penetration resistance using standard penetration tests (SPT) or cone penetration tests (CPT) or from laboratory testing on high quality samples. Empirical relationships have been produced by correlating the SPT N (Seed and Idriss 1971, Seed et al. 1985), CPT qc (Robertson and Wride, Suzuki et al. 1995; Moss et al. 2006), shear wave velocity (Andrus and Stokoe 1997; 2000) and seismic dilatometer paratmers (Marchetti et al. 2008) and the the estimates of the SCR of a number of sites which had or had not had liquefaciton during major earthquakes in the past (Youd et al. 2001; Seed et al. 2003) (Figure 1).

Discussion of state of the practice or uncertainty CRR is beyond the scope of this paper. Semple (2013) discussed problems with liquefaction criteria and their application in Australia and provided a thorough review of the current state of liquefaction susceptibility, including the relatively recent considerations such as low plasticity silts/clays from Bray & Sancio (2006) and as seen in Christchurch (Bray et al. 2014).

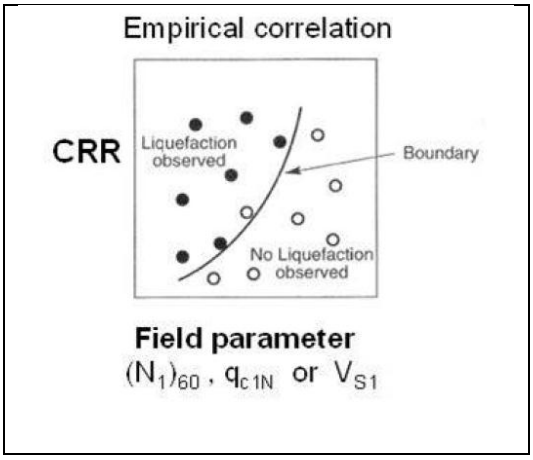

Figure 1: Liquefaction triggering boundary.

The CSR used in the simplified procedure for liquefaction triggering analysis is the ratio of average, or equivalent, shear stress induced by the earthquake to the in-situ effective vertical stress. Seed and Idriss (1971) proposed that the average equivalent CSR for liquefaction triggering assessment is about 0.65 times the peak shear stress, and may be estimated as:

$$CSR = 0.65 \cdot \frac{\sigma_v}{\sigma_v'} \cdot A_{\max} \cdot r_d$$

Where σ_v is the total vertical stress, $\sigma_{v'}$ is the effective vertical stress, A_{max} is the maximum acceleration (taken as peak ground acceleration, PGA), and r_d is the non-linear shear stress reduction factor with depth.

While A_{max} defines the maximum ground acceleration it provides no information on the duration of shaking. The importance of design magnitude in liquefaction assessments is the provision of an indication of duration of shaking or the number of strong motion cycles.

The convention for assessing liquefaction triggering is to determine CSR normalized to the duration of a M7.5 earthquake, denoted $CSR_{7.5}$. This is achieved by modifying the CSR by a magnitude-duration weighting factor, DWF after Idriss and Boulanger (2008) and calculated as:

$$DWF = (6.9*EXP(-M / 4)-0.058)$$

The magnitude-duration weighted cyclic stress ratio, $CSR_{7.5}$, is calculated as:

$$CSR_{7.5} = CSR / DWF$$

To estimate a CSR, these assessments need design ground motions (PGA) and design earthquake magnitude. Groundwater is assumed to be near the surface unless subsurface information proves otherwise.

3 DESIGN CODE LIQUEFACTION GUIDANCE

In active seismic regions, most seismic design codes require liquefaction analysis and provide specific guidance on the assessment methodology. For example ASCE 7-10 requires a Geotechnical Investigation Report, for high risk structures, with an assessment of consequences of soil strength loss, including slope instability, liquefaction, total and differential settlement, surface displacing due to faulting or seismically induced lateral spreading or flow.

ASCE 41-04, seismic evaluation of existing buildings, requires that liquefaction susceptible, saturated, loose granular soils that could jeopardize the building's seismic performance shall not exist in the foundation soils at depths within 50 feet under the building for Life Safety and Immediate Occupancy. If these are encountered a detail study is required.

The NZ Transport Agency Research Report 553 – "The Development of Guidance for Bridges in New Zealand for Liquefaction and Lateral Spreading Effects", presents a clear set of available procedures for analysis and design of bridges based on most recent research findings. A recent development following the 2011 Christchurch Earthquake is the implementation of liquefaction settlement/lateral spread displacement tolerances in the building codes by NZ MiBE. These define vertical and lateral displacements to varying degrees under SLS and ULS events according to liquefaction risk maps that need to be addressed in the design. Structures in areas identified to have moderate to significant land damage from liquefaction require a site specific investigation.

In Australia, AS1170.4 does not consider the effect of a structure from related earthquake phenomena such as settlement, slides, subsidence, liquefaction of faulting. Seismic design for infrastructure (bridges, roads, wharfs, tanks, pipelines) is formally excluded from AS1170.4 (2007), but many infrastructure specific codes, such as AS5100.2 Bridge Code, refer back to AS1170.4 for the basis seismic hazard. AS5100.2 guidance on liquefaction is limited to stating that the possibility of soil liquefaction shall be investigated where saturated sandy and silty soils within 10m of the ground surface have SPT N <10.

Where Australian specific infrastructure seismic design codes do not exist, such as LNG Tanks, international codes are referenced. These often provide liquefaction guidance relying on the seismic hazard sourced from their country of origin, therefore AS1170.4 must be interpreted for application in these codes.

The application of seismic hazard from AS1170.4 (2007) in liquefaction triggering assessment requires significant interpretation which creates an uncertainty in design.

3 DESIGN GROUND MOTIONS CONSIDERATIONS

In Australian practice, liquefaction triggering assessments generally start with AS1170.4 (2007) to derive base ground motion levels by extracting a "Z" value for a site. The "Z" represents the PGA with a 1/500 annual probability of exceedance for bedrock ground conditions. Following the procedures in AS1170.4 the "Z" value is scaled by a probability factor (k_p) according to the importance level of the structure and by factors relating to ground conditions (site sub-soil class).

3.1 DESIGN LIFE, IMPORTANCE LEVEL, & DESIGN RETURN PERIOD CONSIDERATIONS

In most modern seismic codes, the design ground motion is determined from an acceptable risk of earthquake occurrence over the lifetime of a structure. For a design life of 50 years at a 90% confidence level (10% exceedance of design) the return period is 475 years or an annual probability rounded off to 1/500. This is the "normal" structure design level in most international codes.

Design for a more important structure might consider a 98% confidence level which represents 2% in 50 years and would have a 1/2500 annual probability of exceedance. Following the same logic, a structure with a design life of 100 years and a 10% chance of exceedance of design would have an annual probability of exceedance of 1/1000.

AS1170.4 defines the consequence importance level following AS1170.0 based on building type, occupancy, and purpose (emergency response) (Table 1). These are aligned with many international codes.

Table 1: Importance Level AS1170.0

Importance Level	Description
1	Minor structures (failure not likely to endanger human life)
2	Normal structures and structures not falling into other levels
3	Major structures (affecting crowds)
4	Post disaster structures
5	Exceptional structures

In deriving seismic hazard for design, the importance levels are assigned a probability factor (k_p) representing the annual probability of exceedance (return period). The greater the importance, the higher the risk, and the annual probability of exceedance for design.

In practice there is conflicting guidance in the derivation of design annual probability of exceedance that requires consideration and interpretation. This is exemplified in AS5100.2 (Bridge Code) where a proposed revision and the Austroads Bridge Design Guidelines for Earthquake (2012) provide conflicting advice. AS5100.2 generally follows the AS1170.4, annual probability of exceedance, except for the Importance Level 4 (Bridge Design Class 4) structures for essential emergency response, where 1/2000 is recommended compared to 1/2500 in AS1170.4.

Austroads suggests that all bridges be designed for the ultimate (damage control) limit state under a design (1/2000 year) ground motion to ensure that after the earthquake the bridge shall retain its structural integrity. Importance Level

4 will be designed for the serviceability limit state under the design (1/2000) year earthquake. Note that the basis for the 1/2000 annual probability of exceedance is a design life of 100 years and a 5% chance of exceedance of design.

To add to the confusion, AS1170.4 (from AS1170.0) suggests a 1/2500 annual probability of exceedance for an Importance Level 4 structures, yet the BCA (2014) suggests a 1/1500.

Table 2 is a summary of the different annual probability of exceedance

Table 2: Annual Probability of Exceedance for Importance Level Comparison

Importance Level	IL 2	IL 3	IL 4
Austroads	1/2000	1/2000	1/2000
A5100.2 (AS1170.4)	1/500	1/1000	1/2000
AS1170.4 (AS1170.0)	1/500	1/1000	1/2500
AS1170.4 (BCA)	1/500	1/1000	1/1500

Lesson learned from recent earthquakes show that the resilience of a community can be directly related to the functionality of its infrastructures. With transport, power and electricity and water functioning a community is able to respond and recover quicker. If a major earthquake occurs, it would be difficult to imagine society accepting that a modern major bridge is not functioning as it was not designed for the extreme event.

3.2 UPDATE TO AS1170.4 HAZARD MAP

The ground motions provided in AS1170.4 (2007) are based on the probabilistic seismic hazard analysis (PSHA) conducted by Gaull et al. (1990) with revision by McCue et al. (1993).

Geoscience Australia 2012 (Leonard 2013) have developed a revision to this map and recommended it as an update to the hazard map in AS1170.4. As shown in Figure 2, the GA 2012 generally shows lower hazard than AS1170.4, and the 1/2500 spectra is closer to the AS1170.4 (2007) 1/500 spectra. The GA 2012 model is more aligned with current site specific studies where the earthquake catalogue used in the PSHA includes the last 20 years of seismicity, compared to the two decide old AS1170.4 model. Review or comment on the application of the differences in hazard is beyond the scope of this paper, but geotechnical practitioners should be aware of the difference and the potential update to AS1170.4.

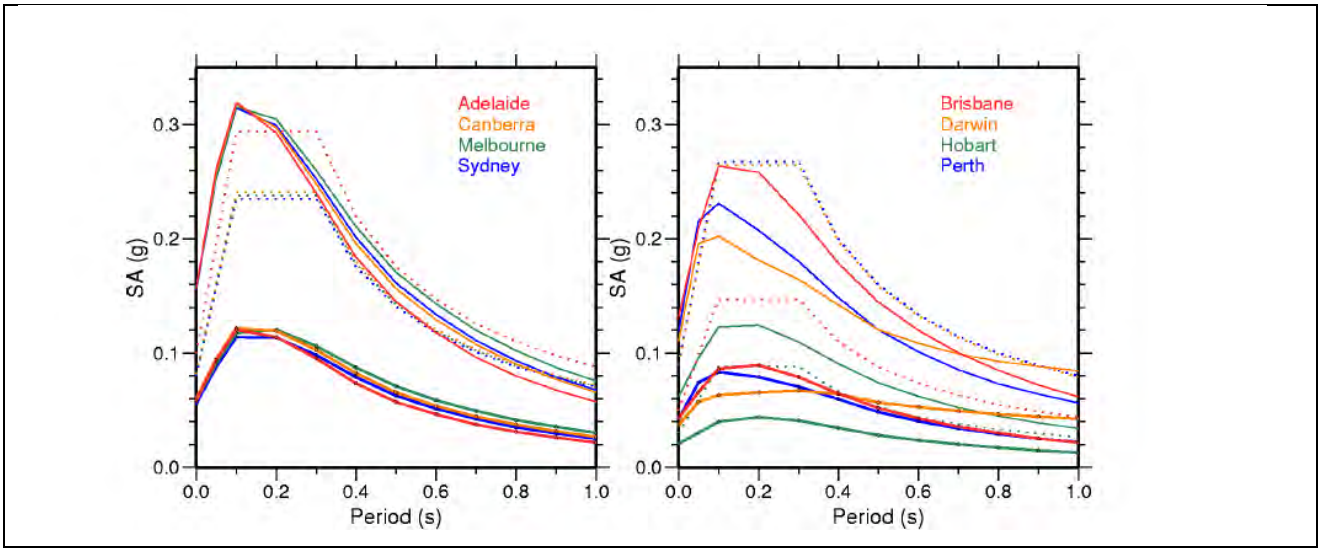

Figure 2: Geoscience Australia National Hazard Map (Leonard 2012) hazard spectra for 1/500 (thin lines), 1/2500 (thick lines) and AS1170.4 for 1/500 (dotted line).

3.3 SITE SOIL SUBCLASS AND SITE RESPONSE CONSIDERATIONS

Earthquake ground motion observed at soil sites can be substantially different from rock sites. The overlying soil deposits modify the earthquake induced bedrock motion as the motion is transmitted up through the soil profile to the

ground surface. This modification is known as site response and is a function of the soil profile geometry, the soil properties and the characteristics of the earthquake excitation.

AS1170.4, and most other seismic codes, provide scaling factors to adjust the bedrock ground motions following site soil properties. The soil profile is classified into a Site Soil Sub-Class based on soil properties. The soil classes are defined by the natural frequency of the soil profile estimated by geotechnical investigation.

Using the simplified method, CSR is derived from the bedrock PGA, scaled for the desired return period, factored by the site soil sub-class, and scaled by the design magnitude to derive a design PGA.

Another method for calculation CSR directly in liquefaction analysis is a site response analysis. The site response analysis eliminates the need to scale for a site soil sub-class, by propagating an earthquake ground motion time-history, representing the bedrock ground motion, through the soil column to calculate the CSR at any location in the soil profile. Depending on the variability of the soil profile and depth, the site response analysis may present very different results to that of the site sub class scaling of AS1170.4.

Figure 3 presents the difference in CSR from a site response analysis compared to CSR derived using the simplified method for 2 different design magnitudes. Site response analysis isn't common in Geotechnical practice here in Australia, but can provide more precision for ground response compared to using the AS1170.4 site soil sub-classes.

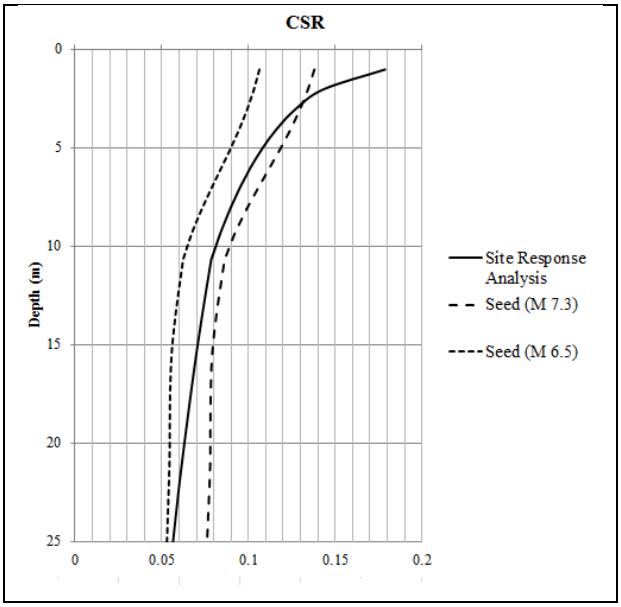

Figure 3: CSR derived from site response analysis and following Seed with M6.5 and M7.3

4 DESIGN MAGNITUDE

For liquefaction triggering assessments in Australia, a critical missing input parameter is the earthquake design magnitude. The design magnitude defines the duration weighting factor (representing the number of shaking cycles) and is included in the calculation of r_d, the non-linear shear stress reduction factor with depth. In active seismic regions around the world, local seismic design code often provides specific guidance on the selection of appropriate design earthquake magnitudes to estimate a CSR. For example ASCE 7-10 recommends using the maximum considered earthquake (MCE) and post-Canterbury Earthquake practice in NZ following NZS1170.5 and MBIE 2012 guidelines specify M7.5 for all liquefaction calculations regardless of the importance level.

Where design magnitudes are not explicitly provided by code, the common method for selecting magnitude is to consider the probabilistic earthquake scenarios that contribute the greatest amount to the ground motion hazard (CalTrans 2012). This is done by examination of the magnitude deaggregation of the PSHA.

In Australian practice, AS1170.4 (2007) and Gaull et al. (1990) with revision by McCue et al. (1993) do not provide enough information to readily extract earthquake design magnitudes or to develop magnitude deaggregation plots. As a result, earthquake engineering practitioners in Australia have applied a number of different methodologies to assign earthquake design magnitude for site-specific studies. These methods range from estimating mean values from regional recurrence curves (Mitchell and Moore, 2007), using the maximum historic earthquake in Australia for a given region, consideration of a range of magnitudes (Yang and Wright, 2010) or choosing a conservative magnitude based on professional judgment.

Mote and So (2013) show in the low seismicity of Australia, liquefaction triggering is sensitive to earthquake design magnitude. Figure 4 shows that for a sand profile in a site soil sub-class D, for a typical "Z" values in Australia (e.g. 0.08g for Sydney) that the selection of a design magnitude above or below a M6.5 will determine whether liquefaction will trigger.

The lack of rigour in guidance on how to select design magnitude in Australia creates significant uncertainty in the liquefaction triggering assessments. The following sections explore a number of methods to select design magnitude in Australia.

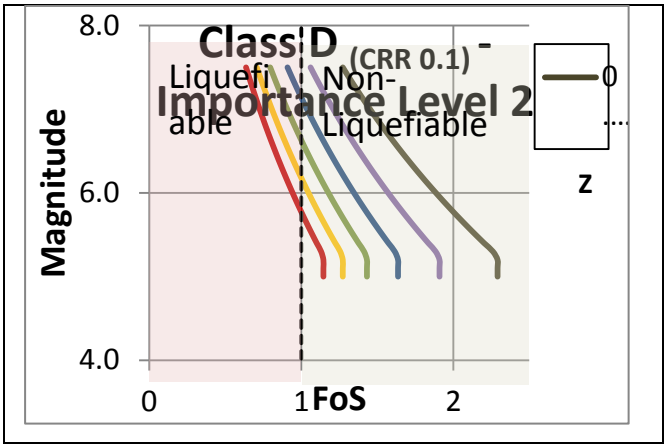

Figure 4: Sensitivity to Liquefaction (taken from Mote and So, 2013).

4.1 APPROXIMATE DEAGGREGATION OF AS1170.4

To understand application of the seismic hazard from AS1170.4 in liquefaction analysis, Dismuke and Mote (2012) developed an approximate magnitude distance deaggregation of the PSHA from AS1170-4 (2007).

The results showed that in the probabilistic modelling of scenario earthquakes, the very close and small earthquakes contribute greatest to the seismic hazard (Table 3). These values are surprising low and reflect the low seismicity nature of Australia. The magnitude of ~5 for the 1/2500 design event, questions the practical application of the magnitude-deaggregation method to derive design magnitudes in low seismicity regions as this design level is supposed to represent the rare event for essential and emergency structures and Australia is capable of much larger magnitude events.

Table 3: Mean Magnitude from Deaggregation of 1170.4 (Dismuke and Mote 2012)

Location	1/500	1/1000	1/2500
Sydney	4.9	5.1	5.2
Melbourne	5.0	5.1	5.3
Perth	4.4	4.5	4.6
Adelaide	5.1	5.2	5.3
Brisbane	4.7	4.8	4.9

4.2 MAXIMUM MAGNITUDES

An alternative magnitude selection method that matches international seismic design codes is using the maximum considered earthquake (MCE). Clark et al. 2012 developed maximum magnitudes estimates for Australia based on paleaoseismic research of past fault ruptures and lengths through the development of neotectonic domains. Figure 5 presents the maximum magnitudes for the 7 neotectonic domains across Australia.

These maximum magnitudes should be considered the upper bound magnitudes in liquefaction assessments.

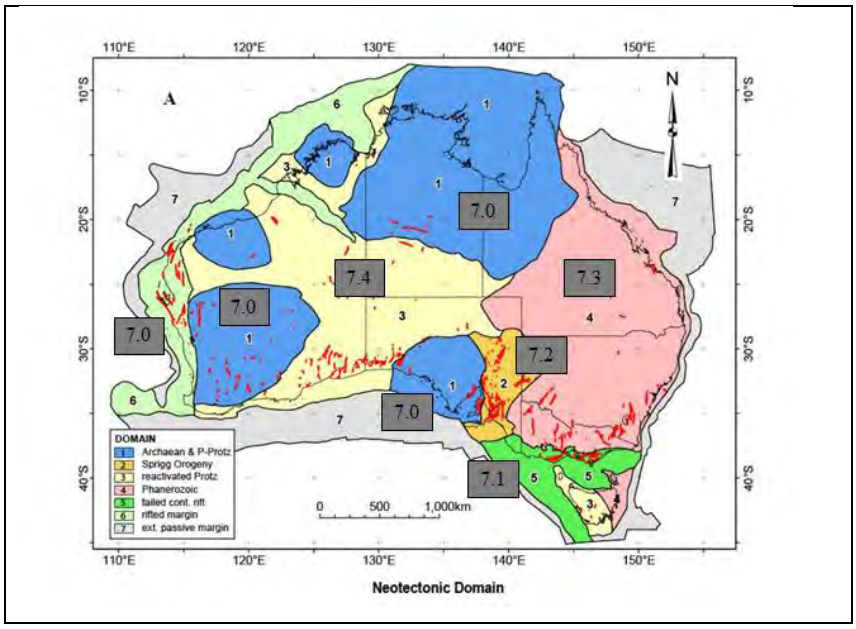

Figure 5: Neotectonic domains (D) and Maximum magnitudes (M_{max}) from Clark et al. (2010).

6 CASE STUDY

To explore the understanding of the seismic inputs to liquefaction assessment in Australia, a case study is presented for a soil profile in Sydney. This is followings the Geoscience Australia publication on Earthquake Ground Shaking Susceptibility of Botany Area, New South Wales (McPherson et al. 2013), which looked at the effect of ground shaking due to the soft soils. This publication did not considered liquefaction potential of the regolith, but the authors note that geotechnical data provide show the regolith is very soft with low shear wave velocities and SPT-N values. The soil profile (Class F from McPherson et al. 2013 in Figure 6) is assessed as a site sub-soil class C and in the upper 5m reports SPT N <10. Groundwater is assumed to be shallow.

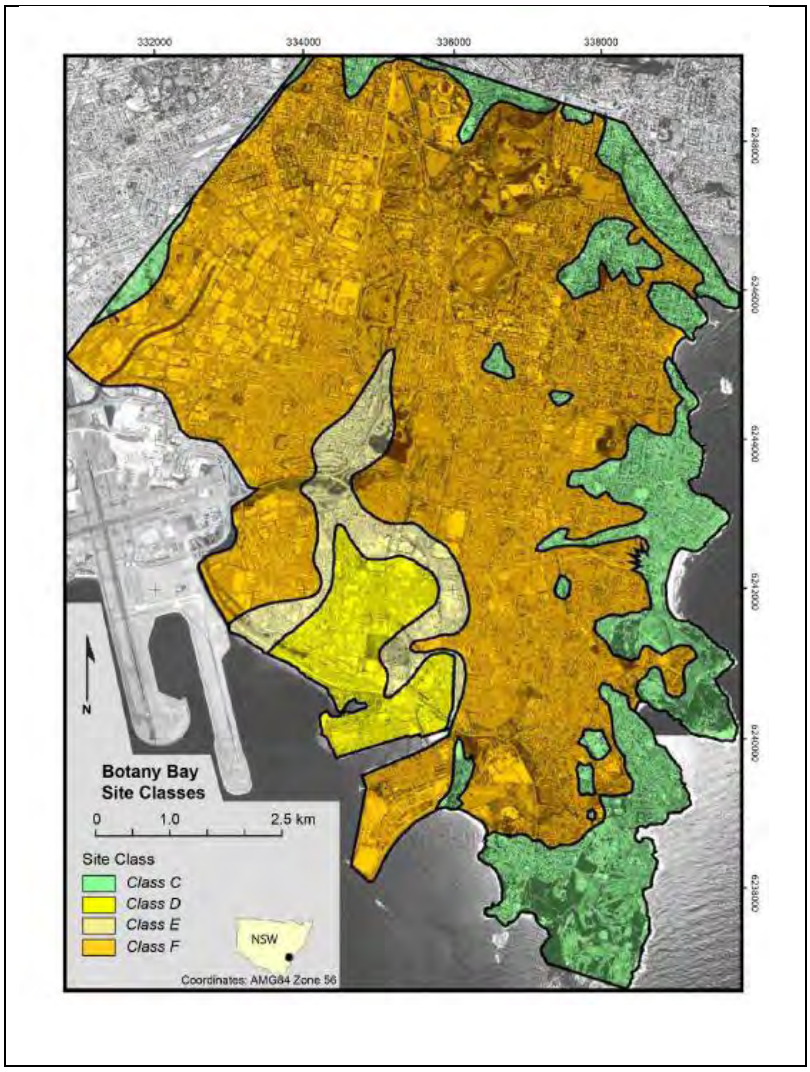

Figure 6: Class F ground conditions (taken from McPherson et al., 2013).

Using Seed et al. 2003 with inputs from AS1170.4 for a 1/1000 and 1/2500 annual probability of exceedance ground motions was considered. CSR was derived using a site response analysis and following the simplified method and using design magnitudes of M7.3 (maximum magnitude) and M6.5 (arbitrary magnitude). The Seed et al. 2003 methodology presents a probability of liquefaction where values greater than 50% are interpreted to have a high probability of liquefying.

The results shown on Figure 6 and Table 4 show for 1/1000 using the simplified method with PGA the design magnitude will determine whether it liquefies or not, but the site response analysis shows liquefaction is highly likely. For the 1/2500 the results show that profile would liquefy, but a lower design magnitude would give suggest liquefaction.

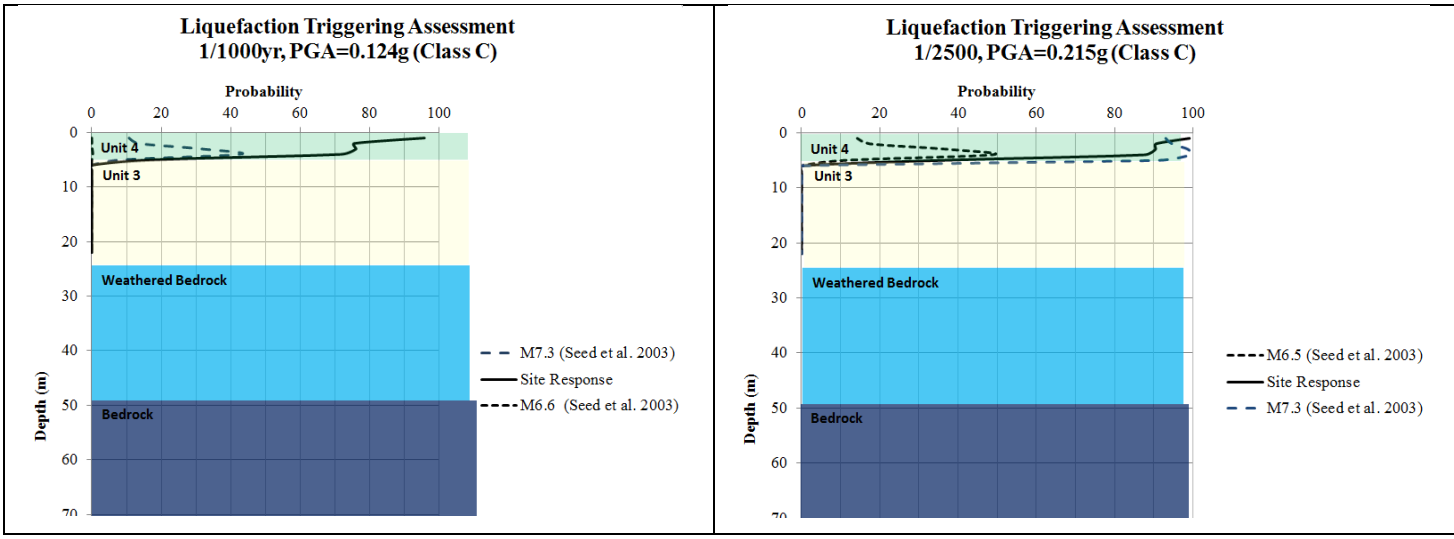

Figure 6: Liquefaction Triggering Probability for 1/1000 and 1/2500.

Table 4: Liquefaction Trigger Assessment Results

Model	Design Annual Level Probability (k_p)	PGA (g)	*Liquefaction*
M6.5	1/1000	0.124	No
M_{max} (M7.3)	1/1000	0.124	Marginal
Site Response	1/1000	NA	Yes
M6.5	1/2500	0.215	Marginal
M_{max} (M7.3)	1/2500	0.215	Yes
Site Response	1/2500	NA	Yes

6 CONCLUSIONS

Following an earthquake the resilience of a community, the ability to respond and recover, can be directly related to functioning infrastructures. Geotechnical resilience design must consideration of liquefaction from a future large earthquake. If a major earthquake occurs, it would be difficult to envision society accepting that a major bridge was not functioning. A key tenant of resilience is understanding risk.

The low seismicity nature of Australia creates a situation where liquefaction triggering is marginal, but very sensitive to the derivation of the seismic inputs. The lack of guidance from AS1170.4 requires interpretation of the seismic input for liquefaction assessments. This paper considered the sensitivity to seismic inputs in low seismicity hazard Australia.

A case study showed that liquefaction assessments in low seismicity regions, liquefaction triggering is sensitive to the selection of design magnitude. As a starting point one should consider using the M_{max} from Clark. The variability in soils and depth show that a performing a site response analysis can provide very a more accurate CSR.

The geotechnical practitioner should understand the design levels and consider a resilient approach, where performance based design is considered to get a community back up and running. Ultimately the infrastructure owners and developers will make design decision based on risk and the code, but it is up to geotechnical practitioners to understand the risk and communicate it.

7 ACKNOWLEDGEMENTS

The authors wish to thank James Dismuke for his helpful collaboration and colleagues including Jack Pappin, Sergei Terzaghi and Tim Thompson for the numerous discussions of liquefaction assessment in Australia.

8 REFERENCES

Andrus and Stokoe 1997; Andrus, R. D., and Stokoe, K. H., II. (1997). „„Liquefaction resistance based on shear wave velocity.‟‟ Proc., NCEER Workshop on Evaluation of Liquefaction Resistance of Soils, Tech. Rep. NCEER-97-0022, T. L. Youd and I. M. Idriss, eds., National Center for Earthquake Engineering Research, Buffalo, 89–128.

ASCE 7-10. 2010. Minimum Design Loads for Buildings and Other Structures. American Society of Civil Engineers Standards.

ASCE 31-03. 2003. Seismic Evaluation of Existing Buildings, American Society of Civil Engineers.

AS1170.0. 2002. Structural design actions – General principles. Standards Australia.

AS1170.4. 2007. Structural design actions - Part 4: Earthquake actions in Australia. Standards Australia.

AS5100.2. 2014. DRAFT Bridge Design – Part 2 Design Loads. Standards Australia.

Austroads 2012. Bridge Design Guidelines for Earthquake AP-T200-12

Andrus and Stokoe 1997; Andrus, R. D., and Stokoe, K. H., II. (1997). „„Liquefaction resistance based on shear wave velocity.‟‟ Proc., NCEER Workshop on Evaluation of Liquefaction Resistance of Soils, Tech. Rep. NCEER-97-0022, T. L. Youd and I. M. Idriss, eds., National Center for Earthquake Engineering Research, Buffalo, 89–128.

Bray, JD & Sancio, RB 2006, 'Assessment of the Liquefaction Susceptibility of Fine-grained Soils', Journal of Geotechnical and Geoenvironmental Engineering, vol. 132, no. 9, pp. 1165-1177.Bray, JD, Cubrinovski, M, Zupan, J & Taylor, ML 2014, 'Liquefaction Effects on Buildings in the Central Business District of Christchurch', Earthquake Spectra, vol. 30, no. 1, pp. 85-109.

Caltrans 2012 Methods for Developing Design Response Spectrum for Use in Seismic Design Recommendations

Clark, D., McPherson, A., and Collins, C., 2010. Mmax estimates for the Australian stable continental region (SCR) derived from palaeoseismicity data. AEES 2010 Conference Proceedings

Collins C., P. Cummins & D. Clark M. Tuttle R. Van Arsdale, 2004, Paleoliquefaction studies in Australia to constrain earthquake hazard estimates. AEES 2004 Conference Proceedings.

Dismuke, J. D. and Mote, T. I. 2012, Approximate Deaggregation Method for Determination of Design Earthquake Magnitudes for Australia. ANZ 2012 Conference Proceedings.

Gaull, B.A., Michael-Leiba, M.O., and Rynn, J.M.W., 1990. Probabilistic earthquake risk maps of Australia. Australian Journal of Earth Sciences 37, 169-187.

Idriss, I.M., and Boulanger, R.W., 2008. “Soil Liquefaction During Earthquakes,” monograph series, No. MNO-12, Earthquake Engineering Research Institute.

Kanai, K., 1961. An empirical formula for the spectrum of strong earthquake motions. Bulletin of the Earthquake Research Institute, University of Tokyo 39, 85-96.

Leonard, M., Burbidge, D., and Edwards, M. 2013. Atlas of Seismic Hazard Maps of Australia. Geoscience Australia Record 2013/2014 GeoCat 77399

Marchetti, S., Monaco, P., Totani, G., and Marchetti, D. (2008) In Situ Tests by Seismic Dilatometer (SDMT). From Research to Practice in Geotechnical Engineering: pp. 292-311.

McCue, K., (Compiler), Gibson, G., Michael-Leiba, M., Love, D., Cuthbertson, R., & Horoschun, G., 1993. Earthquake hazard map of Australia, 1991.

McPherson, A.A. and Hall, L.S. 2007. Development of the Australian National Regolith Site Classification Map. Geoscience Australia Record 2007/07, 37 p.

McPherson,A., Dhu, T., Jones J., and Neville M. 2013. Earthquake Ground Shaking Susceptibility of the Botany Area, New South Wales. Geoscience Australia Record 2013/26 GeoCat 75265

Mitchell P. W. and Moore C. 2007, Difficulties in assessing liquefaction potential from conventional field testing. AEES 2007

Moss, R.E.S., Seed, R.B., Kayen, R.E., Stewart, J.P., Der Kiureghian, A., and Cetin, K.O., 2006. CPT-based probabilistic and deterministic assessment of in situ seismic soil liquefaction potential, Journal of Geotechnical and Geoenvironmental Engineering, ASCE 132(8), 1032-051.

Mote, T. I. and So M. L. 2013. Sensitivity of Liquefaction Triggering Analysis to Earthquake Magnitude. AEES 2013 Conference Proceedings.

NZTA The NZ Transport Agency Research Report 553 – "the development of guidance for bridges in New Zealand for liquefaction and lateral spreading effects",

MiBE 2012. Guidelines for repairing and rebuilding houses affected by the Canterbury earthquake. NZ Ministry of Business, Innovation and Employment.

NZS1170.5 Structural Design Actions – Part 5: Earthquake actions – New Zealand

Robertson, PK & Wride, CE 1998, 'Evaluating cyclic liquefaction potential using the cone penetration test', Canadian Geotechnical Journal, vol. 35, pp. 442-459.Seed, H. B., and Idriss, I. M., 1971. Simplified procedure for evaluating soil liquefaction potential. Journal of the Geotechnical Engineering Division, ASCE, 97(9), 1249–1273.

Seed, H. B., and Idriss, I. M., 1971. Simplified procedure for evaluating soil liquefaction potential. Journal of the Geotechnical Engineering Division, ASCE, 97(9), 1249–1273.

Seed, R.B., K, O., Cetin, R.E.S., Moss, A., Kammerer, J., Wu, J.M., Pestana, M.F., Riemer, R.B., Sancio, J.D., Bray, R.E., Kayen, R.E. and Faris, A. (2003), "Recent advances in soil liquefaction engineering: a unified and consistent framework", Keynote Address, 26th Annual Geotechnical Spring Seminar, Los Angeles Section of the GeoInstitute, American Society of Civil Engineers, H.M.S. Queen Mary, Long Beach, California, USA.

Seed, H. B., Tokimatsu, K., Harder, L. F., and Chung, R. M. (1985). "Influence of SPT Procedures in soil liquefaction resistance evaluations." Journal of Geotechnical Engineering, ASCE, 111(12), 1425-1445.

Suzuki, Y., Tokimatsu, K., Koyamada, K., Taya, Y. and Kubota, Y. (1995), "Field correlation of soil liquefaction based on CPT data", Proceedings of the International Symposium on Cone Penetration Testing, Linkoping,Vol. 2, pp. 583-8.

Yang and Wright, 2010

Youd, T.L., Idriss, I.M., Andrus, R.D., Arango, I., Castro, G., Christian, J.T., Dobry, R., Finn, W.D., Harder, L.F., Hynes, M.E., Ishiara, K., Koester, J.P., Liao, S.S.C., Marcuson, W.F., Martin, G.R., Mitchell, J.K., Moriwaki, Y., Power, M.S., Robertson, P.K., Seed, R.B. and Stokoe, K.H. II (2001), "Liquefaction resistance of soils: summary report from the 1996 NCEER and 1998 NCEER/NSF workshops on evaluation of liquefaction resistance of soils", Journal of Geotechnical and Geoenvironmental Engineering, ASCE, Vol. 127 No. 10, pp. 817-33.Semple, R. 2013 Problems with liquefaction criteria and their application in Australia, Australian Geomechanics Vol 48 No 3 September 2013

DESIGN AND CONSTRUCTION OF A RESILIENT MOTORWAY ON DIFFICULT GROUND

Richard Kelly

Principal, Coffey

Visiting Industry Fellow, Centre of Excellence for Geotechnical Science and Engineering, University of Newcastle

ABSTRACT

Resilience is the ability of assets, networks and systems to anticipate, absorb, adapt to and / or rapidly recover from a disruptive event. Where motorways cross floodplains, a major flood poses the greatest risk of a disruptive event. Deep deposits of soft, compressible materials are often encountered in floodplains making construction of resilient infrastructure difficult and potentially expensive.

In order to optimise the balance between time, cost, resilience and risk the Roads and Maritime Authority of New South Wales (RMS), in conjunction with the Ballina Bypass Alliance, developed a low embankment strategy to minimise the whole of life cost of the Ballina Bypass motorway while allowing the motorway to operate during a 1 in 20 year flood. The low embankments traversed very poor ground conditions and the geotechnical challenge was to estimate performance of the embankments at the design stage, monitor the actual performance of the embankments during construction and to take actions to achieve the strategic goals if required.

This paper presents the low embankment strategy, the associated pavement strategy and discusses the geotechnical elements pivotal to its success.

1. INTRODUCTION

Resilience is the ability of assets, networks and systems to anticipate, absorb, adapt to and / or rapidly recover from a disruptive event. Where motorways cross floodplains, a major flood poses the greatest risk of a disruptive event and historically the Pacific Highway has been closed for periods of time.

Deep deposits of soft, compressible materials are often encountered in floodplains. Embankments constructed on these materials will settle and potentially be unstable. Long term deformations will occur causing embankments to potentially settle below flood level and/or affect pavement performance if action is not taken to improve the ground.

There are several ways of achieving a suitably resilient motorway.

- To eliminate settlement as a constraint a bridge could be built across the floodplain;
- To reduce settlement ground treatment could be provided across the floodplain; or
- Embankments could be built directly on the ground and a whole of life construction and maintenance strategy developed to manage the impacts of settlement during construction and operation.

Deciding which option to adopt required optimisation of conflicting cost, time, performance and risk constraints. For example, a highly resilient solution is to build a bridge across the floodplain but the expense would mean that construction of other sections of the highway could not be afforded. Given that the fundamental driver of the Pacific Highway upgrade is to improve safety, building kilometres of road outweighed flood proofing the Ballina Bypass. The optimum balance was determined to be adopting a low capital cost solution by constructing directly on the soft ground and implementing a whole of life maintenance and intervention strategy to manage the settlements.

The Ballina Bypass was a motorway with a 6km length traversing the floodplain associated with the Richmond River. The location of the motorway is shown in Figure 1 by the dashed line traversing the Holocene sediments.

The Roads and Maritime Authority of New South Wales (RMS), in conjunction with the Ballina Bypass Alliance (BBA), developed a “low embankment strategy” (LES) to minimise the whole of life cost of the Ballina Bypass motorway while allowing the motorway to operate during a 1 in 20 year flood.

The low embankment strategy had the following elements:

- The formation was designed such that the 1 in 20 year flood level was below the pavement level immediately on opening of the Ballina Bypass;

- A post construction settlement of 200mm was allowed to occur before intervening to top up the embankments. After 200mm settlement, the outside lanes would be below water during a 1 in 20 year flood but the inner two lanes would be free of water and trafficable;
- The embankment formation was to be placed shortly after construction commenced and allowed to settle for the maximum time available prior to pavement construction. A minimum settlement time of 17 to 20 months was specified; and
- Monitor the performance of the embankments during the consolidation period and take any actions required to achieve long term whole of life goals.

A pavement strategy was developed in conjunction with the low embankment strategy to allow the pavements to function when subjected to residual settlements.

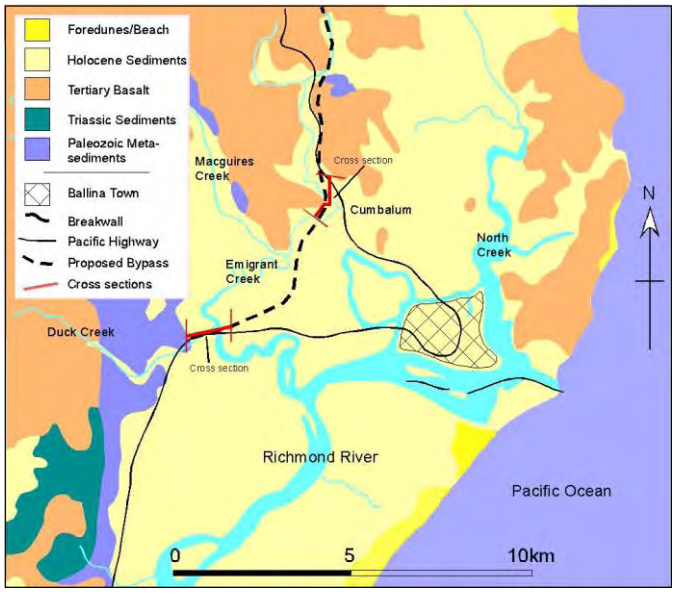

Figure 1: Location of the Ballina Bypass.

The pavement strategy aimed to construct heavy duty pavements using a staged process. On road opening, the pavement would be made from a granular chert material with a seal and an asphalt wearing course. Maintenance allowances and asphalt layers were developed such that a heavy duty deep lift asphalt pavement would be constructed over the design life of the pavement. The pavement strategy is summarised in Table 1.

Table 1: Construction of Staged Pavements

Year	**Staged Pavement: Required Maintenance / Pavement Improvement Interventions**
Construction	300mm chert pavement with spay seal wearing surface
0-1	Repair any initial defects and settlement (Allow 0.25% surface area)
1	Apply 40mm thick asphalt wearing surfacing
2 to 10	Asphaltic Concrete (AC) correction 10% (allowance)
8 to 10[#1]	100mm overlay (Chert or Asphalt)
30	Replace wearing surface including settlement correction (100mm) plus 1% heavy patching
40	Salvage

#1 Overlay thickness will vary from location to location

RMS had extensive experience in the Ballina region with the construction and maintenance of chert pavements. Chert pavements are essentially an unbound granular pavement, with a specific local grading. RMS experience was that chert pavements are a cost efficient and well performed pavement where they:

- are produced from high quality materials;
- are constructed with personnel experienced in chert pavement construction; and
- where particular attention is paid to edge detailing and seal widths.

The construction sequence generally comprised:

- a geotextile separation layer with provision for a bi-axial grid where required;
- a bridging layer of a graded rocky fill;
- an upper zone and select material zone (SMZ) of high quality earthfill material
- full width construction with chert "daylighting" on low side and sealed on high side

RMS requirements stipulated a pavement life for the BBA main line carriageways of 40 years. Due to the potential settlements in the low embankment areas it was considered that a pavement structure which would not require significant rehabilitation to address structural (trafficking) distress within the design period was not appropriate, as extensive planned intervention/maintenance/rehabilitation was expected to be required within the first 10 years of service to address settlement and functional performance issues.

There was considerable uncertainty in both the overall and differential settlement that would occur; hence provision of overlays was expected to be required for shape correction and/or to maintain specified minimum flood levels.

Granular pavements were the preferred option as they are flexible structures which accommodate more differential settlement than the other types of pavements. Full depth or deep lift asphalt solutions can be successfully employed under these conditions. However, they have a higher initial cost than a chert pavement but this was not realised in whole of life terms as overlays are still required and overlays result in under-utilisation of expenditure on the deeper pavement layers.

Given the low embankment areas were susceptible to flooding, water ingress was expected to affect the performance of the pavement materials. As such, it was essential that the materials providing the majority of the structural strength within the pavement comprise materials that are not significantly influenced by their moisture condition.

Maintenance would be triggered by any of the following factors:

- **Safety and function:** The rideability of the road would be affected by shape loss and surfacing defects such as potholes and water ponding arising from differential settlement and flood inundation. The first intervention was considered likely to be triggered by ride comfort;
- **Flood immunity level:** Level restoration to maintain the minimum flood immunity levels. It was considered unlikely that the formation and/or pavement would settle uniformly, and therefore maintenance for shape correction would be required prior to addressing extreme settlement.
- **Pavement distress:** Stripping and flushing were considered likely to trigger resealing activities of granular pavements with sprayed seal surfacings during service. In this type of pavement, surfacing failureswere expected and could be exacerbated by saturation of the underlying granular layers in the case that a flood event occurred. Pavement distress may also occur at isolated locations where extreme differential settlement was concentrated. This was considered most likely to happen at the transitions between ground treatment areas and untreated areas.

It was considered likely that maintenance activities during service, to address both settlement and functional issues, would be undertaken with overlays, or in minor works, with asphalt regulation. When maintenance was undertaken to address functional deficiencies or minor settlement, thicker overlays was expected for the granular pavements. Similar overlay thicknesses were expected when addressing formation settlement.

2. GEOTECHNICAL INPUT

The geotechnical challenge was to estimate performance of the embankments at the design stage, monitor the actual performance of the embankments during construction and to take actions to achieve the strategic goals if required.

2.1 GEOTECHNICAL MODEL

The ground at the southern end of the Ballina Bypass is comprised of a thin layer of over-consolidated crust overlying deep soft to firm Holocene clay over Pleistocene stiff clay. The soft Holocene clay thickness varies from 5m to 28m and has low shear strength, high plasticity and high compressibility. The soft soil is near normally consolidated and is described as dark grey alluvial clay, containing shells and traces of silts. A unit of loose silty sand was occasionally encountered as discontinuous layer or lens within the clays. The land was used for agriculture and mostly sugar cane.

Site investigations included 100MPa piezocone penetration tests (PCPT), dissipation tests, boreholes, hand vane, and down-hole shear vane tests. Laboratory oedometer tests were performed to assess the consolidation parameters.

Over-consolidation ratio (OCR) values were obtained from one-dimensional consolidation tests and from correlations with undrained shear strengths inferred from piezocone test data. Unfortunately many of the oedometer tests showed signs of significant disturbance and interpreting preconsolidation pressures from these tests was difficult. Therefore, the adopted OCR design values were made consistent with the undrained shear strength profile using Equation 1 (Ladd, 1991).

$$s_u = s(OCR)^m \sigma_v' \qquad (1)$$

In Equation 1, s_u is the undrained shear strength, σ'_v is the vertical effective stress, „m" was assumed to by 0.8, „s" = (s_u/σ'_v) for normally consolidated soils and a value of 0.22 was adopted.

The undrained shear strength of the clays was obtained from hand vane, down-hole shear vane and correlations with piezocone tests using an empirical N_{kt} factor of 15.

Rates of horizontal consolidation were obtained from insitu piezocone dissipation tests. The piezocone data for the project were interpreted using the method described by Teh and Houlsby (1991). Rigidity Indices of 20 and 40 were used in the interpretation. The rigidity indices are low and represent soil stiffnesses at strains expected during consolidation. Rates of vertical consolidation, c_v, were obtained by dividing the rate of horizontal consolidation by a factor of 2. They can also be obtained from available one-dimensional laboratory consolidation tests. However, these values are typically much lower than those recorded in the field and were not adopted for design. Field values are considered to reflect the presence of anisotropic fabric in the soil that might not be captured by small scale laboratory tests. In general, the interpreted c_v values were generally in the order of $1m^2/yr$ to $2m^2/yr$ in the Holocene clays. The interpretation of the c_v values was affected by an initial increase in water pressure with time prior to dissipation. This is considered to be a result of desaturation of the filter element as it is pushed through the crust or insufficient de-airing prior to testing.

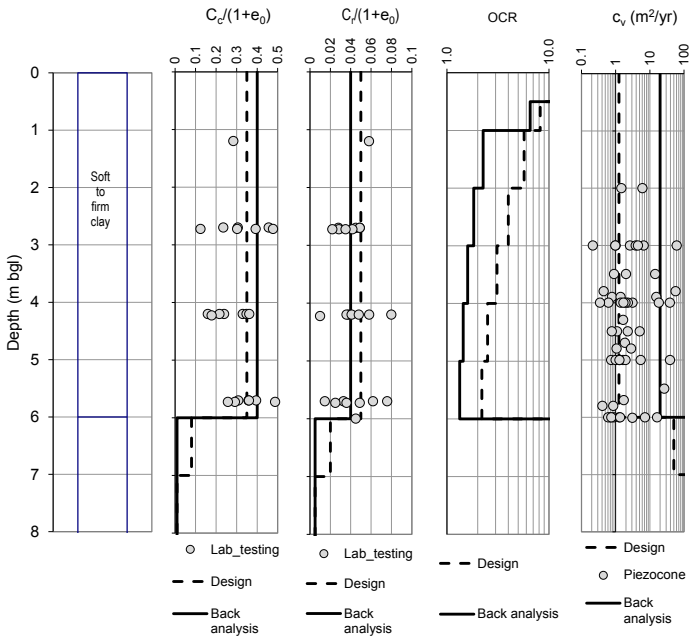

Figure 2: Geotechnical model.

The geotechnical model is summarised in Figure 2 and adopted design profiles are shown by the dashed lines. The design lines were believed to represent a cautious set of parameters. Upper quartile values for the compression parameters were adopted and lower quartile values for the rate of consolidation were adopted.

2.2 DESIGN STAGE SETTLEMENT PREDICTIONS

Settlements were predicted using one-dimensional consolidation theory, a bi-linear void ratio-log effective stress model and a finite difference numerical procedure for the adopted construction staging and geotechnical model.

Predicted settlements were expected to vary from construction performance and therefore an estimate of potential variability was evaluated using Duncan"s (2000) method. Uncertainties of the soil models are associated with evaluating soil and fill properties, with assessed depth of the soft clay deposit and with the unknown presence of sand/silt lenses or layers within clay unit between site investigation locations. The assessment indicated that the settlement may vary by as much as 50% from the predicted values where soft soil thicknesses are greater than 15m. The settlement may vary by 20 to 30% where the depth of the soft soil is less than 15m. The assessed rate of settlement may vary up to 50%.

The predicted settlement is shown in Figure 3 along with upper and lower bounds.

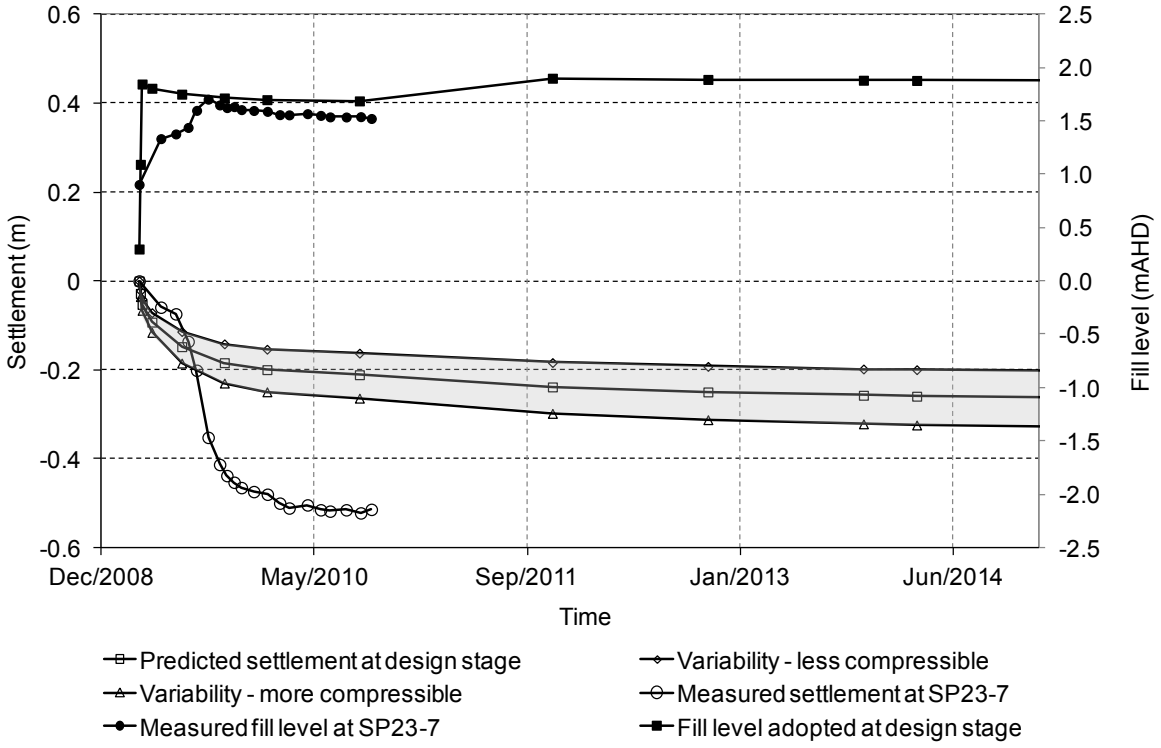

Figure 3: Comparison of predicted and measured settlements.

An intensive instrumentation and monitoring programme was implemented. Settlement plates were installed at 50m intervals staggered on the northbound and southbound lanes. The Observational Method (Peck, 1969) was implemented in the expectation that performance would not match expectation and additional actions might be required to achieve the desired outcomes.

2.3 PERFORMANCE OF THE LOW EMBANKMENTS

Predicted settlement at one particular location is compared with measured settlement in Figure 3. The monitoring data showed that actual settlement of the embankments was substantially greater than estimated at design phase and was greater than the upper bound predicted values up to May 2010. A fast rate of settlement was observed during the early stages of construction. This trend was observed along the entire length of the low embankments to a greater or lesser degree.

The magnitude of the settlement meant that the fill had settled significantly below design level. Additional fill would have to be placed in order to bring the embankment back to design level, but the additional fill would also trigger more settlement during construction and potentially more settlement than could be accommodated by the whole of life pavement strategy.

A remedial strategy was required in order to ensure that the post construction performance met the required maintenance activities and pavement interventions. The first step in this process was to perform back analysis to understand why the soil behaved differently to expectations and to refine the geotechnical model.

2.4 BACK ANALYSIS

Back analysis was performed by varying the compression, OCR and rate of consolidation parameters. These analyses were performed in 2010 and 2011 during construction.

Primary consolidation was observed to be completed when plotting measured settlement data against the logarithm of time. As a result 100% primary consolidation could be approximated with a high level of confidence. For a particular location, various combinations of compressibility parameters were adopted and the settlement analyses were carried out to fit 100% settlement where it was measured. The results of the analyses are shown in Table 1. Values of the empirical parameter „k“ in Table 2 relate to Equation 2 and were varied in the analysis to give different OCR profiles. The values adopted for the back analysis of the low embankments are highlighted in bold.

$$OCR = \frac{k\left(q_t - \sigma_{v0}\right)}{\sigma'_{v0}} \qquad (2)$$

In Equation 2, q_t is the net cone resistance, σ_{v0} is the total initial stress, σ'_{v0} is the initial effective stress and „k“ is an empirical fitting parameter. In Table 2, CRR is the recompression ratio and CR is the compression ratio.

This analysis was performed on a location that had settled 0.83m. A wide range of parameters can be selected to fit the measured settlement. The question is whether or not the parameters are credible. The parameter set adopted was selected because it provided an upper bound to predicted settlement at locations where the soft soils were deep and therefore was considered to be a cautious estimate. Of the adopted parameters, the k value is considered to lie at the low end of the range. The CR values are higher than measured in oedometer tests performed for the Ballina Bypass but are generally consistent with tests on high quality samples currently being performed at the University of Newcastle. At the time of back analysis, this process of back analysis was performed for areas with a range of soft soil depths (not presented in this paper) and the adopted parameters were considered to more adequately represent the range of behaviour than the other parameter sets presented in Table 2.

Table 2: Comparison of parameter combinations

k	CRR	CR	Settlement (m)	Decision
0.15	0.123	0.25	0.83	k implies OCR < 1 for soils greater than 6m depth
0.15	0.04	0.297	0.829	k implies OCR < 1 for soils greater than 6m depth
0.2	0.123	0.3	0.829	
0.2	0.081	0.35	0.828	
0.25	0.135	0.35	0.831	
0.2	**0.04**	**0.4**	**0.83**	**adopted values**
0.25	0.111	0.4	0.83	
0.3	0.15	0.4	0.832	
0.2	0.0001	0.45	0.834	CRR Not Credible
0.25	0.087	0.45	0.829	
0.3	0.135	0.45	0.828	
0.3	0.122	0.5	0.831	CR considered upper bound

This process of back-analysis relies on engineering judgement and to a large extent is an exercise in curve fitting. As such, the parameters cannot be considered absolutely representative of the soil. However, the adopted process does maintain observed trends with depth in OCR values and results in CR and CRR values consistent with subsequent high quality testing. Therefore, the adopted parameters can be considered credible within the confines of a bi-linear one-dimensional model.

A comparison between the measured and back-figured settlements is shown in Figure 4. The back-figured soil parameters are shown in Figure 2. In order to fit the measured settlement, CR values were revised from 0.35 to 0.4, CRR values were reduced to 0.04 from 0.05, the OCR profile was reduced by between one-third and one-half and the rate of vertical consolidation was increased to $20m^2$/yr.

The two most significant differences in the soil parameters are the values adopted for the OCR profile and the rate of vertical consolidation.

Determination of the OCR profile at the design stage was complicated by a lack of confidence in OCR values determined from laboratory testing and lack of sensitivity in the 100MPa piezocone. The back-figured OCR profile corresponds to an „s" value in Equation 1 of 0.3. Although this value appears to be high, Ladd (1991) reports that „s" can be in the order of 0.3 for high plasticity clays rather than the „default" value of 0.22 adopted in design.

Across the area traversed by low embankments, the back analysed coefficient of vertical consolidation ranged from 6 to $125m^2$/year for the top few meters of soil. For deeper soft soil, the coefficient of vertical consolidation was smaller and ranged from 8 to $15m^2$/year. However, where wick drains were used, the back-figured coefficients of consolidation were about $2m^2$/year which is consistent with values adopted from the piezocone dissipation tests. The rate of settlement is a function of the rate of consolidation and also the length of the drainage path. As back-figured rates of consolidation in areas where wick drains were used were similar to values inferred from PCPT tests, it suggests that the difference between design and back-figured values is due to lengths of drainage path being shorter than assumed. The PCPT tests show that clay is uniform with depth and that there are no thin sand lenses present. One possible cause of a short drainage path is the presence of plant roots in the upper 6m of the soil profile (Brian Chandler, AECOM Victoria, personal communication). Sugar cane roots were detected in U75 samples taken in the upper 6m of the clay profile and it is possible that the roots acted as naturally occurring vertical drains. It is also possible that the limitations of the dissipation tests and adopted rigidity index resulted in underestimates of the coefficient of consolidation. Generally speaking, adopting a lower bound for the coefficient of consolidation in design is conservative as it suggests settlement will take longer than it actual, however in the case of the low embankment strategy it was unconservative because more materials were required to construct pavement and potentially more settlement related maintenance could have been required post construction. The compression and recompression ratios were slightly modified to fit the data.

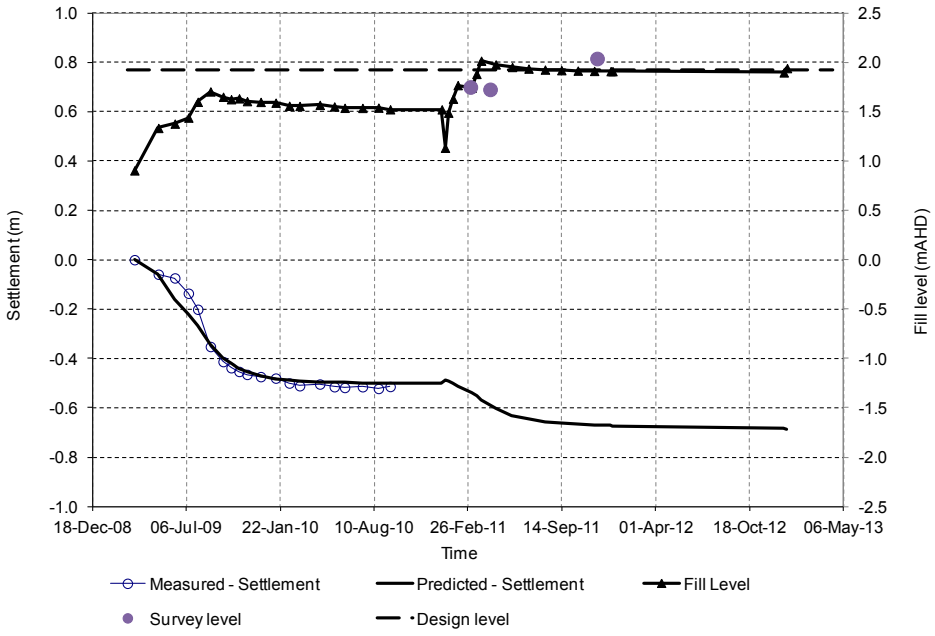

Figure 4: Example of a back analysis - settlement time curve

2.5 REVISED CONSTRUCTION STRATEGY

The fact that there was more settlement and settlement occurred at a faster rate than anticipated meant that additional fill would be required to construct embankments to the design level at road opening and the post construction settlement would be greater than assumed at in the pavement strategy. More interventions would be required at earlier intervals and greater frequencies than the design settlement estimates suggested.

Construction of the low embankments was revised to achieve the long term embankment settlement requirements. The following modifications were made:

- At the southern end of the alignment where the soft soils were deepest, the design vertical alignment was generally higher than required for flood immunity. The vertical alignment was lowered and a lower bound alignment specified that satisfied flood immunity and minimum road design requirements while allowing settlement to occur over time without going below the lower bound alignment;
- Surcharge was placed in some localised areas; and
- Based on the revised geotechnical model, the embankments were constructed to a targeted level above the design level at all locations, and the embankments were allowed to settle such that design level was achieved at the date of road opening.

In addition, it became evident that settlement would occur between placement of each layer of chert pavement. This had the potential to result in more pavement material being placed than provided in the cost estimate. Detailed numerical analyses were performed after the back analyses had been completed to assess the minimum thickness of fill required to construct the pavement to the required level. The predicted settlements are shown in Figure 4. Although these analyses were performed, construction actually occurred at different times to those used in the analyses. Top of fill levels measured during construction are compared with predictions in Figure 4. Measured settlement in February 2011 compare well with predicted settlement. The final pavement level was achieved in November 2011 compared with February in the analysis and this meant that the pavement level at road opening was higher than assessed.

3. CONCLUSIONS

The following conclusions can be drawn from the design, construction and back-analysis of the low embankments:

- Compression parameters and rates of consolidation inferred from conventional site investigation data may not accurately represent actual soil parameters. The highest quality of data is required when embankments are constructed over soft clays;
- Rates of consolidation and overconsolidation ratios were most difficult to estimate;
- Rates of settlement may be high in the upper 6m of the clay deposit due to the presence of roots;
- The Observational Method coupled with detailed back analysis is a vital component of constructing low embankments cost effectively and to achieve design requirements; and
- Low embankments should be constructed by filling sufficiently above design level such that the weight of fill removed when pavements are constructed is greater than the weight of the pavements. This method will prevent additional settlement being triggered by placement of extra fill later in the preloading period. The challenge is to accurately assess how much settlement will occur during the preloading period.

ACKNOWLEDGEMENTS

The author would like to thank the Roads and Maritime Authority of New South Wales, Australia and the Ballina Bypass Alliance for the data. Harry Nguyen, formerly from Coffey, now studying at UTS as a PhD student performed the back analyses reported in this paper.

REFERENCES

Duncan, J.M. (2000), “Factors of safety and reliability in geotechnical engineering”, *Journal of Geotechnical and Geoenvironmental Engineering*, 126(4), 307-316

Ladd, C.C. (1991). "Stability evaluation during staged construction: 22nd Terzaghi Lecture." *Journal of Geotechnical Engineering*, ASCE, 117(4), 537-615.

Peck, R. (1969), “Advantages and limitations of the Observational Method in applied soil mechanics”, *Geotechnique*, 19(2), 171-187

Teh C.I. and Houlsby, G.T. (1991), “An analytical study of the cone penetration test in clay”, *Geotechnique*, 41(1), 17-34

PIPE JACKING THROUGH A RAIL EMBANKMENT

S. Chun[1], J. Hsi[2] and T. Swanson[3]

[1]Tunnel Engineer, [2]Chief Technical Principal - Geotechnics, [3]Senior Engineering Geologist, SMEC Australia, Level 5, 20 Berry Street, North Sydney, NSW, 2060, Australia

ABSTRACT

Pipe jacking through rail embankments inevitably causes ground movements during excavation and construction. Excessive ground movements can lead to embankment instability and rail track distortions which could result in train derailment. Therefore, ground and track movements must be closely monitored during construction in accordance with the respective rail authority standards and geotechnical assessment. This paper presents the project overview, construction method, prediction of ground movements associated with pipe jacking, track deformation design criteria and construction performance for the Gerringong Bypass Belinda Street Culvert where seven 1500mm diameter reinforced concrete pipes needed to be constructed beneath the existing South Coast Line railway embankment. Extensive instrumentation and real time monitoring were undertaken during construction to ensure safety of the rail operation. The measured ground movements were back analysed and the assumptions were calibrated for the prediction of future movements due to subsequent pipe jacking. A contingency plan was implemented to ensure that the settlement criteria and operational safety were met.

1 INTRODUCTION

The Gerringong Upgrade Project is part of the Princes Highway upgrade program which comprises 7.5km of four lane divided highway with a design speed of 100km/h. The project was awarded by the Roads and Maritime Services (RMS) to Fulton Hogan to design and construct the project with SMEC Australia as the Principal Consultant. As part of the upgrade, Fulton Hogan constructed a culvert located under the proposed highway alignment, running from a diversion channel on the west of the Princes Highway, crossing under the South Coast Railway Line and discharging into the south east.

The Gerringong Bypass Belinda Street Culvert (Culvert C4480) is the crossing under the South Coast Railway Line and consists of seven 1500mm diameter (1800mm external diameter) reinforced concrete pipes constructed beneath the existing railway embankment in order to provide additional flood immunity in the area. The pipes were spaced at a nominal separation distance of 2604mm centre to centre with a nominal horizontal clearance of approximately 800mm between adjacent pipes. The distance from the top of the embankment to pipe axis level was approximately 6.4m. The pipes were excavated through Fill and Alluvium consisting of sandy and silty clay. Figures 1 and 2 show various cross sections of the works.

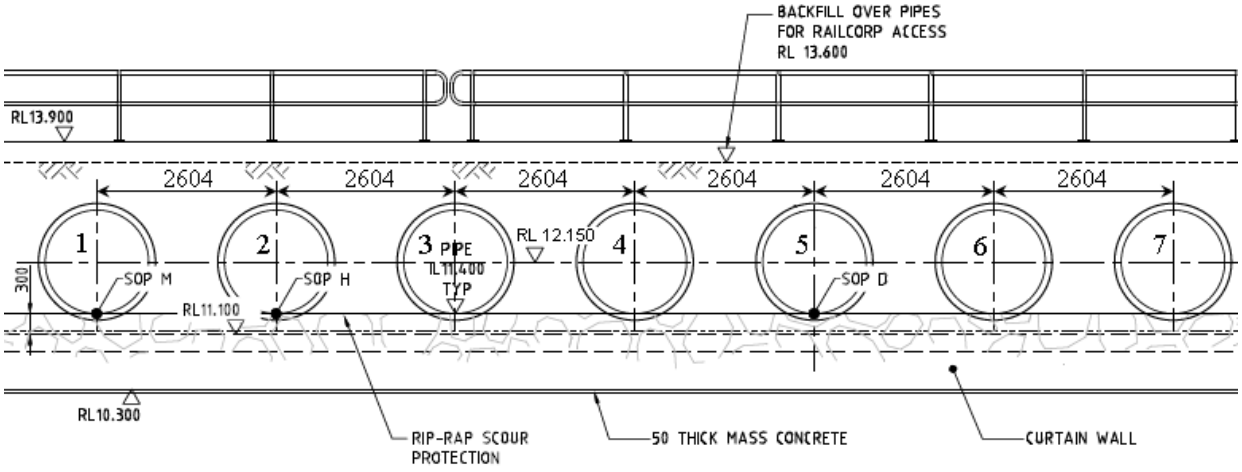

Figure 1: Gerringong Bypass Belinda Street Culvert C4480 finished cross section at embankment toe.

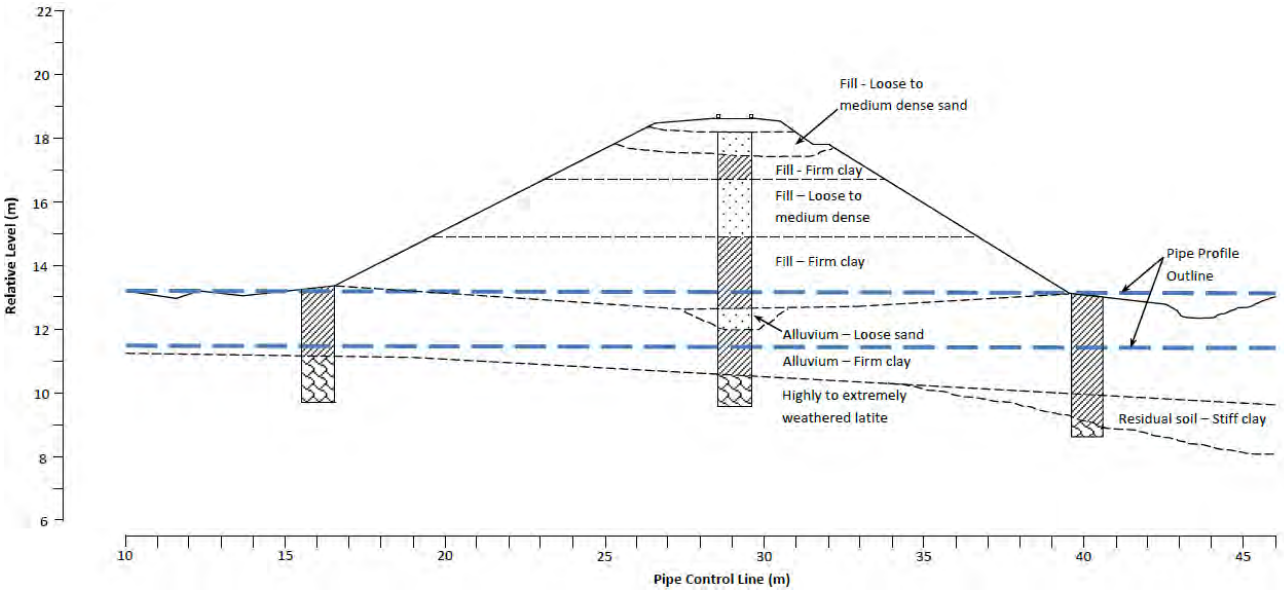

Figure 2: Gerringong Bypass Belinda Street Culvert C4480 embankment cross section.

The installation of the new set of pipes was undertaken by jacking pipes through the embankment so as to minimise disruption to the operation of the railway line. Bothar Boring & Tunnelling carried out the excavation and installation of the pipe underbores as the subcontractor for Fulton Hogan. The pipe jacking operation commenced in May 2013 and was completed in September 2013. Figure 3 shows the culvert alignment plan.

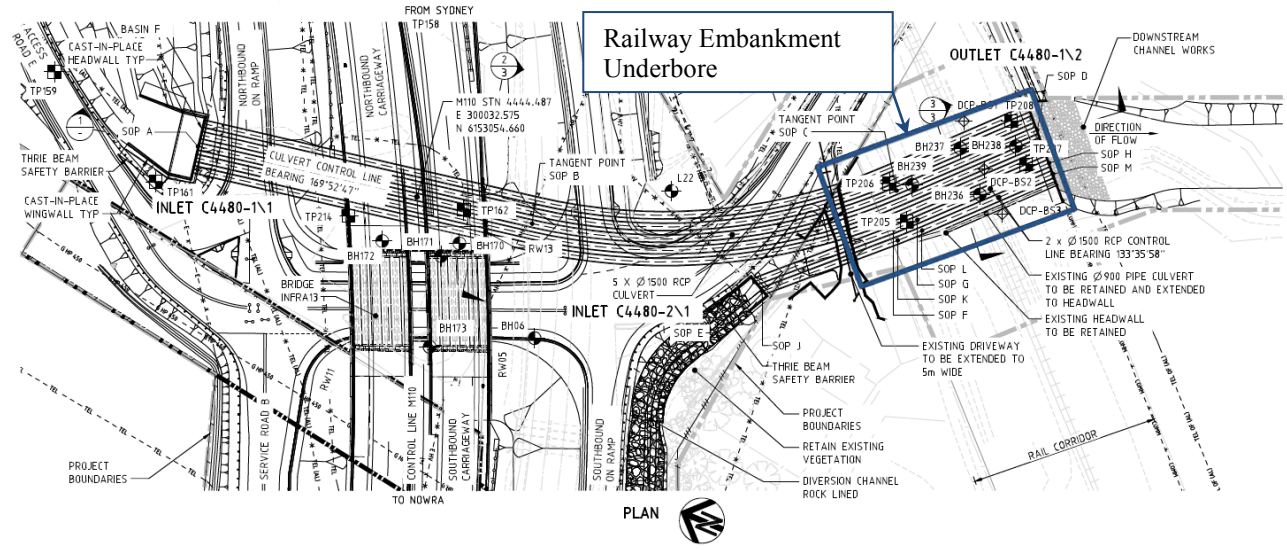

Figure 3: Gerringong Bypass Belinda Street Culvert C4480 alignment plan.

Construction of pipes through live railway embankments using trenchless construction methods such as pipe jacking is common. Tunnelling through rail embankments inevitably causes ground movements. This can lead to embankment instability and rail track deformations which could impair track performance. Therefore, embankment ground movements must be strictly monitored and suitable mitigation measures set in place in accordance with the respective rail authority standards and geotechnical assessment.

This paper presents the project overview, construction method, prediction of ground movements associated with pipe jacking, track deformation design criteria and construction performance for the Gerringong Bypass Belinda Street Culvert. Extensive instrumentation and real time monitoring of the track and embankment were undertaken by Lynton Surveys during construction to ensure safety of the rail operation in accordance with RailCorp Standards. The measured ground movements were back analysed and parameters were calibrated for the prediction of future movements due to subsequent pipe jacking. A contingency plan was implemented to ensure that the settlement criteria and operational safety were met.

2 TUNNELLING METHODOLOGY AND CONSIDERATIONS

2.1 TUNNELLING METHOD

The embankment was excavated using a Hydraulic Arm Tunnelling Machine (HATM) rig. Exit pits and jacking pits with thrust blocks and launch frames were constructed and located at a minimum distance of 2.5m from the toe of the embankment to prevent destabilisation. The HATM rig consists of a Hydraulic Telescopic Excavator (HTE) with a cutting head mounted on a slew ring and fixed in the crown of the shield (Figures 4 and 5). The digging action was obtained by a bucket cylinder mounted within the boom. Excavated material was removed by a hydraulic driven conveyor belt into an electrically driven skip which ran along a set of rails from the HATM back to the jacking pit where it was removed and tipped by an excavator.

Figure 4: Face of HATM rig.

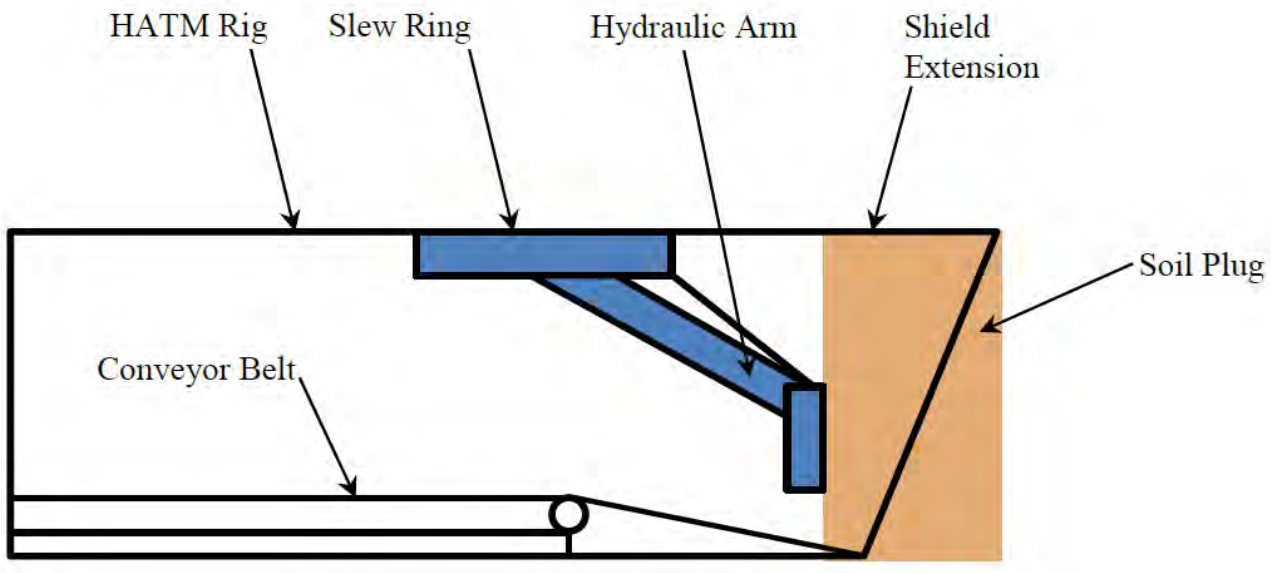

Figure 5: HATM rig schematic.

The cutting head was advanced by means of hydraulic rams exerting pressure off the thrust block. The cutting head produced a 1820mm diameter hole through the existing earth to allow the pipes to be jacked through. After the cutting head was advanced to the full stroke of the hydraulic rams and the rams retracted, the pipe was inserted into the jacking frame to make a continuous line with the cutting head.

The bore was to be cased at all times (steel HATM shield and pipe string). Excavations were to take place in supported ground at all times, i.e. no excavation to take place ahead of the steel shield. The HATM rig selected was configured so that the hydraulic arm could not extend past the face of the shield. The initial underbore design required a sufficient length of soil plug to be maintained ahead of the bore to maintain face stability. Therefore, the hydraulic arm was not to be extended into the soil plug. This was to be monitored by the Designer's Site Geotechnical Representative (DSGR) to ensure that the soil plug was not compromised. This assessment was based on conservative assumptions and was to be recalibrated after the installation of the first pipe.

To prevent local instability due to the HATM rig pushing the soil plug out of the embankment, the advancement rate was to be slowed to a level considered appropriate by the operator. If this did not have the desired effect, there was provision for temporary support around the bore exit. Upon reaching the required location, the ground above the shield was to be supported as the shield is jacked into the exit pit. The shield and equipment were to be split and prepared so that they could be lifted out. This process was then to be repeated for the remaining six pipes.

Each pipe joint was made using a 16mm thick medium density fibre board fixed to the pipe collar before delivery. A water stop and rubber joint sealant was installed under a 6mm thick pre-fabricated steel collar which was cast onto an external rebate in the pipes. The band was to be pulled tight providing a strong and durable water proof connection between adjoining pipe elements.

2.2 TRACK MONITORING AND REMEDIAL ACTIONS

A track monitoring regime was undertaken by Lynton Surveys and a Track Certifier prior to, during and after the boring works was completed. The intention of track monitoring is to notify the construction team of any performance issues during the operation to allow a staged decision making process.

A geotechnical engineer was available to review track monitoring records. A Track Monitoring Plan was produced in accordance with RailCorp Engineering Specification SPC 207 which specifies intervention levels and actions, including track monitoring records distribution. The Fulton Hogan supervisor, Track Certifier and Protection Officer were responsible for implementing the relevant Track Monitoring Plan incident response procedure where out of tolerance ground movement had occurred.

The first pipes were to be installed into the embankment using the HATM without injecting bentonite into the grout ports. The embankment was to be monitored closely at this stage of the operation. If the settlement was less than the alarm levels specified in the Track Monitoring Plan and lateral resistance was low, pipe jacking was to be continued using the same methodology.

If Alarm Level 1 was raised (specified in the Track Monitoring Plan) or significant lateral resistance was encountered, then the following remedial actions were to be implemented:

- Inject bentonite into injection ports near the leading edge of the pipe string to reduce the annulus gap and closure onto the pipe.
- Mixtures of bentonite and/or other materials shall be developed and applied as required to control convergence around the pipe.
- After completion of installation, the annulus shall be fully filled with cement grout.

2.3 INSTALLATION SEQUENCE

The pipes were not installed in sequence and each alternate pipe was installed followed by the intermediate pipes in between. This construction approach was identified as a key factor to limit cumulative settlement due to volume loss of the embankment. The culvert installation sequence consists of:

- Excavation of launch and retrieval pits either side of the railway embankment.
- Construction of launch frame and thrust block within the launch pit and installation of the HATM jacking shield ready for the first pipe jack.
- Advancing the string of jacking pipes beneath the rail embankment at embankment toe level.
- Bentonite injection through injection ports in each pipe if required to limit jacking load and/or control settlement during jacking.
- Grouting of annulus around each pipe if required to limit settlement prior to the installation of the adjacent pipe culvert.

- The above process was repeated for each of the seven pipe culverts to be installed.
- The pipes were installed in the following order (refer to Figure 1): (1) Pipe 3, (2) Pipe 1, (3) Pipe 2, (4) Pipe 5, (5) Pipe 7, (6) Pipe 4 and (7) Pipe 6.
- Permanent works were completed which included a head wall and outlet on the eastern side of the embankment and connection to the upstream culverts and backfilling on the western side of the railway embankment.

2.4 POTENTIAL IMPACTS

The impacts on the railway due to pipe jacking are highly dependent upon the construction methodology and the control measures used to minimise convergence of the ground around the concrete pipe (i.e. closure of the annulus gap). Potential impacts on the railway due to the pipe jacking operation are:

- Vertical settlement at rail track level due to closure (volume loss) of material around the jacking pipe.
- Horizontal movement of the embankment due to jacking loads and disturbance around the jacked pipe strings.
- Potential local instability due to push-out of soil plug ahead of and friction on the shield of the advancing HATM.
- Collapse of the excavated face at the front of the HATM or in case of over-excavation ahead of the HATM shield by the hydraulic arm.
- Instability of the rail embankment due to excavation of jacking and receiving pits.

3 PREDICTION OF GROUND MOVEMENTS

3.1 METHOD OF SETTLEMENT PREDICTION

A method proposed by Peck (1969) and more recently developed by O'Reilly and New (1982), Mair, Taylor and Burland (1996) and Burland (2001) is a commonly adopted approach used for the empirical prediction of ground movements. The method assumes that the transverse ground settlement profile above a tunnel is of a Gaussian form and that ground deformation takes place at a constant volume, so its overall magnitude can be specified as a 'volume/face loss'. The volume loss (VL) is defined as the total magnitude of displacement (i.e. area above the Gaussian profile) expressed as a percentage fraction of the excavated area for the pipe (Figures 6 and 7).

The shape of a settlement trough above a pipe excavation can be represented by a function curve of the form:

$$S = S_{max} \times \exp(-y^2 / 2i^2)$$

Where:

- S is the surface settlement at a transverse distance from the pipe axis.
- S_{max} is the maximum settlement which occurs directly above the pipe axis.
- y is the offset from the pipe axis.
- i is the horizontal distance to the point of inflexion on the settlement trough.

It is assumed that the magnitude of ground movements varies linearly with depth below the surface, which leads to the following expression:

$$i = K \times Z_o$$

Where:

- K is the trough width parameter
- Z_o is the depth to tunnel axis level from ground surface level

The value of K is dependent upon the soil type and according to O'Reilly & New (1982) it varies from 0.4 for stiff clays to 0.7 for soft silty clays and 0.2 to 0.3 for granular materials. The methodology is commonly used in assessing surface movements due to underboring and the results have shown good correlation with actual in-situ measurements.

The maximum settlement, S_{max}, is given by the following equation:

$$S_{max} = VL / [(2\pi)^{1/2} i]$$

According to published data from field measurements, values of VL < 1% can be consistently achieved with modern tunnelling techniques if appropriate control measures are implemented. Results of experimental research specific for pipe jacking (Borghi, 2006) have concluded that volume loss values could be conservatively used for settlement

prediction assuming that full closure of the annulus gap (overcut) around the pipe takes place. Other published data from pipe jacking for sewer installation in Hong Kong (Mok et al, 2007), indicates maximum measured values around VL = 4.0%.

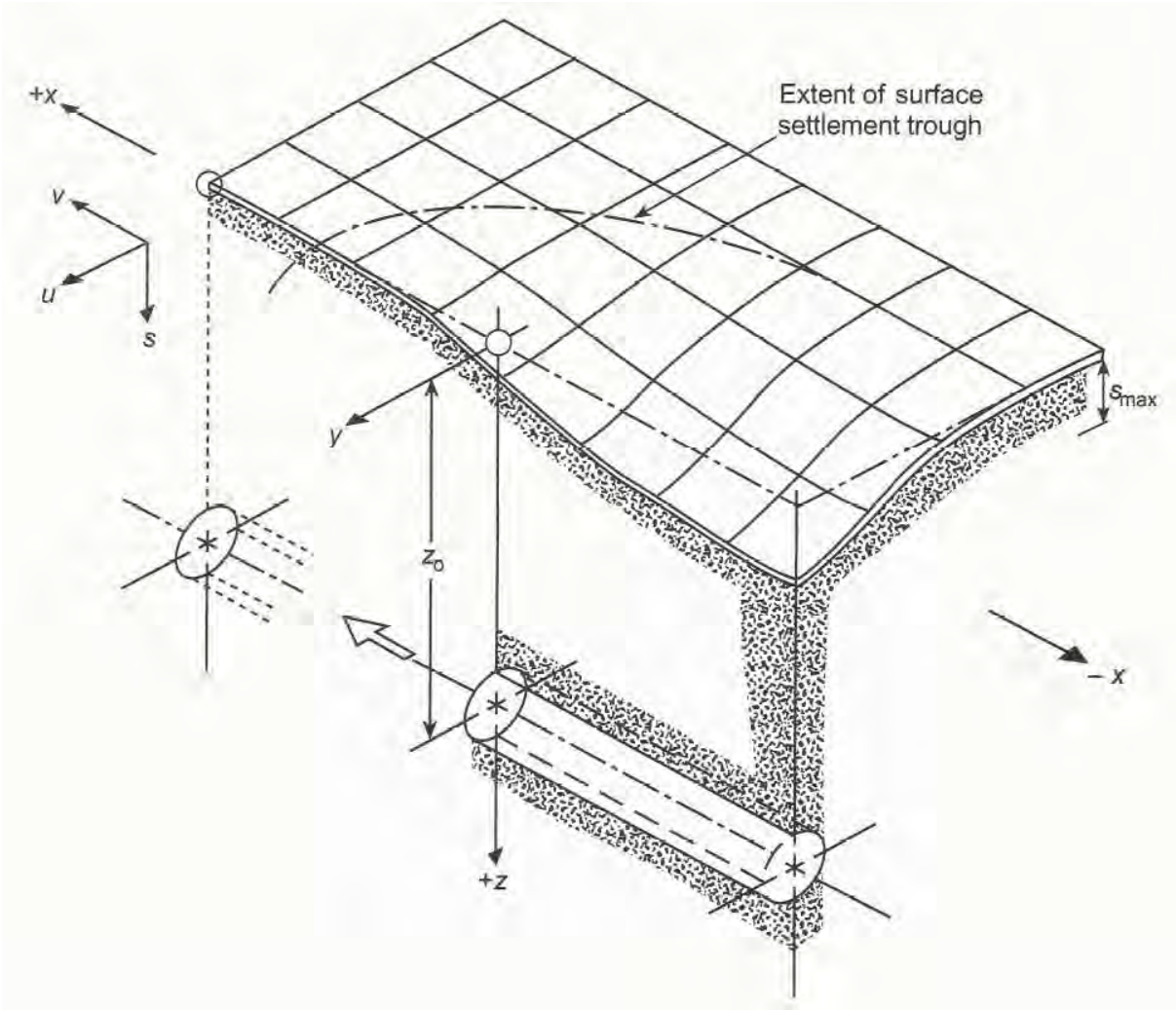

Figure 6: Settlement above an advancing tunnel (Burland 2001).

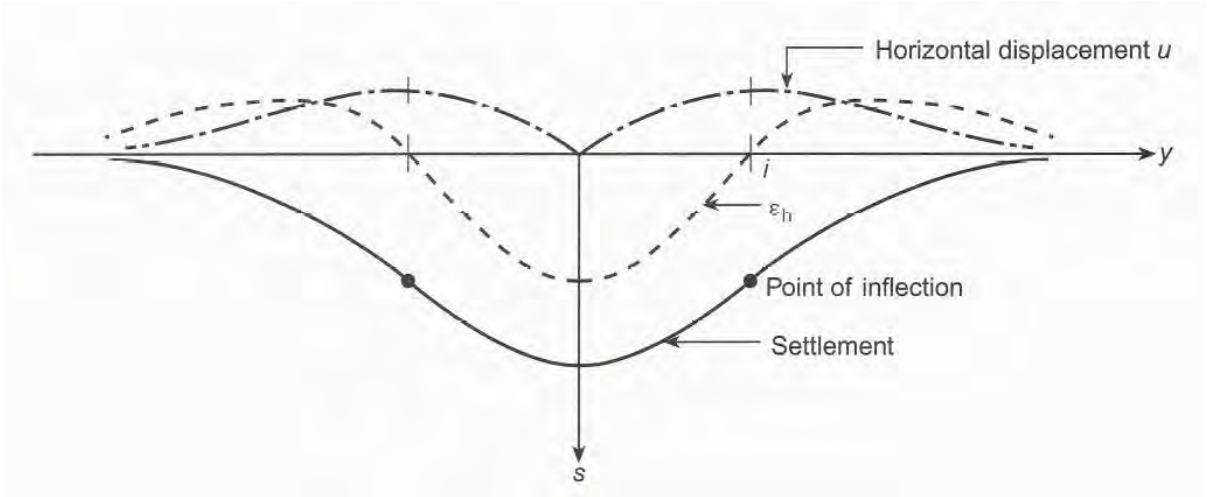

Figure 7: Transverse settlement trough (Burland 2001).

3.2 ASSUMPTIONS OF PREDICTION

The following inputs were assumed in the settlement prediction calculations:

- Ground conditions: The pipes were located along the fill/alluvium transition, embedded approximately 1.2m into alluvium consisting of soft to firm clays. Overlying the alluvium, fill materials were variable and consisted of sandy clays and clayey sands of soft to firm consistency and loose density (see Figure 2).
- Ground and pipe levels: The obvert of the proposed drainage pipes were approximately level with the toe on both sides of the embankment. Ground levels across the rail embankment had been taken from the available survey information. The maximum embankment height from the top of pipe to the rail level was approximately 5.5m, and the batter slopes of the embankment on either side of the rail was approximately 2H:1V.
- The trough width parameter (K) was calibrated to fit the measured settlement profile shape and the volume loss was adjusted to match the maximum measured settlement.
- Predicted settlement troughs for each pipe were superimposed in the back analysis to estimate the combined ground movements.

4 DESIGN CRITERIA OF TRACK DEFORMATION

Excavation of the culvert pipes under the railway line could result in ground movements which would be evident as settlement at the top of the rail embankment. RailCorp Engineering Specification SPC 207 – Track Monitoring Requirements for Undertrack Excavation provides deformation limits and associated rail monitoring intervention levels for changes in track geometry as a result of under track excavation. For a normal track speed of 100km/hr, the limits which apply are summarised in the following table.

Table 1 – Rail monitoring intervention levels for a normal track speed of 100km/hr.

Monitoring Parameters (*Note 1*)	Normal Limits 100%	Gradual movement up to: Alarm Level 1 (*Note 2*) Normal Limits 25% - 50%	Gradual movement up to: Alarm Level 2 (*Note 2*) Normal Limits 50% - 75%	Sudden movement > 50% of Normal: Alarm Level 3 (*Note 2*) Normal Limits 75% - 100%
Track Top (4m)	14 mm	7 mm	9 mm	12 mm
Track Line (8m)	11 mm	6 mm	7 mm	10 mm
Short Twist (2m)	11 mm	6 mm	7 mm	10 mm
Long Twist (14m)	30 mm	15 mm	18 mm	26 mm

Notes:

1. *The monitoring parameters relate to changes to track geometry and are as defined in RailCorp Engineering Manual TMC 202 – Track Fundamentals.*
2. *The definition of "Alarm levels", measurements and notification required and continuation of works following exceedance of the limits are outlined in Section 6.1 of RailCorp Engineering Specification SPC 207.*

The parameter which relates to vertical settlement above the culvert installation is track top, which is the longitudinal level of the track with a chord of specified length (4m chord length). Figure 8 illustrates the definition of the track top measurement. It was assumed that all vertical settlement along the top of the embankment as a result of pipe excavation directly below the rail level would be reflected in the track top measurements.

The track line is the horizontal smoothness of the track without reference to permanent survey marks. This is measured using string lining methods with an 8m long string line. Figure 9 illustrates the definition of the track line measurement.

The track twist is the variation in cross level when measured at different points along the track (every 2m for short twist and every 14m for long twist). The cross level is defined as the level of one rail in comparison to the other when measured along the track (Figure 10).

An assessment of the measured monitoring parameters was required if movements exceeded Alarm Levels 1 and 2 for approval for continuation of works, while all works must cease immediately if Alarm Level 3 was reached.

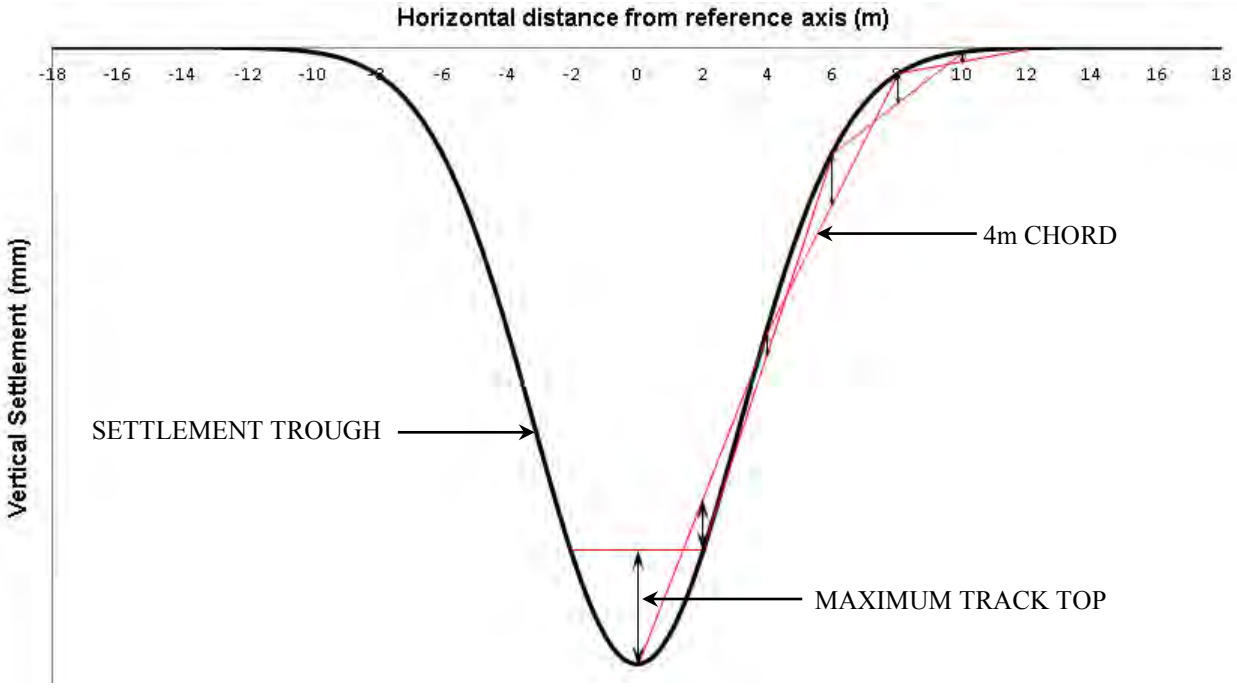

Figure 8: Example of track settlement trough showing track top measurements.

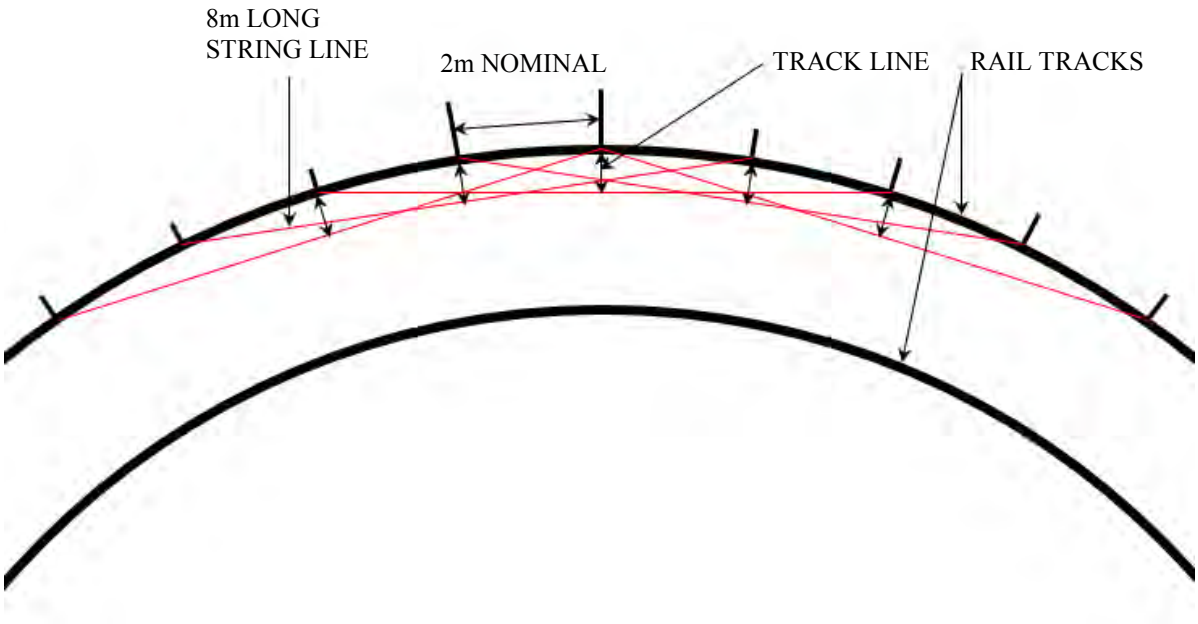

Figure 9: Example of track plan showing track line measurements.

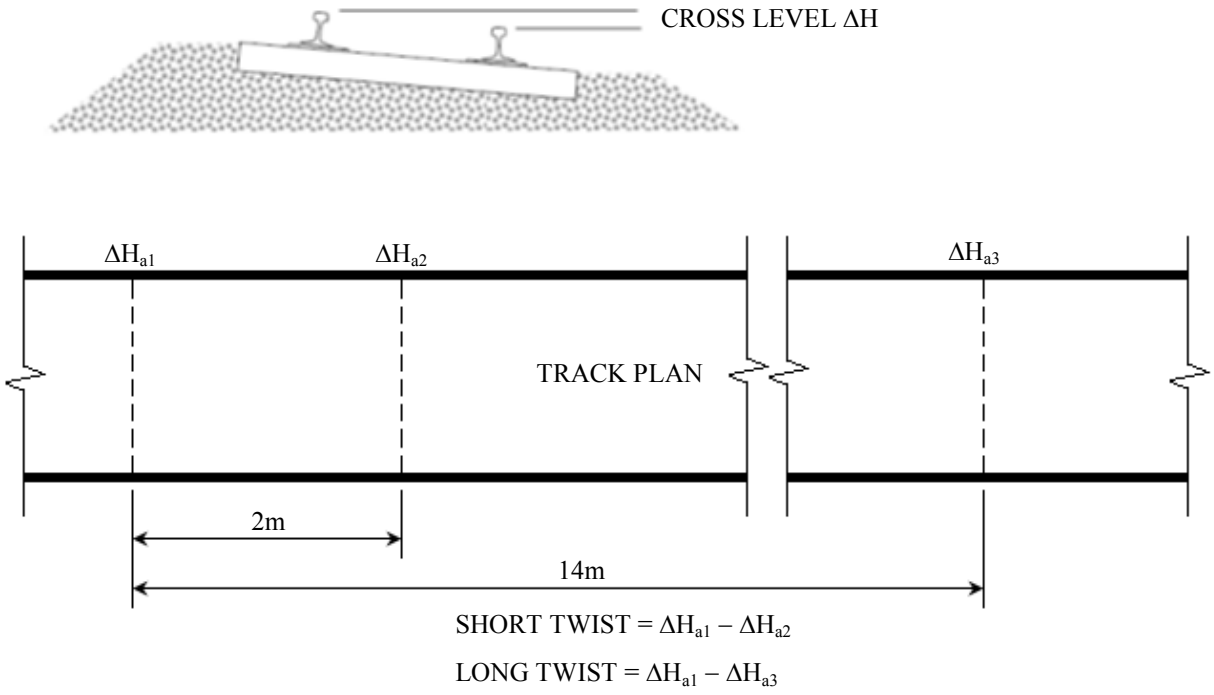

Figure 10: Example of track twist.

5 CONSTRUCTION PERFORMANCE AND BACK ANALYSIS

An initial settlement prediction was carried out using a volume loss of 2.2% and a K value of 0.25. A maximum vertical settlement of 22mm was estimated after construction of all 7 pipes. A maximum vertical settlement of approximately 24mm was recorded along the tracks following excavation and construction of the first two pipes (Pipe 3 and Pipe 1). Although SPC 207 track monitoring parameters for track top, line and twist were below Alarm Level 1, the following tasks were performed:

- Back analyse the measured settlements, recalibrate design parameters to match measured values and predict future ground movements due to subsequent pipe jacking.
- Review/comment on the existing embankment monitoring data and their effects on track performance.

During the back analysis, the settlement trough parameters for each pipe were adjusted to match the measured track vertical settlement profiles from Lynton Survey's real time monitoring data (Figure 11). The calibrated parameters were used to predict future track top and total settlement values during the construction of the 7 culverts. A K value of 0.4 and maximum volume loss of 5.3% were estimated. Table 2 summarises the settlement trough parameters estimated in the back analysis.

Table 2 – Summary of track settlement trough parameters estimated in the back analysis.

Sequence	Pipe 1		Pipe 3	
	Volume Loss (%)	Trough Width Coefficient, K	Volume Loss (%)	Trough Width Coefficient, K
1 (Pipe 3 only)	-	-	2.7	0.48
2 (Pipes 3 & 1)	5.3	0.4	4.1	0.4

Possible sources of the high volume loss, greater than the initial assumption, included:

- Unstable excavation face due to the soil plug not being maintained.
- Ground convergence into the annulus.
- Friction at the embankment exit toe during pipe exit causing lateral ground movement which spreads and drags the top of the embankment down.

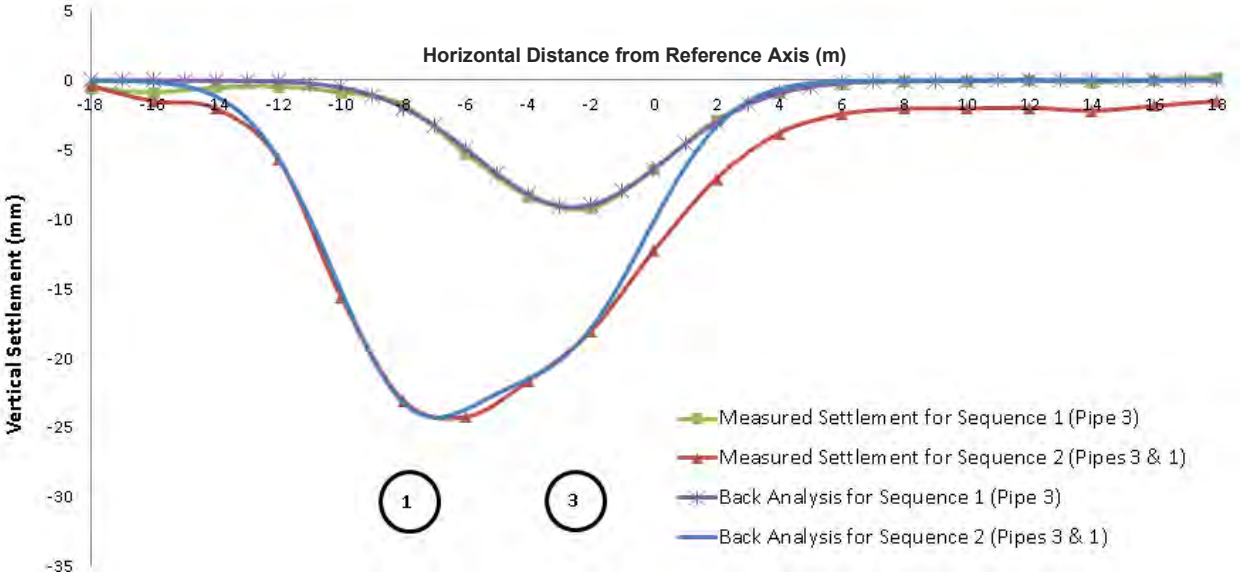

Figure 11: Back analysis of track vertical settlement measurements.

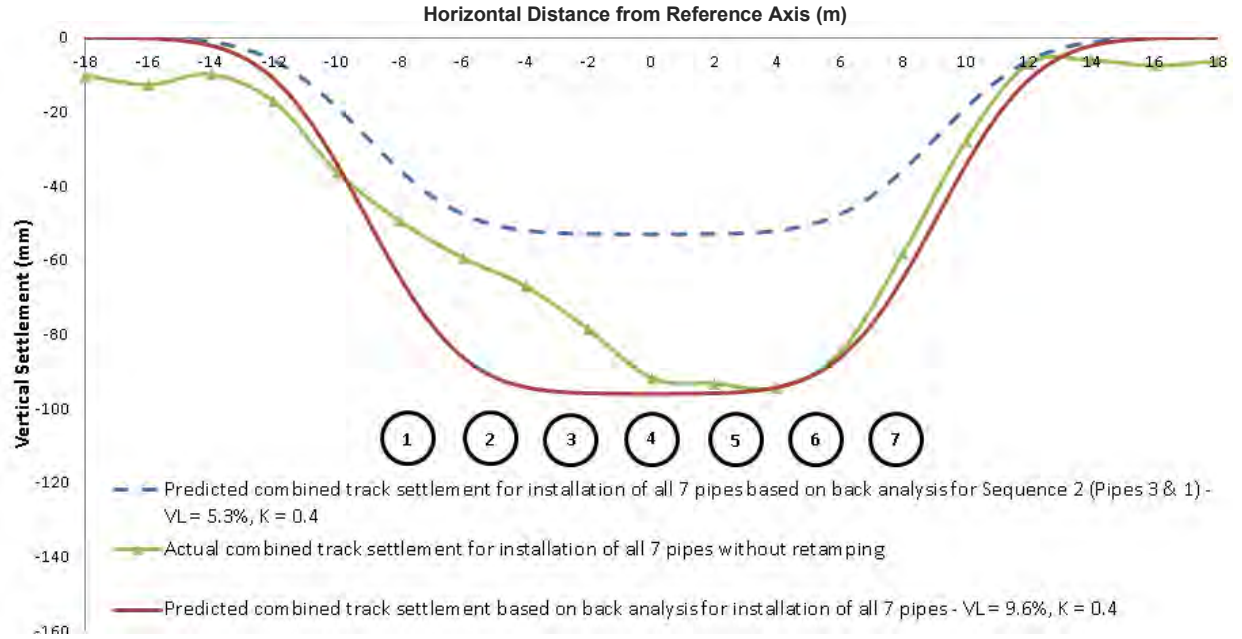

Figure 12: Predicted and actual vertical settlements following construction of all seven pipes.

The revised settlement trough parameters were used to predict future track top and total settlement values during the construction of the seven culverts. The maximum vertical settlement along the track and embankment was estimated to be approximately 53mm after installation of seven pipes (see Figure 12). This magnitude of total embankment settlement is not expected to affect the stability of the rail embankment. The maximum estimated track top value of 6mm was predicted during installation of 7 pipes which is under the Rail Monitoring Alarm Level 1 of 7mm.

Based on the calculated embankment settlements and track top values, the following were recommended:

- The underbore works continue under the current monitoring regime.
- Back analysis and prediction of further settlements to be carried out immediately after the installation of every pipe, if required.
- The embankment total settlement limit to be adjusted to 60mm and this criterion is to be confirmed via further back analysis after the installation of each pipe.
- Construction of rock toe berms at tunnel exits to maintain embankment stability due to lateral thrust load from pipe jacking.

The tracks were retamped twice during construction to ensure track stability of the live railway (see Figures 13 and 14). A maximum settlement of 27mm was recorded following the second retamping and construction completion.

The total combined settlement profile of the track following installation of all seven pipes without retamping was estimated by combining the actual track settlement measurements before and after retamping. A maximum track settlement of 95mm was estimated without retamping. This is higher than the 53mm predicted based on the back analysis of the measured data for the first and second pipes, i.e. Pipe 3 and Pipe 1 respectively. The retamping operations provided a precautionary remedial measure to ensure rail safety. A back analysis was carried out for the installation of all seven pipes based on the estimated combined track settlement without retamping. A final maximum volume loss of 9.6% and a K value of 0.4 were predicted from the back analysis. The combined settlement profiles are summarised in Figure 12. The greater predicted settlements above Pipes 1, 2 and 3 indicate smaller volume loss values, i.e. $\leq$ 9.6%, for earlier installed pipes.

Figure 13: Track profile before retamping.

Figure 14: Track profile after retamping.

6 CONCLUSIONS

Considerable ground movements will not always be detrimental to track performance as long as they do not cause embankment instability and excessive track top, twist and line deformations. Settlement limits may not always be specified by the respective rail authority. Hence, it is imperative that the track monitoring parameters are fully understood before settlement alarm levels are assigned for monitoring during excavation and construction of underbores. Setting an appropriate vertical settlement limit for embankment stability requires detailed engineering assessment and judgement. However, close monitoring of real time data is critical combined with appropriate back analyses and contingency measures to ensure safe construction and operation.

7 REFERENCES

Borghi, F.X., *Soil conditioning for pipe jacking and tunnelling*. University of Cambridge, 2006.

Burland J.B., *Chapter 3 Assessment Methods Used in Design, Building Response to Tunnelling*, Case Studies from Construction of Jubilee Line Extension, London, Volume 1: Projects and Methods, Ed. J. B. Burland, J. R. Standing and F. M. Jardine, Thomas Telford Publishing, 2001.

Mair, R.J., Taylor R.N. and Burland J.B., *Prediction of ground movements and assessment of risk of building damage due to bored tunnelling*. International Conference of Geotechnical Aspects of Underground Construction in Soft Ground, London, UK, 1996: p. 713-718.

Mok, W., Mak, M. and Poon, F., *Sewer installation by pipe jacking in the urban areas of Hong Kong, Part II – performance of workers, lessons learned and improvement proposed*. The Hong Kong Institution of Engineers Transactions, Volume 14, No. 1, 2007: p. 31-43.

O'Reilly, M.P., New B.M., *Settlements above tunnels in the United Kingdom – their magnitude and prediction.* Proc. Of Tunnelling '82 Symposium, London, UK, 1982: p. 173-181.

Peck R.B., *Deep excavations and tunnelling in soft ground*, SOA Report, 7th Int. Conf. SMFE, Mexico City, Sate of the Art Volume, 1969, p. 225-290.

Engineering Specification SPC 207 Track Monitoring Requirements for Undertrack Excavation. Version 1.5, RailCorp, April 2013.

Engineering Manual TMC 202 Track Fundamentals. Version 2.3, RailCorp, June 2012.

APPLICATION OF COMPOUND DEEP CEMENT MIXED WALLS FOR RETAINING STRUCTURES IN EXCAVATIONS

D.S. Liyanapathirana
Associate Professor
School of Computing, Engineering and Mathematics, University of Western Sydney, Penrith, Australia

ABSTRACT

Deep cement mixed (DCM) columns are widely used as retaining structures to support deep excavations due to low cost and their ability in reducing seepage. However, the tensile strength of DCM walls is very low. Hence, large wall sections are necessary to avoid development of high tensile stresses when DCM walls are used to support deep excavations. In this paper application of compound DCM walls, which integrate DCM walls and bored piles, to support deep excavations are investigated aiming to develop resilient design methods for compound DCM walls. Three-dimensional finite element modelling is used in simulating the wall behaviour during deep excavations, considering the full geometry of the compound DCM wall. Numerical model is validated using a case study of a compound DCM wall constructed in Shanghai, China. Finally the use of arched DCM walls with different curvatures in between bored piles is investigated. Results of this study clearly demonstrates the advantages and limitations of increased curvature of compound DCM walls with respect to both ground deformations surrounding the excavation and tensile stresses developed in the compound DCM wall.

1 INTRODUCTION

Deep Cement Mixed (DCM) walls are useful as retaining structures because they can retain earth and act as seepage barriers in the case of deep excavations. Retaining walls made out of DCM columns can be self-supported gravity structures or they can be supported by external elements such as anchors or bracings. However, due to very low tensile strength of cement stabilised soils, DCM walls do not have enough lateral load carrying capacity, which limits the maximum support depth of excavations. Hence different configurations of walls have been used in practice to make use of compressive strength of DCM walls while reducing the tensile stresses developed towards the DCM wall surface facing the excavation. If tensile stresses are developed, there is a tendency to develop cracks in the DCM wall increasing the permeability and deformation of the wall substantially. Normally steel reinforcements are used to increase the capacity of DCM walls to withstand tensile stresses, but the inclusion of reinforcements will increase the cost of retaining structure.

Shao et al. (1998) reported a case study, which used three rows of continuous parallel DCM columns with a discontinuous web structure as a self-supporting gravity wall without any reinforcement or external supports such as anchors or struts. Nicholson et al. (1998) introduced Vertical Earth Reinforced Technology known as VERT walls as a composite gravity wall. In a composite VERT wall system, a row of secant DCM columns are formed at the face of the excavation. Then rows of DCM columns are formed within the gravity retaining wall to provide additional strength. Number of rows and the clear spacing between DCM columns in the VERT wall system depends on the size of the excavation and the ground conditions. Finally DCM columns are capped together using soil slurry spoil from DCM column construction or in situ shallow cement mixing to provide a relieving platform for surcharge loads.

If planar DCM walls are used without steel inclusions, width of the wall needs to be about 50-60% of the excavation depth to minimise the tensile stresses developed over the wall section. In situations where availability of land for retaining wall construction is limited, design of planar walls without reinforcements is a challenge. Therefore DCM walls with steel inclusions are gaining widespread popularity as an excavation support and a seepage barrier in many projects (e.g., Yang 2003, Rutherford et al. 2007 and Gerressen and Vohs 2012). Briaud et al. (2000) reported the behaviour of a full scale VERT wall constructed in a sandy soil at National Geotechnical Experimentation site at Texas A&M University. They proposed to reinforce the front columns and to measure the tensile stresses developed in DCM columns routinely to ensure the factor of safety against cracking. Five modes of deformation; pure shear deformation, rigid body rotation, rigid body translation, rigid body settlement and bending were explained using the deflection values obtained.

In the conventional method of DCM wall construction, overlapping columns are formed by augers rotating about the vertical axis. In 2003, Bauer Maschinen developed Cutter Soil Mixing (CSM) method where rectangular overlapping DCM panels are formed by counter rotating wheels about the horizontal axis (Gerressen and Vohs, 2012). In both

methods, wide flange beams are inserted before the hardening of the cemented soil to increase the lateral load carrying capacity of the retaining structure.

Circular shaped retaining walls were constructed successfully without any reinforcement. This is possible due to the geometry of the wall as it has the capacity to develop compressive stresses while reducing the tensile stresses developed over the wall section. Blackwell (1992) discussed a circular DCM column structure consisting of three concentric unreinforced overlapping rings of 750 mm diameter columns constructed to support manholes. Application of semicircular DCM walls for excavation support were discussed by Stoetzer et al. (2005) and Capelo et al. (2012) using the CSM technology where the circular shape is approximated by a series straight wall panels.

Another construction technology used to minimize tensile stresses developed in DCM walls is the compound DCM walls with a series of arches made of DCM columns. These arches are supported by concrete bored piles at the end of the arches. The lateral load transfer mechanism is totally different to that of a traditional planar retaining wall. Here the arch shape is used to keep the DCM wall predominantly under compression. Hence the geometry of DCM walls with arches makes it possible to use them to support deep excavations without steel inclusions. Shao et al. (2005) reported a case history involving an arch shaped earth retaining structure to support a 9 m deep excavation.

This paper presents the finite element simulation of the above mentioned case study reported by Shao et al. (2005). In this case, the wall is made of a series of arches constructed using secant DCM columns. ABAQUS/Standard finite element program was used for the three-dimensional finite element modelling presented in the paper. Finally a parametric study is carried out to investigate the influence of curvature of the arch section constructed using a series of secant DCM columns on the deformation of the wall and stress distribution within the wall, especially the extent of tensile stresses developed within the arch section.

2 DESCRIPTION OF THE CASE HISTORY

The case study used in this section is an excavation carried out for the construction of an underground sewer line located on Jiangsu Road in Shanghai, China (Shao et al., 2005). The pipe used for the sewer line has an inner diameter of 2.46 m and a thickness of 0.2 m. The excavation is 9 m deep, 160 m long and needs to be at least 4.6 m wide to facilitate the installation of the pipe. A five storey manufacturing building supported by pile foundations is located 2 m away from the excavation. Another five storey building supported by a shallow spread footing is 2.5 away from the excavation. Along the entire length of the excavation, there is a single storey factory building with a basement. The shortest distance between the excavation and the factory building is about 3 m. Hence the ground deformations due to excavation need to be minimized to avoid damages to the existing foundations and buildings supported by them. A compound DCM wall with DCM column arches and bored piles at the toe of the arches was selected to support the 9 m deep excavation. The DCM wall is internally braced by two levels of struts as shown in Figure 1. The base of the excavation was stabilized by chemical grouting to avoid the requirement for higher embedment depth of the wall and to minimise the seepage through the bottom of the wall.

The DCM columns used for the construction of arch wall are 700 mm in diameter. The twin columns were constructed using a double auger mixing machine and they have an effective width of 1 m due to overlap between columns. The circular arch has a span, L, of 4.5 m and a radius, R, of 3.2 m. The effective wall thickness is doubled to 2 m from 5 to 10 m depth to increase the wall stiffness. This increased wall thickness is achieved by using two sets of twin columns. Reinforced concrete bored piles with 600 mm diameter are installed at the toe of the arches. The first level of struts was a reinforced concrete slab with dimensions 400 x 500 mm and it was placed 0.7 m below the surface level. The second level of struts was a set of wide flange beams and they were installed at a level of 5.5 m below the first level of struts, as shown in Figure 1.

The subsurface consists of very soft silty clay and clayey silt deposits from 2 to 15 m below the ground surface. The uppermost 2.0 m thick layer is a fill, which is underlain by a 4.4 m of dark gray soft clay. An 8 m thick soft silty clayey deposit is found at the depth of 6.4 m. The water table is at a depth of 1 m below the ground surface. Soil parameters are summarized in Table 1 (Shao et al., 2005) and discussed in Section 3.1.

The construction was started with the installation of twin DCM columns in arch shape. Then the installation of reinforced concrete bored piles was carried out. Bottom of the excavation was improved by injecting the cement based slurry before the excavation. After that the slab was casted and the excavation was carried out up to 5.5 m. Next, wide flange steel struts were installed and the rest of the excavation was carried out.

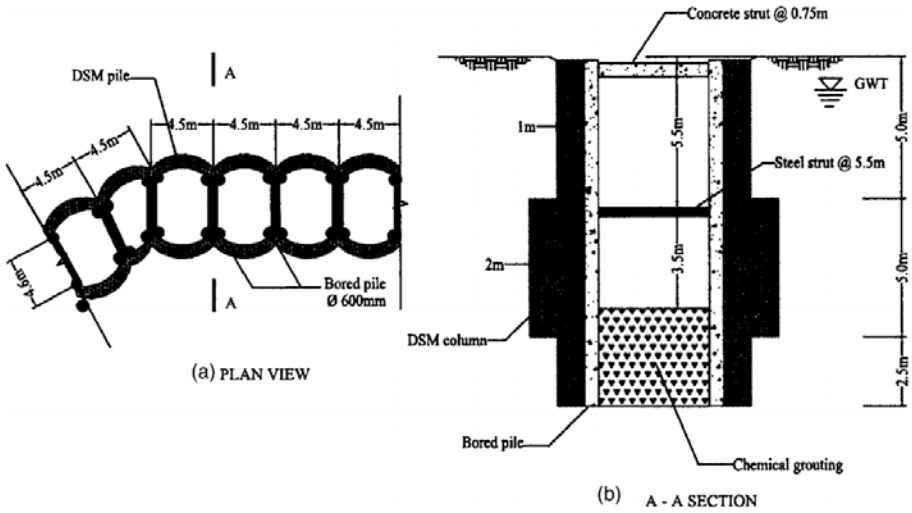

Figure 1: Plan view and cross section of the excavation (after Shao et al., 2005).

Table 1: Material properties used in the finite element model.

Material	Young's modulus of elasticity, E (MPa)	Poisson's ratio, v	Cohesion c' (kPa)	Friction angle, φ' (°)	Unit weight, γ (kN/m^3)
Fill	40*	0.33*	5*	38*	18.5
Soft clay	4.2	0.4*	14	20	19.2
Soft silty clay	15*	0.4*	10	10	18.8
Grouting	420	0.3	20	20	20.0
DCM columns	72.5	0.3	210	25	20.0

Note:* denotes properties assumed based on published data for similar soil types.

3 NUMERICAL MODEL

The case study was modelled considering the three-dimensional geometry using the ABAQUS/Standard finite element program and the results were compared with the measured field data. Due to repetition of arches along the excavation, only one arch section between bored piles was considered in the finite element analysis as shown in Figure 2. Due to the limitation of data availability for the case study, a drained total stress analysis was carried out. Finite element mesh is developed using twenty-node solid continuum elements with reduced integration. The bottom boundary of the finite element mesh is restrained in *x, y* and *z* directions. The two vertical boundaries in the *y-z* plane are restrained in the *x* direction and the other two boundaries in the *x-z* plane are restrained in the *y* direction. The stress-strain behaviour of soil layers and DCM columns were simulated using the Mohr-Coulomb criteria with non-associated flow rule. In ABAQUS/Standard, when the friction and dilation angles are not the same, a non-associated flow rule is used. Although

strain softening behaviour is significant for cement stabilised soils, softening behaviour is not included in the analysis due to unavailability of material properties to simulate the strain softening behaviour. The concrete bored piles and the arch are connected and no relative movement is allowed between bored piles and the toe of the arch. This is a reasonable assumption because the wall and piles are constructed in-situ.

During the finite element analysis, excavation is simulated by removing elements. Due to unavailability of stiffness of struts, it is assumed that once a strut is installed at a particular level, bored piles will not displace laterally in the x direction. In the first step of the analysis first two rows of elements are removed simulating a 1 m deep excavation. Then in the second step, the first set of struts is installed. During analysis steps three to six, 4 m of soil was removed and then the second set of struts is installed. During the last three steps of the analysis another 4 m of soil is excavated, making the total excavated depth to 9 m.

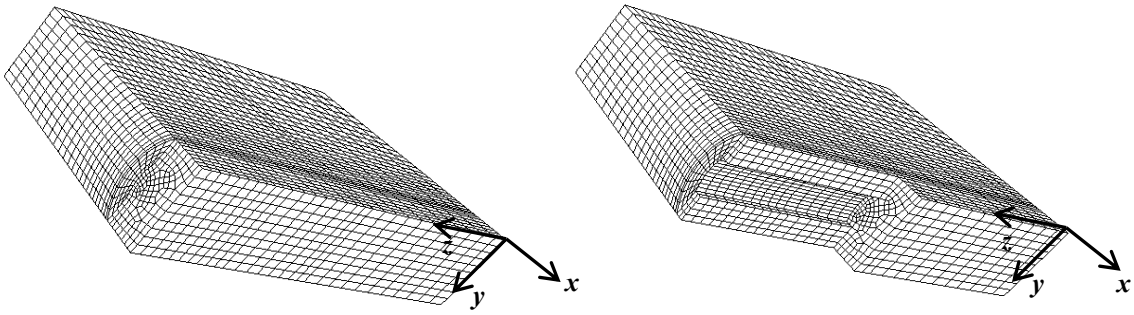

(a) Before excavation (b) After excavation

Figure 2: Finite element mesh before and after excavation.

3.1 MATERIAL PROPERTIES

Soil properties used for the finite element analysis are given in Table 1. Properties for all soil layers necessary to carry out the finite element analysis are not given by Shao et al. (2005). Those properties are selected based on published data for similar soil types. Bored piles are modelled assuming elastic behaviour. Bored piles were assigned a Young's modulus of elasticity of 35×10^3 MPa and Poisson's ratio of 0.3.

Samples were collected from test DCM columns constructed before the wall construction to determine the unconfined compressive strength of cement stabilised soil. For the 15 samples tested, average unconfined compressive strength, $q_{u,}$ was 721 kPa. This value was used to determine the Young's modulus of elasticity and cohesion of DCM columns. For an effective stress analysis, a friction angle of 25 ^{o} to 33^{o} was proposed by EuroSoilStab (2002). Hence in this study, a friction angle of 25° was used. According to Kivelo (1998) and Broms (1999), the cohesion of artificially cemented soil is about $0.289q_u$, which is about 210 kPa for this case. McGinn and O'Rourke (2003) used a value of $150q_u$ for elastic modulus of cement treated soil by wet mixing method. Probaha et al. (2000) and Ellen et al. (2013) proposed $100q_u$ and $300q_u$ respectively. In this analysis $100q_u$ is used and hence the Young's modulus of elasticity of DCM columns was 72.5 MPa.

4 COMPARISON OF RESULTS WITH FIELD MEASUREMENTS

In this section, deformation of the arch during excavation obtained from the finite element analysis is compared with field measurements. To obtain wall deformations, inclinometers were installed at several locations of the DCM wall. Figures 3(a) and 3(b) show the wall deformation after 5.5 m of excavation before installation of the second set of struts. Both measured and finite element results show the same trend. The crest of the arch deforms more than the toe. The measured maximum deformations at the toe and the crest are about 2 mm and 4 mm respectively. Finite element results slightly over predicted the measured deformations.

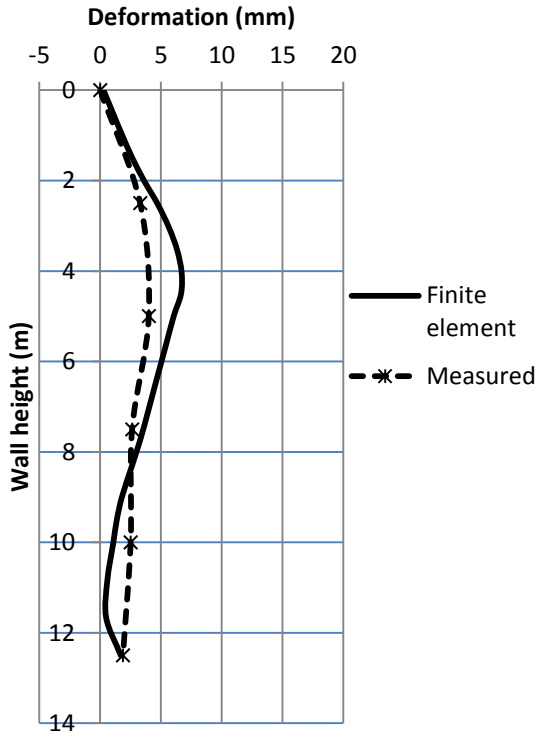

(a) Deformation at the crest of the arch after 5.5 m of excavation.

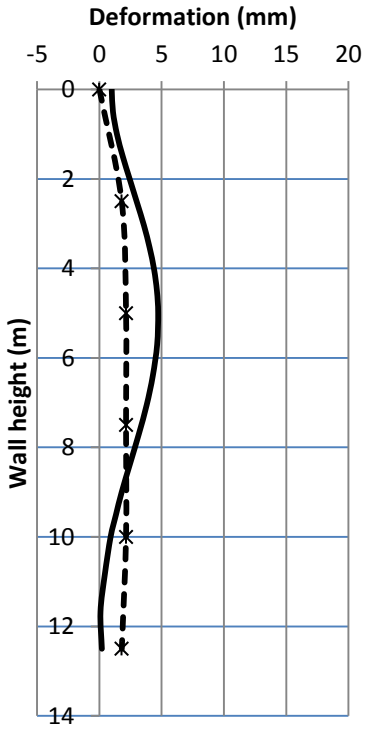

(b) Deformation at the toe of the arch after 5.5 m of excavation.

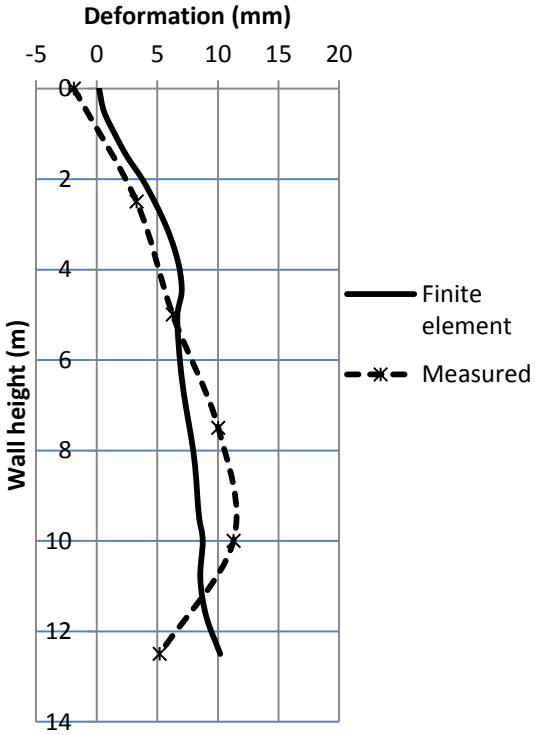

(c) Deformation at the crest of the arch after 9 m of excavation.

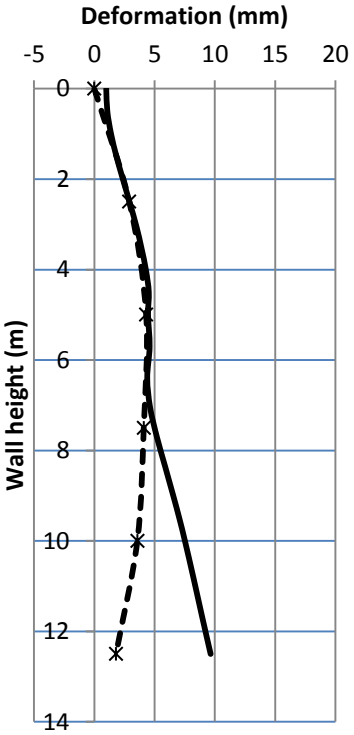

(d) Deformation at the toe of the arch after 9 m of excavation.

Figure 3: Deformation of the wall at the end of 5.5 m and 9.0 m of excavation.

Figures 3(c) and 3(d) show the wall deformations at the crest and toe of the arch after 9 m of excavation. Over the top 8 m of the wall, finite element results agree well with the measured wall deformations but below 8 m, measured wall deformations show that the wall deformation is decreasing towards the tip. According to the finite element results, wall tip is moving towards the excavation. The difference in measured and computed wall deformations beneath the excavation may be due to the difference between actual and assumed soil properties used for the soft silt clay layer around the excavation. Nevertheless, results obtained from the finite element analysis can be explained using Figures 4 and 5. With increasing excavation depth, soil heave over the base of the excavation increases. As a result, soil starts to flow into the excavation increasing lateral deformation of the wall below the excavation depth. When the excavation depth is 7.7 m, soil flow occurs but it is not very high at the wall base level. With increasing excavation depth, soil deformations increase underneath the grout layer below the excavation. Grout layer will try to reduce the soil heave underneath the excavation due to its high stiffness compared to the surrounding soft silty clay but beneath the grout layer, soil lateral deformations are increasing. As a result, lateral deformation of the wall base increases in the *x* direction as observed in Figures 3 (c) and (d).

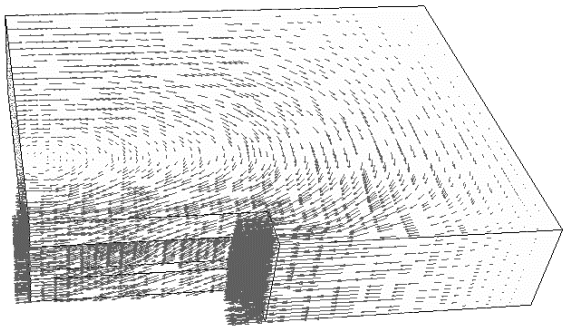

Figure 4: Soil flow around the excavation after 9 m of excavation.

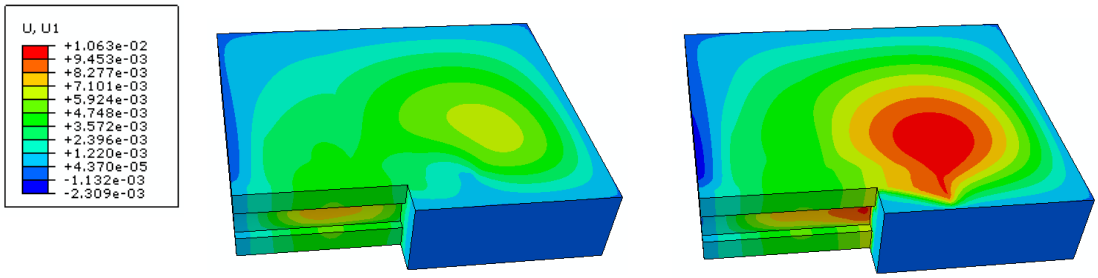

(a) 7.7 m of excavation (b) 9.0 m of excavation

Figure 5: Lateral soil deformation in the x direction.

5. INFLUENCE OF THE CURVATURE OF ARCH ON THE COMPOUND WALL BEHAVIOUR

In this section the effect of curvature of the arch on the compound wall behaviour is investigated. A uniform soft clay deposit is considered for this analysis. The soil and DCM wall behaviour are modelled using the properties given in Table 1. Excavation is simulated as described in the previous section but struts were not used to support the wall. Therefore the depth of excavation is limited to 5 m and the 10 m long DCM wall deformed as a cantilever. Curvature of the arch shaped wall is varied by changing the rise of the arch, h, which is defined as the vertical distance between the toe and the crest of the arch. Figure 6 shows the normal stress distribution in the z direction within the arch wall at the end of 5 m excavation. In this case, due to increased surface area of the arch wall in the yz plane with increasing h, higher lateral earth pressures are applied over the arch with h = 0.75 m than those applied over the arch with h = 0.1 m. Henceforth both compressive and tensile stresses shown in Figure 6 (b) for the arch with h = 0.75 m are higher than those shown in Figure 6 (a) with h = 0.1 m. When h = 0.1 m, tensile stresses are developed not only over the top of the wall but near the base of the excavation as well. However, the arch with higher curvature does not show any tensile stresses below the top of the wall.

Figure 7 shows the deformation of the wall in the *x* direction measured at the crest and toe of the arch. Although toe deforms more than the crest in this case, the difference is marginal. Both toe and crest deformations decrease exponentially with increasing curvature of the arch. Therefore it can be concluded that by increasing the curvature of the compound DCM wall, lateral deformation of the wall can be decreased. In addition, any tensile stresses developed below the top of the wall can be mitigated. However, with increasing curvature, loads applied on the wall increases and as a result, both tensile and compressive stresses developed on the wall near the ground surface increases. Hence, curvature of the wall should be increased carefully by taking into account the tensile load carrying capacity of the wall near the top.

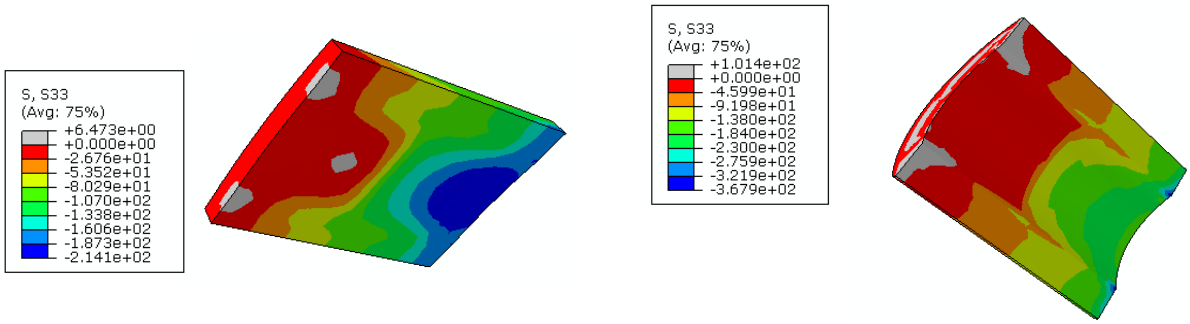

(a) $h = 0.1$ m (b) $h = 0.75$ m

Figure 6. Normal stress distributions in the z direction at the end of 5 m excavation for the 10 m DCM wall.

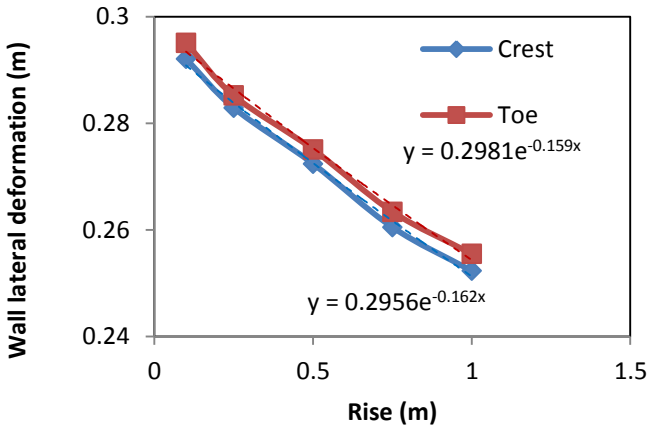

Figure 7: Variation of wall deformation with rise of the arch.

6. CONCLUSIONS

In this paper a case history of a compound DCM wall constructed using DCM columns and bored piles are investigated using a three-dimensional finite element model. The wall section between bored piles is constructed as an arch to reduce the tensile stresses developed in DCM columns. Overall, the measured and computed wall deformations show good agreement. However, when the excavation depth is 9 m, the wall deformation below the excavation computed from the finite element analysis is higher than the measured wall deformation. This may be due to the difference between the assumed soil properties for the soft silty clay layer below the excavation. However, if the soil flow around the excavation base is investigated, it can be justified that the predicted wall movement is acceptable. Using the same numerical model with a uniform soil deposit, a parametric study is carried out varying the curvature of the arch between bored piles. Results from the parametric study show that the increased curvature of the arch has a significant influence on reducing the wall deformation. However, with increasing curvature, surface area of the wall increases and hence the lateral pressures applied over the wall surface increases generating higher compressive and tensile stresses within the wall section. Therefore it can be concluded that wall deformation can be reduced by increasing the curvature of the arch

sections of DCM walls. However, at the same time tensile stresses developed over the arch section may increase developing tensile cracks within the wall, especially closer to the top of the wall.

7. ACKNOWLEDGEMENTS

The author would like to acknowledge the financial assistance provided by the Australian Research Council for this research under the Discovery grant DP1094309.

8. REFERENCES

Blackwell, J. (1992). "A case history of soil stabilisation using the mix-in-place technique for the construction of deep manhole shafts at Rochdale." *Proc. Grouting in the Ground*, London, 497-509.

Briaud, J.L., Nicholson, P., and Lee J. (2000). "Behavior of a Full–Scale VERT Wall in Sand." *Journal of Geotechnical and Geoenvironmental Engineering*, 126(9), 808–818.

Broms, B. B. (1999). "Keynote lecture: Design of lime, lime/cement and cement columns." Int. Conf. on Dry Mix Methods: Dry mix methods for deep soil stabilization, H. Brendenberg, Broms, and B. Holm, eds., Balkema, Rotterdam, Netherlands, 125–154.

Capelo, A., Correia, A.G., Ramos, L.F., Pinto, A., and Tomásio, R. (2012). "Modelling and Monitoring of an Excavation Support Using CSM." *Grouting and Deep Mixing 2012, GSP 228*, 243-250.

Ellen, M.C.B., Berg, R.R., Collin, J.G., Filz, G.M., Terashi, M., and Yang, D.S (2013). "Deep Mixing for Embankment and Foundation Support." *Federal Highway Administration Design Manual* (No. FHWA-HRT-13-046).

EuroSoilStab. (2002). "Development of design and construction methods to stabilise soft organic soils: Design guide soft soil stabilisation." CT97–0351, Project No. BE 96–3177, BREPress, Watford, U.K.

Gerressen, F. and Vohs, T.(2012). "CSM-Cutter soil mixing – Worldwide experiences of a young soil mixing method." Proc. *Grouting and Deep mixing 2012, GSP 228*, pp. 281-290.

Kivelo, M. (1998). "Stabilization of embankments on soft soil with lime/cement columns." *PhD thesis, Royal Institute of Technology*, Sweden.

McGinn, A. J., and O'Rourke, T. D. (2003). "Performance of deep mixing methods at Fort Point channel", Report *to Massachusetts Turnpike Authority*, Federal Highway Administration, and Bechtel/Parsons Brinckerhoff, Cornell University.

Nicholson, PJ, Mitchell, JK, Bahner, EW & Moriwaki, Y (1998), "Design of a soil mixed composite gravity wall." *Soil Improvement for Big Digs*, *GSP 81*, 27-40.

Porbaha, A., Shibuya, S., and Kishida, T. (2000). "State of the art in deep mixing technology. Part III: Geomaterial characterization.", *Proceedings of the ICE-Ground Improvement*, 4(3), 91-110.

Rutherford C.J., Biscontin G., Koutsoftas D., Briaud J.L. (2007). "Design Process of Deep Soil Mixed Walls for Excavation Support." *International Journal of Geoengineering Case histories*, 1(2), 56-72.

Shao, Y., Macari, E. J., and Cai, W. (2005). "Compound Deep Soil Mixing Columns for Retaining Structures in Excavations." *Journal of Geotechnical and Geoenvironmental Engineering*, 131(11), 1370-1377.

Shao, Y., Zhang, C., and Macari, E.J. (1998). "The application of deep mixing pile walls for retaining structures in excavations." *Soil Improvement for Big Digs GSP 81*, 84–95.

Stötzer, E., Brunner, W., Fiorotto, R., Gerressen, F.W. and Schöpf, M. (2006). "CSM Cutter Soil Mixing - A New Technique for the Construction of subterranean walls - Initial experiences Gained on completed projects." 10th international Conference on Piling an Deep Foundations, (534), 7 p.

Yang, DS (2003). "Soil–Cement Walls for Excavation Support." *Earth Retention Systems 2013, A Joint Conference presented by ASCE Metropolitan Section of Geotechnical Group, The Deep Foundations Institute and The International Association of Foundation Drilling*, NewYork City, NY. 1-17

RESILIENT FOUNDATIONS: BUILDING IN REPAIR CAPABILITY

Y. Duraisamy[1] and D. Airey[2]

[1]PhD Candidate, [2]Professor, School of Civil Engineering, The University of Sydney, Sydney, Australia

ABSTRACT

There is considerable literature on strategies for the repair and self-healing of concrete structures. However, in geotechnical engineering there has been much less interest in the repair of foundation elements. Typical remediation strategies involve provision of extra piles or further ground improvement. One of the approaches which is seen as promising in concrete repair is the use of bio-cements. These are solutions where bacterial actions result in the precipitation of a chemical that can act as a cementing agent. The most widely investigated of these is the use of ureolytic bacteria to precipitate calcium carbonate.

The paper provides a review of repair strategies and techniques used in concrete to encourage self-healing should damage occur. It describes the MICP process, and presents data showing how bio-cement can improve the strength and stiffness of sandy soils. Finally the paper reports results from some preliminary laboratory model tests performed to investigate the ability of bio-cement to repair cemented soil columns.

1 INTRODUCTION

In recent years, there has been increasing interest in self healing concrete materials that have the ability to repair cracks. These have the potential to significantly increase concrete durability by preventing access of corrosive agents to the reinforcement and improve their water tightness, and as a result reduce the need for inspection and maintenance. Research into engineering self healing in concrete was first initiated to reduce the amount of cement needed in concrete mixes (Gerilla et al., 2007; Peris Mora 2007) as part of global efforts to reduce greenhouse gas generation. This is a significant initiative as cement production is currently responsible for about 5% of global CO_2 emissions (IPCC, 2013). The inspiration for the study of self-healing concrete is the ability of living organisms to rapidly detect and repair damage. In concrete, degradation usually begins with micro cracks that lead to corrosion and eventually structural failure. The main form of damage is cracking and thus self-healing concretes must have the ability to repair small cracks and fissures autonomously. The feasibility of self-healing in concrete has been discussed in several studies (Neville, 2002, Reinhardt & Jooss, 2003, Li & Yang, 2007 and Edvardsen, 1999).

Previous research work has demonstrated that concrete repair can be produced by three different processes: natural, chemical and biological. This paper is primarily concerned with biological processes as these are considered to have self-healing potential and they have been shown to be capable of repairing concrete materials. For example, Ghosh et al. 2008, have reported that cement based materials created by biological action exhibited better durability and crack repairing performance than normal concrete. The healing potential of these biological processes are directly related to the amount of calcium carbonate that can be precipitated. Calcium carbonate can be precipitated microbially during urea hydrolysis, denitrification, and iron and sulphate reduction processes (Al-Thawadi 2011). Of these, urea hydrolysis has been the most widely investigated and it has been applied in a range of applications which include bio-remediation, concrete repair (Bang et al., 2010, Ramachandran et al., 2001) and bio-grouting (Paassen, 2009, Paassen et al., 2010). The mechanism of bio-cementation involves the precipitation of calcite, which then bonds to the sand particles. The chemical reactions can be described by Equations 1 and 2. Equation 1 describes the hydrolysis of urea which leads to the production of ammonium and carbonate ions. This reaction is catalysed by the enzyme urease, which is common in a wide range of soil microorganisms. It can be readily induced by adding inexpensive substrates, and is involved in several biotechnological applications (Stocks-Fischer et al., 1999, Hammes et al., 2003). In addition to the reaction requiring bacteria to produce urease, control of temperature and pH is also vital.

$$NH_2 - CO - NH_2 + 2H_2O \leftrightarrow 2NH_4^+ + CO_3^{2-} \quad \textbf{(1)}$$

$$Ca^{2+} + CO_3^{2-} \rightarrow CaCO_3 \quad \textbf{(2)}$$

To produce calcium carbonate a calcium source must be provided, which is commonly provided by adding calcium chloride ($CaCl_2$) although a wide range of calcium compounds have been used.

The application of bacteria to assist with repair in the construction industry is not new. Bio-cements have been used to enhance the durability of building structures and the conservation of cultural heritages because of their self-healing potential. Previously, the potential of bacteria to clean concrete surfaces (DeGraef et al., 2005), to improve the strength of cement-sand mortars (Dick et al., 2006, Ghosh et al., 2005), to repair degraded limestone and ornamental stone surfaces (Rodrigues-Navarro et al., 2003) and to repair cracks on the surfaces of concrete structures (Bang et al., 2001, Ramachandran et al. 2003) have been investigated. However, relatively less attention has been given to the possibility of repairing sub-structures and foundations.

In this paper we describe the procedure for creating bio-cemented soil, and demonstrate the ability of the precipitated calcium carbonate to effectively bond a uniform sand. To demonstrate the potential of the bio-cement for ground improvement cemented columns have been created in dry and saturated sand and these have been shown to lead to significant gains in foundation strength and stiffness. During this process it was noticed that the cemented columns broke into two pieces and this has enabled a study of the ability of bio-cement to repair the cemented columns. Three different methods of repair have been investigated.

2 MATERIALS AND METHODS

2.1 SOIL PROPERTIES

The soil used in the triaxial and model tests is Sydney sand, a quartz sand with sub-angular particles. Some of the basic soil properties obtained using Australian standard tests and the particle size distribution are shown in Figure 1.

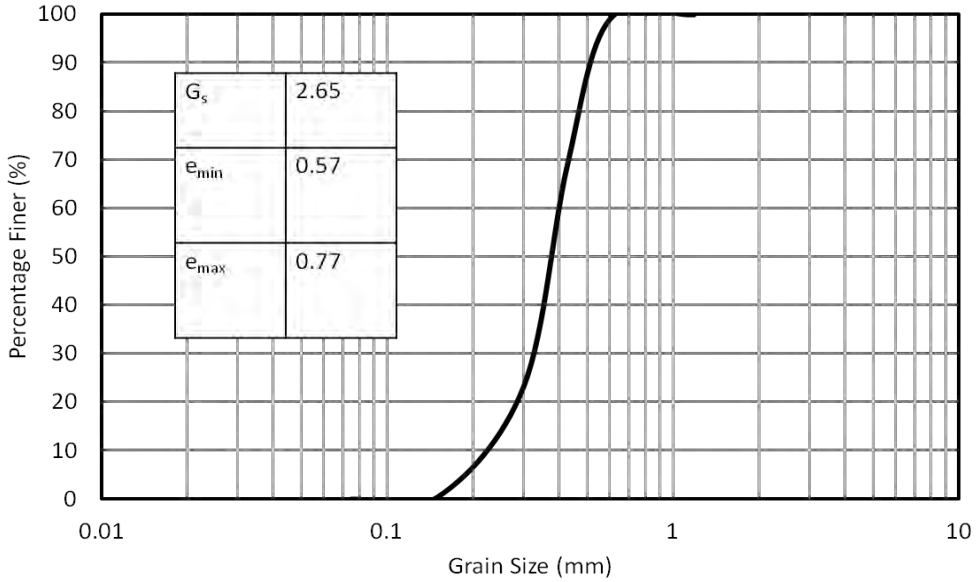

Figure 1: Properties and the particle size distribution of Sydney sand.

2.2 BIO-CEMENTATION

A non-pathogenic microorganism Bacillus megaterium has been used as the urease source to catalyze precipitation of $CaCO_3$. This organism has not received much study, but has been used because previously investigated bacteria were not readily available.

The first step in producing bio-cemented specimens was to culture the bacteria. This involved placing the bacteria (Bacillus megaterium), from American Type Culture Collection (ATCC14581), into a liquid solution comprised of the ingredients shown in Table 1. This mixture was placed in an incubator at a temperature of 30°C for 24 hours.

This produced a highly enriched bacterial solution of 100mL with a bacterial concentration of approximately 9×10^9 cfu/mL. The bacterial solution was then mixed with sand, additional urea, water and calcium chloride and used to create either cylindrical soil specimens or cemented soil columns. The mixture without the sand was also injected into the soil and broken soil columns to enable ground repair. The cultured bacteria continue to multiply in the wet soil mixture, provided sufficient nutrients are available, and facilitate precipitation of calcium carbonate.

Table 1: Liquid medium for bacterial growth

Nutrient Broth	3g	$NaHCO_3$	2g
Urea	15g	Glucose	10g
NH_4Cl	10g	$CaCl_2$	3g

2.3 SAMPLE PREPARATION AND PROCEDURE FOR UCS TESTS

Unconfined compression tests have been used to investigate the effects of the bio-cement on the soil strength and these have been compared with the effects of adding gypsum. To produce bio-cemented samples similar amounts of urea and calcium chloride were used in every mix and the amounts of each were in the range of 0.25% to 20% of the dry weight of the sand. Gypsum cemented samples have been prepared by mixing gypsum, sand and water, with weights of gypsum in the range of 5% to 20 % of the dry weight of the sand.

Specimens were prepared in a split cylindrical mould with lightly greased internal surfaces mounted on a flat base. The sand-cement mixtures were placed loosely in the mould and then lightly tamped to achieve specimens of a uniform dry density, with initial dimensions of 55mm in diameter and 110 mm in height. After 24 hours curing, the split mould was disassembled and samples were left another 6 days to cure. The dimensions of each specimen were checked again before loading. Specimens were then placed on the loading frame and subjected to standard UCS test procedures. An automated loading frame with maximum capacity of 50kN was used to apply a constant displacement rate of 1.14 mm/min.

After completion of the tests on the bio-cemented specimens the amount of calcite precipitated was measured. Sub-samples from parts of the specimens were dried in an oven at 121 °C for 24 hours then weighed. The samples were then flushed with 1M HCL to dissolve the calcite, rinsed with deionized water and then dried for 24 hours. The change in weight of the soil was considered to be the weight of the dissolved calcite.

2.4 PHYSICAL MODEL TEST SET-UP

The objectives of the foundation tests were to demonstrate the ability to create bio-cemented soil columns using ex-situ mixing and to demonstrate the potential of this technique to improve the foundation performance. The procedure for creating the cemented soil columns in this laboratory scale system was designed to be in accordance with deep soil mixing technology. The apparatus shown in Figure 2(a) has been developed for this purpose. It consists of a 600 mm diameter vessel, 500 mm high, which is filled with Sydney sand. The column forming system consists of a vertical frame which enables the lowering and raising of the auger spinning motor, auger and tube holder. In order to maintain experimental consistency and the reproducibility of column formation, a three level travel stop (L1, L2 and L3) mechanism has been used. This enables the column length, the rate of introduction of the cementation liquid and nutrients over the length of the column and the mixing cycles to be controlled accurately and consistently. The speed of the auger spinning motor is adjustable from 5 to 50 rpm. The shaft length of the auger and the blades are 350 mm and 35 mm, respectively.

Cemented soil columns, 38 mm in diameter and extending 200 mm below the surface, have been created in the centre of the confining vessel. To create a cemented column in dry soil, a PVC tube is attached to the fixed frame and placed in the tank to ensure the verticality of the column. While the auger is in the upper L1 position, one third of the dry urea and calcium chloride powders, or gypsum, are carefully poured in using a funnel. The auger is then moved to the middle L2 (position as shown in figure 2(a)) and soil is thoroughly mixed with the additives (gypsum/urea powder) at medium speed. The auger penetration and withdrawal is controlled manually by rotating clockwise at constant speed. After 30 seconds of mixing, the auger is lowered to the bottom L3 position and mixing is continued. This procedure is repeated until the remaining urea and calcium chloride powder (or gypsum) are mixed in. This is followed by pouring in the liquid, either the bacterial solution for the bio-cement or water for the gypsum, before ending with two more cycles (L2 and L3) of mixing at maximum speed. Immediately after finishing mixing the auger is detached from its holder, the column is gently tamped to counter the loosening during auger withdrawal, and the PVC tube is pulled out. The column is then left in the vessel for 24 hours to allow curing to occur before loading. A similar procedure was also used to create cemented columns in wet soil, except that liquid did not need to be added and the bacterial solution was injected using a syringe.

Figure 2(b) shows the experimental setup of the model footing tests. A 90 mm diameter circular footing, 12 mm thick, was placed on the sand surface and the surface was leveled flush with the top of the cemented column. The footings have been vertically loaded to large displacements at a constant deformation rate of 0.076 mm/min. The vertical loads, measured by a 250kg capacity load cell, and displacement, measured by an LVDT transducer, were automatically logged at frequent intervals. A series of tests with bio-cemented columns using different urea amounts, and with gypsum cemented columns with different gypsum amounts have been conducted. Additional tests have been conducted without the cemented columns. Tests have been performed for a range of sand relative densities. To obtain a consistent soil density in the vessel for each test, Sydney sand was poured from a fixed height.

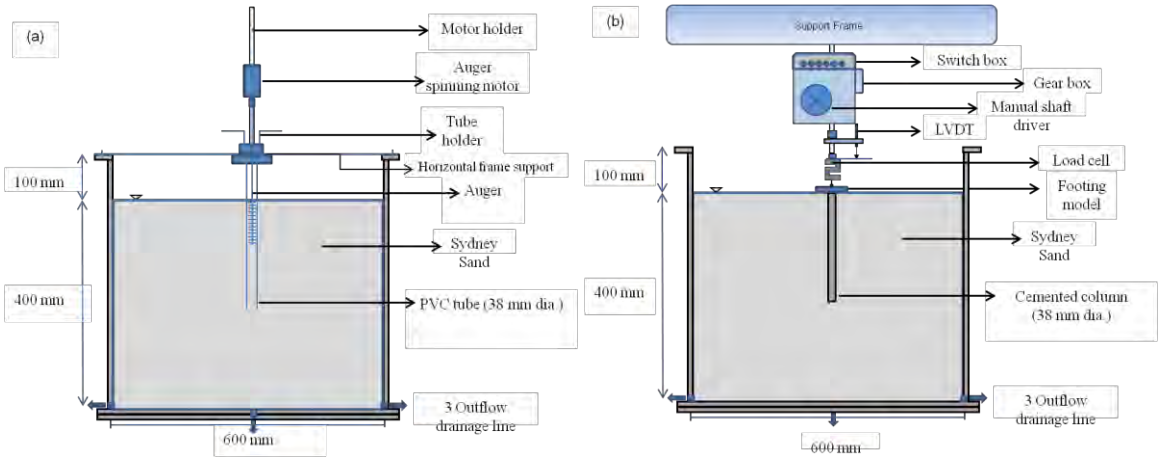

Figure 2: Scematic diagram of (a) column mixing and (b) footing test configuration.

2.5 COLUMN REPAIR METHODS

The physical model tests outlined above were extended to study the potential of bio-cement for repairing damaged pile foundations. As discussed further below, loading of the footing led to all the cemented columns breaking into two, approximately one footing diameter below the surface. Three different strategies were investigated for repairing the damaged columns. In all cases the cemented columns were made by mixing 15% gypsum with the sand. To allow for later repair a glass rod of 8 mm diameter was placed in the centre of the columns after mixing in the gypsum, and this was removed after 2 hours when the gypsum had set leaving behind a hole down the centre of the column for the full length of the cemented column. The column was then left to cure for at least 24 hours before loading the footing. The footings were loaded until a sudden drop in load indicated the breaking of the column. At

this point load was removed and the column repaired. The first repair technique involved injection of the bacterial solution (bacteria and nutrients) around the cemented column in the vicinity of the break as shown in Figure 3a. Five points, equi-spaced around the column were injected with 2 mL of the bio-solution, with each point at a distance of about 40 mm from the centre of the column. The second repair technique involved simply pouring 10 mL of the bio-cement forming solution into the hole in the centre of the column using a funnel as shown in Fig 3(b). The third repair technique also involved pouring 10 mL of nutrients (urea + $CaCl_2$) into the central hole, but in this case no bacteria were added. The third approach was used on columns that had already been repaired using the second method and had been reloaded to failure. The third technique was designed to assess whether residual bacteria from the previous repair could be reactivated by providing additional nutrients. Tests have been performed with the sand surrounding the cemented columns in both dry and saturated states.

(a) (b)

Figure 3: Foundation repair using (a) injection into surrounding sand and (b) pouring solution into the hole in the centre of the column.

3 RESULTS

3.1 UNCONFINED COMPRESSIVE STRENGTH

The variations of the unconfined compressive strength of gypsum and bio-cemented specimens with unit weight are shown in Figure 4(a). This figure shows that the strength increases with dry unit weight, and that a similar trend is observed for both the bio-cemented and gypsum cemented specimens. Interpretation of Figure 4(a) is not straightforward as the increases of unit weight are also associated with increases in the amount of calcite in the bio-cemented specimens, and increases in the gypsum content in the gypsum cemented specimens, and it is well established that the strength of artificially cemented soils increases with both cement content and unit weight. The similarity of the behaviour of soils cemented with gypsum and calcite has been noted in other studies (Ismail et al., 2002), and this is why comparative tests using gypsum are included here. Furthermore, the similar strengths of calcite and gypsum cemented specimens suggest that the method of calcite precipitation is not that important.

Figure 4(b) shows the relations between the amount of urea, which is the same as the amount of calcium chloride, in the bio-cement mixtures and the amounts of calcite precipitated and the UCS. Figure 4 also shows that the amounts of calcite precipitated in each specimen at three locations (top, middle, and bottom) are similar without any consistent pattern. There was less than 5% variance in the calcite distribution which compares favorably to other

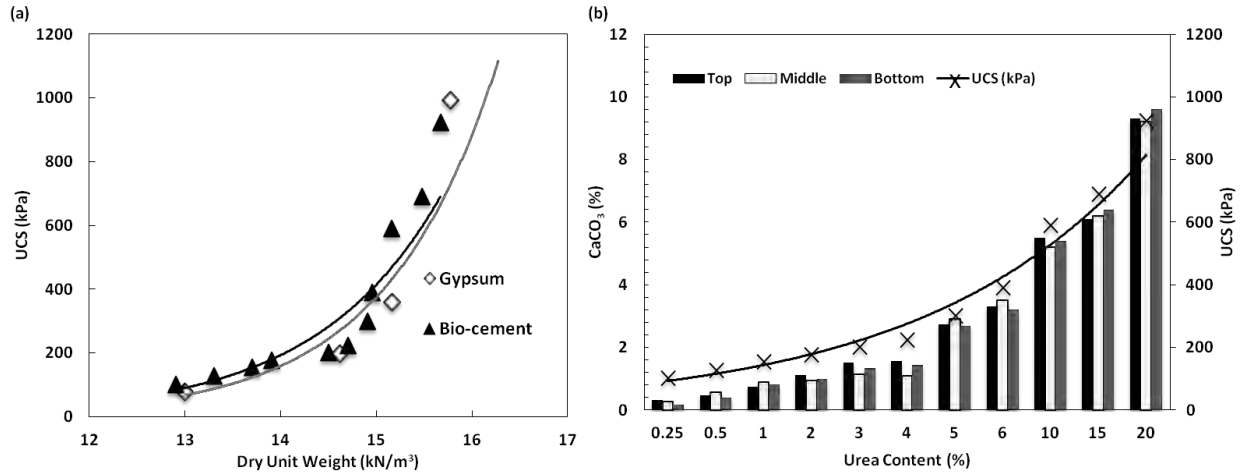

Figure 4: Variations of UCS strength with (a) dry unit weight (b) urea content of bio-cemented sample.

methods used in the past to create bio-cemented specimens (Martinez et al., 2011; van Paassen et al., 2009; Whiffin et al., 2007).

The amount of calcite precipitated is generally reported as the amount of bio-cement and this can be correlated with the UCS strength. This provides a strong linear correlation (R^2= 0.97) which can be described by Equation 3, where C is percentage of calcite precipitated. The trend of linearly increasing strength with increasing calcite content is similar to that previously reported (Al Qabany et al., 2011). Alternatively, the amount of urea required to precipitate the calcite, can be used as a means to estimate and monitor the degree of cementation in this study.

$$UCS(kPa) = 89.9C + 83.7 \quad \textbf{(3)}$$

Analysis of the data shows that the calcite cement is twice as effective as the gypsum, that is the UCS strength with 10% gypsum is similar to the UCS strength with 5% calcite. For example, Figure 4b shows that approximately 5% calcite is produced by adding 10% urea and 10% calcium chloride to the bacterial solution.

3.2 MODEL TESTS

Figure 5 shows the evolution of the average vertical pressure (load divided by area of the footing) with vertical displacement for the model footing tests. Results are shown for surface footings, footings on gypsum cemented columns, and footings on bio-cemented columns. The soil surrounding the columns was Sydney sand with a relative density of about 60% in both dry and wet conditions. As expected, the cemented columns significantly increased the stiffness of the foundation response compared to the tests with no columns, and increasing amounts of both gypsum and bio-cement increased the stiffness and load carrying capacity of the footings. All footings on the dry sand failed in a general shear mode, with a shear plane forming and breaking the column about one diameter below the footing. Failure was associated with a sudden loss in load and tests were terminated when this occurred. In the saturated sand the columns also failed in a similar manner, however this was not evident in the load, deformation responses (Figure 5b) which generally showed a monotonic increase in resistance. The tests in saturated sand also appeared to show a smaller difference than for dry sand between the footings with and without the cemented columns.

In UCS tests it was found that the strength and stiffness of specimens cemented with either gypsum or calcite were similar when the percentage of calcite was half that of gypsum. However, in the footing tests the gypsum cemented columns were superior to the bio-cemented columns with equivalent UCS strengths, providing higher strengths and stiffnesses. This difference was more pronounced in columns mixed in saturated soil where gypsum cemented columns gave almost double the resistance of the bio-cemented columns. These differences are believed to be

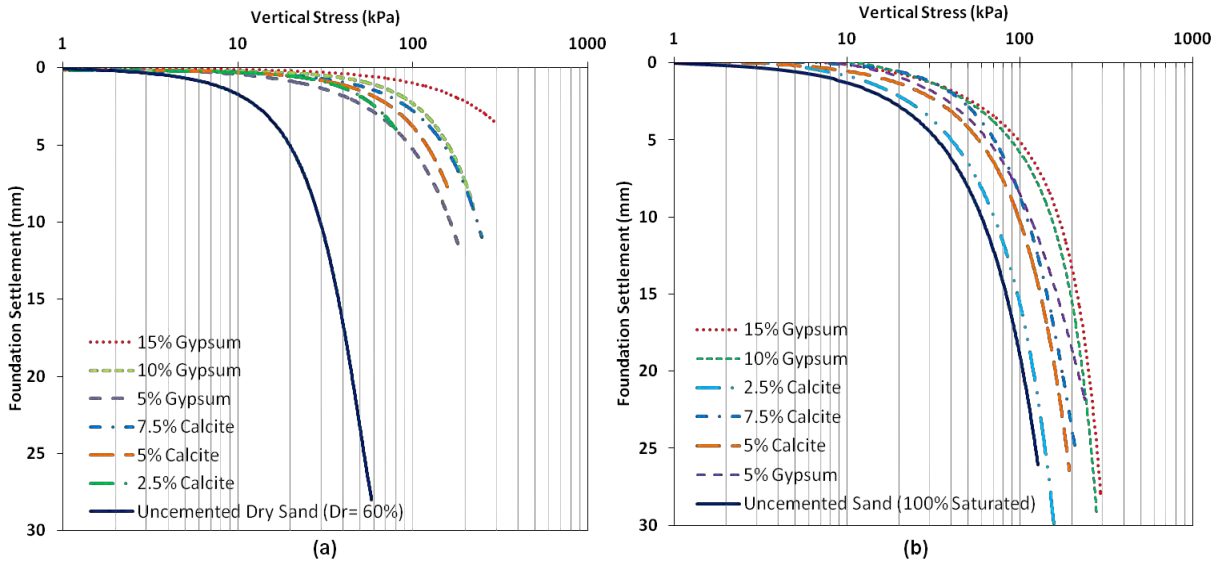

Figure 5: Stress, displacement responses from model foundation tests in (a) dry sand (b) saturated sand.

related to insufficient curing of the bio-cemented columns. By monitoring the shear wave velocity it has been found that about 24 hours is needed for completion of the bio-cementation reaction in UCS specimens (Duraisamy, 2015), but the extra 6 days curing time of the UCS specimens may have resulted in some additional slight strength increase. Under saturated conditions the curing process of the bio-cemented specimens could be affected by the surrounding water. This is possible because dilution by the water may limit changes in pH which are necessary for calcite precipitation. During microbial activity in soil the pore fluid pH increases and calcite typically precipitates when the pH is 8.5 to 9.0 (Stocks-Fisher et al. 1999).

In practice cemented columns are used to control settlements and in these model tests settlement reductions of 50% in dry sand and 32% in saturated sand were observed using bio-cemented columns (7.5% calcite). Similar trends were also observed in other footing tests when the sand surrounding the columns had relative densities of 40% and 50%. Similar settlement reductions have been reported in other model tests using bio-cementation (Martinez and Dejong, 2009). These tests have shown the potential of bio-cementation to create cemented columns of sand, however uncertainty remains regarding the influence of the ambient temperature, which can affect the calcite precipitation; the speed of the mixing auger which can affect the bacterial activity and influence the amount and distribution of calcite; and the curing time required on site.

3.3 COLUMN REPAIR

As noted above all the columns broke about one footing diameter below the tops of the columns. Figure 6 shows the response of the footings on initial loading and in both dry and saturated sand a distinct peak in the stress, deformation response is observed. After unloading, two of the footings were reloaded to show the response without any repair. In each case the stress increased to the value before unloading and then decreased with further deformation. Three methods of repair were then investigated using the bacterial solution to precipitate calcite and restore the columns. In repair method 1 in which the bio-cement is precipitated around the column the foundation stiffness is similar or less than for the failed reloaded column. This suggests that the cement has not been effective in repairing the column, however, the effect of the cement is evident at large settlements where the repaired column shows a higher resistance. In the second repair method where the bacterial solution is poured into a central hole in the column the solution can flow through the region of the break and calcite precipitated there can weld the two parts of the column back together. Evidence that this has successfully occurred can be inferred from the high stiffness and the higher resistance than the reloaded footing seen in Figure 6a for the footing on repaired column 2. The effect of this repair approach does not appear to be so successful in saturated sand (Figure 6b), although even in

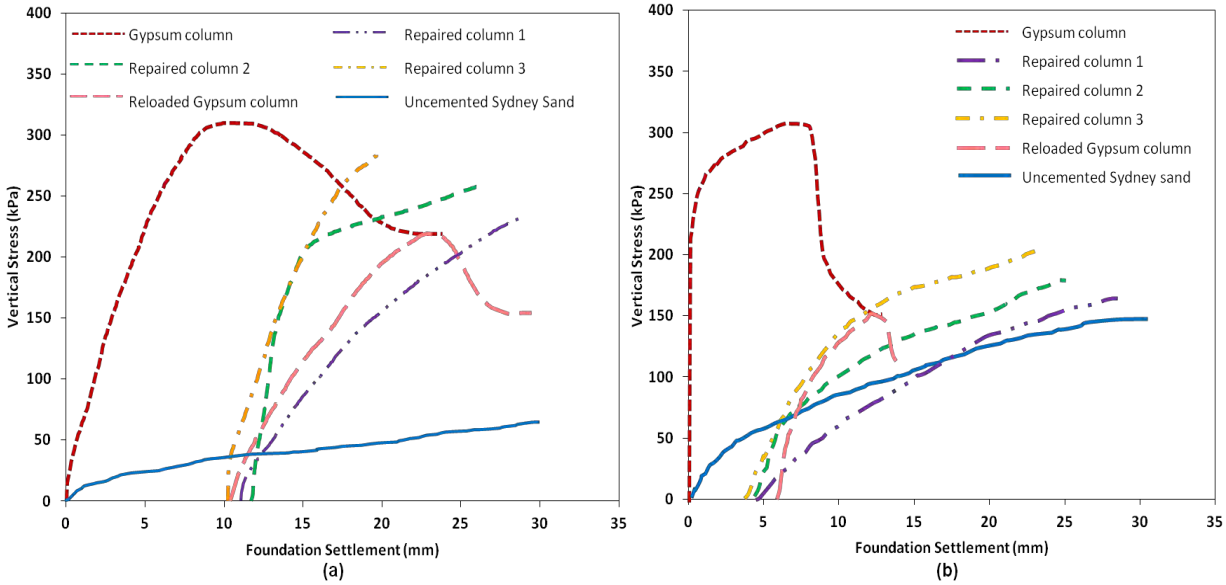

Figure 6: Stress, displacement responses from repaired model foundation tests in (a) dry sand (b) saturated sand.

this case there does appear to be some benefit of the repair at large settlements. In the third repair method the previously repaired column 2, which had been loaded to its breaking point, was repaired again by adding nutrients without any bacteria. The responses in Figures 6a and 6b shows that after this repair (Repaired column 3) the best foundation response was obtained, which suggests that additional calcite has been precipitated. This indicates the potential for self healing exists provided the column has bacteria present at the time of construction and nutrients for the bacteria can be provided as and when required to heal and cracks.

4 DISCUSSION

The challenges of producing uniform and strong bio-cementation have been noted in many studies, and to date none of the methods proposed has proven to be suitable in field application. It has been shown in this study that simply mixing the bacteria, nutrients and soil can produce uniformly cemented specimens suggesting that ex-situ mixing combined with dry soil mixing technologies may provide a viable method for application of bio-cementation. However, it has been noted that obtaining effective bio-cementation in saturated sand is more difficult than in dry sand and further study is needed to investigate whether longer curing periods will result in the same strength for the same amount of precipitated calcite. It was also observed that more nutrients were required to produce a given amount of calcite in saturated sand than in dry sand.

The effects of the repair techniques could also be investigated by extracting the columns from the sand after the loading tests. Two repair mechanisms could be identified. First, in the tests where the bacterial solution was injected around the pile evidence of calcite precipitation on the surface of the column was evident as can be seen in Figure 7a. This precipitation appeared to be primarily filling in cracks in the column surface created during the first loading. There was no evidence of cemented sand surrounding the column, but this may have been because this cementation was broken down during the loading of the repaired column. These observations suggest that injection of bacterial solution in the vicinity of cracks may be effective in sealing them and be able to prevent damage from water entry. Second, when the bacterial solution was poured through the central hole it was able to weld the two parts of the damaged column together as shown in Figure 7b. This observation suggests that there is potential for pile repair providing provision is made for tubes that can enable the bacterial solution to be directed to regions needing repair.

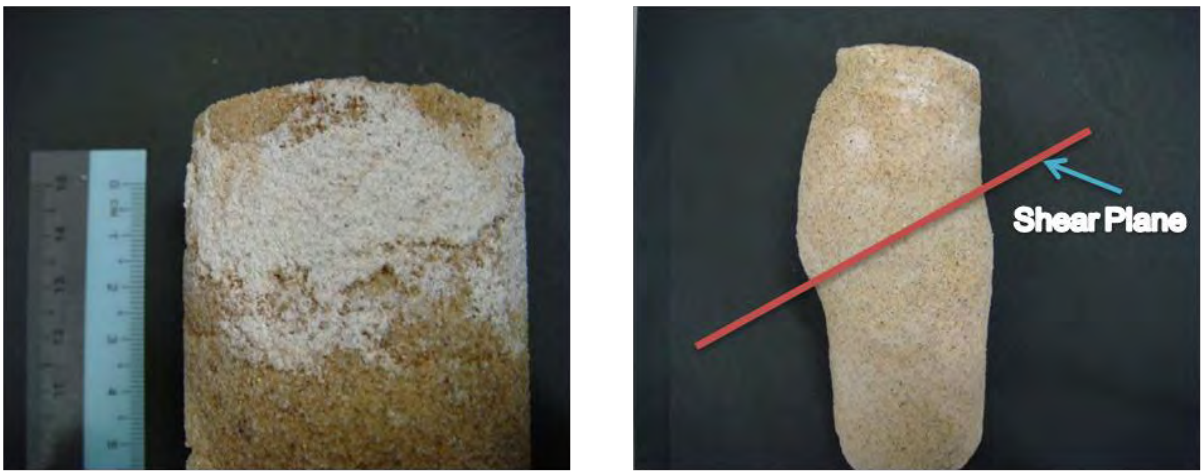

Figure 7: Samples retrieved from model test showing (a) sealing (b) welding effects.

Self-healing strategies generally rely on the bacteria and nutrients being available when repair is required. This can be achieved by encapsulating cells of bacteria and nutrients which are released if cracks occur. The third repair strategy involved simply adding further nutrients and reactivating bacteria from an earlier repair. The success of this approach suggests that incorporation of bacteria in the original soil column may be beneficial for future repair and would require only the release of nutrients to enable self-healing.

Although these tests have shown the ability of bio-cementation to form and repair soil columns the applicability of this approach to real foundations needs further study. In particular, the resilience of the bacteria when subjected to stress and construction handling needs to be demonstrated. Even for cementing agents that are well understood it has been reported (Terashi, 2003) that strength parameters obtained from laboratory treatability studies are usually five times higher than those obtained in the field from deep soil mixing applications.

5 CONCLUSIONS

The patterns of behaviour observed in bio-cemented Sydney sand are very similar to those in specimens bound with gypsum and have been reasonably consistent throughout all the laboratory tests conducted. The laboratory tests have identified the quantities of nutrients required to produce a range of calcite contents and hence soil columns with a range of strength and stiffness. It has also been demonstrated that mixing of soil, bacteria and nutrients can produce specimens with a uniform distribution of cement. Small scale footing tests have been performed on sand improved by bio-cemented columns, where the column creation has modeled the deep soil mixing process. These tests show that bio-cement could be an alternative to existing cementing agents.

The ability of bio-cement to repair broken soil columns, either by injection around the periphery of the column or by injection into a hole in the centre of the column, has been demonstrated. The presence of bacteria can stimulate calcite precipitation when nutrients are provided, and this offers the potential for self-healing foundations.

6 ACKNOWLEDGEMENT

The authors would like to acknowledge the technical support from Mr. Ross Baker and Mr. Sergio de Carvalho.

7 REFERENCES

Al-Thawadi, S.M. *Ureolytic Bacteria and Calcium Carbonate Formation as a Mechanism of Strength Enhancement of Sand*. Journal of Advanced Science and Engineering Research, 2011. **1**(1): 98-114.

Bang, S.S., Galinat, J.K. and Ramakrishnan, V. *Calcite precipitation induced by polyurethane-immobilized Bacillus pasteruii*. Enzyme and Microbial Technology, 2001. 28: 404-409.

Bang, S.S., Lippert, J.J., Yerra, U., Mulukutla, S. and Ramakrishnan, V. *Microbial calcite, a bio-based smart nanomaterial in concrete remediation*. International Journal of Smart and Nano Materials, 2010. **1**(1):p. 28-39.

DeGraef B., DeWindt W., Dick J., Verstraete W. and DeBelie N. *Cleaning of concrete fouled by lichens with the aid of Thiobacill*i. Materials and Structures, 2005. **38**(284): 875-882.

Dick J., DeWindt W., DeGraef B., Saveyn H. VanderMeeran P., DeBelie N. and Verstrate W. *Bio-deposition of a calcium carbonate layer on degraded limestone by Bacillus species*. Biodegradation, 2006. 17: 357-367.

Duraisamy, Y. *Improvement of sand by biocementation*, forthcoming PhD thesis, 2015: University of Sydney.

Edvardsen, C. *Water permeability and autogenous healing of cracks in concrete*. ACI Materials Journal, 1999. **96**(4): 448-454.

Gerilla, G.P., Teknomo, K. and Hokao, K. *An environmental assessment of wood and steel reinforced concrete housing construction*. Building and Environment, 2007. 42: 2778-2784.

Gosh, S., Chattopadhyay, B.D. and Mandal S. *Use of hot spring bacteria for remediation of cracks and increment of durability of structures*. Indian Concrete Journal, 2008. **82**(9): 11-16.

Hammes, F., Boon, N., de Villiers, J., Verstraete, W., and Siciliano, S.D. *Strain-Specific Ureolytic Microbial Calcium Carbonate Precipitation*. Appl. Environ. Microbiol., 2003. **69**(8): 4901-4909.

IPCC (Intergovernmental Panel on Climate Change), *The Climate Change 2013: The Physical Science Basis*. The Fifth Assessment Report, Cambridge University Press, 2013: 867-952.

Ismail, M.A., Joer, H.A., Sim, W.H. and Randolph, M.F. *Effect of Cement Type on Shear Behavior of Cemented Calcareous Soil*, J. Geotech. Geoenviron. Eng., 2002. **128**(6): 520-529.

Li, V.C. and Yang, E. *Self healing in concrete materials*. In S. van der Zwaag (ed) Self healing materials-An alternative approach to 20th centuries of materials science. Springer, The Netherlands, 2007: 161-194.

Martinez, B.C., Barkouki, T.H., Dejong, J.D. and Ginn, T.R. *Upscaling of Microbial Induced Calcite Precipitation in 0.5m Columns: Experimental and Modeling Results*, ASCE Geotechnical Special Publication 211, 2011: 4049-4059.

Martinez, B., and DeJong, J., (2009). *Bio-Mediated Soil Improvement: Load Transfer Mechanisms at the Micro- and Macro- Scales*. Paper presented at the Advances in Ground Improvement.

Neville, A.M. *Autogenous healing-A concrete miracle?* Concrete International, 2009. **24**(11):p. 76-82.

Paassen, L.A. v. *Microbes turning sand into sandstone, using waste as cement*. Paper presented at the 4th International Young Geotechnical Engineers Conference, The Egyptian Geotechnical Society. 2009: 135-138.

Peris Mora, E. *Life cycle, sustainability and the transcendent quality of building materials*. Building and Environment, 2007. 4: 1329–1334.

Qabany, A.A., Mortensen, B., Martinez, B., Soga, K. and Dejong, J. *Microbial Carbonate Precipitation: Correlation of S-Wave Velocity with Calcite Precipitation*, ASCE Geotechnical Special Publication 211, 2011: p. 3993-4001.

Ramachandran, S.K., Ramakrishnan, V., and Bang, S.S. *Remediation of concrete using micro-organisms*. ACI materials journal., 2001. **98**(1): 3-9.

Reinhardt, H.W. and Jooss, M. *Permeability and self-healing of cracked concrete as a function of temperature and crack width*. Cement and Concrete Research, 2003. 33:p. 981-985.

Rodrigues-Navarro, C., Rodriguez-Gallego, M., Ben Checkroun, K. and Gonzalez-Munoz, M.T. *Conservation of ornamental stone by Myxococcus xanthus induced carbonate biomineratization*. Appl. Environm. Microbiol, 2003. **69**(4): 2182-2193.

Stocks-Fischer, S., Galinat, J.K. and Bang, S.S. *Microbiological precipitation of $CaCO_3$.* Soil Biology and Biochemistry, 1999. 31**:** 1563-1571.

Terashi, M. *The State of Practice in Deep Mixing Methods.* Proceedings of 3rd International Specialty Conference on Grouting and Ground Treatment. ASCE Geotechnical Special Publication, 2003. **120**(1): 25-49.

Whiffin, V.S., van Paassen, L.A., and Harkes, M.P. *Microbial Carbonate Precipitation as a Soil Improvement Technique*. Geomicrobiology Journal, 2007. **24**(5): 417-423.

LIMITATIONS ON GEOTECHNICAL RISK MANAGEMENT: DESIGNING FOR RESILIENCE

Tim Davies

Geological Sciences, University of Canterbury, NZ

ABSTRACT

The imprecisions inherent and unavoidable in probabilistically-based risk analysis and management are addressed and shown to be a significant limitation on reliable infrastructure design against the loads resulting from hazard events. The nature of hazard events is outlined and the concept of resilience defined in the context of poorly-quantified and unknown hazards. It is suggested that resilience might be improved by purposefully designing infrastructure to match complex system attributes such as decentralisation, heterogeneity and redundancy. The use of event and effects scenarios in choice of a design event in geotechnical engineering is outlined, and the implications of this strategy explored.

1 INTRODUCTION

The increasing technical ability of geotechnical engineers to characterise and model the nature of both natural and made ground, its response to loads applied to it, and ways of improving that response, are helping to increase the ability of the built environment to withstand the loads generated by specific hazard events. However, in terms of the need for the built environment to function satisfactorily, these abilities are only as good as the knowledge of what events will affect a specific piece of ground during the period of interest – that is, during the design life, which is more or less the next hundred or so years in most cases. Herein I address the inevitable imprecision inherent in estimates of the magnitudes and numbers of events a structure might be exposed to in its design life, and the limitations this imprecision places on the realism of probabilistically-based design loads. This leads to consideration of a different way to decide how an engineering structure might be designed and built to resist geotechnically-derived loads resulting from hazard events.

The term „resilience" is much used nowadays to refer to the ability of something (in our context a unit or system of infrastructure) to survive a major shock (in our context a geotechnical failure of some type, such as foundation collapse or landslide) and to maintain/regain its ability to function effectively during the event and afterwards. Engineering design can obviously enhance the ability of a structure to withstand the loads that a specific anticipated geotechnical event will apply if and when it occurs, but choosing the design event is the tricky bit in this contribution to resilience. Again, if we knew what was going to happen in the design life of a structure we"d be able to design for that – but we don"t.

2 RISK MANAGEMENT

The usual solution to this conundrum is to design a structure so that it will fail in an event of such intensity that it has an acceptably low probability of occurring during the design life; or, increasingly, so that the risk associated with the failure (where risk is probability multiplied by cost of failure) is acceptable. This process is called Risk Management, and it has developed well-defined procedures that result in risk being reduced to such a level that either it is deemed acceptable (e.g. Finlay & Fell, 1997), or that the utility of investment in risk management is optimised in some way. This process obviously requires that the relation between event magnitude and frequency is quantified to an adequate degree.

While for some events (e.g. river floods) substantial quantities of this type of data are available, this is less often the case for geotechnically-related events such as liquefaction, landslides or earthquakes, so the statistical basis for probabilistic design has intrinsic errors. A less well appreciated issue, however, is that even with infinitely accurate statistical data, design based on probability is unavoidably imprecise because – *by definition* – the number of near-design-level events that occur during a design life is small. This means that the infinitely accurate statistics are used to predict the magnitudes of a small number of events, and the magnitudes of events that actually occur will in that case be likely to differ significantly from these predictions. This effect is illustrated in Figure 1, which shows the maximum error in ten averages of various-sized random samples of all the integers from 0 to 99 (whose average is exactly 50). Obviously the smaller the sample, the greater is the deviation of the sample average from 50.0; in particular, when sample size is very small (1 or 2) the error (defined in this way) approaches ± 100%. Applying this to a structure with a design life of 100 years, the

average magnitudes of the ensemble of 1-year events can be predicted to ± 10%, but that of 50-year events has an error of ± 95%. Thus any design based on predicting the occurrence of small numbers of events is liable to extreme errors, even with infinitely accurate probabilities of future event occurrence.

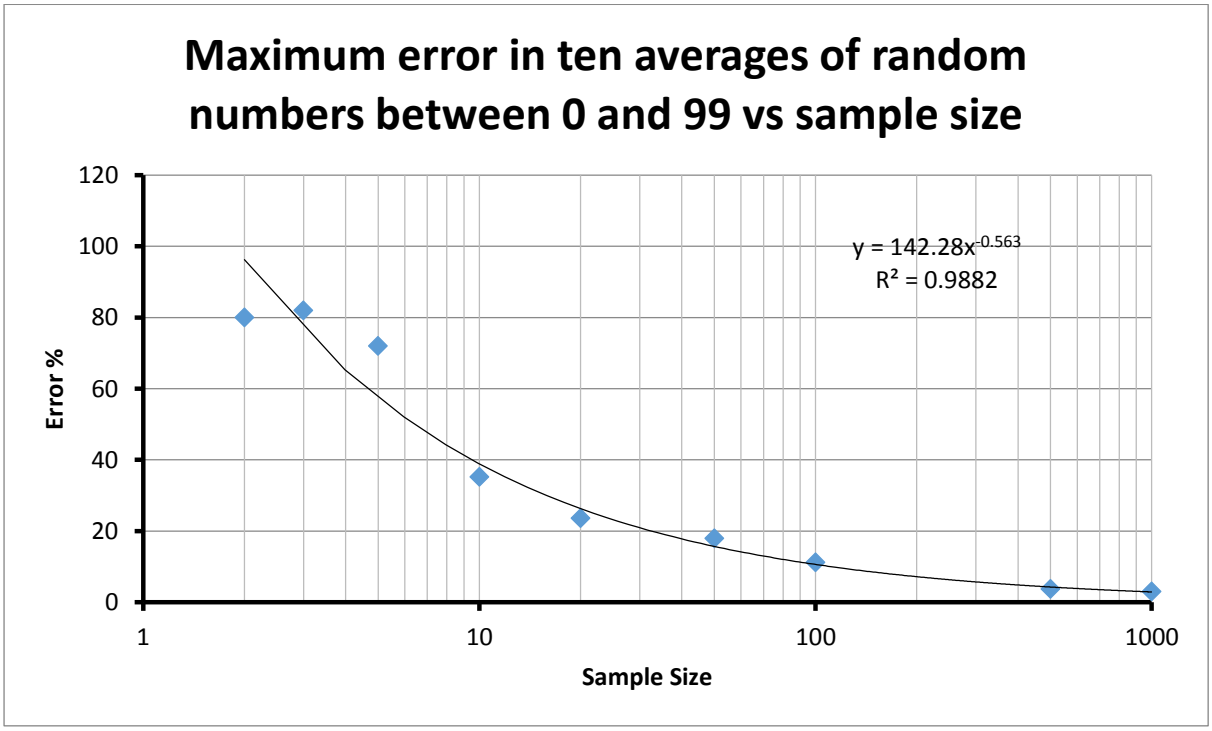

Figure 1: Error in predicting averages of various-sized samples of numbers from 0 to 99.

This situation becomes worse when some utility optimisation procedure is involved (e.g. cost-benefit analysis of event mitigation measures), because in addition to quantified event magnitudes, and thus costs and benefits, being imprecise for the reasons set out in the previous paragraph, the net benefit which is optimised is the difference between two large and imprecise quantities – cost and benefit. Thus the net benefit, which is a much smaller number, has a very much higher imprecision still and its optimisation seems likely to be unrealistic as a design procedure.

A final drawback to the use of event probabilities in design is that very large events, which have very low probabilities, are treated as if they will never occur. In fact, there is absolutely no reason why the next event that occurs cannot be a very low-frequency event. For example, the September 4 2010 Greendale earthquake in New Zealand had a probability of occurrence in 2010 of about 10^{-4} (Stirling et al., 2007), and no rational person would have made a statistically-based decision to prepare for it in that year (or, in fact, in any given year) with a higher priority than preparation for a whole suite of much more likely, if less intense, events. Nevertheless, the 1-in-10,000-year event occurred in 2010. In reality the low probability of the event caused it to be unexpected when it occurred, and this will always be the case when intense events are associated with probabilities. Events become unexpected when they are assigned low probabilities.

Probabilistic design is often justified on the grounds that it defines the most likely event, and that it is rational to design for this rather than for any other event. What is not stated, however, is that in most cases the likelihood of this event is small in absolute terms, and that it is much *more* likely that some other event – that has not been designed for - will occur. For example, if the probability of the most likely event is 10%, then there is only one chance in ten that it will occur, and it is ten times more likely that something else will happen. There is a 90% probability that the design event will not occur.

Thus, reliably designing to avoid ground failure on the basis of probabilistic analysis is very difficult, and there is a strong case for thinking in addition about non-probabilistically-based ways of developing resilient infrastructure.

3 DESIGN FOR RESILIENCE

3.1 SAFE-FAIL DESIGN

One example of a way of preventing ground failure turning into disaster is to *design the failure*, so that the failure mode is known and the consequences foreseeable, even if the time of occurrence and the magnitude of the event that causes failure scale are unpredictable – measures can then be put in place to reduce the impact of the consequences. This is "safe- fail" instead of "fail-safe" design (Park et al., 2013). It renders the failure itself expectable, even if the trigger event is not. This is equivalent having a "fuseplug" in a levee – a length of lower bank that will overtop and wash out before any other part of the bank does, so that the location of failure can be foreseen and the consequences mitigated. It also defines very closely the magnitude of the smallest event that will cause failure; but most important of all, its very existence means that the failure is *expected*, and people will not be taken by surprise when it occurs.

3.2 COMPLEXITY AND RESILIENCE

Most major disasters, by contrast, result from events that are unexpected and take people by surprise, and obviously these cannot be designed for. One of the reasons for unexpectedness has been mentioned above – the event is expectable but is assigned a low probability. Other reasons are that no event of a particular type has ever been experienced or imagined (officially, at least) in the location at which it occurs (an example is the Mt St Helens debris avalanche in 1980: Glicken, 1994); and that while the event type was expected, the event magnitude was not (examples are the 2004 M9.1 Andaman, 2010 M7.0 Haiti, 2010 M8.8 Maule and 2011 M9.0 Tohoku earthquakes, all of which exceeded their maximum credible magnitudes). However, one doesn"t need to know what sort or size of disaster will befall a ship before deciding that lifeboats are a good idea, because the main vulnerability of a ship is that it can sink. It is more useful to think of things that can be done – equivalent to installing lifeboats on a ship – that, whatever the nature of a catastrophe, will reduce society"s vulnerability to the event.

Alternatively, coming from the opposite direction, what characteristics of the way society is organised today lead to vulnerability of infrastructure to unexpected shocks? Some examples include:

- spatial concentration and centralisation, so that all one"s infrastructural eggs are in one basket in a single location;
- short-term economic optimisation and planning, which ignore the possibility of expected but rare events;
- lack of redundancy, so that failure of one component is disastrous;
- component uniformity, so that a failure of one component can trigger cascading failure of equally-strong adjacent components. Component diversity, by contrast, is like biodiversity, it reduces the "brittleness" that leads to sudden and widespread failure;
- top-down governance and communication in order to be better organised, with the result that information about developing crises cannot easily move upwards to decision-makers;
- the operation of systems to eliminate "troublesome" small-scale oscillations in fluxes; this can lead to catastrophic instability on a much larger scale. Steadiness, like uniformity, is potentially destabilising; and
- increasing focus on data-informed decision-making, as a consequence of increased accountability and legal paranoia; as emphasised above, the information carried by data is often spurious, and in addition this diverts attention from events on which data are sparse or absent – usually big events.

The opposite characteristics, which by implication impart resilience to systems, are obvious: decentralisation, long-term planning, redundancy, heterogeneity, unsteadiness, isotropic communication and qualitative decision-making. Interestingly, most of these are also characteristics of the structure or behaviour of *complex dynamic systems*; these are a type of system that is increasingly demonstrated to represent the essential functions and behaviours of many-component, strongly-linked systems such as are found to have evolved in ecology, physiology, finance, geomorphology, sociology and many other fields (e.g. Sornette, 2002). Note that these are the very systems that interact to generate disasters – natural systems and societal systems. Thus there is reason to hypothesise that *complex dynamic system processes are fundamental to disaster processe*s. If this is indeed the case, it has some serious implications for how disasters can be managed or reduced, because one of the major characteristics of complex dynamic systems

is the *emergence* of behaviour patterns at a given scale that cannot be predicted or expected from knowledge or understanding of smaller-scale behaviour; in other words, complex system behaviour is fundamentally and irreducibly unpredictable. Thus, future disasters are fundamentally unexpectable. This corresponds closely to the common experience that major disasters at a given location are unexpected, either in type or in magnitude, and clearly you can"t design to manage the risk of an unknown disaster. Nevertheless, as suggested above, designs that purposefully incorporate characteristics associated with resilience are likely to prove to be more resilient.

But is there any *evidence* that these characteristics do in fact confer resilience? If we think about evolution as the basis of natural system development, the answer is yes. The natural systems of the planet (in particular, species of life-forms, but it is becoming apparent that non-living systems such as rivers behave similarly) - are accepted to have evolved over billions of years as a result of competition with other systems in their environment, and in a context of scarcity of resources. When severely stressed by their environmental systems, species lose those members that are least equipped to survive those stresses, and retain as breeding stock those members better equipped – thus over time a species evolves to become becomes more resilient to the shocks it experiences. Since life began it is accepted that species complexity has increased (albeit punctuated and altered by occasional megashocks, such as mass extinctions), and systems of species have evolved the characteristics and behaviours of complex dynamic systems. It appears that as the systems of Earth have co-evolved over æons, they have all become complex dynamic systems – indicating that such systems are optimally resilient in some sense. The same should apply to societal systems, which have also evolved in competition with neighbouring systems – so how has society developed the less resilient traits bulleted above?

To answer this question authoritatively needs specialised expertise that I lack, but one suggestion is that since humans developed a high level of intelligence and ability to utilise natural resources, human society has increasingly insulated itself from natural systems and is thus decreasingly affected by them – or at least, by the ones it can manage, which are the smaller ones. In this way other priorities than resilience have been able to develop and survive – such as the priority to make as much money as quickly as possible; to exercise maximum power over fellow humans; to minimise personal feelings of insecurity – and these underlie many of the traits listed above. While they may confer resilience to the behaviours of the evolving societal environment, they do not confer resilience to natural system behaviours.

4 SCENARIO-BASED DESIGN

These general considerations are perhaps interesting, but they do not provide the engineer with an alternative to magnitude and probability in designing infrastructure to be resilient to future events. They leave us instead with the uncomfortable feeling that the future is unknowable, and therefore cannot be designed for. While this is true, the situation is more hopeful in reality.

While the future events that will trigger disasters will be of unknown type, unknown magnitude, unknown time of occurrence and unknown location, the societal effects that can result are less unknown. Irrespective of whether the triggering *event* is a tsunami, earthquake, eruption or tornado, the resulting *effects* on society are relatively common: destruction of assets, death and displacement of people, interruption of commerce. How a disaster affects society depends more on the characteristics of society than it does on the characteristics of the trigger event. For example, an identical earthquake to that which hit Tokyo in 1923 will have very different effects when it next occurs in the same location. Again, we cannot know where major landslides will be caused by earthquakes in mountain ranges, but we do know they will block rivers, and since we know where the towns are located that are vulnerable to landslide dambreak floods on rivers, we can figure out what the effects can be. Thus the unknown nature, size, location and time of a trigger *event* is not crucial to usefully characterising its potential *effects*.

This indicates that useful information about what can happen to society in future disasters can be derived from knowledge of past disasters, combined with physical and social science, by developing disaster *scenarios* as a basis for future planning and design. Science, community knowledge and historical/paleo-data provide information on what types of event are possible at a given location, and how big they can be; selecting one of these, the scenario of effects on society can be developed relatively easily, including the longer-term effects of interruption to commerce. By generating a limited suite of scenarios, the likely range

of societal effects can be estimated; this knowledge can then form the basis of community planning to reduce vulnerability to the scenario effects.

Again, this is all very well when expressed in general terms. How can the idea be applied to specific geotechnical design considerations? Let"s think about landslide risk management…

5 GEOTECHNICAL RESILIENCE; EXAMPLE

Consider a typical landslide hazard situation. An existing development at the base of a hillslope is affected by a small landslide during heavy rain some years after the development was completed. No other information is available on the history of landsliding in this area, but some geomorphic indications of past slope instability are found during a post-landslide investigation. The conventional response to this situation would be to carry out limited geotechnical investigation and analysis of the slope, develop a numerical model of its stability under heavy rainfall (calibrated, note, by one data point representing the one known landslide), and establish what rainfall intensity and precursory moisture content are required to cause a landslide sufficiently large to be considered unacceptable. If these conditions occur, according to meteorological data, at an unacceptable frequency or probability, then action is required; if the frequency is acceptable, then nothing needs to be done.

Note, first, the sources of imprecision in this procedure. How well do the geotechnical data represent the full suite of ground conditions across the whole slope? What assumptions underlie the numerical model? Is one data point adequate to calibrate the model? What is the length of rainfall data record, and the corresponding statistical precision? What is the design life of a building? These call into question the robustness of a "do nothing" decision, or in other words the extent to which the people living at the base of the slope are in fact safe. The model may indicate a 10^{-4} per annum chance of damage, but, even if it is accurate this does not mean that no damage can occur in any given year, or in the 100-year expected life of the development. The model may be wrong, and the true probability may be 10^{-2}; and even though the site is then 100 times more dangerous than calculated, it may well be the case that no further landslide occurs with in the 100-year design life. Where is the reality in all this? In addition, who decides what probability of damage or death is acceptable, and acceptable to whom?

If, on the other hand, the frequency appears unacceptable, then action is required either to engineer the slope to reduce the risk; to strengthen or protect the buildings so that a landslide does little or no damage; or to abandon the site, immediately (if feasible) or gradually. Any of these is in reality a useful contribution to risk reduction, but whether the residual risk attending any strategy except abandonment is acceptable is, as noted in the previous paragraph, not simple to determine. Thus, basing a design to counter a geotechnical hazard on magnitude-frequency data is not simple, and is in fact fundamentally unsatisfactory (Wong, 2014). Although based on accepted procedures, much of the rationale is spurious.

A resilience-based approach to the situation, by contrast, starts from the simple and irrefutable observation that an unexpected hazard event has occurred. It can be reliably inferred from this that landslides will occur again on this slope, and thus present further hazards to the development - the hazard is now expected. When, where and how big these landslides will be is unknown. Some scenario landslides can be generated, based on the known occurrence and the geomorphic indications, together with perhaps an idea of the largest conceivable event so that scenarios can be aligned with respect to this; the effects of these on the development can be estimated, and the consequent local and regional impacts on building values, community sociology, commercial activities and regional development can be estimated (note that developing scenarios for the latter impacts will require considerable collaborative work with the community). With these impacts in mind, the community and its officials together can then work out how they wish to respond to the hazard threat. This may, as before, involve slope engineering, and/or building protection and/or partial or wholesale site abandonment; the significant point is that the scenarios provide much more useable information on landslide effects than did the numerical/probabilistic data. No probabilities are attached to the scenarios, because it cannot be known which of them will occur first – all we know is that they all can, and in fact will, occur on some unknown days in the future. In addition, because the scenarios are understandable by everyone involved – from lay people to government department heads and politicians – the community has available a much sounder and broader basis for making realistic and acceptable decisions.

Certainly, in this latter case, there is still a need for detailed geotechnical input for slope engineering, and for building protection and strengthening, but again the point is that this design is now based on a realistic picture of what will happen on the site one day, rather than a probabilistic view of what will happen on average every few thousand years. In essence, the possibility of a poorly-constrained probabilistic decision resulting in unacceptable damage and deaths is avoided. If damage and deaths do occur – and this cannot be ruled out, except by abandonment – then the situation is ameliorated by the fact that the community has taken a genuine part in the decision that led to this, and will therefore accept responsibility along with their professional advisers; a witch-hunt is much less likely because the decision process has been inclusive, open and transparent. This should be comforting to engineers designing structures that might kill people one day.

6 DISCUSSION

6.1 ACCOUNTABILITY

One significant criterion for assessing the feasibility of a design methodology is to think about what will happen at a court of enquiry following a disastrous failure. An enquiry tends to put a lot of weight on demonstrating that approved conventional procedures have been properly followed. Thus suggesting that a conventional procedure is irrational, as herein, tends to generate understandable scepticism and reluctance to adopt any different procedure, no matter how rational. This is a serious disincentive to seriously consider arguments such as those made herein. In this context, it is possibly useful to think of design for resilience as a procedure that can complement probabilistic design, rather than replacing it. In reality the imprecisions that accumulate in probabilistic design allow plenty of scope to implement resilience concepts, and involvement of a community in designing for its future is (or should be) in any case an ethical requirement of most professional disciplines. Thus pragmatic considerations suggest incorporating resilience considerations into conventional design rather than abandoning the latter in the short term, irrespective of its shortcomings.

6.2 GEOMORPHOLOGY

In the hypothetical example above, it is clear in retrospect that the hazard could perhaps have been anticipated had a competent geomorphologist been consulted with respect to the initial hazard assessment of the development, and that might have led to more thorough investigation of the landslide hazard at the outset. Regrettably, geomorphologists are still under-utilised in everyday geotechnical engineering, and indeed generally in engineering site investigations. The latter usually focus on ground conditions from a foundation perspective, perhaps gleaning a deeper geological perspective from engineering geology if the situation appears to warrant it (a decision usually left to the often inadequate geological knowledge of the engineering consultant). However, where hazards may be subtly-indicated, if at all, a geomorphologist can often bring valuable insights on future landform events such as river aggradation and slope instability from an understanding of the geomorphological setting and history of the site.

7 CONCLUSIONS

Examination of the assumptions underlying probabilistic risk management leads to the conclusion that, where the target sample size is small (as in hazard and design event contexts), the technique is of little value in selecting a rational design event to reliably reduce the occurrence of future damaging events in a specific location.

Scenario-based design, by contrast, can avoid probabilities entirely and deal only with event- and effects-scenarios, by whose selection and use communities and experts can work together to decide on the nature and level of protection required against future hazard events and their consequences.

For reasons of professional accountability, however, it is probably more realistic to suggest that scenario-based design is implemented initially to complement standard probabilistic design procedures.

8 REFERENCES

P.J. Finlay and R. Fell, 1997. Landslides: Risk perception and acceptance *Canadian Geotechnical Journal* 34: 169-188

J. Park, T. P. Seager, P. S. C. Rao, M. Convertino and I. Linkov 2013. Integrating Risk and Resilience Approaches to Catastrophe Management in Engineering Systems. R*isk Analysis, Vol. 33, No. 3, 2013* DOI: 10.1111/j.1539-6924.2012.01885.x.

Sornette D. 2002. Predictability of catastrophic events: material rupture, earthquakes, turbulence, financial crashes and human birth. *Proceedings of the National Academy of Science* 9: SUPP1 2522-2529.

Stirling M., N. Litchfield, W. Smith, P. Barnes, M. Gerstenberger, G. McVerry, J. Pettinga 2007. Updated Probabilistic Seismic Hazard Assessment for the Canterbury Region, *GNS Science Consultancy Report 2007/232 - ECan Report U06/6 August 2007*

Wong, H.N. 2014. Is landslide risk quantifiable and manageable? In: Zhang et al. (ed) *Geotechnical Safety and Risk IV* Taylor & Francis Group, London, ISBN 978-1-138-00163-3. 101-111.

RESILIENT GEOTECHNICS - PAST FAILURES AND FUTURE SUCCESS

Philip Davies[1]

[1] *Principal Geotechnical Engineer, Golder Associates Pty Ltd, NSW, Australia (pdavies@golder.com.au).*

ABSTRACT

The concept of resilience applied to engineering systems has gained importance in recent years. Geotechnically, all infrastructure assets interact with the ground and so resilient geotechnical solutions must meet a range of plausible conditions including not only stability and serviceability, but increasingly, repairability, growing demands, climate change and impacts from surrounding works.

Resilience may be described as the ability of a system to adjust its functioning in response to changes while satisfying performance, economy and safety objectives. In the infrastructure engineering context, the notion of resilience can apply to fixed assets, but more perhaps more influentially it applies to the organisations that design, construct and operate those assets. This paper documents historic examples of geotechnical and other engineering failures where geotechnical resilience was deficient, and lessons learnt which can be used to increase resilience in future applications. Failures are reviewed in the lights of „traditional" or „linear" safety engineering concepts which include contributing factors such as people, processes and products. The evolution of safety engineering concepts is also examined by looking at improving risk management, design standards and construction processes towards Resilience Engineering (considering both assets and organisations), where risk is actively managed to achieve superior outcomes. Despite these advances over time, recent failures show that some of these lessons must be painfully re-learned; wisdom is difficult to teach.

Looking forward towards to achieving resilience in future infrastructure design, this paper considers global economic, social, and environmental factors which interact with the field of geotechnics, and how this discipline plays a role in creating robust, flexible infrastructure organisations and assets which are safe, secure, and resilient to what the future may hold. Examples of how climate change and changing societal needs may impact projects are discussed alongside future research trends and emerging geotechnical innovations such as Building Information Management (BIM) and performance based design.

Collectively, the failure examples, risk management guidance and Resilience Engineering concepts herein are provided so that geotechnical practitioners can benefit from case history learnings and can apply new tools to future geotechnical engineering challenges. By knowing what to do, what to look for, what to expect and what has happened (historically and in the project timeframe) then safe, reliable *and* efficient infrastructure can be created.

1 INTRODUCTION

The objective of this paper is to reflect on past, present and future engineering practices which respectfully weaken or enhance the creation of resilient infrastructure. In the context of this discussion, a useful definition of „Resilience Engineering" is that proposed by the „father" of the emerging field, Erik Hollnagel in his seminal publication *Resilience Engineering: Concepts and Precepts* (2006):

"*The intrinsic ability of a system to adjust its functioning prior to, during, or following changes and disturbances, so that it can sustain required operations under both expected and unexpected conditions*."

This definition implicitly includes the conventional definition of safety, whereby „*the ability to sustain required operations*" may be seen as a requirement to satisfy ultimate (and serviceability) limit state requirements. This definition, however, also requires the ability to function under „*both expected and unexpected conditions*" rather than merely just avoid failure. It is this ability that makes the system both safe and efficient, which in turn makes Resilience Engineering attractive and worth exploring.

The notion of resilience as a new systems approach to understanding of safety, risk and performance under competing economic and workload pressures is a relatively new concept with wide-ranging applications beyond geotechnical engineering including ecology, computer networks, economics and industrial / organisational safety. Only selected Resilience Engineering concepts are presented herein, alongside more traditional risk management concepts, illustrative case-histories and historical learnings as they relate to mainly geotechnical aspects of infrastructure design, construction and operation.

Considering the types of infrastructure challenges facing geotechnical engineers, it is worth noting that port and maritime engineers often face relatively high geotechnical risks compared to other forms of civil engineering due to sites being pre-disposed to soft and unfavourable ground with significantly fluctuating groundwater and tidal conditions and the frequent need for retrofitting / deepening old works, generally without existing drawings and with large failure consequences. For this reason, and also the author‟s experience bias and interest towards these projects, many of the following case histories have a maritime engineering flavour.

Ultimately all infrastructure assets interact with the ground and their integrity relies substantially on the performance of geotechnically designed elements. In terms of safety, the challenge is to create „tough‟ rather than „brittle‟ designs (and/or systems of work) which can adapt to, and absorb disruptions and disturbances, even those that fall beyond the capabilities that organisations or assets are trained or designed for (think: World Trade Centre). The future-proofing of infrastructure requires both training of practitioners and incorporation of resilient and reliable geotechnical components which can absorb future environmental changes, potential changes in use and/or impacts by other works.

The following sections focus mainly on geotechnical engineering challenges during design, construction and operation with the aims of reinforcing lessons learned from past failures and understanding how new tools and techniques can be used to create safe and efficient infrastructure.

2 FORMATIVE LESSONS IN EARLY ENGINEERING

On reflection, we are unfortunately spoilt for choice with historical examples of geotechnical and engineering failings, most of which provided hard lessons at the time for the developing engineering community operating on a largely trial and error basis. As drawings and texts became more widespread during the medieval period (5th to 15th century), the use of this written, transferrable knowledge helped to disseminate design concepts and facilitate construction of increasingly large scale and complex religious structures such as cathedrals and mosques.

In his informative paper „*How to design a cathedral: some fragments of the history of structural engineering*”, Professor Jacques Heyman (1992) describes how 13th century sketchbooks by Villard de Honnecourt show that cathedral building was anything but an amateur occupation. In that era, there was no distinction between architect or engineer; the head of such building projects was known as a „master of the work‟, having completed a long, largely practical training regime from apprentice through journeyman and foreman.

Such masters had a firm grasp of both aesthetic „architectural‟ design of Gothic and Renaissance styles and also technical aspects of masonry design including lining, levelling, plumbing and vaulting arrangements. Interestingly, the overriding view at the time was that it was the *shape* of the structure that governed its stability and hence the importance of geometry greatly overwhelmed that of theoretical stress calculation. Scaled models were also used as a test-bed for new or complex features, and to engage with project sponsors.

The bulk of surviving writings on ancient building design dwell on rules relating to geometry with, perhaps, an intuitive understanding of the resulting stresses. The results, however, align surprisingly well with modern structural engineering principles. Success on these early landmark projects depended on the relatively informal involvement of experienced craftsmen and women who could apply rules of precedence, empiricism and „well winnowed experience‟ (Burland, 1987). In today‟s terms, this senior involvement has evolved into formal and auditable review processes.

Lasting examples of these impressive structures include the magnificent c.17 Ottoman Sultan Ahmed (Blue) Mosque in Istanbul, featuring the largest religious dome in the world, and the imposing Lincoln Cathedral in England which was commenced in 1088. The latter was reputedly the tallest building in the known world for over two hundred years between 1311 and 1549 until the spire embarrassingly toppled, following repeated previous failures in 1185 (earthquake) and 1237 (alterations), as described by Jarvis (2014). It is worth considering the advice from a scholar of the period, the 11th century philosopher Solomon Ibn Gabriol, whose reflections on life can be extended to contemporary engineering practice and the Resilience Engineering concepts herein:

“*The first step in the acquisition of wisdom is silence, the second listening, the third memory, the fourth practice, the fifth teaching others*”.

Understanding the evolution from these early trial and error approaches towards methodical design and construction using Resilience Engineering concepts, requires us firstly to reflect on the features and shortcomings of early landmark projects. These contain some fundamental lessons that our predecessors have benefitted from and which are equally important today. Examples and salient lessons from three case histories spanning the Medieval to Victorian periods are explored below. That they are all British may be due to the pioneering nature of UK constructions at that time and also that documentation of these projects during construction and following completion was more comprehensive than from similar projects in different parts of the world at that time.

St Davids Cathedral, Pembrokeshire, Wales (1181 onwards)

Nestled in a picturesque grazing valley, construction of the present Cathedral began in 1181. While specifics of geotechnical conditions are scant, the site is sloping and founded at least in part on alluvial soils adjacent to the Alun River. Anecdotal accounts (Lloyd *et al.*, 2004) indicate that foundation problems occurred at an early stage due to the terrain and „uncertain" foundation conditions. No prizes, then, for identifying the first lesson (often since repeated) that rudimentary investigations, or even desk study and inspection by a seasoned geological eye, can assist in identifying ground engineering risk before major works begin.

Problems affected the new cathedral building from early stages, resulting in the collapse of the new tower in 1220. When one of the largest earthquakes to originate in Britain occurred on 20 February 1247, the structure was significantly impacted, owing partly to the inadequacy of the original foundations and corresponding vulnerability. The resulting effects caused the walls at the west end of the nave to lean outwards as shown in Figure 1.

Descriptions of the earthquake in the annals discussed by Luard (1865) speak of buildings being shaken up to the point of collapse, dishes being thrown off tables and people running out terrified, indicating an estimated earthquake intensity around magnitude 5-6 with a likely epicentre in Wales. As described with latin translations in Lloyd *et al.* (2004), the severity of the earthquake damaged ("corruit") the cathedral of St Davids and "rupes scissae sunt" (stones were split). While some damage was experienced, the overall design was sufficiently robust such that total collapse did not occur (i.e. ultimate limit state was not reached).

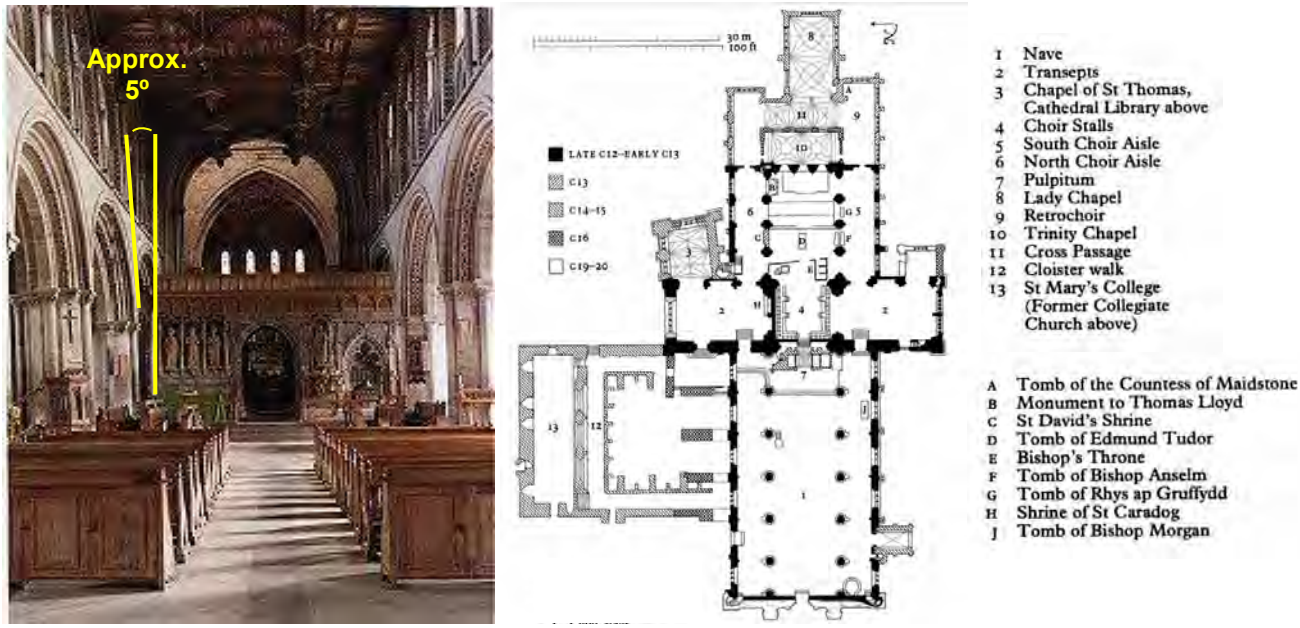

Figure 1: St Davids Cathedral (photo / image souce: www.stdavidscathedral.org.uk / Lloyd *et al.*, 2004).

By chance more than design, the cathedral design was sufficiently resilient such that the post-earthquake condition was repairable. This present day notion of designing (intentionally) for an acceptable, repairable damage condition which is intermediate between ultimate and serviceability states under an unusual event has merit and is discussed in later sections.

Following additions and minor reconstruction during the middle-ages (between about 1250 and 1400), a wooden ceiling rather than stone vault was built in the 16th century to reduce loading. This is visible at the top of the photograph in Figure 1. The resulting magnificent pendant ceiling from made from Irish Oak is one of the most spectacular pieces of carpentry in Wales. This simplistic approach of adjusting the design in response to observed performance actually aligns well with the „observational approach" to construction practice which was first coined by Peck (1969). In essence, this reflective practice cycle can be applied to any project and always starts with a prediction of what you expect to happen. If observations are unexpected then reflection is required to manage risk and refine predictions of future performance (See Figure 2).

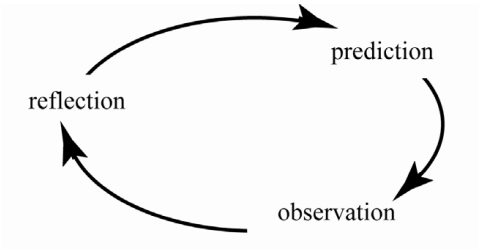

Figure 2: Reflective Practice Cycle.

Following later periods of disrepair and then reconstruction, strengthening works for earthquake affected areas included underpinning which involved an *„audacious feat of engineering of which the architect was justifiably proud*". Other structural problems affecting the façade also required temporary support, then replacement in the 1880"s (Lloyd *et al.* 2004). After nearly 1,000 years of evolving design and construction which has exhibited some elements of resilient engineering, this structure and centrepiece of celtic culture remains as prominent and beautiful landmark.

Thames Tunnel between Rotherhithe to Wapping, London, England (1825 – 1843 and beyond)

As meticulously documented by Sir Alec Skempton *et al.* (1994), the Thames Tunnel running between Rotherhithe and Wapping in London was built by Sir Marc Brunel between 1825 and 1843 and was the world's first subaqueous tunnel. Marc Brunel employed his nineteen year old son Isambard as resident engineer on their first job together.

Despite repeated catastrophic inflows from the overlying river into the tunnel workings, the determination and ingenuity of the Brunels" overcame the challenges and developed pioneering technology including the tunnel shield, soil nails, improved investigation techniques and detailed recording systems involving written notes, observations and sketches made during each shift. Now, more than 160 years after it was completed, the oldest tunnel on the present London Underground was recently upgraded to form part of the new £1bn East London Railway Line, prepared for the 2012 Olympics.

The elder Brunel invented and patented a tunnelling shield to deal with the waterlogged Woolwich and Reading Beds and soft (and foul) riverbed sediments beneath the Thames. The shield comprised a cast iron structure (Figure 3) that moved forward as the ground was excavated, with bricklayers constructing the double tunnel behind. Face excavations were undertaken by sequentially removing oak planks one at a time and cutting the soil behind to a depth of four inches (about 100mm). This process required 36 miners, each in his own cell in the shield.

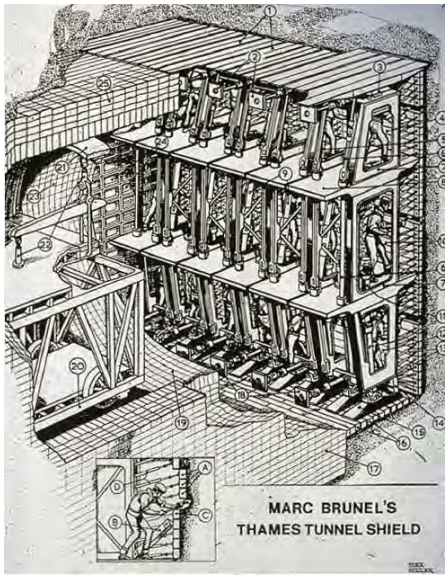

Figure 3: The first ever tunnel shield (photo sourced from www.tunnelsonline.info).

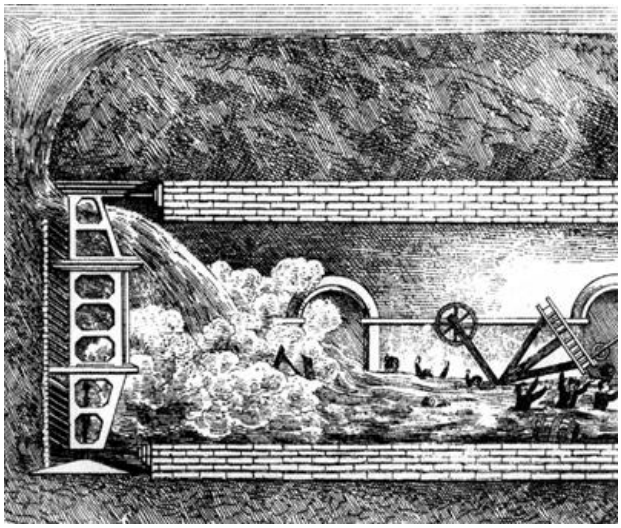

Figure 4: The fatal irruption of January 1828 (photo sourced from www.wiley-vch.e-bookshelf.de).

With a sufficiently thick and stiff clay layer above the tunnel crown and below mixed riverbed sediments this process could be completed without significant ground loss at the face, but where the clay cover was thin (< 6 ft or 2 m), significant water and running sand and silt inflows occurred, causing large settlements and breakdown of the clay ahead

and above the face. In April 1827, flowing spoil from the tunnel face included identifiable riverbed materials apparently including coal, bones, pieces of China (Brindle, 2013) and later a spade interpreted as being dropped by barge workers above (Skempton, 1994). Isambard hired a diving bell to inspect the riverbed which was now covered by so little that on pushing a hollow tube through the mud he could converse with a miner in the tunnel. The intriguing account by Brindle (2013) also relays that Isambard also took his mother down to the riverbed in one diving bell inspection – truly a project of family interest.

In May 1827 about 1,000 tons of soil and an enormous volume of water ran into the workings, requiring plugging of a riverbed sinkhole with 2,500 tons of clay filled bags placed by barges. Fortunately the 100 or so workers managed to escape, however a later inundation in January 1828 resulted in the death of six workers (Figure 4) and Isambard himself was carried unconscious from the tunnel. A seven-year cessation of work followed while new funding arrangements were sought.

These irruptions showed how critical it was to delineate the type and distribution of soil materials at the tunnel crown and face. When this issue became tragically apparent during construction it was realised that early boreholes using a worm drill yielded unsatisfactory information. A second phase of investigations with auger and casing tubes, gave significantly better results, and, along with more detailed riverbed bathymetry, enabled strategic pre-placement of many clay bags at riverbed level to mitigate tunnel face instability. Again, the value of the reflective practice cycle is demonstrated.

On re-starting in 1835, a system of iron bars driven into the face was used to provide temporary support in poor ground. This system of soil nailing was used to facilitate replacement of the old shield and to provide intermittent support during the remaining tunnel drive. Water inflows during construction were typically 100-300 gallons per minute (8-23L/s), and sometimes up to about 1200 gallons per minute (91L/s) in poor ground areas. Ultimately, a total of five uncontrollable river irruptions occurred into the tunnel workings, leading to a modest overall advance rate of about 25m per year during productive work. On completion, the Thames Tunnel was hailed as one of the new wonders of the world, and on its first day of opening 50,000 people walked through the tunnel. Subsequently, a million visits were chalked up in the first 15 weeks and a Royal visit by the year end.

That the project continued and succeeded in the light of such high groundwater inflows, regular uncontrolled irruptions and even fatalities, suggests that the risk appetite then was significantly greater than would be tolerated today. Looking beyond the difficulties, we should also acknowledge the level of perseverance, innovation and personal commitment shown by the Brunel‟s, which ultimately led to step-change advances in construction techniques that have benefitted society since that time. In the author‟s view, this more conventional notion of personal resilience, involving mental toughness, versatility, innovation and capacity to deal with challenge or adversity, at an individual leadership level is an essential element of project (and career) success.

19th Century, Port Infrastructure, UK

Early accounts describing port infrastructure challenges in the 19th century are neatly captured by Jarvis (2011). These include discussions held at the UK Institution of Civil Engineers in 1857, decades before the geotechnical discipline was formally recognised. At that time, civil/maritime engineering topics from around the British Empire included deep problematic muds in Southampton Docks, retaining wall movements at Kidderpore Docks (Calcutta, India) and caisson construction using the „*Indian method of well sinking*‟.

Jarvis also describes the two worst port construction disaster case histories in UK history. These provide powerful insights into the technical, human and organisational risks which are as relevant today as then. These disasters both occurred in 1909 and together, they triggered some of the first legislative maritime labour, construction and design guidelines which have evolved to guide design and protect construction workers today.

The first example relates to the modernisation of Vittoria Dock (*sic*), Birkenhead, near Liverpool. During demolition work inside a large timber cofferdam, uncontrolled inflow and collapse occurred, killing 14 people. Two primary failure causes were cited, including poor/overstressed design and high groundwater pressure. Significantly, informal post-failure enquiries described the cofferdam as „workmanlike‟ suggesting no record of any formal calculation, drawing, or considered construction process, unlike the more diligent documentation of Brunel.

Later that year at Alexandra Dock in Newport, South Wales, another large (18.2m deep) temporary timber retaining structure collapsed with the estimated loss of between 20 and 39 men and widespread damage (See Figure 5).

Figure 5: Pre and Post- cofferdam image, Alexandra Dock, Wales, July 1909 (Photo source: Jarvis, 2011).

The uncertain number of workers affected is a telling indicator of the lack of employer control. While a „general drawing" was produced by a titled „sub-agent", the actual temporary support design was effectively undertaken by a poorly educated „ganger" (four levels of management below the Principal Contractor) who was conveniently and posthumously blamed. Other organisational failings included arbitrary design changes, sporadic/undocumented feedback meetings and a failure to communicate effectively across societal class-based hierarchies.

The Birkenhead failure was seen as a blameless incident, even „*incidental to their calling*" for dock construction workers of the day. However, the ensuing Newport incident was a tipping point that triggered parliamentary reform including extension of factory worker laws to construction workers. Failure themes in these early case histories, which have been unfortunately repeated since, include:

- Poor planning, organisation and management including inadequate ground investigation;
- Hierarchical roadblocks to communication;
- Inadequate recognition of, or response to, variable site conditions – especially tidal and groundwater effects;
- An absence of systematic recognition, documentation or management of risks or safety in design; and
- A failure to disseminate and act on punishing lessons learnt by others – in the case of Newport, only a few months and Counties apart.

3 EMERGENCE OF DESIGN GUIDANCE

Improvements in the early 19th century came in the form of societal awareness of the need to improve safety and risk management at work, in parallel with the appearance of learned societies and improved workplace legislation. Some key milestones are discussed below, again, focussing mainly on civil/maritime engineering developments in the interests of brevity.

Development of industry associations, design guides and design standards have improved the way that infrastructure works have been specified and engineered. One maritime example, founded in 1852, is the Permanent International Association of Navigation Congresses (PIANC). This is a global organisation providing guidance for sustainable waterborne transport infrastructure for ports and waterways (see www.pianc.org).

Similarly, the industry funded Construction Industry Research Association (www.ciria.org) has produced a number of seminal civil engineering and geotechnical design guides including benchmark manuals on site investigations, seawall design, rock materials and groundwater control.

In the United States, coastal engineering has traditionally been the domain of the military, who for instance, have produced a number of useful guides including The Military Handbook of Seawalls, Bulkheads, and Quaywalls and the well-known Naval Facilities Engineering Command (NAVFAC), Foundations & Earth Structures Design.

Some relevant contemporary maritime design codes include, for example, British Standards BS6349 Maritime Structures (2012-13), Australian Standards AS4997 Guidelines for the Design of Maritime Structures (2005), and AS4678 Earth Retaining Structures (2002). Australian users should note that AS4678 is not intended for use with structures over 15m height (of which many quay walls are), and excludes slopes flatter than 70°, which would exclude many revetment structures.

Over time, international design standards have generally moved away from global safety factoring towards assessment of stability and serviceability performance requirements. This enables more specific and appropriate factoring of

individual actions according to design cases under consideration (i.e. ultimate, serviceability and earthquake). It is worth noting that serviceability performance is a significant risk for port owners/operators due to the commercial drivers around asset availability and maintenance cost. Given the commercial importance of operational reliability, suggested strategies to control this risk are presented in the following sections of this paper.

Lagging behind the evolution of design standards, are formal journals about failure/forensic engineering in which lessons about failures can be documented and shared more widely. The ICE only began publishing the regular Forensic Engineering Journal in 2011, well over than a hundred years following the cited civil engineering failures.

4 LEARNING FROM FAILURE: ENGINEERING RISK MANAGEMENT AND RESILIENCE CONCEPTS

Some key developments in the journey from trial and error based approaches in the early 19th century, to the concepts of safety engineering, established risk management practices and emerging field of Resilience Engineering are discussed below.

4.1 UNDERSTANDING FAILURE MODELS: FROM 'LINEAR' TO 'COMPLEX' SYSTEMS

All engineering projects are delivered through a complex set of designing and constructing processes. Despite improvements in the design process, as documented above, failures still occur due to poor design, poor translation of design intent, or poor implementation (i.e. construction).

Several authors have proposed models that outline conditions leading to failures. Over time there has been a shift from failure models that treat accidents as the outcome of a series of events along a linear pathway, to accidents arising from the interaction of a multitude of events in a complex system. Examples of linear system failure models include „The sequence-of-events model", „Man-made disaster theory" and „The latent failure model" which are discussed further below.

With the emergence of resilience concepts in safety engineering, more complex system models have been proposed such as „Normal accidents theory", „Control theory", „High reliability theory" and „Resilience Engineering ". An extensive discussion of all these theoretical accident models is provided by Hollnagel (2006) and Dekker *et al.* (2008). Only a brief description is provided below with examples and case histories to link them to the themes of this paper.

Figure 6 (from Furuta, 2014) schematically shows the evolution of these failure models over time from linear to complex systems (at top). Notable disaster events are also shown and illustrate how the importance of key factors has changed over time as our collective ability to address the various causal factors has changed (improved?) with time.

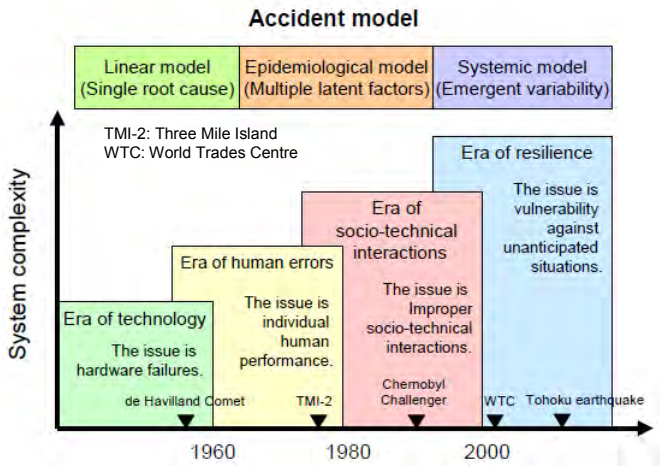

Figure 6: Changing focus of safety systems (Furuta, 2014).

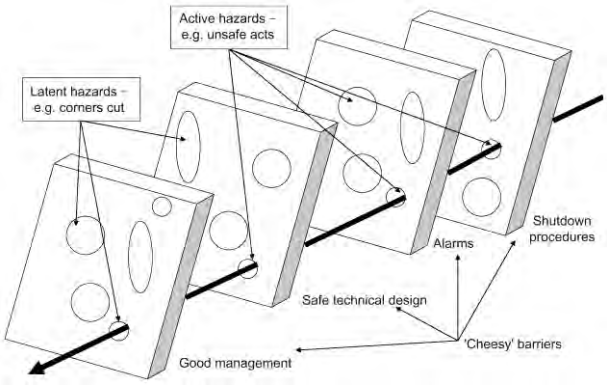

Figure 7: Reasons Swiss Cheese Model - a pathway to failure. (Source: Reason, 1990).

4.1.1 LINEAR FAILURE MODELS

A simple, linear way of conceptualizing how events interact to produce an accident is to imagine them as a sequence, or chain, of events resulting in a mishap. This has also been called the domino model, using the analogy that an accident is the endpoint in a string of falling dominoes (Hollnagel, 2006). This notion also requires a root cause, or trigger at the beginning of the chain that sets everything in motion (the first domino brings down the rest, one by one).

Extended failure models involving multiple parallel or converging sequences forms the basic premise of many risk analysis methods and tools such as fault-tree analysis, probabilistic risk assessment and critical path models. As discussed in Section 9.1, these approaches can be very useful to inform risk management decisions.

Another failure model that emerged from 1960"s to the early 1980"s includes the notion of barriers - a separation between the source of hazard and the object or activity that needs protection. Using the analogy above, barriers can be seen as blockages between dominoes that prevent the fall of one affecting the next, thereby stopping the chain reaction.

Reason (1990) proposed a „Swiss cheese" model to explain different barriers that stop failure of a system. As shown on Figure 7, these barriers include a range of measures and good management practices. Each of these barriers can be represented as separate slices of cheese containing holes that will occur during the life of a project. The holes in each barrier move around and appear and disappear as issues are identified and resolved. It is when holes line up through all the individual slices that a path to failure is completed.

The idea of separating sources of hazard from objects or processes that must be protected by a linear series of barriers is also sometimes thought of as a way of reducing hazard „energy" as it works through system. For example, road safety strategies also aim to reduce the amount of hazard „energy" (i.e. kinetic energy) by controlling release of harmful energy by introducing „barriers" such as speed limits, salting of icy roads, energy absorbing wire-rope median barriers, and passenger airbags (Rosness *et al.*, 2004).

Within the same family of linear systems thinking, the „latent failure model", also termed the „incubating accidents" model by Turner and Pidgeon (1997), involves the concept whereby a build-up of adverse factors creates the pre-condition for failure. A useful analogy describing the onset of failure in such a system is that of an inflating balloon. Imagining pressure as representing the likelihood of failure, then as a balloon grows in size, so does failure potential. Adverse events contribute to an accumulation of pressure and hence failure probability. The size of the balloon (and hence failure probability) can be reduced by letting air out. For example, this could be due to effects of management decisions that remove some of the risk.

If the pressure of events builds up until the balloon is very stretched, then only a small trigger event, such as a needle or lighted match is needed to burst the pressure pent up in the system. The trigger is often mislabelled as the cause of the accident, as the over-stretched balloon is an accident waiting to happen. Team leaders should look for evidence of the building pressure in the balloon – to spot the accident waiting to happen – and diagnose the necessary actions to reduce risk.

Figure 8: Post-failure photo of Nicoll Highway Collapse.

Figure 9: Landslide at Aberfan in 1966 (photo sourced from www.nuff.ox.ac.uk).

A classic example of a geotechnical failure viewed using this analogy is the Nicoll Highway disaster in Singapore which occurred in 2004 when a 30m deep section of cut and cover tunnel collapsed killing four and injuring three (Figure 8). The original design misinterpreted the local geology (missing a buried channel of alluvium) and overestimated the soil shear strength in its analysis. The pressure in the balloon was hence high from the outset. This was compounded by an under-design of the strut-waler support system connections by 50% where splays were omitted.

Signs of trouble such as buckling of plate stiffeners and accelerating ground movements were not appropriately recognised or escalated. At this point, the catalogue of errors and internal communication failures was an accident waiting to happen. The trigger to the „balloon burst" and rapid collapse was initiated by forced sway failure in lower struts which was an inevitable consequence of the design errors. A recap of learning"s from the 1909 Newport dock

disaster in Section 2, above, reveals remarkably similar people and process failings similar to Nicoll Highway over 100 years later. Even the appearance of the end result is hauntingly similar (compare Figures 5 and 8).

In Turner‟s 1976 study of the 1966 Aberfan coal stockpile disaster in Wales (Figure 9), the geotechnical factors behind failure were caused by elevated pore pressures in the accumulated rock and shale waste dump, which rapidly deteriorated into a fluidised flow-slide on 21 October 1966, killing 116 children and 28 adults. On closer inspection, Turner found that the failure exhibited „incubating‟ type characteristics having wider causal factors which were common to other disasters including:

- Rigidities in institutional beliefs
- Distracting decoy phenomena, neglect of outside complaints
- Multiple information-handling difficulties
- Exacerbation of the hazards by strangers
- Failure to comply with regulations
- A tendency to minimize emergent danger.

This work showed that disasters were not necessarily “created overnight” as the pre-failure conditions had been incubating for periods of up to years. A second observation was that the Aberfan failure and other man-made disasters he examined were not caused by a single factor but by a mix of disaster triggering events which had accumulated over time.

This was an important step towards linking multiple causal factors in more complex interrelationships and brings us to the emergence of Resilience Engineering concepts which is a more recent systems approach to understanding safety and risk. This approach brings with it the ability to build-in systems and controls to absorb change, error and disturbance in complex systems such as engineering projects without breaking down, without catastrophic failure. Truly resilient systems go beyond these protection measures towards enhancing the capacity and performance of infrastructure.

4.1.2 COMPLEX FAILURE SYSTEMS – TOWARDS RESILIENCE ENGINEERING

As discussed in the previous section, implementation of combined operational and engineering measures (or barriers) make many systems or projects relatively safe from pre-determined single point failures; that is, they are protected against particular adverse design events or failings of people, products of processes which would otherwise directly lead to bad outcomes.

Resilience Engineering departs from conventional safety risk management approaches based on componential approaches (e.g. elimination, removal, near-miss analysis, calculation of failure probabilities). Instead, Resilience Engineering looks for ways to enhance the ability of systems, organisations or projects, to monitor and revise risk models, to create processes that are robust yet flexible, and to use resources proactively in the face of disruptions or ongoing production and economic pressures.

Here, the word „system‟ can be read as „project‟, and in the context of this paper, perhaps more specifically „infrastructure project‟. Dekker (2008) identifies that a system‟s resilience includes properties such as:

- **buffering capacity**: knowing the size or kinds of disruptions the system can absorb or adapt to without a fundamental breakdown in performance or in the system‟s structure;
- **flexibility**: the system‟s ability to restructure itself in response to external changes or pressures;
- **margin**: how closely the system is currently operating relative to one or another kind of performance boundary;
- **tolerance**: the brittleness of a system and whether the it gracefully degrades as stress/pressure increase, or collapses quickly when pressure exceeds adaptive capacity.

These properties can be considered alongside adverse disturbing forces such as tensions created by the need to carry out work under time pressure or other resource constraints, resulting in a „resilience triangle‟ (Rasmussen, 1997) with boundaries defined by functionally acceptable performance, economy and safety. In cases where crossing the boundary is irreversible, an error or an accident may occur. The dynamic interplay between these different constraints and objectives is illustrated in Figure 10.

This illustrates how multiple pressures act to move the operating point of the organization or project in different directions. For example, management pressures towards efficiency can drive any given risk position towards unacceptable safety or workload outcomes. Conversely a desire to take the path of least effort (i.e. taking short-cuts or laziness) can compromise safety or efficiency, or excessive focus on robustness can reduce efficiency and risk economic failure.

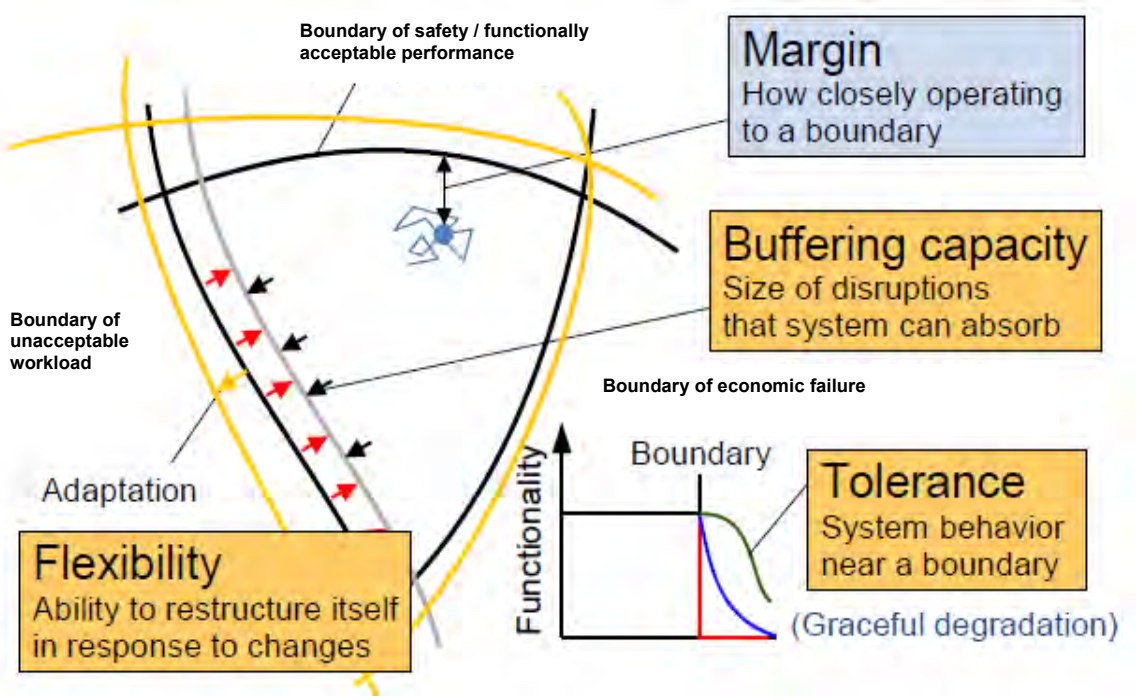

Figure 10: The resilience triangle bounded by constraints: safety, workload and economics (adapted from Furuta, 2014).

The case of the space shuttle Columbia disaster in 2003 is extensively used by Dekker (2006) to explore patterns that have helped shape the ideas behind Resilience Engineering. Some of these causal factors have their basis in the earlier models described by Turner previously, including:

- Drift toward failure as defences erode in the face of production pressure.
- An organization that takes past success as a reason for confidence instead of investing in anticipating the changing potential for failure.
- Fragmented distributed problem-solving process that clouds the big picture.
- Failure to revise assessments as new evidence accumulates.
- Breakdowns at the boundaries of organizational units that impede communication and coordination.

The fourth point affecting the Columbia mission, involves the failure to recognise and act on new evidence resonates strongly with aforementioned civil engineering failures – especially the Nicoll Highway, discussed above. The key here is to identify and have the courage to revise once-plausible designs as new evidence comes in. Revising assessments successfully requires getting a "fresh" view, often by bringing in people new to the situation; through interactions across diverse groups with diverse knowledge and tools; and or through new visualizations which capture the big picture and reorganize data into different perspectives.

Resilience Engineering therefore requires practices to provide decision support for balancing production and safety trade-offs, and creation of feedback loops that enhance the organization‟s ability to monitor and revise risk models and protect safety. This can include monitoring for effective cross-checks when risky decisions are made or understanding the brittleness of a design by undertaking sensitivity studies (discussed further in Section 7).

In an infrastructure context, project leaders need sufficient awareness to know when to relax the pressure on throughput and efficiency and make trade-off decisions to sacrifice production over risk – especially when approaching safety boundary conditions. Ironically, it is at the very times of higher pressure and focus on acute goals that resilience behaviour is needed to keep these production/safety trade-offs in balance.

When operating under production and efficiency pressures, evidence of increased risk on safety may be missed or discounted. As a result, organizations act in ways that are riskier than they realize or want, until an accident or failure occurs. This is one of the factors that create the drift toward failure signature in complex system breakdowns. For example, the need to make aerospace operations reliable also makes them very complex, resulting in layers of obscuring processes and procedures which can themselves present unintended hazards.

Since the application of linear systems approaches to safety engineering, researchers such as Perrow (1984) have identified that adding many barriers and redundancy can paradoxically, add complexity and reduce clarity so that when

even small things start going wrong it becomes very difficult to see the problem and get off an accelerating pathway to failure. Indeed the case of an aircraft crash involving a Boeing 737 leaving Cyprus in 2005 reported by Dekker (2008) demonstrates that even highly prescriptive barrier-based and codified systems can result temporary inability to cope effectively with complexity, in this case due to misunderstandings caused by poor language skills. In these cases training of Resilience Engineering principles may help such as having the courage to speak up, identifying the consequences of ambiguous/hazardous/decoy information, understanding the „brittleness" of safety situations and understanding the trade-offs between commercial pressure and accident risk.

In the words of Adjunct Professor Tim Sullivan (experienced consultant appointed as Mine Warden to the 2007 Yallourn Coal mine collapse), the people responsible for maintaining safety can sometimes *„fail to hear the sound of the bus coming"*. With this in mind a classic example of incrementally increasing safety risk is captured by the following case history in Petroski (2000), reproduced from Dekker (2008). This case is reproduced in full below due to the exceptional clarity of these concepts conveyed:

CASE: TEXAS A&M UNIVERSITY BONFIRE (PETROSKI, 2000)

The Texas A&M University bonfire tragedy is a case in point. The accident revealed a system that was profoundly out of control and that had, over a long period, marched towards disaster. On November 18, 1999, a multi-story stack of logs that was to be burned in a traditional football bonfire collapsed while being built by students at the Texas A&M University [Figure 11]. Twelve students working on the structure were crushed to death as the structure collapsed. Twenty-seven others were injured. It was the worst such disaster at a college campus in the United States and was devastating within the tight knit community that prided itself on its engineering college. An independent commission was established to investigate the causes of the collapse. Extensive and expensive engineering studies were conducted that showed that the collapse was the result of specific aspects of the structural design of the bonfire. It revealed that the collapse happened because the bonfire had evolved from being a conventional bonfire into a large scale construction project. That project had never been competently designed or analyzed and was largely carried out by unsupervised amateurs.

The bonfire was a Texas A&M football tradition that extended over many years. It began in 1928 as a haphazard collection of wooden palettes. It grew gradually, increasing in scale and complexity each year until the 1990's when it required a crane to erect. In 1994 a partial collapse occurred but was attributed to shifting ground underneath the structure rather than structural failure per se.

The catastrophe five years later overwhelmed the medical facilities of the area. The response to the failure made it clear that no one imagined that this sort of disaster was possible, let al.one likely. In hindsight, it seems incredible that this should be the case. Even here hindsight misleads us into believing that the inevitability of this particular sort accident should have been apparent. It was not at all obvious before the fact. The relative lack of failure over many years produced a sense that failure was unlikely, even though the growing structure over the years was taking the system in that direction. Each increment in complexity and scale was too small to signal that the system was becoming dangerous in new ways. The bonfires of the late 1990's reached new heights without anyone understanding what those heights meant. The inability to recognize that the system was unsafe was a property of the system itself, a property essential to the development of the accident situation.

Figure 11: Texas A&M University Bonfire (Source: ww3.hdnux.com/photos, www.ruhr-uni-bochum.de).

Against the backdrop of success, warning signals like the partial collapse could be discounted. The partial collapse was treated as an incident. It was not large enough to garner the sort of attention needed for the kind of detailed examination that would show how dangerous these new bonfires were. Only a truly catastrophic failure was enough to produce a new look at what the bonfire had become. The group managing the bonfire had marched into tragedy with their eyes open but unable to interpret what they were seeing.

This illustrative example fits very closely with the incubating failure model in which almost all of the causal factors identified by Turner (1976) are satisfied. Reflecting on this with the benefit of hindsight, it is worth asking ourselves if the same pathway would have been followed, had the parties responsible for the bonfire displayed the following characteristics of a resilient organisation:

- **Preparedness/anticipation** - is the organization proactive in picking up on evidence of developing problems versus only reacting after problems become significant?
- **Opacity/observability** - does the organization monitor safety boundaries and recognize how close it is to „the edge" in terms of degraded defences and barriers? How widely are safety concerns distributed throughout the organization?
- **Flexibility/stiffness (brittleness)** – is the organization or processes nimble enough to adapt to change, disruptions, and opportunities? How quickly could something go wrong and go out of control?

Resilience is not necessarily about reducing negatives (incident recording, rule violations, etc.), it"s about identifying and then enhancing the positive capabilities of people and organizations that allow them to adapt effectively and safely under pressure. For example, systems which encourage learnings, feedback and open communication about system failures should be encouraged and rewarded. The degree to which the reporting of safety concerns and problems is truly open and encouraged provides another significant source of resilience within the organization. Assessing the organization"s response to incidents indicates if there is a learning culture or a culture of denial.

Recognising that there are infinite permutations of complexity involved in large scale engineering projects, the author considers it helpful, as a starting point, to focus on the three key risk management categories which contribute towards failure or shortcoming in performance. These are the „3Ps" being people, processes and products. These factors reinforce the concept that in addition to technical issues, engineers have to deal with a wide range of human and organisational issues including social, political and legal systems.

5 ROLE OF PEOPLE

Paraphrasing the first axiom of Worden *et al.* (1976), „*All social systems have inherent flaws or defects*". This can often lead to human factors in failures. Organisational and cultural situations may exacerbate the potential for failure and unfortunately these may be difficult for those close to or within teams or certain cultural environments to identify. The importance of multiple human or organisational factors in failure is complex because failures may not be solely linked to mistakes by individuals. Rather, they may also be impacted by organisational and/or cultural context.

Individual human frailties lie behind many failures. Although many people related risks are mitigated through safety rules, prescriptive procedures and management processes, people don't always do what they are supposed to do. This can arise through apathy, malice, laziness, stupidity, confusion or a whole range of other rational and irrational reasons.

This uncertain aspect of human behaviour screams out „unreliability alert!"; an erratic, unpredictable form of variability that we should aim to engineer out of systems through more automation, better education or indoctrination in safety, stricter procedures, and/or (in fact, ideally), tighter monitoring of workplace behaviour. As history shows, "human error" is often the product of factors that lie deeper inside the operation and organization. To help mitigate this embedded people risk, review processes involving people from outside an organisation or team may be of great benefit as they may be able to assist in the identification of risk unseen by people buried in detailed design (think: the master cathedral builder who knows when things „look wrong").

In design and construction applications, such people may be appointed on projects as internal reviewers, or as independent verifiers. Imagine the scenario of a Project Director / Reviewer on a large scale infrastructure project who has to come to the aid of a struggling design team to address a critical, high pressure issue. By involving themselves in design they are no longer able to offer the critical independent insight and review necessary to maintain an awareness of emerging risks. In this sense, Isambard Brunel may have been better off away from the tunnel face where he could make objective assessments of site behaviours and project risk.

Generally issues may be most easily addressed where all parties involved in a project have agreed to share risk and reward. Alliance contracts, for example, help to focus people on flaws and risks in a collaborative way. However,

Alliance forms of contract delivery are becoming less common due to the overall perception of reduced client value. Alternatives such as design-and-construct, or design/construct only delivery models involve multiple corporate interfaces which can inhibit collaboration between parties and over-prioritise commercial drivers. As an industry seeking a pathway towards Resilience Engineering, we, as individuals and industry societies, should openly discuss with and encourage project sponsors to engage with collaborative delivery models where parties are incentivised across a range of non-commercial key performance indicators.

Also important is the role of leadership in the prevention of failure. Factors include leadership „authority" and „style" and culture setting. For instance, a culture of blind „obedience to authority" was partly to blame for the Newport disaster. Ultimately, though the underlying philosophy of Resilience Engineering, is not to focus on human error at all, but instead focuses on the ability of the organisation, system or project to overcome people risk.

6 ROLE OF PRODUCTS

Product failures in the sense of conventional forensic engineering commonly relates to the unplanned behaviour of manufactured materials or members which then trigger collapse.

Examples of poor „product" design include Ronan Point apartment building collapse in London in 1967 which occurred due to a localised explosion of a burst gas pipe. The resulting cascading failure of multiple floors highlighted poor design of the prefabricated connections. This concept was also identified as important in the World Trade Centre in 2001, and prompted checking of the capacity of structures against total collapse mechanisms due to explosions.

Arguably, these types of manufactured product failures are an extension of process or people failures, either due to poor design, specification or quality control, or because of inadequate structural redundancy. In the context of this paper, geotechnical failures such as excessive movement or collapse of a structure could be viewed either as either a „product" failure of the ground as a natural material with assumed or interpreted properties; or as a „process" failure of the design to account for the intrinsic variability and uncertainty of the ground and its interpreted properties. For the purpose of this discussion, geotechnical uncertainty is captured and discussed below as a „process", risk rather than a „product" risk.

7 ROLE OF PROCESSES

Unlike other engineering disciplines in which the strength of materials may be well understood, controlled and quality tested prior to and during construction, the ground is a variable material. Conventionally a limited number of investigation locations, such as boreholes, will be undertaken which cover only a small proportion of the overall volume of ground occupied by any project. From this information geotechnical engineers develop an inferred model of the geological conditions and corresponding material properties.

The investigation, design, construction and monitoring process is a well-developed routine applicable to most port infrastructure works, but which has many pitfalls for the unwary. Good design will also consider the robustness or efficient forms of redundancy in a design. This risk assessment process is important, even where design and construction risks have considered and addressed all reasonable standards. Most designers are conscious of providing some additional safety margin or redundancy for critical elements of design which prevent collapse type failure mechanisms. This must be balanced against the cost of such comfort, but it can make a pivotal difference in cases where unforseen loads apply to structures. Examples of poor design process include failures of port structures in Malaga and Barcelona (Del Campo *et al.*, 2011). These caisson structures were postulated to have collapsed due to:

- Lack of information on the in-situ ground conditions below the structures (a theme common to many of the cases in this paper);
- The foundation for the structures were insufficient to transfer applied loads;
- Structural and filling operations being completed by different contractors;
- The nature of reclamation fill was poorly understood and it was placed very quickly to maximise production;
- The sequence of filling caused a "lake" inland of the structures which then unintentionally acted as dams; and
- The tidal and wave variability was not considered during the design.

In both of these projects water had an impact on the failures, both in terms of hydrostatic pressures on a structure and excess pore pressures generated by rapid placement of fill. More active risk and interface management processes and review between designer and contractor would have reduced risk in this situation.

Another significant opportunity to mismanage process risk involves numerical modelling. In recent times the use of sophisticated geotechnical models to assess behaviour of the ground has become routine. However, failures have occurred due to misinformed or incorrect use of complex models, such as the Nicoll Highway Collapse. When considering the results from any model it is useful to consider the anonymous adage that "*All models are wrong - but*

some are more useful than others". Respected Imperial College Professor David Potts (2003) also discussed potential difficulties associated with numerical modelling as follows:

- There is no standard strategy for implementation of nonlinear models;
- Some constitutive models seem to be unable to give reasonable predictions;
- Even for apparently simple problems, the results of numerical modelling can be very dependent on the decisions made by the user;
- Useful numerical modelling requires skilled operators who have a detailed understanding of; soil mechanics, the underpinning theory for the numerical algorithms, limitations of constitutive models and are knowledgeable about the software that is being used.

This is not to say that use of numerical modelling is not an appropriate tool. Rather, reviews should always be completed by experienced practitioners and appropriate benchmarking or independent checks undertaken. Key questions to ask about numerical models include:

- Are we getting the answers that we think we are getting?
- Are we getting the answers that we need?
- Can we justify/understand the results using back of the envelope calculations?

Going beyond deterministic design approaches, reliability-based design (RBD) is a design approach involves evaluation of key input variable uncertainties, enabling the designer to convey to stakeholders the confidence level associated with design outcomes such as stability, settlement, etc. Using RBD is not possible with a working stress design (WSD) approach but rather limit state design. This can require development of numerous sets of input parameters and associated partial factors, which requires greater work on the part of the designer. However, this approach does lend itself to appropriate factoring of a greater variety of load cases and scenarios such as groundwater fluctuation in response to flooding events and earthquakes, both of which are important in geotechnical engineering terms.

Problems such as time-dependent settlement can be framed usefully in probabilistic terms and can provide a rational basis for adopting risk positions on key issues having significant commercial or safety implications. The extra time and effort involved with undertaking reliability based design may be justified where risks are significant. Reliability analyses such as those outlined by Duncan (2000) can be done with relatively little additional effort and provide a logical framework for choosing FoS values that are appropriate for the degree of uncertainty and the consequences of failure.

These methods provide a measure of confidence in the spread of outcomes, noting that probability of failure should not be viewed as a replacement for factor of safety, but as a supplement. Indeed calculation of both factor of safety (FoS) and failure probability is better than computing either one alone. Although neither FoS nor failure probability can be assessed with high precision, both have value and each enhances the value of the other. Hence the use of such sensitivity analyse and RBD approaches aligns well with the notion of Resilience Engineering which requires an understanding of the brittleness of a system (or design) so that appropriate controls can be applied to stay within the optimum areas within the „resilience triangle" (Figure 10).

8 TOMORROW'S WORLD

This section looks at some global and local societal, economic and environmental trends and considers how what risks and opportunities these present to geotechnical and infrastructure engineering. With this in mind, the final sections of this paper look at how these trends may act on geotechnical and engineering practitioners, and how these tensions may be dealt with by adopting Resilient Engineering principles.

8.1 GLOBAL MEGATRENDS

Significant shifts in environmental, economic and social conditions that will play out over the coming decades may be termed a „megatrend". A recent CSIRO study (Hajkowicz, 2012), identified six interrelated megatrends affecting the world and Australia over an indicative time frame of 20 years. These are:

- **Competition for natural resources.** The earth has limited supplies of natural mineral, energy, water and food resources essential for human survival and maintaining lifestyles. In Australia, the population is expected to reach 34m by 2035 (ABS)
- **Biodiversity at risk.** Many of the world's natural habitats, plant species and animal species are in decline or at risk of extinction.
- **Global economic shifts.** Coming decades will see the world economy shift from west to east and north to south (Figure 12).

- **Ageing population.** Australia and many other countries that make up the Organisation for Economic Cooperation and Development (OECD) have an ageing population.
- **Increasing connectivity.** This megatrend recognises increased connectivity where individuals, communities, governments and businesses are immersed into the virtual world to a much greater extent than ever before.
- **Higher expectations.** This is a consumer, societal, demographic and cultural megatrend. There is a rising demand for experiences over products and the importance of social relationships is increasing.

For the purposes of this paper, the Author has added one other trend:

- **Demand for Transport Infrastructure:** In Australia, travel demand will increase by 60% by 2035 (DoIT) and congestion will cost AU$20bn p.a.by 2020.

How are these megatrends and local changes linked to the notion of resilient engineering? Table 1 below, explores some of these issues and what they could mean to engineers in Australia.

Table 1: Megatrends: Challenges and Opportunities for Engineers

Megatrend	*Engineering Risk or Challenge*	*Engineering Opportunity*
Competition for natural resources	• Increasing cost of raw materials to society. • Responsible and ethical development of resources in developing countries with unrest / political constraints (i.e. ebola, ISIL)	• Investment / demand for improved exploration, extraction, processing and generation of energy from conventional fuels. • Investment in new technologies for alternative materials, fuels and energy sources.
Biodiversity at risk	• Challenge to promote genuinely sustainable infrastructure development. • Associated effects of climate change (See Section 8.2)	• Opportunity to re-develop brownfield sites thereby preserving natural habitat. • Greater use of recycled materials. • Factoring in potential effects of climate change to improve robustness and design life (See Section 9).
Global Economic Shifts	• Reducing engineering resilience due to rapid economic development and engineer skills shortages. Example: major infrastructure failures in South Korea in 1990"s.	• Greater harmonisation and collaboration between international consultants and contractors creates shared knowledge and experience. • Increased demand in containerised shipping and associated port facilities. Berth upgrades also required to accommodate larger vessels due to widening of Panama Canal.
Ageing Population	• Reducing pool of taxation and funding for public projects.	• The ageing population and engineering practitioners are an asset who could be engaged as mentors and to disseminate knowledge.
Increased connectivity	• Potential over-reliance / dependency on IT / IM systems to perform safety critical tasks.	• Telecommuting / teleconferencing and associated offset in transport demand and resources use. • Adoption of BIM and associated improved efficiencies, reduced re-work and improved infrastructure versatility (See Section 9.2)
Great expectations	• Society expectations of high levels of transport user satisfaction (journey times reliability, comfort levels) requiring increasing levels of engineering.	• Increasing disposable incomes and access to motor and air travel driving investment in transport infrastructure.
Demand for Transport Infrastructure	• Limitations on Infrastructure development due to 3-4 year Political & Budgetary cycles. • Widening infrastructure gap (Demand Vs expenditure, Figure 13). • Continuing societal demand for reducing transport fatality rates.	• Requirements for other sources of revenue (Private Public Partnerships (PPPs); capture community funds such as superannuation investments; develop new user-based sources). • Innovation to find greater efficiency and durability in design and construction (See example below). • Improvements in transport safety engineering and automated transport systems. Example: Rio Tinto"s driverless trucks have now moved more than 100 million tonnes of earth in the Pilbara.

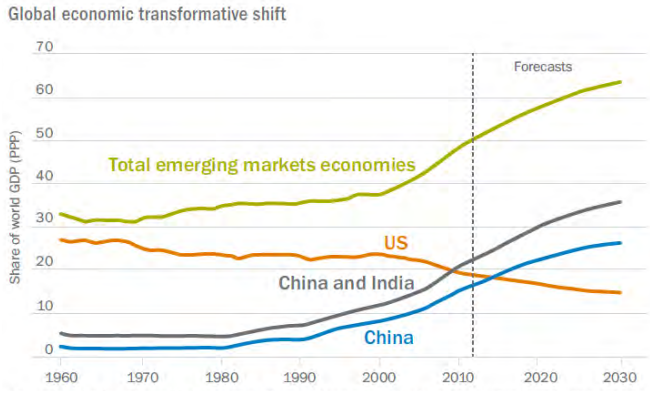

Figure 12: Global Transformative Shift (Source: The Conference Board Economy Database, Maddison (2010).

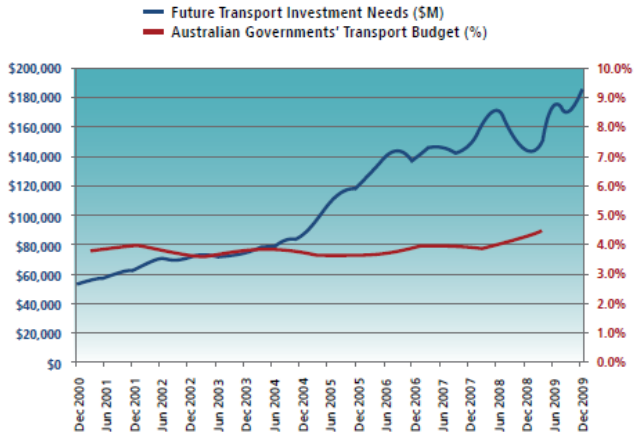

Figure 13: Future Australian Transport Needs (Source: National Transport Commission, Annual Reports).

An over-arching megatrend reaching across those identified above relates to the effects of climate change, the specifics of which are discussed in the Section 8.2, below. This is possibly the greatest single challenge affecting the engineering community (and community at-large) and so an example of the actual and projected challenges associated with extreme weather events and rising sea levels are explored using a real-world example in Section 9.

8.2 CLIMATE CHANGE

Into the future, climate change presents an emerging challenge to performance durability of coastal structures. Research presented in Figures 14 and 15, below suggest that sea level has risen by about 200mm over the last 130 years and may rise between about 200mm and 800mm by 2100. Design standards now incorporate a requirement to consider these impacts in design.

The Intergovernmental Panel on Climate Change (IPCC) has found that warming of the climate system is unequivocal and that anthropogenic greenhouse gases are very likely responsible. Predictive work indicates that this warming will accelerate into the future due to continued anthropogenic greenhouse gas emissions and this will influence sea level. While there is uncertainty about the rate and amount of future rise, there is a high degree of confidence that sea level will continue to rise, and possibly accelerate, over the next century and beyond, through a combination of mechanisms including thermal expansion of the ocean, melting of glaciers and ice caps and changes in terrestrial storage.

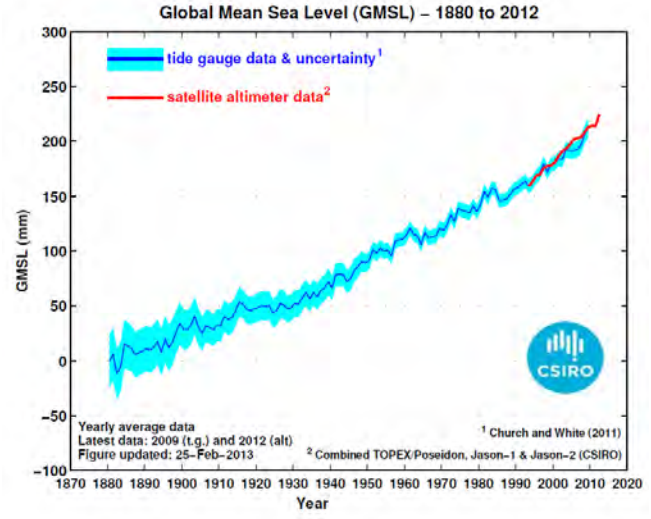

Figure 14: Past Sea Level Rise (Source: IPCC 2007 Fourth Assessment Report).

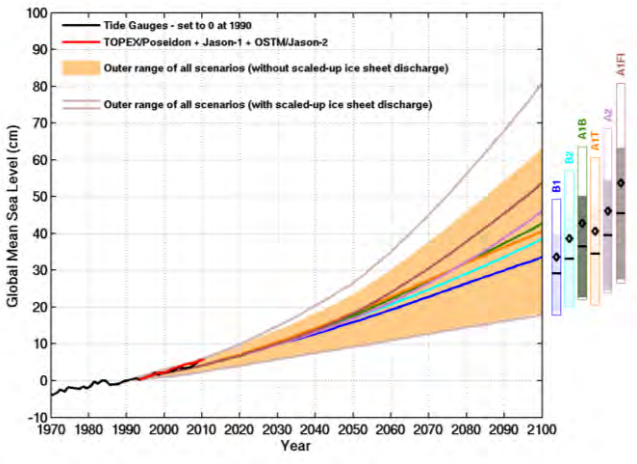

Figure 15: Future Sea Level Rise (Source: IPCC 2007 Fourth Assessment Report).

The three scenarios developed by CSIRO for sea level rise between 2030-2100 (relative to 1990) are presented in Table 2, below.

Table 2: Three global sea-level rise scenarios, 2030-2100 (metres)

Year	*Scenario 1 (B1) Low Rise (m)*	*Scenario 2 (A1F1) Moderate Rise (m)*	*Scenario 3 High Rise (m)*
2030	0.13	0.15	0.2
2070	0.3	0.5	0.7
2100	0.5	0.8	1.1

The potential impacts of sea level rise in Botany Bay are shown graphically in Figure 16. Associated increasing financial impacts of extreme Australian weather events are also shown in Figure 17, underscoring the need to build-in resilience to infrastructure.

Figure 16: Sydney region predicted inundation for Scenario 3 high sea level rise (1.1m) in 2100 (Dept. Climate Change and Energy, 2014).

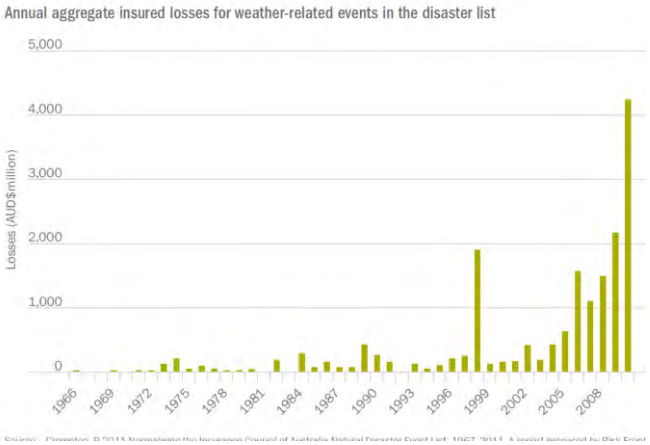

Figure 17: Insured Australian losses due to weather related events (Source: IPCC Fourth Assessment Report, 2007).

Sea level rise is not a static design parameter and is projected to increase over time at an accelerating rate. Given that differing coastal areas, communities and commercial organisations will have varying capacity to adapt to sea level rise, there will be differing "tipping points" beyond which adaptation becomes either uneconomic or unworkable from an engineering perspective. In general, some design flexibility and pre-planning is needed to consider eventualities beyond the timeframe of immediate interest. Typically for significant Australian government projects such as major port upgrades and waterside urban regeneration projects having a design life of 100 or so years, the infrastructure must be designed to accommodate a 0.9m sea level rise.

The challenge for smaller scale local government funded infrastructure or upgrade projects relates to the limited financial capacity of the agencies and developers to overcome these same issues. Coastal engineering options include for one-way flood valves for stormwater pipes intersecting tidal waterways, use of wave deflection capping structures, more widespread use of seawalls and revetment structures and/or use of adaptable, relocatable structures rather than permanent fixtures.

9 REAL-WORLD EXAMPLES OF RESILIENT ENGINEERING

9.1 CASE OF A STORM DAMAGED PORT RE-DESIGNED FOR TOMORROWS WORLD

To illustrate how design choices can impact performance and capacity to withstand adverse environmental design effects of wind and wave action, the published case of a storm damaged port in the Philippines serves as a useful example to explore the notion of resilience. The case history described by Wallis and Sandeford (2007), describes a port development for a new open cut mine which was extensively damaged by a „Super Typhoon" in 2006. Because the facility had a relatively short design life of 7 years, risks were accepted by the designers and owners by designing for a lower return period typhoon event.

A rational approach to the design of structures subjected to intermittent, severe events is to use a statistical approach determine the design criteria for the project structures, based on the economic life of the project. Although the design was strictly code compliant, it was less resilient than assets designed to withstand longer return period (more adverse)

events because it was designed for a lesser, more frequently occurring design load, corresponding to an event having a lower return period. However, on any given day, events equivalent to, or worse than, the designed-for event can happen. As discussed below, the lower the ULS design event severity, the higher the probability that the asset will be exposed to the ULS event, even taking into consideration the reduced design life. In the case of the Philippines port example, an event exceeding the ULS capacity occurred during the life of the structure.

To illustrate the design challenge, it is worth exploring the relationship between typhoon recurrence, design life and how future sea level rises might affect the capacity of existing infrastructure to absorb climatic changes such as sea level rise. Based on published data estimating the return period of typhoon recurrence (Table 3), it is possible to represent this graphically as Shown on Figure 18. In accepting reduced design life, the consequences of losing key assets (such as wharf structures) should be considered and cost-benefit studies for various return periods for various return periods undertaken, remembering that the minimum capital cost may produce the maximum unreliability.

In 2006, a „super typhoon" described as „*the worst for many years*" affected the Philippines port area. Design wind speed for project was 200kmh, and based on report by Guard et al. (1999) this corresponds to a recurrence interval of about 1 in 30 years. It is worth noting that the definition of design speed as recommended by the World Meteorological Organization (WMO) and used by most weather agencies, is the average speed measured over a 10-minute period at a height of 10 m above ground.

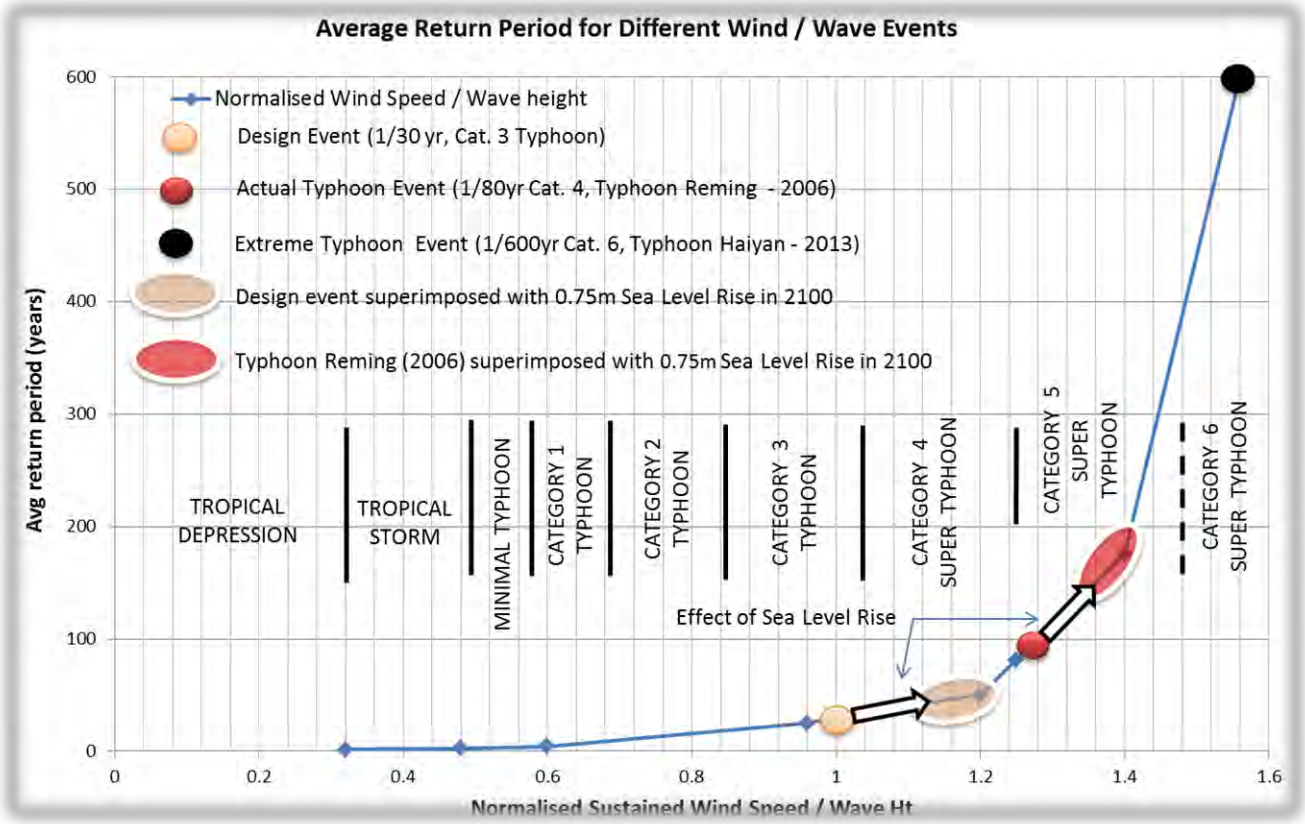

Figure 18: Return Periods for Various Wind Events.

Damage to port infrastructure may be due to combinations of wind and waves, hence the two conditions are often considered separately in design of any particular asset. Considering cranes and revetments, for instance, the capacity of these structures is governed by wind and waves, respectively.

Considering firstly sustained wind speed as a governing cause of damage for the case history in question, it can be seen that the 200 km/hr sustained wind speed design condition approximates to a roughly 1 in 30 year event, based on published data (Guard et al., 1999), as shown graphically on Figure 18. The documented „Super Typhoon" Reming which hit the port in 2006 reached sustained wind speeds of 250 km/hr, which, by interpolation corresponds to an event having a return interval of about 80 years. For comparison, the Super Typhoon Haiyan, known in the Philippines as Typhoon Yolanda in 2013 is also shown in Figure 18. Haiyan was the strongest storm ever recorded at landfall, and unofficially the strongest typhoon ever recorded in terms of wind speed with maximum ten-minute sustained winds at

275 km/h (170 mph), unfortunately killing more than 6,000 people in the Philippines alone. Based on data published by Guard et al. (1999), the estimated return period for this event is 1 in 600 years.

The likelihood of any particular asset experiencing these events in any given period can be assessed using Figure 19, which shows likelihood of events occurring over a range of typical design life intervals. For example, the probability of occurrence of a rare (or severe) event such as Haiyan with a 1/600 year return period would be only 0.05 (5%) over a 100 year design life.

For the case history in question, the design sustained wind speed adopted was 200km/h (1/30 year return period) and this was selected on the basis that the design life was relatively short at 7 years. This puts the probability of occurrence at about 0.21 (21%) in the seven year design life as shown in Figure 2.

When the „Super Typhoon" Reming occurred near the end of construction in 2006 (red dot in Figure 19), this rarer 250km/h wind speed event (1/80 year return period) had only a 8% chance of occurring during the 7 year design life, however, it underlines the principle that adverse events can occur at any time during the design life. The likelihood of the 2013 Haiyan type event occurring would only be about 1%, however, interestingly this also occurred within the 7 year design life of the development (constructed in 2006).

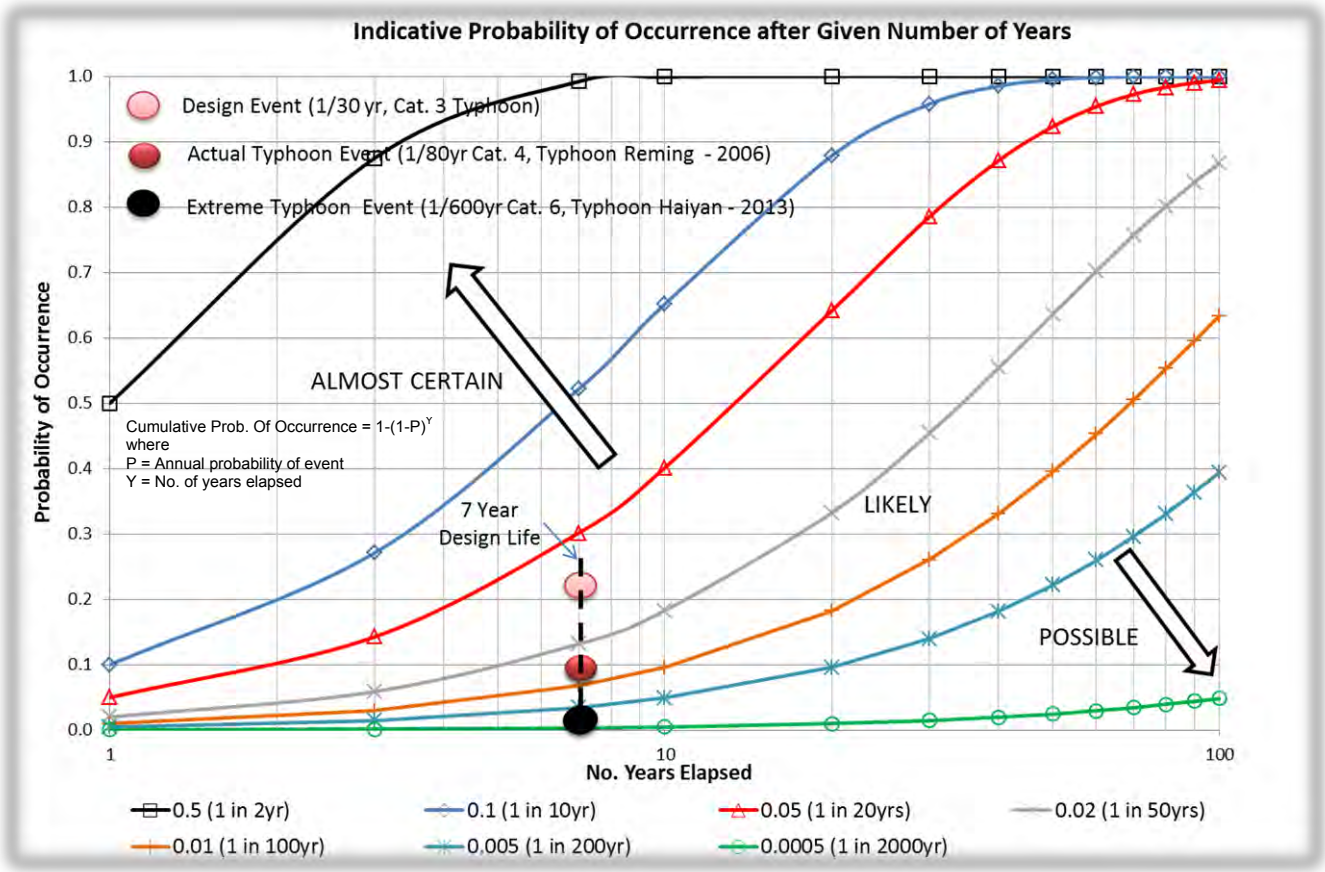

Figure 19: Probability Curves for Various Return Periods and Design Life.

It is uneconomic to design for the worst possible loads if they can rarely happen, but reflecting on the logic of adopting the selected 1/30 year design event for a 7 year design life, the client arguably adopted an unwise risk position. In this case, a cost-benefit assessment of designing for the 1/80 year event may have shown this to be a relatively good return on investment.

In general terms, risk is defined as the product of hazard/likelihood and consequence and this is the basis of what is often called the hazard-consequence matrix approach for risk assessment in either a qualitative or a quantitative context. One only needs to refer to the various National Standards, such as the Australian Standard on Risk Management (AS/NZS 4360:2004) which was first published in 1995. The Australian Geomechanics Society has developed a specific landslide risk management document entitled „Landslide Risk Management Concepts and Guidelines". This can be illustrated using the semi-quantitative framework published by the AGS (2007). Assuming that the infrastructure ultimate limit state (ULS) condition is designed for the same outcome (i.e. damage is limited to „Medium"; unserviceable, but not destroyed), then the relative risk of designing for a range of events is presented in Table 3.

Table 3: Comparison of Risk Outcomes for Varying Design Events

Design Event	*Return Period*	*Probability during 7 year design life[1] (%)*	*Annualised Probability (%)*	*Likelihood Category[2]*	*Target ULS Consequence Category[2,3]*	*Risk Category[2]*
Adopted design event (period 2006 to 2014)	1/30yr	21	3	Almost Certain	Medium (Low cost to achieve)	Very High
Super Typhoon Reming (2006)	1/80yr	8	1	Likely	Medium (Moderate cost to achieve)	High
Super Typhoon Haiyan (2013)	1/600yr	1	0.1	Possible	Medium (High Cost to achieve)	Moderate

1. From Figure 2.
2. Risk framework taken from AGS Risk Management Guidelines, 2007.
3. „Medium" Consequence defined as Moderate damage to some of structure, and/or significant part of site requiring large stabilisation works.

Table 3 shows that the position adopted by the client in the case history was a „Very High Risk", defined in AGS as "*Unacceptable without treatment. Extensive detailed investigation and research, planning and implementation of treatment options essential to reduce risk to Low; may be too expensive and not practical*." Ultimately, in the case study presented here, the additional cost of carrying out the repairs before production (and thus revenue generation) was possible, but imposed considerable financial strain on the company.

If the client had chosen to invest in a more conservative risk position by designing the works to withstand the more adverse Typhoon Reming event which eventuated during the relatively short 7 year design life, then using this framework, the risk category would be „High", defined as "Unacceptable without treatment. Detailed investigation, planning and implementation of treatment options required to reduce risk to Low." With a cost-benefit analysis, this may have been a more attractive outcome for the client and project investors. Adopting the most conservative position of design for an extreme event like Haiyan, the Risk outcome reduced to „Medium", defined by AGS as "*May be tolerated in certain circumstances.. but requires investigation, planning and implementation of treatment options to reduce the risk to Low*." Given that the subject site was a mining type infrastructure project involving a relatively high initial capital investment followed by a slow revenue increase over a limited production life, the up-front investment required to achieve the safest outcome may have been too expensive.

As summarized in Wallis and Sandeford (2007), key points to consider relating to the risk position adopted in relation to weather events are:

- Consequences to project continued viability if an important facet (such as the export wharf) is closed down by an event outside the adopted design criteria;
- Additional cost of designing for a higher return period;
- Consider a cost-benefit study for various return periods before selecting the design standard to be adopted; and
- Remember that minimum cost may produce maximum unreliability.

Considering associated wave impacts on this type of port infrastructure and the potential for future sea level rise due to climate change, it is also possible to explore how the vulnerability of existing assets may change, and also how future projects may need to be designed to incorporate resilience to accommodate environmental change. Recognising that the relationship between wind speed and wave impact is complex and depends on many factors including the sensitivity of assets to each variable, the effects of sea level rise can be approximated using the simplistic assumption that that design wave heights are proportional to sustained wind speed. Hence, assuming that the „base case" design wave heights adopted for the published case history of 6.4 m (berth) and 3.8m (reclamation) correspond to the 1/30 year return period „base case" design wind speed event, then it is possible to estimate the change in risk by scaling these cases to other scenarios including extrapolation for sea level rise. Hence, normalising for the 1/30 year return period wind event and calibrating the design wave event against it, various other wave events can be scaled according to the relative size and recurrence of corresponding wind events.

Adopting a 800 mm rise in sea level from Figure 15, and correcting by 50 mm to account for the estimated rise that has already occurred since the 1990 benchmark, the effect of a 750 mm sea level rise to the year 2100 can be estimated by adding this elevation change to the design wave heights, above. This is an approximate approach because the majority of damage associated with wave action would be due to wave energy which is a function of wave height rather than wave level; however, superimposing sea level rise on storm events would undoubtedly have adverse effects considering

storm surge and flooding. Although not considered here, research work by Palmer and Räisänen (2002) suggests that the likelihood of future extreme weather events may also increase, which would be additive to the effects of sea level rise. Based on their probabilistic analysis of 19 global climate model simulations with a generic binary decision model, they estimated that the probability of total boreal winter precipitation exceeding two standard deviations above normal will increase by a factor of five over parts of the UK over the next 100 years, and that there would be corresponding implications for flooding in Bangladesh.

Assuming the impacts of wind and waves are equivalent in terms of damage potential for comparison purposes, then the normalised effect of increasing the design wave height due to sea level rise from are shown graphically in Figure 18. It can be seen from this plot that the effect of future sea-level rise (taken as being synonymous with increase in wave height when superimposed with any given event) is to move up the characteristic curve and effectively up-scale the impact of any given event in today"s terms. Adopting this simplistic approach, the estimated amplifying effects of sea level rise on storm events on two assets published in the Wallis and Sandeford case history are summarised in Table 4.

Table 4: Comparison of Risk Outcomes for Varying Design Events

Asset	*Design event Return Period*	*Estimated Wave Height (Normalised)*	*Sea Level Rise, SLR (Year 2100)*	*Design Wave Height + SLR (Normalised)*	*Equivalent Design Event Return Period (inc SLR in year 2100)*
Berth Structure	1/30 yr (Design Base Case)	6.37m (1)	0.75 m	7.12 (1.12)	1/50yr
	1/80 yr (Typ Reming 2006)	7.96 m (1.25)	0.75 m	8.71 m (1.38)	1/150 yr
	1/600 yr (Typ Haiyan 2013)	9.94 m (1.56)	0.75 m	10.69 m (1.68)	1/700 yr
Reclamation	1/30 yr (Design Base Case)	1 (3.80m)	0.75 m	4.55 m (1.20)	1/70 yr
	1/80 yr (Typ Reming 2006)	4.75 m (1.25)	0.75 m	5.50 m (1.45)	1/230 yr
	1/600 yr (Typ Haiyan 2013)	5.73 m (1.56)	0.75 m	6.68 m (1.75)	1/1000 yr

SLR – Sea Level Rise

Table 4 shows that for reclamation structures in this region, the adverse effects of sea level rise (and inferred wave height) could result in having to design for events having return periods two or three times longer than anticipated without these future effects.

9.2 SAFETY IN DESIGN

A relatively new requirement of designers in Australia and internationally is the need to consider Safety in Design (SID). In Australia, this requirement became mandatory from 1st January 2013. The legislation requires that designers of all new structures and renovations report on the health and safety aspects of the design (a „Safe Design Report"). In addition, the designer is required to ensure „as far as is reasonably practicable", that a structure is designed to be without risks to the health and safety of direct users or those impacted by the works. A recent example of safety in design failure relates to an incident at the Italian Port of Genoa. Nine people were killed after the container ship „Jolly Nero" collided with a control tower. Here, it is immediately apparent that the tower position and lack of protection against ship collision (Figure 20) was a major SID shortcoming.

Figure 20: Port of Genoa Control Tower before and after incident (Source: Sydney Morning Herald, The Australian).

9.3 A CASE FOR REPAIRABILITY LIMIT STATE

The notion of a „repairability" or „damageability" limit state, is a performance based design criterion intermediate between serviceability and ultimate limit states and is becoming increasingly recognised as a way of providing resilience at reasonable cost. This approach specifies that the design is governed by limiting movements or other agreed metrics whereby the repair cost corresponding to the damage of the structure is within an acceptable repair cost and/or economic loss.

Functional objectives are to provide continued viability of structure with some interruption of service. This may involve limited damage to non-structural elements or contents and repairable damage to structure. In terms of structural performance, stresses would be anticipated as being above the elastic limit with displacements and slightly bigger than damage threshold. These concepts are most commonly applied to earthquake resistant design, which sometimes involve a further breakdown of limit states and structural importance categories.

For instance, the Structural Engineers Association of California suggests categories of „Fully Operational", „Operational" (light damage, economically repairable"), „Life-Safe" (repair possible but may not be economically practical) and „Near Collapse" (structural collapse prevented, repair not possible). Potential occupancy types include „Safety Critical" facilities (nuclear power stations), „Essential" facilities (hospitals, emergency services) and „basic facilities" (all other structures). The appropriateness of using design categories for varying event magnitudes can be expressed as a matrix as shown below in Figure 21.

Damage to a Structure ⇨

Magnitude of Actions ⇩

	Serviceability Limit State	Repairability Limit State	Ultimate Limit State
High frequency, low impact	Δ∞□		
Medium frequency, medium impact	Δ∞	□	
Low frequency, high impact		Δ	∞□

Note: Δ Important Structure ∞ Ordinary Structure □ Repairable Structure

Figure 21: Concept of Repairability State (data sourced from Honjo, 2010).

By way of example, in relation to a seismic design on a recent port project, a minimum L.E. safety factor of 1.1 was specified for seismic global, sliding, overturning and liquefaction. Seismic bearing capacity requirements were not explicitly specified by the owner but were discussed and developed during detailed design. Design requirements included completion of a site-specific seismic hazard study; design for serviceability and ultimate design earthquake events of 1 in 100 („serviceability earthquake") and up to 1 in 1000 („ultimate earthquake") annual exceedance probability (AEP), respectively. Dynamic analyses considering spectral shape factor, soil dynamic and inertial loading were also required for design (Figure 22).

As design progressed, discussions ensued around tolerable safety factors for seismic bearing capacity because the apparent global bearing capacity factor of safety was relatively low (less than 1.5). This included debate on the appropriate use of input motion, appropriate factoring of peak acceleration values and the applicability of conventional (simple) bearing capacity theory for the design of gravity retaining walls including concepts of local yielding. The designers argued that full bearing failure could not develop without invoking a fully global mechanism, and that consideration of local bearing pressures, toe yielding and corresponding wall movements were more rationally assessed using dynamic analyses rather than a simplistic bearing factor of safety.

The dynamic gravity wall behaviour was typified by localized yielding at the toe and heel regions of the counterfort structure, characterized by the occurrence of plastic failure within a PLAXIS finite element model. The predominant mode of movement behaviour under earthquake loading was found to be translational rather than rotational (tilting). Critical seismic crane gauge displacement criteria were subsequently developed from these analyses.

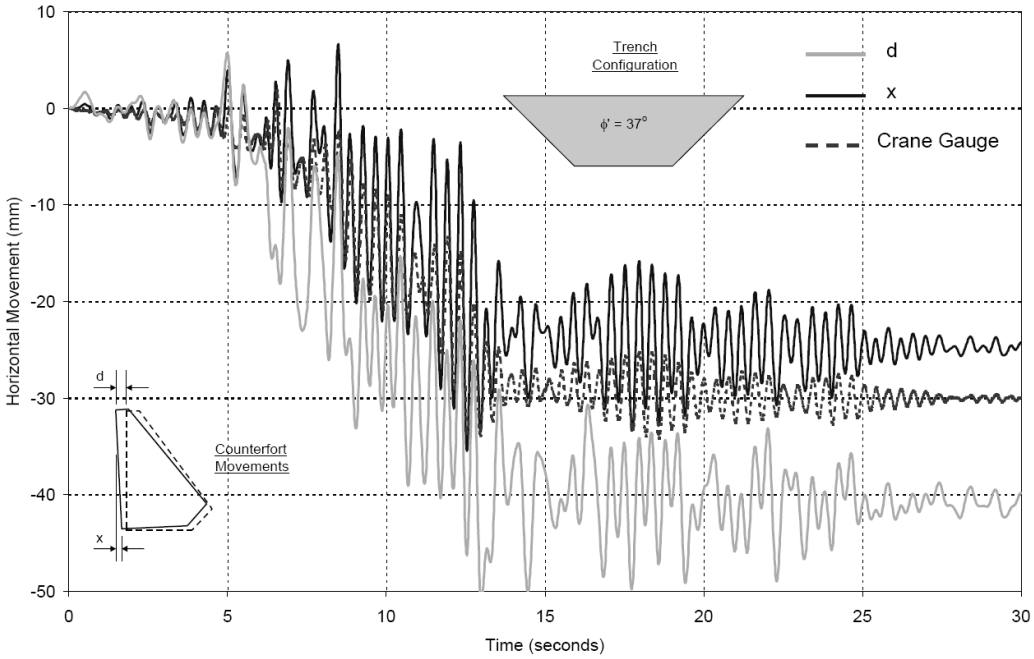

Figure 22: Dynamic Analysis of a Quay Wall Struture.

The design team successfully argued for a displacement based approach to design in lieu of an agreed factor of safety for seismic global bearing. This displacement-based seismic design enabled the client to make informed, risk based decisions around the notion of tolerable movements, damage and operational outcomes such as crane gauge movement and potential cost of repairs under different event scenarios.

9.4 GEOTECHNICAL DATA MANAGEMENT AND BUILDING INFORMATION MANAGEMENT (BIM)

In future, as the data demands on engineering projects of increasing size and complexity grow, there is an emerging need to build in scalable information sharing systems which allow remote access and sharing across diverse design and construction teams. Indeed, failing to provide such information management tools leads to potential risk related to delay, obsolete information, clashes and re-work.

Smart infrastructure in the form of digital technologies provides opportunities to improve productivity and contribute to sustainability. For example, in recent years road-mounted camera and sensor systems can detect congestion, collisions and road works, providing motorists with alerts and re-routing suggestions, reducing travel times, reducing fuel consumption and energy demand. For example, coordinated signals on Melbourne‟s Monash Freeway have saved 16,500 litres of petrol and led to a 40 tonne reduction in greenhouse gas emissions a day, as well as rerouting traffic, at a relatively low cost. This is a good example of how adaptive technology and feedback process can be utilised to improve the utility of existing infrastructure assets.

Starting with geotechnical data management, Child et al. (2014) describes how the traditional paper based investigate-report-design approaches can be significantly improved by efficiencies gained through centralization of data and integration across collaborative platforms. Furthermore, work by Chandler (2014) explores linkages between geotechnical data management and increasingly widespread Building Information Management (BIM) systems. BIM is gaining global popularity as a value creating collaboration through the entire life-cycle of an asset, underpinned by the creation, collation and exchange of shared 3D models and intelligent, structured data attached to them.

A graphical example of the transformation of geotechnical data management is shown in Figures 23 and 24 below. The representation shows a move from the sequential reporting process in Figure 23 towards a more fluid process whereby centralised data is constant, allowing controlled collaboration with other disciplines. In this way, the various stages of geotechnical investigation, model development and refinement, site characterization, interpretation and design inputs can be advanced and updated in parallel, where appropriate using relevant using visualizations generated by 3D and GIS packages linked to the same cloud-based data source. As a legacy, this data can also be made available in the form of a digital archive providing a repository of easily accessible as-built information, thereby adding resilience in the form of capacity to upgrade and avoid clashes.

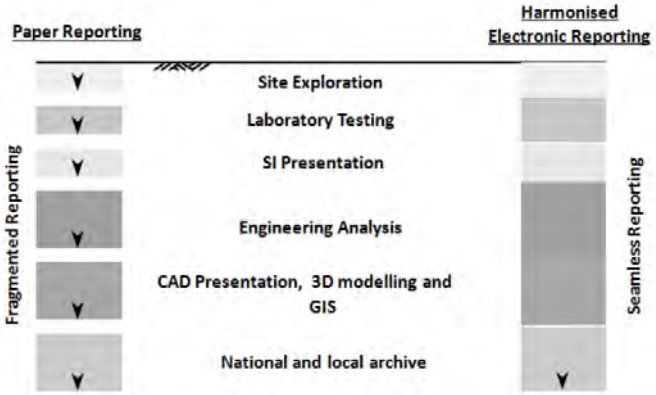

Figure 23: The traditional geotechnical data journey (Source: Chandler and Hutchinson, 1998)

Figure 24: The future of geotechnical data management (Source: Child *et al*. 2014).

Although the concept of BIM (coined in 1992) pre-dates the relatively recent advancements in geotechnical data, it has taken some time for government policies to create key driver for its use on major infrastructure projects. In 2011, the UK Government announced that all publicly funded infrastructure projects must integrate collaborative 3D BIM (with all project and asset information, documentation and data being electronic) into major projects within an overall push to introduce 20% savings across the construction industry by 2016 (estimated as £1-2.5 billion per annum). Beyond this, BIM will potentially deliver greater value in the post-construction phase, through improved ongoing management of assets at individual, portfolio and national levels by allowing for the modelling and optimization of running costs, improving energy efficiency and reducing carbon emissions – in other words improving infrastructure resilience.

The benefits of supply-chain integration in the construction sector are largely understood in terms of performance improvement, greater project „certainty" and reduced risk. One of the key factors in achieving successful integration in design and delivery is the accuracy, effective flow and intelligent use of information, which BIM facilitates. These concepts are well aligned with Resilience Engineering philosophies.

The BIM process encourages the development and exploitation of centralized digital models enabling greater interdisciplinary collaboration, increased efficiency and optimised project performance with reduced mistakes, clashes and re-work. The general features of BIM types are described in terms of the number of model „dimensions" (2D, 3D, 4D, etc). These are briefly described below:

- 2D – 2D Models containing flat drawing, line images or CAD renderings which depict geometric construction elements.
- 3D – 3D Models including walkthroughs, clash detection, project visualisation, virtual mock-up models, prefabrication.
- 4D – Models with the additional dimension of time. By adding „time" to the information in the project model, it is possible to review the construction of the building as it progresses. For large complex projects or those on challenging sites, this can be particularly useful as it can be used to examine critical path activities, logistical issues such as deliveries and craneage, and to assist with building methodology.
- 5D – Models with the additional dimension of Cost. The ability of BIM models to contain cost information and quantity schedules allow costings for a given design to be produced faster; allowing option appraisals, accelerated iterative design processes and budget control.

Integration of geotechnical „layers" into BIM systems are generally focused at the 3D level as time and cost dimensions tend to reside in the realm of construction management and delivery. The benefits of moving away from a sequential reporting-design-drafting design framework towards a collaborative design process accessing shared information is shown schematically in Figure 25 below. Considering curve 1, in a typical traditional project, as progress moves from preliminary design to documentation and into construction phases, the ability to impact the costs and functional capabilities declines, and inversely (curve 2) the costs of such changes are greater with time. The majority of team efforts enabled by CAD peaks during the construction documentation phase.

In a collaborative design process, key participants are brought in earlier, and clear goals are set and the preferred design process (curve 4) shifts efforts to an earlier point in the design cycle, spending more time up front to make better design

decisions. With this process, using BIM as a catalyst, construction documentation becomes a by-product of the design effort. Adoption of this type of process where more cost and effort is spent earlier in the project will lead to an overall increase in efficiency and optimised project performance.

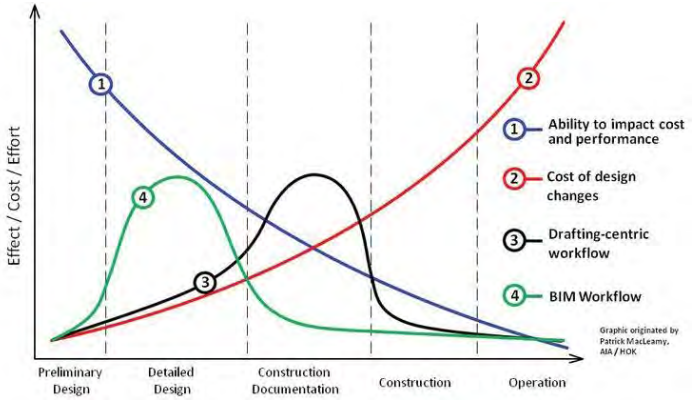

Figure 25: Design Process Curve (Source: Patrick MacLeamy, AIA/HOK).

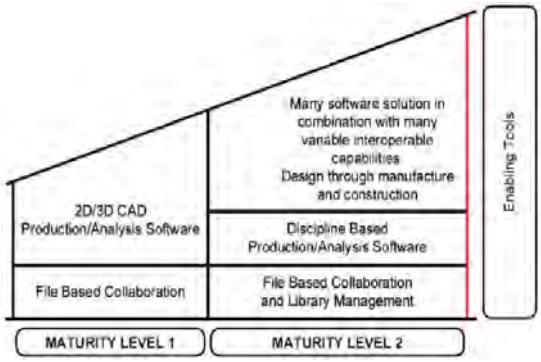

Figure 26: Summary of BIM Level framework (Source: adapted from www.bimtaskgroup.org/).

The various levels of BIM sophistication are measured in Maturity Levels (0 to 3) after the Bew-Richards BIM maturity model. The maturity model is also used to define the supporting infrastructure required at each level of capability (Figure 26). The UK government expects all public contracts to run to BIM level 2 in 2016 and onwards, as standard.

With investment only required in a limited number of digital-tools, BIM is available to anyone because principally it is more a way of working than a fixed system or product. It is the process of information modelling and information management in a team environment. Examples of Geotechnical processes could include the provision of instructions to drillers, transferring data from hand-held devices on site, remote monitoring and client access. Depending on permissions, these can create a new level of transparency and service across key stakeholders.

The availability of geotechnical information across BIM platforms during the whole process from conception, to design, construction and maintenance provides a positive risk management tool, as demonstrated by its recent use in the UK in relation to the M25 motorway project in the UK (after Chandler *et al*. 2014). The M25 motorway that circles London is one of Europe's busiest highways. In 2009, England‟s Highways Agency awarded a AUD$10 billion contract to the Connect Plus consortium for future development, operation and maintenance of the M25 motorway. BIM was adopted to help accelerate the widening contract to enable opening for the 2014 London Olympics.

Tenderers for the M25 project had access to all geo-environmental data via an on online data-room integrated with the BIM compatible Highways Agency Geotechincal Data Management System (HA GDMS). HA GDMS is the principal tool for the management of geotechnical hazards and risks throughout the full life-cycle of the UK highway network from initial feasibility studies, through design and construction, into operation and towards decommissioning or redevelopment. This is by definition a continuously improving, resilient engineering system. The system contains a national model of all highways-related geotechnical assets and boreholes held by the HA and their agents, including mapping, aerial photographs and LIDAR. Related to the model are geotechnical reports, geotechnical inspections and maintenance records.

Integrating this HA GDMS data with a BIM system achieved the following benefits which helped meet the aggressive design-build schedule:

- The integrated design model helped the team visualize all above ground and underground components key elements (like retaining walls) and also related safety and access zones.
- Improved understanding of critical space constraints producing a coordinated, accurate design model allowing construction of several new cuttings and embankments under tight tolerances, while maintaining 3 lanes of live traffic in each direction during construction.
- Elimination of potential clashes between geometrically complex new elements and existing assets were identified that would otherwise be very difficult to detect using 2D documentation.

- Rapid access to critical BIM model allowing re-design and just-in-time design change ordering to optimise cost and schedule related to extensive use of steel sheetpiling.
- At construction stage, updating of the design model to incorporate additional as-built elements including new retaining walls, point clouds from laser scans, and temporary works.
- Linking the project team, including on-site construction personnel, with a consolidated, accurate construction model meaning that everyone could access the same up-to-date project information.

Ground modelling always requires interpolation and judgment when interpreting geotechnical conditions and ground risk. Work required to identify and manage geotechnical risk by ground engineers would be the same without BIM. However, the platform provides tools to assist with the understanding and sharing of this information. Ground modelling is a process of gradual refinement, often requiring multiple phases of investigation. With an initial model in place, BIM can assist with design of ground investigations and quantities for geotechnical structures and earthworks. Setting-out data can then also be fed directly into surveying equipment or extracted as 2D/3D drawings.

10 CONCLUSIONS

This paper reflects on past, present and potential future engineering demands and practices which respectfully weaken or enhance the creation of resilient infrastructure. The desired state of a resilient engineered system, project or organisation may be described as the ability of that entity to adjust its functioning in response to changes while satisfying performance, economy and safety objectives.

Remembering the ancient philosophy quoted earlier in this paper that the acquisition of wisdom involves silence, then listening, commitment to memory, practice, then teaching others, the selected case histories presented above describe the journey from trial and error based approaches towards Resilience Engineering.

Valuable lessons are shared from the past which continue to shape how geotechnical practitioners manage in-ground risk today. Linear systems of safety engineering such as Reasons Swiss cheese model and Turners incubating accidents model identify potential contributory factors in failure including misguided beliefs, decoy phenomena, information-handling difficulties, failure to comply with regulations and a tendency to minimize emergent danger.

As explored in the case history of a storm-damaged port, Resilience Engineering (as it applies to infrastructure), can apply directly to the capacity of fixed assets to absorb change. However, as case-histories show, the concept is perhaps more influential in the hands of organisations and individuals that design, construct and operate those assets, considering the people, products and processes that are involved through the project life cycle. Rather than placing multiple barriers to risk, adverse outcomes can be more effectively mitigated by recognising and enhancing the positive capabilities of people and organizations that allow them to respond to risk effectively and safely under pressure.

More recently, Resilience Engineering has emerged as a natural evolution from the principles of safety engineering and organizational reliability. Successful, highly reliable engineering organizations (and individuals) of the future will become skilled at the following basics of Resilience Engineering:

- Detecting signs of increasing organizational risk, especially when production pressures are intense or increasing – i.e listening for the „sound of the bus coming“;
- Having the resources and authority to make extra investments in safety at precisely these times when it appears least affordable; and
- Having a means to recognize when and where to make targeted investments to control rising signs of organizational risk and re-balance the safety and production trade-off.

These resilience-enhancing mechanisms may help produce an organization or project that creates foresight about changing risks before failures occur, by offering new directions for measuring and maintaining safety in complex systems. Furthermore, Resilience Engineering looks for ways to enhance the ability of systems, or more widely, organizations, to monitor and revise risk models and create processes that are robust yet flexible.

Key recommendations for Resilient Engineering are presented and include:

- Application of Resilience Engineering principles which aim to satisfy the three competing requirements of performance, safety and economy. Established and emerging tools include safety in design, BIM, safety in design and monitoring systems.
- Maintaining vigilance against the common „incubating factors“ arising from risk sources being „3Ps“, being people, processes and products.

- Considering in design increasingly adverse environmental effects such as extreme wind and wave events, selecting appropriate return intervals and selection of design events to manage risk over the range of conditions (including climate change) expected over the design life.
- Taking into account other global megatrends such as demographic changes, regional economic shifts, biodiversity and the continuing demand for transport infrastructure.
- Consideration of performance or reliability based design approaches and repairability limit states on larger projects where critical assets must be designed to remain functional, and where governing issues may relate to managing damage and repair costs. These can provide a logical framework for understanding the confidence of predicted movements and safety outcomes (serviceability and stability) and can also help with understanding of design „brittleness".
- Moving geotechnical data management to cloud-based, collaborative platforms which are refined over the full life-cycle of projects from initial feasibility studies, through design and construction, into operation and towards decommissioning or redevelopment. This is by definition a continuously improving, Resilient Engineering system.
- Learning and teaching lessons from case histories. This will continue to be highly important to the ongoing development of geotechnical engineering and particularly in port and maritime projects. Knowledge sharing, lessons learnt registers and forensic study are all elements of a designer"s toolbox.

Dealing effectively with geotechnical risk on infrastructure projects presents challenges to designers, builders, owners and operators alike. Common issues include large and important assets sited in challenging sites where waves and water play a dynamic role. As individuals and organisations involved in the design, construction or procurement of port assets, we are all risk managers and should strive to challenge embedded assumptions and uncertainties and adopt these principles of Resilience Engineering.

11 ACKNOWLEDGEMENT

This paper builds on previous work which was developed closely with my good friend and colleague James McIlquham.

12 REFERENCES

Australian Geomechanics Society Landslide Taskforce, *Practice Note Guidelines for Landslide Risk Management*, Australian Geomechanics, March 2007, Vol 42 No 1.

Australian Government Department of Infrastructure and Regional Development, *Trends Infrastructure and Transport to 2030*, 2014, http://www.ags.org.uk/publications/GoodPracticeGuidelines.pdf

Brindle, S., *Brunel: The Man Who Built the World*, 2013, Hachette, UK.

Burland, J.B., *The teaching of soil mechanics: a personal view,* Proceedings of the European Conference on Soil Mechanics, 1998, 3:1427-1448.

Chandler, R. and Hutchinson, R. *Formatting for the Future*, Geotechnics for Developing Africa: Proceedings of the 12th regional conference ISSMGE, 1998.

Chandler, R.J., McGregor I.D., G R Morin, http://www.keynetix.com/wp-content/uploads/2013/07/ChandlerMcGregorMorinFinal.pdf

Child, P., Grice C Chandler R, *The Geotechnical Data Journey – How the Way We View Data is Being Transformed*, Information Technology in Geo-Engineering, 2014, D.G. Toll et al. (Eds.) IOS Press.

Chowdhury, R. and Flentje, P., *Perspectives for the future of Geotechnical Engineering*, Proceedings of the International Conference on Civil Engineering For the New Millennium: Opportunities and Challenges, Bengal Engineering College, Shibpur, India, 2007.

Davies, P., McIlquham, J., Port Geotechnics – What Failures Can Teach Us, Coasts & Ports 2013 Conference, National Committee for Coastal and Ocean Engineering, Engineers Australia, PIANC and IPENZ, 2013.

Dekker, S., Hollnagel E., Woods D., Cook R.., *Resilience Engineering : New directions for measuring and maintaining safety in complex systems*, Final Report, November 2008, Lund University School of Aviation

Del Campo, *et al*. *Failures of Harbour Walls at Malaga and Barcelona*, Bulletin of Engineering Geology and the Environment 2011, 70, pp 1-6.

Duncan, J.M., *Factors of safety and reliability in geotechnical engineering*, Journal of Geotechnical and Geoenvironmental Engineering, 2000.

Furuta, K., Presentation on *What is Resilience Engineering ?*, Resilience Engineering Research Center, 2014, www.cse.sys.t.u-tokyo.ac.jp/furuta/teaching/resilience/resilience.pdf.

Godfrey, P. *Control of Risk – A guide to the systematic Management of risk from construction*, CIRIA Special Publication 125, 1996.

Guard, C., Hamnett M., Neumann C., Lander M., Siegrist Jr. G., *Typhoon Vulnerability Study for Guam*, Water and Environmental Research Institute of the Western Pacific (WERI) at the University of Guam, 1999, Report Number: 85.

Hajkowicz, SA, Cook H, Littleboy A. *Our Future World: Global megatrends that will change the way we live*. *(2012 Revision)*. CSIRO, 2012.

Heyman, J., Villard, Vitruvius, Honnecourt V.D., *How to Design a Cathedral: Some Fragments of the History of Structural Engineering*, Proceedings of the ICE - Civil Engineering, 1992, Vol 92, pp 24 – 29 http://www.icevirtuallibrary.com/content/article/10.1680/icien.1992.18045

Hollnaegl, E., Nemeth C.P., and Dekker S., *Resilience Engineering Perspectives*, 2008, Ashgate.

Hollnagel, E., Woods, D. D. & Leveson, N. C. (Eds.) *,* 2006 Aldershot, UK: Ashgate.

IPCC, *3rd Assessment Report*, 2007.

Jarvis, A., *Investigating nineteenth century dock construction disasters*, Proceedings of the ICE - Forensic Engineering, 201, Volume 164, Issue 3 Volume 164, pages 109 – 115.

Lloyd, T., Orbach J., Scourfield R., *The Buildings of Wales – Pembrokeshire*, 2004, ale University Press.

Morin, G., Hassall, B., Chandler, R., *Case study - The real life benefits of Geotechnical Building Information Modelling*, Information Technology in Geo-Engineering, 2014, D.G. Toll et al. (Eds.), IOS Press,

Musson, R., *The seismicity of the British Isles to 1600*, British Geological Survey Open Report, 2008, pp 102.

Mylius, A., *Design and construction failures caused Singapore tunnel Collapse*, NCE Magazine, 2005.

Palmer, T.N., and Räisänenhttp://www.nature.com/nature/journal/v415/n6871/full/415512a.html - a2 J., *Quantifying the risk of extreme seasonal precipitation events in a changing climate*, Nature, 2002, 415, 512-514, doi:10.1038/415512a

Peck, R.B., *Advantages and limitations of the observational method in applied soil mechanics*, Geotechnique1969, 19, No. 1, pp. 171-187.

Potts, D.M., *Numerical analysis: a virtual dream or practical reality?*, Geotechnique, 2003, 53, 6, pages 535–573.

Rasmussen, J., *Risk management in a dynamic society: A modelling problem,* Safety Science, 1997, 27(2/3), pp183-213.

Reason, J., *The Contribution of Latent Human Failures to the Breakdown of Complex Systems*, 1990, 327 (1241), pp 475–484.

Rosness, R., Guttormsen, G., Steiro, T., Tinmannsvik, R.K., & Herrera, I.A., *Organisational accidents and resilient organizations: Five perspectives (Revision 1)*, 2004, Report no. STF38 A 04403. Trondheim, Norway: SINTEF Industrial Management.

Skempton, W., Chrimes M.M., *Thames Tunnel: geology, site investigation and geotechnical problems*, Géotechnique, 1994, Vol. 44 PG 191 – 216, http://www.icevirtuallibrary.com/content/article/10.1680/geot.1994.44.2.191

Structural Engineers Association of California, *Vision 2000 - A Framework for Performance-based Design*, California Office of Emergency Services, 1995.

Turner, B.A., and Pidgeon, N.F., *Man-made Disasters*, 2nd Ed, Oxford, Butterworth-Heinemann, 1997.

Worden, K. *et al*., *The fundamental axioms of structural health monitoring*, Proceedings of the Royal Society, 2007, Vol. 463 No. 2082, pp 1639-1664.

NORTH STRATHFIELD RAIL UNDERPASS
A ONE PASS SYNTHETIC FIBRE REINFORCED SHOTCRETE LINING FOR A VERY SHALLOW COVER TUNNEL

M. C. Kitson[1] and E. J. Nye[2]
[1,2]*Mott MacDonald Australia Pty Ltd*

ABSTRACT

The single track North Strathfield Rail Underpass (NSRU) consists of two dive structures either end of a 148m long driven tunnel. The underpass is for diesel hauled freight trains up to 1.5km in length. The tunnel excavation dimensions are 7 to 8m in height and 9m in width with has a horseshoe shaped profile. The permanent tunnel structural lining consists of synthetic fibre reinforced shotcrete. The ground cover over the crown of the tunnel varies between 2.5m and 3.5m. The ground profile is predominately Ashfield Shale with graded weathering from the surface to fresh shale. Finite Element analysis, calculated the stresses in the shotcrete lining, was also used to assist in predicting surface settlements. Apart for the initial steel canopy tubes no other steel support is installed in the driven tunnel (a first for civil transport tunnel in Australia). A repeated grid pattern of thirty-five grouted 12m long fibreglass dowels ensured tunnel face stability. The tunnel face was mapped daily. The 12m long canopy tube array installations are staggered relative to the 12m long face dowels by 4.5m. The excavation/shotcrete support cycle advanced in increments and the next cycle cannot commence until the initial 150mm thickness of shotcrete has reached an early strength of 6MPa. Early strength measurements of the shotcrete are a vital part of the construction. At the tunnel face, to support the train live loads, there are three levels of redundancy, the canopy tubes, the shear capacity of the ground slot to the surface and the structural/deflection capacity of the rails. The synthetic fibres in the shotcrete provide shrinkage crack control, residual strength if cracking occurs due to deformation and enhanced durability of the tunnel lining compared any alternative using steel such as steel lattice girders(and with no electrical stray current issues). Both the macro and micro synthetic fibres (the latter in the final 100mm fire protection layer placed over a spray-on waterproofing membrane) will reduce potential fire event related shotcrete spalling. Surface settlement minimisation relies on the construction methodology with the shotcrete over the arch always being very close to the tunnel face not allowing the ground to relax. Real time surface settlement monitoring was carried out using robotic scanning theodolites aimed at reflective prisms. In tunnel monitoring included convergence taping and optical targets. Excavation of the driven tunnel commenced in February 2014 was completed in late August.

1. INTRODUCTION

The NSRU project is designed to grade separate south bound diesel haled freight trains from the electrified suburban rail network north of Sydney at North Strathfield Railway Station. The freight line will pass under three heavily trafficked suburban railway lines and one line currently not in use. The original concept for the underpass included a cut and cover tunnel that would take between three and five years to construct due to the very limited number of track possessions available during any one year. The subsequent reference design stage, developed a driven tunnel option which was further refined during the detailed design phase to have a shotcrete final lining reinforced with synthetic fibres. During the reference design the underpass was also moved northwards 60m to take advantage of more favourable geological conditions. The shallow cover over the driven tunnel necessitated that the tunnel design and construction methodology minimise surface settlements so that there would be no speed restrictions placed on the operation of the existing train services. This was achieved using a combination of canopy tubes and the placement of the shotcrete lining as close as possible to the excavated face of the tunnel. The final driven tunnel length was 148m with the ground cover between 2.5m and 3.5m. The tunnel excavated dimensions were around 8m high by 9m wide. No disruption to train services occurred during the construction of the tunnel. This paper describes some aspects of the design development from the reference design stage through to the detailed design and other minor changes made during the construction phase. An unforeseen 800mm wide dyke was also intersected by the tunnel, though there was some speculation before construction commenced that an anomaly could exist about half way along the tunnel length.

To ensure that tunnelling operations did not impact upon the integrity of existing track infrastructure, a need was identified to design and implement a 24 hour a day, 7 days per week Automated Deformation Monitoring System (ADMS). This was also required to operate within existing client maintenance specifications (Gonzalez, et al 2014).

2. DESCRIPTION OF PROJECT

The NSRU is one of the first projects to be undertaken under the Northern Sydney Freight Corridor Program. This program includes a number of infrastructure projects to improve freight and passenger rail services along the 155 kilometre rail corridor between Sydney and Newcastle, and is a joint federal and state government funded project under the Nation Building Program. The NSRU is being delivered by Transport for NSW(TfNSW) under an Alliance contract with the John Holland Group and Bouygues Constructions Australia. A design JV of Sinclair Knight Merz and Parsons Brinckerhoff were the lead designers with Mott MacDonald Australia as the driven tunnel designer.

A plan of the skewed driven tunnel traversing beneath the railway tracks is shown in Figure 1 and a section schematic in Figure 2.

Figure 1: Tunnel plan alignment.

The project involves the construction of a new rail underpass (dives plus driven tunnel) between North Strathfield Station and the Strathfield Junction which will allow the UP Freight movements to the Flemington Goods Loop to be provided via a route beneath the UP Relief, UP Main, DN Main and the DN Relief, thereby eliminating conflicting at-grade movements. The dive structures either end of the driven tunnel are around 350m long each. Trains using the underpass driven tunnel are travelling south down the northern dive across and out through the southern dive. The tunnel alignment (the UP Relief Line) is on a reverse curve of 400m radius with a down gradient on the north dove of 2.8% and on the south dive of 2.2%.

For the tender, the Alliance had developed their own tunnel design and construction methodology which differed quite significantly from the approach taken by the designer for the reference design(Nye, 2013). The reference design had also referred to lattice girders and the builder proposed light steel sets and continuous grout bags to make contact with the rock. The reference design had flagged the possible use of fibre only reinforcement in the shotcrete and not using lattice girders.

The final detailed design of the tunnel lining progressed on the basis of a synthetic fibre reinforced shotcrete without steel sets or lattice girders and this form of tunnel lining has now been successfully constructed.

Also the reference design was developed as a heading and bench excavation and it was anticipated that for such a short tunnel the builder would use or have available a small road header. For efficiency of the construction and to allow large plant to pass each other in the tunnel the Alliance requested that the tunnel be a full height heading excavation and the tunnel at least 1.5m wider. Additional calculations were made by the designer to confirm that this would have minimal additional impact on the predicted surface settlement. Another advantage of a full height heading was the seamless shotcrete lining over the full tunnel profile adding to its durability and lower permeability. This construction change had no impact on the final structural lining shotcrete design thickness which was 250mm.

The reference design driven tunnel was 170m long. This was reduced to 148m by allowing the piling works in the southern dive structure to be constructed closer to the operating railway line.

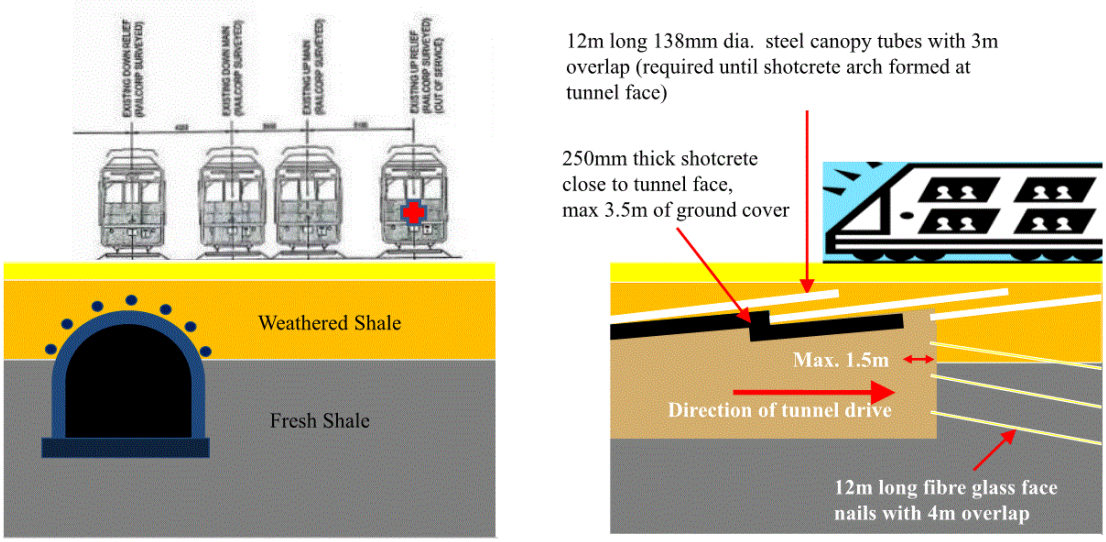

a) Tunnel Cross Section b) Tunnel Long Section at Tunnel Face

Figure 2: Schematic Cross section of tunnel and railway tracks, 3.5m maximum ground cover. Tunnel traverses the tracks on a skew.

A proposed 25mm passive fire protection layer in the driven tunnel reference design was removed and replaced with a final 100mm thickness shotcrete layer (increased from 75mm thickness) and containing micro fibres to reduce spalling of the shotcrete. This final layer of shotcrete also will protect the spray-on waterproofing membrane. The tunnel lining has been designed to resist without collapse, a 4 hour duration hydrocarbon fire even allowing for a significant loss of the overall lining thickness. The design fire size had been increased significantly from that used in the reference design.

3. GENERAL BACKGROUND DISCUSSION

Before launching into the details of this project paper it is important to understand some of the drivers to its design and the construction method adopted.

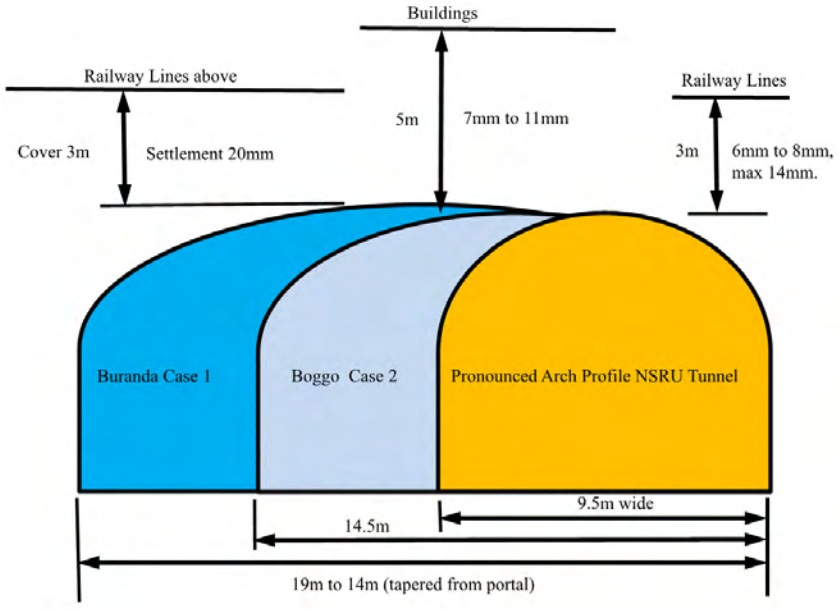

Figure 3: Comparing previous shallow cover tunnels with the NSRU tunnel.

Firstly, as shown in Figure 3 the NSRU tunnel is very shallow but compared to the two Brisbane tunnels (Buranda and Boggo), also excavated in weak rock, the tunnel is narrower and more importantly has a pronounced curved profile over the tunnel crown. The Boggo Road Busway Tunnel had lattice girders embedded in shotcrete as the temporary support, and this was then followed by an in-situ concrete lining for the permanent support. Shotcrete spray trials on lattice girder sections were conducted at the start of the project to assess whether the shotcrete and lattice girders could be used as permanent support. Figure 4 are a series of photographs taken from these trials at Boggo Road. It can be readily seen that voids have formed around the steel lattice girder elements within the shotcrete, which in the long term would be expected to result in steel corrosion followed by shotcrete spalling. The formation of these voids is accentuated by the use of a curing accelerator in the shotcrete which is necessary for its overhead sprayed application in a tunnel.

Figure 4: Evidence of shadowing of shotcrete (when used with accelerator) around steel lattice girders.

The curved profile of the NSRU tunnel is important to ensure that the arch is basically acting in compression and that there are no bending moments and hence no significant tensile stresses in the shotcrete. The synthetic fibres used in the NSRU tunnel provide a reserve of flexural capacity but they were not expected to be mobilised and this was the case in practice with absolutely no longitudinal cracking evident in the crown of the tunnel. It would also appear that fibres negated any visual evidence of shrinkage cracking in the shotcrete.

The other issue at the NSRU tunnel (say compared to Boggo Road) was that the cover was so low that the idea of having an initial ground support (which would also have to negate all of the possible ground settlement) then followed by an in-situ concrete lining would in effect reduced the ground cover. There was simply not enough room to fit a thicker tunnel lining because of the constraints associated with the track vertical alignment and the track gradients.

4. SITE INVESTIGATIONS

Some of the site investigation boreholes and test pit excavations that were located within the rail corridor track zone had to be carried out during the long week-end track possessions in June 2011 and September 2012. Golder Associates carried out the site investigations on behalf of TfNSW with inputs from both the designers and their geotechnical consultant Douglas Partners. Additional boreholes were also drilled outside track possessions where they were not located in the rail danger zone.

The boreholes drilled on the track during the weekend possessions were drilled to a maximum depth of 11m using a small tracked drilling rig.

Visual inspection of the corridor at reference design during a track possession revealed surface rock outcrops on the east embankments extending from the southern end of North Strathfield Railway Station up to the Pomeroy Street Road Bridge. This was the prime factor leading to moving the tunnel alignment northwards from the original concept design cut and cover tunnel as it was anticipated that the geology improved together with a slight improvement in ground cover for a driven tunnel.

The site investigation failed to detect an 800mm wide dyke within a 2m wide shear zone that was intersected at an oblique angle during the tunnel excavation, Figure 5. Though not of great consequence to the project in terms of tunnelling progress, given that the tunnel construction methodology included canopy tubes that could accommodate ground changes quite readily, Figure 6. The interpretation of the groundwater levels discussed later may have identified this dyke, however, the presence of a dyke seemed a highly unlikely event even though the possibility was discussed

Test pits were excavated between sleepers in critical locations along the track to determine the depths of the ballast and the ballast sub-base during track possessions. After the award of the contract to the Alliance excavated additional test pits at the south end and west side of the tunnel as this was likely to be the worst near surface material.

Figure 5: 800mm wide dyke in tunnel face.

Figure 6: Canopy tube installation with shotcrete lining in foreground.

5. GEOLOGICAL MODEL

From the site investigation data it was possible by interpolation to develop a geological long section with cross sections taken through the tunnel at 10m intervals. The typical mixed face conditions consisted of extremely low), to low strength (Unit 1) Ashfield Shale in the crown, with low to medium strength shale (Unit 2) down to the tunnel spring line and high strength shale in the lower half of the tunnel (Unit 4). Above the shale bedrock there was an undulating layer of residual clay of variable thickness underlying fills and railway ballast. The residual soil thickness was very thin above the northern half of the tunnel as the railway is in cutting, and increases in thickness in the southern half as the railway transitioned into an embankment (refer to Table 1 for the Geological profile and parameters).

The geological long section indicated a fractured rock band (Unit 3) would be encountered near to the invert over much of the tunnel. The daily geotechnical mapping determined that the fractured rock band was in fact linked to thrust faulting associated with the dyke and shear zone, which was aligned nearly parallel with the tunnel. The series of thrust faults had lots of bedding shears due to the fault movements giving an increased fracturing in the face and floor. Apart from the dyke and shear zone that intersected the tunnel 60m from the north portal and suddenly terminated within the 2m wide shear zone at the 90m point, the geological interpretation has proven to be very accurate.

Table 1: Geological profile and parameters

#	Strata	Thickness	Description	UCS	Range E (MPa)
Material above the tunnel crown of the driven tunnel					
1	Ballast	500mm	Gravel and cobbles	-	100 - 200
2	Capping L-1	250mm	Clayey gravel/gravelly clay	-	50 -100
3	Capping L-2	250mm	Silty gravel/ sandy gravel	-	50 -100
4	Filling	0 to 1000mm	Mostly sandy gravel	-	60 -100
5	Residual Clay	0 to 1000mm	Mostly stiff to very stiff residual clays	-	12 - 20
Material intersected at the tunnel face of the driven tunnel				**Min. UCS (MPa)**	**Range E (MPa)**
6	Rock Unit 1	1m to 3m in the tunnel face	Extremely low to very low strength, fractured to highly fractured	0.5	100 - 200
7	Rock Unit 2	1m to 4m in the tunnel face	Low to medium strength, fractured	2	300 - 500
8	Rock Unit 3	0.5m to 2.5m in the tunnel face	Medium to high strength, fractured to highly fractured	7	700 - 1000
9	Rock Unit 4	3m to 6.5m in the tunnel face	Medium to high strength, unfractured, RQD > 70%	15 - 25	2000

The 800 mm thick dyke within a 2.0m wide shear zone was intersected approximately 58m from the north portal on the eastside tunnel wall. The vertical dyke was aligned obliquely to the tunnel at approximately 15 degrees to the alignment centre line. The dyke when first encountered was medium to low strength however it deteriorated rapidly when conjugate faults crossed the dyke (at 80m point) perpendicular to the tunnel alignment. The dyke consisted of stiff clay with a contrasting golden colour compared to the surrounding dark grey shale rock (Figure 5). The dyke sheared material was more susceptible to weathering and had weathered to a soft to firm clay in the tunnel crown and firm to stiff clay below the spring line.

An additional 23 fibre glass dowels where installed in the upper tunnel face at around the 79m point in additional to the standard 35 face dowels pattern that had just been installed at 76m point. A second round of 19 additional face dowels were installed in the upper tunnel face at the 89m point prior to the dyke finishing within the shear zone around 4m short of the west tunnel wall. Interestingly the dyke had little or no impact on the surrounding Unit 4 shale rock below the tunnel springline while a deeper more weathered zone developed in the Unit 2 shale above the spring line. The

increased weathering on the uphill side of the dyke may be the result of wetting and drying effects on the shale rock as the groundwater finds its way around the weathered dyke which acts like a dam to the groundwater.

From a lining design perspective it was important that the Unit 4 shale be at or above tunnel spring line so that the walls of the tunnel would be constrained laterally. This point is discussed further in Section 6.

During the detailed design various sources of information were used in the kinematic assessment including a stereo net projection of the data from the Optical Tele-viewer and RaaX imagining data was produced of both the Common Joint & Fault Sets in Ashfield Shale Table 1 from Deep Excavtion in Shale: (Andrews & Braybrooke, 2001) and the Metro West Borehole 3103_130. The typical Joint Sets / Faults / Shear Zones / Dyke encountered during tunnelling have been summarized on Table 2 below and in Figure 7 DIPs 6.0 stereonet.

Douglas and Partners our geotechnical sub-consultant provided three potential rock planar and wedge failure cases based on their experience with Ashfield Shales. The three cases included:

- a small planar failure of a 45 degree wedge (**Minor Joint Set J6- 28/180**) occurring on the face, which was assessed using Rocplane to determine the bolt loads and Unwedge for the Tunnel shotcrete sidewalls;
- a large wedge occurring on the face and Tunnel shotcrete side walls from the intersection of two persistent major joint sets at 60 degrees (**Major Joint Set J2 - 60/020**) and 70 degrees (**Major Joint Set J3 - 70/290**) intersecting the face were assessed using Unwedge.;
- planar failure of a large persistent 70 degree wedge (**Major Joint Set J1- 85/185**) on the face, which was assessed using Rocplane along the length of Tunnel at 10m chainage intervals;

Table 2: Joint Sets / Faults / Shear Zones / Dyke encountered during tunnelling

Tunnel Bearing	*Defect Type*	*Dip*	*Dip Direction*	*Quantity Mapped*	*Persistence (m)*	*Peak Defect Property*		*Comments*
						Friction (degrees)	*Cohesion (kPa)*	
163° to 154°	JM1	**89**	**020**	33	10	28	0	Joint Set with a single small Fault
	JM2	**85**	**343**	47	10	28	0	Potential for Large Planar Failure x 2
	JM3	**84**	**275**	90	10	28	0	Shear Zone with Dyke (800mm)
	JM4	**82**	**073**	38	10	28	0	Joint set with small shear zone
	With Minor sets							
	Jm5*	**76**	**310**	83	3	25	0	Small Fault where wedge broke out
	Jm6*	**37**	**018**	13	3	25	0	Shear Zone crossed Dyke
	Jm7*	**49**	**158**	16	3	25	0	Shear Zone / Thrust Faults
	Jm8*	**72**	**119**	26	3	25	0	Fault 4 east side wall beyond dyke
	Major Features							
	FT9	**41**	**269**	46	>100m	20	0	Thrust Faults 1&2 Aligned parallel to tunnel prior to Dyke
	B10	**10**	**091**	15	>10	27	0	Bedding
	Joint Swarm	**85**	**085**	8	>10	25	0	Joint Swarm at Southern Portal

Note * indicate minor joint sets

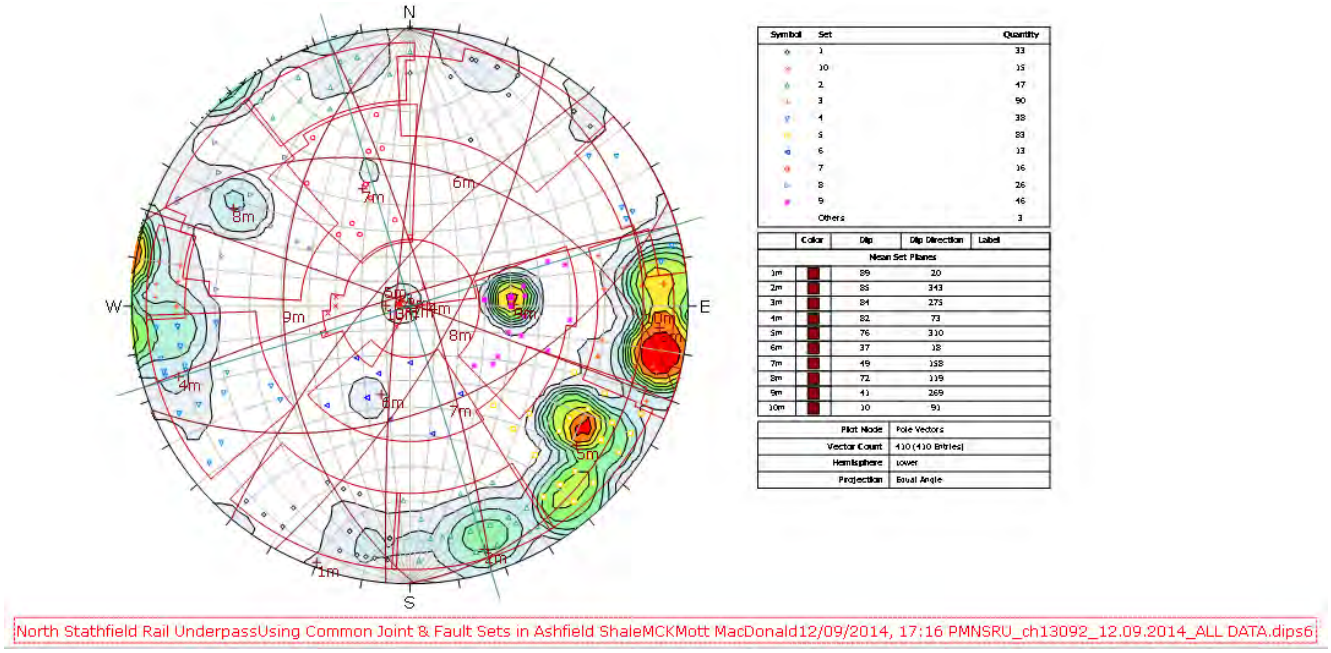

Figure 7: showing DIPs 6.0 stereo-net showing Joint Sets & Fault / Dykes encountered during construction

The daily geotechnical mapping assessed rock failure mechanisms for the tunnel during constructions which are summarized in Table 3. From the start of tunneling at the northern portal a series of thrust faults FT9 (41/269) were intersected that were aligned parallel to the tunnel alignment. The thrust faults caused lots of bedding shears that increased the amount of fracturing in the face and invert. Prior to encountering the 800mm wide dyke, joint set JM2 (85/343) caused the potential for two large potential planar failures at dip angles of around 70 degrees, which had been one of the Douglas and Partners potential rock planar expected failure mechanisms that had resulted in the requirement for 35 No. standard pattern face dowels.

Two rows of additional side wall dowels at 1.5m x 1.5m pattern spacing were installed into the side walls where the dyke and shear zone were entered and left the tunnel. Beyond the 2.0m wide shear zone with the 800mm wide dyke, a fault was encountered in the eastern wall Jm8 (72/119) which was also aligned near parallel to the tunnel alignment. The fault created a hanging wall and it was decided to continue the two rows of additional side wall dowels through the faulted section. The poorest rock conditions where encountered at the southern portal where the rock have been sheared to highly fractured rock by two intersecting shear zones (Joint Swarm (85/085) and JM3 (84/275)) creating a joint swarm.

Table 3: Typical rock failure mechanisms encountered during tunnelling

Geotechnical Domain	***Wall Azimuth (°)***	***Typical rock failure mechanisms***
Tunnel South Wall - Tunnel Face	341	A few large potential planar wedge were encountered **2m (85/343) and** small planar wedge **JM2 (85/343)** intersecting bedding shears**;** Wedge failures were typically **JM2 (85/343), JM3 (84/275)** intersecting **Jm5 (76/310)** and random bedding shears intersecting **Fault 1 & 2 (41/269)**; and Potential toppling failure **JM1 (89/020) and JM2 (85/343)** on the bedding **B10** (**10/091**).
Tunnel East - Side Wall	253	Occasional over break on **Jm5 (76/310)** and planar failure **3m (84/275)**; Some small wedge failure on **JM3 (85/275)** intersecting **Jm5 (76/310)**;
Tunnel West - Side Wall	073	Occasional small over break on **JM4 (82/073)** Some small wedge failure on **JM4 (82/073)** intersecting **Jm8 (72/119)**;

Face stability is an important issue when constructing a shallow rock tunnel beneath multiple live railway lines. There are essentially three types of deformation mechanisms associated with the face stability and they are pre-convergence settlement that occurs ahead of the tunnel face (which extends out in front of the tunnel and may indicate poorer ground conditions ahead of the tunnel face); convergence that occurs at the face (settlement that occurs during excavation and prior to the ground support being installed) and extrusion of material in the face (face loss). If face stability is not maintained then it may lead to excessive settlements, spalling, large over-break, and potentially to a face collapse.

The stability of the tunnel face was maintained by installing 12m long fibreglass face dowels on a 9m advance sequenced with a 4m overlap. The 35 No. fibreglass dowels were installed in a standard pattern of 1.0m x 1.0m grid in four rows in the top half of the tunnel face, with 2 rows spaced a 1.0m x 2.0m grid in the lower half of the face, which was combined with a 50mm thick layer of shotcrete in the top half of the face. The 12m long fibreglass dowels effectively create a stiffened core of material ahead of the tunnel. In the more competent rock the fibre glass dowel provide support to key rock wedges.

The highly weathered faulted dyke material that was encountered at the 80m point comprising soft to firm clay in the tunnel crown and firm to stiff clay below the spring line had caused pre-convergence settlement ahead of the tunnel face. It was agreed to install an additional 23 No. fibreglass dowels that reduced the dowel spacing to 0.5m x 0.5m pattern across the face. The large number of dowels in the face effectively created a stiffened core of ground ahead of the tunnel face and this helped to reduce the pre-convergence settlement. Shotcrete was also spayed on the upper half of the face to seal the clays from the moisture and to reduce face loss from squeezing of the clays, and to prevent loosening of the highly fractured rock mass below the residual soils. The timely application of shotcrete onto the face and arch straight after the excavation finished also helped to reduce convergence settlement that was observed in the real time track monitoring prior to the support being installed.

Confining the face of the tunnel with the dowels and shotcrete helped to reduce the magnitude of surface settlement. However but this will not be significant compared to the overriding influence of the canopy tubes in combination with the stiff shotcrete lining which will closely follow the tunnel face excavation.

6. STRUCTURAL DESIGN OF TUNNEL LINING

The tunnel support design is closely aligned with the construction sequence described in Section 2 and shown in Figure 2b). The canopy tube array over the arch of the tunnel has to partially support the ground and live loading with the fibre reinforced shotcrete lining following very closely behind. The shotcrete is applied in layers starting with an initial thickness of 150mm at the tunnel excavated face and then up to 250mm with 3m of the tunnel face. The canopy tubes have to support ground up to a 2-m span (length wise along the tunnel) allowing for any unforeseen overbreak. The shotcrete taken up to the tunnel face over the arch and walls had to have reached 6MPa before the next excavation cycle of one metre in length can commence to provide both strength and stiffness.

The tunnel lining is what is called a one pass lining. Fibre reinforced shotcrete alone is the tunnel permanent support over the arch and tunnel walls. There is no requirement for lattice girders or steel sets (and as explained in Section 3 these would adversely impact on the lining durability). The tunnel lining behaves as a “confined arch” due to the confinement of the arch by the surrounding rock (ranging from Unit 1 to the better Unit 4) and therefore the compressive thrust in the arch will always be maintained close to the neutral axis of the shotcrete lining.

The two-dimensional plane strain linear elastic finite element analysis was used to model the tunnel lining as a continuation of the continuum of the surrounding rock mass. The compressive stress in the tunnel arch is reasonably uniform with a magnitude over the arch of around 4 MPa (this compares with the Ultimate Strength of the concrete in compression of 40MPa at 28 days). The maximum tension in the lining was 0.25MPa on the inner face in the crown of the tunnel and was easily within the capacity of the fibre reinforced shotcrete tensile capacity if it were to occur. The loading on the model included live loading with trains above and on adjacent tracks and combinations thereof.

In addition to the 2D FE analysis we also carried out 3D FE analysis with train loadings over the tunnel using STRAND7. The results were not included in the design reports for this project submitted to the Alliance or to TfNSW. They proved, however, that the lining stresses predicted by the 2D FE models were conservative.

The canopy tubes were designed as simple continuous members with assumed loading and calculated loadings. There is no single design approach as the mode of loading is very complex. The loads were broken down into individual elements and simple beam calculations used for different loadings or load combinations. For example if the ground

above the canopy tubes moves down as a block then the shear capacity of the canopy tubes is the most important criteria and for which the factor of safety is very high. The bending capacity of the canopy tube is limited by the capacity of the threaded joint (if at the point of maximum bending moment) and is around half that of the main casing. In practice additional steel was inserted in the canopy tubes during construction when the excavation span was increased from 1.3m to 1.5m in the form of single reinforced bars. This was to provide a section of uniform strength. The canopy tubes were fully grouted but the grout only allowed the full steel capacity to be used in the analysis (no local buckling assumed once fully grouted). Direct rail wheel loads were reduced at the tunnel crown to allow for the distribution of load under the tracks. Separate calculations determine the stresses in the rails if one or two sleepers were removed (simulating high localised settlement in the tunnel). These calculations demonstrated a high factor of safety overall for the loading assumed to be applied to the tunnel.

The tunnel invert is permanently drained. The tunnel drainage system is described in Section 7. A nominal external ground water pressure with 3m head above the invert of the tunnel has been taken to check the wall for bending and shear capacity, which are satisfactory. The wall could be in compression with a stress of 2MPa. The dive structures either ends of the driven tunnel are 350m long and are also permanently drained.

In principle the tunnel shotcrete walls should bond to the shale rock and this would negate any water pressure applied directly to the wall (and water travelling between the rock and the back of the wall). However, in the field if in some locations this bond did not develop then additional support in the form of cement grouted permanent dowels would be an option. In actual tunnel construction weep holes at 3m centres have been installed along both walls. Approximately 20% of these weep-holes, which were drilled to 2.5m in depth, actually had intermittent, minor water flows. For all practical purposes the tunnel in its current state, even before the application of the membrane and final shotcrete layer is dry.

Further to the discussion about shotcrete bonding to shale (which is applicable to the near vertical walls of the tunnel) there is very little published or actual test information in Sydney. The reference (Hahn and Holmgen) does provide some general test data (but not from Sydney). The range of shotcrete bond strengths against fine grained shales reported varied from 60 KPa (lower bound) to 290KPa (upper bound). For design purposes an Ultimate shotcrete/shale bond strength value of 100 KPa was adopted. The shear capacity of fibre reinforced shotcrete is also an important parameter in addition to bond. Actual test data using fibre reinforced shotcrete (steel or synthetic fibres) has been published. According to these tests there is an excellent correlation between AS3600 $v = 0.34\sqrt{f'_c}$ and at 28 days, shear capacity = 2.15 MPa, however for early strength shotcrete the following formula can be used v = 0.28 fc' 0.6 – 0.11. These are ultimate strengths so for working stresses an F of S of 1.5 has been applied. These figures also compare well with the Euro-code values.

The tunnel was constructed without lattice girders or steel sets as they are not required. There are numerous other examples in tunnels where lattice girders (although used) provide no structural support (Boggo Road and the M5 East Exit Ramp). There are also tunnels with shotcrete only (recent Cross Rail station caverns and cross-passages) and other tunnel examples available in numerous other references. The tunnel lining is totally dependent on the shotcrete to gaining sufficient strength to support the tunnel. In an arch profile it only takes around 6 to 7 hours to gain strength (with an accelerator) and within days the shotcrete is actually stiffer than steel lattice girders. There are two reasons for this, firstly the large area of shotcrete relative to the area of steel and secondly the shotcrete arch is acting in compression by a combination of the arch profile and the confinement of the surrounding rock. In the permanent state there is no obvious failure mode of the shotcrete arch with a compressive stress of up to 4 MPa in a shotcrete with a design characteristic strength of 40MPa. High flexural capacity of the shotcrete is not a requirement for the success of the tunnel structural lining design. This assertion is based on the fact that the tunnel walls are rock tunnel preventing the arch from sagging at the crown and thus always acting in compression.

While the probability of a major fire in the tunnel is extremely low as the return interval for such an event is much greater than 10,000 years, nonetheless the tunnel has been designed to at least not collapse after a hydrocarbon fire of 4 hours duration in the tunnel, it is probable that there would be 150mm of shotcrete lining remaining. Our analysis shows that the ground above the tunnel would arch and that the stress in the remaining shotcrete would at the apex of the arch (which provides the surface rock with confinement) would have a uniform compressive stress of around 2MPa (this is under dead load only with no train live loading). If there was a fire larger than even in the most extreme fire case assessed to date we believe that the tunnel could be backfilled from the surface and the surface track reinstated with the lines operational within approximately one week. While the tunnel is being rebuilt the freight trains could be diverted back to the existing surface tracks.

Another issue that was raised during the detailed design was the possible impact of vibration caused by trains passing overhead during the initial application of the shotcrete. Some investigation of this issue was carried out with the conclusion that there would be no impact. Calculations estimated a possible maximum displacement of the canopy tubes of 0.1mm. During construction vibrations due to passing trains were for all practical purposes non-existent.

7. GROUND WATER AND DRAINAGE

Prior to the start of tunnelling the groundwater table level was approximately 2.6m below ground level (typically 11.0m AHD) between the northern portal and the 90m point and then drops down to approximately 4.5m below ground level (8.0m AHD) between 90m to the southern portal. A possible reason for the groundwater change was initially believed in the detailed design phase was that the groundwater was damming behind a geological barrier like a dyke across the alignment of the tunnel.

Both the driven tunnel and the dive structure at either end of the tunnel are permanently drained. The combined predicted flow rates from these two structures was predicted to be the order of 0.1 to 0.5 litres/second with potential for higher short-term inflows. The actual ground water inflows to date have been very much less than predicted with only localised seepage points along the tunnel either through purposefully drilled weep holes in the lower wall (drilled at 3m intervals along the tunnel) or in circumferential defects in the shotcrete lining which have occurred at only about 6 locations within the tunnel itself (caused by a probable cold joint in the shotcrete at the staging point for the installation of the face nails spaced at 9m intervals along the tunnel).

Initially, circumferential 450mm wide core drains will be applied over the structural shotcrete lining on areas where tunnel lining seepage has occurred, which is at a very limited number of locations along the tunnel. Additional core drains were installed at 4.5m intervals along the tunnel and to take the groundwater seepages from the base of the side wall weep holes down to the sub-track slab drains. A cement based smoothing layer is next applied prior to the membrane application.

Over the smoothing layer a spray-on membrane will be applied over the arch of the tunnel to spring-line level on both walls over the initial tunnel shotcrete structural lining. The membrane will be applied over the smoothing layer which is around 10mm to 20mm in thickness. This layer will be applied by firstly spraying it onto the shotcrete surface and then rolled or brushed to obtain the desired smooth finished surface.

For the spray-on membrane BASF MasterSeal 345 (or equivalent) was proposed in the tunnel waterproofing specification, but Tam800 has now been applied to the tunnel. Both are water based products that are safe to use without specialised applicators. The Tam800 product is applied in two different contrasting colours and this may result in a final membrane that is at least easier to monitor its application thickness. The membrane will have a minimum thickness of around 5mm. The bond strength of the membrane to both shotcrete surfaces (dry and newly applied over the membrane) is typically around 1MPa for these products.

The invert of the tunnel is fully drained to prevent uplift forces acting under the track slab with perforated pipes running in gravel filled trenches excavated in the shale rock and running down both sides of the tunnel to the drainage sump at the low point of the tunnel. The low point sump in the tunnel also acts as a flame proof trap. The low point sump then drains by gravity to the north portal groundwater pump well. This drain was installed by directional drilling and pipe jacking a one pass reinforced concrete pipe for the 100m long drain. The south dive structure groundwater is transferred directly to the tunnel low point sump and then to the north portal sump. The groundwater from the north dive structure does not enter the tunnel but is directed to the northern pump well located outside the tunnel portal. Surface rain water flows from both the dive structures are diverted prior to entering the tunnel into the pump sumps located at each portal. In addition to waterproofing measures in the tunnel spoon drains run along the base of the tunnel walls in the track slab and any seepages from the lower wall if they occurred are directed to the sub-track slab drains.

The waterproofing membrane over the tunnel arch is designed to prevent long term drips developing in the tunnel crown and becoming a maintenance issue for the overhead wiring, the track rails and fixtures and the tunnel services on the tunnel walls. For durability the tunnel is classified as B2 and this is based on a sample of ground water taken within the rail corridor but not close to the tunnel.

8. SHOTCRETE

The tunnel profile with circular arch profile has been specifically developed to ensure that there is no flexure in the lining and that the loads applied result in a tunnel lining purely in compression. The maximum compressive stresses in the shotcrete lining determined from Finite Element (FE) analysis are a little under 4 MPa (dead plus live load). For

this reason the shotcrete needed to gain an early strength of 6MPa (aided by the use of an accelerator) before the next excavation cycle could commence. This strength level was achieved after about 7 hours. The full dead load would also not be applied at the face, but the live load due to the trains passing above from calculation and assuming no distribution along the rails would be around fifty percent of the total load. The structural shotcrete had to have a design life of 100 years and as such, the shotcrete mix includes fly ash and silica fume, both of which enhance the durability of the mix. The shotcrete mix was developed through a number of iterations during the construction phase despite having shotcrete trials and testing carried out many months before the commencement of construction. The key parameters refined during the shotcrete trials included accelerator percentage, cementitous content, steel fibre vs plastic fibres, fibre contents, shotcrete life, and additives balance. The focus on achieving the 6MPA strength gain as quickly as possible without compromising the 28 day strength was a key focus. The macro synthetic fibres used in the structural shotcrete were Barchip60 with a dosage rate of 6kg/m^3 – the selection of the synthetic fibres required a reduction in the specified thoughness criteria, however this offered lining performance, commercial and durability benefits to the project. The 100mm fire protection shotcrete layer over the TamSeal 800 spray-on waterproofing membrane is the same mix design as the structural layer but with Duomix 6mm long synthetic fibres designed to reduce explosive spalling and with a dosage rate of 2kg/m^3.

The bond between the spray-on membrane and shotcrete will be checked on-site, however, typically for these products the bond between the both the underlying shotcrete and the sprayed shotcrete onto the membrane, it is expected that this bond strength will not be less than 1 MPa.

Measured strength gain of cored or site tested shotcrete (with fibres) are given in Table 5 below, together with the elastic modulus calculated using the following AS3600 formula at Clause 6.1.2, $Ec = 0.043\rho^{1.5}\sqrt{fc}$. In which ρ is the density of the shotcrete in kg/m^3 and fc is the compressive strength. The initial values up to the 3 days strengths are significantly less than taken at the time of design. However, even the one day old stiffness of the shotcrete is significantly more than the surrounding rock and certainly much greater than the overlying extremely weather shale, fill and track ballast.

Table 4: Shotcrete Mix Design

Material	Weights (kg/m^3)	Comments
Cement (kg/m^3)	370	The shotcrete mix design was modified twice during construction to improve the early strength gain without the addition of more accelerator (which is applied at the shotcrete nozzele). Modifications included reducing the flyash content from 25% to 20% and replacing the loss with cement. The percent of 10mm aggregate and sand was also reduced in the final modified shotcrete mix design.
Flyash	100	
Silica Fume	30	
10mm	520	
Man. Sand	570	
Fine Sand	530	
Admixture	4800	Polymer-based Superplasticiser
Admixture	650	Retarder
Additive	6	BARCHIP (Polyfibre)
Water	215 litre/m^3	
Slump	130 mm	

Table 5: Summary of shotcrete strength and stiffness gain with time

Time	Strength (MPa)	Elastic Modulus (MPa)
7 hrs	6	12 000
1 day	10	15 000
3 days	21	22 000
7 days	33	27 000
28 days	40	32 000

9. SETTLEMENT AND MONITORING

Surface settlement and in tunnel monitoring formed a critical part of the works both prior to and when tunnel excavation progressed under the live railway lines.

The principle at the core of the tunnel lining design and construction was that the shotcrete should be applied as close to the tunnel face as practical so that in effect, the ground does not relax. The canopy tube array installed ahead of the

excavation ensures that even during the excavation process the ground has had little opportunity for movement prior to the placement of the shotcrete. The face nails have similar though less influence on surface ground movement. Figure 8 is a typical screen shot of surface settlement profiles relative to the advancing tunnel.

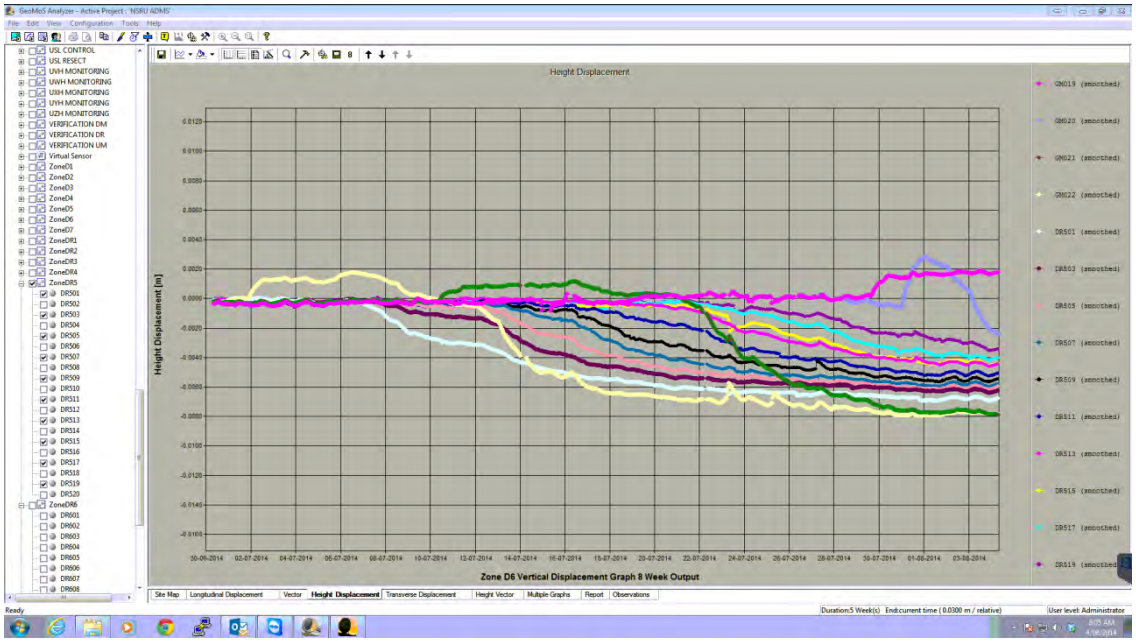

Figure 8: Typical settlement plot track monitoring (screen capture).

During the construction phase tunnel excavation commenced with 1.3m length excavation cycles and the surface settlements observed before passing under the first live railway track were the order of 5-6mm (7 excavation cycles between canopy tube array installations which are 9m apart, 12m long canopy tubes with 3m overlap). Through the daily Permit-To-Tunnel (PTT) process used on site the excavation cycle length was later increased to 1.5m. Excavation cycle lengths were subsequently reduced to 1.3m, then back down to 1.0m when the 800mm wide dyke was intersected. Later reverting back up to 1.3m as the ground conditions then improved and back up to 1.5m again after passing the last live track.

The maximum recorded surface settlement was 15mm at around the half-way point along the tunnel excavation, at which point the dyke coincided with the tunnel crown. Due to the increase in observed surface settlement other mitigation measures were applied including reducing the excavation cycle back to 1m, installing additional face dowels in soft material high in the heading and increasing the tunnel lining thickness from 250mm to 300mm. The maximum settlement started to develop just prior to the dyke and further investigation is required because in addition to the dyke excavation progress in the tunnel also increased prior to the mitigation measures listed above were adopted.

At the design stage the Design Settlement Report listed the following:

“The following summarises our conclusions:

1) The geometry of the tunnel arch (a pronounced curved arch profile) in combination with relatively strong rock strata (at least to tunnel spring-line level, with more weather rock above) is very favourable to achieving low surface settlement values.

2) The construction method proposed has a reliable history of achieving both predicted and low settlement values in similar weak rock tunnels.

3) The 2D finite element model predicts surface settlement in the order of one millimetre. Compared to say Boggo Road which used the same FE analysis approach that did not allow initial relaxation of the ground (pseudo 3D effect in a plain strain FE model, due to the forward installation of canopy tubes) this is a much lower prediction which may be the result of the circular arch profile compared to the flat arch. Either way the approach gave a very

accurate estimate of the surface settlement (calculated 7mm plus 3mm (judgement) and gave 10mm which matched the actual).

4) The magnitude of surface settlement is greatly dependent on the construction sequencing being followed and the quality of construction workmanship. These two factors are considered the controlling drivers on the magnitude of settlement as the theoretical predictions are so low.

5) Our interpretation of the geological profile is that during excavation of the driven tunnel there will be a lowering of the water table, however, changes in the water table will not have significant impact on the predicted surface settlements both in the short and long term.

6) The theoretical settlement values predicted from the FE analysis due to tunnelling construction works are less than a few millimetres, however, these are guide only and for this reason our judgemental estimate of the surface settlement due to the tunnel works is around 5mm."

It is always interesting to review predictions made during the design and while the settlements were higher there were reasons for this, although the actual settlements had no impact whatsoever on the operation of the trains. Rail twist, which is more important that uniform settlement values of the track were always within railway limits with no alarms triggered.

10. CONSTRUCTION

Tunnel excavation commenced on the 7th February 2014, initial progress was slow, with the first 9m of tunnel excavation taking 16 days to complete. Nineteen 12m long 139mm diameter steel canopy tubes were installed over the arch every 9m length of tunnel starting from the tunnel portal. There is a 3m overlap between canopy tube arrays. The excavation cycle was 1.3m with an initial 150mm of shotcrete sprayed over the arch and walls of the tunnel with additional shotcrete layers added immediately behind the face section building up the thickness to a final 250mm. A pattern of 35 face nails 12m long were installed at 4.5m into the excavation from the start of each canopy tube array. By staggering the canopy tubes and face dowels by 4.5m, a delay in construction was achieved which allowed the following shotcrete lining to gain more strength before the next series of excavation cycles.

Apart from observed standard tunnel design support, additional measures were taken based on the mapped geology and deformation readings. For example, when the dyke was intersected on the east wall of the tunnel two rows of permanent fibre glass dowels up to 10m long were installed on this section of the wall. Additional convergence of the side wall was also noted, around 3.5mm, in the vicinity of the dyke. Further along from where the dyke intersected the tunnel, ground conditions deteriorated in the centre of the face of the tunnel with some associated additional surface settlement observed. While it would be difficult to quantify all the components of observed settlement, with certainty, face relaxation of the tunnel was occurring. To mitigate this movement additional fibreglass face dowels were inserted in the top third of the tunnel face.

The excavation cycle along the tunnel varied thus the number of cuts within each 9m long array length varied correspondingly. For 1m length excavations, nine cuts between canopy tube array installations and for 1.3m cuts seven and for 1.5m cuts six. The tunnel excavation was being carried out after environmental approvals were granted, on a 24 hours per day seven days per week basis. The Alliance from 108m onwards along the tunnel changed the scheduling of the work such that shotcrete was delivered only in the early morning and reduced the shifts down to two 10 hour shifts with the final 1.5m long excavation cycle up to the south portal. The adjusted shift pattern and advance optimisation allowed for consistent shotcrete timing and mitigated lost time due to variability in curing time and inconsistent shotcrete supply.

In addition to plastic depth markers attached to the exposed ground surface, in order to further prove that the thickness of structural shotcrete is in excess of the design minimum, the Alliance has developed, in conjunction with local based software developer 12d solutions, a system of thickness verification whereby measurements are taken normal to the design profile on both the underlying (rock excavation) and underlying surfaces (shotcrete). A concept to measure the thickness during shotcrete application has been proven and further trials are being considered to further support the construction cycle.

While the waterproofing membrane has not been installed at the time of writing of this paper its installation is expected to go smoothly as for all practical purposes the shotcrete lining is almost dry as the shotcrete lining has little or no defects and there are no voids within the shotcrete matrix.

It is worth noting that there are many disadvantages of using steel sets or lattice girders in the same situation. Apart from the complexity of erecting lattice girders in such a large tunnel (and probably it would have to be a heading and bench operation and not a full face tunnel as used here) there is the issue of obtaining continuous and consistent

contact with the excavation profile. Shotcrete on the other hand because it can be spayed directly onto the rock surface provides immediate and consistently continuous support. And because of the sheer volume (hence larger cross-sectional area) of shotcrete the lining is stiffer than alternative steel support that is spaced at intervals of at least 1m along the tunnel. The shotcrete only method is more advantageous for full face excavation because it is simple, continuous, provides high durability and construction safety (robotic application of shotcrete). The need for delivery and site storage of heavy and cumbersome steel components to a small and confined construction site is also eliminated.

11. ACKNOWLEDGEMENT

For permission to publish this paper from the Transport for New South Wales and the excellent work environment created by the Alliance.

12. SUMMARY AND CONCLUSIONS

1) The construction of the NSRU tunnel has proved conclusively that a shotcrete only lining applied close to the tunnel face in combination with the canopy tubes is an extremely effective construction method in this particular geological setting with very shallow ground cover. Without the need to erect lattice girders or steel sets the construction process was significantly simplified and the durability of the tunnel shotcrete lining, which forms the final lining without embedded steel has been considerably enhanced. The alternative to a one pass structural lining would have required a larger excavation further reducing the ground cover and perhaps to a point where the driven tunnel solution may not have been achievable (considering here both technical issues and approvals).

2) Compared to the initial cut and cover tunnel option proposed which required track possessions, the driven tunnel could be constructed continuously without disruption taking at least three years off the original construction program.

3) Shotcrete can be applied directly to the excavated surface while steel sets and lattice girders require some form of blocking which in practice can never be as effective as the intimate contact between the ground and sprayed shotcrete (which can be applied over both the tunnel arch and tunnel face in the same operation, if the latter is required). Using this construction method, settlement predictions are not only reduced but are also more predictable.

4) The tunnel was excavated as a full height heading which would have been less practical had lattice girders been used. Erecting these in an 8m high face would have required additional resources and transportation costs. In contrast the shotcrete was applied robotically and progressively by spraying with mechanical plant without the need for men to be close to the face.

5) The use of synthetic fibres with the shotcrete also proved to be successful. There is also no evidence of shrinkage cracking in the shotcrete lining. For all practical purposes the structural lining is near watertight. There is also a significant cost saving by using synthetic fibres compared to steel fibres. And as with the permanent fibre glass dowels used as a mitigation measure in the tunnel walls in the dyke zone, no possible electrical earthing and bonding issues.

6) The flexibility of the shotcrete only approach to tunnel support was made more apparent when a dyke was intersected. To increase the stiffness of the lining it was just a simple matter of increasing the shotcrete thickness (in this case from 250mm to 300mm , and this was taken as a precautionary measure). Permanent fibreglass dowels were also installed along the tunnel walls on both sides of the tunnel in the vicinity of the dyke.

7) The standard fibre glass dowel pattern of 35 dowels was effective at pre-supporting the tunnel face through various poor ground conditions consisting of mixed face conditions with a typical weathered shale profile that was intersected by faults and sheared zones in which one contained an 800mm wide dyke. An exclusion zone of 3m from the tunnel face was maintained, to protect the worker from potential rockfall and falling wet shotcrete. During the drilling of Canopy Tubes and fibreglass dowels, when the tunnel crew had to work within 3m of the tunnel face, the fibreglass dowels were combined with a minimum 50mm thickness of shotcrete. Additional dowels to the standard pattern were installed when a series of faults intersected the dyke and this helped reduce pre-convergence settlements (that occurred ahead of the tunnel face) by creating a stiff core of ground in front of the tunnel face. There were no incidents like a rock fall.

8) The timely application of shotcrete to the upper face of residual soils sealed the clays from the moist air and also helped reduce convergence settlement that occur during and after excavation until the ground support can be installed.

9) Geotechnical site investigations are more difficult to carry out in an operating rail, nonetheless there was sufficient information to interpret geology along the full length of the tunnel. While a dyke was intersected and not identified by the site investigation it has little real impact on tunnel excavation progress and the construction method was able to accommodate changed geological environment without significant modification.

10) The broad geological model developed for the tunnel proved to be very accurate. The shotcrete arch acted as a compression member without flexure because the high level of Unit 4 rock in the tunnel walls ensured that the lining behaved as per design. No cracking in the shotcrete associated with possible flexure in the tunnel crown has been observed at any point along the tunnel.

11) The PTT process was used very successfully on this project. With a high level of focus on risk of settlement, the process was used to closely monitor settlements and ground conditions and instruct mitigation measures or optimisation as appropriate. Through the PTT process it was possible to enhance tunnel excavation productivity by increasing the excavation cycles in steps between 1m, 1.3m to 1.5m depending on ground conditions and live loading.

12) The maximum surface settlement was around 15mm but this movement was not reflected in the lining deformations which were in the range of 1mm to 2mm in the tunnel crown within the tunnel. Typical surface settlements were between 5-8mm. At springline level tunnel convergence was never greater than 3.5mm across the full width of the tunnel. At no time were either the short or long twist criteria for the railway tracks exceeded.

13) While surface settlement values were higher than predicted at some locations this can be partially offset by the change to the larger tunnel profile taken for the reference design, the geology and particularly the dyke and its localised effect on the immediate surrounding geology, the excavation cycle length changes and also magnitude of settlement and rate of tunnel advance. Groundwater disturbance and possible ground consolidation in the zone above the tunnel arch together with train live loading are other possible contributing factors.

13. REFERENCES

Andrews P., Braybrooke J. 2001. Common Joint & Fault Sets in Ashfield Shale (Table 1). *Deep Excavation in Shale: AGS Mini-symposium "Excavation Retention"*, Sydney Australia: Australian Geomechanics Society.

Gonzalez, M. ,Kitson M. , Mares D., Muir B., Nye E., Schroeter T. 2014. The North Strathfield Rail Underpass – Driven Tunnel Design And Construction, *15th Australian Tunnelling Conference 2014*, Sydney Australia: AusIMM.

Nye, E. J. 2013. North Strathfield Rail Underpass Shallow Cover Driven Tunnel. *Rapid Excavation and Tunneling Conference*, pp 150 – 158. Washington DC, USA: Society for Mining, Metallurgy, and Exploration.

INNOVATIVE DESIGN OF REINFORCED SOIL WALL ON A STEEP SLOPE SUBJECT TO LAND SLIP RISKS

Qijing Yang[1] and Simon Yau[2]
[1] Regional Technical Director, [2] Technical Director, Hyder Consulting Pty Ltd
Level 5, 141 Walker Street, North Sydney, NSW 2065

ABSTRACT

This paper presents a case study of an innovative reinforced soil wall (RSW) design on steep slope using site-won material that is not in full compliance with Roads and Maritime Services (RSM) QA specification R57. The steep slope was impacted by a landslip occurred in February 2010. Firstly the local geology and the landslips occurred along the project corridor are briefly described. The key design and material requirements for RSW have been reviewed with respect to the use of site-won material. A detailed strategy is presented on how to deal with the potential risks of using the non-compliance site-won fill material to the specification R57. A comprehensive laboratory testing regime of the site-won material and large-scaled pullout tests of RSW reinforcement were undertaken. With the test results and engineering judgement, the design was proceeded with the following key assumptions/factors: 1) the allowable fines (<75 microns) content of up to 25%, clay (<2.4 microns) content of up to 7%; 2) the use of reduced friction angle of 30 degrees; 3) a 10% reduction in the calculated pullout capacity of reinforcement; and 4) 1.5 times sacrificial allowance as per R57. These were to cater for long term corrosion on steel reinforcement and to ensure longevity and integrity of the RSW. A heavy rainfall in February 2010 resulted in two significant landslips within the project corridor, with the larger one being immediate at the down slope of the reinforced soil wall (RW01). This event required us to carry out an additional geotechnical investigation and landslip remedial works to ensure the long term global stability of RW01. Three dimensional effects were considered in the assessment of the slope instability in the construction stage review.

1 INTRODUCTION

The design of the reinforced soil walls (RSW) for RMS projects and some other building development projects is often based on RMS specification R57 within the New South Wales and sometimes across Australia. One of the key design requirements on the RSW fill is the fines (<75 microns) content limit of not greater than 15%. A Design Alliance, comprising Roads and Maritime Services (formerly Roads and Traffic Authority) and Hyder Consulting was formed to undertake the detail design for the Great Western Highway Upgrade at Bullaburra West. The Design Alliance team investigated the feasibility of the use of site-won material from the proposed rock cuttings with higher fines content for construction of the reinforced soil walls within the project corridor. At the start of the project the Design Alliance team held a workshop and planned a series of sampling and testing programs in order to gain the confidence in preparing a comprehensive documentation for design and construct of the proposed RSWs using site-won material.

This paper describes how a rigorous planning and implementation process was carried out together with specialist testing so as to determine the design parameters appropriate for this project. In addition this paper discusses the impacts of landslips occurred in February 2010 during the detail design phase of the RSWs, in particular a large landslip at the Brown property access road. The remedial design of the Brown property access landslip to achieve a minimum factor of safety against the global instability of RSW RW01 is also presented in this paper.

2 PROJECT DESCRIPTION

This project consists of a 2 km highway upgrade to a separated dual carriageway of the Great Western Highway from 400 m west of Genevieve Road, Bullaburra, to Tableland Road, Wentworth Falls. The existing section of highway is one lane in each direction with overtaking lanes, and generally runs uphill from east to west, with a significant 8.5% grade up Bodington Hill. The project main elements of works, as shown in Figure 1, comprise eleven retaining walls including three RSWs (RW01, RW02 and RW04), three cuts, four property accesses including Brown Property Access and four Basins (only the permanent basin was shown and the other three temporary ones were not shown), one fauna underpass and three underbores underneath the Main Western Railway for drainage works (not shown). Cut03 is approximately 370 m long cut into the Bodington Hill on the southern side of existing Highway. Cut02 is approximately 150 m long into the Mohawk between the existing highway and the main western railway. Reinforced soil wall RW01 is about 150 m long with a maximum height of 14m, RW02 is 80 m long with a height of 10 m and RW04 is 50 m long with a maximum height of 6 m. One of the project challenges was to use the site-won material from Cut03 and Cut02 for RW01, RW02 and RW04 as shown on Figure 1. The other challenge was the remedial design of landslips induced by February 2010 storm event, in particular the landslip at Brown property access road, which would have an impact on the global stability of RW01.

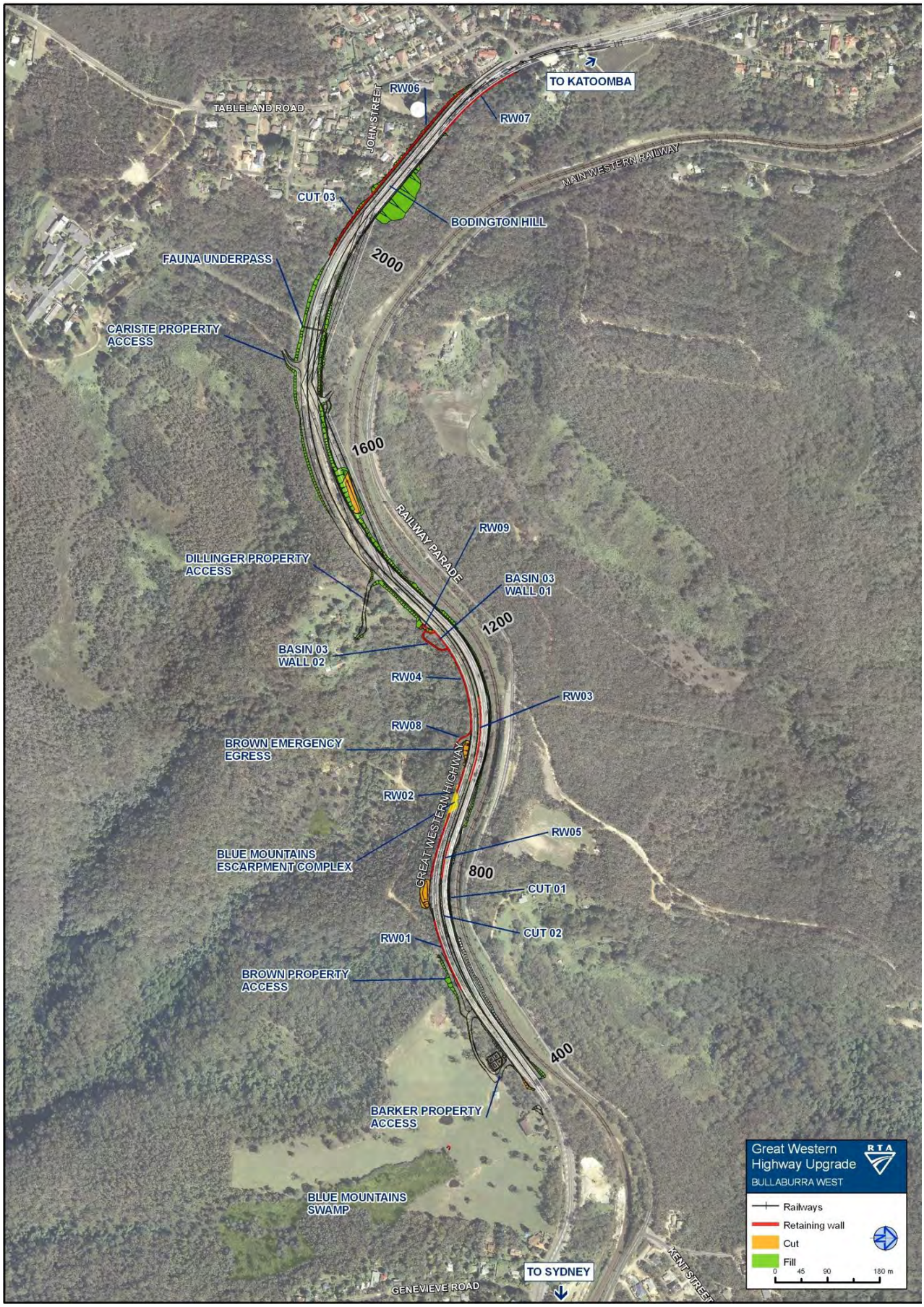

Figure 1: Locality map showing key elements of proposed works.

3 LOCAL GEOLOGY AND SITE CONDITIONS

3.1 GEOLOGICAL SETTINGS

Reference to the Katoomba 1:50,000 geological map (Sheet 8930-1) indicates that the Bullaburra West upgrade project sites are underlain by the Banks Wall Sandstone (BWS) of the Triassic period. The BWS is generally described as quartz sandstone slightly lithic, with minor interbedded claystone. Subsurface conditions within the site generally comprise varying thicknesses of sandy soils overlying sandstone bedrock and there are numerous rock outcrops and cuttings along the highway corridor.

BWS across the project site is generally red to orange brown, typically extremely to highly weathered, extremely low to very low strength, highly friable, medium to fine grained and has closely spaced joints/fractures. Ironstone veins are frequently encountered within the sandstone matrix at varying depths.

3.2 LANDSLIPS

During a storm event in February 2010 three landslips occurred over the project corridor. These are at:

- Station 635 – This was a relatively small slip with a width of about 10m around the toe of the embankment of the access road to the Brown's property.
- Station 660 – This was a large-scale landslip that occurred at the edge of the access road to Mr Brown's property.
- Station 1150 – This was a major landslide that occurred at the identified uncontrolled fill area. It was found from the historic data that a similar scale of landslide occurred around 1960.

The primary cause of the landslip was the erosion/washout induced by either surface water or seepage through the embankment or at the interface between embankment and bedrock.

The landslips that occurred across the project corridor complicated the detailed design process and documentation. The remedial design strategy for the landslips that occurred at Station 660, which would have an impact on the RSW RW01 global stability, is briefly described in this paper.

4 GEOTECHNICAL UNITS AND DESIGN PARAMETERS

4.1 GEOTECHNICAL UNITS

A concept site investigation was undertaken by RMS prior to tendering. An additional site investigation was carried out jointly by Hyder and RMS between 2009 and 2010. A geotechnical factual report was prepared by RMS in March 2010. Hyder subsequently prepared an interpretation report in April 2010. An addendum to the geotechnical factual report was prepared for the Brown property access investigation in May 2011 by RMS, and the results were interpreted by Hyder in June 2010. A summary of the geological units, depth range and characteristics for the project based on the geotechnical interpretative report is presented in Table 1.

Table 1: Geotechnical profile of project site

Geological Unit	Depth Range (m)	Description	Comments
Unit 1A	0-2	Fill: Sand and or Sandy soil of residual origin, medium dense to dense.	Generally encountered at most of the drilled boreholes and the thickness of the layer various along the project corridor
Unit 1B	0-9.9	Fill and Colluvium: Sand and Gravelly Sand, dense to very dense.	Maximum depth of 9.9m encountered at down slope of the Bodington Hill cut and approximate 6-8m fill was encountered at Brown access road.
Unit 2A	>20	Banks Wall Sandstone: Highly to moderately weathered, low to medium strength sandstone bedrock.	Generally greater than 20m with no indication of strength increase with depth observed from all boreholes drilled across the project site.
Unit 2B	0-3	Banks Wall Sandstone: Extremely to highly weathered, extremely low to very low sandstone bedrock.	Occasionally present within Bodington Hill cut as identified from mapping and borehole drilling.

4.2 GEOETCHNICAL DESIGN PARAMETERS

As part of the geotechnical investigation targeted soil sampling and testing was carried out during the detail design stage. Some samples were collected from the borehole auger drilling, cores and some from the bulk excavation trenches done at the existing Bodington Hill cut. The test results indicated that most of the indices as per R57 were satisfied except for the fines content (passing 0.075mm) being higher than 15%. A series of shear box testing was also carried out to assess the shear strength of the remoulded Banks Wall Sandstone. The shear strength test results yielded the friction angle ranging from 28 degrees to 40.5 degrees (Yang *et* al 2012). A summary of the geotechnical parameters adopted for use in the project is presented in Table 2.

Table 2: Adopted geotechnical design parameters for each unit

Geological Unit/Description	Unit Thickness (m)	Unit Weight (kN/m^3)	Effective Cohesion (kPa)	Effective Friction Angle (Deg)	Young's Modulus (MPa)	Permeability (m/s)
Unit 1A – Loose to very dense sand	11.4	17-19		30-38	10-80	-
Unit 1B – Uncontrolled fill	4.6	16		30	5	-
Unit 2A(1)- Extremely low to very low strength sandstone	12.6	22	23	37	100-300	1.0e-7
Unit 2A(2)- Extremely low to very low strength sandstone	12.6	22	30	44	100-300	1.0e-7
Unit 2A(3)- Extremely low to very low strength sandstone	12.6	22	15	37	100-300	1.0e-7
RSW Fill		20	0	30	60	1.0e-7

Note: a) Unit 2A(1) - Applicable to the design of soil nail wall, piled and other retaining walls; b) Unit 2A (2) - Only applicable to slope stability of the reinforced soil wall design; and c) Unit 2A (3) - Parameters used for underbore modelling to predict the settlement.

5 DESIGN CONCEPT DEVELOPMENT

At the concept design development stage a number of retaining wall options were considered. These includes a) piled wall with ground anchors; b) counterfort retaining wall; c) gravity retaining wall; and d) reinforced soil wall. The reinforced soil wall option was preferred for its low cost advantage. However the cut and fill material balance was an issue in that large quantities of material surplus from Cut01, Cut02 and Cut03 would have to be disposed due to presence of high fines contents, should imported fill be required for the RSW construction. As such further sampling and testing works were undertaken to assess how much fines were in the material won from these cuts.

6 REINFORCED SOIL WALL DESIGN CONSIDERATONS

The design of reinforced soil wall for this project required careful consideration of the following key issues: a) use of site-won material and material characterisation; b) consideration of durability aspects of the RSW system; c) constructability of the RSW on steep hillside; d) the landslip impact on RSW stability; and e) achieving R57 global stability requirements.

6.1 REVIEW OF RSW DESIGN CRITERIA

The specific requirements for RSW design that are either subject to further consideration or interpretation are summarised in the Table 3. R57 only allows the use of one type of RSW fill material that is defined as inert, durable material with fines less than 15% passing of 75 microns. AASHTO (2010) has similar design requirements for the RSW to those of R57. It is, however, noted that BS8006 (1995, 2010), Hong Kong Geospec 2 (1989) and subsequent Geoguide 6 (2002) allows the use of two types of fill, i.e. Type I - granular fill with fines less than 10% passing of 63 microns; and Type II - cohesive fill with fines between 10 to 45% passing of 63 microns. It can be seen that requirements of Type I material is virtually the same among R57, BS8006, AASHTO and Hong Kong Geospec 2 or Geoguide 6 except for different sieve diameter for the fines.

A summary of the key RSW material requirements and stability analysis acceptable factors of safety (FoS) and factors is presented in Table 3.

Table 3: RSW fill requirements and key design criteria

Reference	Design Method	Key RSW Fill Requirements and Design Criteria
Table R57.10 / BS8006	Property Index of RSW Fill	R57: Fines<0-15%, LL<30% and PI<12% for Fines. BS8006: LL≤ 45% and PI≤ 20% for Type II, less than 2 microns 0-10%.
Generally Acceptable Industrial Practice	Conventional global stability analysis	• A minimum global factor of safety shall be 1.5. All load factors are set to be 1.0. Earthquake load is not considered. Groundwater level is set to be at the actual groundwater level.
R57 Clause 4.7.3	Global stability analysis under earthquake	• A minimum global factor of safety shall be 1.35. Load factor for static loads is set to be 1.0. Load factor for traffic (live) load and earthquake load is set to be 0.5 and 0.75 respectively. Ground water is set to be at ground surface level.
Generally Acceptable Industrial Practice	Global stability analysis under extreme conditions – flooding	• A minimum global factor of safety shall be 1.2. All load factors are set to be 1.0. Earthquake load is not considered. Water level is set to be at the ground surface in front of RSW.
R57	External Design (Sliding, bearing and overturning)	• The interaction factors for sliding, bearing and overturning are to be greater than 1.05 Load Factors for Load Cases A), B), C), D), E and F are the same as per Standard RMS R57.

A comparison between R57 and BS8006 regarding the allowable electrical and chemical limits of RSW fill is shown in Table 4. It can be seen that the key parameters are virtually the same between these two design guidelines. With reference to AASHTO 2010, it is noted that similar testing requirements are set for granular RSW fill. The fundamental difference is that only BS8006 and Geoguide 6 permit the use of cohesive soil for the RSW.

Table 4: Comparison of allowable electrical and chemical limits of RSW fill

Code Reference	Allowable Limits		Allowable Limits		
	R57	**R57**	**BS8006 (1995)**	**BS8006 (1995)**	**AASHTO (2010)**
	Submerged[1]	Non-Submerged	Submerged	Non-Submerged	
pH	5-10	5-10	5-10	5-10	5-10
Resistivity (ohm m)	≥ 30	≥ 10	≥ 30	≥ 10	≥ 30
Organic Content (%)[2]	N/A	N/A	≤ 0.2	≤ 0.2	≤ 1.0
Redox Potential (volts)[3]	N/A	N/A	≥ 0.4 (Type I) ≥ 0.43 (Type II)	≥ 0.4 (Type I) ≥ 0.43 (Type II)	N/A
Microbial Activity Index[3]	N/A	N/A	≤ 5	≤ 5	
Chloride Ion Content (% by weight)	≤ 0.01	≤ 0.02	≤ 0.01	≤ 0.02	≤ 0.01
Sulphate Ion Content (% by weight)	≤ 0.05	≤ 0.10	≤ 0.05	≤ 0.10	≤ 0.20
Total Sulphate Content (% by weight)	N/A	N/A	≤ 0.10	≤ 0.20	

Notes: (1) Submerged structure means a structure that is periodically submerged in water but excluding marine condition and contaminated or saline water. (2) The measurement of organic content shall be carried out for clayey soils where more than 15% passes a 63 microns BS Sieve Size. (3) The measurement of either redox potential or microbial activity index shall be carried out for clayey soils with an organic content in excess of the specified.

6.2 RSW FILL CHARACTERISATION

In order to better characterise the fines content from Cut02 and Cut03 the Design Alliance team undertook additional borehole drilling and coring as well as in-situ trench sampling from the existing Bodington Hill cut. Sampling and the testing procedures were kept as close as possible to normal field excavation and compaction for the reinforced soil wall. It was acknowledged that the samples obtained from auger drilling appeared to have much higher fines contents than those crushed bulk samples from the Bodington Hill cut as shown in Figure 2.

It has been noted from Figure 2 that, except for those samples taken by auger drilling, the fines content for the rock samples from Bodington Hill range from 15% to 25%. The fines content of the rock samples from the eastern cutting (in the vicinity of Cut 02) is more variable, ranging between 7% and 24%. The hydrometer testing results indicates that the clay content (less than 2.4 microns) is typically ranging from 3% to 10% based on samples from test pits where fines of less than 75 micron is less than 25%. It has been concluded that the testing results of the cored samples and trench excavation samples are more realistic, noting the treatment of sample would result in an increase in fines by 2% to 4%.

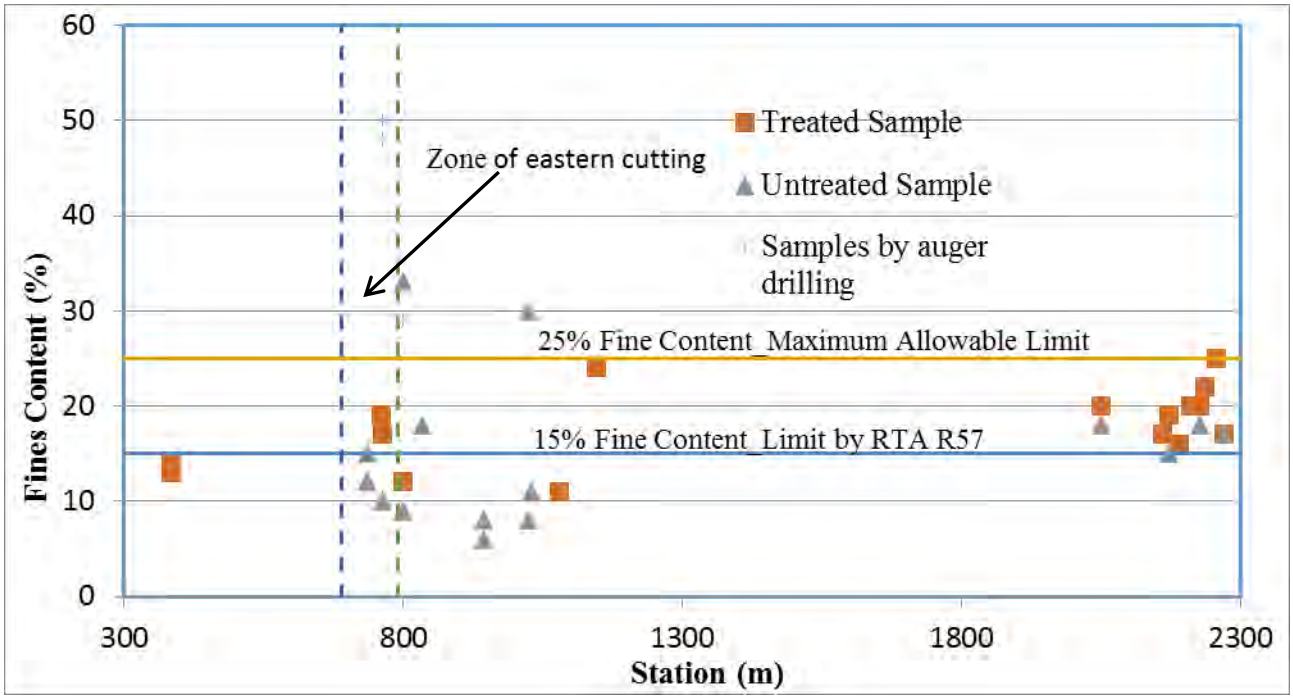

Figure 2: Fines contents of recovered samples from borehole and trenches along project alignment.

6.3 DURABILITY CONSIDERATION

Due to the higher fines content within the RSW fill a research of the corrosion allowance was undertaken to determine how much sacrificial allowance should be adequate at various stage of the design life. It is noted that the requirements for the electrical and chemical limits with respectively to the pH value, resistivity and Chloride ion content are identical for R57, BS8006 and AASHTO. The Sulphate ion content and the organic content in AASHOT 2015 are relatively higher than those in R57 and BS8006. This was based on the findings that most constructed RSWs experienced a slower corrosion rate on the reinforcements than allowed in the design, which has a typical factor of 2 as reported by Elias (1990, 2009). However BS8006 requires additional testing for redox potential and microbial activity index for cohesive fill as shown in Table 4. The authors believe that this is due to the fact that R57 only allows the use of inert, durable material with fines not more than 15% passing 75 microns. After review of these published codes or specifications the Design Alliance team decided to refer to Hong Kong Geospec 2 (1989) which specified the use of Type II fill with fines up to 45% and clay up to 15% and an additional 50% sacrificial thickness to the metallic reinforcement.

Hong Kong Geoguide 6 (2002) indicates that the effects of loading and construction damage to metallic reinforcement may not be time dependent. Corrosion, which is related to the electrochemical nature of the soil and the air/water requirement, is time dependent and is considered as a reduction in net reinforcement cross-sectional area with time. For the conditions pertaining to reinforced soil, the effects of individual factors are additive and not interdependent. Thus rates of corrosion, for example, do not vary with load intensity.

Based on the above assessment Tables 57.9 and 57.13 in R57 were revised to include an increase in the steel corrosion allowances to cater for the potential higher level of corrosion due to presence of high fines content. The revised specific details for minimum sacrificial steel thickness on each hot-dip galvanized steel surface exposed to corrosion within reinforced the fill material are shown in Table 5 and Table 6:

Table 5: Minimum sacrificial steel thickness for hot-dip galvanized steel soil reinforcement (mm)

Design Life (Years)		**5**	**10**	**20**	**30**	**50**	**100**
Structural Location	Land Based i.e. out of water	0	0.1	0.3	0.5	0.9	1.35
Structural Location	Fresh Water Based	0	0.15	0.5	0.65	1.05	1.5

Note: (1) Linear interpolation may be used for intermediate values; (2) These values may not be applicable in the presence of stray electrical currents from adjacent power sources. In such cases values must be assessed by specific study.

Table 6: Sacrificial steel thickness for steel facing connections/facing elements and other steel components (mm)

Design Life (Years)		**5**	**10**	**20**	**30**	**50**	**100**
Structural Location	Land Based i.e. out of water (1)	0	0.15	0.5	0.65	1.05	1.5
Structural Location	Fresh Water Based (2)						

Note: (1) Linear interpolation may be used for intermediate values; (2) These values may not be applicable in the presence of stray electrical currents from adjacent power sources. In such cases values must be assessed by specific study.

6.4 PULLOUT CAPACITY

The research work by Bobet (2002) has found that RSW fill with high fines content is likely to lower the pullout capacity of reinforcement under saturated condition. In addition the degree of saturation and transportation of moisture is important to the shear strength at the interface of the reinforcement against the RSW fill. Bobet (2002) also noted that when the permeability of the RSW fill is lower than 10e-5 m/s the dissipation of the pore water pressure is very slow, and that the pullout capacity of reinforcement may be reduced by up to 50% when a small percentage of fines is present within the RSW fill. As such the Design Alliance team proposed a pro-typo laboratory test to determine the pullout capacity of two reinforcement systems. These specialist pullout tests using the materials collected from the excavated trenches in Bodington Hill cut were undertaken on two RSW systems by the Australian Defence Force Academy (ADFA) of the University of NSW in Canberra, i.e. Reinforced Earth System and VSL Retained Earth System.

6.5 SUMMARY OF KEY FACTORS CONSIDERED FOR THE NON-COMPLIANCE MATERIAL

Based on assessment and discussion with the RMS, the following measures were undertaken to mitigate the adverse effects resulting from use of site-won crushed sandstone with a fines content of up to 25%:

- Based on the grading results discussed above, increased the upper limits for particles smaller than 75 micron and 2.4 micron in reinforced fill material to 25% and 7% respectively in revised R57 for this project.
- Adoption of a slightly conservative design value of constant volume frictional angle of 30 degrees for reinforced soil fill.
- Reduction of the design values of the coefficient of interaction by 10% for pullout capacity as stipulated in the Specification R57 based on ADFA testing results.
- Provision of a dedicated drainage system using gravel wrapped in geotextile behind to minimise groundwater pressure built-up behind the RSW
- Provision of a clay liner on top of the RSW block to minimise infiltration into the RSW.
- Placement of a geotextile behind the facing panels to prevent the escape of fines from the RSW block.

7 RSW WALL CONSTRUCTABILITY AND DETAILS

7.1 RSW CONSTRUCTION STRATEGY

The Design Alliance commissioned a specialist contractor to undertake a concept design of the proposed reinforced soil walls (RW01, RW03 and RW04) along the westbound carriageway where the retained height was greater than 6 m. This particular proprietary wall type was selected for several reasons, including cost efficiency, construction method and sequencing, materials management, spatial constraints and safety.

To balance the earthworks throughout the project, it was intended to re-use the crushed sandstone as the reinforced fill material where possible on the RSWs. The site-won sandstone from Cut03 was proposed for use in RW02 and RW03.

Material from the eastern cutting (Cut02, Station 705 to 800) was proposed for use in RW01. Sandstone from temporary excavations needed for RW01 and RW02 was proposed for use in RW04. Significant temporary work was expected for the construction for these RSWs due to steep hillside.

A typical cross-section of the proposed reinforced soil wall is shown in Figure 3. A dedicated drain was applied to control the potential seepage from the uphill side and divert the seepage to the subsoil drain to a dedicated outlet points. A geosynthetic clay liner was provided at the top surface of the reinforced fill material at 2% grade to prevent subsurface water flows/infiltration into RSW fill. The water collected from the clay liner would then be drained away through a vertical drainage blanket at the rear of the RSW. To this end it is unlikely that there will be significantly free water entering the RSW block.

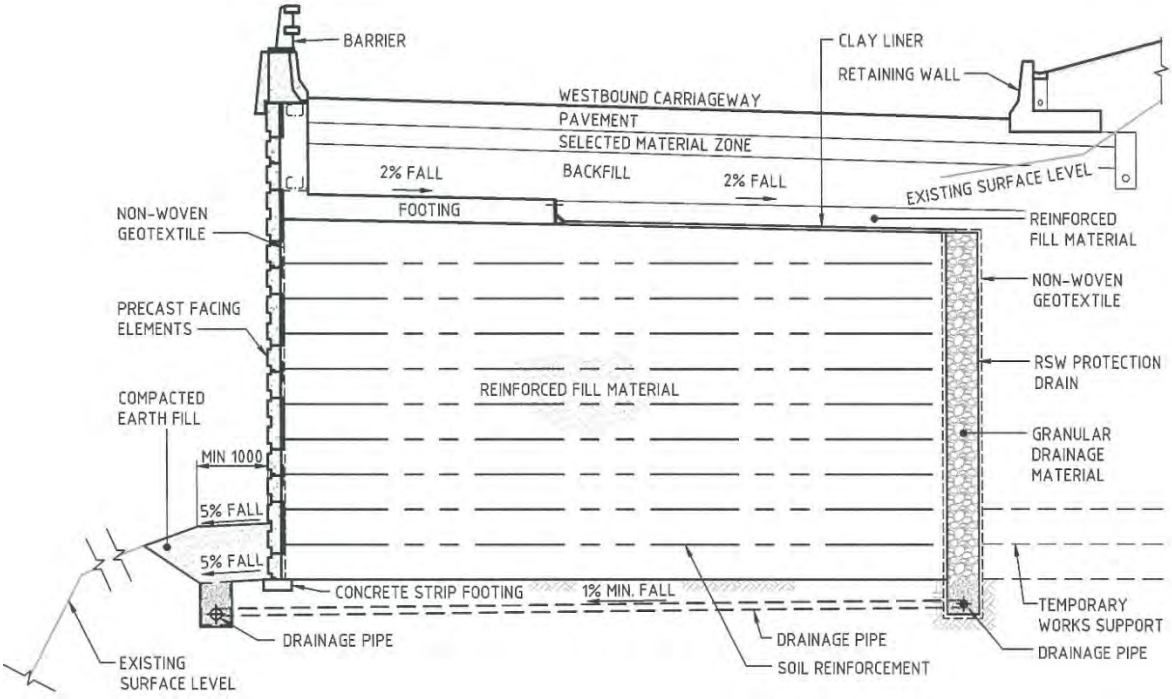

Figure 3: Typical cross-section of RSW wall.

The internal stability check was carried out by the specialist contractor, while the external stability was carried out by Hyder. It was found that the length of the RSW block was governed by the global stability rather than internal stability.

7.2 INTERNAL STABILITY CHECK

The internal stability check was carried out for all the load cases as per R57 with due consideration of the factors summarised in Section 6.5. An interaction factor of 1.05 rather than 1.0 was adopted to facilitate a slightly higher safety margin due to some uncertainties in soil electrical and chemical properties. The RSW internal stability checks against rupture, pullout, connection strength at the face panel and wedge failure were undertaken with due consideration of the following:

- Steel reinforcement with appropriate corrosion allowance made as per revised R57;
- 10% reduction in pullout capacity of reinforcement at the interface between steel and soil; and
- Use of a friction angle of 30 degrees for the RSW block.

7.3 EXTERNAL STABILITY CHECK

The external stability checks of the RSW were carried out for load cases A to F as stipulated in R57 in order to satisfy the following failure mechanisms: Ultimate Limit States: a1) Bearing failure; a2) Sliding; a3) Slip failures and b) Serviceability Limit State: Settlement, b1) tilting, eccentricity, rotational and lateral movement; and b2) Slip failures. These were carried out by the specialist contractor and Hyder.

It was found that the width of the RSW block was governed by the global stability of the potential slip plane either beyond or just passing the bottom corner of the RSW. This suggested that global stability is critical in determining the size of the RSW block width and the constructability of the RSW, in particular RW01 which is very close to the existing highway that has to remain open at all time.

The global stability of the existing embankment was analysed based on the rock and soil parameters discussed in the previous sections. This analysis indicated that the existing slopes were close to the minimum required factors of safety

of 1.35, prior to the additional loads from the retaining wall. Note that the global stability analysis assumed the design water table on the downslope side of the retaining wall to be at the proposed surface level as per R57.

A lower factor of safety than 1.35 was calculated for the sections that were impacted by landslip occurred at Brown's property access road. As such landslip remediation was carried out prior to completion of detail design.

8 LANDSLIP REMEDIATION

In order to maintain the access road to Brown's property and enhance the factor of safety against slope instability after construction of the RSW RW01, remedial works were required for the landslip approximately between Station 660 and Station 700.

A workshop was held by the Design Alliance to discuss the strategy of the Brown's landslip remedial works. It was agreed that two cases were to be investigated:

- Case 1: The minimum factor of safety against global failure of retaining wall RW01 without repair works to the existing Brown slip;
- Case 2: The minimum factor of safety of RW01 following repair works.

Three remedial options were considered: a) Rockfill re-profiling – use rock fill deposited on the slope face to stabilise the slope to achieve the required factor of safety; b) Gabion wall - construction of a gabion wall along the shoulder of the existing access road to Brown's property; and c) Piled wall – construction of a contiguous piled wall along the edge of existing access road.

The option of rockfill re-profiling was preferred for ease of construction, low cost and project program advantage. A maximum slope angle of 29 degrees should be maintained to achieve a minimum factor of safety of 1.35 for the RW01. In addition a rockfill containment bund was required at the toe of the slope prior to the placement of the rockfill for ease of construction. To avoid saturation of soil at the upper part of slope and subsequently instability of the slope, a drainage pipe was designed to discharge stormwater from uphill catchment beyond the point at least 16 m away from the slope crest.

It was found that the calculated factor of safety of RW01 at about Station 660 without any remedial works was approximately 1.27 as shown in Figure 4, which did not satisfy R57 requirement of 1.35. With the consideration of the remedial works the calculated FOS was enhanced to 1.40 as shown in Figure 5.

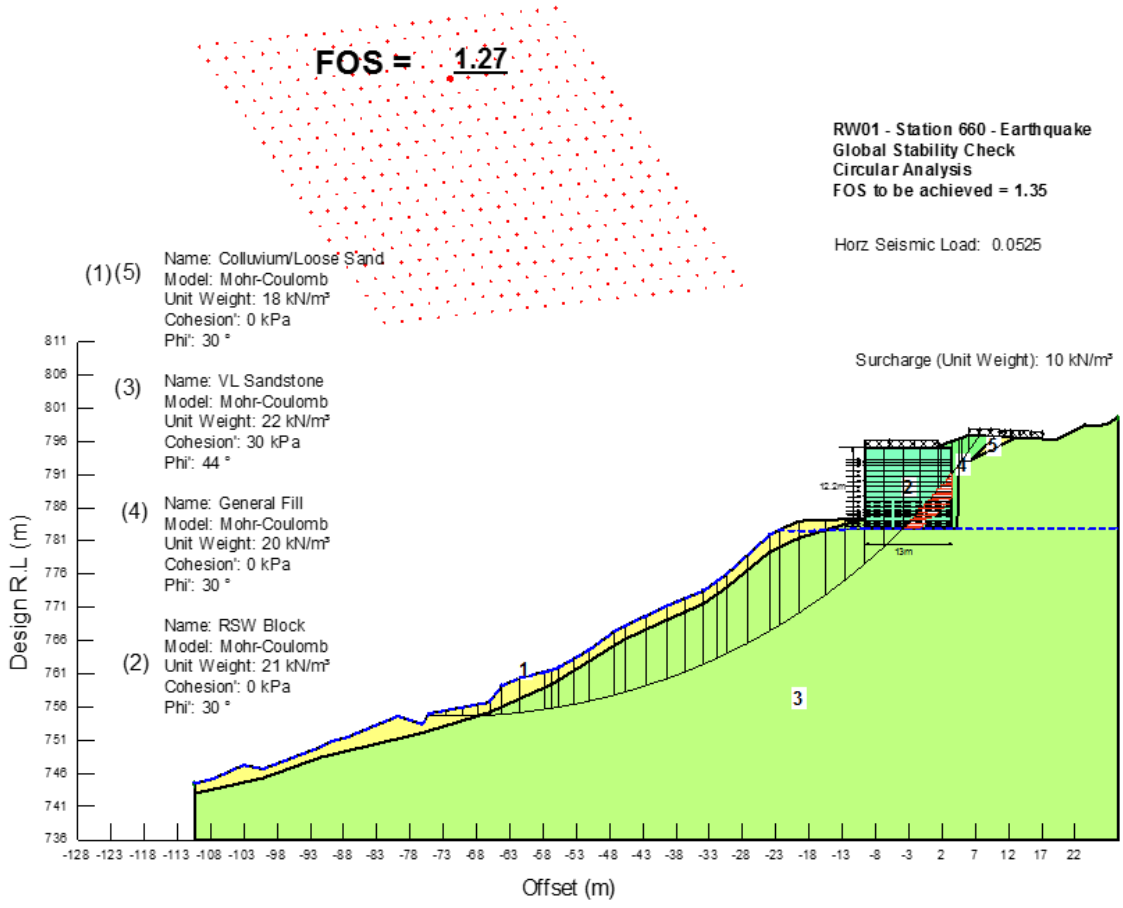

Figure 4: Calculated FoS of Slope without remedial works.

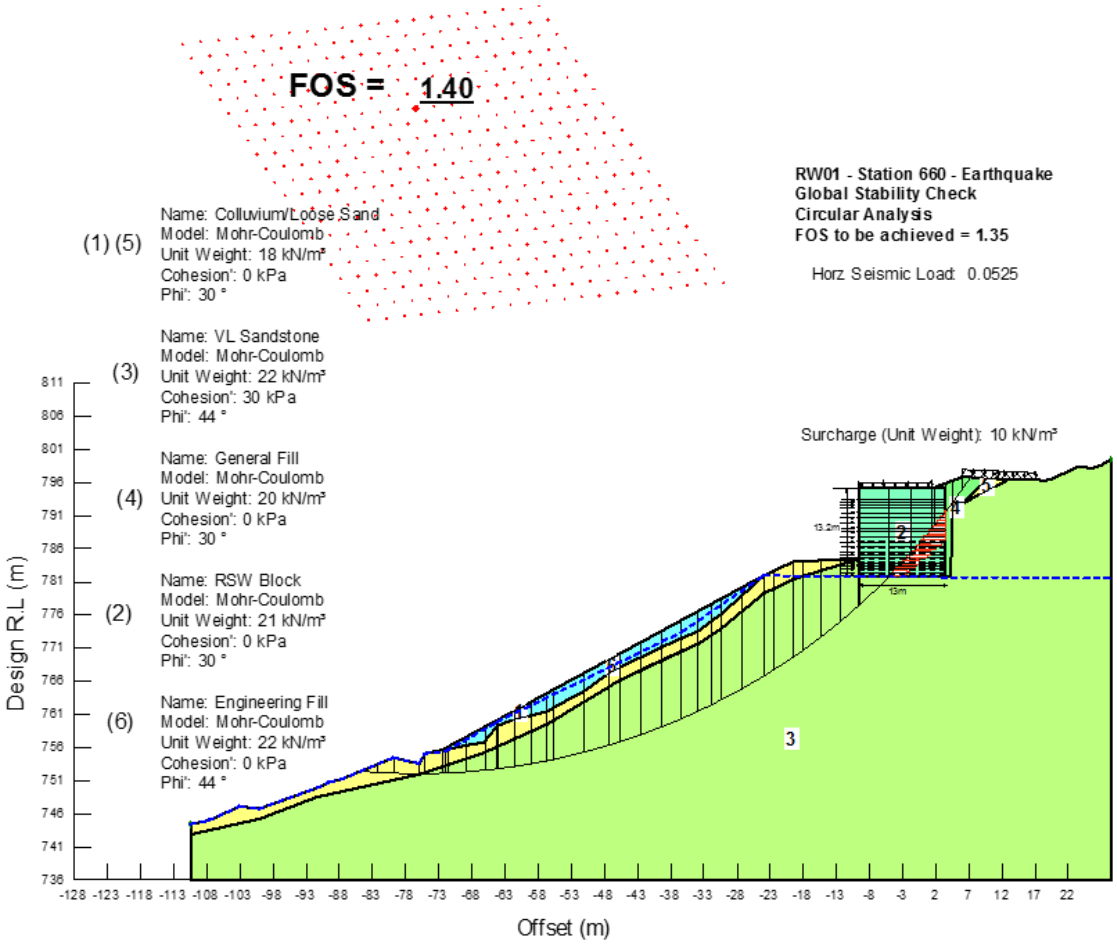

Figure 5: Calculated FoS of Slope after remedial works.

The documented concept design of the RSWs was therefore assessed to be in compliance with the R57 specification. The obligation for the Contractor following contract award was to design and construct all project RSWs including RW01 in accordance with R57 and R58. In this regard the Contractor was required to engage an engineering consultant to undertake external design of the RSWs whilst the internal design was being undertaken by a specialist contractor.

9 CONSTRUCTION STAGE ISSUES

During the construction the contractor reported that a minimum factor of safety of 1.35 as per R57 could not be attained for an RW01 section approximately between Station 675 and Station 705 by adopting the original reference design. The lowest computed FoS was about 1.20.

Review carried out by Hyder identified a number of factors that might contribute to the contractor not achieving a satisfactory FoS against global instability, namely: a) Browns slip restoration work (see below) altered the downslope profile below RW01; b) Design Alliance used previous survey profile, i.e. original down slope profile; and c) Use of relatively conservative design assumptions and parameters by the contractor.

Hyder undertook an independent slope stability assessment for RW01 at the cross sections of concern, and a summary of calculated FoS is presented in Table 6.

Table 6 Summary of calculated factors of safety at each station based on 2D Slope/W analysis

Station	660	675	685	695	700	710
Calculated FoS	1.41	1.27	1.20	1.22	1.24	1.37

An average FoS of the 30m wide block between Station 675 and Station 705 is calculated to be 1.24, based on the individual FoS of each of the four sections in Table 6. A FoS of 1.43 can be achieved when the side cohesion and friction resistance on both sides are considered. This implies when 3D effects are taken into account an increase in FoS of approximately 13% from the 2D analysis result, which is within lower end of the 3D enhancement of 10% to 50% found by other researchers such as A. Li et al (2009, 2010), Fredlund et al (2011) and Stark T (2012). This finding was presented to RMS at a workshop, and it was recognised that for a very long (>100m) and deep-seated (>10 m) slope to

fail, resulting from a lower FOS of 1.24 (average over 30 m) than required 1.35, the probability is very remote. This is particularly supported by the fact that it is unlikely for groundwater table to rise to the ground surface and to fully saturate the entire down slope given the steep terrain and measured standing water table in rock is well below the surface. To this end RMS accepted the minimum FOS of 1.24 (average, using 2D analysis) as a concession case for RW01. It was however emphasised that the 3D enhancement effect must be assessed on a case by case basis and should not be broadly applied to any of the 2D slope stability analytical results.

10 CONCLUSIONS

This paper has presented a case study of the use of site-won non-compliance fill material to R57 for construction of RSW walls by a systematic early planning, testing and design. It is found that there are limited guidelines available as to the permeability of the RSW fill when the fines content is close to 15%. The relaxation of fines passing of 75 microns up to 25% and 2.4 microns up to 7% were set for the RSW fill in a revised R57. This was coupled by: 1) the use of a lower pullout capacity of reinforcement by 10%; 2) the use of a friction angle of 30 degrees for the site-won fill; 3) an additional sacrificial allowance by 50%; and 4) provision of a groundwater management system including a clay liner above the RSW and a vertical drainage behind the RSW. These mitigation measures were devised to ensure a successful design of RSW using site-won material. The remedial works for the landslip in the vicinity of Brown's property access road were critical for the overall stability of the RSW wall - RW01. During construction due consideration of 3D effects in the slope stability analysis for the lower than standard R57 FoS of 1.35 was proved to be the best outcome for project.

It is suggested that further research be carried out to assess if the use of high fines content RSW fill material will yield satisfactory performance during its service life. Moderate proportion of fines such as this project case (up to 25% passing 75 micron and 7% passing 2.4 microns) may be considered for future projects with appropriate mitigation measures, including electrical and chemical limits testing as per BS8006. From a durability point of view R57 should be modified accordingly to include appropriate tests such as the organic content and potential acid sulphate soil to assess the corrosiveness of the fill material when the fines passing 75 microns is up to 15%.

At the time of writing this paper the westbound dual carriageway has been completed and the traffic switched onto the new traffic lanes being supported by the three RSWs. It has been reported that the RSWs have been performing within the expectation.

11 ACKNOWLEDGEMENTS

The views expressed in this paper are the authors' professional opinions only. Special thanks are due to Mr. Max Anandappa who was the RMS interface manager for the design alliance and Mr. Joseph Mak of RMS who was the specialist reviewer for RSW design. Without their support and contributions this paper would not be possible. The authors are also grateful to the Bullaburra West Design Alliance for the permission to the publication of this paper. The contribution from the Alliance members to the results presented in this paper is greatly appreciated.

12 DISCLAIMNER

Neither the author/s, contributors, nor their respective organisations make any representation or warranty as to the accuracy, completeness or suitability or otherwise of the information contained in this paper and shall have no liability to any person in connection therewith.

13 REFERENCES

AASHTO (2010), *AASHTO LRFD bridge design specifications*, Fifth Edition, American Association of State Highway and Transportation Officials.

Bobet, A. (2002), *Design of MSE walls for fully saturated conditions*, FHWA/IN/JTRP 2002/13, School of Civil Engineering, Purdue University, prepared in Cooperation with the Indiana Department of Transportation and the U.S. Department of Transportation Federal Highway Administration.

BS8006 (1995), *Code of practice for strengthened / reinforced soils and other fills*, British Standard.

BS8006-1 (2010), *Code of practice for strengthened / reinforced soils and other fills*, Vol. 1, British Standard.

Elias, V. (1990), *Durability/corrosion of soil reinforced structures*, FHWA/R-89/186, Federal Highway, Administration, U.S. Department of Transportation, Washington, DC, p. 173.

Elias V, Fishman, K. L., Christopher B. R. and Berg R. R. (2009), *Corrosion/degradation of soil reinforcements for mechanically stabilized earth walls and reinforced soil slopes*, FHWA-NHI-09-087, U. S. Department of Transportation, Federal Highway Administration, Nov. 2009.

Fredlund, M. D., Lu, H. and Fredlund, D.G. (2011) *Three dimensional limit equilibrium slope stability benchmarking*. https://www.google.com.au/search?q=three-dimensional+limit+equilibrium+slope+stability+benchmarking&hl=en-AU&gbv=2&oq=&gs_l=.

Geotechnical Engineering Office (1989), *Guide to reinforced fill structure and slope design*, Geospec 2, Civil Engineering Department, The Government of the Hong Kong Special Administrative Region.

Geotechnical Engineering Office (2002), *Guide to reinforced fill structure and slope design*, Geoguide 6, Civil Engineering Department, The Government of the Hong Kong Special Administrative Region.

Hyder Consulting (2008), *Geotechnical interpretative report for Wentworth Falls East, Great Western Highway upgrade*, May 2008.

Hyder Consulting (2010), *Geotechnical interpretative report, Great Western Highway upgrade at Bullaburra West*, Report No FF0001-AA002486-AAR-01, 16 April 2010.

Hyder Consulting (2010), *Geotechnical interpretative report, Great Western Highway upgrade at Bullaburra West*, Report No FF0001-AA002486-AAR-02, 28 June 2010.

Li, A. J., Merifield, R.S. and Lyamin A.V. (2009), *Limit Analysis solutions for three dimensional undrained slopes*, Computers and Geotechnics, Vol. 36, pp 1330-1351.

Li, A. J., Merifield, R.S. and Lyamin A.V. (2010). *Three dimensional stability charts for cohesive frictional and purely natural slopes based on limit analysis methods.* Canadian Geotechnical Journal, 2010, 47(12): pp 1316-1334.

Roads and Traffic Authority (2007), *RTA QA specification R57 – design of reinforced soil wall*, Ed2/Rev1, Infrastructure Contract Branch, Roads and Traffic Authority of New South Wales.

Roads and Traffic Authority (2010), *Compilation of factual geotechnical information - HW5 - Great Western Highway Upgrade at Bullaburra West*, Report No G4045/1, Volumes 1, 2,3 ,4 and 5, 26/03/2010.

Roads and Traffic Authority (2010), *Additional geotechnical investigation for detail design - HW5 - Great Western Highway upgrade at Bullaburra West*, Report No G4045/2, 26/05/2010.

Stark, T. (2012), *Three-dimensional slope stability methods in geotechnical practice*. 51st Annual Geotechnical Engineering Conference, University of Minnesota. http://tstark.net/wp-content/uploads/2012/10/CP56.pdf.

Yang, Q. J., Yau, S. and Chen J. (2011), *Rock mass characterisation for rock cutting and slope stability design*, Advances in Geomechanics, Perth, Australia, Nov 2011.

TOWARDS A RESILIENT DESIGN: L-SHAPED BARRIER-IMPACT LOAD MODELLING ON REINFORCED SOIL WALL STRUCTURES

P. Wanis[1] and T. Fitzpatrick[2]

[1]Senior Design Engineer, [2]Design Engineer, The Reinforced Earth Company, Australia

ABSTRACT

It has always been a challenge to model the effect of crash barrier loadings on Reinforced Soil Wall (R.S.W.) structures due to the complexity of their design and the manner in which the load is transferred through each soil reinforcement layer of the R.S.W. structure. Current design practices in Australia rely heavily on the designers experience and the individual knowledge the impact crash barrier loadings have on the R.S.W. structure. Each designer has an individual approach to the same problem. Relevant codes do not adequately cover this issue and leave it up to the designer‟s experience. This paper outlines and discusses a design beyond the current codes and how codes and standards can be enhanced. There is a clear necessity to provide a systematic, well proven and tested approach to the manner in which the loading on the R.S.W. structure from the crash barrier is interpreted, modelled and analysed.

1 INTRODUCTION

An R.S.W. structure is a soil block formed by the association of earth and soil reinforcement. Flexible, linear soil reinforcing elements are placed in a granular earth fill. Frictional forces between the soil and the soil reinforcing elements provide a cohesive strength to the earth fill forming a composite material, „Reinforced Earth®“. The most common case of an R.S.W. structure is where it supports the access embankment for an overpass. Therefore, the top of the R.S.W. structure must allow for the effects of traffic surcharge and impact. In general, the road surface consists of asphalt pavement which provides far less structural resistance for the incorporation of crash barriers than a concrete pavement. For the purpose of crash barrier design, the crash barrier has to be assumed to take the full impact load without any support from the asphalt pavement.

In the case of L-shaped barriers, the footing is intended to provide stability for the barrier to resist impact loads and to reduce the influence of these impact loads on the R.S.W. structure by distributing the load over a wide area (Briaud et al 2012). The resistance is generated by the inertia force required to lift the slab. The impact load then generates additional stresses in the R.S.W. structure soil reinforcement in addition to the static loads due to gravity. The dynamic design loads are specified using both a pressure distribution approach and a line load approach.

Australian Standards currently do not provide any clear guidelines in relation to the effect crash barrier loadings have on R.S.W. structures. As a result there are no design analysis programs currently available that adequately examine the impact loads and their net effect on the R.S.W. structure. The accurate design of R.S.W. structures with an incorporated crash barrier system requires a good understanding of the relevant failure modes and the magnitude and distribution of impact loads transferred from the crash barrier system onto the R.S.W. structure. The manner in which the design has been approached can often be dictated by information provided by the external designers. This information may be unrealistic however; it can control the design where it is not possible to provide a clear alternative which can be adequately backed up by the relevant codes.
This paper aims to:

i) Provide information on how codes and standards can be enhanced.

ii) Recommend a new design approach for the accurate interpretation and modelling of crash barrier loading on R.S.W. structures based on current Australian Standards and other relevant international standards.

2 THEORY

2.1 LOADS

2.1.1 Permanent Loads

The soil above the crash barrier footing and the concrete crash barrier self-weight has to be considered in the analysis. The magnitude and line of action must also be calculated. Therefore, the geometry of the crash barrier and depth of soil plays a significant role in the analysis of the system. As shown in Figure 1, there are several different crash barriers systems that are already in place and have been built for various projects. Table 1 shows the value of the permanent loads (working) and point of action behind the wall facing.

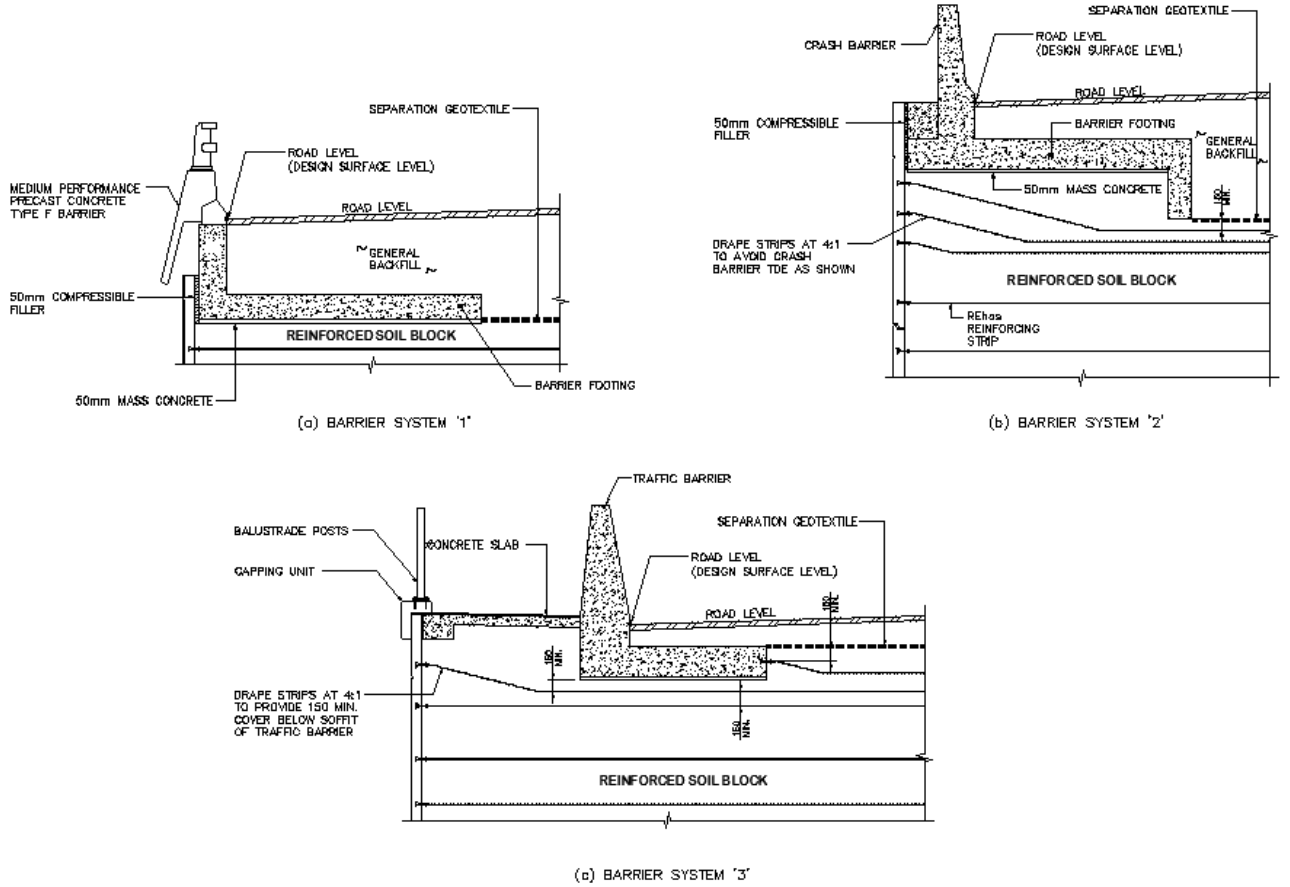

Figure 1: Different Crash Barrier Geometries

Table 1: Permenant Loads – Working

Barrier System	Weight $_{Soil}$ (kN/m)	Weight $_{Concrete}$ (kN/m)	Weight $_{Total}$ (kN/m)	Distance between Weight $_{Total}$ line of action & wall facing (m)
1	72	45	117	1.88
2	32	61	93	1.95
3	12	48	60	3.10

2.1.2 Live Loads

The vehicle vertical load must be considered in the design. Many guidelines are available for the value of the vertical load to be incorporated in the design based on Australian Standards and technical specifications as follows:

1- Australian Standards AS5100; Bridge Design Code, Part 2: Design loads, road traffic vary between W80 wheel load, A160 axle load, M1600 moving traffic load, S1600 stationary traffic load and heavy platform load. The majority of these loads are equivalent to 20 – 25 kPa.

2- Australian Standards AS/NZS 3845; Road Safety Barrier Systems, Clause 3.5 suggests using the mass of the vehicle in the analysis as shown in Figure 2.

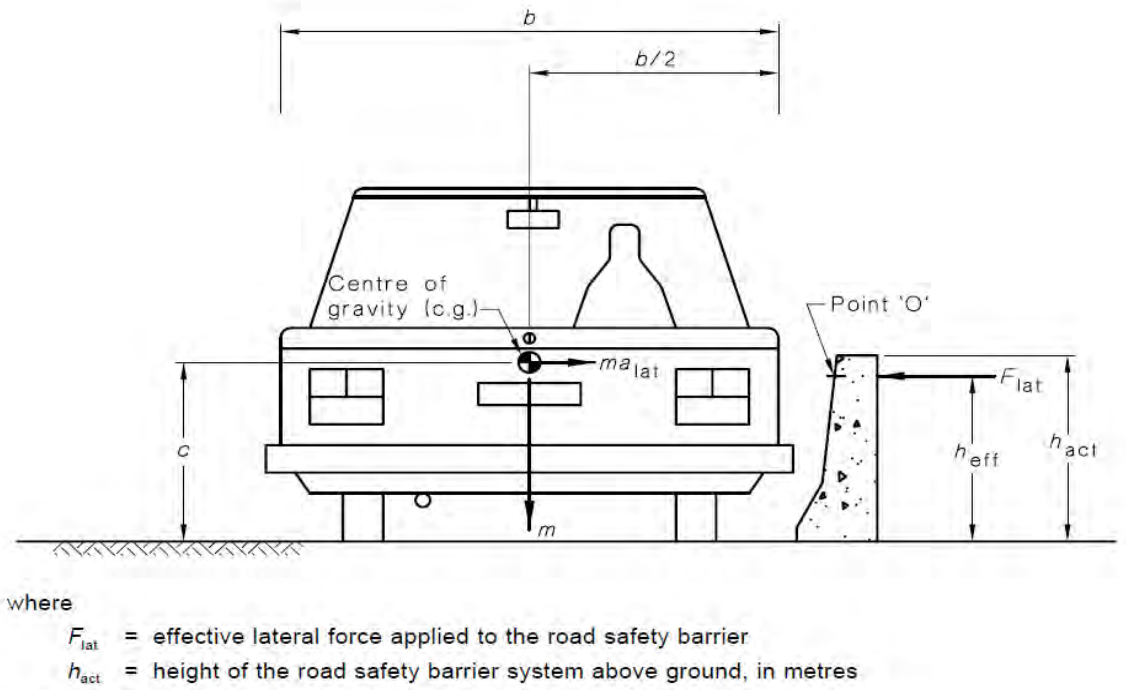

Figure 2: Suggested vertical load to be used in the analysis as per AS/NZS 3845.

3- The information on owner product specifications (mainly for heavy vehicles and dump trucks) is available for the public. These specifications include information regarding: total vehicle weight, load distribution over the front and rear axle, vehicle dimensions and pay load. Table 2 shows the load distribution details for a CAT 797B Mining Truck (Gross Vehicle Weight 624T). By using this information designers can model the live loads to be considered in the analysis accurately and as per site conditions.

Table 2: CAT 797B Mining Truck Weight Distributions Details

Weight Distributions - Approximate	
Front Axle - Empty	43.5%
Rear Axle - Empty	56.5%
Front Axle - Loaded	33.3%
Rear Axle - Loaded	66.7%

2.1.3 Collision Loads

Similar to the vertical live load, many guidelines are available in Australian Standards and technical specifications for different levels of vehicular collision loads. They vary depending upon the crash barrier performance level as follows:

1- Australian Standards AS5100; Bridge Design Code, Part 2: Design loads Clause 11.2.2 "Traffic barrier design loads" and Appendix A. The classification is based on the crash barrier performance level as per Table 3, the direction and notations for these loads are shown in Figure 3.

Table 3: Traffic Barrier Design Loads as per AS5100.

Barrier performance level	Ultimate transverse outward load (F_T) **(kN)**	Ultimate longitudinal or transverse inward load (F_L) **(kN)**	Vehicle contact length for transverse loads (L_T) and longitudinal loads (L_L) **(m)**	Ultimate vertical downward load (F_V) **(kN)**	Vehicle contact length for vertical loads (L_V) **(m)**	Minimum effective height(H_E) **(mm)**
Low	125	40	1.1	20	5.5	500
Regular	250	80	1.1	80	5.5	800
Medium	500	170	2.4	350	12	1100
Test level 6 (36 T articulated tanker)	750	250	2.4	350	12	1400
Greater than Test Level 6 (44 T articulated van)	1000	330	2.5	450	15	1400

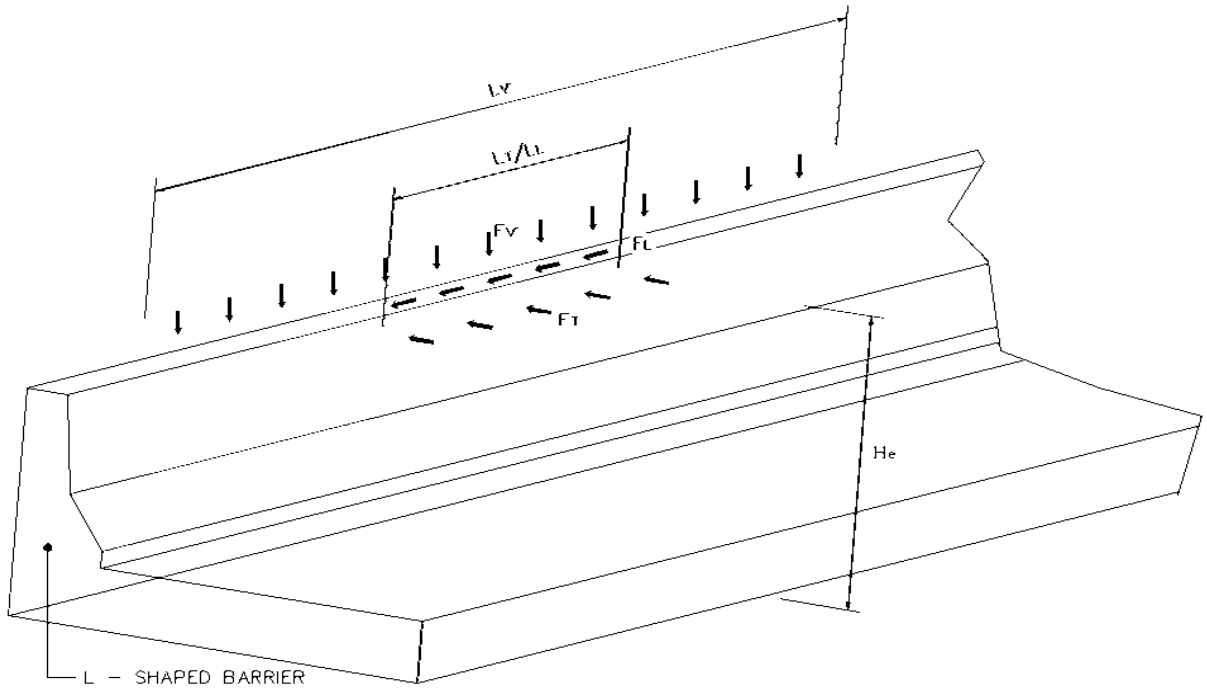

Figure 3: Crash Barrier Load Directions and Distributed Length as per AS5100.

2- Australian Standards AS/NZS 3845; Road Safety Barrier Systems, Appendix C Tables C1 and C2 summarize the design loads and distributed length based on type of vehicle and category of test level. Table 4 shows a summary of this information.

Table 4: Traffic Barrier Design Loads as per AS3845.

Corresponding AS5100 barrier performance level	Type of vehicle	Longitudinal length (L_T) **(mm)**	Category	Design Load **(kN)**	Minimum height above road surface **(mm)**
Low	Pick up or small vehicle	1200	Test Level 2	100	535
			Test Level 3	100	535
Regular	Van or truck with single rear axle	1070	Test Level 4	300	820
Medium	Truck with rear tandem axles	2400	Test Level 5 <	700	1500

2.2 LOAD CASES

Australian Standards AS4678; Earth-Retaining Structures, Appendix J gives some guidelines for the load combinations that have to be checked for the R.S.W. structure design. The load factors that should be used in the design for R.S.W. stability are as per Table 5.

Table 5: Load Factors as per AS4678.

Dead load	0.80 (min.)	1.25 (max.)
Live load	0.00 (min.)	1.50 (max.)

The combinations of these load factors that should be used in the design are shown in Table 6.

Table 6: Static Load Combination as per AS4678.

Load Case	1 (static)	2 (static)	3 (static)
Weight of the R.S.W. Structure	0.80	1.25	1.00
Earth Pressure from Backfill	1.25	1.25	1.00
Live Load on R.S.W. Structure	0.00	1.50	0.00
Live Load behind R.S.W. Structure	1.50	1.50	0.00

There is no reference in Australian Standards AS4678; Earth-Retaining Structures on how to incorporate the collision loads, so guidelines from Australian Standards AS5100; Bridge Design Code, Part 2: Design Loads can be used. According to AS5100.2 Clause 22.2(c), the Permanent effect + Ultimate collision load case has to be considered. The permanent effect load factor can be obtained from Table 5.2 of the same standards which refers to a load factor of 1.2 or 0.85 to be considered for the dead load factor, depending upon whether it reduces or increases safety. However, for the

ultimate collision load factor AS5100.2 Clause 11.2.2, states that a load factor of 1.0 is to be used. Therefore Table 6 can be modified to include the collision load cases as per Table 7.

Table 7: Static Load Combination as per AS4678 and Collision Load Combination as per AS5100.

Load Case	1 (static)	2 (static)	3 (static)	4 (collision)	5 (collision)
Weight of the R.S.W. Structure	0.80	1.25	1.00	0.85	1.20
Earth Pressure from Backfill	1.25	1.25	1.00	1.25	1.25
Live Load on R.S.W. Structure	0.00	1.50	0.00	0.00	1.50
Live Load behind R.S.W. Structure	1.50	1.50	0.00	1.50	1.50
Collision Load	0.00	0.00	0.00	1.00	1.00

2.3 MAXIMUM SOIL PRESSURE

In order to properly examine the effect of the collision load combination on the R.S.W. structure, the maximum soil pressure at the soffit of the crash barrier footing due to collision load has to be calculated. The collision load will be transferred to the soffit of the crash barrier footing as an equivalent vertical pressure and horizontal load.

2.3.1 Vertical Pressure Calculation

For R.S.W. structure design purposes, by considering 1.0m section of the crash barrier, depending upon the load case, the maximum soil pressure diagram will be one of the following:

2.3.1.1 Triangular soil pressure (generally Load Case 4 in Table 7)

An equation for the maximum soil pressure q and the effective footing length B‟ can be obtained from Figure 4 (load case 4) where it is obvious that the base area is not fully effective by the amount B-B‟. The area of the pressure distribution must be equal to the total vertical load ($\Sigma F_Y = 0.0$) and acts at B‟/3 from the toe through the triangle centroid. Also the summation of the moment of all forces is equal to zero at any point ($\Sigma M = 0.0$). Therefore q and B‟ can be easily determined based on these two equations.

2.3.1.2 Trapezoidal soil pressure (generally Load Case 5 in Table 7)

An equation for the maximum soil pressure q1 and q2 can be obtained from Figure 4 (load case 5) where it is obvious that the total base area is fully effective. The area of the pressure distribution must be equal to the total vertical load ($\Sigma F_Y = 0.0$) and acts at its centroid. Also the summation of the moment of all forces is equal to zero at any point ($\Sigma M = 0.0$). Therefore q1 and q2 can be easily determined based on these two equations.

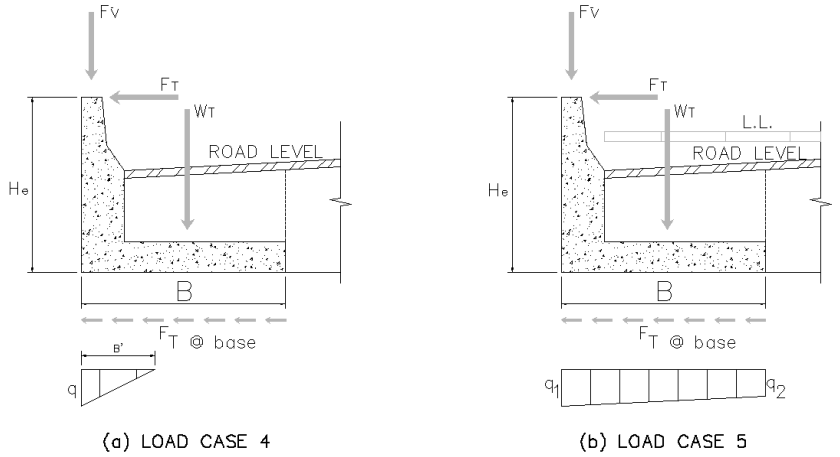

Figure 4: Maximum Soil Pressure at Soffit of Crash Barrier Footing for Load Case 4 and Load Case 5.

2.3.2 Horizontal Load Calculation ($F_{T\ @\ base}$)

The analysis can be undertaken by assuming the distribution of the transverse load at 45° to the horizontal from the point of application of the load to the soffit of the crash barrier as shown in Figure 5. End effects such as expansion joints should be considered to determine the effective distribution length. Referring to Figure 5, $F_{T\ @\ base} = F_T / L_{Teff}$

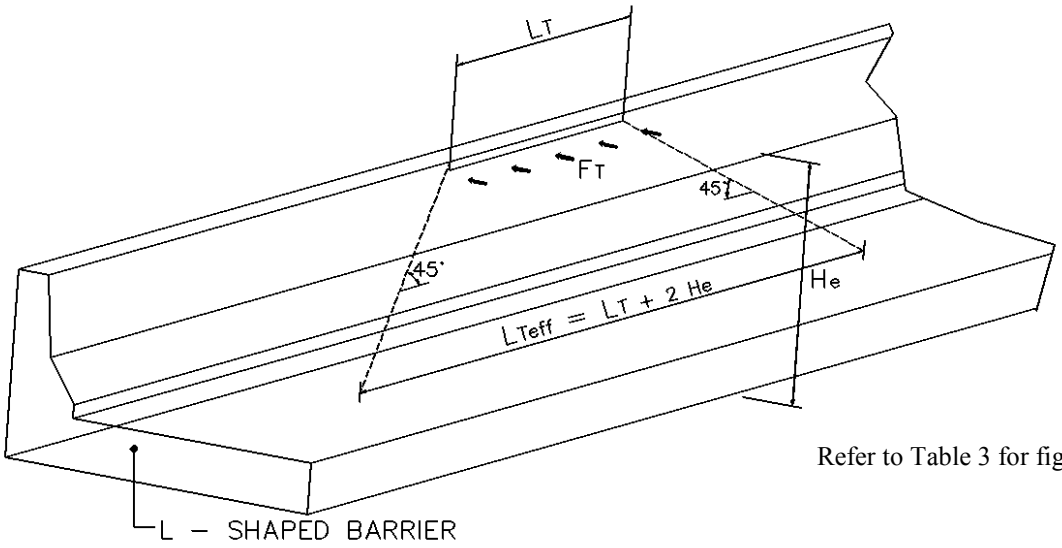

Refer to Table 3 for figure notations

Figure 5: Collision Transverse Load Distribution.

3 CURRENT PRACTICES

In Australia, the code that governs the design of R.S.W. structures is the Australian Standards AS4678; Earth-Retaining Structures. AS4678 offers limited guidelines for the crash barrier load effect on the R.S.W. structure in Appendix J Clause J10.1 (b) which states: "In some cases, the retaining structure may support other amenities such as sound barriers or New Jersey kerbs that may attract loadings, e.g. wind loads or traffic impact loads. The effect of such loads should be checked for the global and internal stability of the retaining structure."

Additionally, there are no guidelines for the load cases to be considered with such a special loading. Also from experience, the authors have seen many approaches for the distribution of the crash barrier load through to the soffit of the crash barrier footing. Australian Standards AS5100; Bridge Design Code defines the distribution width at the top of the crash barrier however, the manner in which the load is transferred to the soffit of the crash barrier is not clear and is left open for interpretation.

There are varying methods and methodologies taken to examine the net impact on the R.S.W. structures by designers. This has resulted in the implementation of overly conservative designs to account for the uncertainty regarding the manner in which the loads are transferred and transmitted through the R.S.W. structure. More importantly, there is a risk that the effects of load transfer onto the R.S.W. structure are being underestimated by inexperienced designers and therefore the full effect of collision impact on the R.S.W. structure are being inadequately designed for.

4 DESIGN APPROACHES

As Australian Standards do not adequately provide guidelines for the effects for crash barrier loading on R.S.W. structures, designers have turned to both the USA and UK Standards to examine their methodologies. Both have examined the crash barrier effects in more detail, particularly the USA where the crash barrier impact on the R.S.W. structure is outlined in AASHTO LRFD. However, neither approach has been implemented in their entirety for the approach proposed in this paper.

4.1 AASHTO LRFD

AASHTO LRFD Bridge Design Specification (SI) examines the design of three main components:

1. Barrier-moment slab system
2. R.S.W. structure reinforcement
3. R.S.W. facing panel

The barrier-moment slab design examines two failure modes in addition to structural failure; sliding and overturning. For sliding, the barriers factored resistance is examined, it must be greater than the factored static load applied over the length of the slab ($F^* > ØR$). In regards overturning, the factored moment resistance must be greater than that of the factored moment applied ($M^* > ØM_R$). The moment applied is the factored equivalent static load times the relevant lever arm.

AASHTO LRFD also outlines the design approach for the effect of the crash barrier on the R.S.W. structure in Clause 11.10.10.2. It specifies the concentrated horizontal load that the upper layers of soil reinforcement have to resist. The soil reinforcement"s resistance has to be examined at both pull-out and tensile failure. AASHTO LRFD sets out the relevant factors to be considered as part of the design as well as the relevant load cases. Interestingly the force distribution for pull-out calculations is greater than that used for tensile calculations because the entire base slab must move laterally to initiate a pull-out failure due to the relatively large deformation required according to AASHTO LRFD.

4.2 BRITISH STANDARDS

British Standards base its design on two main effects:

1. Local Effects: examines the area in the vicinity of the collision.
2. Global Effects: examines the structure as a whole.

Both effects examine sliding, toppling and rupture of the base slab. However, it is only the Global Design that examines the effect on the R.S.W. structure. The design examines both the Ultimate and Serviceability Limit State Design to ensure that the design requirements from a structural and useability perspective are met.

For loads due to vehicle collisions, BSI British Standards BS 8006-1:2010 Annex E requires the following collision loads to be applied uniformly over a 3m length at the top of the traffic face of a high level of containment parapet:

1. A horizontal transverse load of 500kN
2. A horizontal longitudinal load of 100kN
3. A vertical load of 175kN

The code also recommends that any load effects be distributed both vertically and horizontally through any up-stand plinth. The load is distributed at a 1:1 ratio through the structure. Also clear guidelines are given for the live load and load combinations to be considered in the design.

5 RECOMMENDED APPROACH

Having reviewed the current practices and approaches, The Reinforced Earth Company commenced researching a new design analysis approach that would take into account the current Australian Standards as well as other international codes where aspects were not adequately covered under the Australian codes. This new approach had to take into account the varying range of crash barrier performance levels and geometries. It also had to place emphasis on examining the effect of loading and its distribution at each soil reinforcement layer. The program was required to be flexible to easily cater for geometry, soil reinforcement and loading changes. However, the main purpose of implementing a new design analysis approach was to introduce a clear and systematic method of design, backed up with the relevant codes that could be easily reviewed by clients and external designers (relevant stakeholders). The following steps summarise the design steps taken in this approach.

5.1 STEP 1: CALCULATE THE DESIGN ACTION EFFECT ON TOP OF THE R.S.W. STRUCTURE

This can be calculated using force equilibrium equations as discussed in Section 2.3.1 of this paper. It is recommended to use Meyerhof pressure distribution where the pressure beneath the soffit of the crash barrier footing is assumed to be uniform over an effective width as shown in Figure 6 and given by B_{ref} = B-2e. Two load cases (L.C. 4 & L.C. 5) should be considered in calculating the **vertical** Meyerhof pressure as per Table 7.

Calculation of the **horizontal** shear load based on barrier performance level following the guidelines as per Australian Standards AS5100 Bridge Design Code and the approach discussed in Section 2.3.2 of this paper.

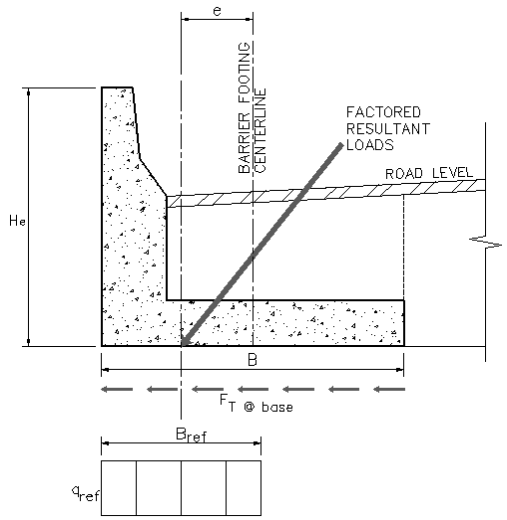

Figure 6: Meyerhof Pressure Distribution.

5.2 STEP 2: DISTRIBUTION OF THE DESIGN ACTIONS ON EACH SOIL REINFORCEMENT LAYER

This includes the calculation of the vertical pressure at each layer due to the vertical Meyerhof soil pressure. Also the calculation of the horizontal pressure due to the horizontal shear load at barrier soffit footing level. Both can be done using the guidelines from Australian Standards AS4678 Earth-retaining Structures Clause J10.4 and Figure J8.

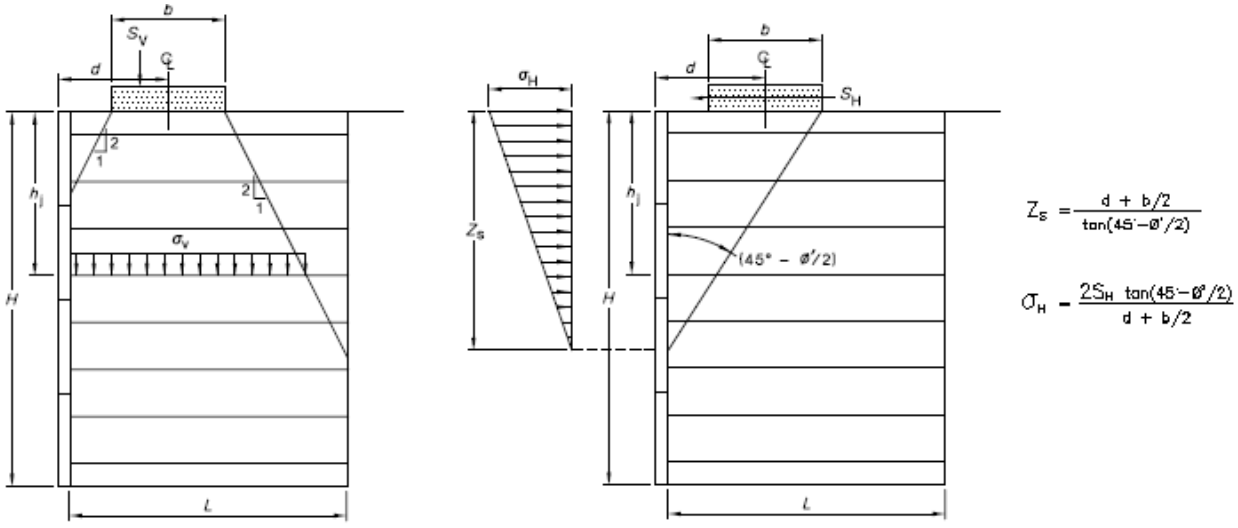

(a) Vertical Strip load Dispersion (b) Horizontal Shear load Dispersion

Figure 7: Dispersal of vertical strip load and horizontal shear load through reinforced fill as per AS4678 Figure J8.

5.3 STEP 3: DESIGN

a) Examine the internal design of the R.S.W. structure at each soil reinforcement layer, taking into account the additional horizontal and vertical pressures for each load case. The design should ensure that the soil reinforcement does not pull-out or rupture. Accordingly, the soil reinforcement's resistance has to be examined for both pull-out and tensile failure. In examining the pull-out capacity of the soil reinforcement, its full length is considered to be effective in resisting pull-out due to the impact load (following AASHTO LRFD Bridge Design Specifications Clause 11.10.10.2; Australian Standards do not currently examine this). The soil reinforcement frequency and length should be amended to achieve optimum design as required. The location of each soil reinforcement layer relative to the loaded area will have a significant effect on the load distribution across each layer.

b) Examine circular and linear slip failures with a stability analysis program by modelling the barrier footing and applying the vertical Meyerhof pressure and the horizontal shear load on top on the R.S.W. structure.

c) Check the wall facing capacity, taking into account the additional horizontal and vertical pressures for each load case. The wall facing should have sufficient structural capacity to resist the maximum design pressure.

6 APPROACH VERIFICATION

Having researched and developed the above design approach, it was required to fully verify its results before this design approach was fully implemented. An analysis was carried out using PLAXIS 2D version 8.2, a finite element computer program. This allowed the modelling of the combined R.S.W. structure, foundations and crash barrier loading. The crash barrier loading was modelled as per Section 5.1 above, the Meyerhof pressure was assumed to act at barrier soffit footing level combined with the horizontal load.

A selected output from PLAXIS 2D analysis is shown in Figure 8 which clearly demonstrates the manner in which the stresses are transferred from the crash barrier footing through to the R.S.W. structure along the wall facing. These stresses are then transferred to the soil reinforcement which act to resist the additional stresses. The results from this analysis are consistent with the stress distribution assumed in the recommended design approach.

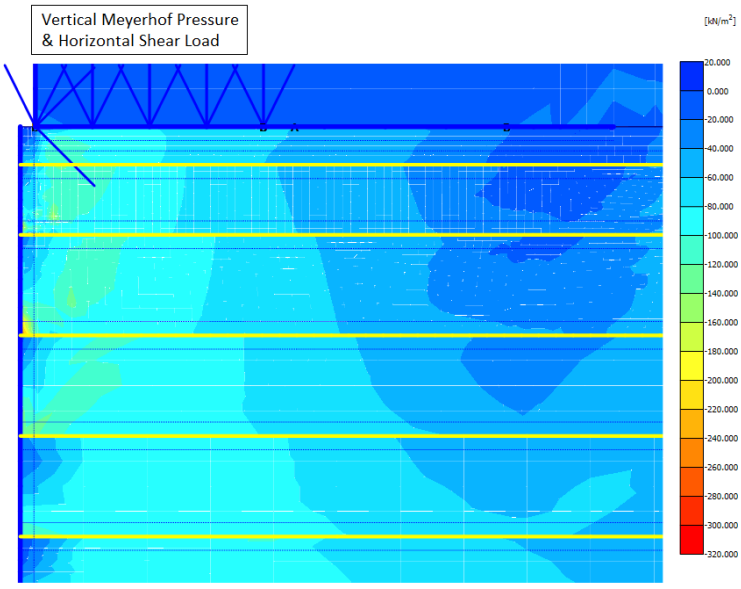

(b) Effective Mean Stress (kPa)

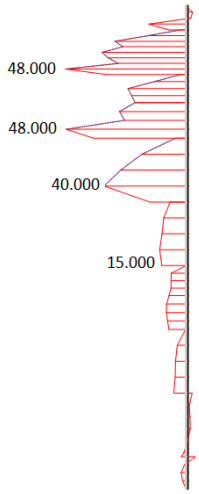

(a) Approximate Shear Stress @ Facing (kPa)

Figure 8: PLAXIS 2D version 8.2 analysis results.

7 CONCLUSIONS AND RECOMMENDATIONS

A step by step systematic design approach has been developed that incorporates force equilibrium with all available guidelines from the Australian Standards. This approach has been verified using a finite element analysis program. The net effective pressure resulting from all forces acting on top of the crash barrier is examined for its effect on external and internal stability on the R.S.W. structure taking into account the most critical load cases.

Having examined Australian and other international standards, it is essential that the Australian Standards are enhanced to provide a clear design approach for the R.S.W. structure design under collision loading that specify the following:

1. The load cases to be considered and the manner in which this loading is transferred from the top of the crash barrier through to the soffit.
2. The full length of the soil reinforcement should be considered effective in resisting pull-out due to the impact load.
3. A consistent traffic barrier design loading specification (transverse load, vehicle contact length and effective height) across all Australian Standards.

It is essential that the stress distribution of the collision load in the three dimensions through the R.S.W. structure is fully understood. Currently, to the author‟s knowledge, the only research being carried out in this area has been completed by the Texas Transport Institute in conjunction with The Reinforced Earth Company USA. With such little research and full scale testing being carried out, it is an area that needs much further development of knowledge and understanding and for that to be translated into applicable design standards.

8 ACKNOWLEDEMENTS

The authors acknowledge The Reinforced Earth Company Australia for permission to publish this paper and are grateful to colleagues, for their excellent works and invaluable contributions during detailed design and development of this approach. The authors wish to thank Geoffrey Chan and Rocco Bressi for their input on this paper.

9 REFERENCES

American Association of State Highway and Transportation Officials (2007). *AASHTO LRFD bridge design specifications*, 4rth Ed. AASHTO, Washington, D.C.

Briaud, J.L.; and Saez, D. (2012) "Design Guidelines and Full Scale Verification for MSE Walls with Traffic Barriers Impacted by Vehicles" *ANZ 2012 Conference, 563-585.*

BSI British Standards BS 8006-1:2010 Code of practice for strengthened/reinforced soils and other fills.

CATERPILLAR 797B Mining Truck, *Safety section, www.CAT.com*

Foundation Analysis and Design - Fifth Edition by Joseph E. Bowles, P.E., S.E. *Chapter 8: Spread Footing Design - Eccentrically Loaded Spread Footings.*

National Cooperative Highway Research Program (NCHRP Report 663) *Design of Roadside Barrier Systems placed on MSE Retaining Walls, 2010, http://utc2.edu.vn/Uploads/File/AASHTO%20LRFD%202012%20BridgeDesignSpecifications%206th%20Ed%20(US).PDF*

Queensland Government, Department of Main Roads, Structures Division/Network Operations and Road Safety Division, *Technical Specification QR MCE-SR-007 Design and Selection Criteria for Road/Rail Interface Barriers initial issue 15 June 2009.*

STANDARDS AUSTRALIA. *Bridge Design Code Part 2: Design Loads AS5100.2*, Standards Australia, 2004.

STANDARDS AUSTRALIA. *Earth-Retaining Structures AS4678*, Standards Australia, 2002.

STANDARDS AUSTRALIA. *Road Safety Barrier Systems AS3845*, Standards Australia, 1999.

Tasmanian Government, Department of Infrastructure Energy and Resources, Transport Infrastructure Branch, *Road Safety Barriers, Design Guide - Part B.*

DESIGN CHALLENGES OF ROAD WIDENING IN SOFT GROUNDS: CHARACTERISATION TO NUMERICAL ANALYSIS

S. Zargarbashi[1], J. Alinur[2], J. Gniel[3] and Craig Curnow[4]
[1]Senior Geotechnical Engineer, Principal[4], Golder Associates Pty Ltd, Sydney, Australia
[2]Geotechnical Engineer, Golder Associates Pty Ltd, Brisbane, Australia
3Associate, Golder Associates Pty Ltd, Melbourne, Australia

ABSTRACT

This paper presents challenges involved in robust geotechnical design for upgrading an existing motorway, which is founded on soft soil. A critical review is presented on current approaches adopted for soft soil characterisation using results of laboratory and field tests commonly applied in Australian practice. Particular attention is given to assessment of undrained shear strength, overconsolidation ratio (OCR), primary and secondary compression (creep) indices and coefficient of consolidation. Some of the limitations of finite element analysis using 2D PLAXIS software, as a commonly used tool, and its 'soft-soil creep model' are also highlighted. Analytical approaches are presented which were used in a case study to overcome these limitations and help with deformation analysis of soft soils undergoing creep, as well as the design of rigid inclusions taking into account 3D effects.

The case study project upgrade works involved widening of the motorway embankment and in turn extension of existing culverts, which were located in a river floodplain. Preload and wick drains were considered for soft soil improvement to meet residual and differential settlement criteria over the design life of the new pavement. Rigid inclusions were also designed for the new culvert extension to reduce potential differential settlement between the proposed extension and existing culverts.

1 INTRODUCTION

Transport infrastructure in Australia has been mostly built along the congested eastern and southern coastal belt where soft and compressible alluvial and marine clay deposits are often encountered around watercourses and paleochannels. These soft deposits present significant challenges to design, construction and performance of major infrastructure currently being built or upgraded in Australia. This is due to their high compressibility and low bearing capacity that can adversely affect stability and settlement performance of structures.

To overcome these challenges and to enable a resilient geotechnical design for such infrastructure, it is crucial that fundamental features of soft soils are well understood and characterised through an appropriate laboratory and field testing program. Test results should be meticulously interpreted to extract design parameters, and appropriate material models should be applied for stability and deformation analyses. It is also important that limitations of present material models and commercial software are appreciated and appropriately dealt with to obtain reliable outcomes.

This paper presents challenges involved in robust geotechnical design for upgrading an existing motorway, which was founded on soft soil. The upgrade works involved widening of the motorway embankment and in turn extension of existing culverts, which were located in a river floodplain. Preload and wick drains were considered for soft soil improvement to meet residual and differential settlement criteria over the design life of the new pavement. Rigid inclusions were also designed for the new culvert extension to minimise potential differential settlement between the proposed extension and existing culverts.

A critical review is presented on current approaches adopted to extract design parameters using results of laboratory and field tests, which are commonly applied in Australian practice. Particular attention is given to assessment of shear strength, overconsolidation ratio (OCR), primary and secondary compression (creep) indices and coefficient of consolidation. Some of the limitations of finite element analysis using 2D PLAXIS software, as a commonly used tool, and its 'soft-soil creep model' are also highlighted. Analytical approaches are presented which were used in this design to overcome these limitations and help with deformation analysis of soft soils undergoing creep, as well as design of 3D rigid inclusions.

The reader should note that 'soft soil' terminology used in this paper represents very soft to firm soils.

2 CASE STUDY PROJECT BACKGROUND

The subject project (confidential) comprises an upgrade of an existing major motorway from 4 lanes to 6 lanes, with provision for an additional 2 lanes (8 in total). The upgrade mainly involves widening of existing motorway embankments and median infilling as well as realignment of the motorway in one section. There are two main areas with 'soft soils' requiring early works ground treatment. These sections are low-lying, each about 1 km in length and are underlain by soft, compressible Holocene-age deposits of various thickness, up to a maximum depth of around 10 m depth (Figure 1). There are box culvert structures traversing the existing carriageways which require extension to account for the proposed embankment widening.

The case study presented in this paper is part of early works implemented to reduce the construction time and risks for a main contract using preload and ground treatment that can be carried out without significantly limiting future design refinement. In particular, this paper describes the finite element stress-strain analysis at a proposed culvert extension. The analysis was undertaken to assess the ground displacements, stability conditions as well as structural analysis of the piled foundation for the proposed culvert extension.

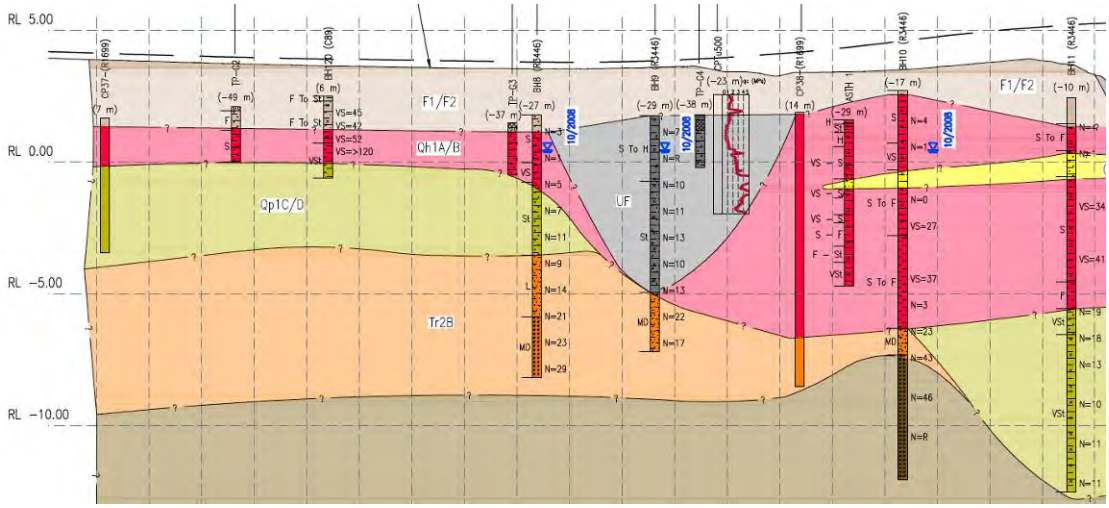

Figure 1: Sample stratigraphy along the section of the motorway around the case study

3 SOFT SOIL CHARACTERISATION

Sections 3.1 to 3.4 provide a critical literature review of different methods utilised to characterise soft soils, and cover a range of laboratory and field tests currently used in Australian practice. The design parameters adopted for the study project and associated selection processes are described in Section 3.5. As is typical of projects in the pre-tender phase, there were limited laboratory and field test results available for this early-work design, so the available results didn't include all the tests discussed in this section.

3.1 SHEAR STRENGTH

Stability performance, in particular short-term stability, of road embankments founded on soft ground is often a design challenge, as it is adversely affected by low bearing capacities of soft soils. Thus, a robust and prudent design necessitates appropriate evaluation of shear strength of soft soil deposits using laboratory and field tests.

Short-term stability of embankments on soft grounds is often controlled by the undrained shear strength (S_u) of saturated soft foundation materials, as soft soils are mostly located around watercourses and paleochannels, where groundwater levels are usually near the surface. Upon embankment loading, excess pore water pressure develops within saturated soft soil deposits of low permeability. This excess pore water pressure gradually dissipates over time and, in turn, effective stress and shear strength increase. However, if at any stage during or immediately after construction, the induced shear stress exceeds the average undrained shear strength of soft soil deposits, embankment failure can occur under undrained or partially drained conditions.

Therefore, to assess stability of an embankment during and after construction, it is crucial that the initial undrained shear strength profile and its subsequent increases due to consolidation be thoroughly assessed for a robust design. The initial shear strength profile may be evaluated using laboratory or field testing as discussed in the following sections; however, to assess the subsequent increases of S_u due to ongoing consolidation, the variation of the

undrained shear strength ratio, S_u/σ'_v, should also be studied (σ'_v is vertical effective stress or consolidation pressure). Experimental studies conducted since the early 1970's (e.g. Ladd and Foott, 1974; Larsson, 1980, Ladd, 1991) suggested that undrained shear strength ratio can be approximated by the following relationship:

$$\frac{S_u}{\sigma'_v} = S(OCR)^m \quad (1)$$

Where S=the normally consolidated value of S_u/σ'_v, OCR= overconsolidation ratio, and m =the strength increase exponent. S and m can vary significantly by soil type. Their recommended values for different soil types are presented later in this section.

Nevertheless, Ladd and Degroot (2003) and various other authors have shown that the undrained shear strength of normally consolidated inorganic clays can be approximated using the following relationship:

$$S_u = 0.22 \times \sigma'_v \quad (2)$$

To initial shear strength profile and the undrained shear strength ratio-OCR relationship can be evaluated using laboratory and field tests. The type and extent of testing are determined based on the degree of refinement required for the undrained strength analysis. Three levels of testing may be considered in regard to sophistication and expenses (Ladd, 1991), as follows:

Level A - for detail design of major projects and sites where foundation materials expected to show significant anisotropy in terms of shear strength and stress-strain relationship, or where soils have unusual features such as fissuring or high organic content, etc. This level also applies to the project where lateral deformations during construction are on interest (e.g. excavation adjacent existing sensitive structures).

Level B - for preliminary or tender design of major projects or detail design of less important projects involving "ordinary" soils with low to moderate anisotropy.

Level C - for preliminary feasibility or concept design and also to verify whether initial strengths inferred from in situ and laboratory Unconsolidated Undrained (UU) test programs are reasonable.

3.1.1 Laboratory Strength Tests

There are many types of laboratory testing equipment developed to measure soil shear strength under certain drainage conditions and stress paths. Nevertheless, variations of simple direct shear box and triaxial shear testing apparatus are commonly available in commercial laboratories and used in practice. Depending on the level of the project sophistication and importance, described above, the following laboratory test programme is recommended (Ladd, 1991):

Level A – Due to the effect of intermediate principal stress and anisotropy on the shear strength, a test program should ideally include CK_oU triaxial tests, where samples are consolidated under K_o (at rest) conditions to represent actual site conditions and sheared under undrained conditions. Samples should be tested for different modes of failure (e.g. compression and extension). Conventional CK_oU triaxial tests, however, generally would give conservative peak shear strengths for plain strain problems (Ladd et al., 1977). Alternatively, the test programme could include direct simple shear and plane strain compression/extension tests.

Testing of samples at different OCRs enables the site specific S and m in Eq. 1to be established.

Level B - CK_oU direct simple shear testing is recommended for Level B to obtain S_u/σ'_v versus OCR relationships for stability analyses using isotropic strength profile (Ladd, 1991). Alternatively CK_oU triaxial compression and extension tests may also be used, however, they would require more soil, more experience and effort to obtain reliable results, and hence are more expensive.

Isotropically consolidated triaxial compression tests should not be relied on in Level B projects. It has been shown that these tests could significantly overestimate the in-situ average shear strength for most soils.

Level C – at this level the empirical correlation of Eq.1 can be used. In absence of site-specific correlations, Ladd (1991) suggests the following values for S and m:

- Sensitive marine clays (Plasticity Index, I_P<30% and Liquidity Index, I_L>1):

  S= 0.20, with normal standard deviation of 0.015, and m=1;
- Homogeneous sedimentary clays of low to moderate sensitivity (I_p=20% - 80%):

  S=0.20+0.05I_p, or simply S=0.22, and m=0.8;
- Varved clays:

  S=0.16, m=0.75; and
- Sedimentary deposits of silts and organic soils and clays with shells:

  S=0.25, with normal standard deviation of 0.05, and m=0.8.

3.1.2 Field Tests

Laboratory test results can sometimes be misleading for soil characterisation as they are based on testing small discrete samples collected from limited and specific depths which are also subject to sampling distrubance. In-situ field tests, however, enable assessment of a broader range of soil properties and provide an opportunity for an economical tool for soil profiling. The in-situ tests commonly used in Australia include Standard Penetration Test (SPT), Field Vane Test (FVT), Piezocone Penetration Test (CPTu) and the Marchetti Dilatometer Test (DMT). The SPT is not considered further in this paper as the authors consider it is of limited use for clays and gravelly soils and, in any event, is rarely used for soft soil characterisation. Other tests have also limitations in term of applicability as discussed below.

FVT provides a reasonable evaluation of undrained shear strength of relatively homogeneous clay deposits (i.e. clays without shells, granular layers varves, fibres, etc.) for preliminary design. However, it should be noted that the undrained shear strength assessed by FVT should be reduced by a correction factor as indicated by Bjerrum (1972, 1973). Chandler (1988), among others, suggested a correction factor as a function of Plasticity Index (PI) and time to failure, as presented in Figure 2.

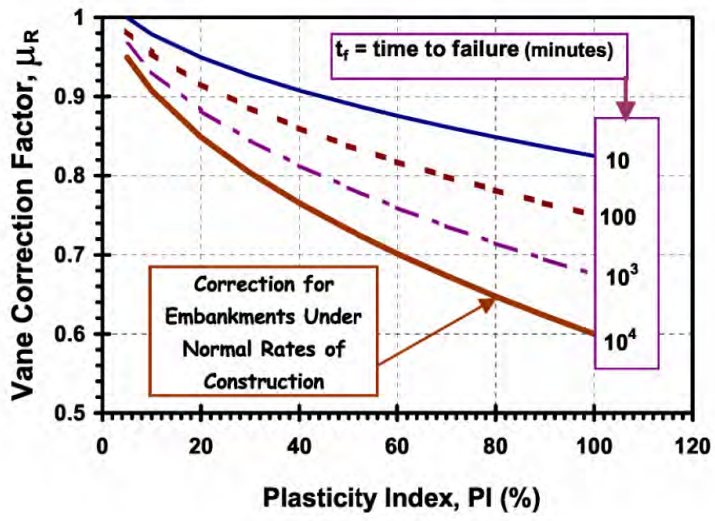

Figure 2: Proposed correction factor to raw field vane shear data from plasticity index (after Chandler, 1988)

CPTu is one of the most common field tests used for soft soil characterisation. It is relatively economic, quick and provides continuous results ideal for capturing spatial variations of soil properties (Campanella and Robertson, 1988). The peak undrained shear strength ratio can be estimated using CPT cone resistance as follows:

$$\frac{s_u}{\sigma'_{v0}} = \left(\frac{q_t - \sigma_{v0}}{\sigma'_{v0}}\right)(1/N_{kt}) = Q_{tn}/N_{kt} \qquad (3)$$

where q_t is cone resistance, and N_{kt} is a cone factor that varies between 10 and 20, with an average value of 14. For sensitive clays ($8<S_t<16$) N_{kt} should be reduced (Robertson, 2009a). Sensitivity (S_t) of clays may be estimated using:

where $F_r=[f_s/(q_t-\sigma_{vo})]100\%$ is CPT normalised friction ratio. For large and important projects (Levels A and B projects), site-specific N_{kt} should be determined using laboratory and FVT results. In the authors' experience, a reasonably accurate assessment of N_{kt} can be made by calibrating the results of the continuous CPT shear strength profile to discrete FVT measurements made in nearby boreholes or test holes.

Marchetti DMT is also inexpensive and relatively quick tool for soil profiling. However, the empirical relationships presented for DMT have limitations and need site-specific calibration for major projects (Ladd, 1991). Having said that, the original correlation for determining c_u from DMT recommended by Marchetti (1980) is as follows:

$$c_u = 0.22\,\sigma'_{vo}\,(0.5\,K_D)^{1.25} \quad (5)$$

where K_D is horizontal stress index from DMT test.

3.2 OVERCONSOLIDATION RATIO

Stress-strain behaviour of soils is highly stress history dependent. Therefore, it is crucial that the initial stress history of the deposit and its evolution during construction be comprehensively assessed. Pre-consolidation pressure (σ'_p) is commonly used to evaluate the deposit initial stress history[1].

Pre-consolidation pressure, known as 'maximum past pressure' that acted on the soil, represents a yield stress that divides recompression (elastic) from virgin compression (plastic or irrecoverable) during one-dimensional compression. Jamiolkowski et al. (1985) indicated four different mechanisms which can cause over-consolidation (OCR[2]) values greater than 1 within horizontal clay deposits: 1. *Mechanical*, due to removal of overburden pressure or lowering water table, 2. *Desiccation*, due to evaporation or freezing, 3. *Aging or secondary compression*, due to drained creep, and 4.*Physico-chemical*, due to natural cementation and related phenomena. Wong (2006a) provides further discussion on these mechanisms with particular emphasis placed on the effects of ageing.

For young man-made deposits such as dredged materials and mineral processing wastes, the aging and physico-chemical mechanisms can be neglected. While for natural deposits, all of the mechanisms could effectively contribute to actual OCR of the deposit (Ladd, 1991).

Determination of σ'_p profile plays an important role in analysis of soft soils, as it governs the initial in-situ undrained strength and represents the boundary between recompression with little deformation and small increase in S_u and virgin compression involving substantial rate of compression and strengthening of the soils. Different methods are used in practice to evaluate σ'_p including: laboratory consolidation tests and correlation with field test results.

3.2.1 Laboratory Tests

The most common laboratory test used in practice is incremental oedometer tests (1D-consolidation test) using a load increment ratio ($\Delta P/P$) of unity, which is often required to be reduced to about 0.5 to obtain a better fitted curve in the vicinity of σ'_p *(Ladd, 1991)*. The test procedure and its result interpretation are well described in the literature (e.g. Casagrande, 1936, Schmertmann, 1955) and known by geotechnical engineers. Boone (2010) presents a critical appraisal of common methods used for interpretation of preconsolidation pressure using oedometer tests and proposes a new, simplified approach. However, it is worthwhile to highlight that users should be aware of the limitation of different interpretative techniques presented in the literature, as some might be only applicable to special classes of clays, e.g. structured clay, which could introduce significant errors if generalised to other types of clay. The authors consider Casagrande (1936) method is an appropriate method for ordinary clays, and for structured clays Schmertmann (1955) technique can be applied to correct the compression curves.

3.2.2 Field Tests

FVT, as mentioned before, can provide a reasonable measure of undrained shear strength of homogenous clays. It can also be used to evaluate OCR using Eq. 1, as follows:

[1] In general, soil behaviour not only depend on can be stress path dependent
[2] Over Consolidation Ratio: ratio of σ'_p to in-situ initial vertical effective stress (σ'_{v0}).

$$OCR = (\frac{s_{u(FV)}}{\sigma'_{v0}} . \frac{1}{S})^{\frac{1}{m}} \quad (6)$$

where $s_{u(FV)}$ is corrected undrained shear strength from FVT. As *S* and *m* could significantly vary for different soil types, site-specific correlations should be established.

There are also a few correlations presented in literature between OCR and CPT test results. The most common relationship is as follows (Robertson, 2009a):

$$OCR = k(\frac{q_t - \sigma_{v0}}{\sigma'_{v0}}) = kQ_{tn} \quad (7)$$

where *k* is the preconsolidation cone factor with an average value of 0.33, with an expected range of 0.2 to 0.5. A higher value of *k* is recommended in aged heavily consolidated clays. Its value should be adjusted based on previous experience in the same deposit, where possible.

Further to this, a quick assessment of pre-consolidation pressure and OCR for inorganic clays can be made by comparing the calibrated shear strength profile derived from the CPT to the theoretical normally consolidated shear strength profile calculated using Eq. 2. However, CPT interpreted OCR may not always be reliable because, as indicated by Blight (1986a, 1986b), no universal correlations can be made between penetration pore pressure-cone resistance data and stress history. This is because the shear induced pore pressure, which varies with OCR is small compared with the total pore pressure measured by the cone pressure cells. Also, cone-resistance-undrained shear strength correlations need site-specific data.

In the authors' experience, Marchetti DMT provides more reliable results than CPTu in evaluation of soil stress history (i.e. OCR) of cohesive deposits and K_0, at–rest coefficient of lateral pressure. Nevertheless, it should be noted that some of the empirical relationship presented for DMT have limitations and need site-specific calibration for major projects (Ladd, 1991).

Marchetti (1980) presented an imperial relationship between OCR and K_D for fine-grained soils, based on DMT results carried out at over 40 Italian sites, which is still commonly used:

$$OCR = (0.5K_D)^{1.56} \quad (8)$$

Similar equations have been published by others based on DMT testing at different sites (Mayne and Martin, 1998; Kamei and Iwasaki, 1995), of which most have similar forms to Eq. 3. The equation form is also confirmed by analytical studies (Finno, 1993) and is influenced by soil shear strength, stiffness and compressibility (Robertson, 2009b). Therefore, for detailed design of large projects, the authors consider this equation may need to be compared to site-specific data and calibrated if required.

3.3 PRIMARY AND SECONDARY COMPRESSION INDICES

Relatively strict settlement criteria often apply to major roads and highways in Australia which sometimes are in effect up to a century after their construction. These criteria are used to essentially reduce maintenance costs for road pavements and to satisfy the drivers' comfort which is governed by change in grade of the pavement. Meeting these tight criteria is often a major challenge and can have a significant impact on the project cost. The reliable prediction of settlements in soft soils requires a reasonable understanding of their compressibility and time-dependent settlements (i.e. primary consolidation and creep) behaviour. This is achieved by undertaking laboratory and field tests or adopting empirical correlations to determine primary and secondary compression indices and consolidation coefficient (C_v). The latter parameter is discussed in the next section. This section presents the most common approaches to assess primary compression (c_c) and unloading-reloading compression (c_r) indices as well as secondary compression or creep index (c_α) which define compressibility of soils under applied pressure.

1D-consolidation tests with incremental load stages are the most common and commercially available laboratory test used to determine soil consolidation parameters. Typically, end of primary consolidation (EOP) void ratios (*e*) are plotted versus applied consolidation pressure (σ) in the *e*-log σ plane. c_c and c_r are calculated as the slope of the normally consolidated (NC) compression curve and unloading-reloading curve, respectively.

For each loading stage, variation of *e* versus time is typically plotted in *e*-log *t* plane. If settlement reading is continued long enough after EOP, the shape of the *e*-log *t* plane often consists of three linear segments representing initial compression, primary consolidation and secondary consolidation. It is important that settlement reading is

continued at least for one log cycle of time after EOP, otherwise c_α, the slope of the secondary consolidation segment *e*-log *t* plane, can be overestimated.

Some of commercial laboratories present only the assessed values of c_α with test certificates and do not present the time plots. Nevertheless, the authors recommend that these plots are sought from commercial laboratories so geotechnical engineers can verify the reliability of assessed c_α value; which its over or under estimation could result in significant design and maintenance costs, respectively.

Although consolidation testing can be expensive and time consuming, it is considered crucial in major projects (i.e. Level A and B projects). For less critical design, several empirical correlations have been presented in the literature to estimate compression indices using Atterberg limits and natural moisture content. These correlations provide an easy and inexpensive alternative method based on which the scope of the geotechnical laboratory program can be reduced to confirmatory investigation of the consolidation properties; hence reducing the amount of required consolidation testing. In the authors' experience, these correlations are used in less important projects (Level C) or to verify and obtain further data in combination with consolidation tests on more important projects.

3.3.1 Primary Compression Index

Correlations for primary compression index, which are widely used in practice and also considered in the case study presented later in this paper, are summarised in Table 1.

Table 1: Selected empirical correlations for primary consolidation index.

Soil	Equation[1,2]	Reference
All Clays	$c_c = 1.15(e_0 - 0.35)$	Nishida (1956)
Inorganic Clays	$c_c = 0.30(e_0 - 0.27)$	Hough (1957)
Undisturbed NC Clays	$c_c = 0.009(LL - 10)$ (±30% error)	Terzhagi and Peck (1967)
All Clays	$c_c = 0.01325 I_p$ or $c_c = 0.01 W_N$	Koppula (1981)
All Clays	$c_c = 0.009 W_N + 0.005 LL$	Koppula (1986)
All Clays	$c_c = 0.012 W_N$	US Army (1990)

Note: 1. LL=Liquid Limit, I_p = Plasticity Index, W_N= Natural moisture content and e_0= initial (in-situ) void ratio.

2. In these equations, Atterberg limits and W_N are in percentage, not decimal.

3.3.2 Secondary Compression Index

Soil creep or secondary compression is considered one of the controversial concepts in geotechnical engineering practice. There are differing opinions on aspects ranging from the reference time when creep settlement is thought to begin to the general applicability of some of the $c_c - c_\alpha$ correlations presented in the literature. Nonetheless, it is widely accepted that for the purpose of settlement analysis, the creep reference time is at EOP. Mesri and Godlewski (1977) introduced the concept of c_α / c_c that for any natural soil, the ratio of c_α to c_c is constant for any time, effective stress, and void ratio during secondary compression. Therefore, the value of c_α / c_c together with EOP *e*-log σ curve completely defines the secondary compression behaviour of any consolidating soil. This concept has been validated for variety of soils and peat (e.g. Fox et al., 1992) and used for preloading design for soft ground (Mesri and Choi, 1985).

To assess site-specific c_α / c_c values, special attention should be given to selection of $c_c - c_\alpha$ pairs. They should be selected for the same time, effective stress and void ratio, as graphically depicted in Figure 3.

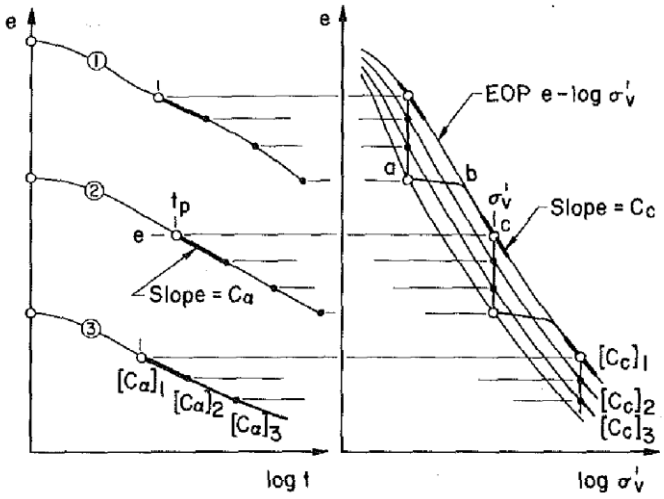

Figure 3: Corresponding values of c_α and c_c at any instant (e, σ'_v, t) during secondary compression (after Mesri and Castro, 1987)

The ratio c_α / c_c is independent of time and its total range of values for all soils are in the range of 0.01 to 0.07 (Mesri and Vardhanabhuti, 2005). Table 2 shows the typical range of this ratio for different soils.

Table 2: Values of c_α / c_c for geotechnical materials (Mesri and Castro, 1987; Mesri and Vardhanabhuti, 2005)

Material	c_α / c_c
Granular soils including rockfill	0.02±0.01
Shale and mudstone	0.03±0.01
Inorganic clays and silts	0.04±0.01
Organic clays and silts	0.05±0.01
Fibrous and amorphous peats	0.06±0.01

3.4 COEFFICIENT OF CONSOLIDATION

Coefficient of consolidation controls the rate of consolidation settlement and in turn strength gain achieved over time. The laboratory 1D-consolidation test is used to estimate the vertical coefficient of consolidation, C_v ,whereas a piezocone (CPTu) with pore pressure dissipation test data or flat dilatometer (DTM) can be used to estimate the horizontal coefficient of consolidation, C_h . The general trend associated with coefficient of consolidation is that the C_v values are stress dependent and that higher values are to be expected for effective stresses less than the preconsolidation stress.

Nonetheless, it is generally assumed to be constant within the interest range of stress. This is one of several simplifying assumptions made in the Terzaghi theory of 1D-consolidation. Therefore, even the best estimates of C_v or C_h from high-quality laboratory tests typically only result in predictions of consolidation settlement rate within one order of magnitude of observed values. The laboratory value of C_v is usually less than the value measured in the field (Sebatini et al., 2002). The authors, based on their previous experience, consider that actual C_v value can be 2 to 3 times larger than the value measured in the laboratory. Therefore, it is recommended that laboratory C_v values are compared to the values for C_h obtained from field dissipation tests to select a design value. Although the rate of horizontal consolidation can be greater than that in the vertical direction, for most relatively isotropic soils the ratio of lateral to vertical consolidation is not greater than two (Table 3). Nevertheless, it should be noted that in highly stratified soils such as varved clays a ratio of ten or more is anticipated (Sabatini et al., 2002). Furthermore, Figure 4

presents a correlation for C_v which can be used to judge the reasonableness of computed C_v values obtained from oedometer test data (U.S. Navy, 1971).

Table 3: Suggested anisotropic permeability of clays (after Jamiolkowski et al., 1985)

Nature of clay	$k_h / k_v = c_h / c_v$
No evidence of macrofabric or layering, or only slightly developed macrofabric, essentially homogeneous deposits	1 to 1.5
From fairly well to well-developed macrofabric, e.g. sedimentary clays with discountinious lenses and layers of more permeable material	2 to 4
Varved clays and other deposits containing embedded and more or less continuous permeable layers	3 to 15

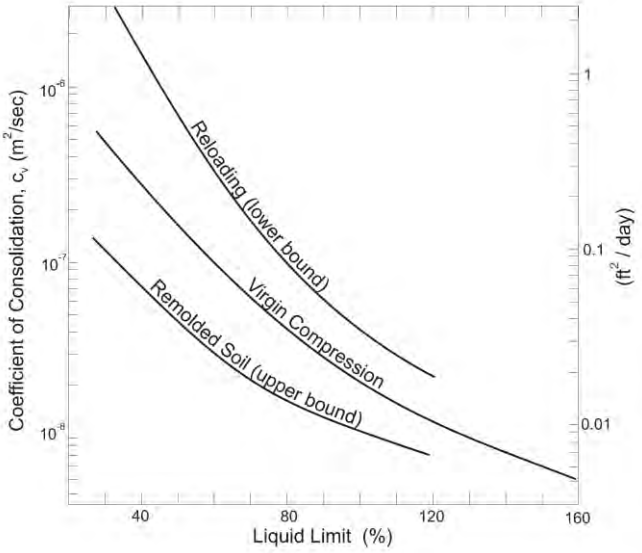

Figure 4: Correlation of coefficient of consolidation with liquid limit (after U.S. Navy, 1971 and Sebatini et al., 2002)

3.4.1 Field Dissipation Tests

Piezocone (CPTu)

During cone penetration excess pore pressures are generated in the soil around the cone. The dissipation rate of this excess pore pressure is controlled by soil permeability and its compressibility. Therefore, interpretation of its dissipation curve could enable estimation of quantities such as permeability and coefficient of consolidation. The initial cone generated pore pressure and its dissipation over time have been modelled based on the cavity expansion theory with critical state soil models, with coupled or uncoupled consolidation analysis. Different methods have been used to capture its initial distribution of the pore pressure around the probe such as strain path method (Baligh and Levadoux 1986), large strain finite element analysis (Houlsby and Teh 1988) or cavity expansion (Burns and Mayne 1998, Chang et al 2001) for which different equations have been presented in the literature relating dissipation data to coefficient of consolidation.

Teh & Houlsby (1991), based on the strain path method, provide the most reasonable results among others especially at U=50% (U, being average consolidation ratio). They indicate that for monotonic pore water decays generally associated with soft to firm clays and silts, where the readings always decrease with time, the following expression may be used to determine coefficient of radial consolidation:

$$C_h = \frac{T^* r^2 \sqrt{I_R}}{t} \tag{9}$$

In which T^* is a modified time factor from consolidation theory, r is the probe radius (17.8 mm for 10-cm^2 cones), $I_R = G / s_u$ (G being undrained shear modulus) is rigidity index (generally ranges between 50 and 500) and t is the

measured time during dissipation (usually at t_{50} representing 50% consolidation). There are other solutions presented for the modified time factor T^* based on different theories. For the particular case of 50% consolidation, the respective time factors are T* = 0.118 for the mid-face porous element (u_1 position) and T* = 0.245 for the shoulder porous element (u_2 position).

For relatively short dissipation tests, where determination of t_{50} from the normalized excess pore pressure curve is not possible, Teh (1987) proposed the following equation on the basis of square root time plot of dissipation results:

$$C_h = (m / M_T)^2 . r^2 . \sqrt{I_R} \tag{10}$$

Where m is initial slope of the linear part for square root time plot of normalised excess pore pressure curve, M_T is a coefficient equal to 1.15 for the typical u_2 position and 10-cm^2 cone.

Determination of t_{50} is quite straight forward for monotonic dissipation curves when the ultimate pore pressure (u_0, hydrostatic water pressure at the time of the test) is known either from a long enough dissipation reading or measured groundwater level. Nevertheless, non-standard dissipation curves are observed, particularly for pore pressure transducers located at the shoulder (u_2 position) or the shaft of a cone (u_3 position). These differences may be due to shear-induced dilatancy of over-consolidated clays or sandy soils, and unloading effects for soil elements moving from the tip to the shoulder of a cone (Sully et al., 1999). In order to be able to use above equations, exclusively developed for monotonic dissipation curves, Sully et al. (1999) have proposed two correction methods to convert these curves to monotonic ones. The first method involves shifting the origin of time to that point where the measured pore pressure is a maximum (Figure 5a). The second method fits a square root of time plot to the post-maximum pore pressure dissipation curve in order to back-extrapolate the value of the initial pore pressure, as depicted in Figure 5b. However, care should be taken as shifting the origin of time ignores the effect of pore pressure redistribution in the vicinity of the cone before the measured pore pressure reaches its maximum, which could result in over-estimation of t_{50} and in turn underestimation of the value of C_h. Chai et al. (2012) have proposed an imperial relationship based on their numerical analysis of radial consolidation around piezocone which correct t_{50} measured using the above methods.

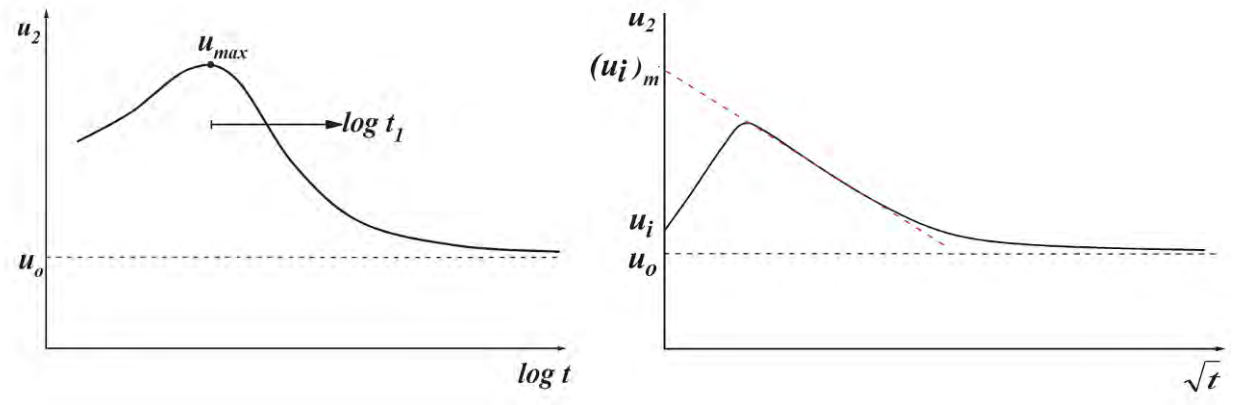

(a) (b)

Figure 5: Correction for dilatory dissipation: (a) logarithm of time plot, (b) square root of time plot (after Sully et al., 1999)

Marchetti DMT Dissipation Tests

Similarly, DMT can also be used to monitor dissipation rates of penetration pore water pressure. To the authors' knowledge, there is no theoretical method published specifically for flat dilatometer penetration. However, the theoretical solutions developed for CPTu have been used to interpret DMT dissipation results by assuming an equivalent radius of the DMT blade and using equations similar to Eq. 9 with nominated empirical values for T^* to estimate C_h (e.g. Robertson et al., 1988).

Marchetti and Totani (1989) proposed a method consisting of sequential 'A readings' (the contact pressure measurement) at several times, while the blade is stopped at a specific depth, until the 'A reading' is stabilised. They suggest that $C_h . t_{flex}$ is constant (t_{flex} being the time associated with the contraflexure point in the A-log t curve), and would range between 5 to 10 cm^2. Marchetti and Totani's method or other DMT based methods may also be used to

estimate consolidation properties, however, it should be noted that the empirical factors used in these methods show some notable variations and extra care should be taken to select and verify appropriate site specific factors.

3.5 SELECTED DESIGN PARAMETERS USED IN CASE STUDY

The inferred geotechnical data in the vicinity of the case study as well as selected design values are shown in Figure 6. The geotechnical parameters for design were based on the assessment of field and laboratory tests, as described above, as well as from experience in similar geological deposits in the project region.

The undrained shear strength of the Holocene alluvium determined from field vane shear tests (peak values corrected for plasticity) and laboratory triaxial tests indicated good correlation with CPTu adopting a N_{kt} of 12 (Figure 6a). However, overconsolidation ratio assessed from laboratory consolidation tests were slightly lower than inferred from CPTu (Figure 6b).

There appears to be a large scatter in results of empirical relationships used for determining the modified primary compression index. However, the published relationship considered in this paper by US Army (1990) indicates the best correlation with project specific laboratory data, as depicted in Figure 6d.

A $c_\alpha / c_c = 0.04$ is assessed based on limited consolidation test results available in this area, which shows a good agreement with the typical ratios presented in Table 2 for inorganic clays. The ratio of 0.04 is used to correlate c_α based on some other older consolidation test results with no secondary compression index reported (Figure 6e)

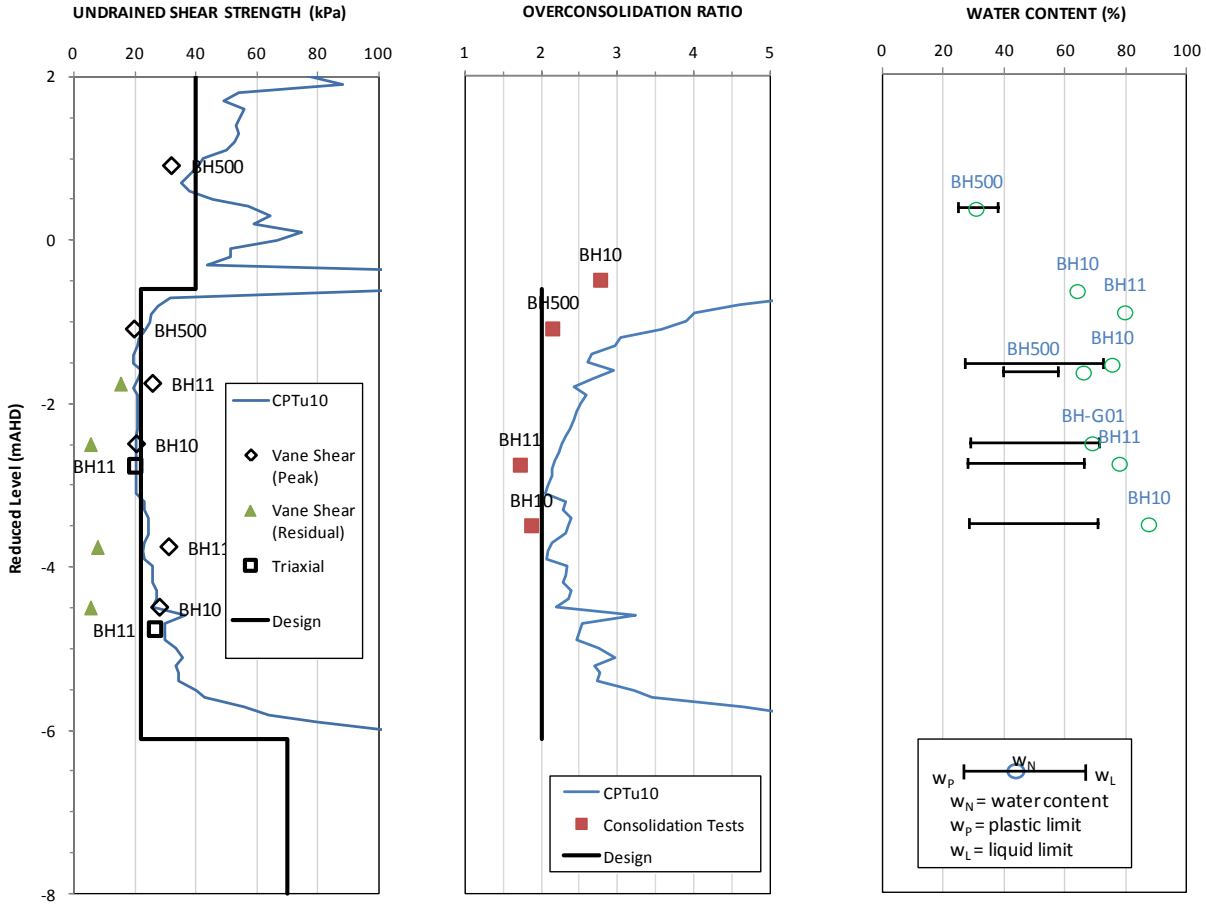

(a) (b) (c)

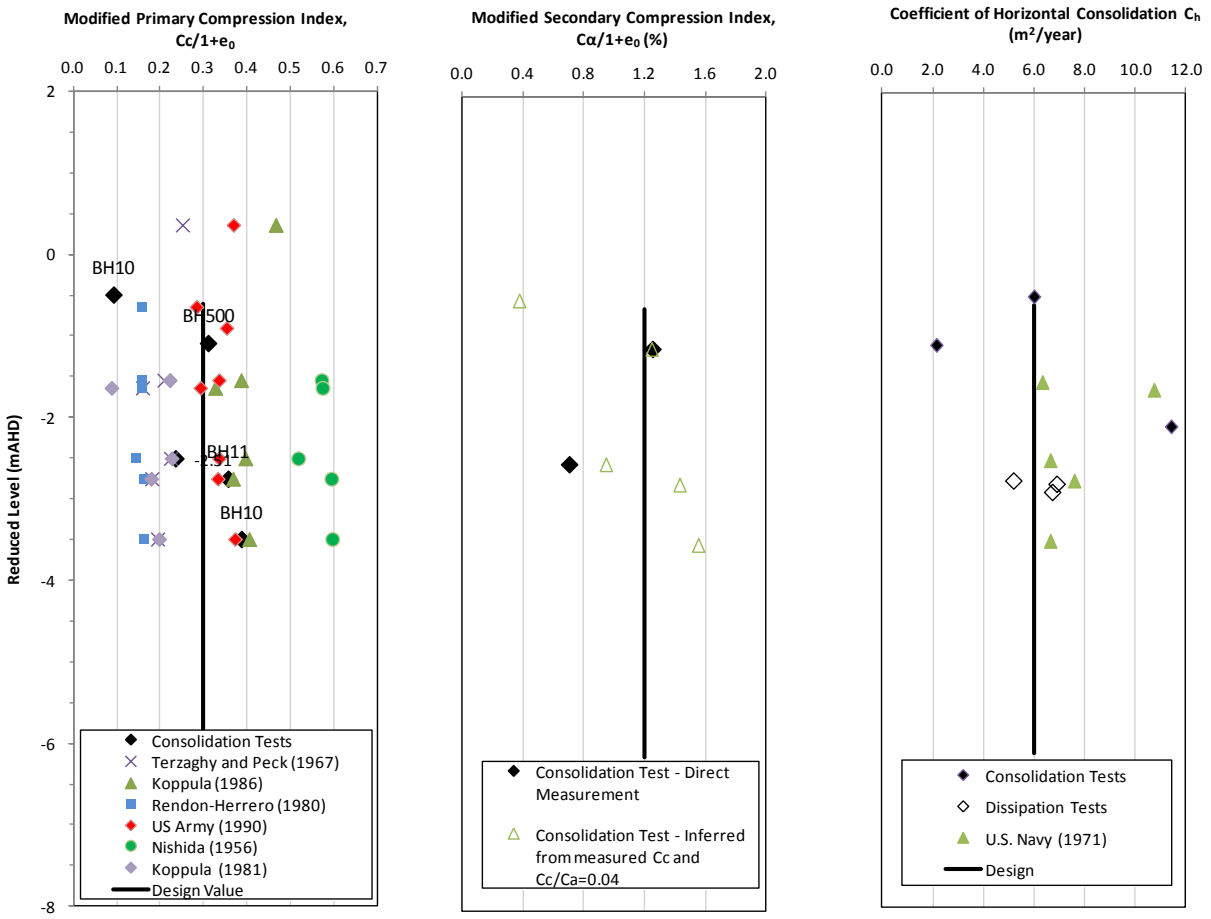

(d) (e) (f)

Figure 6: Typical material parameters obtained through laboratory and field testing and selected design values.

4 RECOMMENDATIONS FOR SITE INVESTIGATION

A comprehensive geotechnical site investigation (SI) is one of the crucial initial steps in every project which enables safe, resilient and economic design, and identifies potential mechanical and chemical hazards related to the ground. No universal approach can be recommended for site investigations as their extent, planning, approach and sampling and testing methods adopted will depend on the site-specific circumstances and the project requirements. Standards such as BS5930-1999 'Code of practice for site investigations' or, to some extent, AS1726-1993 'Geotechnical site investigations' set out the minimum requirements for a geotechnical site investigation and provide some guidelines for planning and design of SI, methods and testing, etc. However, further to specifying type, location and target depths of field and laboratory tests, there are other factors to be considered. Such factors could significantly increase usefulness of SI results and improve soft ground characterisation, and potentially result in a more reliable and economic design with significant potential savings in the project construction or maintenance costs. Some of these factors are highlighted as follows:

- Site investigations for soft ground, in particular for the detailed design stage, should allow for a combination of CPTu (with dissipation tests), DMT, FVT, and appropriate laboratory shear and consolidation tests. As discussed in Section 3, some of these tests have advantages over others and it would be useful to consider a balance of different field and laboratory test results;
- It would be useful that the above field and laboratory tests are undertaken in the vicinity of each other at a few locations within the same soft soil deposit and at similar depths. This would enable selection and validation of site-specific correlations, where appropriate, as discussed in Section 3;

- The quantity of tests will not guarantee a successful site characterisation, but the quality of test results is also important. It is critical that field and laboratory test equipment is calibrated and standard testing procedures are strictly applied in the field and laboratory. For instance, it is important that the CPT and DMT equipment is appropriately calibrated and piezocone pore pressure porous elements are saturated and de-aired before testing; and
- It is then important that geotechnical engineers supervising site investigations be completely familiar with the standard field testing procedures and calibration of field test equipment, and periodically request field testing contractors to demonstrate calibration of their equipment, as appropriate.

Furthermore, to facilitate the interpretation of test results, the authors also recommend:

- Groundwater level is measured at the time of CPT tests and be reported with CPT results;
- *e-log t* curves for each loading stage of consolidation tests are also presented with the test results to enable geotechnical engineers to verify the assessed consolidation parameters; and
- Consolidation reading at each stage is continued at least one log cycle of time after EOP (and preferably more within the range of applicable stresses) to enable reasonable estimation of the secondary compression index (c_α).

5 FINITE ELEMENT ANALYSIS

Common practices in soft ground profiling and characterisation were reviewed in Section 3. The final part of a geotechnical design would be geotechnical modelling and numerical analysis (if warranted). One of the most commonly used commercial finite element analysis software products used in the geotechnical practice is 2D PLAXIS. In this section, comments are provided about the PLAXIS material models which can be adopted for consolidating soil deposits, different approaches used to model wick drains (usually used in soft ground improvement) and modelling of rigid inclusions or piles using 2D PLAXIS.

5.1 MATERIAL MODEL

One of the most important steps in setting up a numerical model for an engineering problem is adoption of appropriate material models. 2D PLAXIS provides users with different models for soils among which *Soft Soil* (SS) and *Soft Soil Creep* (SSC) models can be used to simulate consolidation of isotropic soft soils. The SSC model also incorporates concepts of viscoplasticity in order to capture time-dependant creep deformations. Both models adopt Mohr-Coulomb (MC) failure criterion.

These models can predict soft soil behaviour with reasonable accuracy. However, this not only depends on the quality of basic input parameters, which include compressibility indices and shear strength parameters, but also the accurate calibration of the model as further discussed below:

5.1.1 Calibration for Rate of Consolidation

It is a common practice that a constant value is nominated for coefficient of consolidation (C_v) of soil units, based on Terzaghi's theory of 1D-consolidation. Nevertheless, there is no input C_v value to the SS or SSC models. PLAXIS calculates rate of consolidation directly based on coefficients of permeability (k_h and k_v), which are model inputs, and coefficient of volume compressibility (m_v), which is assessed at each loading step, based on the current stress state and the input compressibility parameters.

To achieve similar consolidation results as those anticipated based on the design C_v value, the input coefficient of permeability for each material should be estimated using the following equation:

$$k_v = C_v . m_v . \gamma_w \tag{11}$$

Where, $m_v = \dfrac{\Delta e}{(1+e_0).\Delta\sigma'_v}$, $\Delta\sigma'_v$ is the applied pressure (e.g. average surcharge due to a new embankment), e_0 is initial void ratio, Δe is the change of the void ratio due to the applied pressure, and γ_w is unit weight of water. It should be noted that m_v is not constant and depends on the current value of the effectives stress. However, its average value may be simply calculated using a formulated spread sheet when initial OCR and compressibility indices of the layer are known. Then the equivalent k_v can be estimated using Eq. 11.

Alternatively, for preliminary analysis and in the absence of test results, a $k_v = 10^{-9} m/\sec$ can be considered for soft clays, as k_v for the majority of soft clays ranges between $5\times10^{-9} m/\sec$ and $5\times10^{-8} m/\sec$ (Mesri and Choi, 1985).

5.1.2 Calibration of M-parameter

The SS and SSC models have a cap yield surface to delineate elastic and plastic strains. In both models, a M-parameter determines the height of this elliptical cap yield surface and in turn controls the coefficient of lateral stress in normal consolidation (K_0^{nc}). By default, $K_0^{nc} = 1 - \sin\phi$ is considered in both models (ϕ is the friction angle of the material). On this basis the M-parameter is calculated automatically such that the simulation of an oedometer test will give the most realistic results. It should be noted, however, that the SSC model in PLAXIS V8 (or older versions) adopted an M-parameter such that the simulation of an undrained triaxial test gave the best results (Waterman and Broere, 2004), using the following equation:

$$M = \frac{6.\sin(\phi)}{3 - \sin(\phi)} \tag{12}$$

This equation yields a smaller value than the automatically calculated default value. It should be noted that the M-parameter would affect calculated displacements but would not affect undrained shear strength in these models, as the both models use a MC failure criterion. Therefore, to obtain more realistic results, the M-parameter can be adjusted by changing default K_0^{nc} value in regard to the purpose of the analysis.

5.1.3 Calibration of SSC model for ageing effect

The cap yield surface in the SSC model continuously expands over time with a decreasing expansion rate. This enables the model to simulate the ageing effect in the soft soils (Schmertmann, 1991). The rate of the cap expansion is affected by any change in the stress state; an increase in stress, even when the stress remains within the elastic region, increases the rate of the cap expansion. Similarly, a decrease of stress decreases in the velocity of the cap expansion. However, the cap never stops expanding.

The above artificial ageing effect could affect the creep settlement analysis as the creep rate at which PLAXIS displacement calculation starts depends on the current value of OCR, which is continuously changing over time in this model. So to obtain more realistic creep settlements, it is important that the ageing effect, or in other words the amount of creep settlements occur due to the self-weight of the layer before a new load applies, is taken into the account (Wong, 2006). It is proposed then the default OCR=1 is selected for the soft soil, and after the stress initialisation of the PLAXIS model, a plastic nil step is considered with a time period of Δt (may be called 'geological time period') estimated as follows (Waterman and Broere, 2004):

$$\Delta t \cong \exp\left(\frac{\lambda^* - \kappa^*}{\mu^*}.\ln(OCR)\right) \tag{13}$$

In which $\lambda^* = c_c/[2.3(1+e_0)]$, $\kappa^* = 2.c_r/[2.3(1+e_0)]$ and $\mu^* = c_\alpha/[2.3(1+e_0)]$ are modified compression index, modified swelling index and modified creep index, respectively. The value of OCR in this equation is the design value selected through the soil characterisation practice. In the cases where the design value for soft soil OCR changes with depth or the geotechnical model comprises more than one soft soil unit with different compressibility indices and/or OCR, one may resort to considering an average OCR value in Eq. 13 with or without an initial OCR>1 profile for different units to account for the ageing effect.

Alternatively, the SS model can be adopted for soft soils to calculate primary consolidation settlements using PLAXIS. Creep settlements can then be separately calculated using other methods (e.g. Mesri and Choi, 1985, Wong 2006b, etc.), possibly with a formulated in-house spreadsheet, where the user could appropriately control the creep starting time and the creep rate, depending on the loading history. In the authors' experience, this latter approach can provide more realistic results when compared to the PLAXIS SSC model, particularly for modelling staged construction involving unloading (e.g. surcharge removal). In several case studies assessed by the authors, the current PLAXIS formulation seems to overestimate the creep rate during and after unloading. Whilst acknowledging this may be associated with improper use or calibration of the geological time step, the concept can be difficult to rationalise and a simpler analytical approach based on well stablished principles is therefore appealing. The authors note a similar finding by Wong (2006b).

5.2 WICK DRAINS

Wick drains are installed by pushing the wick drain (and anchor plate) into the ground using a mandrel. The process can disturb a zone of soil around the centre of the drain referred to as the *smeared zone*. This smearing can break down the natural structure and drainage pathways in the soil, reducing horizontal permeability and effectively reducing some of the benefits the wick drains are designed to provide.

The diameter of the smeared zone, d_s, can vary substantially from the equivalent diameter of the wick drain, d_w, depending on the soil type, the size and type of equipment used to install the wick drains and the experience of the contractor installing them. Likewise, the horizontal permeability of the smeared zone, k_s, can be significantly lower than that of the parent soil, k_h. Therefore, design is not just sensitive to the soil parameters adopted, but is also heavily dependent on construction practices.

There are various methods available to design wick drain treatments. The most straightforward typically comprise analytical solutions that are based on radial consolidation theory and apply corrections for the diameter and permeability of the smeared zone. As an example, Yeung (1997) provides a practical analytical design approach by presenting design curves used to calculate wick drain spacing, assuming different ratios of k_h/k_s and d_w/d_s. Values of k_h/k_s and d_w/d_s range from 5 to 10 and 2 to 3, respectively, depending on the level of conservatism warranted in design.

Finite element approaches can be adopted where more robust analysis is required. This is typically undertaken by modelling wick drains using one of the following approaches:

- Modelling wick drains as individual drains in plane-strain and correcting for 3D effects.
- Modelling the soil mass with a vertical permeability equivalent to that treated with wick drains (CUR 191).
- Modelling the soil mass with a horizontal permeability equivalent to that treated with wick drains, after CUR 191, Indraratna (2000) and other works by the same author.

Modelling of individual drains is time consuming. In the authors' experience, reasonable results have been yielded more efficiently using the equivalent vertical and horizontal permeability approaches set out above.

5.3 RIGID INCLUSIONS

Box culvert structures for the case study project were considered to be structural elements with strict settlement criteria. After a period of ground treatment options assessment the client required that culvert extensions be supported on piles embedded beneath the soft soil deposits in deeper stiffer/denser materials. Piles typically comprised 0.6 m diameter CFA piles on a 2.4 m centre-to-centre grid. In addition to vertical loading from the box culverts, the piles needed to be designed to resist bending moments and shear forces due to lateral displacements in the soft soils underlying adjacent non-pile supported embankments.

One method to estimate bending moments and shear forces in the piles invovles modelling pile rows in 2D plane-strain finite element analysis (e.g. PLAXIS) using plate elements. Pile properties are 'smeared' in the out-of-plane direction based on the pile spacing, and thus each row of piles is effectively analysed as a 'wall'. This method has the clear drawback of not allowing for 3D effects assoicated with soil continuity between piles. Plate elements in 2D models completely separate the soil at both sides of the element. This may be an appropriate simplification when piles have a small out-of-plane spacing compared to the pile diameter (e.g. spacing-to-diameter ratio < 2 to 3). However, for piles with a larger spacing-to-diameter ratios, and particularly in soft soil deposits where soil can more readily 'flow' between, and independent from the pile, such a method does not accurately resemble pile-soil interaction. The outcome is that bending moments and shear forces in the pile may be overestimated.

The selected design method adopted for the project allows for 3D effects associated with soil flow around the piles by first calculating the 2D free-field soil displacement below the culverts (i.e. without piles) in a plane-strain finite element PLAXIS analysis. The soil displacements are then input into the program PYGMY, which analyses the behaviour of single piles under general lateral loading. In this case, the user applies soil displacement and peak soil pressure to the pile. Soil resistance is represented by p-y springs. To perform analysis of pile groups, different multiplying factors (termed p multipliers) are applied depending on the individual piles position relative to the group (e.g. leading pile, trailing pile, side-by-side pile, etc.). The p-multipliers are based on the research of Dunnavant and O'Neill (1986) and O'Neill et al. (1990).

The two-stage process of using PLAXIS and PYGMY results in estimated bending moments and shear forces which are in general less than the method using plate elements in PLAXIS alone. It is noted that PLAXIS 2D (2012) includes a relatively new material model called 'embedded pile row' which is intended to improve the modelling of pile-soil interaction of a row of piles in the out-of –plane direction, which was not utiltised in this design. A 3D

approach, for instance using 3D PLAXIS, can also be adopted to overcome the above issue by allowing soil flow around the piles, but 3D models are more time consuming to build and compute and are mostly considered for detailed design on complex projects.

6 ANALYSIS RESULTS

Preliminary settlement analysis in the vicinity of the proposed culvert extension indicated that 2 m surcharge (in addition to preload) would be required for a period of 9 months to meet the settlement criteria. Construction considerations in this area mandated that staging comprised placement of a 0.7 m working platform, pile construction and wick drain installation on both sides of the culvert, immediately followed by placement of the preload and surcharge. A PLAXIS model (Figure 7) was developed to assess: a) internal forces of piles induced by lateral displacement of soft soils underlying adjacent non-pile supported embankments, and b) post construction total and differential settlements. Another model was also developed at a transverse direction to assess potential impact on the existing embankment, and to assess the stability of the new embankment and filling rates, which is not presented in this paper.

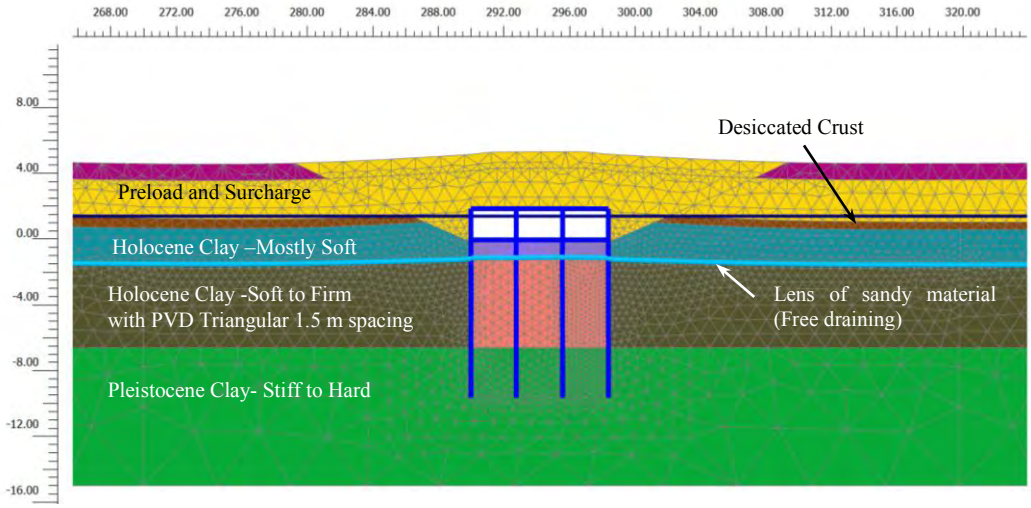

Figure 7: PLAXIS geotechnical model.

Initial analyses indicated that the outer row of piles were likely to experience un-factored bending moments of 460 kN.m for 0.6 m diameter piles, which were greater than the design limit. As a result one of the recommended options was that one outer row of 'shielding' piles be installed. The shielding piles were to be installed beyond the edge of the culvert at the same spacing as the main culvert piles (i.e. 2.4 m c/c spacing), and be provided with a minimum 2.5 m wide top slab (beyond the edge of the culvert) to support the overlying soil and traffic loads.

The shielding piles would provide settlement reduction as well as some protection from lateral soil movements to the piles supporting the culverts. In this sense they were considered ground improvement, and did not require design in strict accordance with AS 2159. The piles could therefore carry higher structural stresses and lower factors on geotechnical strength. It was also considered prudent to design a joint detail into the connection between the culvert base slab and the slab over the shielding piles, to allow some rotation while transferring horizontal loads (a pin connection).

Further to Section 5.3, this analysis utilised PYGMY to calculate pile internal forces using 2D free-field soil displacement. Figure 8a shows a comparison between free-field soil lateral displacements, and pile displacements predicted by PLAXIS and PYGMY. The bending moment diagram of outer piles (at the edge of the culvert), with pinned head, estimated by PYGMY has also been compared with those estimated by PLAXIS in Figure 8b. As shown in this figure, the corrected pile bending moments, estimated by PYGMY, are over 20% less than those predicted by PLAXIS for this case where piles have 4d (i.e. 2.4 m) spacing (d is pile diameter). This reduction of pile bending moment due to 2D to 3D correction would increase to a certain threshold value when the pile spacing increases. It is anticipated that the reduction would be negligible when the pile spacing is 3d or less (Carder and Easton, 2001).

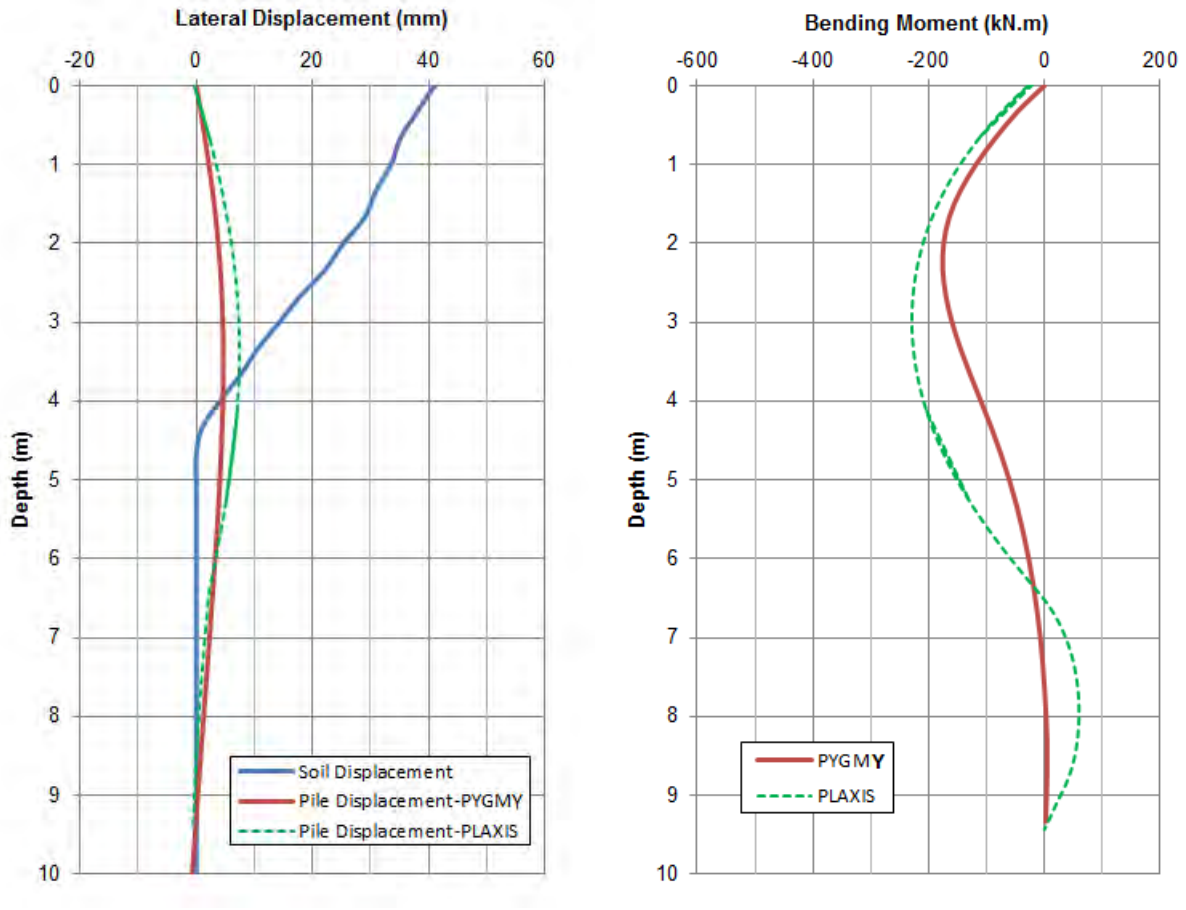

(a) (b)

Figure 8: (a) Lateral soil and outer pile displacements, (b) PYGMY vs PLAXIS pile bending moment diagram (600 mm dia. piles with 2.4 m c/c spacing).

7 CONCLUSIONS

Embankment construction or widening over soft ground presents several geotechnical design challenges including stability and settlement. This paper provided a critical literature review of the current approaches to characterise soft soils and select key design parameters. The advantages and limitations of the major laboratory and in-situ field tests were discussed, as follows:

- Different field and laboratory test methods may be used to determine undrained shear strength including CPT, field vane shear, DMT and laboratory triaxial or direct shear testing. The undrained shear strength profile could be assessed using undrained shear strength ratio according to Ladd (1991) to assess the undrained shear strength profile.
- The test program and types of testing selected as part of site characterisation would depend on the level of project sophistication and importance and recommendations were provided in this regard.
- Assessment of overconsolidation ratio is generally made through interpretation of 1D laboratory consolidation tests. However estimates of OCR can also be obtained from field vane, CPT and DMT, although in these cases, correlations usually need site-specific data.
- Compression indices are assessed from interpretation of 1D laboratory consolidation tests. A number of empirical correlations have also been presented which provide an easy and inexpensive alternative method based on which the scope of the geotechnical laboratory program can be reduced to confirmatory investigation of the consolidation properties.

- The constant c_α / c_c concept introduced by Mesri and Godlewski (1977) defines secondary compression behaviour of any soil. Site specific values should be determined by selection of c_α / c_c pairs, selected for the same time, effictive stress and void ratio.
- Coefficients of consolidation are usually determined using laboratory 1D-consolidation tests. However, interpretation of CPTu and DMT dissipation tests could also be used to determine C_h and/or C_v. It is highlighted that the laboratory value of C_v is usually found to be less than the value measured in the field. Even the best estimates of coefficients of consolidation from high-quality laboratory tests could result in estimation of the rate of consolidation settlement with an order of magnitude difference from observed values in the field.

Furthermore, recommendations were provided for site investigations mainly emphasizing on:

- Inclusion of variety of laboratory and field tests within the program, and to undertake different types of tests at a few locations in vicinity of each other and at the same depth. This is to facilitate establishment of site-specific correlation factors, as discussed in this paper.
- Quality of test results which could be affected by the test procedures, calibration of test equipment and operators skills.

Finally material models of 2D-PLAXIS and their limitations were discussed. Some methods were proposed for correct calibration of the models to obtain reasonable results. Different approaches in numerical modelling of wick drains were presented, and some of the drawbacks of modelling rigid inclusions or piles using 2D-PLXIS were highlighted and recommendations were provided to overcome such issues.

8 REFERENCES

Baligh, M. M. *Undrained deep penetration, I: Shear stresses*. Géotechnique, 1986a, 36(4): p. 471-485.

Baligh, M. M. *Undrained deep penetration, II: Pore pressures*. Géotechnique, 1986b, 36(4): p. 487-501.

Bjerrum, L. *Embankments on soft ground: SOA Report*, Proc. Speciality Conference on Performance of Earth and Earth-Supported Structures, ASCE, 1972, 2: p. 1-54.

Bjerrum, L. *Problems of soil mechanics & construction on soft clays*. Proceedings, 8th International Conference on Soil Mechanics & Foundation Engineering, 1973, Vol. 3, Session 4, Moscow: p. 111-159.

Boone, S.J. *A critical reappraisal of "preconsolidation pressure" interpretations using the oedemeter test.* Canadian Geotechnical Journal 2010, 47: p. 281-296.

Carder, D. R. and Easton, M. R., *Analysis of performance of spaced piles to stabilise embankment and cutting slopes.* TRL Report TRL493, 2001, Crowthorne: TRL Limited.

Casagrande, A. *The determination of the pre-consolidation load and its practical significance*. Proc. 1st Int. Conference on Soil Mech. and Found. Engrg., Cambridge, Mass.,1936, 3: p. 60-64.

Chai, J., Sheng, D., Carter, J. P. and Zhu, H. *Coefficient of consolidation from non-standard piezocone dissipation curve,* Computers and Geotechnics, 2012, 41: p. 13–22.

Chander, R.J. *The in-situ measurement of the undrained shear strength of clays using the filed vane*. Vane Shear Strength Testing in Soils: Filed and Lab Studies, STP 1014, ASTM, West Conshohocken, PA, 1988: p.13-44.

CUR 191 (1997), *Achtergronden bij numerieke modelling van geotechnische constructies*, deel 2. Stiching CUR, Gouda.

Dunnavant, T. W. and O'Neill, M. W.*Evaluation of design oriented methods for analysis of vertical pile groups subjected to lateral load*, Numerical Methods in Offshore Piling, Institute Francais du Petrole, Laboratoire Central de Ponts et Chausses, 1986: p. 303-316

Engineering and Design- Settlement Analysis, Department of the Army U.S. Army Corps of Engineers, 1990, Engineer Manual No. 1110-1-1904

Finno, R.J. *Analytical interpretation of dilatometer penetration through saturated cohesive soils*. Géotechnique, 1993, 43(2): p. 241-254

Fox, P., J., Tuncer, B. E., and Li-Tus, L, *Cα/Cc concept applied to compression of peat*, Journal of Geotechnical Engineering, 1992, ASCE, 118 (8): p. 1256-1263

Hough, B. K., *Basic Soil Engineering,* The Ronald Press Co., New York, N. Y., 1957: p. 114-115.

Houlsby G. T., Teh C. I., *Analysis of the piezocone in clay*, Proc. of the International Symposium on Penetration Testing, ISOPT-1, Orlando, 2, Balkema Pub., Rotterdam, 1988: p. 777–83.

Indraratna, B., and Redana, I.W. (2000). Numerical modelling of vertical drains and well resistance installed in soft clay. Can. Geot. J., 37(1): p. 132-145.

Jamiolkowski, M., Ladd, C. C., Germaine, J. T., and Lancellotta, R, *New development in field and laboratory testing of soils: Theme Lecture 2*. Proc. 11th International Conference on Soil Mechanics and Foundation Engineering. 1985, San Francisco, 1: p. 57-153.

Kamei T. and Iwasaki K. *Evaluation of undrained shear strength of cohesive soils using a flat dilatometer*, Japanese Society of Soil Mechanics and Foundation Engineering, Soils and Foundations, 1995, 35 (2): p. 1-13

Koppula, S. D. Statistical estimation of compression index, ASTM Geotchnical Testing Journal, 1981, 4 (2): p. 68-73.

Koppula, S.D. Dicussion: consolidation parameters derived from index tests. Géotechnique,1986, 36(2): p. 68-78.

Ladd, C. C , and Foott, R. *New design procedure for stability of soft clays*. Journal of Geotechnical Engineering, ASCE, 1974, 100(7),): p.763-786.

Ladd, C. C, Stability Evaluation During Staged Construction. Journal of Geotechnical Engineering, 1991. 117(4): p. 540-615.

Ladd, C.C., and DeGroot, D.J. (2003). *Recommended Practice for Soft Ground Site Characterisation – Arthur Casagrande Lecture.* Proc. 12th Pan-American Conf. on Soil Mech. And Geot. Engr., Massachusetts Institute of Technology, MA, USA.

Ladd,C.C, Foott,R., Ishihara,K., Schlosser, F., and Poulos, H.G. *Stress-deformation and strength characteristics: SOA report*. Proc.9th Int. Conference on Soil Mech. And Found. Engrg., 1977, 2: p. 421-494.

Larsson, R. *Undrained shear strength in stability calculation of embankments & foundations on clays*. Canadian Geotechnical Journal, 1980, 17 (4): p. 591-602.

Marchetti, S. *In-situ tests by flat dilatometer*. J. Geotech. Eng., 1980, 106 (3): p. 299–321.

Marchetti, S., and Totani, G. *Ch evauations from DMTA dissipation curves*, Proceeding of XII International Conference on Soil Mechanics and Foundation Engineering, Rio de Janeiro, 1989, 1: p. 281-286.

Mayne, P. W., and Martin, G. K. *Commentary on Marchetti flat dilatometer correlations in soils*. Geotech. Test. J., 1998 21(3): p. 222–239.

Mesri G. and Vardhanabhuti. *Secondary compression*. Journal of Geotechnical and Geoenvironmental Engineering, ASCE, 2005, 131(3): p. 398-401.

Mesri, G. and Godlewski, P. M. Time- and Stress-Compressibility Interrelationship. Journal of the Geotechnical Engineering Division, ASCE, 1977, 103: p. 417-430.

Mesri, G., and Castro, A. *Ca/Cc concept and K_0 during secondary compression*. J. Geotech. Engrg., ASCE, 1987, 113(3): p. 230-247.

Mesri, G., and Choi, A. M., *Settlement Analysis of Embankments on Soft Clays*, J. Geotech. Engrg., ASCE, 1985, 111(4): p. 441-464.

Navy, U. S., *Soil Mechanics, Foundations and Earth Structures*, NAVFAC Design Manual DM- 7, Washington, D.C., 1971.

Nishida,Y. *A brief note on compression index of soils*, Journal of Soil Mechanics and Foundations Division, ASCE, 1956, 82(3): p. 1027-1-1027-14.

O'Neill, M. W., Reese, L. C. and Cox, W. R. *Soil behaviour for piles under lateral loading*, Proceedings 22nd Annual Offshore Technology Conference, Houston, OTC 6377, 1990: p. 279-287

Rendon-Herrero, O. *Universal Compression Index Equation*, Journal of Geotechnical Engineering Division, ASCE, GT11, 1980: p.1179-1199.

Robertson P. K., Sully J. P., Woeller D. J., Lunne T., Powell J. J. M., Gillespie D. G. *Estimating coefficient of consolidation from piezocone tests*, Canadian Geotechnical Journal, 1992, 29: p. 539–550.

Robertson P.K. *CPT-DMT Correlations*, Journal of Geotechnical and Geoenvironmental Engineering, 2009a, 135: p.1762-1771.

Robertson P.K. *Interpretation of cone penetration tests- a unified approach*, Canadian Geotechnical Journal, 2009b, 46: p.1337-1355.

Sabatini P. J. , Bachus R. C. , Mayne P. W. , Schneider J. A. , Zettler T. E. *Evaluation of soil and rock properties*, Federal Highway Administration of the US, Report No. FHWA-IF-02-034, 2002.

Schmertmann, J. H. *Suggested method for performing the flat dilatometer test.* Geotech. Testing J., ASTM, 1986, 9(2): p. 93-101.

Schmertmann, J. H. *The mechanical aging of soils.* Journal of Geotechnical Engineering, ASCE, 1991, 117(9): p. 1288-1330.

Schmertmann, J. H. *The undisturbed consolidation of clay*. Trans., ASCE,1955, 120: p.1201-1233.

Schmetrmann, J.H., *Guidelines for using the CPT, CPTu and Marchetti DMT for geotechnical design- Vol. 3- DMT Test Methods.* Report No. FHWA-PA-87-024+84-24 to PennDOT, and Data Reduction, 1988

Skempton, A.W. *Notes on the Compressibility of Clays*, Quarterly Journal of Geological Society of London, 1944, 100: p. 119-135.

Sully P. J., Robertson P. K., Campanella R. G., Woeller D. J., *An approach to evaluation of field CPTU dissipation data in overconsolidated fine-grained soils*, Canadian Geotechnical Journal, 1999, 36: p. 369–381.

Teh C. I., Houlsby G. T., *An analytical study of the cone penetration test in clay*, Géotechnique, 1991, 41: p. 17–34.

Teh, C.I. *An analytical study of the cone penetration test*. D.Phil. Thesis, Oxford University, UK.

Terzaghi, K. and Peck, R.B. *Soil Mechanics in Engineering Practice*, John Wiley & Sons Inc. New York, 1967.

U.S. Army Corps of Engineers, *Engineering and Design- Settlement analysis,* Engineering Manual EM *1110-1-190, 1990.*

Waterman, D., Broere, W., *Application of the SSC model - Part I*, 2004, PLAXIS Bulletin.

Wong, P. K., *Preload Design, Part 1 –Review of Soil Compressibility Behaviour in Relation to the Design of Preloads*, Australian Geomechnics Society Sydney Chapter 2006a Symposium: p. 23-32.

Wong, P. K., *Preload Design, Part 2 – An Analytical Method Based on Bjerrum's time line principal and comparison with other design methods*, Australian Geomechnics Society Sydney Chapter 2006b Symposium: p. 33-42.

Yeung, A.T. *Design Curves for Prefabricated Vertical Drains*, Journal of Geotechnical and Geoenvironmental Engineering, August, 1997: p. 755 – 759.

SUSTAINABILITY CONSIDERATIONS FOR GROUND IMPROVEMENT TECHNIQUE USING CONTROLLED MODULUS COLUMNS

H. H. Nguyen[1], H. Khabbaz[2], B. Fatahi[3], P Vincent[4], and M. Marix-Evans[5]

[1]PhD Student, [2]Associate Professor, [3]Senior Lecturer, Centre for Built Infrastructure Research, University of Technology Sydney (UTS), NSW, Australia
[4]Technical Manager, Menard Bachy Pty Ltd, Sydney Office,
[5]Design Manager, Fulton Hogan Australia Pty Ltd, Australia

ABSTRACT

Sustainability is becoming an ever more important consideration for the selection of ground improvement methods on construction projects around the world. When considering this criterion, the controlled modulus column (CMC) technology emerges as one of the relatively novel technologies that are capable to deliver valuable and sustainable outcomes. CMC installation is a vibration free process and produces very limited soil cuttings, making CMC suitable for improvement of soft ground, contaminated sites and ones adjacent to sensitive structures. Besides, CMC uses grout only without the use of steel reinforcement; hence carbon footprint estimated for CMC is generally lower than those for traditional piling techniques. Besides these valuable aspects, it is believed that this technology can still be advanced to contribute more to the sustainable development, owing to ongoing research works and practical experience. This paper summarises the key sustainability aspects of using CMC technology and highlights some potential aspects for further development. Future research directions are discussed to enhance sustainable design practice. These include general discussions on the issues of economic design with trial field tests, the use of recycled industrial by-products for grout mix, improved design, maximising the resiliency of structures and the energy consumption. The CMC installation effects on the surrounding soils and environment are also discussed sensibly in this paper.

Key words: Ground improvement, CMC, sustainability, resilience, installation effects, lateral displacement

1 INTRODUCTION

The *sustainability* concept has been increasingly accepted to be a key aspect in engineering design and construction, most noticeably in government supported projects. Since geotechnical engineering is one of the key parts of construction, geotechnical engineers have opportunities with power to deliver project outcomes that are not only economical, safe but also sustainable. Ground improvement techniques aim to increase ground bearing capacity, improve stability, and reduce short and long term ground settlements. These techniques have an impact on environment, local ecological systems and ground conditions. Appropriate techniques are increasingly demanded due to decreasing available and favourable land for construction and redevelopment of urban areas. Today a large number of ground improvement methods exist in the industry, with each serving a limited number of purposes. Selection of one or a combination of two or more methods requires deep understanding of various ground treatment methods. Decision making should rely on trials, design requirement, project budget and time restraint, ground and site conditions. Alongside with control of quality, durability, cost and safety, authorities also require design and construction of infrastructure to consider environmental outcomes, forming important aspects of sustainable development.

Although sustainability in geotechnical engineering has been addressed by a number of authors (Abreu et al., 2008; Holt et al., 2010; Jefferson et al., 2007), little attention on sustainable development has been placed during the process of geotechnical design and implementation. The geotechnical community should set out specific sustainability outcomes with tangible results to be achieved within a set time frame. At this stage it will be very likely that any sustainability policies/requirements attached to the contract works may receive mixed responses from businesses.

To target sustainability outcomes in geotechnical engineering and ground improvement works, three major "triple bottom line" Economic, Environment and Social impact proposed by Elkington (1997) should be followed in combination with "financial, social, human, natural and produced" factors. Economic benefits and social reactions should not be considered as barriers for sustainable development. In fact, adoption of sustainable solutions should be considered to enhance the competiveness in bidding and winning projects. Today sustainability in geotechnical engineering targets (i) reduction in energy consumption, (ii) lower carbon emission during implementation and (iii) decrease in material usage. This should be accompanied with increased use of reused, recycled or green materials and locally available materials instead of importing (Mitchell and Kelly, 2013). Geotechnical engineers should be aware of and equipped with methods of sustainability assessment (e.g. how carbon footprint is estimated).

One way to achieve those outcomes would be through technological innovations. One of the relatively new innovative ground improvement methods is the controlled modulus column (CMC) ground improvement technique. This technology was first developed in France. Today CMC has become a method of choice for many projects having tight construction schedule or with concerns related to soft soils and contaminated ground. CMC possesses several features that are distinct from those of more traditional methods such as prefabricated vertical drains, stone columns, deep soil mixing or piled embankment foundation. CMC has been used considerably in Europe with increasing popularity in the US. The technique has recently been used in a number of projects in Australia, mainly involving construction of bridge approach embankments, port development and warehouse foundation with the aim to reduce both total and differential settlements and to accelerate construction sequence (Fok et al., 2012; Wong and Muttuvel, 2012). The Gerringong Upgrade project is one of the recent projects where CMC have been successfully utilised for bridge and road construction (Fulton Hogan, 2013).

This paper summarises the key sustainability aspects of using CMC technology and highlights some aspects that are potential for development. Future research directions are discussed to further enhance sustainable design practices. These include fuel consumption during operations, economic design with trial field tests, the use of recycled industrial by-products for grout mix, improved design, maximising the resiliency of structures and the energy consumption. The remainder of the paper will discuss the current state of art in assessing installation-induced displacement of the surrounding soils.

2 CONTROLLED MODULUS COLUMNS AND SUSTAINABILITY

2.1 CMC TECHNOLOGY

CMC technique has been described well in the texts by Plomteux et al. (2004) and Pearlman and Porbaha (2006), amongst others. CMC aims to reinforce soils that are often prone to settlement and having low bearing capacity by using a system consisting of non-reinforced and cement-based grout columns inserted into the ground. Both ground and columns are overlain by a granular layer, which is used to transfer the loading from upper structures to CMC and the surrounding soils. The presence of this layer over isolated columns makes CMC system suitable to support uniform loading applied over a relatively large area. CMC reduces total and differential settlement, better than stone columns and the quality is more controlled than with deep soil mixing techniques.

The CMC installation process involves penetration of a rotary displacement auger into the ground under the torque and downward thrust provided by the drilling rig; which is followed by grout injection through the hollow stem of the drilling tool while the tool is withdrawn (Figure 1). The specially designed auger comprises a short partial flight segment near the tip, the middle segment welded with helically wound blades and the uppermost portion with counter-rotating flight segment (Figure 2), which enables lateral soil compaction during installation.

Figure 1: CMC auger (Gerringong Upgrade project, 2013)

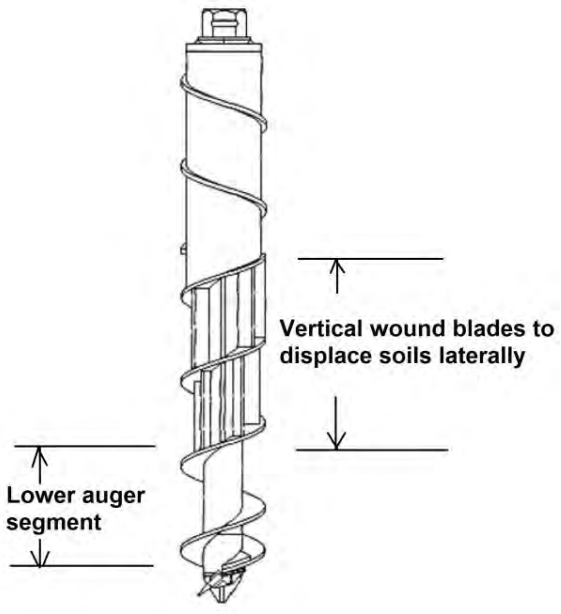

Figure 2: Patented CMC auger (Cognon, 2004)

2.2 SUSTAINABILITY ASPECTS OF CMC

The key contribution of CMC technology to the sustainable development is the production of very limited soil cuttings to the ground surface, thanks to the auger that is specially designed to displace soils laterally. This feature is particularly useful for construction projects involving contaminated or landfill sites, making CMC a cost-effective ground improvement technique associated with the reduction of cost for spoil disposal and handling compared to the contiguous flight auger (CFA) piling or bored piles (Masse et al., 2011; Walker et al., 2011). Besides performing well in soft or loose soils, CMC is also suitable for soils with significant organic content or acid sulphate soils. Integrity pile testing by Kirstein and Wittorf (2013) indicated that CMC can also be performed well in very soft soils although additional vertical drains had to be installed in the soft soil surrounding the columns. Environmental benefits can also be achieved through a vibration free and quasi-static installation process, as opposed to dynamic vibratory methods e.g. stone columns or driven piles. This allows CMC to be installed near sensitive structures.

The second advantage of CMC over other traditional methods is associated with a high production rate, which means overhead cost saving and suitable for projects with tight construction schedules. Hole drilling and concrete injection are carried out in one go without risk of hole collapses. Experience shows that many bored piling project suffered extended delay due to the unforseen ground conditions. CMC column strength develops quickly, does not rely on the surrounding soil strength, and is effective in settlement control. Hence CMC is often selected to support bridge approach embankment, to fast track the bridge construction (Plomteux and Lacazedieu, 2007; Plomteux et al., 2004).

Thirdly, with CMC, saving can be achieved by various ways. Using displacement auger, the risk of necking is minimised leading to saving in the volume of injected grout. The load transfer layer functions in place for a more costly structural pile caps and concrete slabs. Fok et al. (2012) indicated that a 10 to 15% cost saving was achieved by using CMC compared to the deep soil mixing technique. Sometimes up to 30% in saving could be achieved (Angelo, 2007). When making judgement in terms of time, cost and long term performance (Higgins, 2014), it is considered that CMC may be positioned between deep soil mixing and piling with quick results and lower post construction settlement (Figure 3).

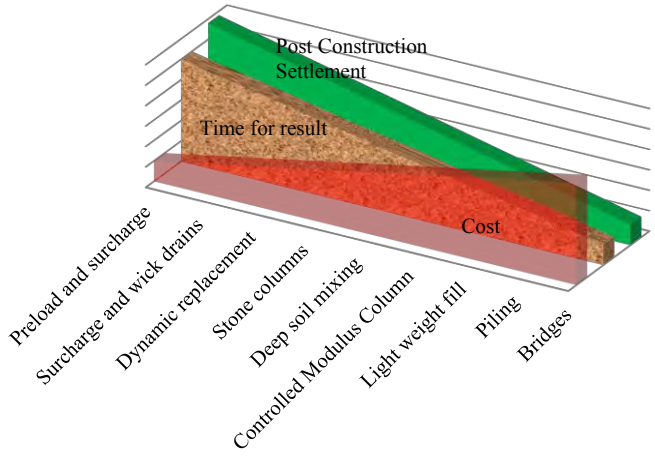

Figure 3: Cost, time for result, and performance considerations (modified after Higgins, 2014)

When scoring sustainability for a ground improvement method, the estimated carbon footprint can often be an important indicator. Carbon footprint is the sum of all emissions of CO_2 in a year, induced by ground improvement activities and by the production of materials used in construction. The estimated carbon footprint from CMC operation and related materials is considered lower than those from traditional piling methods by approximately 25% (Masse et al., 2011; Spaulding et al., 2008; Walker et al., 2011). Those emissions were calculated assuming no steel is used for CMC and that production of steel generally emits more carbon dioxide than cement related products.

Today, access to new tools to assess several environmental indicators for various competing solutions allows for the rapid comparison of ground improvement techniques and assists both contractors and clients in retaining the ~~"b~~best for project" schemes. Figure 4 illustrates such a comparison being performed on a range of solutions in accordance with the European Norm 15804.

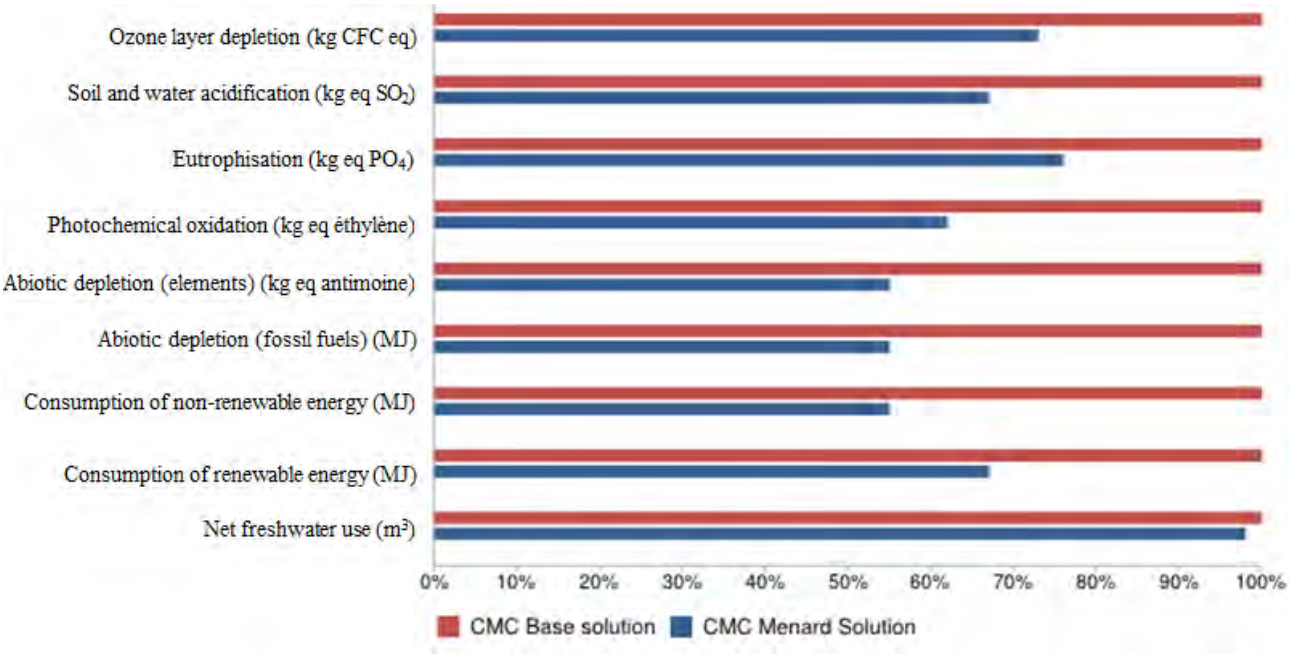

Figure 4: NF EN 15804 Indicators – Comparison of various CMC schemes (Prism solution – Menard Bachy)

Sustainable development also means design for durability and robustness to maximise the future resilience of a structure. The quality of CMC columns are subject to a real time monitoring system where installation parameters are recorded, allowing the operator to adjust the drill rate and installation depths, in combination with prior column design and drawings. This is particularly important for a site having varying ground profile with depth and/or with heterogeneous soils. Durability of the grout columns within a specific design life also relates to the properties of the mix i.e. the ability of the columns to resist chemic attack and weathering. Although the grout column will somewhat deteriorate with time, addition of fly ash can improve column durability. In fact, grout incorporating high volume fly ash was found to create grout columns with very low pemeability and a high resistance to the passage of chloride ions (Bilodeau et al., 1994).

Every ground improvement method serves just a limited number of purposes. Decision making in selection of ground improvement methods will have to rely on the project requirement, local sustainability policies, ground, site conditions and others. Specifically within its functions, there are still areas for future development of CMC, which will be discussed in the next section.

2.3 POTENTIAL DEVELOPMENT IN TERMS OF SUSTAINABILITY FOR CMC

Many potential development approaches can be underlined when dealing with sustainability for controlled modulus columns (CMC). They are summarised in this section.

1. Economic design, an important aspect of sustainable development, can be achieved by various ways. In a CMC system, the load transfer layer provides arching effects, allowing structural or embankment loads to be transferred to the columns and to the founding stratum. Wong and Muttuvel (2012) carried out a limited study, indicating that it may be possible to reduce the thickness of the load transfer layer and the use of geotextiles for embankments that are sufficiently high. Similarly, for warehouse building constructions, due to the presence of the concrete floor slabs, geogrid reinforcement was rarely placed within the load transfer layer (Masse et al., 2011). Such economic designs are currently carried out on a case-by-case basis and no standardised method has been proposed. In fact, if the load transfer layer is not provided, the soil arching developed in the embankment fill alone may break due to traffic dynamic loads, seismic effects and flooding. Further rigorous numerical and experimental investigations are required.

In medium to large projects, the economic design proposal can be confirmed by construction of CMC test pads. The purposes of the test pads are not only to optimise the final design but also for design optimisation in future projects. According to Farouz (2014), with every $1 spent for the rigid inclusion test pads, $4 of savings could be achieved in the long run.

2. Grout mix design may be modified with further considerations of using industrial by-products such as ground blast-furnace slag, coal ash and fly ash with various contents, depending on the design strength requirements. The most appropriate grout mix for good pumpability is a specially designed lean sand-mix mortar or pea-gravel concrete, often with fly ash to increase workability. Concrete has been considered less costly than grout and has been increasingly used

in the US and Europe for CFA and displacement columns (Brown et al., 2007). Whether concrete or grout, the mix producers should make more use of local materials rather than importing in order to reduce the transport cost and fuel consumption. To increase tensile strength for columns, some recycled fibres such as polypropylene and recycled carpet may be added to the grout mix. The addition of fibres was found to reduce the cement content for stabilising poor clayey soils, particularly for applications associated deformations under seismic loading (Fatahi et al., 2013). Sustainability relates to savings in design and building resilient structures; however, such designs should have sufficient testing and verification to meet strength and durability requirements.

3. The installation effects are rarely taken into account to estimate columns' skin friction capacity. Designers seem to have little confidence in the use of increased soil parameters in actual design and no systematic approach has been established. In fact, most CMC or rigid inclusions in general, are installed through soft or loose soils and founded on stiffer founding stratum. The installation of displacement columns, despite causing compaction effects, usually creates a thin smeared or disturbed zone around the columns, depending on the type of auger and soil types. For column installation in loose sands, soils are densified everywhere immediately after installation. For clayey soils, strength gain and column set-up can be achieved at later stages depending on the amount of generated excess pore water pressure (Carter et al., 1980). A recent numerical study was carried out by Rivera et al. (2014) to study the increase in the radial effective stress σ'_r and the earth pressure coefficients K in clayey soils due to CMC installation. Figure 5 shows some increase in K value at the end of construction within a zone of up to 10 times column radius r_0. Although the results of this study is very useful, field test and performance verification have not been carried out. Further studies should be accompanied with thorough site investigation before CMC design and employing recent technology advancement e.g. the National French ASIRI project by Simon and others (2012a).

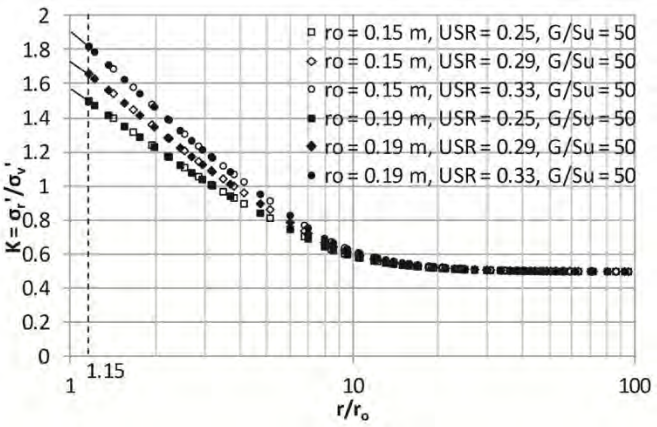

Figure 5: Distribution of radial effective stress in terms of K at the end of construction with varying CMC radius r_0, varying undrained strength ratio (USR = s_u/σ'_v) and a constant soil rigidity index G/s_u of 50 (Rivera et al., 2014)

4. The performance of CMC installed in expansive soils is unknown. Although deep columns can be designed to bypass such soil horizons, CMC should also be able to resist potential tension and uplift effects. While CMC are non-reinforced and relatively weak in tension, the shaft may fail under excessive tension and the column may move upwards when the clay expands (Manjriker, 2006). In such cases, one of the possible solutions would be to add fibre reinforcement to the grout mix to provide additional tensile strength for the columns. In fact, it was found that the tensile strength of the cement-treated clay increased with the addition of carpet fibres (Fatahi et al., 2012). Figure 6 presents a sample of cement-treated clay with added geofibres.

Figure 6: A typical fibre reinforced cement-treated clay sample

5. Sustainable development also means design to maximise the future resilience of a structure against slope instability and seismic loadings. CMC is typically non-reinforced and often designed to mainly support uniform vertical loading. If CMC columns are located at the batter of embankment, or subject to seismic events, the column capacity to resist negative bending moment may be of particular concern. Under such non-vertical or dissymmetric loading, the excessive shear forces and bending moments may be induced.

To support reinforced soil wall (RSW) blocks at a site near Newcastle, one of the seismically active zones in Australia, the outer rows of CMC were reinforced with steel bars (Wong and Muttuvel, 2011). High strength grout may be required if additional strength is required to resist cracks developed in negative bending resisting elements. In addition to the capacity of CMC columns, quality and thickness of the Load Transfer Platform strongly affect the intensity of shear forces and bending moments in the columns, and therefore the behaviour of foundation, under seismic effects (Simon, 2012b). Similar to design approach using micropiles presented in the French national project on micropiles (Juran and Weinstein, 2008), some CMC columns may be installed symmetrically inclined in small angles to make use of the axial capacity . If implemented, this solution may potentially replace other costly solutions such as using larger and/or reinforced columns. The use of CMC or other rigid inclusions in seismic related projects is still a general concern to the designers, demanding a set of general design guidelines.

6. The amount of carbon footprint from a CMC system is generally less than other traditional piling methods. CMC columns normally have smaller diameters compared to typical bored piles. Also CMC columns are not normally designed to socket into hard stratum. Considering only the diesel consumption of the machinery during installation, however, displacement methods may require larger torque and vertical force than using continuous flight auger methods for an equivalent column diameter. Research by NeSmith and Fox (2009) indicated that the installation effort required to drill a new hole adjacent to the previously drilled hole was higher due to densified soils caused by the installation effects. While CMC auger has been optimised to significantly reduce the soil resistance, future research on auger geometry would further reduce soil resistance and hence the energy consumption.

7. Although CMC is a vibration free method, large displacement caused by the installation process could cause damage to the surrounding built environment (Brown, 2005) if proper installation sequence is not considered during implementation. If the soil deformation is excessive, the shape of the adjacent CMC may not be maintained, leading the reduction in the bending stiffness. This particular concern, relevant to sustainable development, will be presented in the following section. Recommendations for the required improvement in predicting lateral displacement and simulation of the CMC installation are provided.

3 DISPLACEMENT EFFECTS ON SURROUNDING ENVIRONMENT

The movement of the CMC auger into the ground causes lateral displacement of the soils surrounding the column. The displacement effects become more apparent in a number of circumstances, e.g. design of closely spaced columns in order to reduce differential settlement at the surface of the embankment. As a result, the installation-induced displacement at a new column could cause damage to freshly grouted surrounding columns. While the long term CMC elastic modulus ranges between 1,000 and 10,000MPa, the fresh grout is often wet, plastic and viscous. If the freshly-grouted columns are subject to soil movement, the verticality of the column may be adversely affected and hence a reduced bending moment capacity can be expected, potentially causing column cracking. Within the first 24 hours of the grout setting time, the grout has not cured to gain sufficient stiffness and could be susceptible when subject to external loading. Similarly, if installation is carried out near a bridge abutment or an existing sensitive structure, the displacement may cause lateral movement and impose additional load on the bridge piles or structures. Such effects can be a major concern for piling contractors and geotechnical engineers (Brown, 2005; Hewitt et al., 2009; Plomteux et al., 2004). As recommended by French National project on rigid inclusions (Simon, 2012a), for inclusions executed with displacement piling technique, the minimum distance between columns is recommended to be approximately four diameters i.e. $S_{min} = 4D$. As a comparison, in a much less displacement method like CFA, it is considered risky to install piles within a centre-to-centre distance of less than three column diameters from adjacent piles cast within the previous 24 hours (NSW Roads and Maritime Services, 2010). If ground conditions are unfavourable, then the spacing should be increased. Based on author's experience, the displacement effects of non-displacement type CFA piling can sometimes adversely affect sensitive structures at close proximity. Therefore, it is important for engineers to become aware of the piling displacement effects, especially with displacement installation techniques like CMC.

Plomteux et al. (2004) highlighted the risk involving construction of CMC columns with a spacing of 1m near the bridge abutment piles. The proposed construction method was modified with CMCs installed in two different interleave passes, each with 1.4m x 1.4m grids (Figure 7).

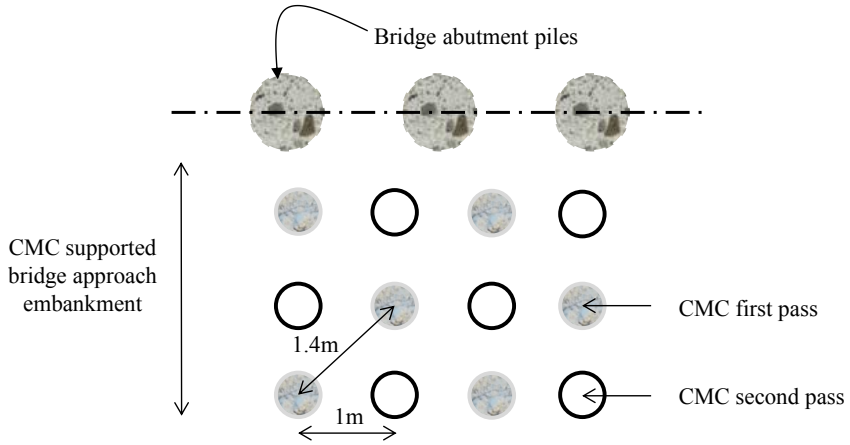

Figure 7: Modified CMC installation layout (modified after Plomteux et al. 2004)

Another installation sequence of displacement columns was reported by Hewitt et al. (2009), where columns closer to the existing embankment were installed first and then the rig worked away from the existing embankment to avoid accumulated installation-induced stresses. Although reported results from these modified installation patterns were positive, there is no solid justification for those selected patterns and how efficient they were in comparison to other possible installation patterns. To date the magnitude of such installation induced displacement remains unclear and, hence, requires further investigation. Optimisation of the CMC installation patterns requires (1) accurate assessments of the lateral displacement of the surrounding soils due to column installation, specific to CMC technique and (2) a good understanding of the soil structure interaction. The assessments should involve rigorous numerical, analytical and physical modelling techniques. Knowing the extent of installation effects on neighbouring structures will contribute to the selection and evaluation process of ground improvement techniques.

3.1 SOIL RESPONSE DURING AND POST INSTALLATION

CMC installation process involves formation of a cavity by the auger penetration together with simultaneous rotation in a clockwise direction. Soil cuttings at the auger tip are carried upwards between auger flights, towards the auger segments with helically wounded blades, where the soils undergo further destructuration and are displaced laterally. As a result, the surrounding soils are brought into passive state of stress during installation. At the same time, soil elements are also displaced vertically (Ahmadi et al., 2005; Hird et al., 2011). According to Basu and Prezzi (2009), the ratio of vertical and horizontal displacement mainly depends on the ratio of the vertical penetration rate and the rotation speed. Unlike jacked-in and driven piles, CMC techniques involve augering prior to soil compaction by the displacement body. The augering remoulds the soils causing significant soil disturbance. Through numerical modelling, Pucker and Grabe (2012) indicated that the higher ratio of the auger rotation speed over the vertical penetration rate, the larger lateral displacement occurs. In addition, installation induced displacement is quite distinct at different portions of the CMC. Ground heave normally occurs near the ground surface, to depths ranging from approximately 2.5m to 4.0m (Krasiński, 2014; Larisch et al., 2013). In the middle region of the column, the installation results in a remarkable increase in soil density and stress level. Near CMC column base, the stress increase is insignificant (Krasiński, 2014). This is in contrast with a jacked or driven pile, where the base is the most influenced portion.

Most current investigations were carried out for cohesionless soils (Basu and Prezzi, 2009; Pucker and Grabe, 2012). During installation sand behaves under drained conditions since the excess pore pressure dissipates quickly. As the auger reaches the elevation of a soil element located in the vicinity of the soil/column interface, the total and effective stresses generally increases. However, as the auger passes that soil element, the soil within 1 diameter (1D) from the column centre is loosened up because of the slight change in auger's cross section, from the displacement body towards the drill rod (Pucker and Grabe, 2012). Outside this very thin zone, the soil generally densified significantly within a distance of 2D. Within this 2D zone, it is noted that dense sand tends to dilate slightly due to strong shear stresses induced by the auger, in addition to the compaction induced by the displacement body (Mahutka et al., 2006). Overall, the extent of densified zone ranges from 6D for dense sand to a greater distance of approximately 8D for loose sand. Long term effects in sand are considered as creep-induced ageing phenomenon (Lim and Lehane, 2014), which has not been thoroughly investigated in the literature.

The behaviour of saturated cohesive soils during installation is often assumed to be undrained due to rapid auger penetration. Little change in the volume is expected with the generation of excess pore pressure. Due to large deformation caused by the installation, the soils closer to the column fail in shear, which forms a region called "plastic zone", extending to a radius $R = r_0[G/s_u]^{1/2}$, where r_0 is the column radius, s_u is the undrained shear strength and G is

the soil shear modulus (Randolph and Wroth, 1979). Outside the plastic zone is ―elastic zone" where excess pore water pressure is assumed zero. Generally the response of clay to cavity expansion depends on the over-consolidation ratio. For normally consolidated clay, there is an increase in both total stress and excess pore pressure Δu, but a decrease in effective stress (Ladanyi, 1964). For over-consolidated clay, the total and effective stress increase everywhere but Δu, after increasing within a narrow zone near the column wall, becomes negative in the next surrounding zone (Ladanyi, 1964). It should be noted that for a structured clayey soil due to increase in the mean effective stress as well as deviatoric stress, cementation degradation may occur influencing the deformation of the ground immediately or long time after the installation (Nguyen et al., 2014).

Immediately after installation, the peak excess pore pressure falls off rather quickly (Randolph and Wroth, 1979). Excess pore pressure decays during consolidation inducing elastic viscoplastic deformation together with soil strength gain. At the end of consolidation, radial effective stresses around the column is greater than the in-situ horizontal effective stresses in the undisturbed ground with decreasing magnitudes with increasing distance from the column centre within a zone of approximately 10 times the column radius (Rivera et al., 2014).

3.2 ASSESSMENT METHODS

The response of soils to the installation is time dependent. Compared to installation effects in the long term, short term effects on the surrounding soils and existing structures (e.g. increase in stress and displacement) are more evident, causing more concerns for practitioners. The short term effects due to CMC installation will be discussed here. Since very limited assessment of CMC installation effects has been reported, the existing assessment methods for various piling and ground improvement techniques most relevant to CMC will be discussed herein.

3.2.1 Analytical techniques

Pile jacking or Cone Penetration Testing (CPT) is often simulated using cavity expansion theory. The theory is well described by Yu (2000). Unlike jacked and driven piles, the penetration of CMC auger into the ground includes soil loosening by auger flights in addition to the displacement effects. Therefore, CMC installation is not simply a cavity expansion process, but rather affected by the partial flight auger rotation, significantly reducing the normal stress on the column shaft that would be estimated by cavity expansion theory (Basu and Prezzi, 2009). The cylindrical cavity expansion theory is more applicable for the middle section of CMC. Closer to the column tip the installation resembles spherical cavity expansion. Near the ground surface the confining stress is significantly lower and vertical strain is dominant with the occurrence of heaving effects. Furthermore, since the column is drilled incrementally, the cavity expansion theory cannot simulate the installation process precisely. Despite these limitations, cavity expansion method may be used for preliminary assessment due to its simplicity compared to more complicated methods.

Cavity expansion theory has been applied to assess installation effects of driven piles and other vibratory methods such as stone columns. The predicted lateral displacement due to a closed-ended driven pile reported by Pestana et al. (2002) agreed quite well with the deflection measured using inclinometers. Typical equations used to estimate the radial displacement due to cavity expansion are presented here for illustration.

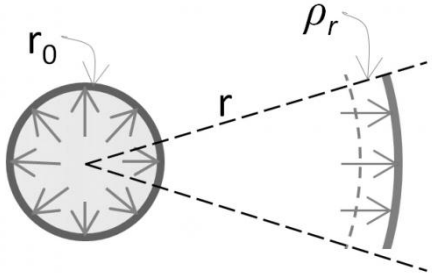

Figure 8: Lateral displacement of a soil element at a radius *r* due to cavity expansion

As shown in Figure 8, for an isotropic homogenous soil medium, a soil element located at a radius *r* from the centre of the cavity will be displaced a radial distance of ρ_r, due to undrained cavity expansion from an initial cavity of zero radius to a cylindrical cavity having a radius of r_0. A radius of r_0 represents the size of a stone column or CMC. The radial displacement ρ_r can be readily derived by assuming a constant volume of soil before and after undrained cavity expansion, as shown in Equation (1).

$$\rho_r = \sqrt{r^2 + r_0^2} - r \tag{1}$$

From some well-known solutions of undrained cylindrical cavity expansion presented by Yu (2000), Kelly et al. (2011) introduced Equation (2) to estimate soil displacement at various depths due to undrained cylindrical cavity expansion

from zero initial radius in infinite cohesive soil medium. The soil rigidity index (G/s_u) can be obtained from the field tests e.g. Seismic Dilatometer testing (SDMT). The undrained finite cavity expansion solution in an infinite soil mass with critical state soils are presented in Yu (2000).

$$\rho_r = s_u/(2G)(1 + \ln(G/s_u))(r_0/r)^2 r \quad (2)$$

3.2.2 Numerical methods

Installation effects can be assessed more accurately using the finite element method (FEM) or the finite difference method (FDM) including the use of more realistic soil models. Since the soils is strongly affected by the CMC auger rotation, ideally numerical simulation should include augering effect, which becomes very complex and can only be done in a 3D system (Pucker and Grabe, 2012). As illustrated in Figure 1, the auger is asymmetric, making simulating augering effect impossible in a 2D axisymmetric model. Simplified numerical methods have been used by various authors to serve specific research goals. One less complex, yet difficult method, is the numerical simulation of the vertical penetration of a pile/column or other penetrating tools, which is initially positioned above the ground surface. Other less complex studies include the penetration of the tool preinstalled in the soils before simulation starts (Larisch et al., 2013), or the simulation of cavity expansion from a finite cavity using prescribed horizontal and/or vertical displacements e.g. by Castro and Karstunen (2010) and Rivera et al. (2014). Typical outputs of three dimensional analyses simulating horizontal cavity expansion are shown in Figures 9 and 10.

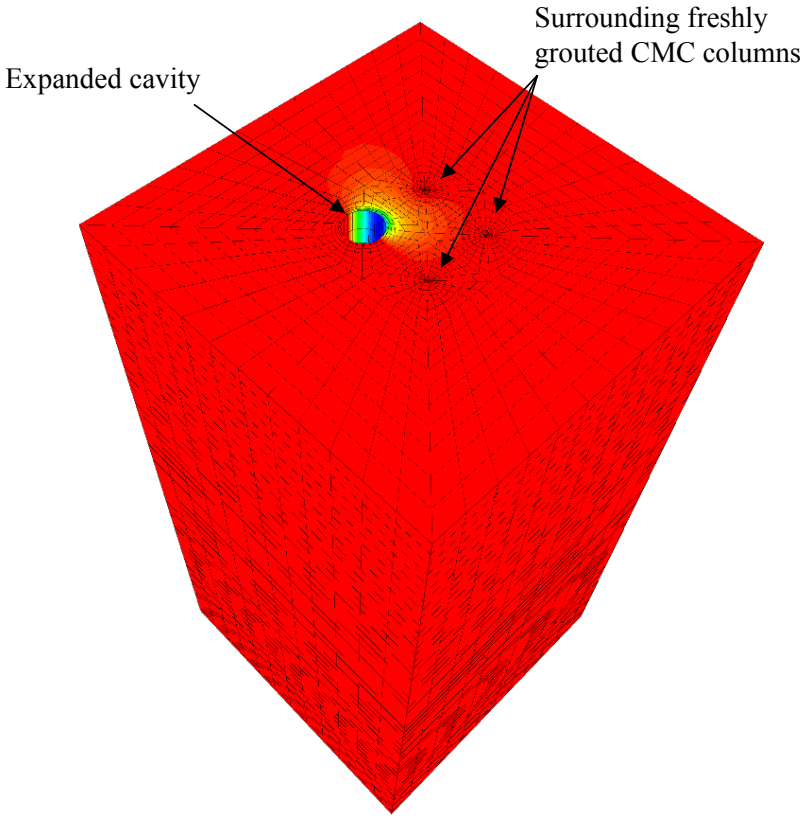

Figure 9: Contour of lateral soil displacement due to undrained cavity expansion performed in FLAC^{3D}

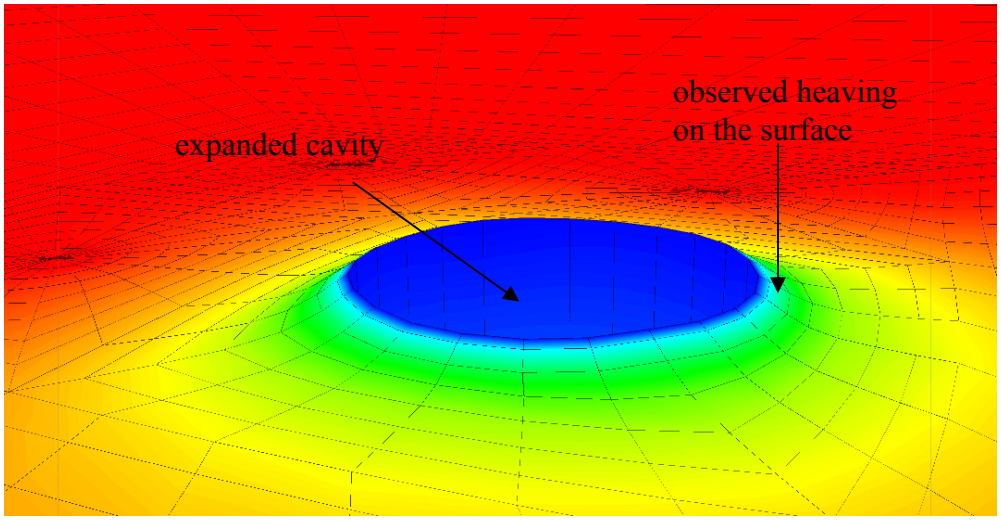

Figure 10: Heaving effects due to undrained cylindrical cavity expansion in FLAC^{3D}

Cavity expansion methods and effects of initial radius on predictions

Numerically, there are two types of cavity expansion (i) from an existing cavity (ii) from a cavity with an initial zero radius. Although column installation resembles cavity creation from an initial zero radius, numerical expansion must necessarily be modelled from a finite radius rather than from zero radius to avoid numerical difficulties (e.g. infinite circumferential strain). In fact, the restriction of numerical expansion from a finite radius in place for a zero initial radius would cause no inconsistency in the final results (Carter et al., 1979). If undrained cavity expansion is assumed, the required size of the final cavity at the end of the expansion r_f can be readily estimated using Equation (3), which relates the initial size r_i of the cavity and the actual column radius R_c (Figure 11). The initial size of the cavity may have to be adjusted to avoid excessive mesh distortion while maintaining reasonable numerical accuracy.

$$r_f = \sqrt{r_i^2 + R_c^2} \tag{3}$$

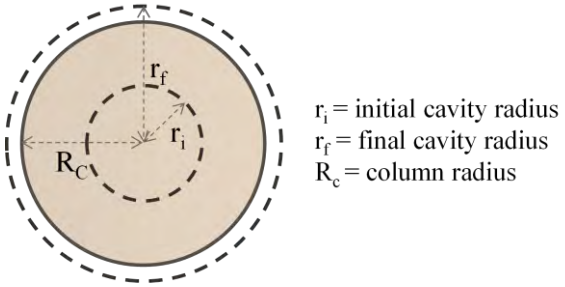

Figure 11: Cavity expansion from an existing cavity with a radius of r_i to a final radius of r_f

It is quite common to double the size of an existing cavity e.g. Krasiński (2014), Rivera et al. (2014) and Castro and Karstunen (2010). Krasiński (2014) simulated the installation of a screw displacement column using PLAXIS by creating an initial cavity with a radius equal to half column radius, and then doubled that cavity to the full size of column radius in an axisymmetric model. For simulation of the installation of a drilled displacement column as in Basu and Prezzi (2009), a "finite initial radius" r_i of 0.015m was specified compared to a final column radius r_f of 0.165m. While a smaller initial radius results in better prediction, a larger amount of expansion $\Delta r = r_f - r_i$ will be required, which may eventually lead to heavily distorted mesh, especially with the use of fine mesh.

Heavy mesh distortion and complex soil/auger interface

One of the simple methods to assess lateral soil displacement is to expand a cavity with the application of horizontal and vertical displacement at the nodes along the existing initial cylindrical cavity (Ahmadi et al., 2005). This method can be performed using several commercially available software packages such as FLAC and PLAXIS, or their 3D counterparts. The packages are equipped with Updated Lagrangian analysis (e.g. "large strain mode" in FLAC and "Update Mesh" in PLAXIS). The analysis allows grid-point coordinates updated at each step. It is noted that the numerical accuracy increases with a fine mesh, but in combination with a large amount of required cavity expansion,

excessive mesh distortion sometimes occurs. For more advanced analyses e.g. numerical modelling of the penetration of a column/pile or a drill tool into the ground, extreme large deformation often occurs, causing mesh to heavily distort. Various authors have used advanced numerical technique to deal with large deformation problem and complex contacts between soils and the penetrating tool. Those methods include the Arbitrary Lagrangian – Eulerian (ALE) adaptive meshing and Coupled Eulerian–Lagrangian (CEL) analysis, both available in commercial FEM software package ABAQUS, with ALE available in ANSYS Multi-Material LS/DYNA program. Compared to ABAQUS/Standard, ALE in ABAQUS/Explicit is more robust and can handle a large variety of problems including severe distorted mesh, hence will be discussed further. ALE mesh is allowed to move independently of material deformation. In the first step, the explicit Lagrangian analysis is performed. The resulted distorted mesh will require a new improved mesh. In the second step, the Eulerian analysis is performed, where variables in the previous analysis is transferred into the new mesh. ALE can deal with large deformation problem; however, since elements and connectivity (i.e. topology) do not change, high quality mesh may not be maintained during extreme deformation.

In contrast, CEL (only in ABAQUS/Explicit) has spatially fixed mesh. Eulerian and Lagrangian bodies within the same model can interact via a contact definition e.g. a Lagrangian auger travelling into Eulerian yielding soil. Chosen portions of a CEL model can be modelled as Eulerian or Lagrangian. Since the Eulerian mesh is fixed in CEL, soil displacement has to be calculated by integrating node velocities of the Eulerian mesh recorded along a predefined path over time (Pucker and Grabe, 2012). The installation of a screw displacement auger into dry sand was numerically simulated using CEL as in Pucker and Grabe (2012), however the results were not adequately verified against field measurements. Overall, although both ALE and CEL seem to be the promising solutions to the very large strain problems, CEL is more computationally friendly since a fixed mesh means no mesh distortion and less solution convergence. These ABAQUS/Explicit analyses, however, seem to offer only single-phase possibility with either fully drained or total stress undrained condition analyses (Elkadi et al., 2014). Also, ABAQUS/Explicit currently only allows total stress or frictionless contact between bodies. The challenge would be to create a user's subroutine into ABAQUS to enable undrained effective stress analysis and frictional contact.

Soil models

Since soils are subject to complex loadings during installation, constitutive models adopted should capture highly non-linear inelastic behavior, decay of excess pore pressure, loading and unloading paths and density changes. Well-established models such as Mohr Coulomb (MC) and modified Cam Clay (MCC) are incorporated in most of the commercial software packages. Also some consideration should be taken to account for the cyclic effects induced by the action of the drill auger (Pucker and Grabe, 2012). The MC failure criteria if used should account for stress-dependent stiffness. For MCC model, since the soil surrounding the column is likely to be in critical state, this model can be quite representative. It can be noted that above water table, soils may be partially saturated and thus excess pore pressure should be predicted considering coupled flow-deformation behaviour of unsaturated soils.

Compared to MC and MCC, hypoplasticity is a relatively new type of soil model and has been increasingly utilized to solve large deformation problems (Larisch et al., 2013; Pucker and Grabe, 2012). Various hypoplasticity models exist, noticeably by von Wolffersdorff (1996) for sand and modified version by Mašín (2005) for clay. Von Wolffersdorff (1996) model for granular materials incorporates the intergranular strain and dependency of friction angle and stiffness on density changes and compaction. The model requires 13 parameters including critical state friction angle and void ratio. Despite included advanced features, determination of a large number of model parameters may be a challenge. Meanwhile, clay hypoplasticity model developed by Mašín (2005) combines mathematical structure of hypoplasticity models with basic principles of the critical state soil mechanics. This model requires five parameters, similar to those of MCC model; however, it can provide a smooth transition between overconsolidated and normally consolidated states. Unlike MC, this hypoplasticity model correctly predicts the state dependent soil stiffness. Implementation of these models is a difficult task since they are not built-in in most commercial software packages.

3.2.3 Physical modelling

No laboratory scale simulation of installation effects for CMC has been reported in the literature, possibly due to many challenges associated with preparing auger model, setting up driving tools that can control torque and vertical crowd and complicated on-sample instrumentation. Hird et al. (2011) used an alternative approach to simulate the screw displacement auger without the use of on-sample instrumentation. Transparent artificial soils contained in a chamber with observable window allowed the displacement field to be captured by photographs and analysed using "particle image velocimetry" technique. Such studies indicated that the soil displacement in downward and horizontal direction depends very much on rotation speed of the auger and the penetration rate. Although useful, rigorous scaling is hard to be achieved to translate the results into behaviour of a prototype CMC and artificial soils like glass offers little practical usefulness. Despite expected shortcomings, small scale models may provide roughly similar trends of lateral displacements in full scale field tests.

Field measurement of lateral soil displacement is more indicative although field tests are not often readily available for verification of theoretical analyses. The required field instrumentation and monitoring scheme are often expensive. Also the equipment may be prone to damage during execution.

Rare but limited field tests were carried out by Suleiman et al. (2013), comprising installation of a 320mm-diameter CMC with four surrounding reinforced CMCs acting as reaction piles, instrumentation and one subsequent load test. The CMC was installed in very soft sandy organic soils with a thickness of approximately 6m. The instrumentation included four push-in pressure sensors and four shape acceleration arrays (SAA) to capture stress change and displacement in soft silty soil throughout column installation and testing. Each SAA was inserted together with a PVC casing into a predrilled hole. Two out of the four SAAs did not fit well with the pipes, and hence sand was used to fill the gap. In addition, strain gauges attached to a steel bar were inserted into the freshly grouted column, along the vertical axis, in order to measure the column strain developed during the load tests. The test outputs indicated that the strain gauges located near the CMC tip did not function, which may have been damaged during installation, or also during the steel bar insertion. At the end of CMC installation, an increase in horizontal stress by 2kPa was recorded within 1D (i.e. one diameter) distance from the CMC, by 8kPa within 2D distance, and then with decreasing trend with increasing distance from the CMC. Some stress relaxation by approximately 2 to 3kPa was recorded at the end of the installation. After installation, the stress recorded around the central CMC increased and was greater than stresses recorded at the end of the installation. The maximum soil displacements recorded at radial distances of 450mm, 750mm and 1050mm from the centre of the CMC were approximately 13mm, 8mm and 3mm respectively. The recorded soil displacement showed a clear decreasing trend with increasing distance from the CMC.

Good contracting practice also calls for early trials and excavation of ~~"c~~alibration" columns in order to confirm that the combination of selected design parameters (grid spacing/column diameter for a given type of soil) and retained methodology do not present a risk to the structural integrity of the columns installed. Figure 12 illustrates such trials presenting good quality columns with well-formed shafts and regular diameter. The presence of small and localised cracks is generally acceptable as with most type of unreinforced concrete structures.

Figure 12 : Typical shape of excavated columns presenting sound characteristics

In addition, static load testing is also a routine form of trial to confirm both the integrity and the performance of both calibration columns during initial stages of construction and production columns throughout the works. If appropriately specified, results of static load tests can provide useful information to the practicing engineers about structural and geotechnical capacities. Typical static load test results for CMC columns are shown in Figure 13.

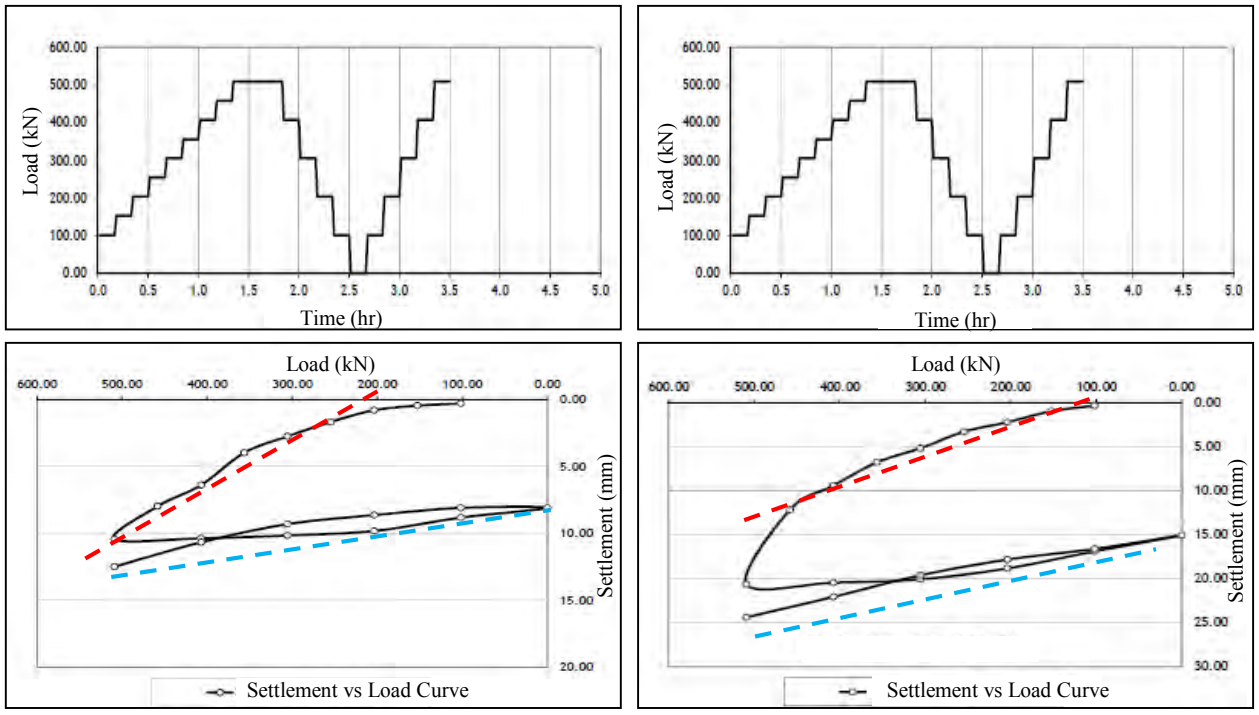

Figure 13: Typical static load test results

4 CONCLUSIONS

The evaluation of controlled modulus column (CMC) technology with respect to the sustainability has been taken into consideration. Evidently CMC provides a sustainable solution to the ground engineering including eliminating cost for spoil disposal, a high production rate, project saving through the use of displacement methods and load transfer layers, controlled quality and durability, and lower carbon emission in comparison to piling. Research directions to improve CMC for sustainable development have also been discussed including economic design with trial field tests, the use of recycled industrial by-products for grout mix, rigorous design, maximising the resiliency of structures and the energy consumption during operations.

The concern over the CMC installation effects on the existing structures and the adjacent columns has also been addressed in this paper. Numerical methods are the most appropriate techniques to assess the resulting stress and displacement fields in the surrounding soils. Selection of a modelling technique and soil model, which are able to account for extreme displacement, are of paramount importance. The results can be checked using preliminary assessment guidelines such as the cavity expansion theory. The other challenge is associated with the verification methods including small and full scale model testing. It is recommended that future CMC projects allow more field measurements as a basis to improve the assessment methods.

5 REFERENCES

Abreu, D., Jefferson, I., Braithwaite, P. and Chapman, D. 2008, 'Why is sustainability important in geotechnical engineering?', *Geosustainability and geohazard mitigation, Proceedings of Geocongress*, pp. 9-12,208.

Ahmadi, M.M., Byrne, P.M. and Campanella, R.G. 2005, 'Cone tip resistance in sand: modeling, verification, and applications', *Canadian Geotechnical J.*, vol. 42, no. 4, pp. 977-93.

Angelo, W.F. 2007, 'Lateral soil displacement gains ground on U.S. projects', *Engineering News-Record*, vol. 258, no. 11, 19 March 2007, p. 16.

Basu, P. and Prezzi, M. 2009, *Design and applications of drilled displacement (screw) piles*, 2326-6325, Publication FHWA/IN/JTRP-2009/28. Joint Transportation Research Program, Indiana Department of Transportation and Purdue University, West Lafayette, Indiana.

Bilodeau, A., Sivasundaram, V., Painter, K. and Malhotra, V. 1994, 'Durability of concrete incorporating high volumes of fly ash from sources in the USA', *ACI Materials Journal*, vol. 91, no. 1.

Brown, D., Thompson, W.R. and Lazarte, C.A. 2007, *Geotechnical Engineering Circular (GEC) No. 8 - Design And Construction Of Continuous Flight Auger Piles*.

Brown, D.A. 2005, 'Practical considerations in the selection and use of continuous flight auger and drilled displacement piles', *ASCE-Geotechnical Special Publication*, no. 129, pp. 251-61.

Carter, J.P., Randolph, M.F. and Wroth, C.P. 1979, 'Stress and pore pressure changes in clay during and after the expansion of a cylindrical cavity', *Int. J. for Numerical and Analytical Methods in Geomechanics*, vol. 3, no. 4, pp. 305-22.

Carter, J.P., Randolph, M.F. and Wroth, C.P. 1980, 'Some aspects of the performance of open- and closedended piles', *Numerical methods in offshore piling*, pp. pp 165-70.

Castro, J. and Karstunen, M. 2010, 'Numerical simulations of stone column installation', *Canadian Geotechnical J.*, vol. 47, no. 10, pp. 1127-38.

Cognon, J.M. 2004, *Concrete pile made of such a concrete and method for drilling a hole adapted for receiving the improved concrete pile in a weak ground*.

Elkadi, A.S.K., van Lottum, H. and Luger, H.J. 2014, 'A 3D coupled Eulerian-Lagrangian analysis of the dynamic interaction of jack-up legs with the seabed', *Numerical Methods in Geotechnical Eng.*, CRC Press, pp. 1255-9.

Elkington, J. 1997, 'Cannibals with forks', *The triple bottom line of 21st century*.

Farouz, E. 2014, 'CBIS Project- Ground Improvement Approach CH2MHill'.

Fatahi, B., Fatahi, B., Le, T. and Khabbaz, H. 2013, 'Small-strain properties of soft clay treated with fibre and cement', *Geosynthetics International*, vol. 20, no. 4, pp. 286-300.

Fatahi, B., Khabbaz, H. and Fatahi, B. 2012, 'Mechanical characteristics of soft clay treated with fibre and cement', *Geosynthetics International*, vol. 19, no. 3, pp. 252-62.

Fok, N., Qiu, T., Vincent, P. and Kreminsky, M. 2012, 'A case study of ground improvement using semi-rigid inclusions for breakwater road bridge', paper presented to the *International Conference on Ground Improvement and Ground Control*, Wollongong.

Fulton Hogan 2013, 'Gerringong Upgrade Project - Mt Pleasant to Toolijooa Road', <http://www.fultonhogan.com/Global/EPL%20Reports/EPL%20Monthly%20Report%20Aug%202013.pdf>.

Hewitt, P., Summerell, S.J. and Huang, Y. 2009, 'Bridge Approach Treatment Works On The Coopernook To Herons Creek Section Of The Pacific Highway Upgrade', *Sydney Chapter Symposium*

Higgins, R.B. 2014, 'Pacific Highway - Create public value for money', Presentation for Roads Australia.

Hird, C., Ni, Q. and Guymer, I. 2011, 'Physical modelling of deformations around piling augers in clay', *Geotechnique*, vol. 61, no. 11, pp. 993-9.

Holt, D.G.A., Chapman, D.N., Jefferson, I. and Braithwaite, P.A. 2010, 'Sustainable Geotechnical Design', *GeoFlorida* pp. 2925-32.

Jefferson, I., Hunt, D.V.L., Birchall, C.A. and Rogers, C.D.F. 2007, 'Sustainability indicators for environmental geotechnics', *Proceedings of the ICE - Engineering Sustainability*, vol. 160, pp. 57-78.

Juran, I. and Weinstein, G. 2008, *Forever-Synthesis of the Results and Recommendations of the French National Project on Micropiles.*, Schnabel Engineering: Dallas TX.

Kelly, R., Muttuvel, T. and Chan, K. 2011, 'Lateral Displacements in Soft Soil Due to Installation of Vibro-Stone Columns Using the Dry Method', *Geo-Frontiers*, ASCE, pp. 549-56.

Kirstein, J.F. and Wittorf, N. 2013, 'Improvement of soft fat clay using rigid inclusions and vertical drains', paper presented to the *18th Int. Conf. on Soil Mechanics and Geotechnical Eng.*, Paris.

Krasiński, A. 2014, 'Numerical simulation of screw displacement pile interaction with non-cohesive soil', *Archives of Civil and Mechanical Engineering*, vol. 14, no. 1, pp. 122-33.

Ladanyi, B. 1964, 'Expansion of a cavity in a saturated clay medium', *J. of Terramechanics*, vol. 1, no. 2, p. 96.

Larisch, M.D., Nacke, E., Arnold, M., Williams, D. and Scheuermann, A. 2013, 'Simulation of auger displacement pile installation', *Int. J. of Geotechnical Eng.*

Lim, J. and Lehane, B. 2014, 'Characterisation of the effects of time on the shaft friction of displacement piles in sand', *Géotechnique*, vol. 64, no. 6, pp. 476-85.

Mahutka, K., König, F. and Grabe, J. 2006, 'Numerical modelling of pile jacking, driving and vibratory driving', *Numerical modelling of construction processes in geotechnical engineering for urban environment. Taylor and Francis, London*, pp. 235-46.

Manjriker, G. 2006, 'Design of Driven Piles and Pile Groups', *The Foundation Engineering Handbook*, CRC Press.

Mašín, D. 2005, 'A hypoplastic constitutive model for clays', *Int. J. for Numerical and Analytical Methods in Geomechanics*, vol. 29, no. 4, pp. 311-36.

Masse, F., Pearlman, S., Walker, M. and Swift, S. 2011, 'Sustainable Use of Controlled Modulus Columns in Brownfield Redevelopment Projects', paper presented to the *"Case studies and recent advances in ground improvement"- A Specialty Seminar presented by ASCE Metropolitan Geotechnical Group*, New York, NY.

Mitchell, J.K. and Kelly, R. 2013, 'Addressing some current challenges in ground improvement', *Proceedings of the ICE - Ground Improvement*, vol. 166, no. 3, pp. 127-37.

NeSmith, W. and Fox, J. 2009, 'Practical Considerations for Design and Installation of Drilled Displacement Piles', *Contemporary Topics in Deep Foundations*, American Society of Civil Engineers, pp. 438-46.

Nguyen, L.D., Fatahi, B. and Khabbaz, H. 2014, 'A constitutive model for cemented clays capturing cementation degradation', *International Journal of Plasticity*, vol. 56, no. 0, pp. 1-18.

NSW Roads and Maritime Services 2010, 'Concrete Injected (CFA) Piling - QA Specification B63'.

Pearlman, S.L. and Porbaha, A. 2006, 'Design and monitoring of an embankment on controlled modulus columns', paper presented to the *Transportation Research Board*, Washington DC.

Pestana, J., Hunt, C. and Bray, J. 2002, 'Soil Deformation and Excess Pore Pressure Field around a Closed-Ended Pile', *J. of Geotechnical and Geoenvironmental Eng.*, vol. 128, no. 1, pp. 1-12.

Plomteux, C. and Lacazedieu, M. 2007, 'Embankment Construction on Extremely Soft Soils Using Controlled Modulus Columns for Highway 2000 Project in Jamaica', *Proceedings of the 16th Southeast Asian Geotechnical Conference, Kuala Lumpur, Malaysia 8 - 11 May 2007*.

Plomteux, C., Porbaha, A. and Spaulding, C. 2004, 'CMC Foundation System for Embankment Support—A Case History', *GeoSupport*, pp. 980-92.

Pucker, T. and Grabe, J. 2012, 'Numerical simulation of the installation process of full displacement piles', *Computers and Geotechnics*, vol. 45, pp. 93-106.

Randolph, M.F. and Wroth, C.P. 1979, 'An analytical solution for the consolidation around a driven pile', *Int. J. for Numerical and Analytical Methods in Geomechanics*, vol. 3, no. 3, pp. 217-29.

Rivera, A.J., Olgun, C.G., Brandon, T.L. and Masse, F. 2014, 'Numerical modeling of controlled modulus column installation in soft soils using a linear elastic perfectly plastic soil model', *Proceedings of NUMGE*, CRC Press, pp. 571-6.

Simon, B. 2012a, *ASIRI 2012, Amélioration des sols par inclusions rigides*, Presses des Ponts et Chaussées, Paris.

Simon, B. 2012b, 'General Report - session 5 - Rigid Inclusions and Stone Columns', paper presented to the *ISSMGE - TC 211 International Symposium on Ground Improvement IS-GI*, Brussels, 31 May and 1 June 2012

Spaulding, C., Masse, F. and LaBrozzi, J. 2008, 'Ground improvement technologies for a sustainable world', *Civil engineering of American Society of Civil Engineers*, vol. 78, no. 4, pp. 891-8.

Suleiman, M.T., Ni, L., Davis, C., Lin, H. and Xiao, S. 2013, *Instrumented Static load test of CMC*, Lehigh University.

von Wolffersdorff, P.A. 1996, 'A hypoplastic relation for granular materials with a predefined limit state surface', *Mechanics of Cohesive-frictional Materials*, vol. 1, no. 3, pp. 251-71.

Walker, M., Masse, F. and Swift, S. 2011, 'CMC an attractive alternative structural magazine', *Structure Magazine*, pp. 13-5.

Wong, P. and Muttuvel, T. 2012, 'Economic Design of Controlled Modulus Columns for Ground Improvement ', paper presented to the *11th Australia New Zealand Conference on Geomechanics (ANZ 2012)*, Melbourne, Australia.

Wong, P.K. and Muttuvel, T. 2011, 'Support of Road Embankments on Soft Ground using Controlled Modulus Columns', paper presented to the *Proceedings of the International Conference on Advanced Geotechnical Engineering, Perth, Western Australia*, Perth, Australia.

Yu, H.-S. 2000, *Cavity expansion methods in geomechanics*, Kluwer Academic Publishers, The Netherlands.

RISK BASED APPROACH IN A SPILLWAY UPGRADE

Jayanta Sinha[1], John Sukkar[2]and Guresh Ahuja[3]
[1]Project Manager, [2]ManagerDam Safety, [3]Project Manager
[1,2,3]State Water Corporation, NSW, Australia

ABSTRACT

In line with worldwide best practice, major dam upgrades are currently being undertaken in New South Wales (NSW) to ensure the continued safe operation of these assets in line with the Dam Safety Management Guidelines set out by Australian National Committee on Large Dams (ANCOLD) and NSW Dams Safety Committee requirements. Burrendong Dam, which is one of the major dams owned by State Water, is located in the greater Murray Darling River catchment on the upper reaches of the Macquarie River. The dam is currently being upgraded to increase the flood handling capacity of the spillway to cater for extreme flood events.

The conventional spillway design was found to be expensive therefore State Water embarked on a risk based approach to reduce the risk below As Low as Reasonably Practicable (ALARP). Saddle Dam A, which is located approximately 1.5km east of the existing spillway, was considered to be a viable option for an auxiliary spillway. The main issue was, however, the presence of a shear zone containing brecciated rock and clay gouge, which consisted of broadly graded silty sandy gravels and sandy clays. Hence, the potential for piping and foundation erosions were identified as the major risks for the project. The conventional design approach of a traditional concrete apron slab with ground anchors was found to be very expensive. Therefore, the erosion risks for not providing an apron slab to protect the shear zone were thoroughly investigated. The geotechnical conditions were analysed in order to satisfy the nominal criteria for energy dissipation of spillway discharge flows into the natural environment with an acceptable degree of erosion risk. The outcome of this analysis led to a significant reduction in cost as well as risk.

This paper focuses on the analysis and design of the geotechnical aspects adopted in the risk based approach, which led to significant cost savings to the spillway upgrade project. This paper is intended to provide valuable information for geotechnical professionals handling similar types of projects – especially where there is a potential to reduce cost by accepting a risk based approach.

1 BACKGROUND

Burrendong Dam is in the greater Murray Darling River catchment on the upper reaches of the Macquarie River, downstream of the confluence with the Cudgegong River in central-west New South Wales. The dam is located approximately 32 kilometres upstream of the township of Wellington. Construction of the dam was completed in 1967, and its primary purposes are for river regulation, hydro-electric power generation and flood mitigation. The dam is owned and operated by State Water Corporation.

The main embankment of Burrendong Dam is a zoned-earthfill embankment constructed across the Macquarie River. The intake and outlet works are located near the right abutment of the main embankment. Two earthfill saddle dams and a concrete primary spillway are located along a ridge separating the Cudgegong River from the Macquarie River reach downstream of the main embankment. Spillway flows are controlled by seven radial gates, and are discharged into Macquarie River approximately 2.5km to 3km downstream of the main embankment. Some of the features of Burrendong Dam are shown on Figure 1.

The State Water Portfolio Risk Analysis has shown that Burrendong Dam does not meet current deterministic standards for flood capacity. The PRA outcomes led to the conclusion that the spillway capacity of the dam was inadequate, and had to be upgraded to improve the safety of the dam against larger flood events.

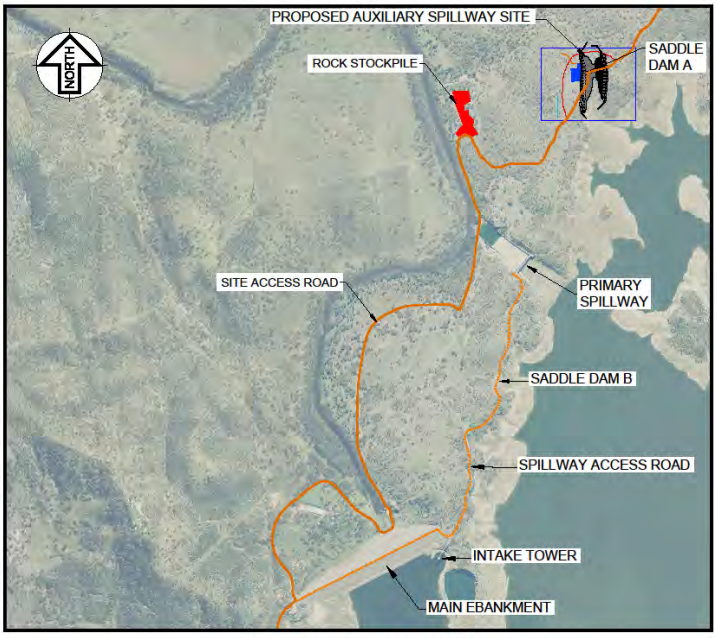

Figure 1: Layout of the dam

Following extensive investigations, a two stage upgrade was adopted as the strategy to reduce the risk of the dam from being overtopped during extreme flood events. Stage 1 consisted of raising the dam by 1.8m, and Stage 2 was to construct 120m wide auxiliary spillway to increase the outflow capacity of the dam.

The saddle dams were found to be the attractive options for the new auxiliary spillway. The existing Saddle Dam B is located between the main embankment and the existing gated spillway, and Saddle Dam A was located approximately 1.5km east of the existing gated spillway. Saddle Dam A was adopted as the preferred location for the auxiliary spillway due to its position away from the main spillway and favourable hydraulic behaviour. Due to financial constraints, the challenge for the project was to manage the geotechnical and hydraulic conditions in developing a risk based spillway design to optimise the overall cost, which would make the project viable to State Water.

The option for upgrading the existing gated spillway was estimated to be in the order of $30M to $40M. On the other hand, the option of an auxiliary spillway at Saddle A was estimated to be in the range of $10M for a conventional type concrete apron spillway to $5M for a risk based partially erosive spillway (if triggers), which were acceptable to State Water.

Construction of the auxiliary spillway has been completed in August 2014 at a cost of $5M. The hydraulic analysis and concept designs were carried out in house by State Water. Geotechnical investigations and detailed designs were undertaken by NSW Public Works (Public Works Report, 2013) and URS Pty Ltd (URS Detailed Design Report, 2013), respectively. The construction works were undertaken by Bardavcol Pty Ltd.

This paper mainly focusses on the geotechnical challenges encountered at the Saddle Dam A site, and the assessments that lead to the optimum cost effective design and construction of the spillway. Aspects of hydraulic characteristics and their impact on erosion are also discussed.

2 GEOLOGY AND GEOTECHNICAL ASPECTS

The investigations at the Saddle Dam A included geological mapping of a trench and a series of vertical cored boreholes. The trench was 1.5 m deep and extended 134 m across the gully parallel to the axis of the existing saddle dam (shown in Figure 2). Rock cores were drilled in the left and right shoulders, at the centre of the saddle dam and in the centre gully floor downstream of the dam.

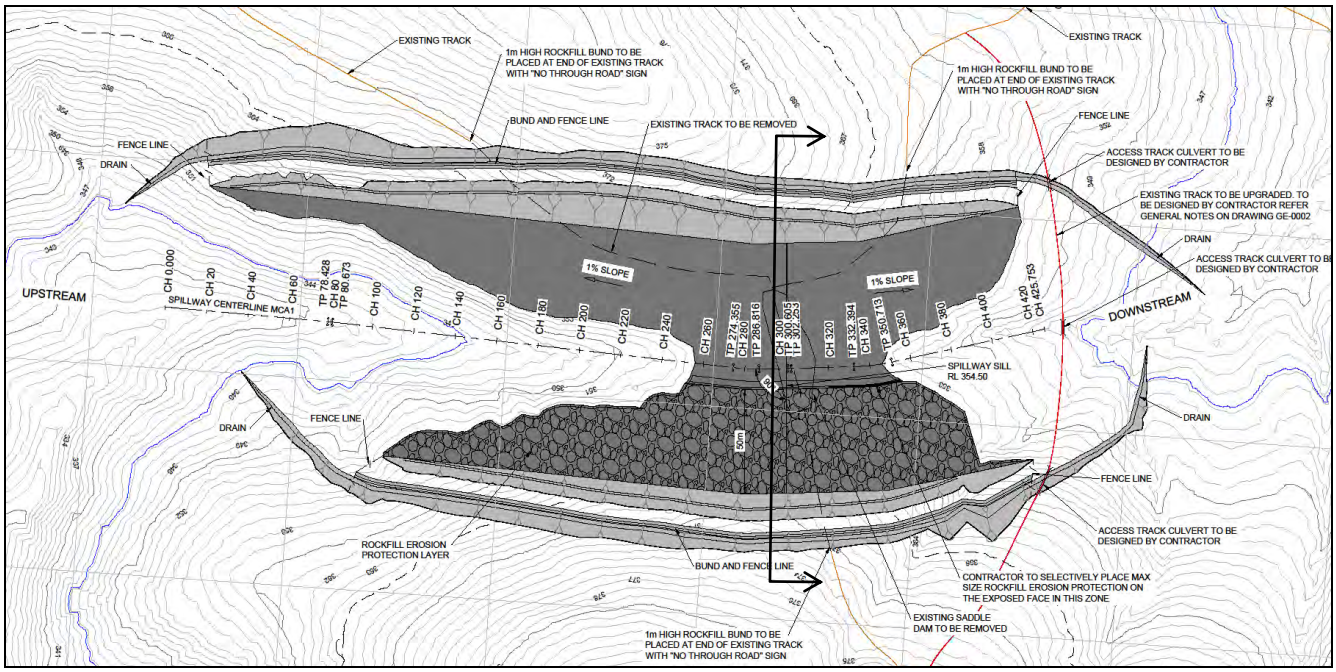

Figure 2A: Plan

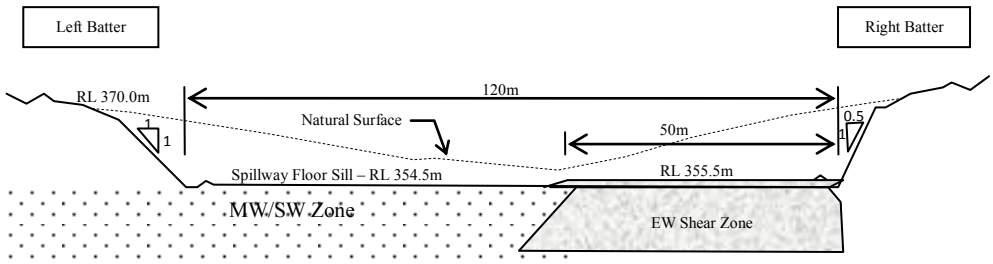

Figure 2B: Cross-section

Figure 2: Spillway layout at Saddle Dam A

The regional geology of the area consists of a Hill End Synclinorial Zone, which forms part of the Lachlan Fold Belt. The underlying bedrock geology is indicated to be of inter-bedded meta-sandstones and meta-siltstone rocks of the Devonian age Crudite Group. Several major fault zones are indicated to pass through the saddle dam site. The defect orientations were logged and plotted across the trench and were split into three groups that correlate with the areas in the spillway floor, and in the spillway walls with the representative stereonets plotted for each section and the whole trench. The orientation of the bedding and joints was identified to vary across the site. Two major joint sets were identified with two other minor joint sets also identified. The joints were generally found to be iron stained, occasionally in filled with calcite, rough and discontinuous with very close to close spacing increasing with better weathering grade and depth. The open surface defects were generally in-filled in the slightly weathered rock. Bedding was moderately spaced.

Shears were dominant features in the saddle, and were observed to be generally sub-parallel to the bedding but other orientations were also observed. Calcite stringers and veins up to 100mm thick and sandy clays (extremely weathered meta-sandstones) were associated with the shear zones. The potential for dykes was also noted in the area. The meta-siltstones were apparently more weathering resistant than the meta-sandstones. The soil to rock interface was noted to be irregular with highly or moderately weathered rock underlying the soil. No ground water was observed. Point load tests were not possible due to the fractured nature of the rock**.** In general, decreasing weathering grade from soils and extremely weathered rock to slightly weathered rock was observed across the site, and fresh rock was not encountered.

The spillway foundation was to be at a depth of approximately 14m cut into predominantly meta-siltstone that is slightly weathered (SW) on the right and moderately weathered (MW) on the left. There is an approximately 1-2m thick zone of lesser quality rock and soil near the surface. The spillway floor was proposed to be at RL 354.5m, approximately two thirds of which is inferred to comprise moderately weathered rock and one third extremely weathered (EW) sheared meta-sandstone.

The data indicated that the bedding was adversely oriented with dips out of the slope allowing potentially unstable planar failures for the left batter. Further reviews of these defect orientations established that the left batters should be 2H:1V and 1H:1V in EW to HW and in SW to MW materials, respectively. The right batters were designed at 2H:1V and 0.5H: 1V in EW to HW and in SW to MW materials, respectively. The channel bench widths were set at 1m to prevent vehicle access to comply with Work Health and Safety requirements. The highly weathered material was expected to persist up to 3m in this area. This slope has been revegetated to further improve the stability and provide erosion protection.

In light of the above findings, allowance was made in the design for the use of shotcrete for as a risk based treatment of the batters. Areas, which were prone to erosion and degradation, could lead to undermining of the slope and minor rock falls. The areas identified during construction such as highly fractured areas, shear zones, and dykes, were considered for local treatment with shotcrete. Allowance for rock bolts was also made to improve safety in areas, where random adversely oriented defects were expected to potential slides or toppling hazards, which could compromise the integrity of the spillway or the safety of workers. The use of these strengthening measures was considered in the risk based estimate, as well as in the contract as provisional sums. The need for these strengthening measures was assessed on site at the time of construction.

3 SPILLWAY DESIGN CONSIDERATIONS

Extensive hydraulic modelling was carried out by State Water by using MIKE21 to establish the geometry of the auxiliary spillway required to pass various flood events, including 1:10,000 AEP, 1:20,000 AEP and Probable Maximum Flood (PMF). The velocities along the spillway channel obtained from the above modelling are presented in Figure 3.

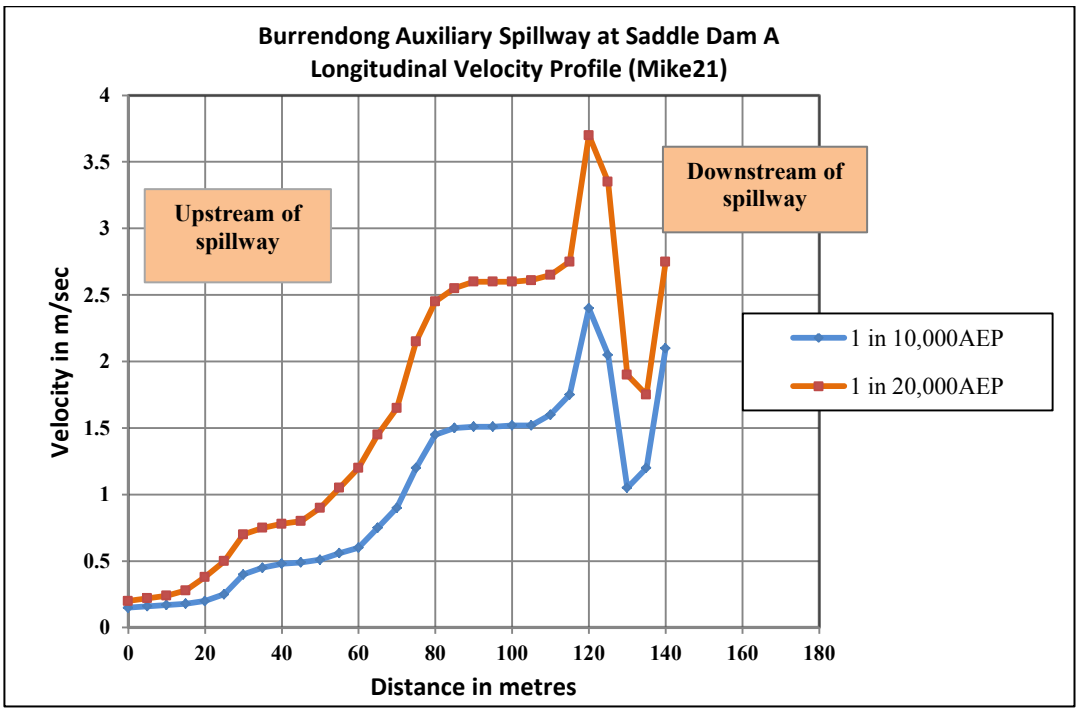

Figure 3: Longitudinal Velocity Profiles for flood events

It can be seen from the above figure that the velocities are low through the auxiliary spillway, and then accelerating through the downstream gully. The spillway entrance sill level was set at RL 354.5m with a base width of 120m. These velocities indicated that there would be significant erosion, if no protection works are incorporated in the design.

Therefore, erosion protection was considered as one of the critical elements in the design of the spillway, which could influence the overall viability of the project in terms of its cost. A conventional solution including concrete apron with anchors was found to be very expensive, whereas a risk based solution was financially very attractive, provided that the erosion risks during flood was acceptable to State Water. Therefore, the assessment of erosion and its potential resistance to uncontrolled flows were investigated to optimise the spillway design.

The assessment of the potential for erosion was carried out by using the method proposed by Annandale (Annandale, G.W, 1995) for erosion of rock masses. The erosion indices are presented in Table 1.

The floor of the auxiliary spillway was founded predominately within moderately weathered meta-sandstone and meta-siltstone. The rock mass was adopted as fractured, and is characterised by a relatively low Rock Quality Designation (RQD) (typically < 50%). A 20-30m wide shear zone comprised of extremely weathered meta-sandstone is inferred to strike parallel to the channel on the right hand side of the channel floor (see Figure 2). The investigations indicated that the shear zone and EW material extends to depths greater than 10m depth below FSL (RL 344m AHD).

Table 1: Erosion indices (EI)

Rock Mass Unit	EI
EW sheared meta-sandstone	0.15-0.55
MW meta-sandstone rock	11-440
SW meta-sandstone rock	20-380

The primary erosion mechanisms were considered to be:

- Surface erosion of exposed rock mass in the unlined sections, including left and right batter faces and channel floor;
- Headcut erosion initiating in the natural gully downstream of the spillway channel and progressively eroding back through the channel floor (shown in Figure 4). Head cut occurs when an erosion gully forms at a point of weakness and flow concentration then flow into the gully and forms a back roller which progressively erodes the face of the gully such that it extends towards the source of flow. The shear zone was considered to be the most vulnerable area to this form of erosion, but it could also trigger elsewhere as well.

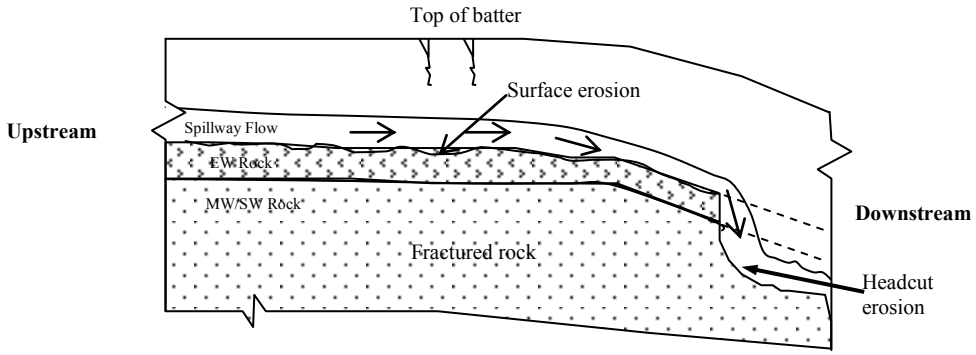

Figure 4: Erosion mechanism at spillway floor

The Stream Power values for various spillway discharges through the auxiliary spillway were based on HEC-RAS modelling, and are provided in Table 2. At the downstream edge of the spillway channel floor, the model predicted locally higher velocities of 2.4m/s and 3.7m/s, respectively for the 1 in 10,000 and 1 in 20,000 AEP flood events (see Figure 3). The Stream Power will also be locally higher in the area of the higher velocities. These locally higher velocities at the downstream end of the spillway floor were considered critical for the surface erosion assessment.

Table 2: Estimated Stream Power Values

Flood Event (AEP)	Surface Erosion		Headcut Erosion
	Velocity (m/sec)	Stream Power (kW/m^2)	Stream Power (kW/m^2)
1 in 10,000	2.4	0.2	12-22
1 in 20,000	3.7	0.6	22-34
PMF	9.0	6.2	>500

4 STREAM POWER ASSESSMENT AND EROSION INDICES

The Stream Power and Erosion Index (EI) values are presented in Figure 5. EI values have been calculated as outlined in Annandale (Annandale, G.W, 1995). It can be seen that in the case of the flood frequencies 1 in 10,000 AEP to 1 in 20,000 flood events, surface erosion of the EW shear zone material is predicted to start occurring, however surface erosion of the MW and SW rock is unlikely to occur including within the area of the locally higher velocity at the downstream end of the spillway channel floor. Head cut erosion is predicted to occur relatively rapidly within the EW material as the EI for this material plots well above the threshold line, as indicated in Figure 5.

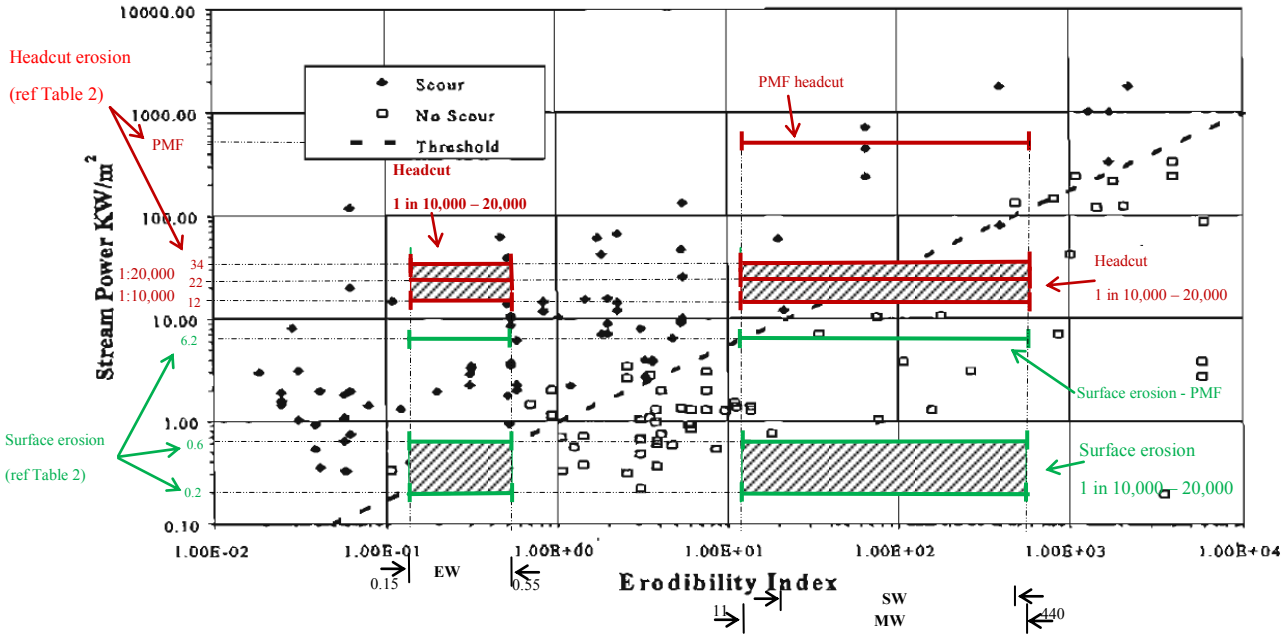

Figure 5: Prediction of Erosion using Annandale (1995)

Head cut erosion is also predicted to occur in the MW and SW rock mass but at a much slower rate based on the EI values plotting on either side of the threshold erosion line. The rate of head cut advancement is discussed further below.

For the PMF event, surface erosion is predicted to occur relatively rapidly within the EW shear zone material, however surface erosion is unlikely to occur for the MW and SW rock. Head cut erosion is predicted to occur relatively rapidly within the EW material and MW/SW rock as the EI for this material plots well above the threshold line for the PMF event.

In order to estimate the rate of advancement of head cut erosion within the unlined earth spillway, NRCS earth spillway erosion model (NRCS, 1997) was utilised. The results of the assessment are shown in Table 3.

Table 3: Estimated Rate of Head Cut Advancement

Flood Event (AEP)	EW Shear Zone		MW Rock	
	Average Rate of Head Cut Advance (m/hr)	Distance of Head Cut Advance (m)	Average Rate of Head Cut Advance (m/hr)	Distance of Head Cut Advance (m)
1:10,000	1.5 – 3.3	36 - 80	0 – 1.1	0 - 24
1:20,000	12 - 16	>400	0 – 2.6	0 - 88
PMF			93 - 145	>>200

For the 1 in 10,000 AEP flood event, the estimated average rate of head cut advancement is 1.5 m/hr to 3.3 m/hr within the EW shear material. The estimated duration of discharge through the auxiliary spillway is 24 hours. The estimated distance of head cut advancement is less than the spillway channel length and so for this event, head cut erosion is unlikely to progress far enough upstream within the EW material or MW rock to cause an uncontrolled release through the saddle feature. For the 1 in 20,000 AEP flood event, the estimated average rate of head cut advance is 12 m/hr to 16 m/hr, and the predicted distance of head cut advancement over the duration of spillway flows (34 hours) is significantly greater than the spillway channel length. Therefore, for the 1 in 20,000 AEP event head cut erosion is likely to occur across the full length of the channel within the EW shear material and lead to an uncontrolled release by deep erosion through the saddle feature. However, head cut erosion within the MW rock is unlikely to head cut across the full length of the channel. For the PMF event, rapid head cut erosion is predicted within the EW shear zone and also the MW rock, and this is likely to lead to an uncontrolled release by deep erosion through the saddle feature.

The following points summarised the findings of the above analysis:

- For the 1 in 10,000 AEP event, the unlined spillway is likely to experience surface erosion and head cut erosion within the EW shear zone material. However, this is unlikely to lead to an uncontrolled release of the reservoir. Surface erosion is not predicted to occur within the MW and SW rock.
- For the 1 in 20,000 AEP event, the unlined spillway is likely to experience surface erosion and head cut erosion within the EW shear zone and MW/SW rock. If left unprotected, then head cut erosion within the EW shear zone is likely to be sufficient to cause an uncontrolled release by deep erosion in the base of the channel floor. However, this is unlikely to lead to an uncontrolled release of the reservoir. Surface erosion is not predicted to occur within the MW and SW rock.
- For the PMF event, significant head cut erosion of the EW shear zone and MW/SW rock is predicted to occur and this is likely to lead to an uncontrolled release of the reservoir by deep erosion of the spillway channel floor.

5 OPTION DEVELOPMENT

Option 1 consisted of placing a layer of rock rip rap protection over the erodible EW shear zone to prevent it being eroded for spillway discharges up to the 1 in 20,000 AEP event. The rip rap layer at the downstream end of the channel would slow the head cut erosion through the erodible EW material. The purpose would be to allow this coarser rockfill to collapse into any head cut erosion features that develop in the gully downstream of the channel to stop or slow the advancement of the head cut. Option 2 consisted of constructing a conventional anchored reinforced concrete slab and downstream cut-off wall in addition to the rip rap protection over the EW shear zone. The concrete slab would be 10m wide, 120m long and 0.3m thick. The slab would also serve as the flow control sill. The downstream cut-off wall would be at least 2m deep into the fractured rock mass. The side batters would also be protected with shotcrete, mesh and rock bolts over a 10m wide zone in line with the concrete slab. Option 2 represents a more conventional approach to providing erosion protection. Option 3 was to use shotcrete with rock anchors as an erosion protection at the floor of the spillway. Option 4 was similar to Option 2 except a deep, structural cut-off wall would be constructed at the downstream end of the slab to prevent head cut erosion through the auxiliary spillway channel for flood events up to the PMF. A deep cut-off wall would be required in this case due to the significant depth of erosion that could develop within the fractured rock mass and EW shear zone under large spillway flows. Investigations indicate the EW shear zone extends at least 10m below channel invert level and probably extends significantly below this. This option was discussed, and it was agreed not to pursue it due to the likely significant construction costs (i.e. $10M - $20M), which was considered to be not warranted for addressing the business risks associated with deep erosion of the auxiliary spillway channel.

Options 1 and 2 were selected for further consideration and are discussed below. An assessment of the risks of an uncontrolled release by deep erosion in the base of the spillway channel floor was carried out to select the level of

erosion protection measures for the spillway channel. The key issue from the erosion assessment was whether head cut erosion is likely to initiate at the downstream end of the channel, and then whether there is sufficient time for it to progress over the full length of the spillway channel. This is not considered to represent a dam safety risk as the rate of enlargement of the "breach" through the very broad natural saddle feature would not be sufficient to cause a significant flood wave on top of the already large discharges from the primary and auxiliary spillways. The estimates of the probabilities of the preliminary risk assessment are provided in Table 4.

Table 4: Probability of Uncontrolled Release

Option	Estimated Incremental Cost Over Base Case	Annual Probability of Uncontrolled Release
Base case - No erosion protection measures	Nil	1 in 11,000
Option 1 - Rip rap protection over shear zone	\$0.6M	1 in 40,000
Option 2 - Rip rap protection over shear zone, plus anchored concrete slab	\$2.5M	1 in 180,000

The results in Table 4 indicate that the estimated annual probability of an uncontrolled release is 1 in 11,000 with no erosion protection measures. This probability is dominated by the potential for head cut erosion through the erodible EW shear zone for flood events rarer than 1 in 10,000 AEP. The probability of uncontrolled release can be reduced to 1 in 40,000 if localised rip rap protection measures are provided over the EW shear zone (Option 1). This option provides erosion protection measures designed for the flood events up to 1 in 20,000 AEP event. The estimated construction cost increase for providing the rock rip rap protection works is in the order of \$0.6M. For this option, the residual risk is dominated by head cut erosion within the MW rock mass for events rarer than 1 in 20,000 AEP. Further risk reduction could be achieved by constructing an anchored concrete slab with a cut-off wall at the downstream end in addition to the rip rap protection measures over the EW shear zone (Option 2).

The estimated construction cost increase for Option 2 is in the order of \$2.5M and the probability reduces to 1 in 180,000. This represents more than an order of magnitude of reduction in the business risk compared to that of an uncontrolled release with no erosion protection measures. Option 1 was adopted as the preferred option.

The preferred option for the erosion protection measures that was selected by State Water comprises constructing a layer of rockfill rip rap material over the more erodible shear zone. The design intent of the erosion protection measures are summarised as follows;

- To provide protection over the more erodible Extremely Weathered shear zone materials so that the erosion resistance is more comparable to the moderately weathered rock areas of the spillway floor; and
- To reduce the likelihood of an uncontrolled release caused by excessive erosion within the floor of the spillway channel consistent with the outcomes of the spillway erosion risk assessment described above. The grading characteristics of the rockfill protection layer have been selected by assessing the size of rock particles required to resist erosion caused by large spillway flows passing over a rip rap layer.

6 ACKNOWLEDGEMENTS

The authors acknowledge Mr Michael Neville, Senior Geologist, NSW Department of Commerce for the geotechnical investigation of the site. State Water Major Projects developed the concept design, which was further refined and developed by URS Pty Ltd in the detailed design phase. Authors would also like to thank Dr Mark Foster, Senior Principal, URS for his excellent input in stretching the risk boundaries and reducing overall project cost. The authors would also like to thank Mr Gurmeet Singh, Specialist Senior Hydrologist, State Water Corporation for his invaluable help in providing relevant information on MIKE21 outputs.

7 REFERENCES

1. NSW Public Works Report, *Burrendong Dam Upgrade (Stage 1B): Saddle A Spillway: Geotechnical Investigations,* 2013.
2. URS Pty Ltd., *Detailed Design Report - Burrendong Dam Auxiliary Spillway*, Dec 2013
3. Annandale, G.W. *Erodibility*, Journal of Hydraulic Research, 1995 vol. 33, pp. 471 – 494.

EXPLORATION OF A NOVEL PLATE ANCHOR GEOMETRY WITH A VIEW TO REDUCING MATERIAL USAGE

Angus Dyson[1], Matthew Bennett[2] and Pierre Rognon[3]
[1,2]Research Assistant, [3]Senior Lecturer,
Particles and Grains Laboratory, School of Civil Engineering, The University of Sydney, NSW, 2006, Australia.

ABSTRACT

Soil anchors are often used to stabilise structures. Various anchor designs have been developed with the aim of achieving higher pull-out capacity at lower cost. Examples include plate, helical, grouted and drilled shaft anchors. Presented herein is a series of experiments investigating the anchoring properties of root-like fractal shapes. The pull out resistance and resilience (pull-out resistance after an initial displacement) of a plate anchor with a root-like shape in a model granular soil comprising 50μm glass beads is compared to that of a plain plate anchor. Results show that such root-like shapes are characterised by a higher pull-out resistance per unit volume of anchor material, and a higher resilience than plain shape anchors.

By focusing on a particular anchor shape in a model soil, this study pinpoints the potential benefit of using complex shape anchors. These results pave the way for further investigations of various anchors shapes, for instance fractal, wheel or mesh geometries, aiming at finding the shape that optimise the pull-out resistance and resilience.

1 INTRODUCTION

Soil anchors have been used to stabilise structures for thousands of years. Modern construction of transmission towers, utility poles, submerged pipelines, tunnels and offshore structures rely on effective and cost efficient strategies for soil anchoring (Das 2012; Liu et al. 2012). Existing strategies include plate anchors (which are the focus of this study), direct embedment anchors, helical anchors, grouted anchors, anchor piles and drilled shafts. Installation of plate anchors involves excavating soil down to a desired depth, installing the anchor, backfilling and compacting (Figure 1a). Plate anchors are usually circular, rectangular or long strips, and made using concrete, steel or timber. The quality of anchoring is characterized by the pull out resistance F_0, which is the maximum tensile force the anchor can sustain before the soil fails and let it move upward irreversibly.

Several models have been developed to predict the pull-out resistance of shallow anchors as a function of their size and depth. These models all consider that the pull-out resistance is governed by the weight of the soil that would be mobilized when the anchor moves upward (Murray and Geddes 1987; Cheuk et al. 2008; Niroumand and Kassim 2010; Liu et al. 2012; Jung et al. 2013). They differ however, in the estimation of the volume of mobilized soil, delineated by a failure envelope. For a circular anchor of diameter D, cylinders (Majer 1955; Meyerhof and Adams 1968), truncated cones (Downs and Chieurzzi 1966; Veesaert and Clemence 1977) and circular (Baker and Kondner 1966) failure envelopes have previously been proposed (see Figures 1b,c). In any case, the pull-out force can be generally expressed as:

$$F_0 = \rho g A H f(\theta) \quad \textbf{(1)}$$

where ρ is the density of the soil, H the anchor depth, g the gravity, A the anchor surface area in the pull-out direction, and the function f accounts for the shape or the failure envelope, defined by a characteristic angle θ. The shape function is 1 for a cylindrical failure envelope. For a truncated cone failure envelop, it is greater than one and can be expressed as:

$$f(\theta) = \frac{1}{3}\left(1 + 2\frac{H}{D}\tan(\theta) + 2\frac{H}{D}\tan(\theta)\right) + 2\frac{H}{D}\tan(\theta) + 2 \quad \textbf{(2)}$$

The value of θ □□□usually within the range 2/3ϕ <θ< ϕ/2 where ϕ is□□□□□□□□□□□□□□□□□□□□□□□□□□□□□soil.

As a consequence, there are two basic solutions to improve the pull-out resistance of such anchors, burying them deeper or making them larger. However, these two solutions require larger excavations and/or larger amount of material to build the anchor, which increases the construction cost. A third solution is to combine multiple plates spaced along the vertical axis. However, the increase in pull-out force saturates when plates get to close to each other due to a screening effect (Kouzer and Kumar 2009; Kumar and Sahoo 2011). A fourth solution, which is the focus of this study, is to design the anchor shape to improve its anchoring properties.

In this paper, a particular type of anchor shape is investigated, that is inspired tree's root system. The primary role of the tree's root systems is to access nutriments in soil. Another role of roots, equally critical to the tree's survival, is to ensure that the tree can resist wind loading. As a consequence, it is possible that root geometries may present interesting anchoring abilities, which could be used in geotechnical applications. To probe this hypothesis, a set of pull-out experiments of fractal shape anchors were carried out in a model granular soil. Experiments will focus on the anchor pull-out resistance and on their resilience, i.e., their pull-out resistance after an initial displacement.

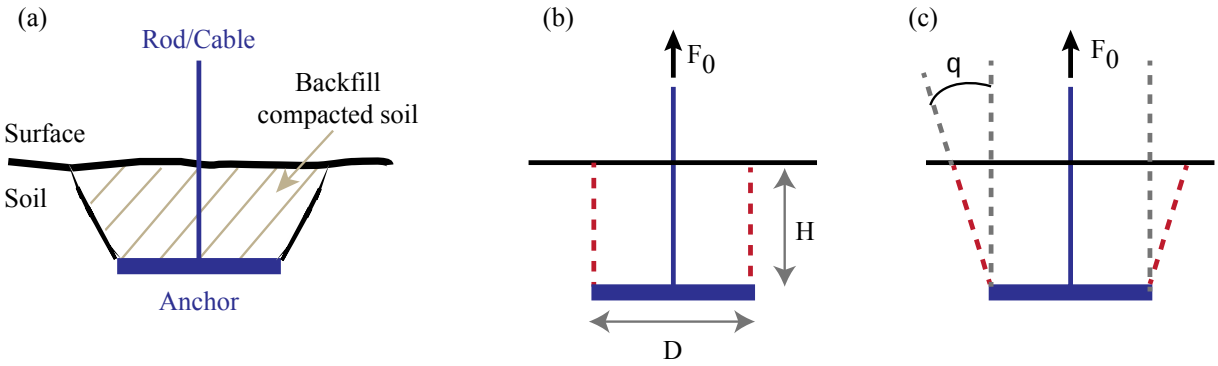

Figure 1. Soil anchoring using shallow plate anchors: (a) schematic of practical setting; illustration of cylinder (b) and cone (c) failure envelopes (red dashed lines) from which existing models deduce the anchor pull-out force F_0 (see Equation (1)).

.

2 PULL-OUT EXPERIMENTS OF FRACTAL ANCHORS

To highlight the effect of the anchor geometry, we have designed a model experimental configuration illustrated in Figure 2. The model soil is comprised of small spherical glass beads of diameter ranging from 50 μm to 60 μm. This model soil is characterised by a relatively low friction angle, $\phi = 21°$. The advantage of using this model soil is that it reaches its maximum density $\rho = 2300$ kg/m^3 irrespective of the mode of preparation. Experiments can then easily be repeated in the same conditions.

The model soil is confined in a square glass tank with 40cm width. An anchor is buried in the soil and connected to a linear stage and a force meter via a shaft of diameter 10mm.

2.1 EXPERIMENTAL PROTOCOL

Each experiment starts with a similar preparation step, which consists in emptying the tank, placing the anchor at a desired depth *H,* and filling the tank with the glass beads. At this stage, the anchor is subjected to a non-null, relatively small tension force that slightly varies from test to tests depending on the filling process. The value of that initial force did not affect the measured pull-out resistance.

Experiments then consist of lifting the anchor upward at a prescribed velocity V^{up}, and measuring the tension force as a function of the displacement.

2.2 ANCHOR DESIGN

We designed two types of anchors, namely plain disks and planar fractals (see Figure 2b,c). The two anchors have the same outer diameter, D = 8cm, and are 4mm thick. They feature a 4mm hole in their centre to fit the shaft connection. Fractal anchors are comprised of six first-generation branches joining in the centre, with a relative angle of 60°. Each sub-generation comprises two sister branches forming an angle of 60°. The branches length decrease by a factor of 1.8 from one generation to another.

The design of this fractal anchor was performed by a recursive algorithm able to produce a stereo lithographic 3D model, which was then 3D-printed. This fractal anchor can be characterized by its surface ratio ϕ:

$$f = \frac{A^{Root}}{A^{Disk}} = 0.47 \quad \textbf{(3)}$$

where A^{Root} is the surface area of the fractal anchor and $A^{Disk}=\pi D^2/4$ is the surface area of the disk of same diameter. Given that the anchors have the same thickness, the surface ratio ϕ directly quantifies how much material is needed to build the fractal anchor as compared to the full disk.

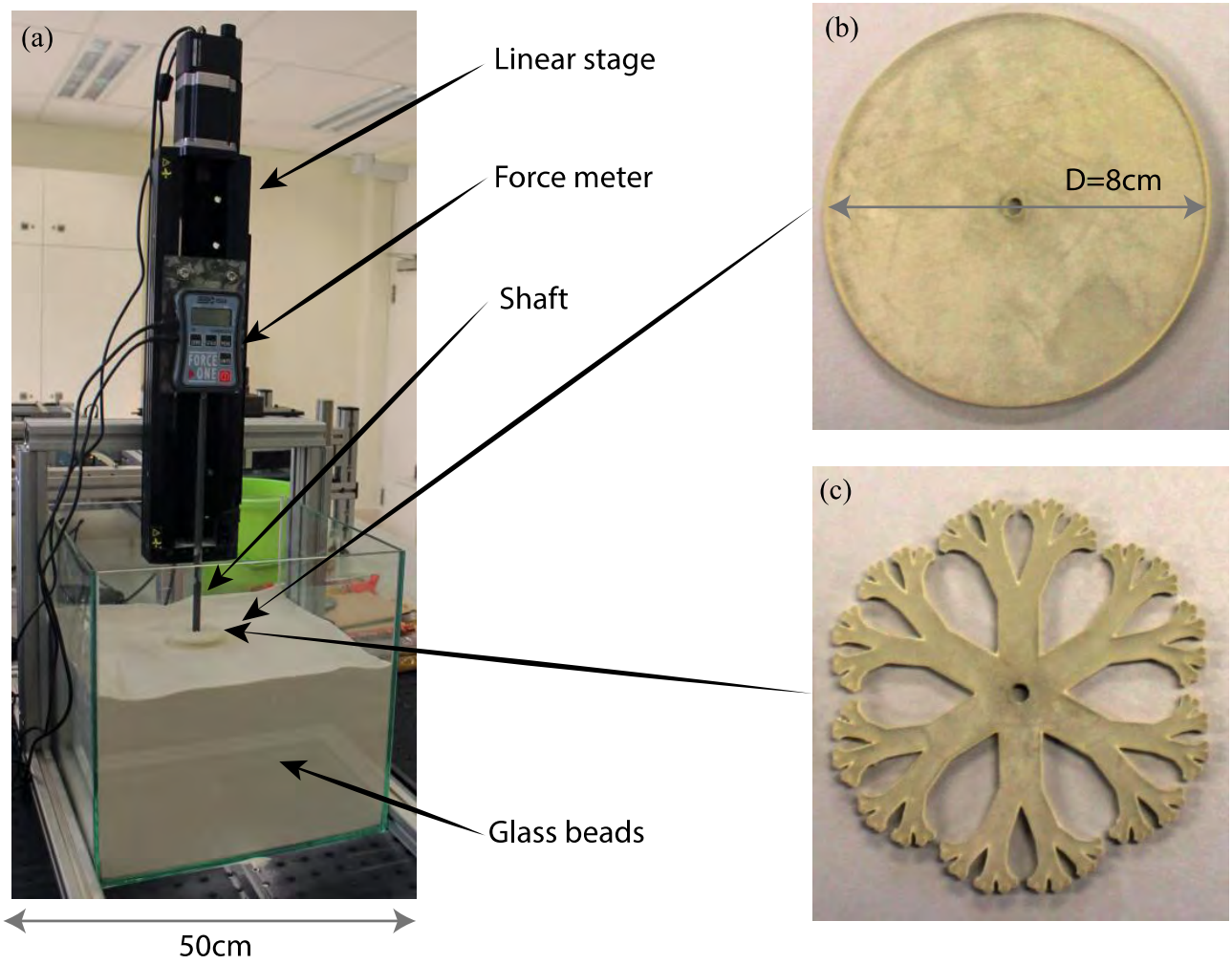

Figure 2. (a) Experimental device to measure the pull-out force; (b) plain disk and (c) fractal anchors.

3 PULL-OUT FORCE

3.1 DISK ANCHOR

Figure 3a shows the force *F(z)* measured by the force meter while pulling out a disk anchor. Initially, the anchor is at a depth *z=H*. As the linear stage lifts up the anchor, the force rapidly builds up and reaches a maximum, and then slowly decreases as the anchors get closer to the free surface, *z=0*. The pull-out force F_0 is defined as the maximum force on such a curve.

We have checked that the value of F_0 is not affected by the proximity of lateral walls, as long as they are farther than a few centimetres from the anchor edge. We have also checked that the value of F_0 is not too sensitive to the mode of preparation: experiments can be reproduced with a variation in F_0 lesser than 5%. Finally, we varied the velocity of

pulling V^{up} between 1mm/s and 20cm/s with no noticeable effect on F_0. Note that the non zero value of the force at the free surface, $F(z=0)$, is due to the formation of a static pile on top of the anchor.

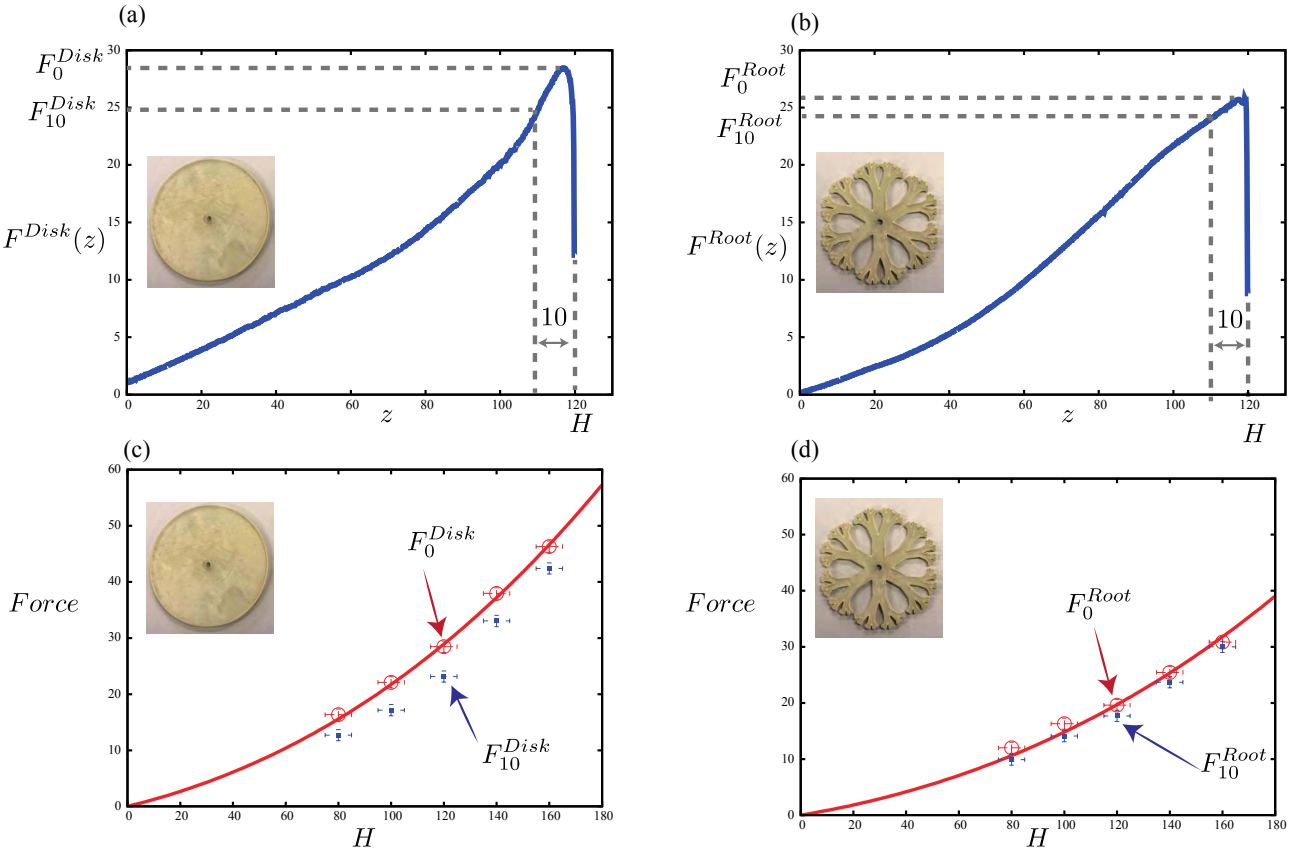

Figure 3. Pull-out force for disk and fractal anchors. Force versus depth z as the anchor moves toward the surface ($z=0$) from its initial position ($z=H=120mm$): (a) disk anchor and (b) fractal anchor. Maximum pull-out force F_0 as a function of the initial depth H: (c) disk anchor and (d) root anchor. (c,d) Each symbol represent on test, error bars account for the force meter accuracy of 1N and the non-uniformity of the free surface of the order of 5mm; red lines represents the model described by Eqs. (1), (2) and (4) (see text for more details). (a-d) forces are expressed in Newtons and distances in millimetres.

3.2 FRACTAL ROOT ANCHOR

Figure 3b shows the force measured while pulling-out a fractal anchor, starting from the same depth $H=120mm$. The force $F(z)$ exhibits a shape similar to that of the disk anchor. However, the value of the pull-out force is lower.

3.3 DEPTH EFFECT

Similar experiments were repeated for both anchors for different depths ranging from 80mm to 160mm, which corresponds to H/D ranging from 1 to 2. Results of the pull-out force F_0 are showed for the disk anchor on Figure 3c. On this Figure, the prediction of the model described in Eq. (1) and (2) is represented by the red line. The density of the glass beads was measured, $\rho = 2300\ kg/m^3$, the surface area of the anchor is known, $A = \pi D2/4 = 50.2\ cm^2$ and the best fit of the data was obtained with an angle $\theta = 13.2°$.Note that this value is consistent with the range $2/3\phi < \theta < \phi/2$ that the friction angle of the glass beads is $\phi=21°$. The quality of the fit shows that the cone failure envelope model is able to capture our results.

Figure 3d shows the results obtained with the fractal anchor. The red line was obtained using Eqs. (1) and (2), also with $\rho = 2300\ kg/m^3$ and $\theta = 13.2°$, and considering the anchor surface area $A^{Root} = \phi\ \pi D2/4 = 23.6\ cm^2$. However, a prefactor $\alpha = 1.47$ needs to be introduced as a fitting parameter to capture the data. Hereafter, α will be refereed to as *shape factor*. The pull-out force of the fractal anchor is then captured by a modified version of the model in Eqs. (1) and (2):

$$F_0^{Root} = \alpha g A^{Root} H f(\varphi) \quad (3)$$

Let us now use these results to compare the pull-out force of a fractal anchor and of a disk anchors made using the same amount of material, i.e., with the same surface area. The pull-out force of the fractal anchor would be α=1.47 times higher than the pull-out resistance of the plain disk.

4 RESILIENCE

The pull-out experiment results showed in Figures 3a,b show the behaviour of the anchoring force once the anchor has moved past the failure point, as illustrated in figures 2 a,b. For both disk and fractal anchors, the force then drops as the anchor moves upward. The drop seems to be more important for the disk anchor than for the fractal anchor. It can be quantified by the following quantity:

$$\mathrm{Re}s = 100 * \frac{F_0 - F_{10}}{F_0} \quad (4)$$

where F_{10} is the anchoring force after an anchor displacement of 10 mm (see Figures 3a,b). *Res* thus measures the percentage of anchoring force after an anchor displacement of 10 mm, relative to the pull-out force. It can be seen as a measure of the anchor resilience, which characterises its pull-out resistance after an initial displacement past the failure point. Large value of *Res* would correspond to a large force drop and a low anchor resilience.

Figure 4 shows the disk and fractal anchors' resilience as a function of the initial depth *H*. The disk anchor loses up to 22% of its force for shallow depth, a value that decreases for deeper anchors. The fractal anchors systematically exhibit much lower value of *Res*, and thus a much better resilience.

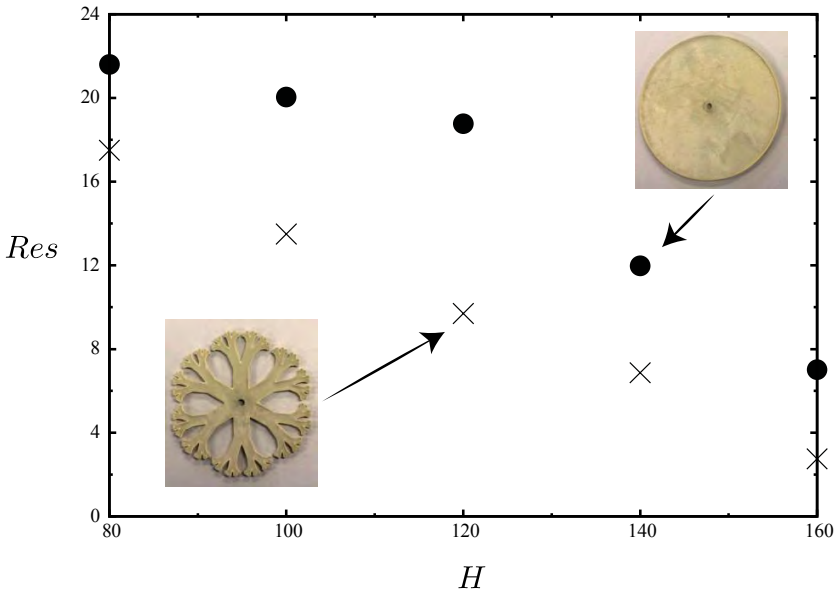

Figure 4. Resilience (%) of disk (circle) and fractal (cross) anchors as a function of the depth *H* as defined in equation (4).

5 CONCLUSION

The experimental results we presented here indicate that fractal root-inspired anchors have interesting anchoring properties in granular soils. Results show that their pull-out resistance can be described by a cone-failure envelope model if a shape factor α is introduced. Focusing on one fractal shape anchor, we obtained a shape coefficient of 1.47, which means that using the same amount of material, a fractal shape would have a superior pull-out-resistance than a plain disk.

Further still, these anchors were found to exhibit interesting resilience properties, represented by the loss in anchoring resistance after the anchor has moved past the failure point. Results showed that fractal anchors are significantly more resilient than plain disk anchors.

These results constitute a first proof of concept suggesting that that complex shape anchors may be an interesting solution for geotechnical applications requiring optimum use of material and high anchor resilience. They pave the way for further investigations of complex anchor geometries, both 2D and 3D, aiming at identifying the shapes that optimise the pull-out resistance, the resilience and the required amount of material. Beyond fractal shapes, other shape such as wheel or mesh shapes may exhibit interesting anchoring properties.

To determine the optimum anchor shape, future work should focus on identifying the relevant geomechanical mechanisms controlling the anchor mechanical response, including soil deformation pattern near the anchor, and mechanisms of arching that may lead to clogging the anchor holes.

5 REFERENCES

Baker, W. H., & Konder, R. L. (1966). "Pullout load capacity of a circular earth anchor buried in sand". *Highway Research Record*, (108).

Clemence, S. P., & Veesaert, C. J. (1977, January). "Dynamic pullout resistance of anchors in sand". In *Proceedings of the International Symposium on Soil-Structure Interaction, Roorkee, India* (pp. 389-397).

Cheuk, C. Y., White, D. J., & Bolton, M. D. (2008). "Uplift mechanisms of pipes buried in sand". *Journal of geotechnical and geoenvironmental engineering*, *134*(2), 154-163.

Das, B. M. (2012). *Earth anchors*. Elsevier.

Downs, D. I., & Chieurzzi, R. (1966, April). "Transmission tower foundations". In *Electric Power@ s Today and Tomorrow* (pp. 335-390). ASCE.

Kouzer, K. M., & Kumar, J. (2009). "Vertical uplift capacity of two interfering horizontal anchors in sand using an upper bound limit analysis". *Computers and Geotechnics*, *36*(6), 1084-1089.

Kumar, J., & Sahoo, J. P. (2011). Upper bound solution for pullout capacity of vertical anchors in sand using finite elements and limit analysis. *International Journal of Geomechanics*, *12*(3), 333-337.

Jung, J. K., O'Rourke, T. D., & Olson, N. A. (2013). "Uplift soil–pipe interaction in granular soil". *Canadian Geotechnical Journal*, *50*(7), 744-753.

Liu, J., Liu, M., & Zhu, Z. (2012). "Sand Deformation around an Uplift Plate Anchor". *Journal of Geotechnical and Geoenvironmental Engineering*, *138*(6), 728-737.

Majer, J. (1955). "Zur berechnung von zugfundamenten". *Osterreichische Bauzeitschrift*, 10(5), 85-90.

Meyerhof, G. G., & Adams, J. I. (1968). "The ultimate uplift capacity of foundations". *Canadian geotechnical journal*, *5*(4), 225-244.

Murray, E. J., & Geddes, J. D. (1987). "Uplift of anchor plates in sand". *Journal of Geotechnical Engineering*, 113(3), 202-215.

Niroumand, H., & Kassim, K. A. (2010). "Analytical and numerical study of horizontal anchor plates in cohesionless soils". *Electronic Journal of Geotechnical Engineering*, *15*, 1-12.

EXCAVATION INDUCED RESPONSE OF PILE FOUNDATIONS

D.S. Liyanapathirana[1] and R. Nishanthan[2]
[1]Associate Professor, [2]PhD Candidate
School of Computing, Engineering and Mathematics, University of Western Sydney, NSW, Australia

ABSTRACT

In urban areas excavations for construction of basements, tunnels and other underground facilities inevitably influence the existing pile foundations. Due to the release of stresses during excavations, confining pressures around existing piles decrease significantly inducing additional deflections and bending moments. It is important to quantify these effects at the design stage, in order to protect the existing structures during nearby deep excavations. In this paper, the impact of excavation induced ground movements on adjacent pile groups is investigated. Numerical simulations based on the finite element method are performed on free-head and capped-head piles in different pile configurations. The problem was modelled considering the three-dimensional geometry, which facilitates to simulate the arching and shielding effect of piles within a group. The response of both interior and peripheral piles is investigated. Results show that the presence of front piles reduces the detrimental effects on the rear piles within the group. In addition the provision of a pile cap significantly reduces the deflection of pile group due to load transfer to the rear piles, which are located away from the wall supporting the excavation. Outcomes of this research will contribute towards the design and construction of resilient pile foundations.

1 INTRODUCTION

In the last few decades, significance of ground deformations on single pile response during nearby excavations was investigated extensively using both theoretical and experimental studies. Theoretical studies were carried out using the finite element method, boundary element method and finite difference method to find out the single pile response adjacent to deep excavations (e.g., Poulos and Chen 1996; Poulos and Chen 1997; Chen and Poulos 1996; Poulos 2005; Xu and Poulos 2000 and Zhang et al. 2011). Leung et al. (2000) and Ong et al. (2006a) carried out centrifuge tests to investigate the single pile behaviour during nearby excavations in sand and clay soils, respectively. However, in the literature, only few research studies have been carried out investigating the pile group behaviour due to excavation induced ground deformations. Some case histories were published in the past, where the pile groups were located very close to deep excavations (e.g., Finno et al. 1991, Goh et al. 2003), but with limited measured data and site conditions.

Chen and Poulos (1996) studied pile group response due to excavation induced lateral movements using finite element and boundary element approaches. First they computed free field ground deformations without considering the pile group using the finite element method. Then the pile group behaviour is investigated applying ground deformations to the pile, using the program PALLAS (Hull 1987), which is based on the boundary element method. They obtained group factors for maximum bending moments for three different values of limiting pile-soil pressures when the pile is located 1 m away from the excavation and the stability number, N, is seven, which is defined as:

$$N = \frac{\gamma H}{c_u} \tag{1}$$

where γ is the unit weight of soil , H is the depth of the excavation and c_u is the undrained shear strength of the soil. According to Chen and Poulos (1996), the group effect is not significant for shallow excavations, where the stability number is less than six. For deep excavations with larger soil movements, group effect has a substantial influence based on the spacing and configuration of piles within the group.

Leung et al. (2003) and Ong et al. (2006b) investigated the pile group behaviour in sandy and clayey soils, respectively, using centrifuge tests. They investigated the behaviour of free-head and capped-head pile groups made of two, four and six piles located behind unsupported excavations. According to their results, when the piles were located in a row parallel to the wall, the effect of pile-soil-pile interaction on the behaviour of individual piles is insignificant compared to the case with piles positioned perpendicular to the wall. In the latter case, the front piles located closer to the retaining wall reduces the adverse effects of excavation induced soil movements on rear piles. Furthermore, provision of a pile cap significantly affects the behaviour of individual piles in the front row. In addition, it was found that peripheral piles in a group experience higher bending moments when compared to interior piles of the same group, which are less exposed to the adverse effects of excavation induced ground movements. They mentioned that since the pile caps are transmitting the bending moments from front piles to rear piles, the design of pile caps significantly influence the behaviour of piles in a group during nearby excavations.

Response of pile groups subjected to excavation induced ground movements is a three-dimensional problem due to the soil flow between adjacent piles and wall. In addition, the pile and ground deformations are coupled in the real situation. Although two step approaches discussed before decouples ground deformations and pile deformations, this assumption is not realistic. Hence in this paper, finite element models involving full three-dimensional geometry of the excavation and pile group were used to study the pile group behaviour during nearby excavations. Centrifuge tests reported by Ong et al. (2006b) were numerically simulated and the shielding effect of piles in a group during deep excavations was investigated by varying the pile group configuration and pile head conditions.

2 DESCRIPTION OF THE CENTRIFUGE TESTS

Centrifuge tests reported by Ong et al. (2006b) shown in Table 1 are used to investigate the shielding effect of piles in a group. In these tests, the behaviour of a pile group adjacent to an unbraced excavation is studied. The model container has prototype dimensions of 27 m x 10 m x 23.5 m. The Kaolin clay was filled up to a depth of 6.5 m above a Toyoura sand layer, which has a thickness of 6.0 m. A Latex bag filled with $ZnCl_2$ solution, which has a unit weight equivalent to the clay, is used to represent the soil region that needs to be excavated. The 1.2 m deep excavation was simulated by draining the $ZnCl_2$ solution in six steps over 2 days in the prototype scale. Piles were modelled using hollow square aluminium tubes with outer prototype dimension of 630 mm. Tests were carried out at a centrifugal acceleration of 50g at the geotechnical centrifuge facility, National University of Singapore.

Table 1. Pile configurations used for the analysis.

Pile configuration	Test	Dimensions	Pile head condition
	T1	*e*=3 m	Free head
	T2	*e*=5 m	Free head
	T3	*e*=3 m, *s*=2 m	Free head
	T4	*e*=3 m, *s*=2 m	Capped head
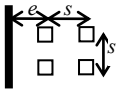	T5	*e*=3 m, *s*=2 m	Free head
	T6	*e*=3 m, *s*=2 m	Capped head

2.2 MATERIAL MODELS AND PROPERTIES

The constitutive behaviour of the clay is modelled using the Mohr-Coulomb model. The finite element analysis simulating the centrifuge tests was carried out assuming the undrained behaviour of clay. Since the clay has a permeability of 1.18×10^{-3} m/day and the excavation was carried out in two days, this is a reasonable assumption. The variation of undrained shear strength of the clay with depth is shown in Figure 1. The top 2.5 m soil crust was found to be over consolidated and soil below that level was normally consolidated. The elastic modulus of the Kaolin clay was calculated using E_c/c_u = 400 (Poulos and Davis, 1980). The internal friction angle and the Poisson's ratio for the undrained Kaolin clay were assumed as zero and 0.49, respectively. Lateral earth pressure coefficient at rest, K_o, is taken as one. The unit weight of the soil is 16.5 kN/m^3 (Ong et al. 2006). The Toyura sand layer below the clay layer was also modelled using the Mohr-Coulomb model with an internal friction angle of 40° and an elastic modulus of 6z MPa, where z is the depth below the ground surface in meters (Ong et al. 2006a). The Poisson's ratio of the sand is assumed to be 0.3. Bending stiffness of square piles used for the experiments is 2.2×10^5 kNm^2 in prototype scale, which is equivalent to the bending stiffness of a 600 mm diameter concrete pile. The pile has an embedment depth of 12.5 m in the prototype scale. A 3 mm thick aluminium plate is used as the wall in the centrifuge test, with prototype bending stiffness of 24×10^3 kNm^2/m and an embedment depth of 8 m. Piles, pile cap and wall are modelled assuming linear elastic behaviour.

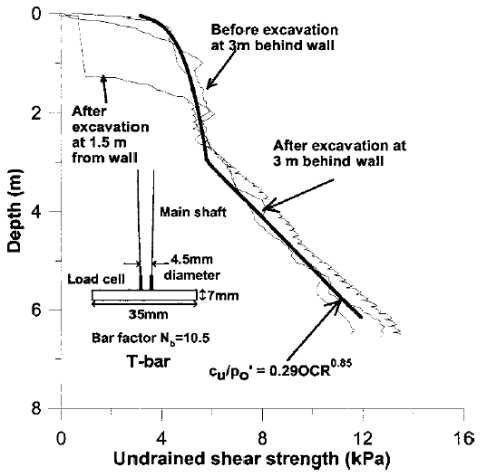

Figure 1: Variation of undrained shear strength with depth (Ong et al. 2006b).

3 FINITE ELEMENT MODEL

A three-dimensional finite element model based on prototype dimensions is used to simulate the centrifuge tests. ABAQUS/Standard finite element program is used to investigate the problem. Due to symmetry of the problem, only half of the geometry is considered for the numerical model.

Soil, pile, pile cap and wall were modelled using twenty-node quadrilateral brick elements with reduced integration formulation. At the bottom of the finite element mesh, horizontal and vertical movements are restrained ($u_x = u_y = u_z = 0$). Nodes over the vertical side faces are free to move in the vertical and horizontal directions along the surfaces of the container and restrained only in the directions perpendicular to the side faces. In the centrifuge model, tips of the pile group extend up to the bottom of the container and the movement of pile tips is restrained only by the surrounding soil and base of the container. If the same restraining conditions are applied to pile tips as for the base of the container, large bending moments will be developed at pile tips, which is not in agreement with the observed bending moments at the pile tip. Hence only the centre of the bottom of each pile is restrained from movements in all directions.

The soil-pile interaction in tangential direction is modelled using the Coulomb friction model, which is governed by a friction coefficient and a limiting displacement for elastic slip. Here a value of 0.3 was selected as the friction coefficient. Based on the typical values reported by Broms (1979), a limiting displacement of 5 mm was selected for the elastic slip to mobilise the full skin friction at the pile-soil interface based on the typical values reported by Broms (1979). The pile-soil interaction in normal direction is modelled using a “hard” contact while allowing separation at the pile-soil interface. Another advantage of allowing slippage and separation at the pile-soil interface is that it will avoid the overestimation of the deflection and bending moment of the pile as shown by Miao et al. (2006).

4 COMPARISON OF FINITE ELEMENT MODEL RESULTS WITH CENTRIFUGE TEST DATA

In this section results from the finite element model are compared with measured data from centrifuge tests to validate the numerical model. Figure 2 shows the computed and measured pile response for the test T3 at the end of 1.2 m depth of excavation. Two free-head piles are used in this test. The front pile is located 3 m away from the excavation and the rear pile is located 5 m away from the excavation. Since this is an unbraced excavation, pile deformations shown in Figure 2(a) are in cantilever shape. Deflection of front pile, obtained from the finite element analysis, is slightly under predicted and the deflection of rear pile is slightly over predicted compared to the centrifuge test results. This may be due to the inhomogeneous soil shear strength parameters in the lateral direction of the soil domain used for the centrifuge test as illustrated in Figure 1. Measured undrained shear strengths show different profiles at distances of 1.5 m and 3 m from the excavation after completion of the excavation. The predicted bending moment profile for the front pile shown in Figure 2(b) agrees well with the measured values during the centrifuge test. However, for the rear pile, computed bending moment slightly over predicted the measured bending moment. In both piles, the maximum bending moment occurs near the mid-height of the pile. For both pile deflections and bending moments developed in the rear

pile are less than those developed in the front pile. The maximum bending moment developed in the rear pile is 30% less than that in the front pile and the maximum deflection developed in the rear pile is 24% less than that in the front pile. These results confirm the shielding effect of front piles on the rear piles.

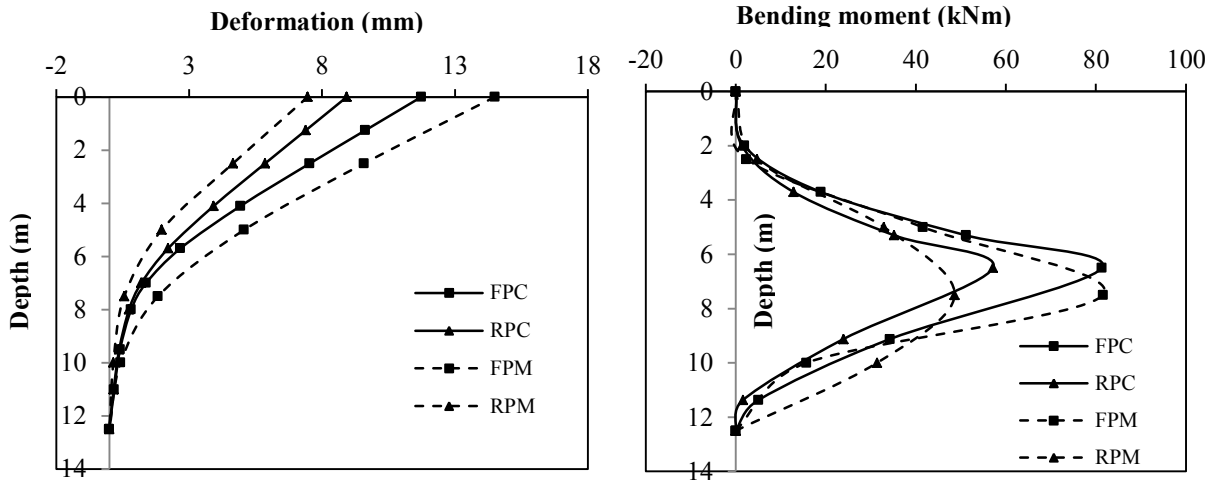

Note: FPC- Computed value for front pile, RPC- Computed value for rear pile, FPM- Measured value for front pile, RPM- Measured value for rear pile.

Figure 2: (a) Pile deflection and (b) Pile bending moment for Test 3.

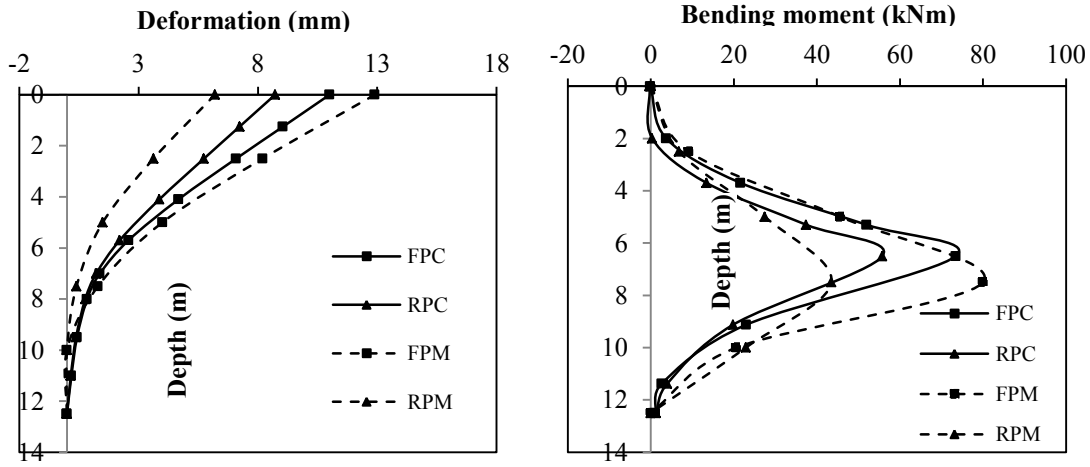

Note: FPC- Computed value for front pile, RPC- Computed value for rear pile, FPM- Measured value for front pile, RPM- Measured value for rear pile.

Figure 3: (a) Pile deflection and (b) bending moment for Test 5.

Figure 3 shows the measured and predicted response for a group of 2 x 2 free head piles (T5) and they are similar to the results given by test T3. In test T5, two piles are located in a line perpendicular to the wall as shown in Table 1. The predicted location of the maximum bending moment slightly differs from the measured one. Due to the arching effect between piles in a row parallel to the wall, the pile deflection and bending moment values are slightly less for test T5 when compared to centrifuge test T3. This difference becomes significant when the ratio of pile spacing over pile diameter decreases. Overall, finite element predictions agree well with the measured pile deflections and bending moments.

Centrifuge tests T3 and T5 consist of free head pile groups. When there is a capped pile group, a concrete pile cap with planar dimensions of 3 m x 1.25 m and a thickness of 1.55 m is used for test T4 and 3 m x 3 m cap with thickness of

1.55 m is used for test T6. Figure 4 shows the bending moment distributions along the pile predicted from the finite element model and the bending moment measured during the centrifuge test. Bending moment predictions from the finite element model are slightly higher than the centrifuge test results. One reason for this difference may be the method adopted to connect the concrete pile cap to the pile group. In the centrifuge test, pile cap is welded to the pile group and in the finite element model, a tie constraint is used to connect the cap to the pile, which represents a fixed boundary condition with zero rotational and translational movements at the pile head. The difference between the degrees of restraint in two cases may have contributed to the difference observed between finite element and centrifuge results. However, the overall bending moment distribution has the same shape.

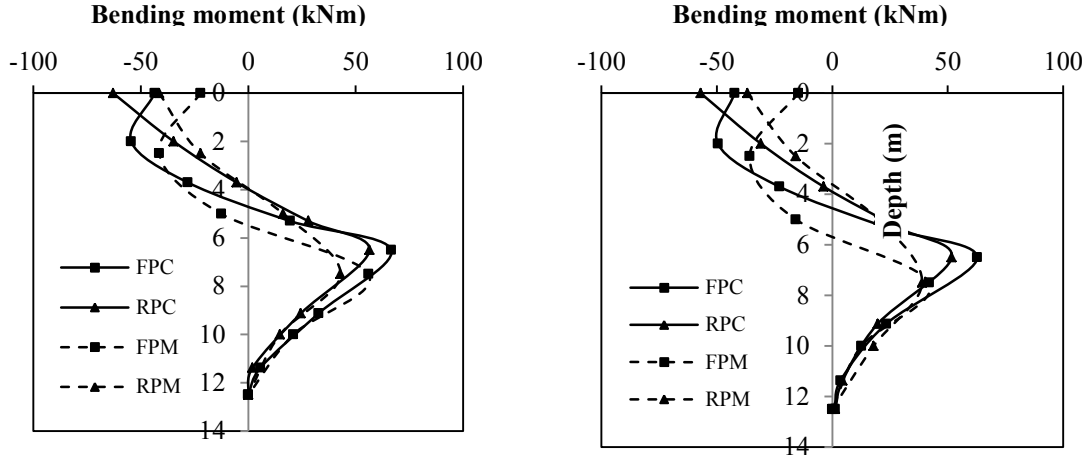

Note: FPC- Computed value for front pile, RPC- Computed value for rear pile, FPM- Measured value for front pile, RPM- Measured value for rear pile.

Figure 4: Pile bending moment for (a) Test 4 and (a) Test 6.

5 SHIELDING EFFECT

Figures 5 and 6 show the comparison of pile head deflection and maximum bending moment, respectively, for rear and front piles in tests T3 and T5 with free head and T4 and T6 with capped head. In these two figures results are also presented for single piles at the corresponding locations for front and rear piles, which are located at 3 m (T1) and 5 m (T2) from the excavation. For tests T4 and T6 with pile caps, bending moment developed at the pile head is negative. Hence both maximum positive and negative moments are given.

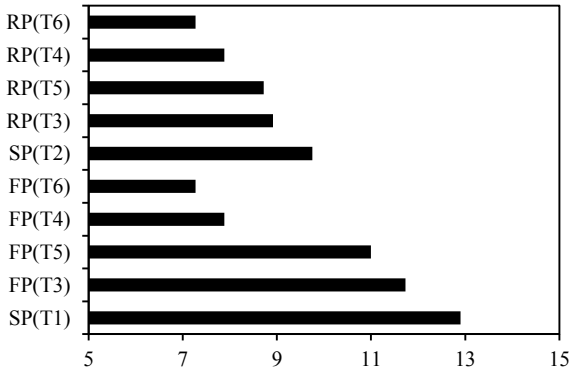

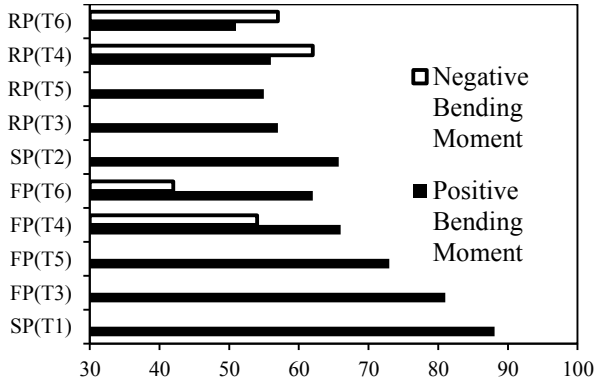

Note: SP- Single pile, FP- Front pile, RP- Rear pile.

Figure 5: Comparison of pile head deflection.

Figure 6: Comparison of maximum bending moment.

According to Figure 5, minimum pile deflections are observed, when there is a pile cap. This is due to the high stiffness of the pile cap. The maximum pile head deflection is the same for both front and rear piles. In this case pile tip is pinned. Therefore both piles show the same deformed shape and do not show any shielding effect from the front pile on the rear pile. For tests T3 and T5 with free head piles, front and rear piles deflect less than single piles at 3 m and 5 m away from the wall, respectively. The reduction in deflection in front pile compared to the single pile at the same location is due to contribution from the rear pile in carrying extra loads imposed on the pile group by excavation induced ground deformations. In both tests T3 and T4, rear piles deform less due to the shielding effect from the front piles. When the number of piles in the group increases from 2 to 4, pile deflection further decreased. This decrease is due to arching between piles along the wall. These observations confirm that the presence of more piles tend to increase the shielding and arching effects on the pile group. In this section only 2 m spacing between piles is considered. However, the ratio between pile spacing and diameter may have a significant influence on the shielding and arching effects of the pile group.

Maximum bending moments for the same set of tests also show a response similar to deflections. When the number of piles increased from 2 to 4, maximum bending moment reduces due to arching between piles parallel to the wall in addition to the shielding effect of the pile group for both free head and capped head pile groups. In capped pile groups, maximum negative bending moment is less than maximum positive bending moment for front piles but in rear piles, maximum negative bending moment is higher than maximum positive bending moment. Overall, maximum bending moments developed in front and rear piles in capped and free head piles are less than those developed in single piles at the corresponding locations confirming the shielding and arching provided by the piles in a group.

6 CONCLUSIONS AND RECOMMENDATIONS

In this study, three-dimensional numerical modelling is used to simulate a series of centrifuge tests carried out at the centrifuge facility at the National University of Singapore. The results obtained from the finite element analysis showed good agreement with centrifuge test results for the free-head piles. In the case of capped piles, computed values are very much higher than the measured values. This is due to the higher pile head fixity developed in the finite element model, compared to the welded pile-cap connection formed in the centrifuge test. The presence of front piles tends to reduce the excavation induced moments in rear piles due to shielding effect. In addition when there are piles in a group parallel to the wall supporting the excavation, arching between piles will further reduce the bending moments developed in rear and front piles. In capped–head piles, the maximum lateral movement is less than that of a rear pile with a free-head. The provision of pile cap helps to moderate the excavation induced lateral movements and maximum bending moments in pile groups.

7 ACKNOWLEDGEMENTS

The authors would like to acknowledge the financial assistance provided by the Australian Research Council for this research under the Discovery grant DP1094309.

8 REFERENCES

ABAQUS Inc.(2013), ABAQUS version 6.11 user's manual, Providence, Rhode Island, USA.

Broms, B. (1979), "Negative skin friction", Proceedings, 6th Asian Regional Conference, Soil mechanics and Foundation Engineering, Singapore, 41-75.

Chen, L.T. and Poulos, H.G. (1996), "Some Aspects of Pile Response Near an Excavation", Proceedings, 7th Australia New Zealand Conference on Geomechanics: Geomechanics in a Changing World, Barton, ACT: Institution of Engineers, Australia, 1996: 604-609.

Finno, R.J., Lawrence, S.A. and Harahap, I.S. (1991), "Analysis of performance of pile groups adjacent to deep excavation", Journal of Geotechnical and Geoenvironmental Engineering, 117 (6): 934-55.

Goh, A.T.C., Wong, K.S., Teh, C.I. and Wen, D. (2003), "Pile response adjacent to braced excavation", Journal of Geotechnical and Geoenvironmental Engineering, 129 (4): 383-386.

Leung, C.F., Chow, Y.K. and Shen, R.F. (2000), "Behaviour of pile subject to excavation-induced soil movement", Journal of Geotechnical and Geoenvironmental Engineering, 126 (11): 947-954.

Leung, C.F., Lim, J.K., Shen, R.F. and Chow, Y.K. (2003), "Behaviour of pile groups subject to excavation-induced soil movement", Journal of Geotechnical and Geoenvironmental Engineering, 129 (1): 58-65.

Miao, L.F., Goh, A.T.C., Wong, K.S. and Teh, C.I. (2006), "Three-dimensional finite element analyses of passive pile behaviour", International Journal for Numerical and Analytical Methods in Geomechanics, 30 (7): 599–613.

Ong, D.E.L., Leung, C.E. and Chow, Y.K. (2006), "Pile behaviour due to excavation-induced soil movement in clay I: Stable wall", Journal of Geotechnical and Geoenvironmental Engineering, 132 (1): 36-44.

Poulos, H.G. and Chen, L.T. (1996), "Pile response due to unsupported excavation-induced lateral soil movement", Canadian Geotechnical Journal, 33(4): 670-677.

Poulos, H.G. and Chen, L.T. (1997), "Pile response due to excavation-induced lateral soil movement", Journal of Geotechnical and Geoenvironmental Engineering, 123 (2): 94-99.

Poulos, H.G. (2005), "The Influence of Construction Side Effects on Existing Pile Foundations", Geotechnical Engineering, 36(1): 51-67.

Poulos, H.G. and Davis, E.H. (1980), Pile Foundation analysis and design, Wiley, New York.

Xu, K.J. and Poulos, H.G. (2000), "Theoretical study of pile behaviour induced by a soil cut", Proceedings of GeoEngineering 2000, Melbourne.

Zhang, R., Zheng, J., Pu, H. and Zhang, L. (2011), "Analysis of excavation-induced responses of loaded pile foundations considering unloading effect", Tunnelling and Underground Space Technology, 26 (2): 320-335.

TRAPEZOIDAL REINFORCED SOIL WALLS – DESIGN DEVELOPMENT AND CHALLENGES

Idy Li[1], Jeff Hsi[2] and Reza Karimi[3]

[1]Senior Geotechnical Engineer, [2]Chief Technical Principal – Geotechnics, [3]Associate Principal Geotechnical Engineer, SMEC Australia Pty Ltd

ABSTRACT

The widening of the existing rail bridges and approach embankments for the Gosford Passing Loops Project necessitated the construction of retaining walls adjacent to existing embankment slopes. Trapezoidally-shaped reinforced soil walls (RSW) were proposed to cater for the various constraints and challenges faced, including allowance for the uninterrupted operation of the existing rail lines during construction. Due to the unconventional wall geometry and load transfer mechanisms, design of trapezoidal RSW is not covered by typical standards and codes, such as RMS R57. The assessment process necessitated consideration of wall design based on first principles, and variations on the conventional assessment of failure mechanisms to ensure the wall achieved the design intent. Numerical modelling was undertaken to verify achievement of wall stability and serviceability requirements. The successful implementation of these walls is demonstrated by the observed stability of the existing rail track and RSW during and after construction, which is further supported by conforming instrumentation records.

1 INTRODUCTION

The Gosford Passing Loops Project forms a part of the Northern Sydney Freight Corridor (NSFC) Program delivered by Transport for NSW (TfNSW), to improve the capacity of the rail freight network between Strathfield, NSW and Broadmeadow, Newcastle. It forms one of three other projects along the existing lines, including North Strathfield Rail Underpass, Epping to Thornleigh Third Track, and Hexham Passing Loop.

The project comprises the construction of two (2) new Passing Loops between Gosford and Narara stations. Each Loop extends approximately 2km in length, providing an alternative route for slower-running freight trains as they are overtaken by passenger services on the existing rail lines. Refer to Photo 1 for an aerial view of the Project site prior to construction.

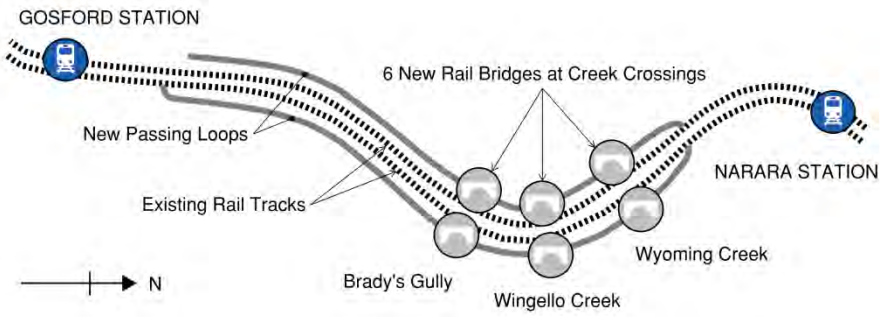

Figure 1: Plan of Gosford Passing Loops project (schematic, based on Transport for NSW, 2014).

The Passing Loops comprise extensions of the existing track footprint to the west and east, by incorporating the width of an additional rail track on the up and down main lines. Existing rail embankments had to be widened to accommodate construction of the Passing Loops to a similar elevation above natural ground. Refer to Figure 1 for a plan view of the Project and Figure 2 for a typical cross section through the proposed embankment widening. Photo 2 shows a typical site where embankment widening was proposed.

The majority of the larger embankment widening sections were located at bridge approaches where the Passing Loops crossed above one (1) of three (3) existing waterways, namely Wyoming Creek, Wingello Creek and Brady's Gully. A total of six (6) bridges were proposed for the Project, with three (3) on each of the up and down main lines.

This paper presents the challenges faced in the design of the proposed widening, the design development and methodologies, assessment outcomes, and the construction performance of the final embankment widening solution, which comprises trapezoidally-shaped reinforced soil walls (RSW).

2 RETAINING WALL – CHALLENGES AND CONSTRAINTS

2.1 REQUIREMENT FOR RETAINING WALLS

The embankment widening comprised fill heights up to 4.3m above natural ground level. Solutions for the widening proved to be a challenge for this project, as site boundary limitations prevented the widened sections from being supported by embankments with self-supporting batters. This limitation necessitated the embankment extensions to be supported semi-vertically with retaining walls, to minimise the footprint of the widened sections. Refer to Figure 2.

2.2 LIMITED CONSTRUCTION SPACE

The geometric extent of the design solution in the direction of the existing embankment was also constrained, as the existing rail line had to remain in full operation during construction of the Project works. This imposed the greatest challenge on the design, as any encroachment into the existing embankment would impact on its stability, potentially introducing risks of deformation or failure, and ultimately endangering passenger and rail safety. Photo 3 illustrates the proximity of the existing rail line to a site where embankment widening was proposed. Accordingly, maintenance of the stability and serviceability of the existing embankment was of utmost importance. Any excavations and / or negative impacts had to be minimised, otherwise temporary stabilisation works would be required.

2.3 WEAK GROUND CONDITIONS

The highest retaining walls were located at bridge abutments where the Passing Loops were expected to cross existing waterways. Due to the proximity to natural watercourses, the subsurface geology was alluvial in origin and of poor strength, consisting of loose density clayey sands and sandy clays of firm consistency. High groundwater levels were observed at or above the existing ground level.

2.4 WALL ARRANGEMENT

A reinforced soil wall (RSW) solution was proposed in favour of other retention systems due to its flexibility to "absorb" movements and deformations expected from the weak ground conditions, as well as its suitability to meet the constrained site conditions.

RSW's comprise a system of mechanically stabilised fill (typically granular), reinforced with a series of tensile straps to effectively form a self-supporting, gravity "block". Concrete panels or blocks are often used to form the wall facia.

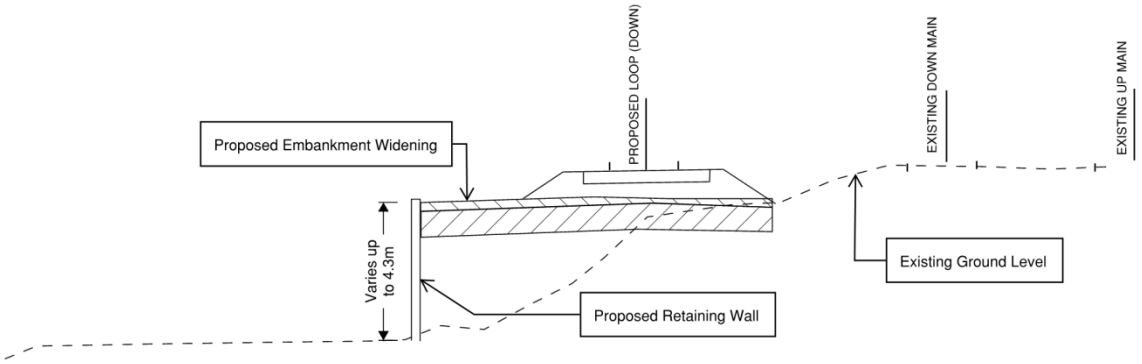

Figure 2: Typical cross section of proposed rail embankment widening.

3 DESIGN DEVELOPMENT

The RSW underwent three (3) stages of development, starting with a conventionally designed rectangular block, and concluding in a trapezoidally-shaped block sitting atop the existing embankment. Details of the design development are summarised below. Reference is made to an example design taken from RSW's designed at Wyoming Creek Underbridge, to facilitate in the reader's understanding of the design process and outcomes. The design stages are summarised below.

- **Stage 1: Initial Design** – The initial RSW design was undertaken using conventional design methods, following RMS QA Specification R57, Design of Reinforced Soil Walls (RMS, 2012), as stipulated in the Project Works Brief. Details of the design methodology are contained in Section 4.1. The resulting designs comprised rectangular RSW block widths which encroached a significant distance into the existing rail embankment. For example, the assessed block width at Wyoming Creek was 7m, refer Figure 3. Installation of the proposed RSW designs required significant excavation into the existing embankment, thereby

necessitating the installation of temporary sheet piles to retain the existing rail tracks at the embankment crest. Due to large deformations predicted at the top of the sheet piles, anchorage mechanisms were proposed in the form of dead men or tie backs attached to top of the sheet piles.

- **Stage 2: Intermediate Design** – Due to the uncertainties and risks posed by the temporary works on the existing embankment in the Initial Design, consideration was made to exploit the stability of the existing rail embankment. Development of the trapezoidally-shaped RSW was born on the theory of "attaching" the RSW onto the embankment – thereby removing the need to excavate into the existing embankment and consequent elimination of the temporary sheet piles. As this wall geometry and design approach is not covered in conventional design codes, assessment of its feasibility was based on first principles, as detailed in Section 4.2. The resulting solution comprised a narrow 1.5m wide "base" at the toe of the embankment formed with cement stabilised sand, upon which the RSW would be constructed. The rear of the RSW comprised a stepped interface following the existing gradient of the underlying embankment. An illustration of the proposed solution at Wyoming Creek is shown in Figure 3 below.
- **Stage 3: Final Design** – In the absence of design standards specifically targeted for the proposed trapezoidal-RSW solution, the Federal Highways Administration (FHWA, 2006) document on "Shored Mechanically Stabilised Earth (SMSE) Wall Systems Design Guidelines" was used as a guiding document. Design refinements were made based on FHWA's (2006) recommendations, eventuating into the Final Design solution, whereby the "base" of the RSW was increased up to 3.5m. The design necessitated a 1H:1V temporary excavation into the existing embankment to accommodate the widened base. Reference can be made to Figure 3 for an illustrative sketch summarising the relative dimensions and design features proposed at the Final Design phase at Wyoming Creek.

4 DESIGN METHODOLOGY

RSW design is typically delineated into two parts, Internal Design, and External Design. In general terms, Internal Design addresses the requirements of the RSW to form a self-supporting, coherent, gravity block; and External Design assessments review the interaction of the RSW with the surrounding ground.

For this Project, SMEC was responsible for the External Design, and a specialist RSW supplier was responsible for carrying out the Internal Design. Accordingly, the design developments and stages mentioned in Section 3 above pertain to developments made in addressing the satisfaction of External Design. The sections below describe the methodologies and theories behind the solutions formulated at each stage of External Design development contained in Section 3. It was assumed that the Internal Design would be adequately addressed by others.

4.1 CONVENTIONAL RSW

Design Specification R57 (2012) was followed for the design of the rectangular RSW block formulated in Stage 1 of the design (Initial Design). R57 (2012) follows conventional RSW design theories, whereby the RSW block provides a means of retention to the adjacent soil mass, resulting in the imposition of destabilising lateral earth pressures on the back of the RSW.

External Design assessments following conventional design theories review the interaction of the RSW and the surrounding ground, with the overarching assumption that the wall acts as a rigid body, against which the soil mass is retained and lateral earth pressures are applied. Typically, External Design assessments comprise:

- Ultimate Limit State: bearing capacity, forward sliding, overturning (tilt), and slip failures
- Serviceability Limit State: settlement, tilting, eccentricity, rotational and lateral movement, and deformation associated with slip failures.

In addition to R57 (2012), there are a number of standards commonly used in Australia and in the international arena which provide guidelines for RSW design which adopt conventional design theories as outlined above. Examples of such standards include, British Standard, BS8006 (2010), "Code of Practice for Strengthened/Reinforced Soils and other Fills", and Australian Standard, AS4678 (2002), "Earth-retaining Structures".

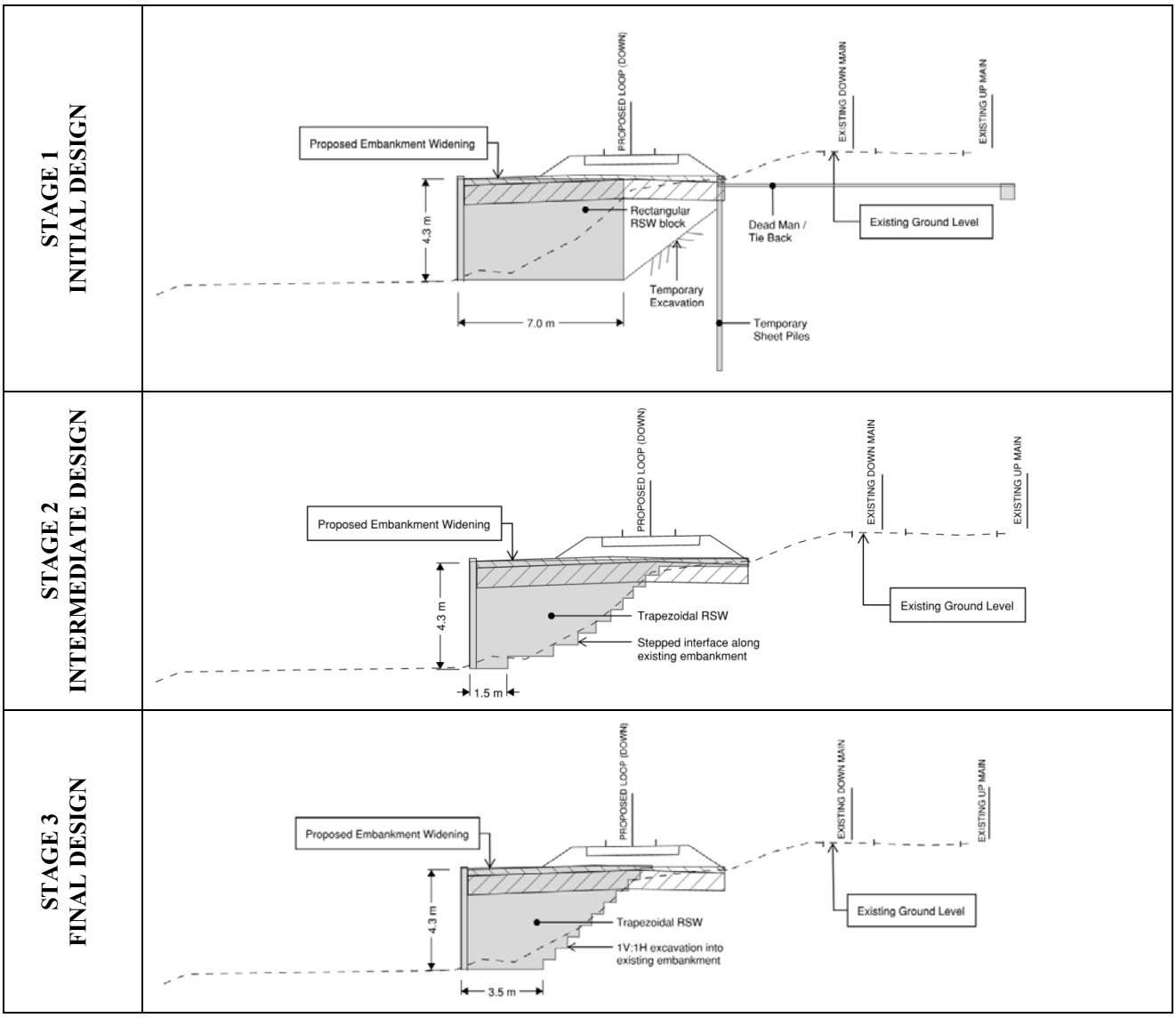

Figure 3: Sketches showing RSW design development solutions at Wyoming Creek.

4.2 TRAPEZOIDAL RSW

As mentioned in Section 3, the concept of trapezoidally-shaped RSW's originated from the theory of "attaching" the RSW block onto the embankment, while exploiting the evident stability of the existing rail embankment. Adherence to conventional RSW External Design theories and standards was no longer applicable, as the RSW block was no longer assumed to retain the adjacent earth fill, and consequently, was not subjected to lateral earth pressures. Accordingly, assessment of External Design failure mechanisms for compliance with R57 (2012) such as bearing capacity, sliding and overturning were no longer considered relevant. Alternative methodologies / design criteria were sought to assess the stability and serviceability of this unique retention system, as presented in the following sections.

It is noted that trapezoidally-shaped walls are covered in R57 (2012), BS8006 (2010) and AS4678 (2002). However, these codes stipulate that such geometries are only applicable for walls founded into sound rock and concrete. Such wall geometries are designed in accordance with conventional design theory, as they are considered to retain adjacent ground materials and consequently are subjected to lateral earth pressures. R57 (2012) provides guidelines to modify the trapezoidal block geometry into an equivalent rectangular shape for the purposes of design calculation and assessment.

4.2.1 First Principles

Design of the trapezoidal RSW-embankment composite system formulated in Stage 2 of the design (Intermediate Design) was undertaken based on first principles. Assuming the RSW block was adequately designed to act as a self-

supporting, coherent unit (i.e. satisfaction of Internal Design requirements), and in the absence of lateral earth pressures on the back of the RSW, consideration of first principles suggests that the feasibility of the system need only be addressed for potential slip failures.

Adopting a minimum base width of 1.5m at the toe of the RSW, trapezoidal RSW blocks were formulated in the Intermediate Design based on the achievement of industry-adopted Factors of Safety (FOS) against slip failure. Limit equilibrium software, SLOPE/W was utilised for this assessment.

Guidance was sought from RSW Internal Designers and suppliers to advise on the shortest practicable wall base width – as minimisation of this dimension would reduce the potential excavation into the existing embankment. A base width of 1.5m to 2m was suggested based on literature reviews and recommendations based on the practical benefit of creating a workable construction platform. It was also suggested that the base could be formed using concrete or cement stabilised sand up to a height where a 1.5m wide base could be created – in the event space limitations necessitated such a "pointed" base.

4.2.2 Reference Design Standards

A literature review indicated that no design standards were available for the proposed trapezoidal RSW-embankment composite solution. However, similarities could be drawn with the "SMSE Wall Systems Design Guidelines" documented by the FHWA (2006). FHWA (2006) provides guidelines for the design of RSW located in front of excavations reinforced with soil nails. This document recognises the stabilising effect of the shoring wall and suggests the consequent elimination of lateral earth pressure loads being imposed on the RSW. For the purposes of External Design, FHWA (2006) suggests that failure mechanisms associated with sliding and overturning need not be considered.

For the RSW formulated in Stage 3 of the design (Final Design), the guidelines presented in FHWA (2006) were used as a basis for the adopted External Design methodology, as summarised below. Load factors and strength reduction factors from R57 (2012) were adopted to address the various load combinations expected during the RSW's lifetime.

- Bearing capacity – Applicable for RSW portion supported on natural ground, as suggested by FHWA (2006). Refer to Figure 4.
- Sliding and overturning – Although earth pressure loads were not considered to exist, destabilising lateral loads from other sources such as earthquake loading and hydrostatic pressure were assessed against the available resistance at the base of the trapezoid.
- Slip failure – Assessment of global slip failures through the existing embankment and supporting ground, due to application of the trapezoidal wall. Modelling of the composite system was undertaken using limit equilibrium software, SLOPE/W.

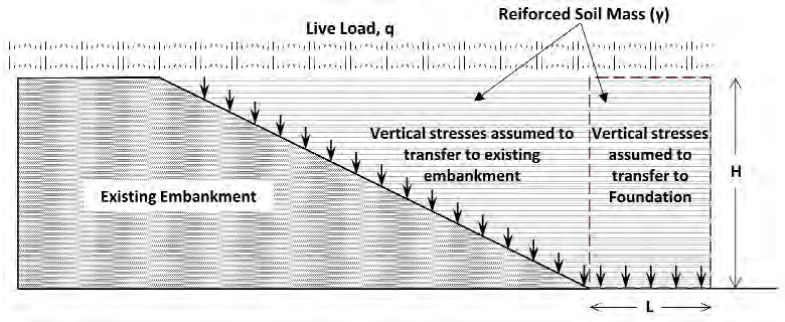

Figure 4: Sketch showing RSW External Design Bearing Capacity Assessment, based on FHWA (2006).

5 NUMERICAL MODELLING

The composite system was modelled using finite element software, PLAXIS 2D, which facilitated in detailed stability assessments and deformation predictions.

5.1 DESIGN INPUTS

The composite system was modelled in stages, simulating the proposed construction sequence, starting with the excavation of the existing embankment, construction of the RSW in 1m to 2m lift increments, up to final completion of the wall. The software facilitated in the assessment of interim stability and expected deformation magnitudes throughout the modelled construction stages.

Freight trains were simulated as pressure loads of 76kPa across a track width of 2500mm. Two train loads were modelled on the existing embankment to simulate the passage of trains on the up and down main lines. One (1) additional train load was modelled on the widened section to simulate train services on the Passing Loop.

5.2 ASSESSED STABILITY

Wall stability at Wyoming Creek was verified through the achievement of FOS against slip failure of 1.35 and 1.6 in the short term and long term design cases respectively, in accordance with standard industry practice. The assessed factors of safety based on the Phi/C reduction method, and potential slip failure plane are shown in Figure 5 and Figure 6 respectively.

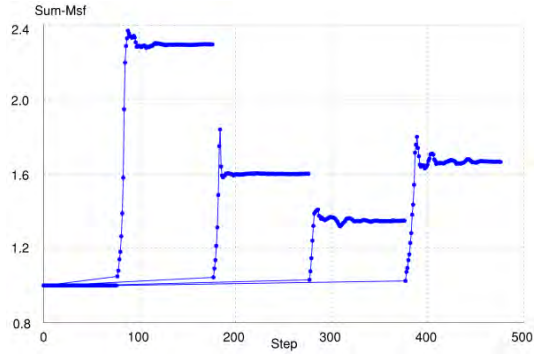

Figure 5: Output of Phi/C reduction (Factor of Safety) for various construction stages at Wyoming Creek (PLAXIS 2D).

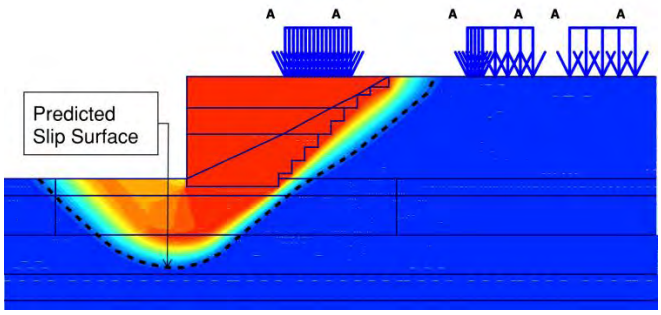

Figure 6: Output of Phi/C reduction (Factor of Safety) of potential slip failure plane at Wyoming Creek (PLAXIS 2D).

5.3 ASSESSED DEFORMATION

Figure 7 presents the deformations predicted within the composite system at Wyoming Creek. The predicted deformations were within the allowable tolerances for the affected structures.

Maximum assessed deformation	Settlement (mm)	Lateral deformation (mm)
Existing embankment	40	35
Existing rail tracks	14	11
Trapezoidal RSW	110	60

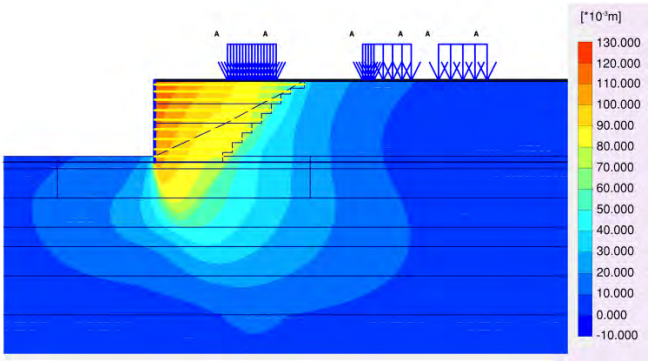

Figure 7: Predicted total deformation at Wyoming Creek.

6 CONSTRUCTION PERFORMANCE

6.1 INSTRUMENTATION

Instrumentation and monitoring were implemented during construction to confirm the performance of the trapezoidal RSW as per the design predictions. A plan showing the proposed instrument locations is provided in Figure 8.

Proposed instrumentation and corresponding trigger levels (in brackets) for RSW at Wyoming Creek comprised the following:

- Settlement plates – located beneath the constructed RSW to capture total ground settlement (90mm)
- Settlement pins – located on the existing embankment, to monitor embankment deformation during and after construction (12mm)
- Survey targets – located at the RSW face to measure wall deformation (90mm vertical, 30mm lateral)

- Track monitoring – surveying of the existing main lines (trigger levels in accordance with track monitoring requirements specified in RailCorp Engineering Specification SPC 207, 2013)

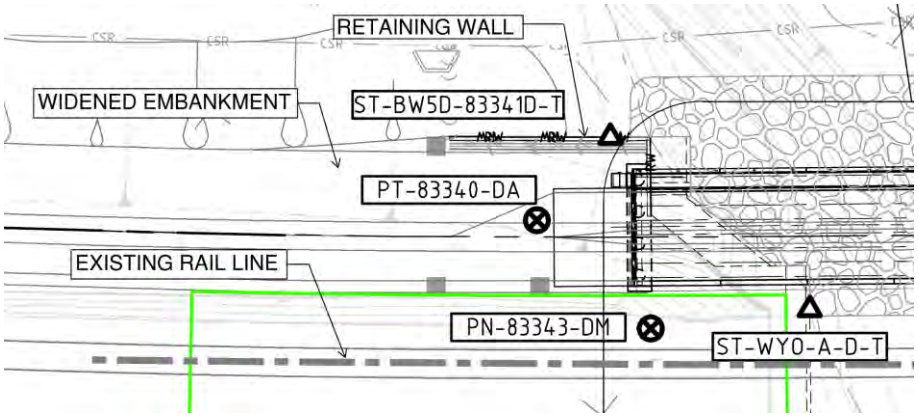

Figure 8: Plan view of proposed instrumentation at Wyoming Creek.

6.2 MEASUREMENTS

At the time of writing, construction of trapezoidal walls on the Project had just commenced, starting with walls at Wyoming Creek Bridge. Settlement plate data registered movements within the predicted values. Although construction works took place in close proximity to the existing rail line, monitoring of the tracks had not registered any excessive movement during excavation of the existing embankment and / or construction of the retaining wall. Photo 4 illustrates the proximity of the works to the existing rail line. The observed stability of the composite system to-date and adherence to the predicted behaviour as demonstrated through the monitoring records, suggests that the wall is performing as expected. Photo 5 provides a picture of a completed trapezoidal RSW at Wyoming Creek. Further monitoring data will be collected to verify the behaviour and performance of this wall and the other trapezoidal RSW.

6.3 CONSTRUCTION

Photos 6 and 7 illustrate typical rail track construction processes and machinery utilised upon completion of the supporting foundation for the new Passing Loops. Similar construction methods are expected to be adopted above the completed trapezoidal RSW.

7 CONCLUSIONS

A trapezoidal RSW-embankment system was adopted to support the embankment widening for the Gosford Passing Loops Project. The concept behind this system exploits the self-supporting characteristics of the existing embankment, and consequent elimination of lateral earth pressures imposed on the overlying RSW. The mechanics behind this system deviates from conventional RSW design theory, such as those followed by typical design standards, R57 (2012). In the absence of specific design guidelines, the External Design feasibility of the composite system was based on first principles, whereby assessment against slip failures was undertaken. Adoption of design guidelines provided in FHWA (2006) "SMSE Wall Systems Design Guidelines" was utilised in the development of the Final Design, which rendered a trapezoidal-RSW with narrow 3.5m base width and a stepped 1H:1V interface with the underlying embankment. Finite element analyses were undertaken to assess stability and formulate deformation predictions. Instrumentation points on the existing track and RSW registered deformations within the expected magnitudes at the time of writing, thereby confirming the observed stability and successful performance both during and post construction.

8 ACKNOWLEDGEMENTS

Acknowledgement is made here to Transport for NSW, Downer Engineering Australia and Robson Civil Projects for their approval to publish this paper.

9 REFERENCES

British Standard (2010) Code of Practice for Strength / Reinforced Soils and Other Fills, BS 8006-1:2010, BSI Standards Publication

Federal Highway Administration (2006) Shored Mechanically Stabilised Earth (SMSE) Wall Systems Design Guidelines, Publication No. FHWA-CFL/TD-06-001, Federal Highway Administration, Lakewood, CO 80228

GEO-SLOPE (2012), SLOPE/W, GEO-SLOPE International Ltd., Alberta, Canada

PLAXIS (2013), PLAXIS 2D, PLAXIS BV, An Delft, Netherlands
RailCorp (2013), Track Monitoring Requirements for Undertrack Excavation: Engineering Specification SPC207, Version 1.5, RailCorp
Roads and Maritime Services (2012) QA Specification R57: Design of Reinforced Soil Walls, Edition 2 / Revision 6, Roads and Maritime Services
Standards Australia (2002) Earth-Retaining Structures, AS4678-2002, Standards Australia International
Transport for NSW (2014), Gosford Passing Loops, viewed 22 June 2014, <http://www.transport.nsw.gov.au/Projects-Northern-Sydney-Freight-Corridor-Program/gosford-passing-loops>
Transport for NSW (2012), Strategic Review Report: Northern Sydney Freight Corridor, Transport for NSW

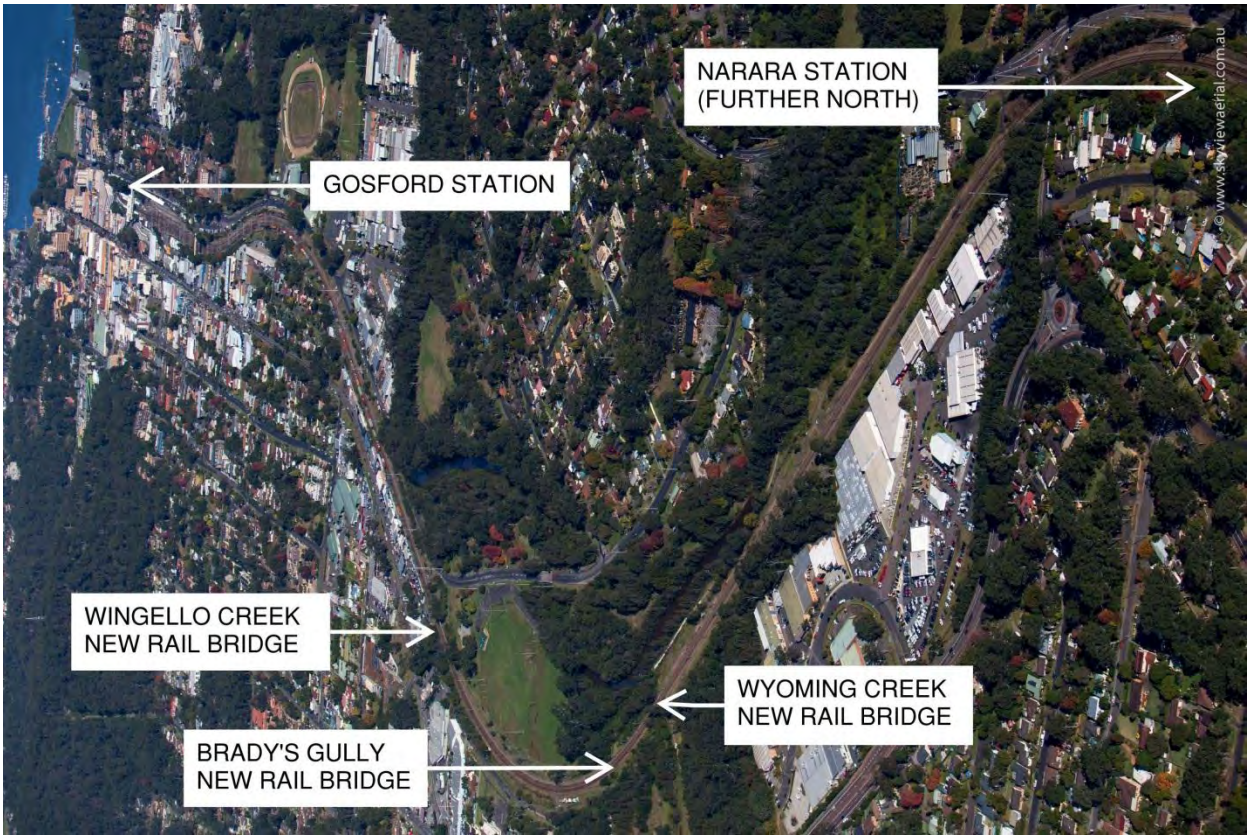

Photo 1: Aerial view Gosford Passing Loops (pre-construction)

Photo 2: Pre-construction – Site of proposed rail embankment widening

Photo 3: Pre-construction – Proximity of proposed embankment widening relative to existing train line.

Photo 4: During construction – Proximity of construction works to existing rail line

Photo 5: Completed Trapezoidal-RSW at Wyoming Creek

Photo 6: Construction of new rail track for Passing Loops

Photo 7: Construction of new rail track for Passing Loops

DESIGN AND CONSTRUCTION OF A GEOFOAM EMBANKMENT OVER SOFT GROUND

B.S. Yoon[1], P. Kidd[2], A. Law[3] and J. Hsi[4]

[1]Senior Geotechnical Engineer, [2]Geotechnical Manager Gold Coast, [3]Manager Geotechnics and Tunnels Northern Region, [4]Chief Technical Principal – Geotechnics, SMEC Australia

ABSTRACT

Development of the new Service Centre required construction of an off-ramp from the existing road together with an internal road network. Together these will provide access to the Service Centre for traffic from the existing roads. The off-ramp and road network were constructed on fill embankments, up to 4m in height, overlying a relatively uniform but very significant thickness of soft clay. In addition, the project site had been subject to a complex history of loading and unloading as a result of previous development on the site and ground improvements adjacent to the site, as part of new Service Centre development. To mitigate the effects of post-construction settlement to acceptable levels, safe and cost-effective ground treatment measures were developed along the preferred road alignment.

This paper provides some background to the project and presents in detail the design and construction methodology adopted for the lightweight fill treatment works using geofoam. The new geofoam embankment had to be constructed within the vicinity of existing and new infrastructures, i.e. pile-supported bridge, existing roads and a new drainage structure.

1 INTRODUCTION

The new Service Centre development, referred to as Banksia Place Stage 1A project, near Brisbane Airport required construction of roadway embankments on soft ground so as to provide an access to the new Service Centre for traffic from the existing airport access roads, i.e. Moreton Drive and Nancy Bird Way. The foundation soils encountered beneath the site comprised very soft and loose alluvial deposits of very significant thickness up to approximately 20m. The site had experienced a complex history of loading and unloading, as a result of the previous extensive upgrade of the Brisbane Airport's road network and ground improvement which was undertaken as part of Banksia Stage 1A project. This improvement included 6 months of preloading with 3.5m surcharge and wick drains. Additionally, the new off ramp from the existing road had to be constructed within close proximity of the existing and new infrastructures which included an existing bridge supported on piles, the existing Brisbane Airport's road network, and drainage structures.

Due to the imposed geotechnical and physical constraints on the project site, construction of the embankments in these areas involved significant risks associated with embankment stability, post construction settlement and potential impact on the existing infrastructures which had tight tolerance in terms of the additional allowable lateral and vertical movements induced by new bulk earthworks.

To develop safe and cost-effective ground treatment measures, the preferred road alignment was divided into discrete zones with similar characteristics including proposed fill height and physical/imposed constraints. Different types of ground treatment method were proposed for each discrete zone in order to mitigate the effects of post-construction settlement to acceptable levels.

This paper outlines some background to the project and presents the design and construction methodology adopted for the lightweight fill treatment works using Geofoam (also known as Expanded Polystyrene, EPS). The Geofoam embankment was constructed on the east corner of Moreton Drive and Nancy Bird Way intersection and had to be constructed within 10m of the existing twin bridge. Figure 1 below shows the project location.

2 BACKGROUND

Brisbane Airport is located approximately 14km north-east of the Brisbane central business district (CBD) and is one of the most important industrial and business areas in the Australia Trade Coast precinct in the state of Queensland. The airport area has therefore been experiencing continuously rapid growth and significant development over the past years.

Together with the State Government's Gateway Upgrade Project that provided improved connectivity to the Australia Trade Coast precinct, an extensive upgrade of the road network around the Brisbane Airport was carried out to alleviate traffic congestion around the airport and to provide much-needed infrastructure for the future growth. A second access roadway to the terminals, that included Moreton Drive linking the Gateway Motorway with the Domestic Terminal and Nancy Bird Way serving the International Terminal, was constructed in 2009.

Since the opening of the new Moreton Drive together with its associated secondary roads, a considerable portion of the overall traffic travelling to and from the terminals has moved onto the new roads. In addition, the construction of the new Brisbane Airport's roads provided an opportunity to provide a new Service Centre within the Banksia Place development precinct on the Eastern corner of the Moreton Drive and Nancy Bird Way intersection roundabout. The new Service Centre development consists of several buildings and restaurants in a central Service Centre, a canopied refuelling area, a carwash and servicing building, and associated driveways and parking areas. Access to the Service Centre is provided by a new off ramp from the Moreton Drive and internal roads to the Nancy Bird Way.

Snowy Mountains Engineering Corporation (SMEC) were commissioned by the Brisbane Airport Corporation Pty Ltd (BAC) to provide design service to facilitate construction of an off-ramp from Moreton Drive and internal road network for the Banksia Place Stage 1A Service Centre precinct.

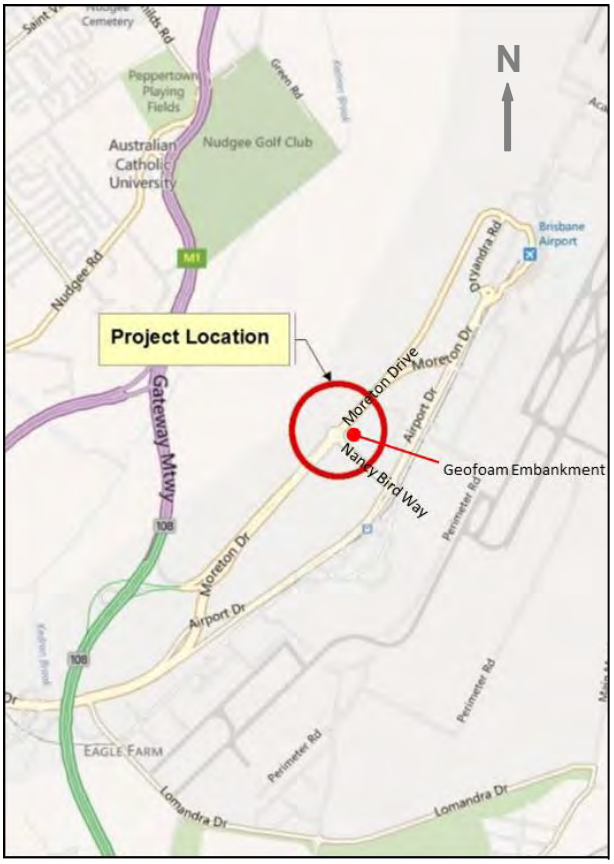

Figure 1: Project location.

As part of the Stage 1A Service Centre development, the site had been undergoing a bulk earthworks strategy to surcharge the Service Centre area at the time of the detailed design proposal. These works were anticipated to be for a period of six months. Upon completion of the bulk earthworks, construction of the off-ramp and internal roads commenced with a planned completion date of February 2014.

The main challenges for the project were the construction of the road embankment on soft ground, requiring safe and economical ground improvement technology for timely delivery of the project, together with a minimal impact of new bulk earthworks on the existing and new infrastructures adjacent to the project.

In particular, the area adjacent to the east corner of Moreton Drive and Nancy Bird Way intersection required construction of the road embankment within the vicinity of the existing twin bridges supported on piles. The bridges had extremely tight tolerance with regard to the additional allowable movements caused by the new bulk earthworks. The soil movement induced by the new bulk earthworks was expected to generate additional lateral forces imposing on the existing bridge piles. According to a preliminary assessment, preloading with 3.5m surcharge and wick drains will give rise to excessive ground movements underneath and adjacent to the embankment which have an adverse impact on the existing bridge piles. Therefore, it decided to adopt lightweight fill (geofoam) together with preloading and wick drains in order to mitigate the ground movement to an allowable range as well as minimise the impact on the nearby bridge structures.

3 GROUND CONDITIONS

3.1 SUBSURFACE CONDITIONS

The site of Banksia Place is located close to the mouth of the Brisbane River, and the subsurface geology generally consists of a sequence of alluvial, fluvial, estuarine and deltaic sediments deposited during the Holocene and Pleistocene ages, overlying Tertiary sediments of the Petrie Formation which typically consists of mudstone, siltstone and sandstone, and basalt.

The Holocene alluvial deposits are typically divided into the Upper Holocene alluvium and Lower Holocene alluvium. Upper Holocene alluvium was formed during the most recent rise in sea level, comprising very soft to firm, grey and brown clay of typically high plasticity, with interlayered silts or sands with some organic content. The underlying Lower Holocene alluvium was deposited in deeper water, comprising dark grey clay of high plasticity, with thin lenses of sandy soils. The clays are typically very soft in consistency, grading with depth to become firm and extending to significant depths, in excess of 20m in places. In some areas of the site, a variably thick sand layer is locally present at the interface between the Upper Holocene alluvium and the Lower Holocene alluvium. The underlying Pleistocene deposits consist of clays, sandy clays or clayey sands. The clays are typically stiff to hard, overconsolidated and of high plasticity. The sandy soils are typically of a medium dense to dense condition.

Groundwater was found at a depth of between 0.2m and 2.2m below natural ground surface level. The depth to groundwater is expected to vary with seasonal changes, tidal changes, and groundwater levels in the local area adjacent to Brisbane River.

3.2 GEOTECHNICAL CHARACTERISTICS

The geotechnical characteristics of the highly compressible soft clays, i.e. Upper and Lower Holocene clays, encountered on the site were evaluated on the basis of the results obtained from a suite of laboratory testing and field investigations, primarily comprising cone penetration tests and boreholes. Key geotechnical characteristics associated with index, deformation and strengths are summarised in Figure 2.

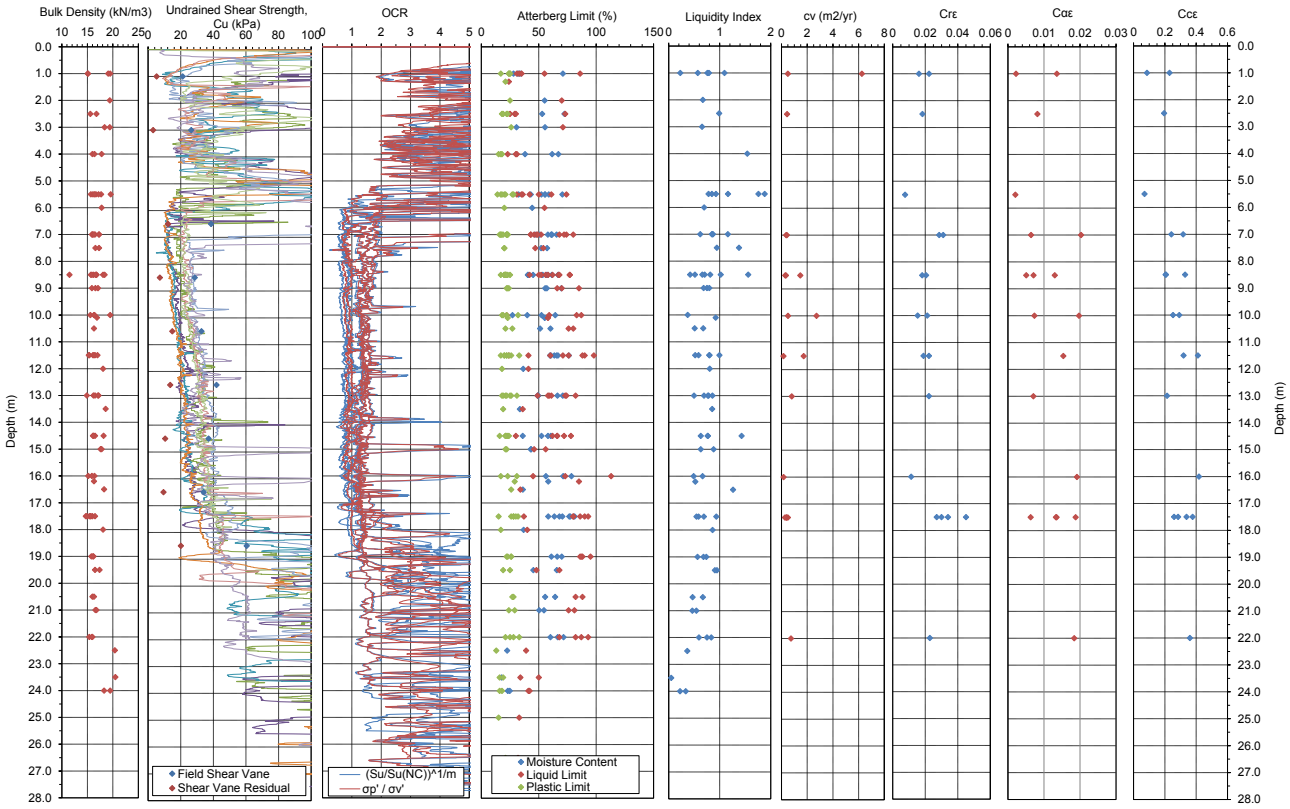

Figure 2: Geotechnical characteristics of subsoils derived based on laboratory and field testing.

Index characteristics were derived using moisture content and Atterberg limits for soil classification. Holocene alluvial soils are typically of a high plasticity with water content (w) of 20-85%, liquid limit of 23-99%, and plasticity limit of 17-33%. For the purposes of settlement estimation, consolidation characteristics including modified compression and recompression indices, $C_{c\varepsilon}$ ($=C_c/(1+e_0)$) and $C_{r\varepsilon}$ ($=C_r/(1+e_0)$), and modified creep index, $C_{\alpha\varepsilon}$ ($=C_\alpha/(1+e_0)$), were utilised, where C_c = coefficient of compression, C_r = coefficient of recompression, C_α = creep index, and e_0 = initial void ratio. The rate of consolidation was defined by the coefficients of consolidation in the vertical and horizontal directions, C_v and C_h. The typical range of geotechnical parameters for both Upper and Lower Holocene alluvial soils are presented in Figure 2. The Upper Holocene layer is highly compressible and relatively rapid consolidation whilst the Lower Holocene layer is expected to consolidate very slowly, taking many years to complete consolidation depending on its thickness and drainage path length. Strength characteristics were determined in terms of undrained strength (S_u) and drained effective strengths (c' and ϕ'). The interpreted S_u for the

Upper Holocene layer shows a great scattering range due to thin layers of silts or sands interbedded at various depths, whilst the Lower Holocene clay shows a trend of a gradual increase in undrained shear strength with depth varying from 10kPa to 20kPa.

4 DESIGN AND CONSTRUCTION

4.1 DESIGN CONSIDERATIONS AND METHODOLOGY

The design of a geofoam roadway embankment over soft soil was carried out in accordance with National Cooperative Highway Research Program (NCHRP) Report 529, web document 65 (Stark et al., 2004a; Stark et al., 2004b) and Transport Research Laboratory (TRL) Contract Report 356 (Sanders and Seedhouse, 1994) that provide the basis of the design framework for a geofoam application in roadway embankments.

The geofoam embankment primarily consists of foundation soil, fill mass including EPS (Expanded Polystyrene)-block geofoam and earth fill (fill cover), and pavement system, as shown in Figure 3. The design requires not only individual design of three major components of the embankment but also external and internal stabilities of the overall embankment taking into account interaction between its components. External stability of the embankment focuses on interaction of the embankment incorporating a mixture of EPS-block geofoam and normal density fills with foundation soil, whilst internal stability considers stability within the embankment itself. Both external and internal stability checks require design considerations for Serviceability Limit State (SLS) and Ultimate Limit State (ULS).

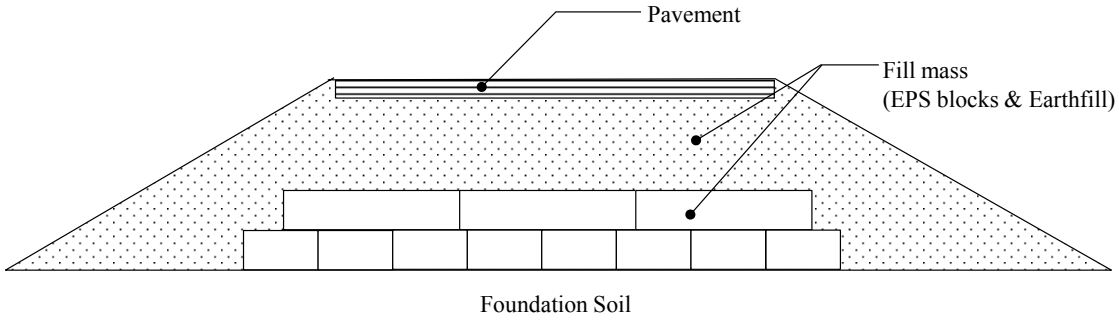

Figure 3: Typical cross section of an EPS-block geofoam embankment.

An overview of the geofoam embankment design procedure is summarised below:

- Gather background investigation information including ground conditions at the project site, maximum design flood levels for a return period similar to the design life of the embankment, temporary or permanent design loads applied to the embankment, and the locations and details of adjacent structures and services.
- Establish representative ground model including subsurface profile and geotechnical parameters.
- Undertake design checks of external (global) stability of the overall embankment that includes total and differential settlement of the soft foundation soil (SLS) and stability of the overall embankment (ULS) in relation to bearing capacity and slope stability under various loading conditions (e.g. hydrostatic uplift (flotation), lateral loading due to water and wind, and seismic loading) to the greatest extent practicable for the design life of the embankment.
- Undertake design checks of internal stability of the embankment including immediate and time-dependent (creep) settlement of the EPS-block geofoam mass due to overlying fill and pavement and stability under water, wind and seismic loadings.
- Undertake design of pavement in order to select suitable pavement type and arrangement.
- Estimate post construction settlement (PCS) that are likely to comprise any remaining primary consolidation settlement of the foundation soils due to dissipation of excess pore water pressure generated as a result of loading and secondary (creep) settlement of the foundation soils as a result of internal compression of the soil structure itself.

4.2 DESIGN CRITERIA

The project was required to fulfil the following design criteria for the geofoam embankment in terms of settlement and stability.

- Design life: 20 years
- Bearing capacity of embankment: FoS = 3
- External stability – Slope stability of embankment: FoS = 1.5
- External/internal stability – Seismic stability of embankment: FoS = 1.2
- External stability – Hydrostatic uplift: FoS = 1.2
- Internal stability – Load bearing (minimum required elastic limit stresses for EPS under pavement systems / within the EPS block): FoS = 1.2
- Post construction settlement of 150mm over 20 years within a structural zone
- Differential settlement gradient within the transition zone less than 1(vertical):200(horizontal)

The area of lightweight fill treatment was specified as a structural zone which was defined as a length not less than 25m within the approach to any structures such as existing bridge and culverts. This structural zone required strict control of the post construction settlement during its design life, whilst the non-structural zone allows the post construction settlement up to 225mm over 20 years.

4.3 GROUND MODEL AND GEOTECHNICAL DESIGN PARAMETERS

A representative ground model for the particular area of lightweight fill was developed based on existing geotechnical information. The geotechnical design parameters adopted for design of geofoam embankment were derived considering the potential variability of the ground conditions. The coefficient of consolidation in the horizontal direction (C_h) was assumed to be $2C_v$, where C_v is coefficient of consolidation in the vertical direction.

The embankment and surcharge fill primarily consist of a silty gravelly sandy clay mixture without any organic material, rocks, stones or any other hard materials that can retain on 75mm sieve size or any other unsuitable material that cannot support pavement.

The design groundwater level was assumed to be present at the ground surface level with hydrostatic pore water pressure distribution. For stability check against hydrostatic uplift, a maximum design flood level was assumed to correspond to finished road surface level.

Table 1: Geotechnical design parameters.

Material	Depth (top of layer) (m)	γ (kN/m^3)	c' (kPa)	ϕ' (°)	E' (kPa)	ν	S_u (kPa)	OCR	$C_{c\varepsilon}$	$C_{r\varepsilon}$	$C_{\alpha\varepsilon}$	C_v (m^2/yr)
Surcharge Fill	-	20	5	30	50000	0.3	-	-	-	-	-	-
Crust	0	18	5	30	8000	0.3	-	-	-	-	-	-
Upper Holocene Clay	0.7	16	2	24	2000	0.3	20	2.1	0.25	0.038	0.01	10
Holocene Sand	2.3	18	0	30	10000	0.3	-	-	-	-	-	-
Lower Holocene Clay	7.0	16	2	24	1000	0.3	Max (10 , 1.54z +0.77)	1.3	0.3	0.045	0.015	2.5
Pleistocene Clay	16.5	17	5	30	15000	0.3	90	2.5	0.04	0.006	0.002	15

4.4 DESIGN PROCEDURE

Design of EPS-block geofoam embankment was carried out with the following steps:

Step 1 – Selection of EPS block type and embankment arrangement

RMAX EPS (expanded polystyrene) geofoam Grade H was initially selected and finally verified during design process. It has the following physical properties: density 24kg/m^3 (equivalent to approximately 1% weight of normal earth fill), nominal compressive strength σ_{c10} = 135kPa at 10% strain, allowable compressive stress σ_{c2} = 100kPa at

2% strain and σ_{c1} = 48kPa at 1% strain, and long term water absorption by total immersion ≤ 3%. The standard commercially available size for the RMAX EPS geofoam for fill use is 5000mm x 1220mm x 600mm blocks.

For cost-effective design, the geofoam embankment arrangement was optimised in order to minimise the volume of EPS-block geofoam, which are generally more expensive than normal fill materials. Two layers of EPS blocks with a total thickness of 1.2m and 1.8m thick overburden consisting of earth fill and pavement were considered to form the geofoam roadway embankment, up to 3m in height. A crest width of the embankment of approximate 11.0m was considered with 1(vertical):2(horizontal) battered side slopes. The depth of soil covering the sides was considered not to be less than 250 mm, measured normally to the planes bounding the installed blocks.

Step 2 – External stability evaluation

Total settlement of an EPS-block geofoam embankment consists of immediate or elastic settlements of both the fill mass and the foundation soil, primary and secondary (creep) settlement of the foundation soil, and long-term creep of the EPS-block geofoam. Immediate or elastic settlements of both the fill mass and the foundation and creep of the EPS-block geofoam assemblage were ignored due to their negligible potential impact on the final pavement construction. On the basis of settlement calculations using one-dimensional consolidation theory, the estimated post construction settlement (comprising primary and secondary settlements) over 20 years was 270mm which exceeded the criteria when compared with the allowable settlement for structural zones (i.e. 150mm). A number of alternatives for foundation improvements were also assessed, including a geofoam embankment with helical screw piles. Prior to placement of EPS-block geofoam, six months preloading of 3.5m surcharge with prefabricated wick drains spacing of 1.0m in triangular pattern was eventually concluded to be most feasible and cost-effective in reducing post construction settlement to an acceptable level, particularly in relation to secondary creep settlements. A maximum primary settlement of 800mm was calculated within the preload area after 6 months of treatment, and a further 100mm post construction settlement over 20 years.

Bearing capacity of the foundation soil and static and seismic stability of the overall geofoam embankment were shown to be satisfactory with the design criteira. For external stability checks, the overburden loads due to the weight ofthe fill mass (EPS blocks and earth fill), pavement and traffic loads was modelled as equivalent pressure that was vertically applied to the surface of the foundation soil. The shear strengths of the EPS blocks, earth fill and pavement were threfore ignored. Use of equivalent pressure instead of modelling the complex behaviour of the EPS-block geofoam embankment has been used in estimating slope stability through the soft soil foundation (Public Works Research Institute, 1992). An example of the external stability check for the simplified EPS-block geofoam embankment is presented in Figure 4.

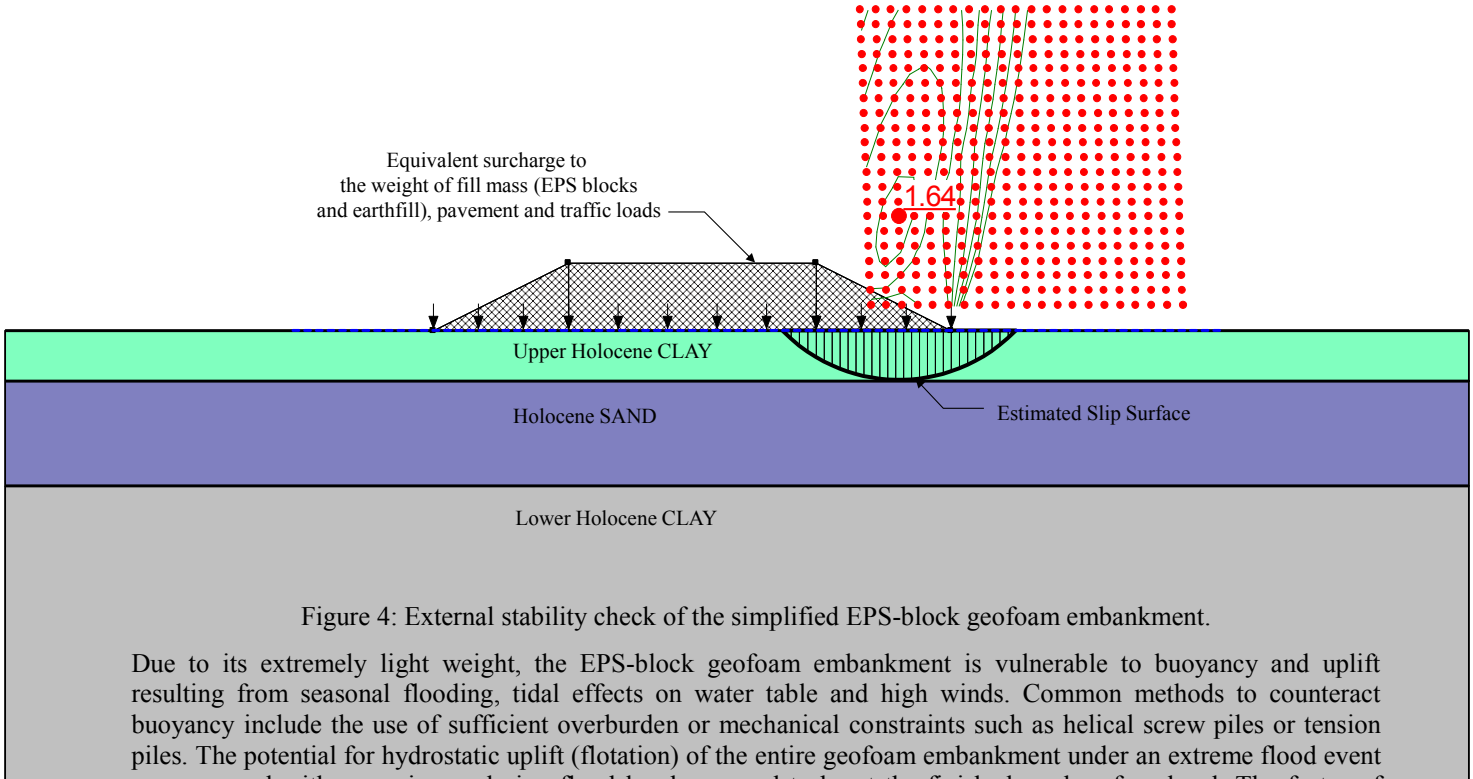

Figure 4: External stability check of the simplified EPS-block geofoam embankment.

Due to its extremely light weight, the EPS-block geofoam embankment is vulnerable to buoyancy and uplift resulting from seasonal flooding, tidal effects on water table and high winds. Common methods to counteract buoyancy include the use of sufficient overburden or mechanical constraints such as helical screw piles or tension piles. The potential for hydrostatic uplift (flotation) of the entire geofoam embankment under an extreme flood event was assessed with a maximum design flood level assumed to be at the finished road surface level. The factor of safety against buoyancy of the embankment is calculated as the ratio of the overburden weight available from the

geofoam embankment to the uplift water force at the base of the embankment. As the geoform is extremely light, sufficient overburden is allowed over the EPS blocks to achieve the required factor of safety. For a road embankment of normal width and moderate height, stability due to lateral loading induced by wind or water is unlikely to be a problem for the completed embankment.

Step 3 – Internal stability evaluation

Internal seismic stability assessment considered failure modes occurring within the geofoam embankment along the following interfaces: 1) between the overburden fill and the EPS blocks, 2) between two consecutive EPS blocks layers and 3) between the EPS blocks and the foundation soil. The internal stability of the embankment was assessed to meet the design criteria with an assumed horizontal seismic coefficient of 0.2.

An EPS geofoam product was selected to have the required properties to support the overlying earth fill, pavement and traffic loads. Such product, when subjected to the estimated loads, will remain to be within the elastic range with an elastic limit stress equivalent to the compressive stress at 1% strain. The analysis indicated that RMAX EPS (expanded polystyrene) geofoam Grade H was appropriate, satisfying the required EPS elastic limit stress for placement underneath the fill and pavement.

Step 4 – Final embankment design

An EPS-block geofoam embankment is inherently susceptible to damage resulting from many potential causes, e.g. petrol and chemical attack, heat and flame, ultra violet light and so on. Geofoam can be protected from most of these risks by being covered with a layer of earth fill and pavement materials. However, these cover materials may be permeable to petrol and other fluids. In the design, the EPS-block geofoam assemblage was encapsulated with impermeable and chemical resistance membrane of 0.75mm in thickness (EnviroLiner 6030) and a 150mm thick lightly reinforced concrete slab (C20/25) was casted in place in order to provide an effective barrier against any chemical spills which could dissolve the EPS-block geofoam. This slab is deemed to be beneficial in improving the distribution of wheel loads. A typical cross section of the EPS-block geofoam embankment is presented in Figure 5 with detailed arrangement of relevant components.

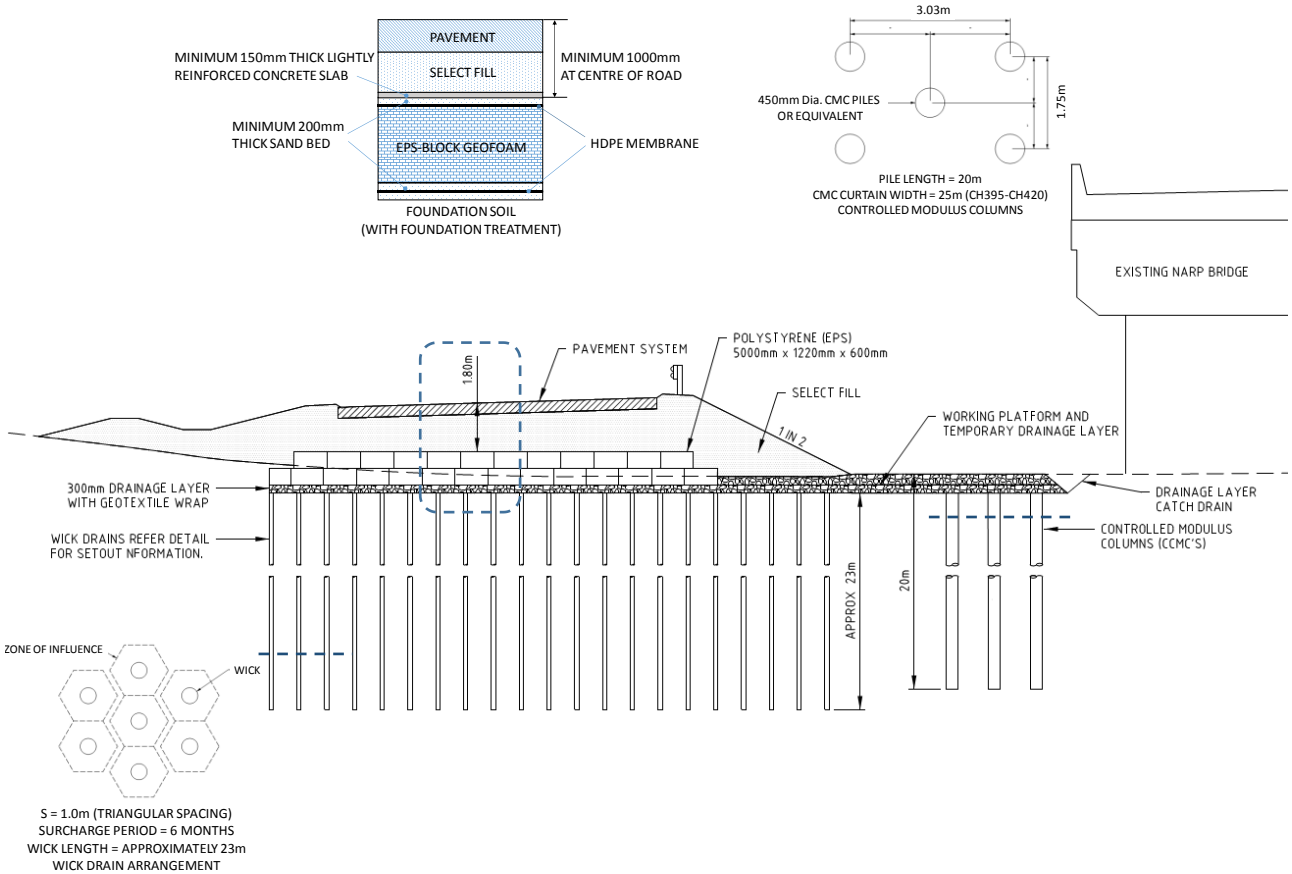

Figure 5: Typical cross section and arrangement of the proposed geofoam embankment.

Where the geofoam embankment adjoins an earth fill embankment, transitional arrangements were designed by adopting progressive reduction in the thickness of the EPS-block over the transition zone. Sufficient length of the transition zone was allowed to minimise differential settlements between different embankment zones and to achieve a settlement gradient of less than 1(vertical):200(horizontal).

4.5 CONSTRUCTION OF GEOFOAM EMBANKMENT

Prior to the placement of EPS-block geofoam to form the roadway embankment, long-term performance of the foundation soils were improved by means of six months preloading with 3.5m surcharge and wick drains (1.0m centre-to-centre spacing in a triangular pattern). The impact of preloading on the existing bridge piles was minimised by three rows of control modulus columns installed to a depth of 20m below ground level between the preload embankment and the bridge (see Figure 5 for details).

(a) Excavation to base level

(b) Foundation preparation

(c) Geofoam installation

(d) Protective membrane installation

(e) Earth fill cover placement

(f) Pavement construction

Figure 6: Geofoam embankment construction.

The site for lightweight fill treatment was firstly prepared by removing the placed surcharge down to the proposed geofoam base. A basal geotextile was placed over the excavated surface on which a bedding layer of sand of a minimum of 200mm in thickness was placed and levelled to prepare a smooth and planar surface. A protective membrane sheet (HDPE) was laid over the bedding sand layer and then covered by another layrer of sand of a minimum of 200mm thickness. This upper sand layer was to allow increased friction between the HDPE membrane and the EPS-block geofoam. The first layer of EPS-block geofoam was placed on the sand bedding layer with staggered joint arrangement where voids and open joints were avoided. The subsequent layer of the geofoam blocks was placed in a similar fashion. The stepped sides of the geofoam generally required the blocks to be resized to suit the required geometry using a hot wire. To prevent displacement of the blocks during construction they were fixed together at intervals with polyurethane-based adhesive or mechanical fasteners. Once geofoam blocks were in place, they were covered and sealed by joining the protective HDPE membranes using extrusion welding as soon as possible. Minor damage to the membranes was repaired with the patch extending at least 200mm outside the damaged area. The overburden earth fill was placed and compacted under controlled and certified conditions. The pavement was finally constructed in accordance with usual practices and rules. Figure 6 shows stages of the geofoam embankment construction.

Any water at or near the ground surface was pumped off until the geofoam blocks are covered by overburden materials with sufficient weight to prevent floatation. A temporary culvert placed on the site during the preloading period was replaced with a permanent one prior to construction of pavement.

5 CONCLUSIONS

The application of lightweight fill (EPS-block Geofoam) was successfully implemented for construction of the road embankment on soft alluvial soils for the new Banksia Place Stage 1A Service Centre development. It has demonstrated that the geofoam embankment can significantly reduce risks associated with embankment construction on soft ground in terms of slope stability, settlement and impact on adjacent structures.

Furthermore, use of EPS-block geofoam allows rapid construction of full-height embankment in a short period of time without any difficulty in handling construction materials. The new Banksia Place Stage 1A Service Centre development was successfully completed and opened in July 2014 as planned.

6 REFERENCES

Public Works Research Institute. (1992). “Design and Construction Manual for Lightweight Fill with EPS” The Public Works Research Institute of Ministry of Construction and Construction Project Consultant, Inc., Japan.

Sander, R.L., and Seedhouse, R.L. (1994). “The Use of Polystyrene for Embankment Construction.” Contractor Report 356, Transport Research Laboratory, Crowthorne, Berkshire, UK.

Stark, T.D., Arellano, D., Horvath, J.S., and Leshchinsky, D. (2004a). “Geofoam Applications in the Design and Construction of Highway Embankments.” NCHRP Web Document 65 (Project 24-11), Transport Research Board, Washington, D.C.

Stark, T.D., Arellano, D., Horvath, J.S., and Leshchinsky, D. (2004b). “Guideline and Recommended Standard for Geofoam Applications in Highway Embankments.” NCHRP Report 529, Transport Research Board, Washington, D.C.